

The first complete mitochondrial genome of a *Lethrus* species (Coleoptera, Geotrupidae) with phylogenetic implications

Réka Zsófia Bubán^{1,2}, Renáta Bőkényné Tóth¹, Csongor Freytag¹, Gábor Sramkó^{2,3}, Zoltán Barta^{4,5}, Nikoletta Andrea Nagy^{4,5}

¹ One Health Institute, University of Debrecen, Nagyerdei krt. 98, H-4032 Debrecen, Hungary

² Department of Botany, University of Debrecen, Egyetem tér 1, H-4032 Debrecen, Hungary

³ HUN-REN-UD Conservation Biology Research Group, University of Debrecen, Egyetem tér 1, H-4032 Debrecen, Hungary

⁴ Department of Evolutionary Zoology and Human Biology, University of Debrecen, Egyetem tér 1, H-4032 Debrecen, Hungary

⁵ HUN-REN-UD Behavioural Ecology Research Group, Department of Evolutionary Zoology, University of Debrecen, Egyetem tér 1, H-4032 Debrecen, Hungary

Corresponding author: Nikoletta Andrea Nagy (nagy.nikoletta@science.unideb.hu)

Abstract

The flightless beetle genus *Lethrus* Scopoli, 1777 (Geotrupidae, Scarabaeoidea) has a large distribution area throughout Eurasia and is characterized by many species, especially in Middle Asia. Despite this diversity and the potential importance as models for speciation, *Lethrus* species are underrepresented in molecular databases. To fill this gap, we report the complete mitochondrial genome of *Lethrus scoparius* obtained using third-generation sequencing technology. The circular mitogenome is 24,944 bp long and has a structure characteristic of coleopterans. It contains 37 genes, including 13 protein-coding genes, two ribosomal RNA genes, 22 transfer RNA genes, and an A+T-rich non-coding region, the control region between the 12S rRNA and tRNA-*Ile* (GAU). The phylogenetic analysis of the superfamily Scarabaeoidea placed *L. scoparius* in the monophyletic family Geotrupidae, which is related to the family Scarabaeidae. The assembled mitochondrial genome is a valuable new genomic resource in the genus *Lethrus* and contributes to a better understanding of the evolutionary history of the genus and the entire family Geotrupidae.

Key words: Circular mitogenome, phylogenetic relationship, phytophagous, Scarabaeoidea, third-generation sequencing



Academic editor: Andrey Frolov

Received: 3 October 2024

Accepted: 3 March 2025

Published: 24 April 2025

ZooBank: <https://zoobank.org/3B9BEE98-798A-4BBE-BA6A-0E81037E42F8>

Citation: Bubán RZ, Tóth RB, Freytag C, Sramkó G, Barta Z, Nagy NA (2025)

The first complete mitochondrial genome of a *Lethrus* species (Coleoptera, Geotrupidae) with phylogenetic implications. ZooKeys 1236: 1–17. <https://doi.org/10.3897/zookeys.1236.138465>

Copyright: © Réka Zsófia Bubán et al.
This is an open access article distributed under terms of the Creative Commons Attribution License (Attribution 4.0 International – CC BY 4.0).

Introduction

The family Geotrupidae is a relatively small, monophyletic group within the large and diverse superfamily Scarabaeoidea (Coleoptera) (Vuts et al. 2014). The species belonging to this group are divided into three subfamilies: Geotrupinae, Taurocerastinae, and Lethrinae (Cunha et al. 2011). The latter group consists of only one genus, *Lethrus* Scopoli, 1777, which comprises about 130 species and is subdivided into several subgenera (Shapovalov 2022). These beetles are flightless and have fused elytra. Most species exhibit sexual dimorphism, in which the males have a pair of tusk-like appendages on the ventral side of their mandibles that the females do not bear (Bagaturov and Nikolajev

2015). Another distinctive feature of these species compared to their geotrupid relatives is that they are phytophagous, feeding on fresh plant material of various species (Shapovalov 2022).

Lethrus is one of the most species-rich genera within the family Geotrupidae, with a wide distribution range in the Palearctic, especially in semi-arid habitats from Central and Southeastern Europe to China and Mongolia (Král et al. 2013; Bagaturov and Nikolajev 2015; Shapovalov 2022). Although some species occur sympatrically, most *Lethrus* species have small allopatric distributions (e.g. Král et al. 2013; Shapovalov 2022). One possible explanation for this patchy distribution pattern is the flightless nature of these species that might have limited their dispersal ability and thus triggered an increased speciation rate within the genus, similar to other examples (Ikeda et al. 2012; Salces-Castellano et al. 2021), especially in the regions of Middle Asia and the Balkans (Scholtz 2000; Bagaturov and Nikolajev 2015; Tóth et al. 2019). Despite the relatively high number of species in the genus and the unique life history traits, there are few molecular resources available for this taxon, both for phylogenetic and ecological genetic purposes.

In a study aimed at elucidating the phylogenetic relationships between the European *Lethrus* species based on targeted mitochondrial and nuclear loci, molecular data on Middle Asian species included as outgroup taxa were presented for the first time (Tóth et al. 2019). They were placed at the basal position of the genus. In this study, one species with a limited distribution area, *Lethrus scoparius* Fischer von Waldheim, 1822, was found to represent a clade subordinate to the European species. This species lives in the western Tian Shan, where individuals inhabit the plains and foothills (Nikolajev 2003). Based on the morphology of the adults, *L. scoparius* shows remarkable differences from the other species of the genus and was therefore described as the only member of the subgenus *Autolethrus* and proposed for further molecular studies to clarify its relationship with other *Lethrus* species (Bagaturov and Nikolajev 2015).

Mitochondrial genomes are important resources for phylogenetic, phylogeographic and population genetic studies at broad taxonomic scales (Cameron 2014; Kern et al. 2020; Zhao et al. 2021) because they are relatively small, simple in structure, have conserved gene arrangements, stable compositions and are maternally inherited (Kern et al. 2020; Jia et al. 2023). Although complete, circular mitochondrial sequences are available for many Scarabaeoidea species, they are scarce in the family Geotrupidae. The sole mitochondrial genome from the genus is that of *Lethrus apterus* Laxmann, 1770 (Nagy et al. 2021), which is fully annotated but incomplete. *De novo* assemblies of mitogenomes using short reads in many cases resulted in partial genomes, without an assembled A+T-rich non-coding region, also known as the control region (CR), and even without genes located near this highly repetitive sequence (e.g. Song and Zhang 2018). With the advances of long-read sequencing platforms, the incompleteness of such assemblies can be addressed.

In this study, we used Oxford Nanopore Technologies (ONT) long-read sequencing to determine the complete mitochondrial genome of *Lethrus scoparius*. It is the first complete mitogenome of the genus and one of the two available circularly assembled mitogenomes in the family Geotrupidae. We describe the structure of the genome, codon usage, nucleotide composition, and gene order.

Additionally, we compare these features with the other complete mitochondrial genomes within the superfamily and examine the phylogenetic relationships of the taxa. The mitochondrial genome presented provides valuable information for future work to uncover the internal relationships within the genus *Lethrus* and at higher taxonomic levels.

Methods

Sample collection and DNA extraction

An adult male of *Lethrus scoparius* was collected on 1 May 2023 in Tian Shan, Kazakhstan (42°23.96'N, 70°27.66'E) and housed at the Department of Evolutionary Zoology and Human Biology, University of Debrecen, Hungary. The species was identified by morphological characteristics (Bagaturov and Nikolajev 2015) and stored in 96% ethanol at 4 °C until DNA extraction. High-molecular-weight (HMW) DNA was isolated from the whole body using a conventional DNA extraction method. Briefly, a lysis buffer with a final concentration of 3 mM CaCl₂, 2% sodium dodecyl sulfate (SDS), 40 mM dithiothreitol (DTT), 250 µg/ml proteinase K, 100 mM Tris buffer (pH = 8.0) and 100 mM NaCl was used (Gilbert et al. 2007). Cell lysis lasted 2 h at 55 °C, during which the sample was inverted several times. After incubation, the sample was centrifuged at 14,000 *g* for 1 min and the supernatant was transferred to a clean 2 ml tube to avoid contamination with chitin in subsequent steps. Then the sample was incubated with 15 µl (10 mg/ml) RNase A (Roche, Switzerland) for 10 minutes at 37 °C. In the next step, 0.5 volume of 7.5 M ammonium acetate was added, and the sample was incubated at +4 °C for 10 min. After incubation, 0.5 volume of a chloroform-isoamyl alcohol mixture (24:1) was added and the sample was incubated for 10 min at room temperature. The sample was centrifuged at 10,000 *g* for 3 min, then the supernatant was transferred to a clean 2 ml tube. After this step, 1 volume of room temperature isopropanol was added, and the sample was incubated at +4 °C for 15 min. After the sample was centrifuged at 10,000 *g* for 3 min, the supernatant was carefully removed from the pellet. The pellet was washed twice with 1 volume of room temperature 70% ethanol and centrifuged at 10,000 *g* for 3 min in between. The pellet was air-dried at room temperature and then dissolved in 65 µl of 10 mM Tris-HCl (pH = 8.0).

The nucleic acid concentration and purity of the sample were measured using a NABI UV/Vis Nano Spectrophotometer (MicroDigital Co., Ltd, Korea). The integrity of DNA was checked by TBE agarose gel (1%) electrophoresis.

Residual RNA contamination was removed by an additional 30-min digestion step at 37 °C with RNase Cocktail™ Enzyme Mix (0.1 U RNase A and 4 U RNase T1) (Invitrogen, USA). Further purification steps were performed with 0.6 volume of Ampure XP (Beckman Coulter, USA) according to the manufacturer's instructions. To remove short DNA fragments, 0.64 volume of Long Fragment Buffer (Oxford Nanopore Technologies, UK) were also added. The decontaminated DNA was dissolved in 20 µl of nuclease-free water (Omega Bio-tek, Inc., USA). The concentration and purity of DNA were checked using a NanoDrop One (Thermo Fisher Scientific Inc., USA), a Qubit 4 Fluorometer (Thermo Fisher Scientific Inc., USA) with the 1x dsDNA High Sensitivity Kit (Thermo Fisher Scientific Inc., USA) and TBE agarose gel electrophoresis (1%).

Library construction and sequencing

The third-generation sequencing library (ONT) was prepared from 1 µg of genomic DNA using the Ligation Sequencing Kit V14 (SQK-LSK114) (Oxford Nanopore Technologies, UK) according to the manufacturer's recommendations. For DNA end repair, the NEBNext® Companion Module for Oxford Nanopore Technologies® Ligation Sequencing (NEB, E7180S) (New England Biolabs, Inc.) was used. 52 ng of the final library was loaded two times onto an R10.4 flow cell (FLO-MIN114). The sequencing run was performed using a MinION Mk1C device for 72 h.

Genome assembly and annotation

The sequencing yielded 9.26 giga base pairs (Gbp) of raw data. The Super high-accuracy model with Guppy 6.5.7 (Wick et al. 2019) was used for basecalling. Raw sequencing reads have been deposited to the Sequence Read Archive (SRA) under the accession number SRR28464392. The quality of the long reads was checked with the R script of MinIONQC 1.4.2 (Lanfear et al. 2019). Reads of the used DNA control strand (DNA CS) were removed with NanoLyse 1.2.0, then NanoFilt 2.8.0 (De Coster et al. 2018) was used to trim both ends of the reads (--headcrop 50, --tailcrop 50) and eliminate reads with low quality (mean quality cut-off 8 (-q 8)) or insufficient length (shorter than 500 bp (-l 500)). The cleaned and filtered reads were analyzed with NanoPlot 1.40.0 (De Coster et al. 2018). The quality filtering resulted in 2,751,077 clean reads with a total length of 6.79 Gbp and a read N50 of 4,124 bp.

Minimap 2.17 (Li 2018) was used to map the filtered reads to the mitochondrial genome of *Lethrus apterus* (Nagy et al. 2021), the closest relative with a fully annotated but incomplete mitochondrial genome. Reads covering more than 70% of the reference mitogenome were accepted as mitochondrial sequences. *De novo* assembly of the mitochondrial reads was performed using Flye 2.9 (Kolmogorov et al. 2019) with the predicted genome size set to 16 kbp and the assembly coverage set to 100 (-g 16k --asm-coverage 100). The assembled sequence was polished using Racon 1.4.10 (Vaser et al. 2017) and medaka 1.7.2 (<https://github.com/nanoporetech/medaka>) with the model r1041_e82_400bps_sup_g615. The annotation of the assembled mitochondrial genome was performed with MITOS2 (Donath et al. 2019) based on the invertebrate genetic code. The annotated mitochondrial genome was visualized using Proksee (Grant et al. 2023).

The AT-, and GC-skew of the sequences were calculated with the following formulas: AT-skew = $(A - T) / (A + T)$; and GC-skew = $(G - C) / (G + C)$ (Perna and Kocher 1995). Amino acid abundances and relative synonymous codon usage (RSCU) values of mitochondrial protein-coding genes (PCGs) were analyzed with Ezcodon (Lee 2018) implemented in EZmito Server (Cucini et al. 2021) using the invertebrate mitochondrial genetic code.

Phylogenetic analysis

The complete circular and annotated mitochondrial genomes of the superfamily Scarabaeoidea were downloaded from NCBI GenBank on 13 January 2025 (Suppl. material 1: table S1). Species represented the families Lucanidae (three

subfamilies), Geotrupidae, Passalidae, Scarabaeidae (six subfamilies), and Trogidae. The mitogenome of the closest relative, *Lethrus apterus*, was also included, as it contains all coding regions needed to reconstruct the phylogenetic tree. In addition, the mitochondrial genomes of *Apatetica glabra* (Staphylinoidea), *Diamesus osculans* (Staphylinoidea), and *Sphaeridium bipustulatum* (Hydrophiloidea) were used as outgroup samples. The nucleotide sequences of PCGs and ribosomal RNA (rRNA) coding genes were collected from the annotations. The sequences of PCGs were aligned with MACSE 2.07 (Ranwez et al. 2018) using the invertebrate mitochondrial code (-gc_def 5), and MUSCLE 3.8.1551 (Edgar 2004) was used to align the rRNA gene sequences. The aligned nucleotide sequences were merged using AMAS.py (Borowiec 2016) to obtain a 13,812 bp long alignment. Phylogenetic reconstruction was performed using IQ-TREE 2.0.3 (Nguyen et al. 2015). All genetic regions were defined as distinct partitions and ModelFinder Plus (Kalyaanamoorthy et al. 2017) was used to find the best fitting partition scheme for the dataset. Branch support was assessed using the SH-like approximate likelihood ratio test (SH-aLRT) (Guindon et al. 2010) and the ultrafast bootstrap (UFBoot) (Minh et al. 2013) with 1000 replicates.

Results

General characteristics of the mitogenome

The assembled mitochondrial genome of *Lethrus scoparius* was complete, circular, and 24,944 bp long. The mitogenome contained 13 protein-coding genes (PCG), two ribosomal RNA genes (rRNA), 22 transfer RNA genes (tRNA), and the control region (CR) (Fig. 1, Table 1). Most of the PCGs and tRNA genes as well as the CR were encoded on the heavy strand, whereas the remaining four PCGs (*nad1*, *nad4*, *nad4l* and *nad5*), eight tRNA genes (tRNA-Cys (GCA), tRNA-Gln (UUG), tRNA-His (GUG), tRNA-Leu (UAG), tRNA-Phe (GAA), tRNA-Pro (UGG), tRNA-Tyr (GUA), tRNA-Val (UAC)), and the two rRNA genes were located on the light strand (Table 1).

The overall base composition of the mitogenome was 41.3% A, 13.6% C, 7.9% G, and 37.2% T, and the A+T content was 78.48%. The AT-skew was slightly positive: 0.052, and the GC-skew was negative: -0.268 (Suppl. material 1: table S2). Descriptive statistics of the protein-coding genes, transfer RNA genes and ribosomal RNA genes, including the amino acid frequency and the codon usage, length distribution and base content are detailed in the Suppl. material 1.

Non-coding and overlapping regions

The largest non-coding region in the mitogenome of *L. scoparius* was the control region at 9,752 bp in length. The CR was located between the 12S rRNA and the tRNA-Ile (GAU) genes and had an A+T content of 80.2%. The base content of this region was 42.04% A, 13.33% C, 6.45% G, and 38.18% T. The AT-skew of the CR had a positive value of 0.048 and the GC-skew had a negative value of -0.348. The second largest non-coding region in the mitogenome had a length of 499 bp and was located between the *nad2* and tRNA-Trp (UCA) genes. In addition, 12 other intergenic spacers were found that were between 1 bp and 40 bp in length (Table 1).

Table 1. Annotation of the mitochondrial genome of *Lethrus scoparius*. The Strand column shows the orientation of the genes, where the + marks the heavy strand and – denotes the light strand. The ovl/nc column indicates the overlapping or intergenic (non-coding) nucleotides, where the positive value means intergenic nucleotides and the negative value indicates overlapping nucleotides.

Gene	Region (bp)	Strand	Length (bp)	ovl/nc	Codons	
					Start	Stop
tRNA-Ile (GAU)	1–67	+	67	0		
tRNA-Gln (UUG)	68–136	–	69	–1		
tRNA-Met (CAU)	136–204	+	69	30		
<i>nad2</i>	235–1,218	+	984	499	ATT	TAA
tRNA-Trp (UCA)	1,718–1,784	+	67	–8		
tRNA-Cys (GCA)	1,777–1,839	–	63	1		
tRNA-Tyr (GUA)	1,841–1,908	–	68	–2		
<i>cox1</i>	1,907–3,445	+	1,539	–5	TCG	TAA
tRNA-Leu (UAA)	3,441–3,504	+	64	–1		
<i>cox2</i>	3,504–4,187	+	684	3	ATG	TAA
tRNA-Lys (CUU)	4,191–4,261	+	71	0		
tRNA-Asp (GUC)	4,262–4,328	+	67	0		
<i>atp8</i>	4,329–4,484	+	156	–7	ATC	TAA
<i>atp6</i>	4,478–5,149	+	672	1	ATG	TAA
<i>cox3</i>	5,151–5,938	+	788	–1	ATG	TA(A)
tRNA-Gly (UCC)	5,938–6,003	+	66	0		
<i>nad3</i>	6,004–6,357	+	354	–2	ATA	TAG
tRNA-Ala (UGC)	6,356–6,421	+	66	–1		
tRNA-Arg (UCG)	6,421–6,486	+	66	3		
tRNA-Asn (GUU)	6,490–6,554	+	65	0		
tRNA-Ser (UCU)	6,555–6,621	+	67	0		
tRNA-Glu (UUC)	6,622–6,688	+	67	–2		
tRNA-Phe (GAA)	6,687–6,752	–	66	–3		
<i>nad5</i>	6,750–8,463	–	1,714	9	ATT	T(AA)
tRNA-His (GUG)	8,473–8,538	–	66	–1		
<i>nad4</i>	8,538–9,874	–	1,337	–7	ATG	TA(A)
<i>nad4l</i>	9,868–10,158	–	291	2	ATG	TAA
tRNA-Thr (UGU)	10,161–10,224	+	64	0		
tRNA-Pro (UGG)	10,225–10,288	–	64	2		
<i>nad6</i>	10,291–10,794	+	504	–1	ATT	TAA
<i>cytb</i>	10,794–11,936	+	1,143	–2	ATG	TAG
tRNA-Ser (UGA)	11,935–12,000	+	66	17		
<i>nad1</i>	12,018–12,929	–	912	40	ATA	TAA
tRNA-Leu (UAG)	12,970–13,030	–	61	–23		
16S rRNA	13,008–14,320	–	1,313	18		
tRNA-Val (UAC)	14,339–14,408	–	70	0		
12S rRNA	14,409–15,192	–	784	0		
CR	15,193–24,944	+	9,752	–		

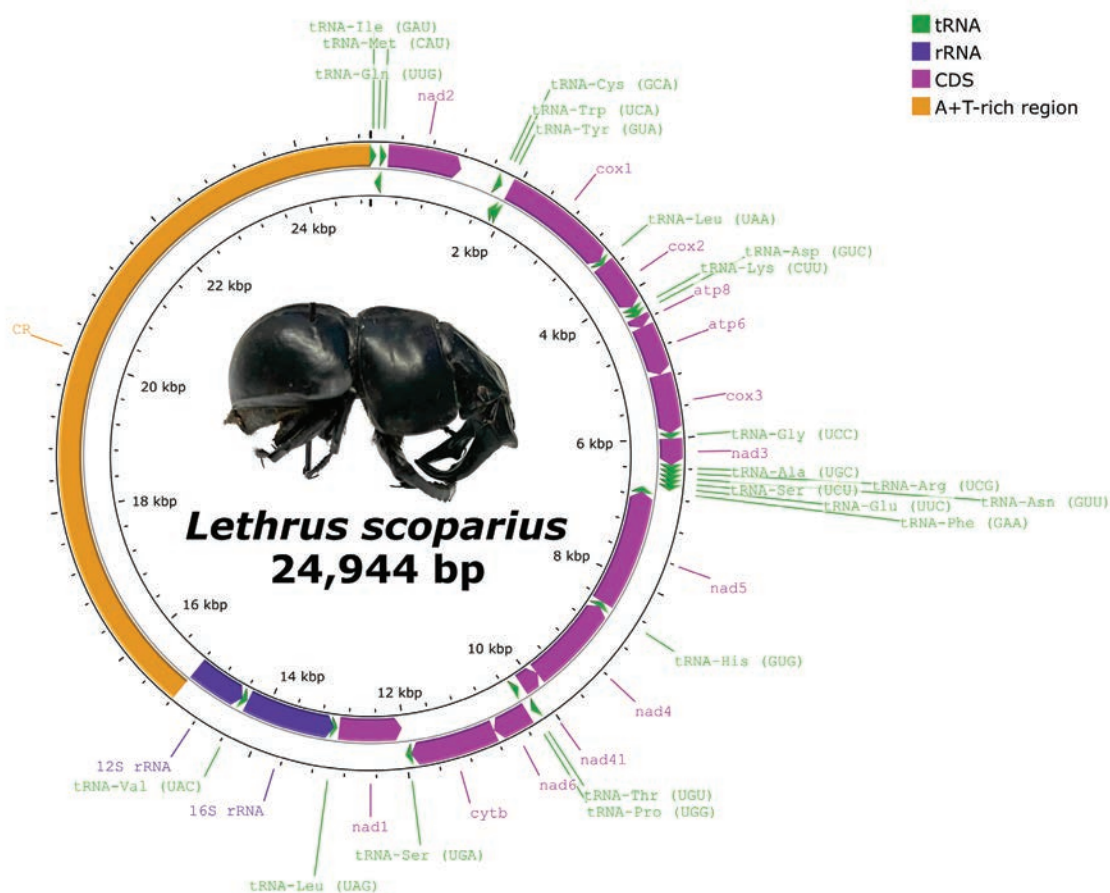


Figure 1. The circular mitochondrial genome map of *Lethrus scoparius*. Genes on the outer circle are located on the heavy strand, whereas the inner circle represents genes on the light strand. Protein-coding genes are shown in purple, tRNA genes in green, rRNA genes in blue, and the control region is represented in orange. Photo taken by RZB.

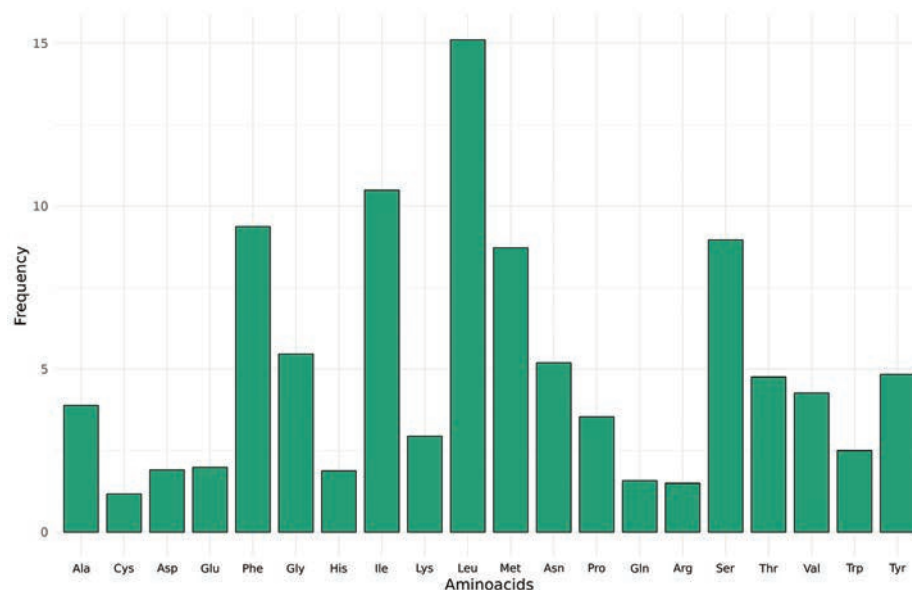


Figure 2. Amino acid frequency of the PCGs in the assembled mitochondrial genome of *Lethrus scoparius*. Three-letter amino acid code is shown on the X-axis and the frequency of amino acids in percentage on the Y-axis.

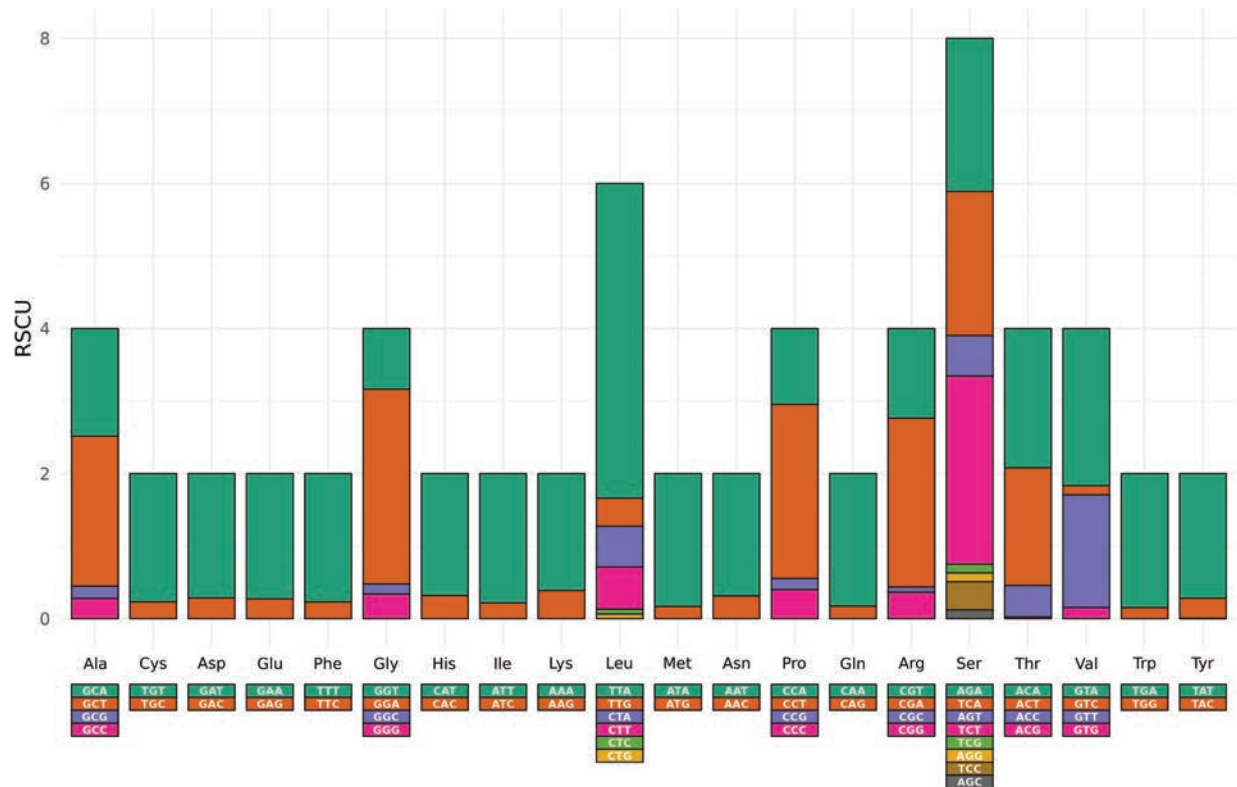


Figure 3. Relative synonymous codon usage (RSCU) of the PCGs in the assembled mitochondrial genome of *Lethrus scoparius*. Codon families and the three-letter amino acid codes are indicated on the X-axis and RSCU values on the Y-axis. Different colors of the bars represent different codons coding for the amino acid.

Several overlapping regions were observed in the mitogenome. The length of these sequences ranged from 1 bp to 23 bp (Table 1). The largest overlapping region was located between the tRNA-*Leu* (UAG) and the 16S rRNA genes. A 7-bp overlap with the “ATGATAA” motif was found between the PCGs *atp8* and *atp6*. In addition, an 8-bp overlap with the “AAGCCTTA” motif was detected between tRNA-*Trp* (UCA) and tRNA-*Cys* (GCA). Finally, an overlap with the “TTAA-CAT” motif was found between *nad4* and *nad4l*.

Phylogenetic analysis

We performed a maximum-likelihood (ML) phylogenetic tree reconstruction based on the nucleotide sequences of the PCGs and rRNA genes of 145 species of the superfamily Scarabaeoidea (Fig. 4). Our analysis revealed two monophyletic groups in addition to the outgroup, one containing the representatives of the family Lucanidae and the other consisting of the species of all four other families. Within the Lucanidae clade, all three subfamilies formed separate monophyletic clusters with the following branching: (Syndesinae (Aesalinae + Lucaninae)). The structure of the other clade was (Trogidae (Geotrupidae (Scarabaeidae + Passalidae))). Within the family Scarabaeidae, the subfamilies Rutelinae and Dynastinae were found to be monophyletic sister groups with the closest relationship to the Cetoniinae. The species of the Melolonthinae were clustered into a paraphyletic group with two main branches. One of these was a sister group to the clade

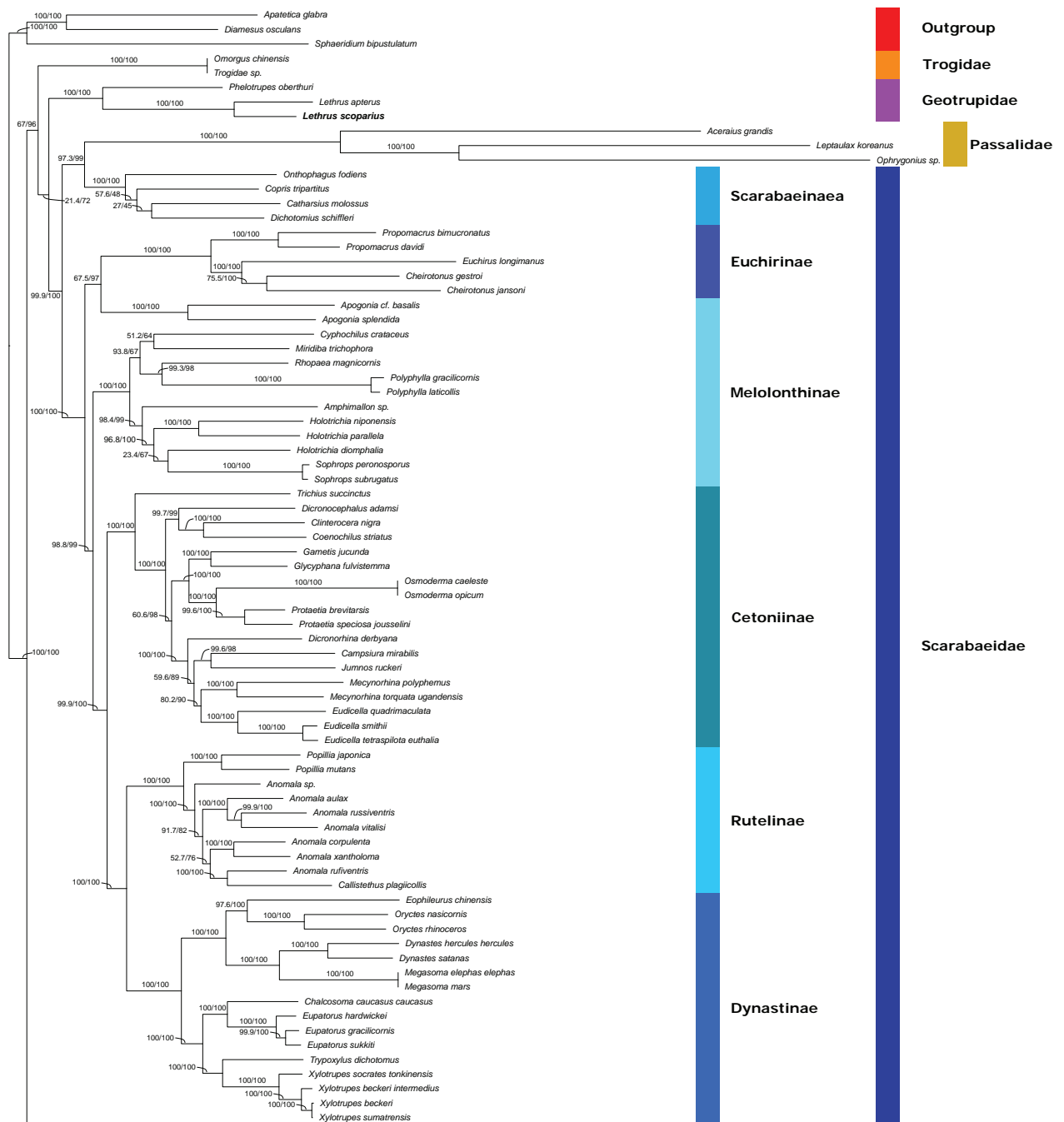


Figure 4. The reconstructed phylogenetic tree of the superfamily Scarabaeoidea based on species with a complete circular and annotated mitochondrial genome in the NCBI GenBank database (split into two parts). *Apatetica glabra*, *Diamesus osculans* and *Sphaeridium bipustulatum* were used as an outgroup. This maximum-likelihood tree was based on the nucleotide sequences of 13 mitochondrial PCGs and two rRNA genes. Branch supporting was evaluated with SH-like approximate likelihood ratio test (SH-aLRT) and ultrafast bootstrap (UFBoot) with 1000 replicates. Colors represent the respective subfamilies (left panel) and families (right panel). *Lethrus scoparius* is highlighted in bold.

((Rutelinae + Dynastinae) Cetoniinae), the other to the subfamily Euchirinae. Interestingly, the paraphyly of the family Scarabaeidae was a result of the cluster consisting of the subfamily Scarabaeinae and the family Passalidae. Within the family Geotrupidae, the two *Lethrus* species were found to have a sister relationship to the third representative of the family, *Phelotrupes oberthuri* Boucomont, 1905.

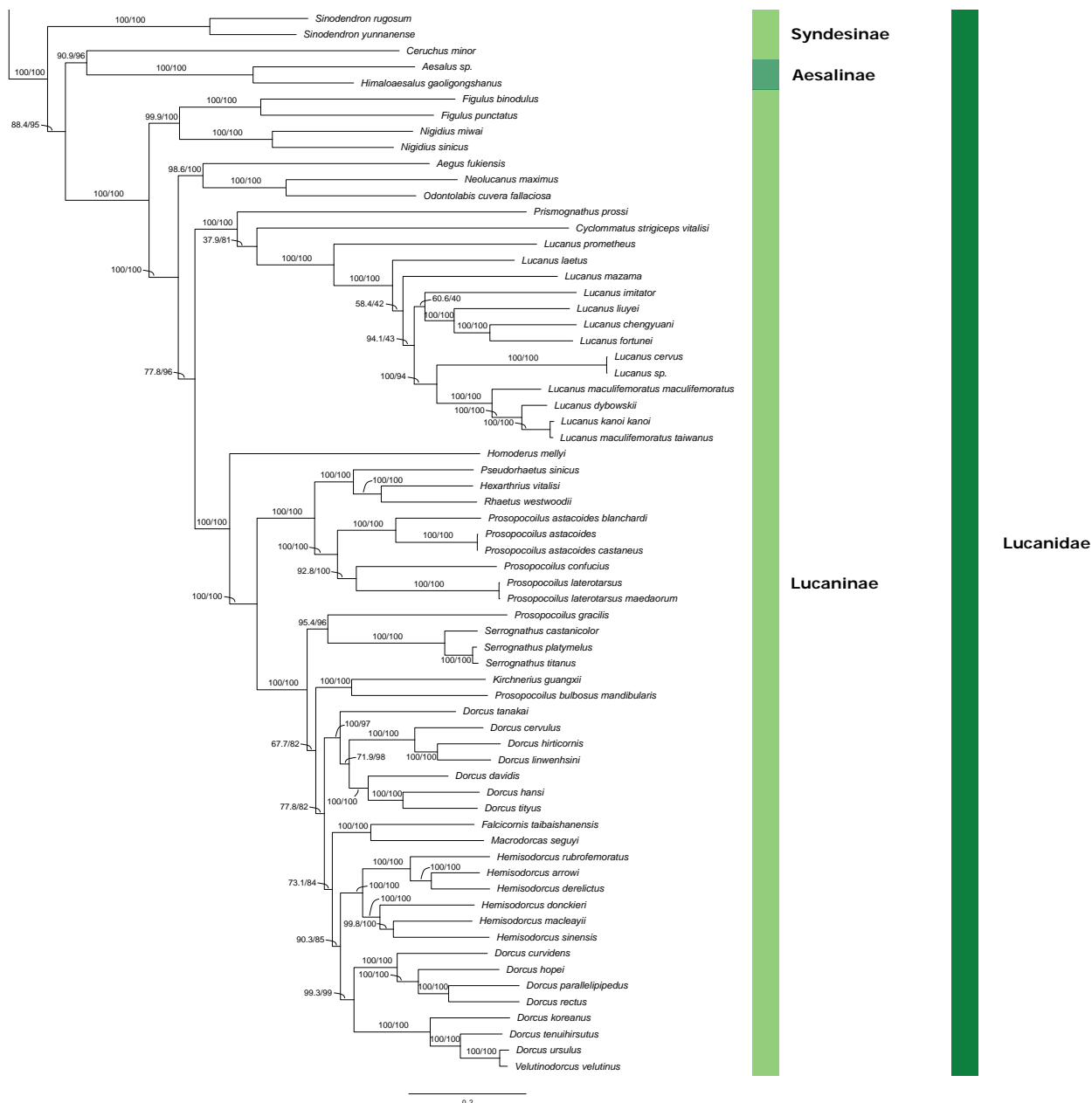


Figure 4. Continued.

Discussion

Lethrus scoparius is a rare Middle Asian earth-boring beetle from the genetically poorly characterized family Geotrupidae. Although *Lethrus* is one of the most species-rich genera in this family, molecular information on this scarabaeoid genus remains limited. In this study, we present the mitochondrial genome of *L. scoparius*, the first complete and well-characterized mitogenome of the genus. The mitogenome is 24,944 bp long and contains 37 genes (13 protein-coding genes, two ribosomal RNA genes and 22 transfer RNA genes) and a control region. The length of our assembled mitogenome is comparable with the elongated genomes found in Hercules beetles (*Dynastes*) (Morgan et al. 2022) and seed beetles (*Callosobruchus*) (Sayadi et al. 2017). The observed arrangement of genes was identical to the order of the insect ancestral mitochondrial genes (Sheffield

et al. 2008). The nucleotide sequence of the genome showed a characteristically high A+T content, as well as a positive AT-skew and a negative GC-skew.

We found several intergenic spacers and overlapping regions of different lengths. Of the observed overlaps, three motifs were proved to be conserved between different arthropod groups. The overlapping motif “ATGATAA” between PCGs *atp8* and *atp6* was also observed in other coleopteran mitogenomes (Wang and Tang 2017, 2018; Shi et al. 2023). In addition, an “AAGCCTTA” overlap motif was found between tRNA-*Trp* (UCA) and tRNA-Cys (GCA), similar to several other insect mitochondrial genomes (Wang and Tang 2017; Wang et al. 2018; Cao et al. 2019). Finally, the overlap of the “TTAACAT” motif between *nad4* and *nad4l* is characteristic of several other arthropod mitogenomes (Huang et al. 2015; Wang et al. 2016, 2018).

To reconstruct the phylogenetic relationships within the superfamily, we used the sequences of all Scarabaeoidea species with a publicly available complete, circular, and fully annotated mitochondrial genome at the date of completing this work. The dataset comprised 145 species resulting in currently the most comprehensive phylogenetic analysis of the superfamily. The basic structure of our reconstructed phylogenetic tree was similar to the phylogenetic relationships found by Ahrens et al. (2014) and Dietz et al. (2023). Previous studies investigating the relationships of the superfamily Scarabaeoidea mostly aimed to clarify the phylogeny within the Scarabaeidae and used members of the other families as outgroups (e.g. Gunter et al. 2016) or included only a few species from them (e.g. Ahrens et al. 2014; Song and Zhang 2018; Dietz et al. 2023). Within the family Scarabaeidae, the subfamily Melolonthinae appeared to be paraphyletic due to the presence of Euchirinae as sister to one of the Melolonthinae lineages. This is in line with the results of Ahrens et al. (2014) and Dietz et al. (2023), who found similar evolutionary relationships based on nuclear and mitochondrial markers. This supports the concept that the species forming the subfamily Euchirinae should be placed in the tribe Euchirini within Melolonthinae (Song and Zhang 2018; Ayivi et al. 2021; Guo et al. 2022). Although a recent study that published the mitogenome of the two *Propomacrus* species concluded that the subfamily Euchirinae forms a separate monophyletic cluster (Yi et al. 2024), the *Apogonia* species that caused the paraphyly within the subfamily Melolonthinae were not included in their analysis. Nevertheless, this taxonomic question would warrant further investigation with an improved set of markers to clarify the relationships between these two taxa.

Another interesting paraphyletic structure was found in our phylogenetic tree between the passalids and the Scarabaeidae. Although this exact relationship has not yet been hypothesized by others, the uncertain position of the family Passalidae is a known problem (see e.g. Dietz et al. 2023). All three members of this family that we included in our analysis were placed on extremely long branches, suggesting long-branch attraction bias – a common phenomenon in mitochondrial sequences (Timmermans et al. 2016). Other recent studies (Gunter et al. 2016; Guo et al. 2022; Dietz et al. 2023) have also placed representatives of the family on long branches, which could be addressed by increasing the number of passalid species with complete mitochondrial sequences.

Our results indicate that Geotrupidae and the clade of Scarabaeidae + Passalidae are sister groups. In the most recent studies, the family Geotrupidae has been considered to be the sister group to Scarabaeidae (Ahrens et al. 2014), Bolboceeratidae (Song and Zhang 2018; Dietz et al. 2023), and Trogidae plus Glaphyridae

(Gunter et al. 2016). The results of Guo et al. (2022) show that the family Geotrupidae occupies different positions depending on the phylogenetic analysis method, although they only used this taxon as an outgroup in their study. Furthermore, the phylogenetic relationships within the family Geotrupidae have so far been analyzed mainly on the basis of larval morphology (Scholtz and Browne 1996; Verdú et al. 2004). Moreover, phylogenetic studies based on molecular markers have not yet included *Lethrus* species as representatives of the family Geotrupidae. Therefore, the mitochondrial sequence of *L. scoparius* is a useful contribution to corroborate the results found based on morphological characters.

The mitochondrial genome presented here is one of the few Scarabaeoidea mitogenomes generated using long-read sequencing technologies (Filipović et al. 2021; Morgan et al. 2022). The advantages of these methods could compensate for the shortcomings of the widely used short-read sequencing platforms. According to the results of Baeza et al. (2024), the latest Oxford Nanopore long-read sequencing chemical methods lead to a very low sequencing error rate, making the short-read polishing step in the assembly process redundant. With this method, the assembly of the non-coding control region, which often contains repetitive motifs, could be performed more accurately (Filipović et al. 2021). Elongated control regions reported in coleopteran species contain several tandem repeats, which have been proposed as informative markers for population genetic studies due to their higher evolutionary rate (Sayadi et al. 2017; Morgan et al. 2022). In addition, both Hercules beetles (Morgan et al. 2022) and seed beetles (Sayadi et al. 2017) have been shown to express specific sites of the control region using transcriptome sequencing data. Although the expression level was very low in both cases, these results suggest a role for these repeat sequences in a mitochondrial function. Our assembly is a novel example of the expansion of control regions in the Scarabaeoidea and suggests that it may be worthwhile to revisit the already assembled mitogenomes to detect expanded control regions and examine their tandem repeat content in the superfamily.

Conclusions

Among the members of the family Geotrupidae, our assembly of the mitogenome of *Lethrus scoparius* and the mitogenome of *Phelotrupes oberthuri* are the only representatives with circularly assembled and fully annotated complete mitochondrial genomes. This sequence provides valuable molecular resources for understanding the phylogeny of this family and the molecular evolution of the mitochondrial genome within the superfamily Scarabaeoidea, and a good example of the high efficiency of third-generation sequencing techniques in assembling mitochondrial genomes.

Acknowledgements

We sincerely thank M.F. Bagaturov for the taxonomic validation of the species investigated. We are thankful for the support of Juhász-Nagy Pál Doctoral School, University of Debrecen, Hungary. We thank for their assistance in fieldwork to Abidkulova Karime (Al-Farabi Kazakh National University, Almaty, Kazakhstan) and Jumanov Smatulla (Aksu-Zhabagly Nature Reserve, Zhabagly, Kazakhstan).

Additional information

Conflict of interest

The authors have declared that no competing interests exist.

Ethical statement

No ethical statement was reported.

Funding

N.A.N. was supported by the National Research, Development and Innovation Office (OTKA PD142602). Z.B. was supported by project no. TKP2021-NKTA-32 which has been implemented with the support provided by the Ministry of Culture and Innovation of Hungary from the National Research, Development and Innovation Fund, financed under the TKP2021-NKTA funding scheme. G.S. was supported by the Hungarian Ministry for Innovation and Technology via an NKFI-FK project (FK137962).

Author contributions

Réka Zsófia Bubán - Conceptualization, Data Curation, Formal analysis, Investigation, Writing – Original Draft, Writing – Review & Editing. Renáta Bókényé Tóth – Methodology, Investigation, Resources, Writing – Review & Editing. Csongor Freytag – Methodology, Investigation, Resources, Writing – Review & Editing. Gábor Sramkó – Resources, Writing – Review & Editing. Zoltán Barta – Conceptualization, Resources, Writing – Review & Editing. Nikoletta Andrea Nagy – Conceptualization, Methodology, Data Curation, Formal analysis, Investigation, Funding acquisition, Writing – Original Draft, Writing – Review & Editing, Supervision.

Author ORCIDs

Csongor Freytag  <https://orcid.org/0000-0002-3356-4182>

Gábor Sramkó  <https://orcid.org/0000-0001-8588-6362>

Zoltán Barta  <https://orcid.org/0000-0002-7121-9865>

Nikoletta Andrea Nagy  <https://orcid.org/0000-0001-7771-830X>

Data availability

All of the data that support the findings of this study are available in the main text or Supplementary Information.

References

- Ahrens D, Schwarzer J, Vogler AP (2014) The evolution of scarab beetles tracks the sequential rise of angiosperms and mammals. *Proceedings of the Royal Society B: Biological Sciences* 281(1791): 20141470. <https://doi.org/10.1098/rspb.2014.1470>
- Ayivi SPG, Tong Y, Storey KB, Yu DN, Zhang JY (2021) The mitochondrial genomes of 18 new Pleurosticti (Coleoptera: Scarabaeidae) exhibit a novel trnQ-NCR-trnI-trnM gene rearrangement and clarify phylogenetic relationships of subfamilies within Scarabaeidae. *Insects* 12(11): 1025. <https://doi.org/10.3390/insects12111025>
- Baeza JA, Minish JJ, Michael TP (2024) Assembly of mitochondrial genomes using nanopore long-read technology in three sea chubs (Teleostei: Kyphosidae). *Molecular Ecology Resources* 25(1): e14034. <https://doi.org/10.1111/1755-0998.14034>

- Bagaturov MF, Nikolajev GV (2015) Overview of distribution of the genus *Lethrus* Scopoli, 1777 (Coleoptera: Geotrupidae). *Caucasian Entomological Bulletin* 11(2): 303–314. <https://doi.org/10.23885/1814-3326-2015-11-2-303-314>
- Borowiec ML (2016) AMAS: a fast tool for alignment manipulation and computing of summary statistics. *PeerJ* 4: e1660. <https://doi.org/10.7717/peerj.1660>
- Cameron SL (2014) Insect mitochondrial genomics: implications for evolution and phylogeny. *Annual Review of Entomology* 59: 95–117. <https://doi.org/10.1146/annurev-ento-011613-162007>
- Cao JJ, Wang Y, Huang, YR, Li WH (2019) Mitochondrial genomes of the stoneflies *Mesonemoura metafiligera* and *Mesonemoura tritaenia* (Plecoptera, Nemouridae), with a phylogenetic analysis of Nemouroidea. *ZooKeys* 835: 43–63. <https://doi.org/10.3897/zookeys.835.32470>
- Chen Q, Chen L, Liao CQ, Wang X, Wang M, Huang GH (2022) Comparative mitochondrial genome analysis and phylogenetic relationship among lepidopteran species. *Gene* 830: 146516. <https://doi.org/10.1016/j.gene.2022.146516>
- Cucini C, Leo C, Iannotti N, Boschi S, Brunetti C, Pons J, Fanciulli PP, Frati F, Carapelli A, Nardi, F (2021) EZmito: a simple and fast tool for multiple mitogenome analyses. *Mitochondrial DNA Part B* 6(3): 1101–1109. <https://doi.org/10.1080/23802359.2021.1899865>
- Cunha RL, Verdú JR, Lobo JM, Zardoya R (2011) Ancient origin of endemic Iberian earth-boring dung beetles (Geotrupidae). *Molecular Phylogenetics and Evolution* 59(3): 578–586. <https://doi.org/10.1016/j.ympev.2011.03.028>
- De Coster W, D’Hert S, Schultz DT, Cruts M, Van Broeckhoven C (2018) NanoPack: visualizing and processing long-read sequencing data. *Bioinformatics* 34(15): 2666–2669. <https://doi.org/10.1093/bioinformatics/bty149>
- Dietz L, Seidel M, Eberle J, Misof B, Pacheco TL, Podsiadlowski L, Ranasinghe S, Guntner NL, Niehuis O, Mayer C, Ahrens D (2023) A transcriptome-based phylogeny of Scarabaeoidea confirms the sister group relationship of dung beetles and phytophagous pleurostict scarabs (Coleoptera). *Systematic Entomology* 48(4): 672–686. <https://doi.org/10.1111/syen.12602>
- Donath A, Jühling F, Al-Arab M, Bernhart SH, Reinhardt F, Stadler PF, Middendorf M, Bernth M (2019) Improved annotation of protein-coding genes boundaries in metazoan mitochondrial genomes. *Nucleic Acids Research* 47(20): 10543–10552. <https://doi.org/10.1093/nar/gkz833>
- Edgar RC (2004) MUSCLE: multiple sequence alignment with high accuracy and high throughput. *Nucleic Acids Research* 32(5): 1792–1797. <https://doi.org/10.1093/nar/gkh340>
- Filipović I, Hereward JP, Rašić G, Devine GJ, Furlong MJ, Etebari K (2021) The complete mitochondrial genome sequence of *Oryctes rhinoceros* (Coleoptera: Scarabaeidae) based on long-read nanopore sequencing. *PeerJ* 9: e10552. <https://doi.org/10.7717/peerj.10552>
- Gilbert MTP, Moore W, Melchior L, Worobey M (2007) DNA extraction from dry museum beetles without conferring external morphological damage. *PloS ONE* 2(3): e272. <https://doi.org/10.1371/journal.pone.0000272>
- Grant JR, Enns E, Marinier E, Mandal A, Herman EK, Chen C, Graham M, Van Domselaar G, Stothard P (2023) Proksee: in-depth characterization and visualization of bacterial genomes. *Nucleic Acids Research* 51(W1): W484–W492. <https://doi.org/10.1093/nar/gkad326>
- Guindon S, Dufayard JF, Lefort V, Anisimova M, Hordijk W, Gascuel O (2010) New algorithms and methods to estimate maximum-likelihood phylogenies: assessing

- the performance of PhyML 3.0. *Systematic Biology* 59(3): 307–321. <https://doi.org/10.1093/sysbio/syq010>
- Gunter NL, Weir T A, Slipinksi A, Bocak L, Cameron SL (2016) If dung beetles (Scarabaeidae: Scarabaeinae) arose in association with dinosaurs, did they also suffer a mass co-extinction at the K-Pg boundary?. *PLoS ONE* 11(5): e0153570. <https://doi.org/10.1371/journal.pone.0153570>
- Guo S, Lin X, Song N (2022) Mitochondrial phylogenomics reveals deep relationships of scarab beetles (Coleoptera, Scarabaeidae). *PLoS ONE* 17(12): e0278820. <https://doi.org/10.1371/journal.pone.0278820>
- Huang M, Wang Y, Liu X, Li W, Kang Z, Wang K, Li X, Yang D (2015) The complete mitochondrial genome and its remarkable secondary structure for a stonefly *Acroneuria hainana* Wu (Insecta: Plecoptera, Perlidae). *Gene* 557(1): 52–60. <https://doi.org/10.1016/j.gene.2014.12.009>
- Ikeda H, Nishikawa M, Sota T (2012) Loss of flight promotes beetle diversification. *Nature Communications* 3(1): 648. <https://doi.org/10.1038/ncomms1659>
- Jia W, Wei J, Niu M, Zhang H, Zhao Q (2023) The complete mitochondrial genome of *Aeschrocoris tuberculatus* and *A. ceylonicus* (Hemiptera, Pentatomidae) and its phylogenetic implications. *ZooKeys* 1160: 145–167. <https://doi.org/10.3897/zookeys.1160.100818>
- Kalyaanamoorthy S, Minh BQ, Wong TKF, von Haeseler A, Jermin LS (2017) ModelFinder: fast model selection for accurate phylogenetic estimates. *Nature Methods* 14: 587–589. <https://doi.org/10.1038/nmeth.4285>
- Kern EMA, Kim T, Park JK (2020) The mitochondrial genome in nematode phylogenetics. *Frontiers in Ecology and Evolution* 8: 250. <https://doi.org/10.3389/fevo.2020.00250>
- Kolmogorov M, Yuan J, Lin Y, Pevzner PA (2019) Assembly of long, error-prone reads using repeat graphs. *Nature Biotechnology* 37: 540–546. <https://doi.org/10.1038/s41587-019-0072-8>
- Král D, Hillert O, Drožová D, Šípek P (2013) *Lethrus (Lethrus) schneideri* sp. n. (Coleoptera, Geotrupidae) from Greece. *ZooKeys* 339: 93–106. <https://doi.org/10.3897/zookeys.339.6132>
- Lanfear R, Schalamun M, Kainer D, Wang W, Schwessinger B (2019) MinIONQC: fast and simple quality control for MinION sequencing data. *Bioinformatics* 35(3): 523–525. <https://doi.org/10.1093/bioinformatics/bty654>
- Lee BD (2018) Python implementation of codon adaptation index. *Journal of Open Source Software* 3(30): 905. <https://doi.org/10.21105/joss.00905>
- Li H (2018) Minimap2: pairwise alignment for nucleotide sequences. *Bioinformatics* 34(18): 3094–3100. <https://doi.org/10.1093/bioinformatics/bty191>
- Minh BQ, Nguyen MAT, von Haeseler A (2013) Ultrafast approximation for phylogenetic bootstrap. *Molecular Biology and Evolution* 30(5): 1188–1195. <https://doi.org/10.1093/molbev/mst024>
- Morgan B, Wang TY, Chen YZ, Moctezuma V, Burgos O, Le MH, Huang JP (2022) Long-read sequencing data reveals dynamic evolution of mitochondrial genome size and the phylogenetic utility of mitochondrial DNA in Hercules beetles (Dynastes; Scarabaeidae). *Genome Biology and Evolution* 14(10): evac147. <https://doi.org/10.1093/gbe/evac147>
- Nagy NA, Rácz R, Rimington O, Póliska S, Orozco-terWengel P, Bruford MW, Barta Z (2021) Draft genome of a biparental beetle species, *Lethrus apterus*. *BMC Genomics* 22(1): 301. <https://doi.org/10.1186/s12864-021-07627-w>

- Nguyen LT, Schmidt HA, von Haeseler A, Minh BQ (2015) IQ-TREE: a fast and effective stochastic algorithm for estimating maximum-likelihood phylogenies. *Molecular Biology and Evolution* 32(1): 268–274. <https://doi.org/10.1093/molbev/msu300>
- Nikolajev GV (2003) Zhuki-kravchiki (Scarabaeidae, Geotrupinae, Lethrini): *Biologiya, Sistematika, Rasprostranenie, Opredelitel'*. [*Lethrus*-beetles (Scarabaeidae, Geotrupinae, Lethrini): *Biology, Systematics, Distribution, Keys*.] Kazakh University, Almaty. 254 pp.
- Perna NT, Kocher TD (1995) Patterns of nucleotide composition at fourfold degenerate sites of animal mitochondrial genomes. *Journal of Molecular Evolution* 41: 353–358. <https://doi.org/10.1007/BF01215182>
- Ranwez V, Douzery EJP, Cambon C, Chantret N, Delsuc F (2018) MACSE v2: toolkit for the alignment of coding sequences accounting for frameshifts and stop codons. *Molecular Biology and Evolution* 35(10): 2582–2584. <https://doi.org/10.1093/molbev/msy159>
- Salces-Castellano A, Andújar C, López H, Pérez-Delgado AJ, Arribas P, Emerson BC (2021) Flightlessness in insects enhances diversification and determines assemblage structure across whole communities. *Proceedings of the Royal Society B* 288(1945): 20202646. <https://doi.org/10.1098/rspb.2020.2646>
- Sayadi A, Immonen E, Tellgren-Roth C, Arnqvist G (2017) The evolution of dark matter in the mitogenome of seed beetles. *Genome Biology and Evolution* 9(10): 2697–2706. <https://doi.org/10.1093/gbe/evx205>
- Scholtz CH (2000) Evolution of flightlessness in Scarabaeoidea (Insecta, Coleoptera). *Deutsche Entomologische Zeitschrift* 47(1): 5–28. <https://doi.org/10.1002/mmnd.4800470102>
- Scholtz CH, Browne DJ (1996) Polyphyly in the Geotrupidae (Coleoptera: Scarabaeoidea): a case for a new family. *Journal of Natural History* 30(4): 597–614. <https://doi.org/10.1080/00222939600770311>
- Shapovalov AM (2022) New species of the genus *Lethrus* Scopoli, 1777 (Coleoptera: Geotrupidae: Lethrinae) from Fergana Valley, Kyrgyzstan. *Zootaxa* 5159(3): 414–424. <https://doi.org/10.11646/zootaxa.5159.3.6>
- Sheffield NC, Song H, Cameron SL, Whiting MF (2008) A comparative analysis of mitochondrial genomes in Coleoptera (Arthropoda: Insecta) and genome descriptions of six new beetles. *Molecular Biology and Evolution* 25(11): 2499–2509. <https://doi.org/10.1093/molbev/msn198>
- Shi F, Yu T, Xu Y, Zhang S, Niu Y, Ge S, Tao J, Zong S (2023) Comparative mitochondrial genomic analysis provides new insights into the evolution of the subfamily Lamiinae (Coleoptera: Cerambycidae). *International Journal of Biological Macromolecules* 225: 634–647. <https://doi.org/10.1016/j.ijbiomac.2022.11.125>
- Song N, Zhang H (2018) The mitochondrial genomes of phytophagous scarab beetles and systematic implications. *Journal of Insect Science* 18(6): 11. <https://doi.org/10.1093/jisesa/iey076>
- Timmermans MJ, Barton C, Haran J, Ahrens D, Culverwell CL, Ollikainen A, Dodsworth S, Foster PG, Bocak V, Vogler AP (2016) Family-level sampling of mitochondrial genomes in Coleoptera: compositional heterogeneity and phylogenetics. *Genome Biology and Evolution* 8(1): 161–175. <https://doi.org/10.1093/gbe/evv241>
- Tóth JP, Bereczki J, Rácz R, Varga Z, Barta Z, Sramkó G (2019) Phylogenetic relationships in the genus *Lethrus* (Coleoptera: Geotrupidae) reveal contrasting evolutionary history in Europe. *Systematic Entomology* 44(4): 899–910. <https://doi.org/10.1111/syen.12364>
- Vaser R, Sović I, Nagarajan N, Šikić M (2017) Fast and accurate de novo genome assembly from long uncorrected reads. *Genome Research* 27: 737–746. <https://doi.org/10.1101/gr.214270.116>

- Verdú JR, Galante E, Lumaret JP, Cabrero-Sañudo FJ (2004) Phylogenetic analysis of Geotrupidae (Coleoptera, Scarabaeoidea) based on larvae. *Systematic Entomology* 29(4): 509–523. <https://doi.org/10.1111/j.0307-6970.2004.00256.x>
- Vuts J, Imrei Z, Birkett MA, Pickett JA, Woodcock CM, Tóth M (2014) Semiochemistry of the Scarabaeoidea. *Journal of Chemical Ecology* 40: 190–210. <https://doi.org/10.1007/s10886-014-0377-5>
- Wang Q, Tang G (2017) Genomic and phylogenetic analysis of the complete mitochondrial DNA sequence of walnut leaf pest *Paleosepharia posticata* (Coleoptera: Chrysomeloidea). *Journal of Asia-Pacific Entomology* 20(3): 840–853. <https://doi.org/10.1016/j.aspen.2017.05.010>
- Wang Q, Tang G (2018) The mitochondrial genomes of two walnut pests, *Gastrolina depressa depressa* and *G. depressa thoracica* (Coleoptera: Chrysomelidae), and phylogenetic analyses. *PeerJ* 6: e4919. <https://doi.org/10.7717/peerj.4919>
- Wang K, Li X, Ding S, Wang N, Mao M, Wang M, Yang D (2016) The complete mitochondrial genome of the *Atylotus miser* (Diptera: Tabanomorpha: Tabanidae), with mitochondrial genome phylogeny of lower Brachycera (Orthorrhapha). *Gene* 586(1): 184–196. <https://doi.org/10.1016/j.gene.2016.04.013>
- Wang Y, Cao J, Murányi D, Li W (2018) Comparison of two complete mitochondrial genomes from Perlodidae (Plecoptera: Perloidea) and the family-level phylogenetic implications of Perloidea. *Gene* 675: 254–264. <https://doi.org/10.1016/j.gene.2018.06.093>
- Wick RR, Judd LM, Holt KE (2019) Performance of neural network basecalling tools for Oxford Nanopore sequencing. *Genome Biology* 20: 129. <https://doi.org/10.1186/s13059-019-1727-y>
- Yi C, Shu X, Wang L, Yin J, Wang Y, Wang Y, Zhang H, He Q, Zhao M (2024) The first report of complete mitogenomes of two endangered species of genus *Propomacrus* (Coleoptera: Scarabaeidae: Euchirinae) and phylogenetic implications. *PLoS ONE* 19(9): e0310559. <https://doi.org/10.1371/journal.pone.0310559>
- Zhao W, Liu D, Jia Q, Wu X, Zhang H (2021) Characterization of the complete mitochondrial genome of *Myrmus lateralis* (Heteroptera, Rhopalidae) and its implication for phylogenetic analyses. *ZooKeys* 1070: 13–30. <https://doi.org/10.3897/zookeys.1070.72742>

Supplementary material 1

Supplementary data

Authors: Réka Zsófia Bubán, Renáta Bókényné Tóth, Csongor Freytag, Gábor Sramkó, Zoltán Barta, Nikoletta Andrea Nagy

Data type: pdf

Copyright notice: This dataset is made available under the Open Database License (<http://opendatacommons.org/licenses/odbl/1.0/>). The Open Database License (ODbL) is a license agreement intended to allow users to freely share, modify, and use this Dataset while maintaining this same freedom for others, provided that the original source and author(s) are credited.

Link: <https://doi.org/10.3897/zookeys.1236.138465.suppl1>

DNA barcoding of passerine birds in Iran

Sahar Javaheri Tehrani^{1,2}, Elham Rezazadeh^{1,3}, Niloofar Alaei Kakhki^{1,4}, Leila Nourani¹,
Vali Ebadi¹, Sahar Karimi¹, Mojtaba Karami¹, Fatemeh Ashouri¹, Asaad Sarshar⁵,
Toni I. Gossmann², Mansour Aliabadian^{1,6}

¹ Department of Biology, Faculty of Science, Ferdowsi University of Mashhad, Mashhad, Iran

² Computational Systems Biology, Faculty of Biochemical and Chemical Engineering, TU Dortmund University, Dortmund, Germany

³ Department of Animal Biology, Faculty of Biological Sciences, Kharazmi University, Tehran, Iran

⁴ Department of Zoology, State Museum of Natural History Stuttgart, Stuttgart, Germany

⁵ Department of Environmental Sciences, Faculty of Natural Resources and Environment, Malayer University, Malayer, Iran

⁶ Research Department of Zoological Innovations, Institute of Applied Zoology, Faculty of Science, Ferdowsi University of Mashhad, Mashhad, Iran

Corresponding authors: Mansour Aliabadian (aliabadi@um.ac.ir); Toni I. Gossmann (toni.gossmann@tu-dortmund.de)

Abstract

Exploring genetic diversity is essential for precise species delimitation, especially within taxonomically complex groups like passerine birds. Traditional morphological methods often fail to resolve species boundaries; however, DNA barcoding, particularly through the mitochondrial cytochrome c oxidase subunit I (*COI*) gene, provides a powerful complementary method for accurate species identification. This study establishes a comprehensive DNA barcode library for Iranian passerine birds, analyzing 546 *COI* sequences from 94 species across 23 families and 53 genera. There is a pronounced barcode gap, with average intraspecific divergence at 0.41% and interspecific divergence at 18.6%. Notable intraspecific variation emerged in the Persian nuthatch (*Sitta tephronota*) and the Lesser whitethroat (*Curruca curruca*), while the European goldfinch (*Carduelis carduelis*) and the grey-crowned goldfinch (*Carduelis caniceps*) showed limited genetic differentiation despite marked morphological distinctions. Phylogenetic analysis revealed significant east-west genetic splits in *C. curruca* and *S. tephronota*, reflecting Iran's geographic and zoogeographic boundaries. These findings demonstrate the effectiveness of DNA barcoding in elucidating biogeographic patterns, emphasizing Iran's key role as an ornithological crossroads for avian biodiversity. Moreover, our results suggest that much of the genetic variation in the *COI* gene arises from synonymous mutations, highlighting the role of purifying selection in shaping mtDNA diversity across species.

Key words: *COI* gene, Genetic diversity, Selection, Species delimitation

Introduction

Genetic diversity is a fundamental aspect of biodiversity, representing the variety of genetic information within and among species (Nonić and Šijačić-Nikolić 2021). This genetic diversity plays a critical role in evolutionary processes such as natural selection and adaptation, driving speciation and shaping the phylogenetic relationships among organisms (Huang et al. 2016; Nonić and Šijačić-Nikolić 2021). Accurate assessment of genetic diversity is also fundamental for species



Academic editor: George Sangster

Received: 2 December 2024

Accepted: 2 March 2025

Published: 24 April 2025

ZooBank: <https://zoobank.org/5F22770E-8678-4A0E-929C-C422020C5350>

Citation: Javaheri Tehrani S, Rezazadeh E, Alaei Kakhki N, Nourani L, Ebadi V, Karimi S, Karami M, Ashouri F, Sarshar A, Gossmann TI, Aliabadian M (2025) DNA barcoding of passerine birds in Iran. ZooKeys 1236: 19–39. <https://doi.org/10.3897/zookeys.1236.143336>

Copyright: © Sahar Javaheri Tehrani et al.
This is an open access article distributed under terms of the Creative Commons Attribution License (Attribution 4.0 International – CC BY 4.0).

delimitation, particularly in cryptic or morphologically similar species, where traditional taxonomic methods may fall short (Hebert et al. 2003; Lohman et al. 2009; Bilgin et al. 2016). Different genetic markers offer varying effectiveness in studying genetic diversity and it is recommended to use fast changing molecular markers (i.e., coding vs noncoding DNA) for closely related species (Abdel-Mawgood 2012). DNA barcoding is a transformative technique in biodiversity research, allowing for the precise identification and differentiation of species through genetic markers. This method utilizes a standardized, short segment of the mitochondrial gene cytochrome c oxidase I (*COI*), typically a 648-base pair region, to serve as a species tag for species identification and delimitation (Arida et al. 2021; Zhang and Bu 2022). This species delimitation relies on DNA barcoding gap, which refers to the difference between mean intraspecific and interspecific genetic distances (Antil et al. 2023) and beyond taxonomy (Chac and Think 2023), this approach has also been employed in studies of biogeography, ecology and biological conservation (Gostel and Kress 2022; Wu et al. 2023). Moreover, genetic diversity levels in mitochondrial DNA are influenced by various factors, primarily mutation rate, selection, and effective population size (Clark et al. 2023). Understanding the selective forces acting on *COI* sequences provides valuable insights into species evolutionary histories and adaptive responses, with important implications for biodiversity conservation strategies and for tracking ecological changes over time (Matzen da Silva et al. 2011).

Birds represent one of the most extensively studied animal groups in DNA barcoding projects (Hebert et al. 2004), achieving species-level identification accuracy ranging from 93 to 99% (Colihueque et al. 2021). This high level of accuracy demonstrates the effectiveness of DNA barcoding in discriminating among sympatric avian species (Colihueque et al. 2021). While the majority of DNA barcoding studies on avian diversity has been concentrated in Europe and North America (Hebert et al. 2004; Johnsen et al. 2010; Bilgin et al. 2016), significant efforts have also been undertaken in other regions, such as the Neotropics (Kerr et al. 2009a, b; Tavares et al. 2011), South Korea (Yoo et al. 2006), eastern Palearctic (Kerr et al. 2009b), Indomalaya (Lohman et al. 2009; Lohman et al. 2010), and Australasia (Patel et al. 2010). Consequently, DNA barcodes are currently available for approximately 41% of bird species worldwide, encompassing approximately 4,300 species from 37 of the 39 recognized avian orders (Colihueque et al. 2021). Despite the expansion of DNA barcode reference databases in species diversity and geographic coverage (Gostel and Kress 2022; Cheng et al. 2023), many regions remain underrepresented, resulting in a notable geographic bias in barcoded species representation (Colihueque et al. 2021). This gap highlights an urgent need for more comprehensive sampling in these poorly documented areas (Gostel and Kress 2022). Furthermore, obtaining the required permits for specimen collection and transporting samples across national borders is often particularly complex, especially for birds (Lijtmaer et al. 2012), which adds to the challenges addressing biodiversity gaps.

Iran is recognized as a globally significant biodiversity hotspot, characterized by its remarkable species richness and high levels of endemism (Aliabadian et al. 2005, 2007; Noori et al. 2024; Rezazadeh et al. 2024). This diversity can be largely attributed to the country's geographic complexity, steep climatic gradients, and pronounced landscape heterogeneity (Noori et al. 2024). Additionally, Iran's unique geographic position serves as a zoogeographical

transition zone where several major biogeographical realms—the Palearctic (both eastern and western), Oriental, and Afrotropical—intersect (Noori et al. 2024). This geographic positioning not only establishes Iran as an ornithological crossroads but also contributes to the notable presence of sister bird species within the country (Aliabadian et al. 2005). However, despite constituting a significantly more important hotspot for diversity, the population structure and genetic diversity of the passerine taxa—representing the most species-rich clade of birds—remain inadequately explored within the country. To address this gap, we have conducted an extensive sampling effort to generate a comprehensive DNA barcoding library of Iranian Passerine birds.

Our main objectives are (i) to evaluate genetic variation in *COI* among passerine birds in Iran—a region characterized by numerous contact zones between passerine species (Aliabadian et al. 2007)—to provide new insights into the efficacy of *COI*-based DNA barcoding; (ii) to identify potential cryptic species; and (iii) to investigate the impact of natural selection on mitochondrial *COI* sequences.

Materials and methods

Taxon sampling

The study area covers the northeastern and western regions of Iran (Suppl. material 1: fig. S1). We examined 546 individuals representing 94 species from all these regions, with 75 species of these taxa (80% of species) represented by more than two individuals. All birds were captured during breeding season using mist nets, identified, and then released following the collection of feather and blood samples. Blood samples were collected from the brachial vein of each bird following standard protocols and preserved in Queen's buffer (Seutin et al. 1991). No birds were harmed during the capture, handling, and blood collection process. For the taxonomy of species, we used the IOC World Bird List v. 14.2 (Gill et al. 2024). The complete list of sampled specimens including information about geographical location, voucher and access numbers are provided in Suppl. material 1: table S1.

Laboratory procedures

DNA was extracted from blood and feather samples using a standard salt extraction method (Bruford et al. 1992), following overnight incubation at 40 °C in an extraction buffer containing 2% sodium dodecyl sulfate (SDS) and 0.5 mg/ml proteinase K. Additionally, 30 µl DTT was added during the initial incubation step for feather extraction. The *COI* gene was selected as the molecular marker of choice, as it is widely recognized, with more than 3,000 papers published on the application of *COI* barcodes for the identification and discovery of animal species (Pentinsaari et al. 2016). Primer pairs and a locus-specific annealing temperature that have been used to amplify this gene region are shown in Table 1. Total PCR reaction volumes were 25 µl, containing 12.5 µl Taq DNA Polymerase Master Mix RED (Ampliqon), 1 µl of each primer with a concentration of 10 µM, 3 µl DNA, and 7.5 µl ddH₂O. PCR products were examined on 2% agarose gels to confirm the successful amplification of the target fragments. The purified PCR products for all specimens were sequenced by MacroGen Inc (Seoul, South Korea).

Table 1. Primer pairs that have been successfully used to obtain bird barcodes. This table includes forward and reverse primer names, primer sequences, annealing temperature, and citation.

Primer Name	Primer Sequences (5'-3')	Annealing Temperature	Citation
BirdF1	TTCTCCAACCACAAAGACATTGGCAC	50 °C	(Johnsen et al. 2010)
BirdR1	ACGTGGGAGATAATTCCAATCCTG	50 °C	(Johnsen et al. 2010)
BirdR2	ACTACATGTGAGATGATTCCGAATCCAG	50 °C	(Johnsen et al. 2010)
PasserF1	CCAACCACAAAGACATCGGAACC	58 °C	(Lohman et al. 2009b)
PasserR1	GTAAACTTCTGGGTGACCAAAGAATC	58 °C	(Lohman et al. 2009b)
AWCF1	CGCYTWAACAYTCYGCCATCTTACC	57.5 °C	(Patel et al. 2010)
AWCR6	ATTCTATGTAGCCGAATGGTTCTTT	57.5 °C	(Patel et al. 2010)

Data analysis

Sequences were aligned and edited in BIOEDIT v. 7.0.1 (Hall 1999). Intraspecific and interspecific distances were calculated using Kimura 2-parameter (K2P) pairwise genetic distances in MEGA v6.0 (Tamura et al. 2013). Average intraspecific distances were determined for species with at least two sequences using MEGA. The K2P model was employed for all sequence comparisons, as it is considered the most effective metric for evaluating closely related taxa (Nei and Kumar 2000; Aliabadian et al. 2013; Carew and Hoffmann 2015). The best-fit model was estimated using JMODELTEST v. 2.1. (Darriba and Posada 2014) based on the Bayesian Information Criterion (BIC). The best model was then used to construct a phylogenetic tree with MRBAYES v. 3.2.0 (Ronquist and Huelsenbeck 2003) to provide a general graphic representation of the pattern of divergence between all species. Bayesian Inference (BI) analysis was carried out using the Markov chain Monte Carlo (MCMC) convergence implemented in MRBAYES v. 3.2.0. Two independent runs with four chains were run simultaneously for five million generations, with trees and parameters subsampled every 1000 generations. The first 50,000 trees (as a conservative 'burn-in') were discarded. Posterior probabilities (PP) were calculated from the remaining trees using a majority-rule consensus analysis.

The phylogenetic tree was rooted with one representative of Galliformes (*Gallus gallus*). Two criteria used for identifying and confirming species based on their DNA barcode if: a) it was monophyletic (i.e., the species formed a single cluster) and b) it did not share a barcode with any other species. Consequently, high intraspecific genetic distances in the *COI* gene are frequently utilized to predict cryptic or potentially new species. In our dataset, this pattern is observed in two species showing elevated genetic distances: the Persian Nuthatch *Sitta tephronota* Sharpe, 1872 and the Lesser Whitethroat *Curruca curruca* Linnaeus, 1758 (Suppl. material 1: table S2). Our dataset includes the Goldfinch *Carduelis carduelis* Linnaeus, 1758 and Grey-crowned Goldfinch *C. caniceps* Vigors, 1831, which hybridize in their contact zone in Iran (Haffer 1977) but have recently been recognized as two full species (Gill et al. 2024). Some members of the *C. curruca* complex may also represent full species (Abdilizadeh et al. 2023), warranting further investigation. For these three taxa, a Neighbor-Joining (NJ) tree was constructed using K2P distances in MEGA. This analysis incorporated the sequences obtained in this study and those deposited in BOLD (<https://www.barcodinglife.org>) from Iran. Furthermore, a haplotype network was implemented in POPART v. 1.7 (Leigh et al. 2015) to

visualize the relationships among haplotypes. Pairwise K2P distances between populations were estimated with the program MEGA, and pairwise F_{ST} values were calculated with DNASP v. 5.1 (Librado and Rozas 2009)

Coding DNA genetic diversity analysis

Based on the *COI* sequence fragments and the subsequent global alignment we obtained genetic diversity at 0-fold and 4-fold sites for all species. For this, we used the vertebrate mitochondrial genetic code with MEGA. We then used the Tajimas_d package from the bfx suite (<https://py-bfx.readthedocs.io/en/latest/>) to calculate nucleotide diversity for each species for 0-fold and 4-fold sites, respectively. We excluded species with zero diversity for either 4-fold or 0-fold sites. One can quantify effective population by dividing genetic diversity with the mutation rate per generation ($\pi = 2N_e * \mu$, where N_e equals the effective population size, μ , the mutations per generation and π is the observed pairwise differences in a population genetic sample). Because we have limited knowledge of mitochondrial gene specific mutation rates for all passerine birds and only rough estimates for generation time, we cannot directly estimate effective population sizes. However, here we use genetic diversity at silent sites as a proxy for effective population size, which is not unreasonable because we restrict our analysis to passerine birds, a taxonomic group with supposedly little variation in mutation rate and generation time (Nguyen and Ho 2016).

Results

COI sequence variation

A total of 546 sequences from 94 passerine bird species were generated and uploaded to the NCBI database (publicly available, Suppl. material 1: table S1), representing 53 different genera and 23 families of Passeriformes. We reconstructed a phylogenetic tree with a Bayesian approach using all the specimens (546 sequences, Suppl. material 1: fig. S2) to provide an initial overview of the species in our dataset. Most nodes in the resulting tree were well resolved and strongly supported with posterior probability (PP) more than 95%, as indicated by bold lines in the tree. Based on our dataset, of the 23 families included in the tree, 20 had high nodal support (≥ 0.95) and three had low nodal support (including Muscicapidae, Emberizidae and Fringillidae). Similarly, 51 of the 53 genera (excluding *Emberiza* and *Luscinia*) appeared monophyletic. Furthermore, all species formed well-supported (PP > 95%) monophyletic groups except *Lanius collurio* which was not monophyletic (i.e., paraphyly occurs) (Suppl. material 1: fig. S2). The mean number of sequences per species was six (1–32). The mean intraspecific K2P distance was 0.41% (range: 0–3.61%), while the mean interspecific distance was 18.6% (range 0.17–29.64%) (Fig. 1). Notably, two species exhibited relatively high intraspecific divergence: *Sitta tephronota* (2.30%) and *Curruca curruca* (3.60%).

Conversely, our analyses revealed low interspecific genetic distance between *Carduelis carduelis* and *Carduelis caniceps* (0.71%), which contrasts with the significant morphological differentiation observed (Suppl. material 1: table S2). In order to illustrate the basic pattern in these taxa, their results were presented in detail in Figs 2–4, respectively.

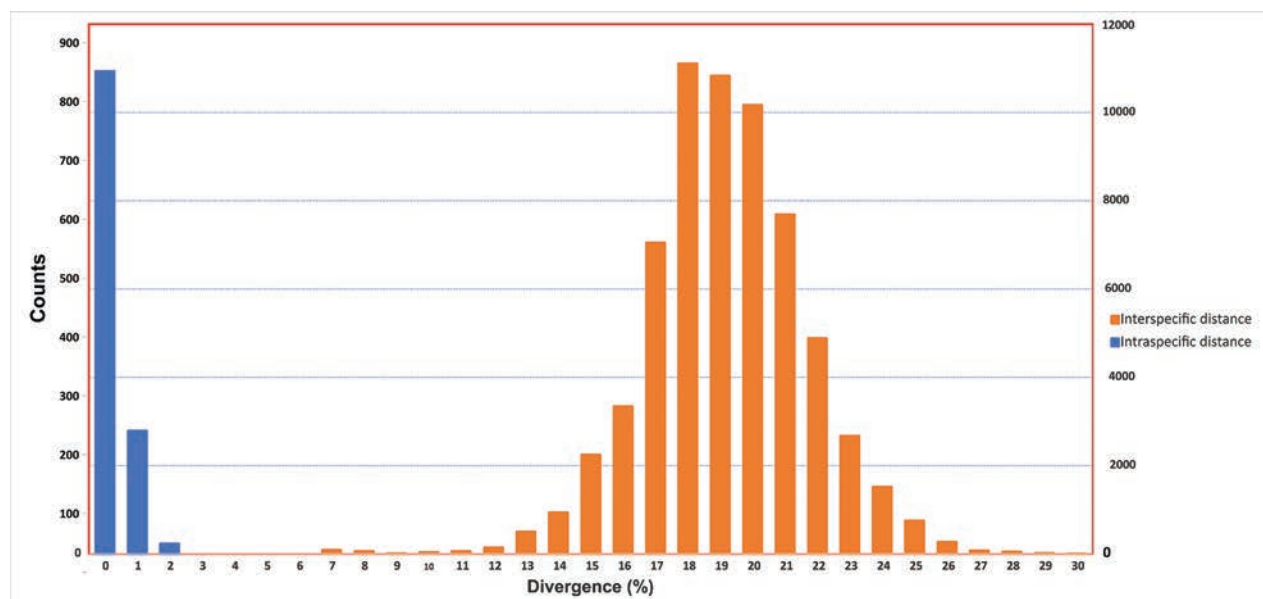


Figure 1. Comparisons of K2P pairwise distances based on the *COI* gene of 96 passerine bird species. Intraspecific distances are indicated with blue bars and interspecific distances with orange bars. Left Y-axis: numbers of intraspecific comparisons; right Y-axis: numbers of interspecific comparisons.

Deep and shallow intraspecific divergences

Sitta tephronota includes three subspecies in Iran, i.e., *S. t. dresseri* (Zagros Mts. in SE Turkey to N Iraq and W Iran), *S. t. obscura* (NE Turkey to the Caucasus and Iran) and *S. t. iranica* (NE Iran and S Turkmenistan). For this species, we analyzed six samples from the western population (*S. t. dresseri*) and seven samples from the eastern population (*S. t. iranica*) (Fig. 2B). Two eastern-western major clades with high support were identified through both NJ and Bayesian analysis (Fig. 2, Suppl. material 1: fig. S2). All *S. t. dresseri* samples formed a strongly supported clade, which is the sister group to another well-supported clade containing samples from the eastern population (Fig. 2A). This differentiation of haplotypes into two clades in the NJ tree was also mirrored by the presence of two haplotype groups in the *S. tephronota* network. In the haplotype network two haplotype groups were separated by 13 base pairs (Fig. 2C). The pairwise F_{ST} and genetic distances between eastern-western populations of *S. tephronota* were 0.91 and 4.1%, respectively (Table 2, Suppl. material 1: table S3). Furthermore, one individual labeled as *S. neumayer* in GenBank (accession number FJ465360.1) and another identified as *S. naumayer* in a GenBank BLAST search both cluster with an eastern subclade of *S. tephronota*.

Curruca curruca is thought to have three breeding subspecies in Iran, including *minula*, *althaea*, and *curruca* and one non-breeding subspecies *halimodendri* Sarudny, 1911. For this species, we primarily analyzed ten samples from the eastern population and six samples from the western population (Fig. 3B). Two major eastern-western clades with high support were identified through both NJ and Bayesian analysis (Fig. 3, Suppl. material 1: fig. S2). Furthermore, the eastern clade (including samples from Khorasan province) is divided into two well-supported subclades. One eastern subclade comprises individuals from the Dargaz region, a high-elevation breeding area. These samples clustered together with strong support (bootstrap 98%) and, when analyzed alongside

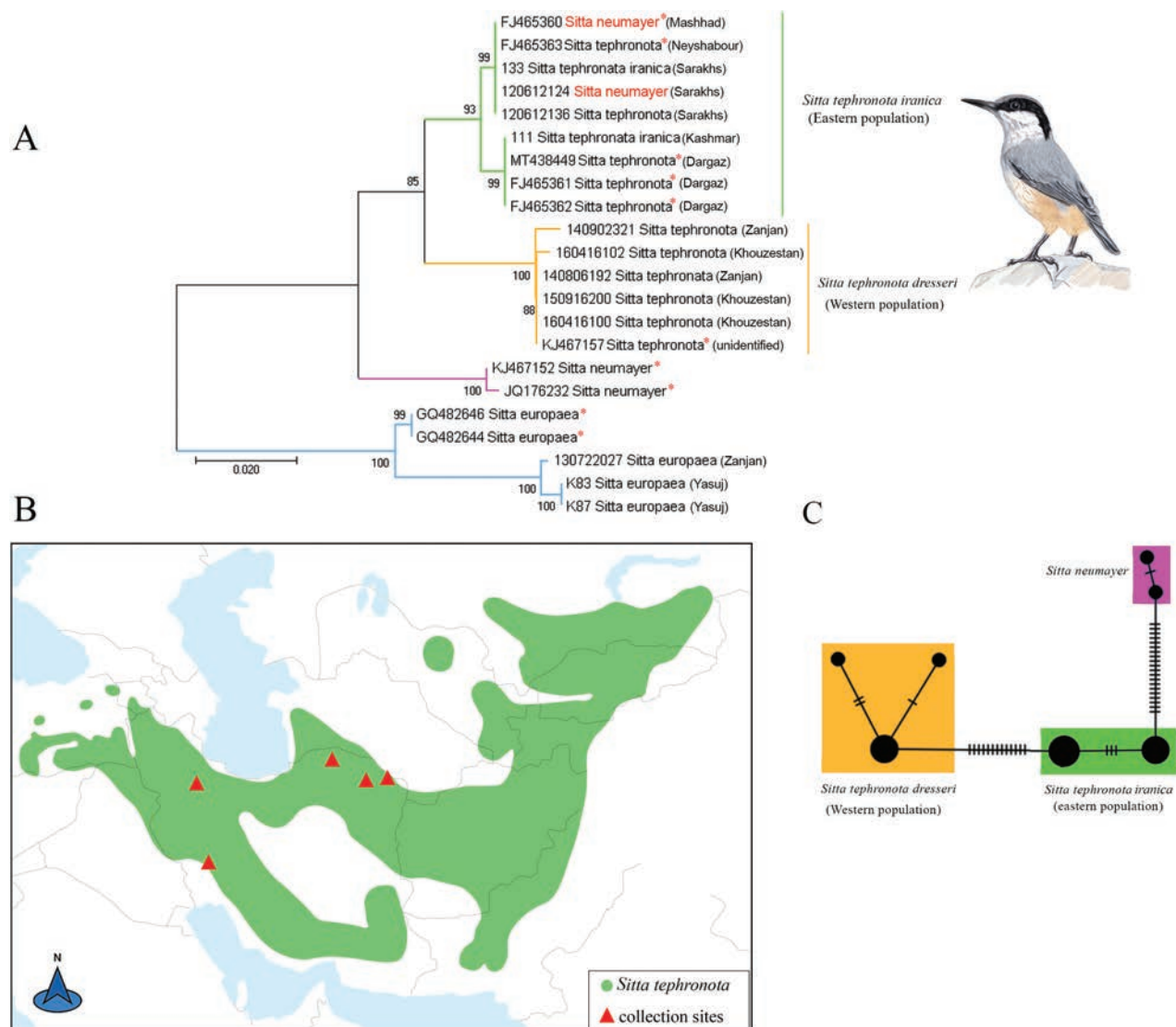


Figure 2. Phylogenetic and haplotype network analysis of *COI* data for *S. tephronota* and the origin of study material **A** neighbor-joining tree, values on the branches shows bootstrap values and, an asterisk indicates Iranian *COI* sequences from GenBank **B** distribution range and collection sites for the samples included in the study. Distribution map of *S. tephronota*, with green indicating areas where the species is native resident according to bird species distribution maps of the world (<https://datazone.birdlife.org>); sampling sites are indicated by red triangles **C** haplotype network, where colors indicate the origin of the haplotypes (orange: western population; green: eastern population; blue: *S. neumayer*) and the number of bars at each branch indicates the number of mutations.

C. c. althaea birds obtained from GenBank (three individuals), confirmed their taxonomic identity (Suppl. material 1: fig. S3).

Another eastern subclade includes individuals from Sarakh, a lower-elevation area near the Turkmenistan border, which are strongly separated from another eastern birds (BB 100%) (Fig. 3A). By adding sequences of *C. c. halimodendri* obtained from GenBank (three individuals from Hormozgan province) they are grouped as sister taxa with unresolved relationship (Suppl. material 1: fig. S3). Additionally, another major, well-supported western clade contains samples from the western part of Iran, within the distribution range of *C. c. curruca* (Fig. 3A). In the haplotype network, these two east-west populations were separated from each other by 21 base pairs (Fig. 3C). The pairwise F_{ST} and genetic distances

Table 2. Pairwise F_{ST} values between the studied subspecies and species of *S. tephronota* and *S. neumayer* estimated from the mitochondrial data.

Subspecies	<i>S. t. iranica</i>	<i>S. t. dresseri</i>	<i>S. neumayer</i>
<i>S. t. dresseri</i>	0.91		
<i>S. neumayer</i>	0.93	0.95	
<i>S. neumayer</i> (potential admixed)	0.50	0.96	0.97

Table 3. Pairwise F_{ST} values between the studied subspecies and species of *Curruca curruca* estimated from the mitochondrial data.

Subspecies	<i>C. curruca</i> ssp? (east)	<i>C. c. curruca</i> (west)	<i>C. c. althaea</i>
<i>C. c. curruca</i> (west)	1.00		
<i>C. c. althaea</i> (east)	0.96	0.99	
<i>C. c. halimodendri</i>	0.70	0.95	0.65

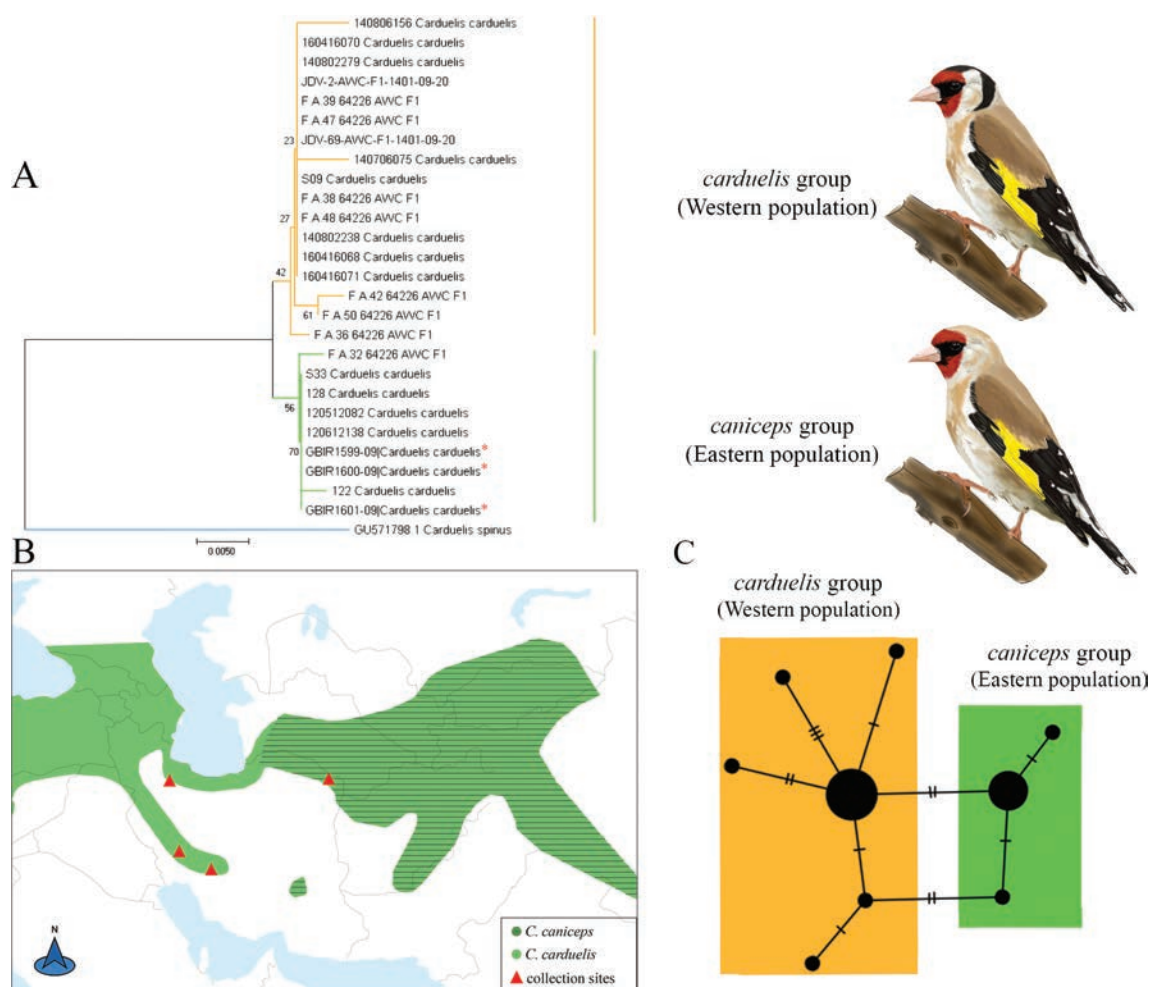


Figure 4. Phylogenetic and haplotype network analysis of *COI* data for *C. carduelis*, *C. caniceps* and the origin of study material **A** neighbor-joining tree, values on the branches shows bootstrap values and, an asterisk indicates Iranian *COI* sequences from GenBank **B** distribution range and collection sites for the samples included in the study. Distribution map of *C. carduelis* and *C. caniceps*, with green indicating areas where the species is native resident according to bird species distribution maps of the world (<https://datazone.birdlife.org>); sampling sites are indicated by red triangles **C** haplotype network, where colors indicate the origin of the haplotypes (orange: western species; green: eastern species) and the number of bars at each branch indicates the number of mutations.

Patterns of COI gene variation

We quantified site-specific coding diversity (i.e., at 0-fold and 4-fold degenerate sites) of each species where we had multiple samples (Suppl. material 1: table S5). For subsequent analysis, we excluded all species with zero diversity at either of these site types and found for all remaining species that the logarithmic ratio of π 0-fold and π 4-fold is negatively correlated with π 4-fold (Fig. 5) which is consistent effective population size scaled effectiveness of selection (James et al. 2016)

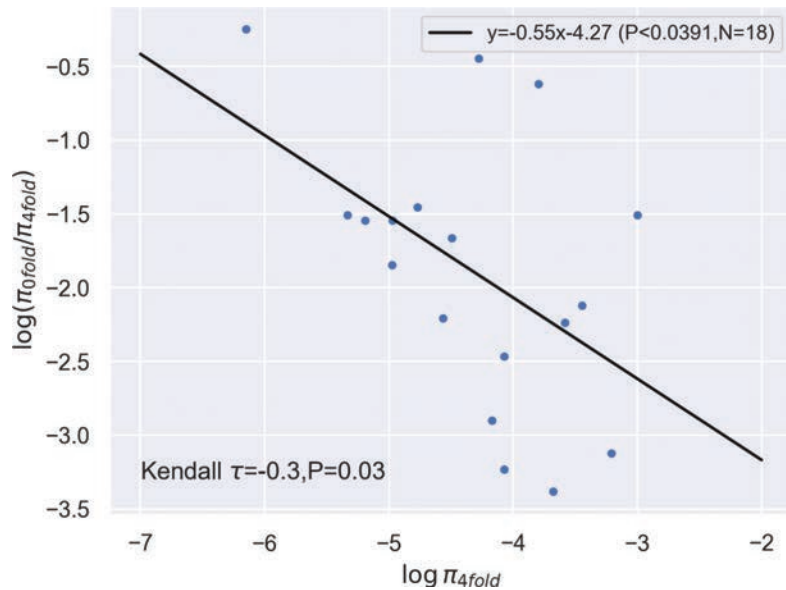


Figure 5. The relationship between $\log(\pi_{0\text{-fold}}/\pi_{4\text{-fold}})$ and $\log(\pi_{4\text{-fold}})$ COI sequences measured for 18 species. The two measures are significantly correlated. The coefficients and p-values of a linear regression as well as Kendall's rank correlation are shown.

Discussion

DNA library for passerine bird species

Here, we provide a DNA barcode reference library for a substantial dataset of passerine birds in Iran, encompassing the identification of 94 distinct species. This study provides an important foundation for understanding the genetic diversity of Iranian passerine birds through DNA barcoding, with extensive sampling from both eastern and western regions. Our results again demonstrate that DNA barcoding is an effective tool for preliminary biodiversity assessments. No species shared sequences or had overlapping clades with any other species, and every passerine species had distinct COI sequences. The development of this DNA barcode library provides a valuable resource for the biodiversity of passerine birds in Iran and will facilitate future studies on the geographic variation and genetic diversity of passerine birds in this area. Our results generally do not resolve phylogenetic relationships above the generic level for Fringillidae, Emberizidae, and Muscicapidae, at the generic level for *Luscinia* and *Emberiza* and, at the species level for *L. collurio*, all of which exhibited paraphyletic patterns in the phylogenetic analysis (Suppl. material 1: fig. S2). Therefore, using only COI alone cannot address higher-level taxonomic

controversies in some cases. To further clarify the taxonomic uncertainties of higher passerine taxa, multiple nuclear markers using phylogenomic approaches (Zhao et al. 2023), potentially combined with detailed morphological comparisons, are required. Below, we discuss our findings in relation to the genetic diversity of the mentioned challenging taxa in Iran and the influence of DNA barcoding in unrevealing biogeographic patterns.

High intraspecific genetic distance and subtle morphological variation

Several DNA barcoding studies of birds have revealed genetically distinct yet morphologically cryptic species (Aliabadian et al. 2013; Saitoh et al. 2015; Bilgin et al. 2016). In our study, we identified two species, *S. tephronota* and *C. curruca*, that may include cryptic species. Both taxa exhibit high intraspecific genetic variation while showing only subtle intraspecific morphological differences. This highlights the challenges in distinguishing cryptic species based solely on traditional morphological methods, as these species may appear similar in morphology but harbor significant genetic divergence (Abdilizadeh et al. 2020). Our results support the subdivision of *S. tephronota* into two major well-supported east (*S. t. dresseri*) – west (*S. t. iranica*) clades (Fig. 2). This genetic split among Iranian populations of *S. tephronota* was first identified by Päckert et al. (2020) in their efforts to clarify the phylogeny of the *Sitta* genus. They included only two samples from Iran, and they discovered a genetic divergence between a sample from eastern Iran (from Dargaz) and an unidentified sample referenced in Pasquet et al. (2014). However, they noted that it remains unclear whether the unidentified sample corresponds to *S. t. dresseri* or *S. t. iranica*. Based on our results, we conclude that this unidentified sample was likely a representative of *S. t. dresseri*, as it clustered with other samples from western Iran.

Moreover, our NJ tree and haplotype network showed that two individuals identified in NCBI as *S. neumayer* were located in the eastern clade of *S. tephronota*. *S. tephronota* has an ecologically and morphologically similar congener, *S. neumayer*, which have overlapping distribution ranges in eastern Turkey and Iran (Mohammadi et al. 2016). These two samples, which were collected from eastern Iran (Khorasan), might be misidentified birds or may represent potential admixed individuals, as it is primarily assumed that hybridization occurs between *S. tephronota* and *S. neumayer* in Iran (Haffer 1977). However, because mtDNA is typically maternally inherited, it is insufficient for identifying interspecific admixed individuals. Biparentally inherited nuclear gene marker is required to complement mtDNA data (Gruenthal and Burton 2005). Therefore, whether these two sister species meet without gene exchange or hybridized to a greater or lesser extent, additional sampling from their potential contact zone is needed. In addition, similar results were found by Elverici et al. (2021), when analyzing mitochondrial *ND2* and *ND3* gene sequences for *S. tephronota* and *S. neumayer*, and they indicated a reciprocal monophyly with no gene flow between birds in the Zagros Mountains and other populations. Furthermore, *S. europaea*, used as an outgroup for *Sitta* phylogenetic tree, exhibits genetic divergence between our samples from the western/northwestern population in Iran (*S. e. persica* and/or *S. e. rubiginosa*) and two other samples representative of the European haplotype. This finding aligns with previous results, which identified two additional Caspian mitochondrial lineages of *S. europaea* from Iran (Nazarizadeh et al. 2016).

The *C. curruca* complex is an intricate model for studying cryptic speciation, presenting challenges in taxonomy due to conflicting morphological and genetic data (Abdilizadeh et al. 2020). Our analysis revealed a basal genetic split in this species between eastern (*C. c. althaea*) and western (*curruca*) subspecies in Iran, supporting previous findings (Olsson et al. 2013; Abdilizadeh et al. 2020; Abdilizadeh et al. 2023). Abdilizadeh et al. (2023) suggested that *C. c. caucasica*, *C. c. zagrossiensis*, and *C. c. curruca* occur in western Iran, and that all are synonyms due to their phylogeographic clustering. Our phylogenetic trees indicate two well-supported subclades within the eastern clade: one consisting of *C. c. althaea*, breeding in eastern Iran (Dargaz), and another sister subclade from lowland northeastern Iran (Sarakhs). However, northeastern Iran is considered part of the distribution range for *althaea* and potentially *C. c. halimodendri* or *C. c. minula* (Shirihai et al. 2001; Votier et al. 2016; Clement 2023). Nonetheless, there remains limited consensus regarding the presence of *C. c. halimodendri* and *C. c. minula* in this region. The only genetic material from this region comes from the study by Abdilizadeh et al. (2020) on samples from the Dargaz region, which were identified as *althaea* birds. It is unlikely that this new subclade represents *minula*, as the new eastern subclade is positioned as a sister group to *althaea*. This contradicts the findings of Olsson et al. (2013), who identified *minula* as a sister taxon of *curruca*. *Curruca c. halimodendri* is another suggested taxon, which is assumed to occur in northeastern Iran (Olsson et al. 2013). Three sequences of *C. c. halimodendri* deposited in GenBank were all collected outside of the breeding season from Hormozgan province (Abdilizadeh et al. 2020). Based on the phylogenetic analysis, which included our samples from Sarakhs (new eastern subclade) and three *C. c. halimodendri* samples from southeastern Iran deposited in GenBank, this new subclade is positioned as a sister subclade with *C. c. althaea*. However, the relationships between *C. c. halimodendri* and this new subclade remain unresolved (Suppl. material 1: fig. S3). Furthermore, this new subclade exhibits lower genetic distance and genetic differentiation with *C. c. halimodendri* compared to *C. c. althaea* (Table 3, Suppl. material 1: table S4). Nevertheless, due to the lack of *C. c. minula* COI sequences in GenBank and the limited sampling from northeastern Iran, we propose that this new subclade represents a sister taxon to *C. c. halimodendri* and *C. c. althea*. However, additional studies, including broader geographic sampling and genetic data, are required to determine whether this new subclade represents a distinct population or a previously unrecognized taxon.

Low intraspecific genetic distance and high morphological variation: a case study of *Carduelis carduelis* and *Carduelis caniceps*

The results revealed a split between two phenotypically different species *C. carduelis* and *C. caniceps*. *Carduelis carduelis* ranges into the Zagros mountains in the west and north of Iran, whereas on the eastern side of its distributional range in Iran, it is replaced by the morphologically divergent species, *C. caniceps*, which ranges further north into south-central Siberia and northwestern Mongolia (Gill et al. 2024). These two species show substantial differences in the plumage coloration and ornaments and there are some conflicts regarding their classification. For example, Dickinson and Christidis (2014) and Clements et al. (2023) consider the taxon *caniceps* as a subspecies group

within *C. carduelis* whereas Gill et al. (2024) consider these two taxa as separate species (i.e., *C. carduelis* and *C. caniceps*). In the NJ tree, the eastern (*C. caniceps*) and western (*C. carduelis*) species formed distinct subclades; however, these subclades were weakly supported, with low bootstrap values. While they appear to form monophyletic groups, the low bootstrap support suggests weak phylogenetic resolution (Fig. 4A). Furthermore, the observed intraspecific genetic distance (0.43%) (Suppl. material 1: table S2) is significantly lower than the average interspecific genetic distances in our dataset. Nevertheless, it is suggested that ornaments may hinder gene flow between distinct or partially distinct populations if shaped by ecological differences or reinforcement, and this ability to modify ornaments, through mechanisms like sexual selection or reinforcement, could influence the formation of new species over time (Cardoso and Mota 2008).

Effect of selection on COI gene

According to population genetic theory, the effectiveness of selection is more pronounced in species with larger effective population sizes (Woolfit 2009; Gossmann et al. 2010, 2012). Here we tested the effect of selection on protein coding mutations in the *COI* gene by contrasting the genetic diversity of mutations that change the amino acid at 0-fold degenerate sites versus those mutations that are silent at 4-fold degenerate sites (James et al. 2016). Species with larger effective population sizes should show relatively fewer amino-acid changing mutations because the selection is more efficient in larger populations. We were able to obtain non-zero coding diversity measures for 18 species and find a correlation between $\log(\pi_{4\text{-fold}}/0\text{-fold})$ versus $\log(\pi_{0\text{-fold}})$. The slope is negative and highly significant which suggests that much of the genetic variation is consistent with population size scaled effects of purifying selection and drift. Our results also suggest that much of the observed variation stems from mutations at synonymous sites.

Biogeographical aspects

The current distribution and genetic makeup of species in Iran reflect its unique biogeographic characteristics (Ficetola et al. 2017; Yusefi et al. 2019). The region's transitional geographic position is exemplified by its diverse assemblage of animal species from distinct biogeographic zones. From the Palearctic realm, notable species include the Red deer (*Cervus elaphus*), Roe deer (*Capreolus capreolus*), Brown bear (*Ursus arctos*), Eurasian lynx (*Lynx lynx*), European green woodpecker (*Picus viridis*), Tawny owl (*Strix aluco*), and Meadow viper (*Vipera eriwanensis*). The Saharo-Arabian zone contributes species such as gazelles (*Gazella subgutturosa*, *G. bennettii*, *G. gazella*), the Cheetah (*Acinonyx jubatus*), Sand fox (*Vulpes rueppellii*), Desert cobra (*Walterinnesia aegyptia*), and Black-striped hairtail butterfly (*Anthene amarah*). From the Oriental realm, the region hosts the Asiatic black bear (*Ursus thibetanus*), Palm squirrel (*Funambulus pennanti*), Indian crested porcupine (*Hystrix indica*), Persian krait (*Bungarus sindanus persicus*), Bay-backed shrike (*Lanius vittatus*), Sykes's nightjar (*Caprimulgus maharattensis*), Striped Pierrot butterfly (*Tarucus nara*), and Baphomet moth (*Cretonotos gangis*) (Noori et al. 2024). In addition to its

role as a biogeographical transition zone, Iran's mountainous topography has played a pivotal role in shaping species distributions and genetic patterns by acting as a barrier and/or corridor, or as glacial refugia during the Pleistocene (Moradi et al. 2024). Mountain ranges such as the Alborz in the north and the Zagros in the west have acted both as barriers to gene flow and as refugia during glaciation periods, contributing to the current genetic differentiation of species. Similarly, the Kopet-Dag in the northeast and the Makran range in the southeast have further limited the distribution ranges of many taxa across the Iranian Plateau, enhancing the biogeographic and genetic diversity of numerous genetic lineages and had a profound impact on the patterns of inter- and intraspecific variation among species (Rajaei et al. 2013; Hosseinzadeh et al. 2020). This biogeographic structure in Iran is even more pronounced in animals with low dispersal abilities and narrow ecological niches, such as reptiles. For example, biogeographic analyses of the snake fauna reveal three distinct groups: one linking the western Zagros and Khuzestan fauna with the Sahara-Arabian region, a second connecting the Kopet Dagh and Turkmen Steppe fauna with the Turanian region, and a third associating the Central Plateau and Baluchistan fauna with the Iranian region (Moradi et al. 2024).

In this study, the patterns of intraspecific divergence observed in *S. tephronota*, *C. curruca*, *C. carduelis*, and *C. caniceps* align with Iran's key zoogeographic boundaries and geographical barriers. These patterns reflect an east-west geographical split within these species that corresponds to the distinct biogeographical realms they inhabit. This highlights the influence of Iran's transitional geographic position, as well as the role of mountains and refugia, in shaping species differentiation and current genetic patterns. In addition, this east-west genetic distinctiveness in our target taxa is paralleled in several other widespread sister Eurasian passerine taxa that have allopatric populations at their southern range margin in Iran, such as the Eurasian nuthatch, *S. europaea* (Nazarizadeh et al. 2016; Päckert et al. 2020), coal tit, *Periparus ater* (Tietze et al. 2011), horned lark, *Eremophila alpestris* (Ghorbani et al. 2020) and great tit, *Parus major* (Javaheri Tehrani et al. 2021).

Conclusions

The present study fills a significant biodiversity knowledge gap in the barcoding data of passerine birds in Iran and demonstrates the utility of standardized DNA-based species delimitation methods in enhancing biodiversity inventories. The observed patterns of intraspecific divergence in *S. tephronota*, *C. curruca*, *C. carduelis*, and *C. caniceps* align with key zoogeographic boundaries in Iran, reflecting an east-west geographical split within these species. This finding underscores the important role of DNA barcodes in revealing phylogeographical patterns, consistent with previous studies that highlight the effectiveness of DNA barcoding in resolving such patterns (Saitoh et al. 2015; Wu et al. 2023). These examples further highlight Iran's pivotal role as a biogeography crossroad for avian diversity, with paired species consisting of a western (European or Mediterranean) member and an eastern (Asian) member (Haffer 1977; Roselaar and Aliabadian 2007). These findings collectively underscore the complex impact of Iran's topography and climatic history on shaping present-day avian genetic diversity (Noori et al. 2024).

Acknowledgments

We gratefully acknowledge Reza Rezaei and Sajad Noori for their assistance in creating the location map for our study and extend our thanks to Justin Wilcox for his support in enhancing the fluency of the English language in this manuscript. We also thank Iran's Environmental Organization for their help during the field sampling and providing the necessary research permits for this study. Additionally, we sincerely thank Shima Noori for her assistance with bird sampling. We are particularly grateful to R. Rezaei for providing the digital drawings of birds. Anonymous reviewers are acknowledged, whose comments contributed to improvement of the manuscript.

Additional information

Conflict of interest

The authors have declared that no competing interests exist.

Ethical statement

No ethical statement was reported.

Funding

This research was supported by Ferdowsi University of Mashhad research grant INSF 4002006 to Mansour Aliabadian and by grant 3971 from Ferdowsi University of Mashhad awarded to Sahar Javaheri Tehrani. Moreover, this project has received funding from the European Research Council (ERC) under the European Union's Horizon 2020 research and innovation programme grant agreement No. 947636.

Author contributions

Investigation: SJT, NAK, LN, VE, SK, MK, FA, MA; Resources: SJT, NAK, LN, VE, SK, MK, FA, AS, MA; Formal analysis: SJT, TIG, ER; Writing – original draft: SJT; Funding acquisition: MA, SJT, TIG; Project administration: MA; Supervision: MA, TIG; All authors read and approved the final version of the manuscript.

Author ORCIDs

Sahar Javaheri Tehrani  <https://orcid.org/0000-0002-4824-1837>

Elham Rezazadeh  <https://orcid.org/0000-0003-4935-0522>

Leila Nourani  <https://orcid.org/0000-0001-7932-2480>

Asaad Sarshar  <https://orcid.org/0000-0002-4325-6706>

Toni I. Gossmann  <https://orcid.org/0000-0001-6609-4116>

Mansour Aliabadian  <https://orcid.org/0000-0002-3200-4853>

Data availability

Sequence data and their accession numbers have been deposited in the NCBI database (<https://www.ncbi.nlm.nih.gov>).

References

Abdel-Mawgood AL (2012) DNA based techniques for studying genetic diversity. *Genetic diversity in microorganisms* 24: 95–122. <https://doi.org/10.5772/33509>

- Abdilizadeh R, Aliabadian M, Olsson U (2020) Molecular assessment of the distribution and taxonomy of the Lesser Whitethroat *Sylvia curruca* complex in Iran, with particular emphasis on the identity of the contentious taxon, *zagrossiensis* Sarudny, 1911. *Journal of ornithology* 161: 665–676. <https://doi.org/10.1007/s10336-020-01772-x>
- Abdilizadeh R, Prost S, Aliabadian M, Shafaeipour A, Lei F, Ahmed Khan A, Olsson U (2023) Admixture and introgression obscure evolutionary patterns in lesser white-throat complex (*Curruca curruca*; Passeriformes; Aves). *Journal of Avian biology* 21: 1–11. <https://doi.org/10.1111/jav.03045>
- Aliabadian M, Roselaar CS, Nijman V, Sluys R, Vences M (2005) Identifying contact zone hotspots of passerine birds in the Palaearctic region. *Biology Letters* 1: 21–23. <https://doi.org/10.1098/rsbl.2004.0258>
- Aliabadian M, Kaboli M, Kiabi B, Nijman V (2007) Contact and hybrid zone hotspots and evolution of birds in the Middle East. *Progress in Natural Science* 17: 1114–1118
- Aliabadian M, Beentjes KK, Roselaar CSK, Van Brandwijk H, Nijman V, Vonk R (2013) DNA barcoding of Dutch birds. *Zookeys*: 365: 25–48. <https://doi.org/10.3897/zookeys.365.6287>
- Antil S, Abraham JS, Sripoorna S, Maurya S, Dagar J, Makhija S, Bhagat P, Gupta R, Sood U, Lal R (2023) DNA barcoding, an effective tool for species identification: a review. *Molecular biology reports* 50: 761–775. <https://doi.org/10.1007/s11033-022-08015-7>
- Arida E, Ashari H, Dahruddin H, Fitriana YS, Hamidy A, Irfham M, Kadarusman, Riyanto A, Wiantoro S, Zein MSA, Hadiaty RK, Apandi, Krey F, Kurnianingsih, Melmambessy EHP, Mulyadi, Ohee HL, Saidin, Salamuk A, Sauri S, Suparno, Supriatna N, Suruwaky AM, Laksono WT, Warikar EL, Wikanta H, Yohanita AM, Slembrouck J, Legendre M, Gaucher P, Cochet C, Delrieu-Trottin E, Thébaud C, Mila B, Fouquet A, Borisenko A, Steinke D, Hocdé R, Semiadi G, Pouyaud L, Hubert N (2021) Exploring the vertebrate fauna of the Bird's Head Peninsula (Indonesia, West Papua) through DNA barcodes. *Molecular Ecology Resources* 21: 2369–2387. <https://doi.org/10.1111/1755-0998.13411>
- Bilgin R, Ebeoğlu N, Inak S, Kirpik MA, Horns JJ, Şekerciöğlu ÇH (2016) DNA barcoding of birds at a migratory hotspot in eastern Turkey highlights continental phylogeographic relationships. *PLoS ONE* 11: e0154454. <https://doi.org/10.1371/journal.pone.0154454>
- Bruford MW, Hanotte O, Brookfield JFY, Burke T (1992) Single-locus and multilocus DNA fingerprint. *Molecular Genetic Analysis of Populations: A Practical Approach* (AR Hoelzel ed.) IRL Press, UK, 225–270.
- Cardoso GC, Mota PG (2008) Speciation evolution of coloration in the genus *Carduelis*. *Evolution* 62: 753–762. <https://doi.org/10.1111/j.1558-5646.2008.00337.x>
- Carew ME, Hoffmann AA (2015) Delineating closely related species with DNA barcodes for routine biological monitoring. *Freshwater Biology* 60: 1545–1560. <https://doi.org/10.1111/fwb.12587>
- Chac LD, Thinh BB (2023) Species identification through DNA barcoding and its applications: A review. *Biology Bulletin* 50: 1143–1156. <https://doi.org/10.1134/S106235902360229X>
- Cheng Z, Li Q, Deng J, Liu Q, Huang X (2023) The devil is in the details: Problems in DNA barcoding practices indicated by systematic evaluation of insect barcodes. *Frontiers in Ecology and Evolution* 2: 8. <https://doi.org/10.3389/fevo.2023.1149839>
- Clark A, Koc G, Eyre-Walker Y, Eyre-Walker A (2023) What Determines Levels of Mitochondrial Genetic Diversity in Birds? *Genome Biology and Evolution* 15: 1–7. <https://doi.org/10.1093/gbe/evad064>

- Clements JF, Rasmussen PC, Schulenberg TS, Iliff MJ, Fredericks TA, Gerbracht JA, Lepage D, Spencer A, Billerman SM, Sullivan BL (2023) The eBird/Clements Checklist of Birds of the World: V2023. Cornell University, New York, USA
- Colihueque N, Gantz A, Parraguez M (2021) Revealing the biodiversity of Chilean birds through the COI barcode approach. *ZooKeys* 1016: 143–161. <https://doi.org/10.3897/zookeys.1016.51866>
- Darriba D, Posada D (2014) jModelTest 2.0 Manual v0. 1.1. https://www.phylo.org/pdf_docs/jmodeltest-2.1.6-manual.pdf
- Dickinson EC, Christidis L (2014) The Howard and Moore complete checklist of the birds of the world. Volume 2. Eastbourne Aves Press, UK.
- Elverici C, Önder BŞ, Perkaş U (2021) Mitochondrial differentiation and biogeography of Rock Nuthatches. *Ardea* 109: 1–13. <https://doi.org/10.5253/arde.v109i3.a5>
- Ficetola GF, Mazel F, Thuiller W (2017) Global determinants of zoogeographical boundaries. *Nature ecology & evolution* 1: 1–7. <https://doi.org/10.1038/s41559-017-0089>
- Ghorbani F, Aliabadian M, Olsson U, Donald PF, Khan AA, Alström P (2020) Mitochondrial phylogeography of the genus *Eremophila* confirms underestimated species diversity in the Palearctic. *Journal of Ornithology* 161: 297–312. <https://doi.org/10.1007/s10336-019-01714-2>
- Gill F, Donsker D, Rasmussen P (2024) IOC World Bird List. 14.1. Release date, 7–22.
- Gossmann TI, Song B-H, Windsor AJ, Mitchell-Olds T, Dixon CJ, Kapralov M V, Filatov DA, Eyre-Walker A (2010) Genome wide analyses reveal little evidence for adaptive evolution in many plant species. *Molecular Biology and Evolution* 27: 1822–1832. <https://doi.org/10.1093/molbev/msq079>
- Gossmann TI, Keightley PD, Eyre-Walker A (2012) The effect of variation in the effective population size on the rate of adaptive molecular evolution in eukaryotes. *Genome Biology and Evolution* 4: 658–667. <https://doi.org/10.1093/gbe/evs027>
- Gostel MR, Kress WJ (2022) The expanding role of DNA barcodes: Indispensable tools for ecology, evolution, and conservation. *Diversity* 14: 213. <https://doi.org/10.3390/d14030213>
- Gruenthal KM, Burton RS (2005) Genetic diversity and species identification in the endangered white abalone (*Haliotis sorenseni*). *Conservation Genetics* 6: 929–939. <https://doi.org/10.1007/s10592-005-9079-4>
- Haffer J (1977) Secondary contact zones of birds in Northern Iran. *Bonner Zoologische Monographien* 10: 1–64.
- Hall TA (1999) BioEdit: a user-friendly biological sequence alignment editor and analysis program for Windows 95/98/NT. In: *Nucleic acids symposium series* 41: 95–98.
- Hebert PDN, Cywinska A, Ball SL, DeWaard JR (2003) Biological identifications through DNA barcodes. *Proceedings of the Royal Society B: Biological Sciences* 270: 313–321. <https://doi.org/10.1098/rspb.2002.2218>
- Hebert PDN, Stoeckle MY, Zemlak TS, Francis CM (2004) Identification of birds through DNA barcodes. *PLoS Biology* 2: e312. <https://doi.org/10.1371/journal.pbio.0020312>
- Hosseinzadeh MS, Fois M, Zangi B, Kazemi SM (2020) Predicting past, current and future habitat suitability and geographic distribution of the Iranian endemic species *Microgecko latifi* (Sauria: Gekkonidae). *Journal of Arid Environments* 183: 104283. <https://doi.org/10.1016/j.jaridenv.2020.104283>
- Huang Z, Yang C, Ke D (2016) DNA barcoding and phylogenetic relationships in Anatidae. *Mitochondrial DNA Part A* 27: 1042–1044. <https://doi.org/10.3109/19401736.2014.926545>

- James JE, Piganeau G, Eyre-Walker A (2016) The rate of adaptive evolution in animal mitochondria. *Molecular Ecology* 25: 67–78. <https://doi.org/10.1111/mec.13475>
- Javaheri Tehrani S, Kvist L, Mirshamsi O, Ghasempouri SM, Aliabadian M (2021) Genetic divergence, admixture and subspecific boundaries in a peripheral population of the great tit, *Parus major* (Aves: Paridae). *Biological Journal of the Linnean Society* 133: 1084–1098. <https://doi.org/10.1093/biolinnean/blab064>
- Johnsen A, Rindal E, Ericson PGP, Zuccon D, Kerr KCR, Stoeckle MY, Lifjeld JT (2010) DNA barcoding of Scandinavian birds reveals divergent lineages in trans-Atlantic species. *Journal of Ornithology* 151: 565–578. <https://doi.org/10.1007/s10336-009-0490-3>
- Kerr KCR, Lijtmaer DA, Barreira AS, Hebert PDN, Tubaro PL (2009a) Probing evolutionary patterns in Neotropical birds through DNA barcodes. *PLoS ONE* 4: e4379. <https://doi.org/10.1371/journal.pone.0004379>
- Kerr KCR, Birks SM, Kalyakin MV, Red'Kin YA, Koblik EA, Hebert PD (2009b) Filling the gap - COI barcode resolution in eastern Palearctic birds. *Frontiers in Zoology* 6: 1–13. <https://doi.org/10.1186/1742-9994-6-29>
- Leigh JW, Bryant D, Nakagawa S (2015) POPART: full-feature software for haplotype network construction. *Methods in Ecology & Evolution* 6: 1110–1116. <https://doi.org/10.1111/2041-210X.12410>
- Librado P, Rozas J (2009) DnaSP v5: a software for comprehensive analysis of DNA polymorphism data. *Bioinformatics* 25: 1451–1452. <https://doi.org/10.1093/bioinformatics/btp187>
- Lijtmaer DA, Kerr KCR, Stoeckle MY, Tubaro PL (2012) DNA barcoding birds: From field collection to data analysis. *Methods in Molecular Biology* 858: 127–152. https://doi.org/10.1007/978-1-61779-591-6_7
- Lohman DJ, Prawiradilaga DM, Meier R (2009) Improved COI barcoding primers for Southeast Asian perching birds (Aves: Passeriformes). *Molecular Ecology Resources* 9: 37–40. <https://doi.org/10.1111/j.1755-0998.2008.02221.x>
- Lohman DJ, Ingram KK, Prawiradilaga DM, Winker K, Sheldon FH, Moyle RG, Ng PKL, Ong PS, Wang LK, Braile TM (2010) Cryptic genetic diversity in “widespread” Southeast Asian bird species suggests that Philippine avian endemism is gravely underestimated. *Biological Conservation* 143: 1885–1890. <https://doi.org/10.1016/j.biocon.2010.04.042>
- Matzen da Silva J, Creer S, Dos Santos A, Costa AC, Cunha MR, Costa FO, Carvalho GR (2011) Systematic and evolutionary insights derived from mtDNA COI barcode diversity in the Decapoda (Crustacea: Malacostraca). *PLoS ONE* 6: e19449. <https://doi.org/10.1371/journal.pone.0019449>
- Mohammadi A, Kaboli M, Ashrafi S, Mofidi-Neyestanak M, Yousefi M, Rezaei A, Stuart Y (2016) Trophic niche partitioning between two Rock Nuthatches (*Sitta tephronota* & *Sitta neumayer*) in a contact zone in Iran. *Journal of Zoology* 299: 116–124. <https://doi.org/10.1111/jzo.12329>
- Moradi N, Joger U, Shafiei Bafti S, Sharifi A, SehhatiSabet ME (2024) Biogeography of the Iranian snakes. *PLoS ONE* 19: e0309120. <https://doi.org/10.1371/journal.pone.0309120>
- Nazarizadeh M, Kaboli M, Rezaie HR, Harisini JI, Pasquet E (2016) Phylogenetic relationships of Eurasian Nuthatches (*Sitta europaea* Linnaeus, 1758) from the Alborz and Zagros Mountains, Iran. *Zoology in the Middle East* 62: 217–226. <https://doi.org/10.1080/09397140.2016.1226547>

- Nei M, Kumar S (2000) *Molecular evolution and phylogenetics*. Oxford University Press. UK. <https://doi.org/10.1093/oso/9780195135848.001.0001>
- Nguyen JM, Ho SY (2016) Mitochondrial rate variation among lineages of passerine birds. *Journal of Avian Biology* 47: 690–696. <https://doi.org/10.1111/jav.00928>
- Nonić M, Šijačić-Nikolić M (2021) Genetic diversity: sources, threats, and conservation. *Life on land. Encyclopedia of the UN Sustainable Development Goals*. Springer, Cham, 421–435. https://doi.org/10.1007/978-3-319-95981-8_53
- Noori S, Zahiri R, Yusefi GH, Rajabizadeh M, Hawlitschek O, Rakhshani E, Husemann M, Rajaei H (2024) Patterns of Zoological Diversity in Iran – A Review. *diversity* 16: 621. <https://doi.org/10.3390/d16100621>
- Olsson U, Leader PJ, Carey GJ, Khan AA, Svensson L, Alström P (2013) New insights into the intricate taxonomy and phylogeny of the *Sylvia curruca* complex. *Molecular Phylogenetics and Evolution* 67: 72–85. <https://doi.org/10.1016/j.ympev.2012.12.023>
- Päckert M, Bader-Blukott M, Künzelmann B, Sun Y-H, Hsu Y-C, Kehlmaier C, Albrecht F, Illera Cobo JC, Martens J (2020) A revised phylogeny of nuthatches (Aves, Passeriformes, Sitta) reveals insight in intra-and interspecific diversification patterns in the Palearctic. *Vertebrate Zoology* 70: 241–262. <https://doi.org/10.26049/VZ70-2-2020-10>
- Pasquet E, Barker FK, Martens J, Tillier A, Cruaud C, Cibois A (2014) Evolution within the nuthatches (Sittidae: Aves, Passeriformes): molecular phylogeny, biogeography, and ecological perspectives. *Journal of Ornithology* 155: 755–765. <https://doi.org/10.1007/s10336-014-1063-7>
- Patel S, Waugh J, Millar CD, Lambert DM (2010) Conserved primers for DNA barcoding historical and modern samples from New Zealand and Antarctic birds. *Molecular Ecology Resources* 10: 431–438. <https://doi.org/10.1111/j.1755-0998.2009.02793.x>
- Pentinsaari M, Heli S, Marko M, Tomas R (2016) Molecular evolution of a widely-adopted taxonomic marker (COI) across the animal tree of life. *Scientific Reports* 6: 35275. <https://doi.org/10.1038/srep35275>
- Rajaei SH, Rödder D, Weigand AM, Dambach J, Raupach MJ, Wägele JW (2013) Quaternary refugia in southwestern Iran: insights from two sympatric moth species (Insecta, Lepidoptera). *Organisms Diversity & Evolution* 13: 409–423. <https://doi.org/10.1007/s13127-013-0126-6>
- Rezazadeh E, Zali H, Ahmadzadeh F, Siahsarvie R, Kilpatrick CW, Norris RW, Aliabadian M (2024) Two new species of brush-tailed mouse, genus *Calomyscus* (Rodentia: Calomyscidae), from the Iranian Plateau. *Journal of Mammalogy* 105: 589–608. <https://doi.org/10.1093/jmammal/gyad116>
- Ronquist F, Huelsenbeck JP (2003) MrBayes 3: Bayesian phylogenetic inference under mixed models. *Bioinformatics* 19: 1572–1574. <https://doi.org/10.1093/bioinformatics/btg180>
- Roselaar CS, Aliabadian M (2007) A century of breeding bird assessment by western travellers in Iran, 1876–1977. *Podoces* 2: 77–96.
- Saitoh T, Sugita N, Someya S, Iwami Y, Kobayashi S, Kamigaichi H, Higuchi A, Asai S, Yamamoto Y, Nishiumi I (2015) DNA barcoding reveals 24 distinct lineages as cryptic bird species candidates in and around the Japanese Archipelago. *Molecular Ecology Resources* 15: 177–186. <https://doi.org/10.1111/1755-0998.12282>
- Sarudny N (1911) *Verzeichnis der Vögel Persiens*. *The Journal of Ornithology* 59: 185–241. <https://doi.org/10.1007/BF02091053>

- Seutin G, White BN, Boag PT (1991) Preservation of avian blood and tissue samples for DNA analyses. *Canadian Journal of Zoology* 69: 82–90. <https://doi.org/10.1139/z91-013>
- Shirihai H, Gargallo G, Helbig AJ (2001) *Sylvia* warblers: identification, taxonomy and phylogeny of the genus *Sylvia*. Christopher Helm, AC Black, London.
- Tamura K, Stecher G, Peterson D, Filipski A, Kumar S (2013) MEGA6: molecular evolutionary genetics analysis version 6.0. *Molecular biology and evolution* 30: 2725–2729. <https://doi.org/10.1093/molbev/mst197>
- Tavares ES, Gonçalves P, Miyaki CY, Baker AJ (2011) DNA barcode detects high genetic structure within Neotropical bird species. *PLoS ONE* 6: e28543. <https://doi.org/10.1371/journal.pone.0028543>
- Tietze DT, Martens J, Sun Y, Liu Severinghaus L, Päckert M (2011) Song evolution in the coal tit *Parus ater*. *Journal of Avian Biology* 42: 214–230. <https://doi.org/10.1111/j.1600-048X.2010.05283.x>
- Votier SC, Aspinall S, Bearhop S, Bilton D, Newton J, Alström P, Leader P, Carey G, Furnes RW, Olsson U (2016) Stable isotopes and mtDNA reveal niche segregation but no evidence of intergradation along a habitat gradient in the lesser whitethroat complex (*Sylvia curruca*; Passeriformes; Aves) *Journal of Ornithology* 157: 1017–1027. <https://doi.org/10.1007/s10336-016-1351-5>
- Woolfit M (2009) Effective population size and the rate and pattern of nucleotide substitutions. *Biology letters* 5: 417–420. <https://doi.org/10.1098/rsbl.2009.0155>
- Wu Y, Hou S, Yuan Z, Jiang K, Huang R, Wang K, Liu Q, Yu Z, Zhao H, Zhang B (2023) DNA barcoding of Chinese snakes reveals hidden diversity and conservation needs. *Molecular Ecology Resources* 23: 1124–1141. <https://doi.org/10.1111/1755-0998.13784>
- Yoo HS, Eah J-Y, Kim JS, Kim Y-J, Min M-S, Paek WK, Lee H, Kim C-B (2006) DNA barcoding Korean birds. *Molecules and Cells* 22: 323–327. [https://doi.org/10.1016/S1016-8478\(23\)17427-9](https://doi.org/10.1016/S1016-8478(23)17427-9)
- Yusefi GH, Faizolahi K, Darvish J, Safi K, Brito JC (2019) The species diversity, distribution, and conservation status of the terrestrial mammals of Iran. *Journal of Mammalogy* 100: 55–71. <https://doi.org/10.1093/jmammal/gyz002>
- Zhang H, Bu W (2022) Exploring large-scale patterns of genetic variation in the COI gene among Insecta: Implications for DNA barcoding and threshold-based species delimitation studies. *Insects* 13: 425. <https://doi.org/10.3390/insects13050425>
- Zhao M, Burleigh JG, Olsson U, Alström P, Kimball RT (2023) A near-complete and time-calibrated phylogeny of the Old World flycatchers, robins and chats (Aves, Muscicapidae). *Molecular Phylogenetics and Evolution* 178: 107646. <https://doi.org/10.1016/j.ympev.2022.107646>

Supplementary material 1

Additional information

Authors: Sahar Javaheri Tehrani, Elham Rezazadeh, Niloofar Alaei Kakhki, Leila Nourani, Vali Ebadi, Sahar Karimi, Mojtaba Karami, Fatemeh Ashouri, Asaad Sarshar, Toni I. Gossmann, Mansour Aliabadian

Data type: docx

Explanation note: **fig. S1**. Sampling locations. Colors and the size of circles represents the number of individuals. **fig. S2**. Bayesian tree of *COI* sequences from 96 species of Iranian passerine birds. Values at nodes show posterior probabilities; full support is indicated with an asterisk. Species that form reciprocally monophyletic clades have been collapsed. Two species showed deep intraspecific divergence: (a) *Curruca curruca* and (b) *Sitta tephronota*; these are marked in blue. Families labeled on the right of the figure. **fig. S3**. Phylogenetic and haplotype network analysis of *COI* data for *C. curruca*. a) Neighbor-joining tree, values on the branches shows bootstrap values and our *COI* sequences are indicated in red. b) Haplotype network, where colors indicate the origin of the haplotypes (Orange: western population; Green: eastern populations) and the number of bars at each branch indicates the number of mutations. **table S1**. List of all Iranian passerine birds that have been sequenced in this study, with voucher numbers and collection localities. Coordinates are given in decimal degrees. **table S2**. Comparisons of K_2P -pairwise distances within species. Distances are calculated for Iranian passerine birds for which two or more sequences were available; species including one individual are not calculated (n/c); three challenging taxa indicated bold and highlighted grey; distances are expressed in percentages. **table S3**. K_2P distances (%) for the populations of *S. tephronota* and *S. neumayer* (*COI* seq), below the diagonal between group average. **table S4**. K_2P distances (%) for the populations of *Curruca curruca* (*COI* seq), below the diagonal between group average. **table S5**. K_2P distances (%) for the populations of *Carduelis carduelis* (*COI* seq), below the diagonal between group average. **table S6**. Genetic diversity at coding sites. Non-synonymous nucleotide diversity π_n , number of non-synonymous nucleotide diversity N , synonymous nucleotide diversity π_s , number of synonymous nucleotide diversity S .

Copyright notice: This dataset is made available under the Open Database License (<http://opendatacommons.org/licenses/odbl/1.0/>). The Open Database License (ODbL) is a license agreement intended to allow users to freely share, modify, and use this Dataset while maintaining this same freedom for others, provided that the original source and author(s) are credited.

Link: <https://doi.org/10.3897/zookeys.1236.143336.suppl1>

First record of the genus *Aspilota* Foerster, 1863 in Argentina (Hymenoptera, Braconidae, Alysiniinae), with the description of the new species *Aspilota murieli* sp. nov. and a key to the Neotropical taxa

Francisco Javier Peris-Felipo^{1,2}, Camila Noemí Villar³, Sofía Belén Forte³, Joel Nazareno Lentini³,
María del Pilar Medialdea³, Analí Bustos³, Federico Pandol-Avalos⁴, Ana Lia Gayan-Quijano²,
Santiago L. Poggio^{5,6}, Sergey Belokobylskij⁷, Mariano Devoto^{3,8}

1 Bleichstrasse 15, CH-4058 Basel, Switzerland

2 Syngenta Crop Protection AG, Rosentalstrasse 67, CH-4058 Basel, Switzerland

3 Universidad de Buenos Aires, Facultad de Agronomía, Cátedra de Botánica General, C. A. de Buenos Aires, Argentina

4 Syngenta Agro S.A., Av. del Libertador 1638, B1638 BGQ, Vicente Lopez, Buenos Aires, Argentina

5 Instituto de Investigaciones Fisiológicas y Ecológicas Vinculadas a la Agricultura (IFEVA), Facultad de Agronomía, C. A. de Buenos Aires, Argentina

6 Universidad de Buenos Aires, Facultad de Agronomía, Cátedra de Producción Vegetal, C. A. de Buenos Aires, Argentina

7 Zoological Institute of the Russian Academy of Sciences, St. Petersburg, 199034, Russia

8 Consejo Nacional de Investigaciones Científicas y Técnicas (CONICET), Buenos Aires, Argentina

Corresponding author: Francisco Javier Peris-Felipo (javier.peris@syngenta.com, peris.felipo@gmail.com)

Abstract

A new species of *Aspilota* without a mesoscutal pit, *A. murieli* Peris-Felipo, **sp. nov.**, is described and illustrated from Argentina. The genus *Aspilota* Foerster, 1863 is recorded from Argentina for the first time. A key to the Neotropical species of *Aspilota* is provided.

Key words: Alysiniinae, *Aspilota*-group, diagnosis, identification key, parasitoid, South America

Introduction

The genus *Aspilota* Foerster, 1863 is distinguished from other members of the subtribe Aspilotina by three key features: paraclypeal fovea extended to the inner eye margin, a closed distal brachial (first subdiscal) cell, and the presence of the vein cuqu1 (2-SR) in the fore wing (van Achterberg 1988; Peris-Felipo and Belokobylskij 2016; Peris-Felipo et al. 2025).

Aspilota species are primarily endoparasitoids of Diptera, Cyclorrhapha, with a focus on the family Phoridae. Records of hosts from other families such as Tephritidae, Anthomyiidae, or Sarcophagidae (Yu et al. 2016) are considered questionable and require further investigation (van Achterberg 1988). The genus comprises approximately 250 species described from nearly all zoogeographic regions.

Current knowledge of *Aspilota* in the Neotropical region is very limited. Prior to this study, only three species had been documented in this realm: *Aspilota stigmalis* Papp, 2012 from Colombia, and *A. nemostigma* Spinola, 1851 and *A. pulchella* Spinola, 1851 from Chile. Unfortunately, our study excludes the



Academic editor:

Mostafa Ghafouri Moghaddam

Received: 17 February 2025

Accepted: 14 March 2025

Published: 24 April 2025

ZooBank: <https://zoobank.org/A2E3BCAB-D01A-4DCC-9497-512BE5950BA0>

Copyright: © Francisco Javier Peris-Felipo et al.
This is an open access article distributed under
terms of the Creative Commons Attribution
License (Attribution 4.0 International – CC BY 4.0).

Citation: Peris-Felipo FJ, Villar CN, Forte SB, Lentini JN, del Pilar Medialdea M, Bustos A, Pandol-Avalos F, Gayan-Quijano AL, Poggio SL, Belokobylskij S, Devoto M (2025) First record of the genus *Aspilota* Foerster, 1863 in Argentina (Hymenoptera, Braconidae, Alysiniinae), with the description of the new species *Aspilota murieli* sp. nov. and a key to the Neotropical taxa. ZooKeys 1236: 41–50. <https://doi.org/10.3897/zookeys.1236.150605>

Chilean species due to two significant challenges. Firstly, we were unable to find the place of preservation of the type specimens for their study and revision. Secondly, the original descriptions of these species are extremely vague. These factors combined made it difficult to identify and select the necessary diagnostic characteristics needed for accurate identification in our research.

In this paper, the genus *Aspilota* is recorded for the first time from Argentina. *Aspilota murieli* sp. nov., characterized by the small size of the upper tooth of the mandible, is described and illustrated. Moreover, an identification key of the available Neotropical species is provided.

Materials and methods

This study was conducted in the Rolling Pampas of Argentina (Fig. 1A), a region characterized by a temperate climate (Cfa/Cfb in the Köppen climate classification) (Soriano et al. 1991; Bianchi and Cravero 2010). The area experiences distinct seasonal variations, with warm to hot summers and cold winters. Average annual temperatures range from 13 °C to 17 °C, with summer highs exceeding 30 °C and winter lows occasionally dropping below freezing. The region is notable for its significant diurnal temperature fluctuations, particularly during summer. Annual precipitation in the Rolling Pampas varies between 800 and 1,200 mm, with the majority occurring in summer (Soriano et al. 1991; Bianchi and Cravero 2010).

The research encompassed 12 fields distributed in the Baradero, Solis, Teodelina and Vedia Districts from Argentina (Fig. 1A). The selected fields, with an average size of 77.25 ha (ranging from 40 to 213 ha), were managed under a rotational cropping system that alternated between corn, soybean, and wheat. Each field was equipped with 10 Malaise traps strategically placed at 10, 50, 100, and 150 m from the field edge (Fig. 1B). Two additional traps were set within 10 × 100 m strips of seminatural vegetation at the field margins. One of these strips was experimentally enhanced with a multifunctional floral margin to promote biodiversity, while the other served as an untreated control.

Trapping was conducted only when crops were present, with traps removed before harvest and reinstalled shortly after sowing. No data was collected during fallow periods. The study spanned two years (July 2022 to April 2024). In the first year (July 2022 to May 2023), traps operated continuously, with bi-monthly collections. The second year (August 2023 to April 2024) involved 15-day trapping periods each month.

Collected specimens were preserved in 70% alcohol and later identified to species. External morphology was examined using a ZEISS Discovery V8 stereomicroscope, with several specimens dissected and slide-mounted in Berlese medium for detailed analysis.



Figure 1. **A** Farms location in Argentina **B** View of a wheatfield with Malaise traps installed.

For the terminology of the morphological features, sculpture, and measurements, see Peris-Felipo et al. (2014); for wing venation nomenclature, see Peris-Felipo et al. (2014) and van Achterberg (1993). Following abbreviations have been used: **POL** (post-ocellar line, shortest distance between inner margins of lateral ocelli), **OOL** (ocular-ocellar line, shortest distance between outer margin of lateral ocellus and inner margin of eye), and **OD** (maximum diameter of ocellus). The species was identified by reviewing the description of the Neotropical *Aspilota* species (Spinola 1851; Fischer 1971; Papp 2012) due to the absence of a key to New World species.

For the molecular methods, the DNA from each sample was isolated using the Quick-DNA Microprep Plus kit (Zymo Research), specifically optimized for small tissue samples, strictly following the manufacturer's instructions. The DNA was eluted in a final volume of 12 µL. DNA concentration was quantified using the Qubit High Sensitivity dsDNA Assay (Thermo Fisher Scientific). For PCR amplification, a 650-bp fragment from the 5' region of CO1 was amplified using the LepF1 and LepR1 primers (Hebert et al. 2003, 2004; Park et al. 2010). Moreover, a fragment of around 666 bp of the 28S rRNA gene was amplified using D2-3665F and D3-4283R primers (Mardulyn and Whitfield 1999). PCRs were carried out in a final volume of 10 µL, containing 2.9 µL of template DNA, 0.5 µM of the primers, 5 µL of Supreme NZYTaQ 2x Green Master Mix (NZY-Tech), CES 1X (Ralser et al. 2006), and ultrapure water up to 10 µL. The reaction mixture was incubated as follows: an initial denaturation step at 95 °C for 5 min, followed by 35 cycles of 95 °C for 30 s, 48.5 °C (LepF1 and LepR1) or 52.7 °C (D2-3665F and D3-4283R) for 60 s, 72 °C for 45 s, and a final extension step at 72 °C for 7 min. The PCR products were bi-directionally sequenced on an ABI 3730xl DNA Analyzer (Applied Biosystems, USA), with the same primers as those used in the PCR amplification. The amplification products were purified using magnetic beads (MagBind, Omega-Bio-tek) prior to sequencing.

The material was imaged using Keyence® VHX-2000 Digital Microscope and post processed in Adobe Photoshop®. The specimens are deposited in the Entomological collection of the Bernardino Rivadavia Natural Sciences Argentine Museum (Buenos Aires, Argentina; **MACN-En**), the Naturhistorisches Museum Basel (Basel, Switzerland; **NMB**), the Zoological Institute RAS (St Petersburg, Russia; **ZISP**), and the F.J. Peris-Felipo Private Entomological Collection (Basel, Switzerland; **PFEC**).

Taxonomic part

Order Hymenoptera Linnaeus, 1758

Family Braconidae Nees, 1811

Subfamily Alysiinae Leach, 1815

Genus *Aspilota* Foerster, 1863

***Aspilota murieli* Peris-Felipo, sp. nov.**

<https://zoobank.org/3D60F943-4189-4308-AE38-D9F87E897DB5>

Figs 2, 3

Type material. Holotype: ARGENTINA • ♀; Buenos Aires Province, Partido de Baradero; 33°55'13"S, 59°37'26"W; 24 m; 10.xi.2022; Malaise trap (Peris-Felipo leg.) (MACN-En).

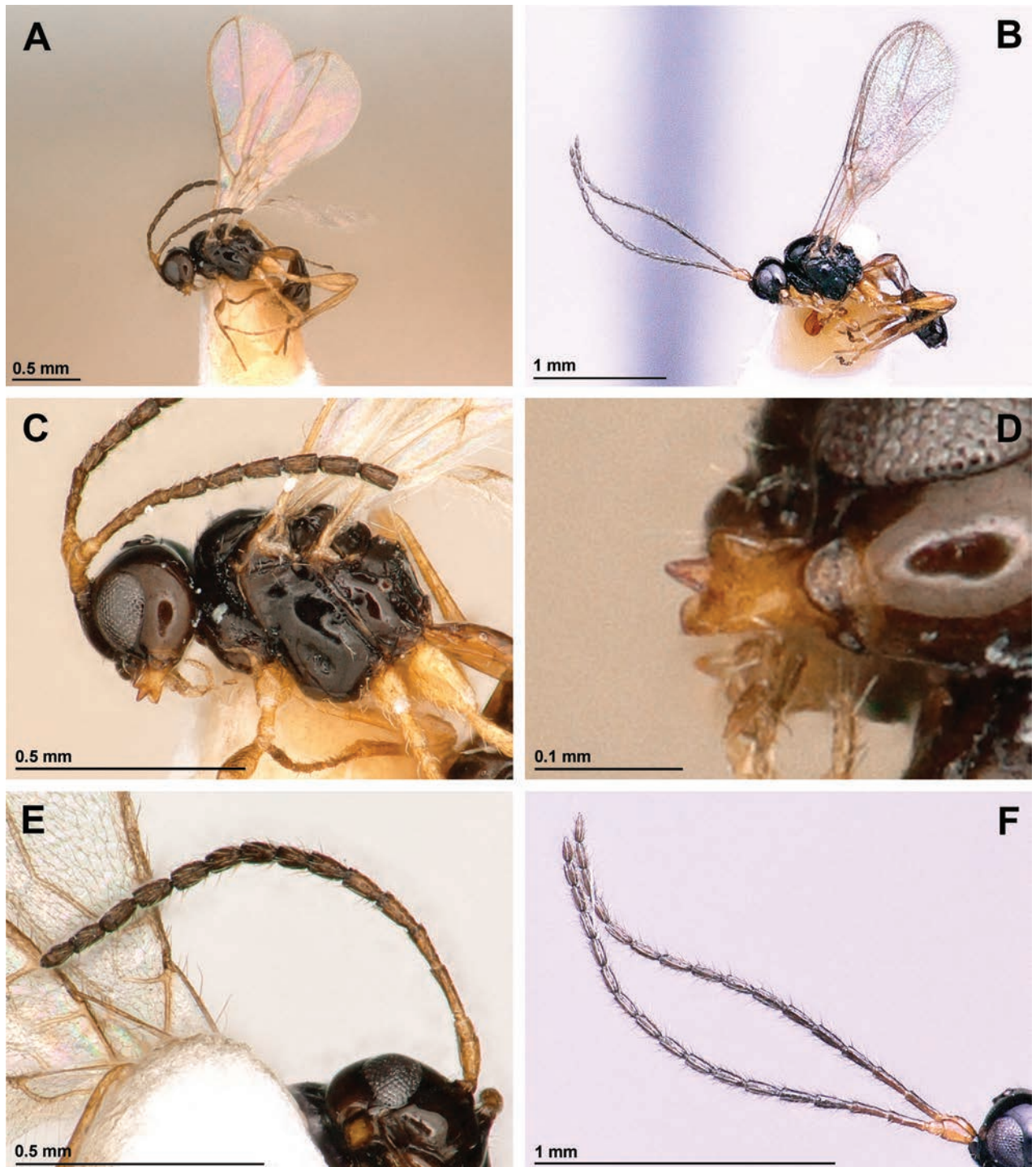


Figure 2. *Aspilota murieli* sp. nov. A, C–E female, holotype B, F male, paratype A, B habitus, lateral view C head and mesosoma, lateral view D mandible D, E antenna.

Paratypes: ARGENTINA • 7 ♀♀; same location than holotype but: 2 ♀♀; 8.ix.2022; 33°56'16"S, 59°37'4"W; 16 m (MACN-En; ZISP); 1 ♀; 5.x.2022; 33°55'16"S 59°37'42"W; 16 m (MACN-En) • 1 ♀; 24.x.2022; 33°55'13"S, 59°37'26"W; 99 m (NMB) • 1 ♀; 23.xi.2022; 33°56'15"S, 59°36'40"W; 19 m (NMB) • 2 ♀♀; 3.x.2023; 33°55'16"S, 59°37'42"W; 18 m (PFEC) • 1 ♀; Buenos Aires Province, Partido de Solis; 5.x.2022; 34°12'10"S, 59°13'22"W; 31 m; Malaise trap (Peris-Felipo leg.) (MACN-En) • 1 ♀; Buenos Aires Province, Partido de Solis; 7.ii.2024;

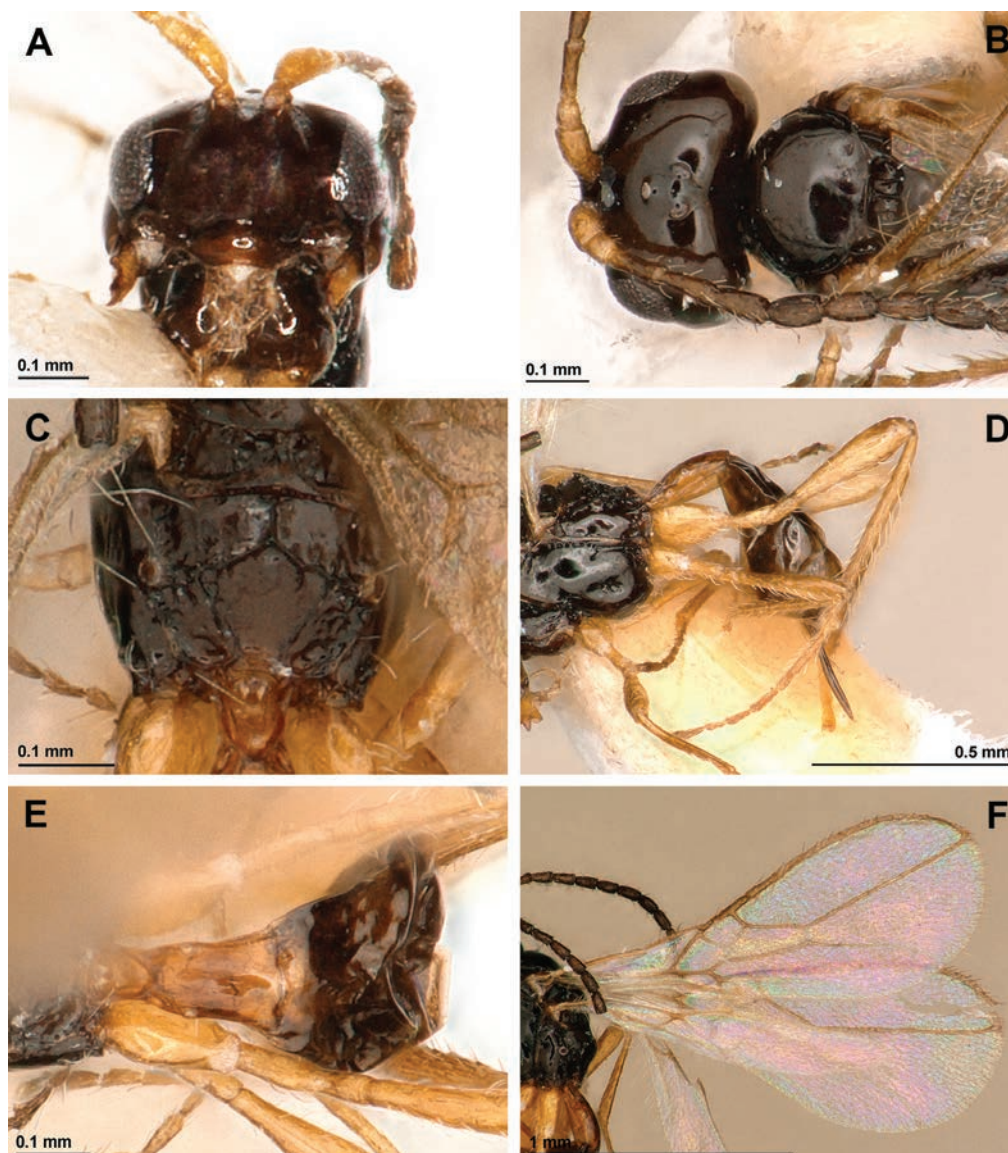


Figure 3. *Aspilota murieli* sp. nov. **A–F** female, holotype **A** head, front view **B** head, dorsal view **C** propodeum, dorsal view **D** hind leg, metasoma and ovipositor, lateral view **E** first metasomal tergite **F** wings.

34°11'29"S, 59°13'44"W; 29 m; Malaise trap (Peris-Felipo leg.) (PFEC) • 2 ♀♀; Santa Fé Province, Partido de Teodelina; 13.x.2022; 34°06'18"S, 61°27'25"W; 97 m; Malaise trap (Peris-Felipo leg.) (PFEC; ZISP) • 1 ♀; Buenos Aires Province, Partido de Vedia; 12.x.2022; 34°27'35"S, 61°48'46"W; 99 m; Malaise trap (Peris-Felipo leg.) (MACN-En) • 1 ♀; Buenos Aires Province, Partido de Vedia; 31.x.2022; 34°29'10"S, 61°47'12"W; 99 m; Malaise trap (Peris-Felipo leg.) (MACN-En) • 1 ♀, 1 ♂, Buenos Aires Province, Partido de Vedia; 10.i.2024; 34°29'10"S, 61°47'12"W; 99 m; Malaise trap (Peris-Felipo leg.) (PFEC) • 1 ♀, Buenos Aires Province, Partido de Vedia, 18.vii.2024; 34°29'25"S, 61°47'45"W; 99 m; Malaise trap (Peris-Felipo leg.) (NMB).

Description. Female (holotype). **Length.** Body 1.4 mm; fore wing 1.6 mm; hind wing 1.2 mm.

Head. In dorsal view, 1.85 × as wide as its median long, 1.5 × as wide as mesoscutum, smooth, with temple rounded behind eyes (Fig. 3B). Eye in lateral view 1.6 × as high as wide and 0.9 × as wide as temple medially (Fig. 2C). POL 1.6 × OD; OOL ~3.0 × OD (Fig. 3B). Face 1.7 × as wide as high; inner margins of

eyes subparallel (Fig. 3A). Clypeus 2.3 × as wide as high, slightly curved ventrally (Fig. 3A). Paraclypeal fovea reaching inner margin of eye (Fig. 3A). Mandible tridentate, weakly widened towards apex, 1.3 × as long as its maximum width (Fig. 2D). Upper tooth distinctly shorter than lower tooth, small and rounded; middle tooth rather long and narrow, longer than lower tooth, acuminate apically; lower tooth widest, obtuse, subrounded distally, weakly curved downwards (Fig. 2D). Antenna (Fig. 2E) 15-segmented, 0.8 × as long as body. Scape 2.0 × longer than pedicel. First flagellar segment 3.7 × as long as its maximum width, 1.2 × as long as second segment. Second flagellar segment 2.6 × as long as its maximum width; third to eleventh segments 1.7–1.8 × as long as their maximum width, 12th segment 1.45×, and 15th (apical) segment 2.0 × as long as their wide accordingly (Fig. 2E).

Mesosoma. In lateral view, 1.2 × as long as high (Fig. 2C). Mesoscutum (dorsal view) 0.75 × as long as its maximum width, smooth, without setae along tracks of notauli (Fig. 3B). Notauli mainly absent on horizontal surface of mesoscutum (Fig. 3B). Mesoscutal pit absent (Fig. 3B). Prescutellar depression smooth, with three carinae (Fig. 3B). Precoxal sulcus present, crenulate, short, not reaching anterior and posterior margins of mesopleuron (Fig. 2C). Posterior mesopleural furrow crenulate in upper half, smooth in lower half (Fig. 2C). Propodeum largely smooth, with pentagonal areola delineated by distinct carinae (Fig. 3C). Propodeal spiracles weakly enlarged, its diameter 0.5 × distance from spiracle to anterior margin of propodeum. (Fig. 3C).

Wings (Fig. 3F). Length of fore wing 2.5 × as long as its maximum width. Radial (marginal) cell ending at apex of wing, 3.7 × as long as its maximum width. Vein r2 (3-SR) 2.3 × as long as vein cuqu1 (2-SR); vein r3 (SR1) 3.1 × as long as vein r2 (3-SR). Nervulus (cu-a) distinctly postfurcal. Brachial (first subdiscal) cell closed distally, 2.6 × as long as its maximum width. Hind wing 6.7 × as long as its maximum width.

Legs (Fig. 3D). Hind femur subclaviform, 3.8 × as long as its maximum width. Hind tibia weakly widened towards apex, 9.2 × as long as its maximum subapical width, 1.05 × as long as its hind tarsus. First segment of hind tarsus 2.4 × as long as second segment.

Metasoma. First tergite long, slightly widened towards apex, 2.0 × as long as its apical width, completely smooth (Fig. 3E). Ovipositor sheath (Fig. 3D) 1.3 × as long as first tergite, 0.4 × as long as metasoma, 0.5 × as long as hind femur, 0.3 × as long as fore wing.

Colour. Body and antenna dark brown. Mandibles, palpi, pterostigma and legs yellowish brown. First metasomal tergite paler than second and third tergites. Wings hyaline.

Variation. Body length 1.3–1.7 mm; fore wing length 1.5–1.9 mm; hind wing length 1.1–1.5 mm. Face 1.60–1.75 × as wide as high. Mandible 1.3–1.4 × as long as its maximum width. Antenna 14–16-segmented. First flagellar segment 3.6–3.7 × as long as its maximum width. Sixth flagellar segment 1.6–1.8 × as long as its maximum width. Vein r3 (SR1) 2.9–3.2 × as long as vein r2 (3-SR). Hind femur 3.65–3.80 × as long as its maximum width.

Male (Fig. 2B, F). Body length 1.2 mm; fore wing length 1.9 mm; hind wing length 1.2 mm. Antenna slender, 18-segmented, about as long as body. First flagellar segment 3.8 × as long as its maximum width. Second flagellar segment 2.6 × as long as its maximum width. Third and fourth segments 3.15×, 5th–11th segments

2.8×, 12th–14th segments 2.5×, and 15th segment 3.0 × as long as its maximum width. Vein r3 (SR1) 3.0 × as long as vein r2 (3-SR). Otherwise similar to female.

DNA sequence data. Sequences obtained as part of this study are deposited in GenBank, accession numbers PV097239 and PV097240.

Etymology. This species is named in honour of Julio Muriel, for his motivational influence, visionary inspiration and his key role as the driving force behind the success of this project.

Comparative diagnosis. This new species is similar to *A. stigmalis* from Colombia (Papp 2012) (Neotropical) and *A. spiracularis* from Mexico (Nearctic) (Fischer 1970). *Aspilota murieli* sp. nov. differs from *A. stigmalis* on having the eye in dorsal view as wide as temple medially (0.8 × as wide as in *A. stigmalis*) and in lateral view 0.9 × as wide as temple medially (1.1 × in *A. stigmalis*), mandible 1.3–1.4 × as long as its maximum width (1.6 × in *A. stigmalis*), scape 2.0 × longer than pedicel (2.5 × in *A. stigmalis*), and vein r3 (SR1) 2.9–3.2 × as long as vein r2 (3-SR) (2.3 × in *A. stigmalis*). On the other hand, this new species differs from *A. spiracularis* on having the head in dorsal view 1.85 × as wide as its median long (1.33 × in *A. spiracularis*), first flagellar segment 3.6–3.7 × as long as its maximum width (5.0 × in *A. spiracularis*), vein r2 (3-SR) 2.3 × as long as vein cuqu1 (2-SR) (1.4 × in *A. spiracularis*), hind femur 3.65–3.80 × as long as its maximum width (4.0 × in *A. spiracularis*), and first metasomal tergite 2.0 × as long as its apical width (1.7 × in *A. spiracularis*).

Key to the Neotropical species of *Aspilota*

Both Spinola's Chilean species, *A. nemostigma* (Spinola, 1851) and *A. pulchella* (Spinola, 1851), have been excluded from the key due to the unavailability of specimens and ambiguous original descriptions, preventing accurate identification for our study.

- 1 Vein r2 (3-SR) 1.4 × as long as vein cuqu1 (2-SR). First flagellar segment 5.0 × as long as its maximum width. First metasomal tergite about 1.7 × as long as its apical width. [Body length 2.4 mm. Mexico] ***A. spiraculis* Fischer** ♀
- Vein r2 (3-SR) 2.3–2.5 × as long as vein cuqu1 (2-SR). First flagellar segment 3.6–3.8 × as long as its maximum width. First metasomal tergite about 2.0 × as long as its apical width.....**2**
- 2 Eye in dorsal view 0.8 × as wide as temple, and in lateral view 1.1 × as wide as temple medially. Mandible 1.6 × as long as its maximum width. Scape 2.5 × longer than pedicel. Vein r3 (SR1) 2.3 × as long as vein r2 (3-SR). [Body length 3.0 mm. Colombia] ***A. stigmalis* Papp** ♀
- Eye in dorsal view as wide as temple, and in lateral view 0.9 × as wide as temple medially. Mandible 1.3–1.4 × as long as its maximum width. Scape 2.0 × longer than pedicel. Vein r3 (SR1) 2.9–3.2 × as long as vein r2 (3-SR). [Body length 1.2–1.7 mm. Argentina]..... ***A. murieli* Peris-Felipo, sp. nov.** ♀♂

Discussion

Species of the genus *Aspilota* are endoparasitoids of Diptera, laying their eggs in larvae and emerging from the host. They have been recorded across multiple zoogeographical regions worldwide. However, until now, knowledge of this

group in the Neotropical region was restricted to Chile and Colombia (Yu et al. 2016). This study provides the first well-documented record of the genus *Aspilota* in Argentina and includes the description of *Aspilota murieli* sp. nov. The genetic data analysis confirms that this species is new to science, with its closest known relative being *A. angusta* Berry, 2007, previously recorded in Australia, Canada, and New Zealand. However, with a genetic similarity of only 94.92%, it is evident that *A. murieli* represents a newly identified species.

The diagnostic morphological traits of the *Aspilota* group align closely with the primary, well-established characteristics of the genus. These include the paraclypeal fovea extending to the inner eye margin, a closed distal brachial (first subdiscal) cell, and the presence of the vein cuqu1 (2-SR) in the forewing. These shared features facilitate genus identification.

The newly developed key for identifying the Neotropical *Aspilota* species, presented in this study, marks an important step toward advancing research on the biodiversity of this genus in the region.

The scarcity of data on this genus in the Neotropics may be attributed to the limited number of specialists focusing on parasitoid wasps and the general lack of entomological studies in the region. Future research on Argentine parasitoid wasps is strongly encouraged to gain a better understanding of their distribution and biology, as many of these species play a vital role in the biological control of fly pest populations.

Acknowledgements

We express our sincere gratitude to Seraina Klopstein and Lucas Blattner from the Naturhistorisches Museum Basel (Switzerland) for their kindness and assistance during our work with the photosystem at the museum. We also appreciate the generosity and support of the owners, managers and technical advisors of “La Donosa” (MSU Agro), “Los Laureles” (Adecoagro), “La Casualidad” (CREA), “Los Montes” (CREA) and “Santa Inés” (CREA) for allowing us to carry out this study on their farms. Additionally, our heartfelt thanks go to Julio Muriel and Hernan Barbero for their invaluable contributions in making this project possible. Finally, we recognize to Neus Marí and AllGenetics & Biology SL (<https://www.allgenetics.eu>) for supporting with the DNA barcoding analyses.

Additional information

Conflict of interest

The authors have declared that no competing interests exist.

Ethical statement

No ethical statement was reported.

Funding

The present work was funded by the project LivinGro® (Syngenta). This study was performed as part of the Russian State Research Project No. 1024031300134-2-2-1.6.14 for SAB.

Author contributions

All authors have contributed equally.

Author ORCIDs

Francisco Javier Peris-Felipo  <https://orcid.org/0000-0001-9929-3277>

Camila Noemí Villar  <https://orcid.org/0009-0008-2756-4670>

Sofía Belén Forte  <https://orcid.org/0009-0004-7551-2120>

Joel Nazareno Lentini  <https://orcid.org/0009-0002-7901-0633>

María del Pilar Medialdea  <https://orcid.org/0009-0008-6214-9472>

Federico Pandol-Avalos  <https://orcid.org/0009-0005-0458-4837>

Ana Lia Gayan-Quijano  <https://orcid.org/0009-0001-1457-3788>

Santiago L. Poggio  <https://orcid.org/0000-0001-9949-9240>

Sergey Belokobylskij  <https://orcid.org/0000-0002-3646-3459>

Mariano Devoto  <https://orcid.org/0000-0003-3098-236X>

Data availability

All of the data that support the findings of this study are available in the main text.

References

- Bianchi AR, Cravero SAC (2010) Atlas Climático Digital de la República Argentina. Ediciones Instituto Nacional de Tecnología Agropecuaria, Buenos Aires, Argentina, 57 pp.
- Fischer M (1971) Revision der nearktischen *Aspilota*-Arten der Sektion D. und Ergänzungen zu anderen Arten-gruppen. Annalen des Naturhistorisches Museum in Wien 74: 91–127.
- Hebert PD, Penton EH, Burns JM, Janzen DH, Hallwachs W (2004) Ten species in one: DNA barcoding reveals cryptic species in the neotropical skipper butterfly *Astraptes fulgerator*. Proceedings of the National Academy of Sciences of the United States of America 101: 14812–14817. <https://doi.org/10.1073/pnas.0406166101>
- Herbert PD, Cywinska A, Ball SL, de Waard JR (2003) Biological identifications through DNA barcodes. Proceedings of Biological Science 270(1512): 313–321. <https://doi.org/10.1098/rspb.2002.2218>
- Mardulyn P, Whitfield JB (1999) Phylogenetic signal in the COI, 16S, and 28S genes for inferring relationships among genera of Microgastrinae (Hymenoptera; Braconidae): evidence of a high diversification rate in this group of parasitoids. Molecular Phylogenetics and Evolution 12: 282–294. <https://doi.org/10.1006/mpev.1999.0618>
- Papp J (2012) Five new braconid species from Colombia (Hymenoptera, Braconidae). Journal of Hymenoptera Research 28: 67–84. <https://doi.org/10.3897/jhr.28.2023>
- Park D-S, Suh S-J, Oh H-W, Herbert PD (2010) Recovery of the mitochondrial COI barcode region in diverse Hexapoda through tRNA-based primers. BMC Genomics 11: 423. <https://doi.org/10.1186/1471-2164-11-423>
- Peris-Felipo FJ, Belokobylskij SA (2016) First record of the genus *Dinotrema* Foerster, 1863 (Hymenoptera, Braconidae, Alysiinae) from the Neotropical region with description of four new species and a key to the New World taxa. European Journal of Taxonomy 179: 1–23. <https://doi.org/10.5852/ejt.2016.179>
- Peris-Felipo FJ, Belokobylskij SA, Jiménez-Peydró R (2014) Revision of the Western Palearctic species of the genus *Dinotrema* Foerster, 1862 (Hymenoptera, Braconidae, Alysiinae). Zootaxa 3885 (1): 1–483. <https://doi.org/10.11646/zootaxa.3885.1.1>
- Peris-Felipo FJ, Santa F, van Achterberg C, Belokobylskij SA (2025) Review of the genera and subgenera of the subtribe Aspilotina (Hymenoptera, Braconidae, Alysiinae), with a new illustrated key. ZooKeys 1229: 133–200. <https://doi.org/10.3897/zookeys.1229.142489>

- Ralser M, Querfurth R, Warnatz H, Lehrach H, Yaspo M, Krobisch S (2006) An efficient and economic enhancer mix for PCR. *Biochemical and Biophysical Research Communications* 347: 747–751. <https://doi.org/10.1016/j.bbrc.2006.06.151>
- Soriano A, León RJC, Sala OE, Lavado R, Deregibus VA, Cauhepé MA, Scaglia OA, Velázquez CA, Lemcoff JH (1991) Río de la Plata Grasslands. In: Coupland RT (Ed.) *Temperate Subhumid Grasslands. Ecosystems of the World. 8, Natural Grasslands.* Elsevier, Amsterdam, 367–407.
- Spinola M (1851) *Ichneumonitos*. In: Gay C (Ed.) *Historia física y política de Chile*, Paris, 471–550.
- van Achterberg C (1988) The genera of the *Aspilota*-group and some descriptions of fungicolous Alysini from Netherlands (Hymenoptera: Braconidae: Alysini). *Zoologische Verhandelingen Leiden* 247: 1–88.
- van Achterberg C (1993) Illustrated key to the subfamilies of the Braconidae (Hymenoptera: Ichneumonoidea). *Zoologische Verhandelingen Leiden* 283: 1–189.
- Yu DS, van Achterberg C, Horstmann K (2016). *Taxapad 2016, Ichneumonoidea 2015.* Taxapad, Ottawa, Ontario. [Database on flash-drive]

An Amazonian hidden gem: a new metallic-colored species of *Ranitomeya* (Anura, Dendrobatidae) from Juruá River basin forests, Amazonas state, Brazil

Alexander Tamanini Mônico¹, Esteban Diego Koch², Jussara Santos Dayrell¹, Jiří Moravec³, Albertina Pimentel Lima¹

1 *Coordenação de Biodiversidade, Instituto Nacional de Pesquisas da Amazônia, Manaus, Amazonas, Brazil*

2 *Programa de Pós-Graduação em Genética, Conservação e Biologia Evolutiva, Instituto Nacional de Pesquisas da Amazônia, Manaus, Amazonas, Brazil*

3 *Department of Zoology, National Museum of the Czech Republic, Cirkusová 1740, 193 00 Prague 9, Czech Republic*

Corresponding author: Alexander Tamanini Mônico (alexandermonico@hotmail.com)

Abstract

The genus *Ranitomeya* has 16 known species, and the last of them was described 13 years ago. The forests of the Juruá River basin are known for their enormous vertebrate diversity, despite being one of the least sampled regions in the entire Amazonia. Our recent expeditions to the region resulted in the discovery of a *Ranitomeya* species with blue-green dorsal stripes and quite peculiar behavior. Here, it is described as a new species using morphological, morphometric, advertisement call, natural history, and genetic data. This new species is strongly nested within the *R. vanzolinii* clade, with interspecific *p*-distances ranging from 2.94 to 3.91%, and it was confirmed in all the delimitation methods used. It differs from its closest relatives mainly by (i) its size (male SVL 15.4–17.7 mm, *n* = 8; female SVL 17.3–18.5 mm, *n* = 5), (ii) its unique color pattern that is metallic pale yellowish green to metallic pale turquoise-green dorsal stripes pattern, limbs metallic chrome with dark carmine spotting), (iii) presence of a conspicuous sulfur yellow spot on the dorsal surface of the thighs, (iv) tadpoles with posterior tooth rows P1 > P2 > P3 in all stages, head translucent brownish and lack of emarginate lateral papillae, and (v) its advertisement call (composed of 21–45 notes, call duration of 647–1,424 ms, note rate of 28–36 notes/s and dominant frequency of 4,996–6,288 Hz).

Key words: Advertisement call, Amphibia, biodiversity, integrative taxonomy, morphology, phylogeny



Academic editor: Luis Ceriaco
Received: 12 January 2025
Accepted: 26 February 2025
Published: 25 April 2025

ZooBank: <https://zoobank.org/BD88CB7C-757A-42EC-85AD-D7061F966B97>

Citation: Mônico AT, Koch ED, Dayrell JS, Moravec J, Lima AP (2025) An Amazonian hidden gem: a new metallic-colored species of *Ranitomeya* (Anura, Dendrobatidae) from Juruá River basin forests, Amazonas state, Brazil. ZooKeys 1236: 51–83. <https://doi.org/10.3897/zookeys.1236.146533>

Copyright: © Alexander Tamanini Mônico et al. This is an open access article distributed under terms of the Creative Commons Attribution License (Attribution 4.0 International – CC BY 4.0).

Introduction

The genus *Ranitomeya* Bauer, 1986 currently comprises 16 recognized species (Frost 2025), with the most recent species being described more than 13 years ago (Brown et al. 2011). These species are distributed throughout northern South America, from the Andean foothills to the Amazonian forests (Frost 2025). Among dendrobatid frogs, the genus *Ranitomeya* has posed significant taxonomic challenges because of its high intraspecific morphological variation and mimicry, especially in coloration patterns. These challenges have been compounded by cases where taxonomic studies lacked support from molecular data (Muell et al. 2022).

Currently, *Ranitomeya* is organized into the following five monophyletic species groups (Muell et al. 2022), which were defined by the phylogenetic placement, morphology, mating systems, and vocalization:

(i) *R. defleri* species group

R. defleri Twomey & Brown, 2009

(ii) *R. reticulata* species group

R. benedicta Brown, Twomey, Pepper & Sanchez-Rodriguez, 2008

R. fantastica (Boulenger, 1884); *R. reticulata* (Boulenger, 1884)

R. summersi Brown, Twomey, Pepper & Sanchez-Rodriguez, 2008

R. uakari (Brown, Schulte & Summers, 2006); *R. ventrimaculata* (Shreve, 1935)

An undescribed species phylogenetically close to *R. uakarii*

An undescribed species phylogenetically close to *R. benedicta*

(iii) *R. vanzolinii* species group

R. cyanovittata Pérez-Peña, Chávez, Twomey & Brown, 2010

R. flavovittata (Schulte, 1999)

R. imitator (Schulte, 1986)

R. sirensis (Aichinger, 1991)

R. vanzolinii (Myers, 1982)

R. yavaricola Pérez-Peña, Chávez, Twomey & Brown, 2010

An undescribed species related to *R. sirensis* from eastern Peru (*R. sirensis* “biolat”)

(iv) *R. variabilis* species group

R. amazonica (Schulte, 1999)

R. variabilis (Zimmermann & Zimmermann, 1988)

(v) *R. toraro* species group

R. toraro Brown, Caldwell, Twomey, Melo-Sampaio & Souza, 2011

In general, numerous studies of the genus have focused on ecological aspects (Lötters et al. 2007), mating systems (Werner et al. 2010; Brown et al. 2011), taxonomy (Brown et al. 2011), biogeography (Muell et al. 2022), and coloration evolution (Vences et al. 2003; Twomey et al. 2023). Despite this, species complexes have been recognized and are yet to be resolved (Brown et al. 2008; Brown et al. 2011; Muell et al. 2022).

The greatest diversity of species is concentrated in eastern-central and north-eastern Peru (Muell et al. 2022), with considerably fewer species along the central Amazonian plain. Meanwhile, despite its vast territorial extension, Brazil has seven species with recorded occurrences (Segalla et al. 2021), and in only two cases their type locality lies on the territory of Brazil (i.e., *R. toraro* and *R. vanzolinii*; Frost 2025). This smaller diversity, aside from being an effect of the species biology, could be caused by a lack of sampling in many areas of the western Brazilian Amazonia.

The forests of the Juruá River basin, a southwestern tributary of the Amazonas River, are known for their enormous vertebrate diversity, despite being one of the least sampled regions in the entire Amazonia (Del-Rio et al. 2021). These knowledge gaps are a result of the exhausting logistics needed to study remote

areas, which make it difficult to develop long-term monitoring that allows understanding of diversity patterns (Moraes et al. 2022). For amphibians, most records come from specific inventories, especially from the upper reaches of the basin (e.g., Pantoja and Fraga 2012; Bernarde et al. 2013; Fonseca et al. 2019). Even inventories in areas where *Ranitomeya* is known to occur did not record them, most probably due to their shyness (Brown et al. 2011), which leads to rare encounters. Taxonomically, the region has a huge potential for finding new species, with several candidate lineages already identified (e.g., Moraes et al. 2022; Souza et al. 2023; Lima et al. 2024; Martins et al. 2024). Added to this, it is known that one of the most notable biogeographic patterns for the basin is that species composition appears to be better divided from the lower to upper reaches of the basin than between river margins (Haffer 1997; Matocq et al. 2000; Azevedo-Ramos and Galatti 2002; Tuomisto et al. 2019).

Our recent expeditions to the Eiru and Juruá rivers resulted in the discovery of a new species of *Ranitomeya* with blue-green dorsal stripes and quite peculiar behavior. In the present study, we describe it as a new species using morphological, morphometric, advertisement call, natural history, and genetic data from four mitochondrial loci.

Materials and methods

Sampling and specimen collection

Adult specimens

Thirteen adult individuals of the new species were manually collected in the RAPELD sampling module of the Comunidade de Santo Antônio (6°47'04.9"S, 69°52'00.3"W), Eiru River, tributary of the Juruá River, municipality of Eirunepé, Amazonas state, Brazil. The specimens were anesthetized and killed with 5% topical lidocaine. Muscle and liver tissue were preserved in 100% ethanol for posterior genetic analysis, whereas the specimens were fixed in 10% formalin and preserved in 70% ethanol. Specimens were sexed by the presence of vocal slits (exclusive to males) and internally by the condition of the gonads. Vouchers were deposited in the herpetological collection of the Instituto Nacional de Pesquisas da Amazônia (INPA-H; Manaus, Brazil) and Museu Paraense Emílio Goeldi (MPEG; Belém, Brazil).

Tadpole specimens

The tadpoles were collected at the same site as the adult individuals. They were euthanized as described above, and fixed and preserved in 5% neutral-buffered formalin. Tadpoles were deposited at INPA-H.

Ethical considerations

Protocols of collection and animal care followed the Brazilian Federal Council for Biology (resolution number 148/2012) and study was approved by the Ethics Committee on the Use of Animals of the Instituto Nacional de Pesquisas da Amazônia - CEUA-INPA (Process No. 35/2020, SEI 01280.001134/2020-63).

Specimens were collected under collection permit number 13777-1, issued by the Centro Nacional de Pesquisa e Conservação de Répteis e Anfíbios of the Instituto Chico Mendes de Conservação da Biodiversidade – ICMBio.

Morphological analyses

Adult morphometrics

Morphometric measurements were taken from eight adult males and five adult females of the new species, following Brown et al. (2011) [snout to vent length (**SVL**), head width (**HW**), head length (**HL**), interorbital distance (**IOD**), upper eyelid width (**UEW**), tympanum diameter (**TD**), eye-tympanum distance (**DET**), eye diameter (**ED**), body width (**BW**), knee-knee distance (**KK**), femur length (**FL**), tibia length (**TL**), foot length / Toe IV length (**FoL**), hand length / Finger III length (**HaL**), fingers I (**L1F**) and II (**L2F**) length, Finger III disc width (**W3FD**), finger width just below III (**W3F**), Watters et al. (2016) [snout length (**SL**), eye-nostril distance (**END**), internarial distance (**IND**), tarsus length (**TaL**), arm length (**AL**), forearm length (**FAL**), Finger IV length (**L4F**); toes I (**L1T**), III (**L3T**) and V (**L5T**) length, Toe IV disc width (**W4TD**), fingers II (**W2FD**) and IV (**W4FD**) discs width, Finger IV width just below disc (**W4F**), and Serrano-Rojas et al. (2017) [snout-nostril distance (**TSCN**), mouth-tympanic distance (**MTD**), Toe III disc width (**W3TD**), toes III (**W3T**) and IV (**W4T**) width just below disc]. Besides these, we also include Toe II length (**L2T**), toes I (**W1TD**), II (**W2TD**) and V (**W5TD**) disc width, toe I (**W1T**), II (**W2T**) and V (**W5T**) width just below disc, Finger I disc width (**W1FD**), and fingers I (**W1F**) and II (**W2F**) width just below disc. Measurements were taken to the nearest 0.01 mm using a stereomicroscope (S8APO, Leica) coupled to a camera (Leica, DFC295), except for SVL, which was measured with a digital caliper to the nearest 0.1 mm. Raw data are provided in Suppl. material 1.

Morphological and coloration description

The format of the description and terminology of the morphological characters follow Kok and Kalamandeen (2008) and Brown et al. (2011). Color in life was described based on photographs taken in the field, following the color catalog provided by Köhler (2012).

Tapdole morphology

Description of the external morphology of the *Ranitomeya* sp. nov. tadpole was based on three individuals, at stage 26, 29, and 39 (Gosner 1960). Morphometric measurements followed McDiarmid and Altig (1999) and Randrianiaina et al. (2011): total length (**TL**), body length (**BL**), tail length (**TAL**), maximum body height (**BH**), maximum body width (**BW**), body height at the nostril (**BHN**), body height at the eyes (**BHE**), body width at the nostril (**BWN**), body width at the eyes (**BWE**), tail muscle width at base (**TMW**), maximum tail height (**MTH**), dorsal fin height (**DF**), ventral fin height (**VF**), tail muscle height (**TMH**), interorbital distance (**IOD**), internarial distance (**IND**), rostro-eye distance (**RED**), rostro-nostril distance (**RND**), rostro-spiracle distance (**RSD**), eye diameter (**ED**), eye-nostril distance (**END**), spiracle length (**SL**), spiracle width (**SW**), spiracle height (**SW**),

vent tube length (**VL**), oral disc width (**ODW**), anterior (upper) labium (**AL**), posterior (lower) labium (**PL**), first anterior tooth row (**A-1**), second anterior tooth row (**A-2**), medial gap in second anterior tooth row (**A-2 GAP**), first posterior tooth row (**P-1**), second posterior tooth row (**P-2**), third posterior tooth row (**P-3**), medial gap in the first posterior tooth row (**P-1 GAP**), lateral process of upper jaw sheath (**LP**), lower jaw sheath (**LJ**) and, finally, upper jaw sheath (**UJ**).

Bioacoustics

Recording protocol

The advertisement calls of sixteen males of the new species were recorded using a digital recorder (PCM-D50, Sony) and unidirectional microphone (K6/ME66, Sennheiser, Germany). Air temperatures (24.3–26.1 °C) and humidity (89–98%) during call recording were measured with a thermohygrometer (7663.02.0.00, Incoterm). Each calling male was recorded for two min using frequency rate of 16 kHz and 16 bits of resolution in mono.

Data deposition

The recordings were deposited in the Fonoteca Neotropical Jacques Viellard of the Universidade de Campinas (**FNJV**; Campinas, Brazil) under access number FNJV 124331 to 124339.

Analyses

Bioacoustic variables were analyzed using Raven Pro 1.6 (Bioacoustics Research Program 2014) with the following configuration: window = Blackman, Discrete Fourier Transform = 2,048 samples and 3 dB filter bandwidth = 80.0 Hz. The following temporal and spectral traits were measured: call duration (**CD**), number of notes per call (**NN**), silence between calls (**SBC**), note duration (**ND**), silence between notes (**SBN**), and minimum (**LF**), maximum (**HF**) and dominant frequency (**DF**). Dominant frequency was measured using the *Peak frequency* function; maximum and minimum frequencies were measured at 20 dB below the peak frequency to avoid background noise interference. Call description follows the call-centered approach of Köhler et al. (2017). The spectrogram and oscillogram were generated in R environment (R Core Team 2019) via the *seewave* package 2.0.5 (Sueur et al. 2008) using a Blackman window, 256 points of resolution (Fast Fourier Transform) and an overlap of 85%. The raw bioacoustic data are provided in Suppl. material 2.

Molecular and phylogenetic analyses

DNA extraction and amplification

Genomic DNA was extracted from ten adult specimens (liver or muscle tissues) from both localities (Suppl. material 3). Genomic DNA was extracted using PureLink™ Genomic DNA (Invitrogen by Thermo Fisher Scientific, Carlsbad, CA, USA). Sequences of four mitochondrial loci [16S rRNA (all specimens),

12S rRNA (6 specimens), cytochrome C oxidase sub-unit 1 – CO1 (six specimens) and cytochrome *b* – *cyt-b* (4 specimens)] were amplified via polymerase chain reaction (PCR) with a general final volume of 15 μ L containing 1.5 μ L of 25 mM MgCl₂, 1.5 μ L of 10 mM dNTPs (2.5 mM each dNTP), 1.5 μ L of buffer 10 \times (75 mM Tris HCl, 50 mM KCl, 20 mM (NH₄)₂SO₄), 1.5 μ L of forward primer (2 μ M), 1.5 μ L of reverse primer (2 μ M), 6.4 μ L of ddH₂O and 0.1 μ L of 1 U Taq DNA polymerase and 1 μ L of DNA (30–50 ng/ μ L). For 12S, we used 12S L13 (5'-TTAGAAGAGGCAAGTCGTAACATGGTA-3'; Feller and Hedges 1998) and 12S Titus I (5'-GGTGGCTGCTTTTAGGCC-3'; Titus and Larson 1996) primers with the following PCR program: 90 s at 94 °C followed by 35 cycles at 94 °C (45 s), 55 °C (45 s) and 72 °C (90 s), and a final extension of 7 min at 72 °C. For 16S, we used 16Saf (5'-CGCCTGTTTATCAAAAACAT-3') and 16Sbr (5'-CCG-GTCTGAACTCAGATCACGT-3') (Palumbi 1996) primers with the following PCR program: 90 s at 94 °C followed by 35 cycles at 94 °C (45 s), 55 °C (45 s) and 72 °C (90 s), and a final extension of 7 min at 72 °C. For COI, we used Chmf4f (5'-TYTCWACWAAAYCAYAAAGAYATCGG-3') and Chmr4r (5'-ACYTCRGGRTGRC-CRAARAATCA-3') (Che et al. 2012) primers with the following PCR program: 60 s at 94 °C followed by 35 cycles at 94 °C (20 s), 50 °C (50 s) and 72 °C (90 s), and a final extension of 10 min at 72 °C. Finally, for *cyt-b*, we used MVZ 15-L (5'-GAACTAATGGCCCACACWWTACGNAA-3'; Moritz et al. 1992) and H15149 (5'-AAACTGCAGCCCCTCAGAAATGATATTTGTCCTCA-3'; Kocher et al. 1989) primers with the following PCR program: 120 s at 95 °C followed by 35 cycles at 95 °C (30 s), 45 °C (60 s) and 72 °C (90 s), and a final extension of 6 min at 72 °C. All the PCR products were visualized in 1% agarose with SYBRSafe (Life Inc.) and purified using the PEG 8000 protocol (Sambrook and Russell 2001) and then submitted to sequencing using the standard protocols of the Big Dye™ Terminator kit (Applied Biosystems, Inc., Grand Island, NY, USA). Forward and reverse amplicons were sequenced in a genetic analyzer (ABI PRISM 3500xL, Thermo Fisher).

Sequence processing

The sequences were subjected to BLAST searches (Altschul et al. 1997) in GenBank to verify whether the target had been amplified, and its quality was checked manually. The consensus sequences of each specimen were deposited in GenBank (Suppl. material 3). To infer the phylogenetic relationships of the new species, a data set containing homologous sequences was retrieved from GenBank (Suppl. material 3).

Sequence alignment

Sequences that represented all the diversity of *Ranitomeya* species were selected, preferably containing material assigned to the type series or from the type locality. Our complete dataset comprises 266 sequences of the four loci (33 for 12S, 120 for 16S, 17 for CO1, and 96 for *cyt-b*) that correspond to 120 terminals. Sequences of each locus were aligned using the MAFFT online server using the E-INS-i strategy for 12S and 16S gene and G-INS-i for CO1 and *cyt-b* (Kato et al. 2019). The final matrix was composed of 120 terminals with a maximum of 2,419 bp (632 bp for 12s, 532 bp for 16S, 656 bp for COI, and 599 bp for *cyt-b*).

Species delimitation and genetic distances

The operational taxonomic units (OTUs) were delimited to confirm the candidate species as a single OTU. Three DNA-based species delimitation methods were used: (1) the pairwise distance-based method Assemble Species by Automatic Partitioning (ASAP; Puillandre et al. 2021) (2) the Bayesian implementation of the Poisson Tree Processes model approach (bPTP; Zhang et al. 2013); and (3) the Generalized Mixed Yule Coalescent method (single threshold GMYC; Pons et al. 2006; Monaghan et al. 2009). All methods were performed with the 16S locus, and additionally ASAP was performed with the 12S and CYTB loci to confirm the delimitation of the new species. OTUs were defined by the majority-rule consensus of the three partitions obtained with 16S locus (i.e., a lineage is considered as an OTU when it appeared in at least two out of the three results). The pairwise interspecific and the intraspecific genetic distances (p-distance and Kimura-2-parameter; Kimura 1980) using pairwise deletion were calculated between the populations of new species and close relatives using MEGA 11 (Tamura et al. 2021).

Phylogenetic tree reconstruction

The phylogenetic analyses were performed with Bayesian inference (BI) using the complete matrix for the four loci via the software Beast 2.6.6 (Bouckaert et al. 2014). Coding loci were partitioned to independently analyze each codon position. Two independent runs on 5×10^7 generations of the MCMC were conducted, with sampling every 5,000 generations. The best nucleotide substitution model was selected using *bModelTest* using the “named extended models” parameters in the MCMC (Bouckaert and Drummond 2017). The clock was set to strict clock model to estimate the evolutionary rates, and the tree prior was Yule, with other priors in default.

Data availability and supplementary materials

Raw data are provided in Suppl. materials: morphometrics (Suppl. material 1), bioacoustics (Suppl. material 2), and gene sequences (Suppl. material 3).

Table 1. Interspecific and intraspecific genetic distances between *Ranitomeya aquamarina* sp. nov. and closely related taxa. Uncorrected p-distances (%; lower diagonal) and Kimura-2-parameter (%; upper diagonal) for sequences in a matrix with 532 characters from 16S mtDNA gene and expressed as percentages. Numbers in bold represent intraspecific p-distance values.

Species	1	2	3	4	5	6	7	8	9	10
1. <i>R. aquamarina</i> sp. nov.	0.00	2.08	4.03	4.05	3.16	3.02	9.97	10.01	3.45	4.74
2. <i>R. cyanovittata</i>	3.89	0.97	3.13	3.96	3.76	3.86	9.14	8.99	4.06	3.63
3. <i>R. aff. cyanovittata</i>	3.05	2.04	0.13	3.13	2.26	3.16	8.16	8.00	2.55	3.27
4. <i>R. aff. flavovittata</i>	3.91	3.06	3.91	0.00	1.62	4.37	10.42	10.57	2.05	5.53
5. <i>R. flavovittata</i>	3.07	2.21	3.07	1.60	0.25	3.73	9.48	9.64	1.68	4.90
6. <i>R. imitator</i>	2.94	3.07	2.94	4.21	3.60	0.60	8.85	9.29	4.01	3.97
7. <i>R. sirensis</i>	9.19	7.67	9.19	9.61	8.78	8.26	1.65	5.65	9.25	6.93
8. <i>R. aff. sirensis</i>	9.27	7.56	9.27	9.78	8.97	8.68	5.40	0.00	9.91	8.01
9. <i>R. vanzolinii</i>	3.35	2.50	3.35	2.02	1.66	3.87	8.61	9.21	0.12	4.65
10. <i>R. yavaricola</i>	4.53	3.19	4.53	5.28	4.69	3.84	6.58	7.56	4.47	0.24

Results

Phylogenetic relationships and genetic distances

Individuals of the new species show no intraspecific genetic variation (16S p-distance = mean 0.0%). The new species is nested within a strongly supported clade grouping *R. vanzolinii* and *R. flavovittata* (Fig. 1). This clade is sister to the clade nesting *R. imitator*. Within this large clade, interspecific p-distances range from 2.94 to 3.91% (Table 1). All these species occur in the Western Amazonian and in the Andean foothills. The new species was confirmed in all delimitation methods, including using 12S and CYTB loci (i.e., ASAP, bPTP and GMYC; Suppl. material 4).

Taxonomic account

Order Anura Fischer von Waldheim, 1813

Family Dendrobatidae Cope, 1865 (1850)

Subfamily Dendrobatinae Cope, 1865 (1850)

Genus *Ranitomeya* Bauer, 1986

***Ranitomeya aquamarina* sp. nov.**

<https://zoobank.org/16207CA5-3CDC-43FB-91E5-51139FBFD1F4>

Figs 2–4, 6–8, 10, Tables 2–4

Chresonymy. *Ranitomeya* sp. Envira – Twomey et al. (2023); *Ranitomeya* aff. *sirensis* – Lima et al. (2024).

Vernacular names. Suggested English name: Metallic poison frog.

Suggested Spanish name: Rana venenosa metálica.

Suggested Portuguese name: Rãzinha-venenosa-metalizada.

Type material. Holotype. • INPA-H 47568 (field number APL 24805; Fig. 2), adult male collected by Alexander Tamanini Mônico and Albertina Pimentel Lima on 15 March 2024, from RAPELD sampling module of the Eiru River, tributary of the Juruá River, municipality of Eirunepé, Amazonas state, Brazil (6°47'04.9"S, 69°52'00.3"W, WGS84, 137 m elevation). **Paratypes.** Twelve adult specimens (7 males and 5 females), same locality as holotype • one male [INPA-H 47561; field number APL 24481] collected on 26 February 2023 by A.P. Lima • 3 males [INPA-H 47563, INPA-H 47564 and MPEG 45220; field numbers APL 24765, 24766 and 24768, respectively] and 3 females [INPA-H 47562, INPA-H 47565 and MPEG 45221; field numbers APL 24764, 247667 and 24769, respectively] collected on 24 March 2023 by A.P. Lima and J. Dayrell • 3 males [INPA-H 47566, MPEG 45223 and INPA-H 47570; field numbers APL 24800, 24808 and 24809, respectively] and 2 females [INPA-H 47569 and MPEG 45222; field numbers APL 24806 and 24807, respectively] collected on 14–15 March 2024 by A.T. Mônico and A.P. Lima.

Generic placement. We assign the new species to *Ranitomeya*, based on the phylogenetic placement (Fig. 1) and the following external characteristics: coloration is bright and aposematic, finger I is greatly reduced and shorter than finger II, finger discs two and four are greatly expanded, dorsal skin texture is smooth (to shagreen), and toe webbing is absent (see Brown et al. 2011; Kahn et al. 2016).

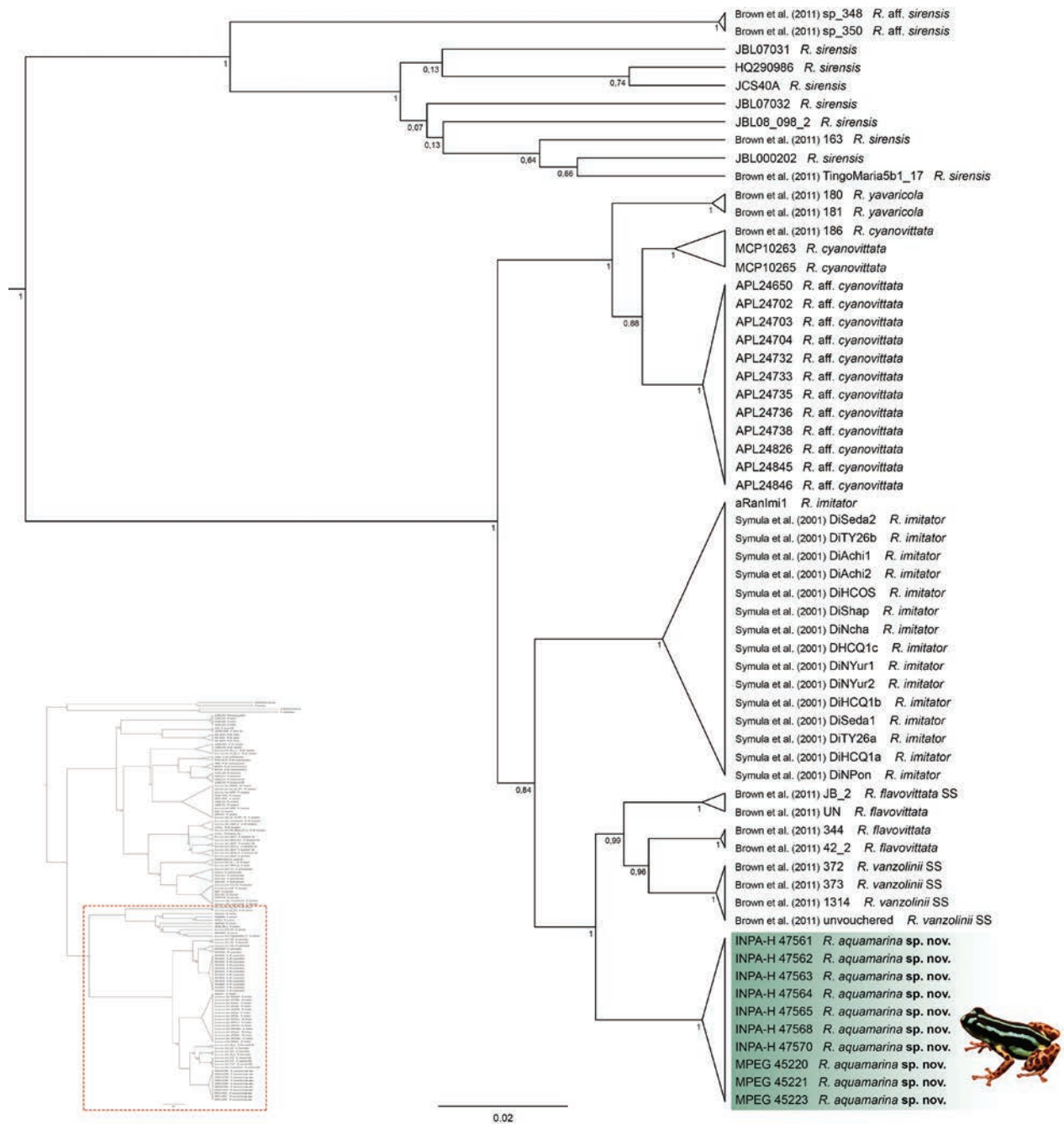


Figure 1. Part of the phylogenetic reconstruction showing the relationships of *Ranitomeya aquamarina* sp. nov. Bayesian inference tree for genes 16S, 12S, COI, and cyt-b. Posterior probability support is shown on the branches. The species name is preceded by the specimen voucher number (continuation of the tree in Suppl. material 5).

Characterization. This new species of *Ranitomeya* is characterized by the following combination of characters: (1) dorsal color jet black with three parallel stripes metallic light yellowish green to metallic light turquoise-green, mid-dorsal stripe extending from between eyes to slightly before the vent, dorsolateral stripes extending from the snout to the groin, where they become medium sulfur yellow; (2) venter jet black with metallic olive-yellow to metallic light yellowish green reticulations on belly, and gular region metallic light yellowish green to olive-yellow; ventrolateral stripes light yellowish green; extending from through the loreal region, to the thighs integrating into the ventral reticulate pat-

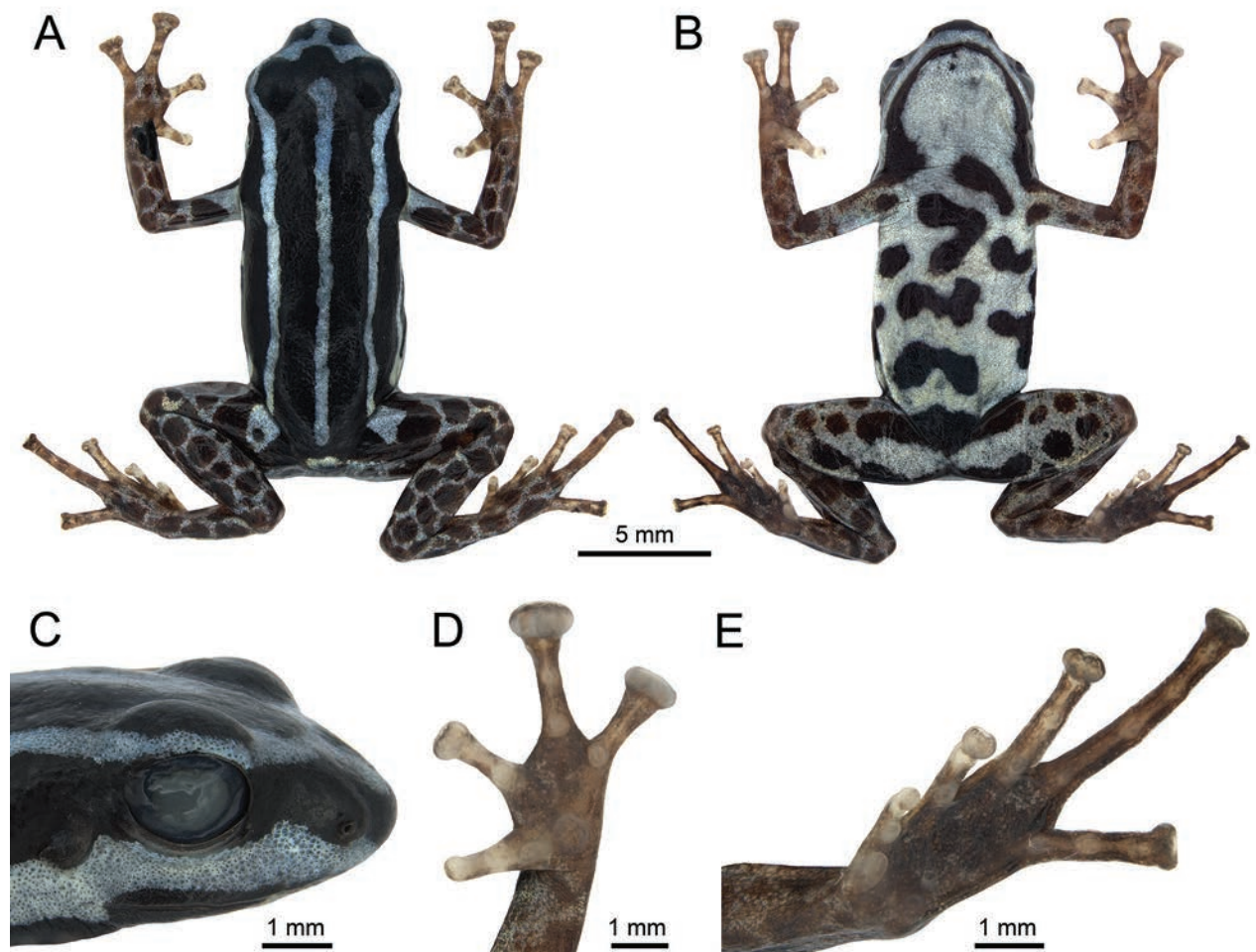


Figure 2. Preserved holotype of *Ranitomeya aquamarina* sp. nov. (INPA-H 47568, field number APL 24805) from Eiru River, municipality of Eirunepé, Amazonas state, Brazil. **A** Dorsal view **B** ventral view **C** lateral head **D** hand **E** foot. Photographs ATM.

tern, becoming medium sulfur yellow on the arms; (3) limbs medium metallic chrome orange with dark carmine spotting, presence of a conspicuous sulfur yellow spot on the dorsal surface of the thighs, forming an ‘ocellus’ like pattern; (4) dorsal skin shagreen to granular, and smooth on head; (5) gular and ventral skin shagreen to granular; (6) limbs smooth to shagreen; (7) SVL in adult males of 15.4–17.7 mm ($n = 8$) and in females of 17.3–18.5 mm ($n = 5$); (8) sexual dimorphism, females with greater SVL, BW and KK; presence of vocal slits in males, located near jaw articulation; (9) head width 0.8–1.0× body width; (10) head width 1.1–1.2× larger than head length; (11) head width 31–34% of SVL; (12) snout moderately long (SL 36–42% of HL), rounded in dorsal view and rounded to protruding in lateral view; (13) *canthus rostralis* rounded, loreal region flat; (14) nostril directed frontolaterally at the angle of the snout, internarial distance 33–39% of head width; (15) tympanum visible, tympanic membrane poorly differentiated, tympanum diameter 38–48% of eye diameter; (16) tongue ovoid, attached anteriorly; (17) dentigerous processes of vomers absent; (18) choanae ovoid and small, located marginally in the maxilla; (19) hand 24–28% of SVL, arm 25–30% of SVL; (20) fingers III > IV > II > I, Finger I 58–68% of Finger II, finger discs rounded on Finger I, and expanded and truncate on fingers III and IV; (21) thenar tubercle elliptical, palmar tubercle large and ovoid; (22) proximal subarticular tubercles ovoid, present in each finger; distal subarticular

tubercle present only on Finger III; (23) knee-knee distance 80–84% of SVL, femur 94–98% of tibia; (24) toes IV > III > V > II > I, Toe I 48–64% of Toe II, finger discs not expanded and rounded on Finger I to elliptical on toes III and IV and truncate on Finger V; (25) outer metatarsal tubercle ovoid, poorly visible; inner metatarsal tubercle elliptical; (26) proximal subarticular tubercles ovoid on all toes, distal subarticular tubercles on toes III–V; (27) advertisement call with 21–45 notes and average call duration of 647–1,424 ms, note rate (28–36 notes/s) and dominant frequency of 4,996–6,288 Hz; and (28) tadpole head translucent in life, and posterior tooth rows P-1 > P-2 > P-3.

Differential diagnosis. External morphology. The new species differs from all currently recognized *Ranitomeya* species (*R. amazonica*, *R. benedicta*, *R. cyanovittata*, *R. defleri*, *R. fantastica*, *R. flavovittata*, *R. imitator*, *R. reticulata*, *R. sirensis*, *R. summersi*, *R. toraro*, *R. uakarii*, *R. vanzolinii*, *R. variabilis*, *R. ventrimaculata*, and *R. yavaricola*) by its unique coloration (light yellowish green to light metallic turquoise-green dorsal stripe pattern, medium metallic chrome orange limbs with dark carmine spotting, and conspicuous sulfur yellow ocellus-like spot on the dorsal surface of the thighs). *Ranitomeya aquamarina* sp. nov. is generally most similar to *R. cyanovittata* and *R. yavaricola* but it can be easily distinguished from *R. cyanovittata* by light yellowish green to light metallic turquoise green dorsal stripes and medium metallic chrome orange limbs with dark carmine spotting (dorsal stripes turquoise blue, limbs with bluish reticulation and black spots; Pérez-Peña et al. 2010) and from *R. yavaricola* by light yellowish green to light metallic turquoise green dorsal stripes with no or only minor breaks and by dark carmine spotting on the limbs (dorsal stripes sage color, formed by points, that can become dashes, limbs solid bronze; Pérez-Peña et al. 2010).

In addition, *Ranitomeya aquamarina* sp. nov. is distinguished by its smaller male SVL (15.4–17.7 mm) from *R. fantastica* (~ 20 mm; Boulenger 1884), *R. imitator* (~ 19 mm; Schulte 1986) and *R. summersi* (17.5–19.5 mm; Brown et al. 2008); and larger than *R. cyanovittata* (13.8 mm; Pérez-Peña et al. 2010), *R. sirensis* (14.7–15.4 mm; Aichinger 1991), *R. toraro* (14.8–15.6 mm; Brown et al. 2011) and *R. uakari* (14.8–15.5 mm; Brown et al. 2006); by its larger female SVL (17.3–18.5 mm) from *R. sirensis* (16.8 mm; Aichinger 1991), *R. toraro* (16.2–16.7 mm; Brown et al. 2011), *R. uakari* (15.7–16.2 mm; Brown et al. 2006); *R. yavaricola* (16.7–16.8 mm; Pérez-Peña et al. 2010); by its greater female head width (5.7–5.9 mm) from *R. cyanovittata* (5.6 mm; Pérez-Peña et al. 2010), *R. sirensis* (5.4 mm; Aichinger 1991), *R. toraro* (5.0–5.3 mm; Brown et al. 2011), *R. uakarii* (5.0–5.2 mm; Brown et al. 2006), *R. yavaricola* (5.1–5.7 mm; Pérez-Peña et al. 2010); by its greater male head length (4.8–5.4 mm) from *R. cyanovittata* (3.6 mm; Pérez-Peña et al. 2010) and *R. sirensis* (3.0–3.8 mm; Aichinger 1991), but smaller than *R. imitator* (~ 6 mm) and *R. yavaricola* (5.5–6.6 mm; Pérez-Peña et al. 2010); by its smaller female head length (5.1–5.2 mm) from *R. toraro* (5.5 mm; Brown et al. 2011) and *R. yavaricola* (5.9–6.3 mm; Pérez-Peña et al. 2010) and larger than *R. sirensis* (4.0 mm; Aichinger 1991).

Bioacoustics. The advertisement call of *R. aquamarina* sp. nov. is distinguished by its longer call duration (647–1,424 ms) from the call of *R. amazonica* (160–360 ms; Brown et al. 2011), *R. benedicta* (100–170 ms; Brown et al. 2008), *R. defleri* (410–620 ms; Twomey and Brown 2009), *R. fantastica* (180–320 ms; Brown et al. 2011), *R. reticulata* (180–290 ms; Brown et al. 2011),

R. summersi (380–500 ms; Brown et al. 2008), *R. uakarii* (260–290 ms; Brown et al. 2006, Brown et al. 2011), *R. vanzolinii* (570–640 ms; Brown et al. 2011), *R. variabilis* (140–440 ms; Brown et al. 2011) and *R. ventrimaculata* (320–380 ms; Brown et al. 2011). Furthermore, it differs by its higher dominant frequency (4,996–6,288 Hz) from the calls of *R. benedicta* (3,190–4,240 Hz; Brown et al. 2008), *R. fantastica* (2,950–3,790 Hz; Brown et al. 2011), *R. reticulata* (4,140–4,480 Hz; Brown et al. 2011), *R. summersi* (2760–3220 Hz; Brown et al. 2008), *R. uakarii* (3,790–4,130 Hz; Brown et al. 2006, Brown et al. 2011), and *R. ventrimaculata* (4190–4400 Hz; Brown et al. 2011); by its lower number of notes (21–45) from the calls of *R. reticulata* (48–94; Brown et al. 2011) and *R. ventrimaculata* (58–63; Brown et al. 2011); by greater number of notes from the calls of *R. fantastica* (10–13; Brown et al. 2011), *R. summersi* (14–16; Brown et al. 2008), *R. uakarii* (14–16; Brown et al. 2006, Brown et al. 2011), and *R. vanzolinii* (16–17; Brown et al. 2011); by its smaller note rate (28–36 notes/s) from the calls of *R. amazonica* (85–138 notes/s; Brown et al. 2011), *R. defleri* (94–104 notes/s; Twomey and Brown 2009), *R. fantastica* (41–57 notes/s; Brown et al. 2011), *R. reticulata* (270–382 notes/s; Brown et al. 2011), *R. summersi* (39–40 notes/s; Brown et al. 2008), *R. uakarii* (50–58 notes/s; Brown et al. 2006; Brown et al. 2011), *R. variabilis* (106–297 notes/s; Brown et al. 2011), and *R. ventrimaculata* (166–181 notes/s; Brown et al. 2011).

The advertisement call of *R. aquamarina* sp. nov. is highly similar to the calls of all other species of the *R. vanzolinii* group, which have long-lasting trills, but it can still be distinguished from the call of *R. vanzolinii*, which has slightly lower note rate of 26–28 notes/s (Brown et al. 2011). On the other hand, based on the literature, the call of *R. aquamarina* sp. nov. is indistinguishable from the calls of *R. flavovittata*, *R. imitator*, *R. sirensis*, and *R. yavaricola* (Pérez-Peña et al. 2010; Brown et al. 2011). There is no available information about minimum and maximum frequencies, note duration and inter-notes interval in these species. In addition, the calls of *R. toraro* and *R. cyanovittata* remain completely unknown.

Tadpole morphology. There is little information available about the tadpoles of the *Ranitomeya* species, but we did find information for ten species (*R. amazonica*, *R. benedicta*, *R. defleri*, *R. flavovittata*, *R. imitator*, *R. reticulata*, *R. toraro*, *R. uakarii*, *R. vanzolinii* and *R. variabilis*). The tadpoles of *R. aquamarina* sp. nov. differ from the tadpoles of all these species by absence of emarginate marginal papillae.

Because there is great variation between the initial (25–27), intermediate (28–32), and final (37–40) stages, we compared them using the ratios between measurements (the characteristics of compared species are given in parentheses). The labial tooth row formula in *R. aquamarina* sp. nov. is 2(2)/3(1) in all stages and differs from the formula of *R. toraro* 2(2)/2(1) (Brown et al. 2011). The ratios (in percentages) tail length/total length are in *R. aquamarina* sp. nov. (63 to 64% in all stages) greater than in *R. amazonica* (45% st. 29, Brown et al. 2011), *R. flavovittata* (57% st. 26; Brown et al. 2011), *R. imitator* (62% st. 26; Brown et al. 2011), *R. reticulata* (41% st. 30; Brown et al. 2011), *R. uakarii* (62%, st. 29; Brown et al. 2011) and *R. variabilis* (37% st. 28; Brown et al. 2011), and smaller than in *R. toraro* (64.2% st. 25; Brown et al. 2011), *R. vanzolinii* (67.9% st. 38; Brown et al. 2011) and *R. yavaricola* (64.4% st. 25; Pérez-Peña et al. 2010). The ratios oral disc width/body width are in *R. aquamarina* sp. nov. (42% at stage 26, 36% at stage 29, and 35% at stage 39) greater than in *R. amazonica* (29% st. 26, 22% st. 29, 33% st. 38; Brown et al. 2011, Klein et al. 2020), *R. flavovittata* (28% st. 26; Brown et al.

2011), *R. imitator* (38% st. 26; Brown et al. 2011), *R. toraro* (36% st. 25; Brown et al. 2011), *R. reticulata* (14% st. 30; Brown et al. 2011), *R. uakarii* (35%, st. 29; Brown et al. 2011), and smaller than in *R. vanzolinii* (38.9% st. 38; Brown et al. 2011).

The ratios tail muscle width/tail muscle height are in *R. aquamarina* sp. nov. (91% at stage 26 and 115% at stage 29) greater than in *R. flavovittata* (63% st. 26; Brown et al. 2011), *R. imitator* (52% st. 26; Brown et al. 2011), *R. amazonica* (76% st. 29; Brown et al. 2011), *R. reticulata* (92% st. 30; Brown et al. 2011), *R. uakari* (88%, st. 29; Brown et al. 2011), and *R. variabilis* (72% st. 30; Brown et al. 2011), and smaller than in *R. toraro* (100% st. 25; Brown et al. 2011).

Posterior tooth row formula of *R. aquamarina* sp. nov. (P-1 > P-2 > P-3 in all stages) differs from the formulas of all other described tadpoles: *R. amazonica* (P-1 = P-2 > P-3, P-3 = 80% of P-1; Brown et al. 2011), *R. benedicta* (P-1 = P-2 = P-3; Klein et al. 2020), *R. flavovittata* (P-1 = P-2 > P-3, P-3 = 80% of P-1; Brown et al. 2011), *R. imitator* (P-1 = P-2 > P-3, P-3 = 55% of P-1; Brown et al. 2011; Klein et al. 2020), *R. reticulata* (P-1 = P-2 > P-3, P-3 = 80% of P-1; Brown et al. 2011; Klein et al. 2020), *R. toraro* (P-1 > P-2; Brown et al. 2011), *R. uakarii* (P-1 = P-2 > P-3, P-3 = 75% of P-1 and P-2; Brown et al. 2011), *R. vanzolinii* (P-1 < P-2 = P-3, P-1 = 44.6% of P-2; Brown et al. 2011), *R. variabilis* (P-1 = P-2 > P-3, P-3 = 75% of P-1; Brown et al. 2011) and *R. yavaricola* (P-1 = P-2 > P-3; Pérez-Peña et al. 2010).

In life, tadpoles of *R. aquamarina* sp. nov. have a translucent brownish head in all stages, which differs from all the other tadpoles described: *R. amazonica* (head and body black to gray; Brown et al. 2011, Klein et al. 2020), *R. benedicta* (head and body dark gray, with a reddish area anterior and posterior to the eye; Klein et al. 2020), *R. imitator* (head beige strongly dotted with yellowish green spots; Klein et al. 2020), *R. reticulata* (head and body gray; Brown et al. 2011), and *R. toraro* (head and body gray; Brown et al. 2011), *R. uakari* (head gray; Brown et al. 2011), *R. vanzolinii* (head and body dark gray to black; Klein et al. 2020), *R. variabilis* (head and body gray; Brown et al. 2011) and *R. yavaricola* (light grey; Pérez-Peña et al. 2010). When preserved, the tadpoles of *R. aquamarina* sp. nov. are cream with brown reticules on the lateral, dorsal, anterior half belly, spiracles, tail muscle and fins and differ from *R. amazonica* (dorsum dark gray and hindlimbs bluish gray, spotted with dark dots; Klein et al. 2020), *R. benedicta* (dorsum and hindlimbs dark gray; Klein et al. 2020), *R. imitator* (beige, densely spotted with gray dots; Klein et al. 2020) and *R. vanzolinii* (dorsum of body grayish brown, tail musculature light yellowish brown and fins translucent; Brown et al. 2011).

Holotype description. Adult male (INPA-H 47568, field number APL 24805, Figs 2–4). SVL 17.1 mm; head width slightly smaller than body width; head width larger than head length; head width 30% of SVL (Fig. 2A, B). Snout rounded in dorsal view and rounded to protruding in lateral view (Fig. 2C). Nostril directed frontolaterally at the angle of the snout, 1.0 mm from the tip of the snout; internarial distance 2.0 mm, 35.6% of head width. *Canthus rostralis* rounded, loreal region flat. Eye-nostril distance 1.5 mm, 74.0% of horizontal eye diameter. Tympanic annulus and tympanic membrane present. Tympanum slightly ovoid, posterodorsal margin hidden by depressor muscle, tympanum 44.4% of eye diameter. Tongue ovoid, attached anteriorly, longer than wide, median lingual process absent. Dentigerous processes of vomers absent. Choanae ovoid and small (0.4 mm), located marginally in the maxilla, not visible in ventral view. Paired vocal slits present, located near jaw articulation.

Forelimbs slender, hands relatively large, 25.9% of SVL. Finger I shorter (66.9%) than Finger II; Finger III > IV > II > I. Discs on fingers III and IV considerably expanded and truncate, disc of Finger II moderately expanded and elliptical, disc of Finger I rounded. Ulnar tubercles absent. Hands lacking lateral fringes and webbing. Palmar tubercle rounded, unpigmented, ~ 4× larger than the subarticulars. Thenar tubercle elliptical, small. Large unpigmented, rounded, proximal subarticular tubercles present on base of each finger. Rounded distal subarticular tubercle visible only on Finger III (Fig. 2D).

Length of legs moderate, femur slightly smaller than tibia, with 93.7% of the tibia length; knee-knee distance 80% of SVL. Relative lengths of appressed toes IV > III > V > II > I. First toe short, Toe I disc not expanded and rounded, Toe II with slightly expanded and rounded disc, toes III–V with moderately expanded discs, III and IV elliptical, and V truncated. Tarsal tubercle absent; feet lacking webbing; lateral fringes poorly developed. Outer metatarsal tubercle ovoid, unpigmented, poorly visible. Inner metatarsal tubercle elliptical, unpigmented. Proximal subarticular tubercles present at base of each toe, large and elliptical on toes I and II, small and rounded on toes III–V, all unpigmented. Distal subarticular tubercles large on toes III and V, and poorly distinguished on Toe IV. Two medial subarticular tubercles diffused on Toe IV (Fig. 2E). Holotype measurements summarized in Table 2.

Skin texture nearly smooth to shagreen on head, becoming weakly granular on the dorsum and limbs. Ventral surface of limbs smooth to shagreen. Gular region and venter shagreen. Arms smooth to shagreen.

In life, dorsal surface jet black (color 300 by Köhler 2012) with three parallel metallic pale yellowish green stripes (color 100 by Köhler 2012) (Figs 3B, 4A), middorsal stripe extends from between the eyes to slightly before the vent. Dorsolateral stripes extend from the snout, where they merge, to the groin. Slightly before the groin, the dorsolateral stripes become metallic light sulfur yellow (color 93 by Köhler 2012), and merge with a medium sulfur yellow (color 94 by Köhler 2012) spot on the dorsal surface of the thigh. Ventrolateral stripes metallic light yellowish green (color 100 by Köhler 2012), extending through the loreal region, without touching the upper labium, to the thighs and integrating into the ventral reticulate pattern; its color leaks slightly on the arms, becoming medium sulfur yellow (color 94 by Köhler 2012) and integrating into the arms reticulate pattern. On the side of the head, the stripe does not reach the nostril, eye, and tympanum. Venter jet black (color 300 by Köhler 2012) with metallic olive-yellow (color 117 by Köhler 2012) to metallic light yellowish green (color 100 by Köhler 2012) reticulations on belly. Gular region fully metallic light yellowish green (color 100 by Köhler 2012; Fig. 3B). Both forelimbs and hindlimbs medium metallic chrome orange (color 75 by Köhler 2012) with dark carmine spots (color 61 by Köhler 2012) in the ventral surface of the thighs proximal to the body. Iris jet black (color 300 by Köhler 2012).

After four months in alcohol, general color pattern remained, but colors faded (Fig. 2A, B). Stripes and limb reticulations become pale cyan (color 157 by Köhler) and ventral surfaces cyan-white (color 156 by Köhler). Forelimb and hindlimb spots become raw umber (color 280 by Köhler 2012).

Variation. SVL ranges from 15.4 to 17.7 mm in males ($n = 7$) and from 17.3 to 18.5 mm in females ($n = 5$) (Table 2). The dorsal stripe pattern is very consistent among individuals (Figs 3, 4). The middorsal stripe is complete and ex-

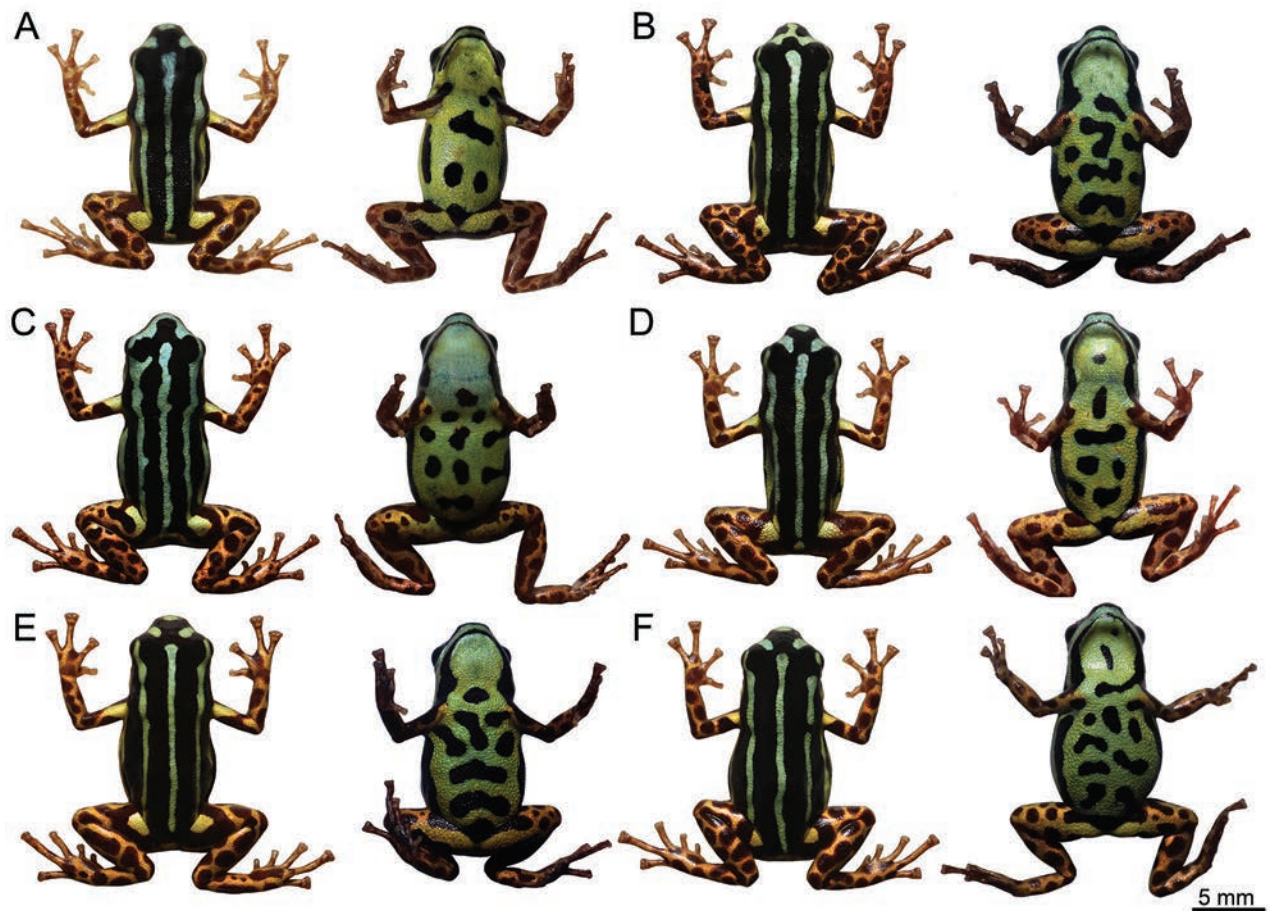


Figure 3. Dorsal and ventral pattern variation of *Ranitomeya aquamarina* sp. nov. in life. Males: **A** INPA-H 47566 **B** INPA-H 47568 [Holotype] **C** MPEG 45223 **D** INPA-H 47570; and Females: **E** INPA-H 47569 **F** MPEG 45222. Photographs ATM.

tends from between the eyes to slightly before the vent, except for one individual, where the stripe interrupted in the scapular region. Dorso-lateral stripes are complete and extend from eyes to the groin (Fig. 4), except for two individuals, where the stripes are interrupted in the arm region (unilaterally or bilaterally).

The head stripes have five patterns in the type series (Fig. 5). The basis is formed by three dots: one on the tip of the snout and another on the underside of each eye. These dots can be connected with the dorsal stripes. Three of the five patterns found do not have the dots connected with the middorsal stripe (Fig. 5A–C), while the other two do (Fig. 5D, E). The most common pattern presents the three unconnected dots ($n = 53.8\%$; Fig. 5A), followed by the pattern of three dots connected with dorsolateral stripes forming a W-shape (Fig. 5B) and three dots connected in the margin of the snout with one of the lateral dots connected with the mid-dorsal stripe (Fig. 5D) ($n = 15.4\%$ each). The less frequent patterns are formed by three dots connected at the margin of the snout (Fig. 5C) or connected with the mid-dorsal stripe forming an O-shape (Fig. 5E) ($n = 7.7\%$ each).

The coloration of the stripes varies from metallic light yellowish green (color 100 by Köhler 2012) to metallic pale turquoise green (color 146 by Köhler 2012; Fig. 3). All individuals show a medium sulfur yellow (color 94 by Köhler 2012) spot in the dorsal surface of the thigh, well-defined in most of them ($n = 84.6\%$; Fig. 3). Limb coloration is very constant, but the spots can vary in their size and quantity, going from denser, small, rounded spots to less dense large merging spots.

Table 2. Morphometric measurements (mm) of adult type specimens of *Ranitomeya aquamarina* sp. nov. Values express mean \pm standard deviation, and range.

Morphometric measurements	Holotype	Males (n = 7)	Females (n = 5)
SVL – Snout to vent length	17.1	16.9 \pm 0.73 (15.4–17.7)	17.9 \pm 0.45 (17.3–18.5)
HL – Head length	5.1	5.1 \pm 0.18 (4.8–5.4)	5.2 \pm 0.05 (5.1–5.2)
HW – Head width	5.7	5.6 \pm 0.34 (4.9–5.9)	5.8 \pm 0.08 (5.7–5.9)
IOD – Interorbital distance	2.3	2.4 \pm 0.10 (2.2–2.5)	2.3 \pm 0.13 (2.2–2.5)
UEW – Upper eyelid width	1.4	1.4 \pm 0.12 (1.2–1.6)	1.6 \pm 0.08 (1.5–1.7)
MTD – Mouth-tympanum distance	0.8	0.7 \pm 0.07 (0.5–0.7)	0.8 \pm 0.08 (0.7–0.9)
TD – Tympanum diameter	0.9	0.9 \pm 0.06 (0.8–1.0)	1.0 \pm 0.09 (0.9–1.1)
DET – Distance from eye to tympanum	0.6	0.6 \pm 0.04 (0.6–0.7)	0.7 \pm 0.05 (0.6–0.7)
ED – Eye diameter	1.0	2.0 \pm 0.11 (1.8–2.2)	2.1 \pm 0.09 (2.0–2.2)
SL – Snout length	2.0	1.9 \pm 0.10 (1.7–2.0)	2.1 \pm 0.11 (1.7–2.2)
END – Eye-nostril distance	1.5	1.4 \pm 0.07 (1.3–1.6)	1.5 \pm 0.07 (1.4–1.6)
BW – Body width	5.8	5.6 \pm 0.28 (5.1–5.9)	6.6 \pm 0.36 (6.2–7.1)
TSCN – Snout-nostril distance	1.0	0.9 \pm 0.07 (0.8–1.0)	1.1 \pm 0.02 (1.1–1.1)
IND – Internarial distance	2.0	1.9 \pm 0.17 (1.6–2.1)	2.2 \pm 0.09 (2.1–2.3)
KK – Knee-knee distance	13.7	13.8 \pm 0.46 (12.9–14.3)	14.7 \pm 0.33 (14.2–15.0)
FL – Femur length	6.6	6.9 \pm 0.21 (6.6–7.2)	7.2 \pm 0.14 (7.0–7.4)
TL – Tibia length	7.0	6.9 \pm 0.37 (6.3–7.3)	7.5 \pm 0.18 (7.2–7.6)
TaL – Tarsus length	3.7	4.0 \pm 0.32 (3.6–4.4)	4.4 \pm 0.16 (4.1–4.6)
FoL – Foot length	7.1	6.7 \pm 0.37 (6.0–7.1)	6.8 \pm 0.38 (6.3–7.2)
LT1 – Toe I length	1.9	1.7 \pm 0.17 (1.5–2.0)	1.9 \pm 0.12 (1.7–2.0)
LT2 – Toe II length	3.0	3.0 \pm 0.16 (2.8–3.3)	3.1 \pm 0.21 (2.9–3.5)
LT3 – Toe III length	4.8	4.9 \pm 0.30 (4.4–5.3)	5.1 \pm 0.29 (4.6–5.3)
LT4 – Toe IV length	7.1	6.7 \pm 0.37 (6.0–7.1)	6.8 \pm 0.38 (6.3–7.2)
LT5 – Toe V length	4.8	4.4 \pm 0.44 (3.9–4.9)	4.8 \pm 0.25 (4.4–5.1)
W1TD – Width of disc on Toe I	0.3	0.4 \pm 0.04 (0.3–0.4)	0.4 \pm 0.06 (0.3–0.5)
W1T – Width of Toe I just below disc	0.3	0.3 \pm 0.04 (0.3–0.4)	0.4 \pm 0.04 (0.3–0.4)
W2TD – Width of disc on Toe II	0.6	0.5 \pm 0.06 (0.4–0.6)	0.6 \pm 0.04 (0.5–0.6)
W2T – Width of Toe II just below disc	0.4	0.4 \pm 0.04 (0.4–0.5)	0.5 \pm 0.02 (0.4–0.5)
W3TD – Width of disc on Toe III	0.7	0.7 \pm 0.08 (0.5–0.8)	0.7 \pm 0.09 (0.6–0.8)
W3T – Width of Toe III just below disc	0.5	0.5 \pm 0.05 (0.5–0.6)	0.6 \pm 0.06 (0.5–0.6)
W4TD – Width of disc on Toe IV	0.8	0.8 \pm 0.09 (0.7–0.9)	0.9 \pm 0.11 (0.7–1.0)
W4T – Width of Toe IV just below disc	0.6	0.7 \pm 0.08 (0.5–0.7)	0.7 \pm 0.08 (0.6–0.8)
W5TD – Width of disc on Toe V	0.7	0.8 \pm 0.08 (0.6–0.8)	0.8 \pm 0.11 (0.7–1.0)
W5T – Width of Toe V just below disc	0.6	0.7 \pm 0.07 (0.5–0.7)	0.7 \pm 0.08 (0.6–0.8)
AL – Arm length	4.5	4.8 \pm 0.23 (4.4–5.0)	5.1 \pm 0.19 (4.8–5.3)
FAL – Forearm length	4.1	4.1 \pm 0.12 (3.9–4.3)	4.2 \pm 0.10 (4.1–4.4)
HaL – Hand length	4.4	4.5 \pm 0.27 (4.0–4.7)	4.6 \pm 0.16 (4.5–4.8)
L1F – Finger I length	2.1	1.9 \pm 0.08 (1.8–2.1)	2.1 \pm 0.07 (2.0–2.2)
L2F – Finger II length	3.1	3.2 \pm 0.21 (2.8–3.5)	3.3 \pm 0.19 (3.1–3.5)
L3F – Finger III length	4.4	4.5 \pm 0.27 (4.0–4.7)	4.6 \pm 0.16 (4.5–4.8)
L4F – Finger IV length	3.5	3.5 \pm 0.26 (3.0–3.8)	3.7 \pm 0.13 (3.5–3.8)
W1FD – Width of disc on Finger I	0.4	0.4 \pm 0.07 (0.4–0.6)	0.4 \pm 0.03 (0.4–0.5)
W1F – Width of Finger I just below disc	0.4	0.4 \pm 0.06 (0.3–0.5)	0.4 \pm 0.04 (0.3–0.4)
W2FD – Width of disc on Finger II	0.7	0.7 \pm 0.08 (0.6–0.8)	0.8 \pm 0.14 (0.7–1.0)
W2F – Width of Finger II just below disc	0.6	0.5 \pm 0.08 (0.4–0.7)	0.6 \pm 0.06 (0.5–0.7)
W3FD – Width of disc on Finger III	1.1	0.9 \pm 0.09 (0.8–1.1)	0.9 \pm 0.10 (0.8–1.0)
W3F – Width of Finger III just below disc	0.7	0.7 \pm 0.08 (0.6–0.8)	0.7 \pm 0.09 (0.6–0.8)
W4FD – Width of disc on Finger IV	0.9	0.9 \pm 0.07 (0.8–0.9)	0.9 \pm 0.09 (0.7–1.0)
W4F – Width of Finger IV just below disc	0.7	0.7 \pm 0.06 (0.6–0.7)	0.7 \pm 0.04 (0.6–0.7)

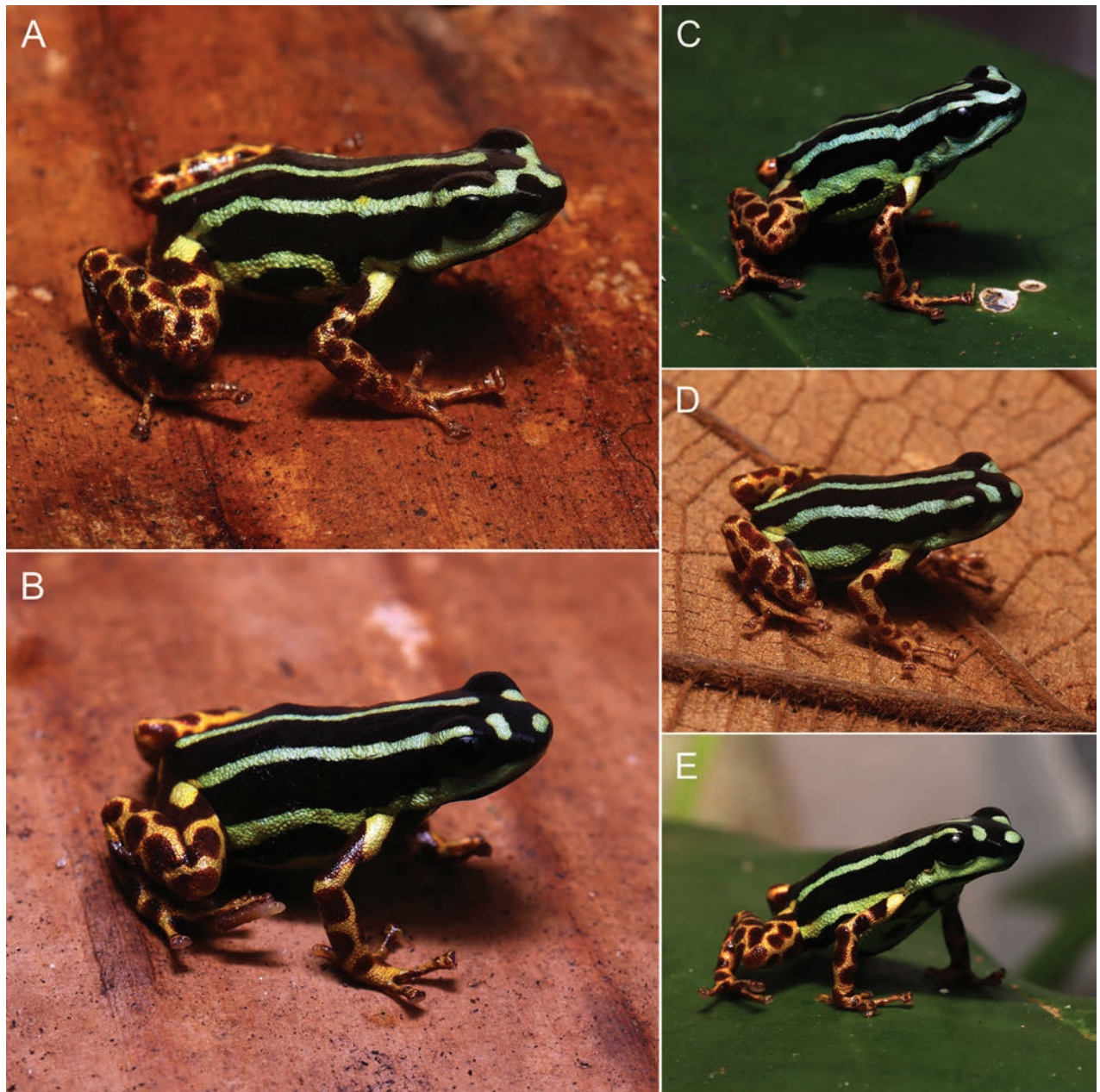


Figure 4. Adult individuals of *Ranitomeya aquamarina* sp. nov. in natural posture **A** holotype, male INPA-H 47568 **B** paratype, female INPA-H 47569 **C** paratype, male MPEG 45223 **D** paratype, male INPA-H 47570 **E** Paratype, female MPEG 45222. Photographs ATM.

Advertisement call. The advertisement call of *Ranitomeya aquamarina* sp. nov. ($n = 7$ males) consist of a long-lasting trill of 21–45 notes ($n = 44$ calls)—most commonly of 32–38 notes ($n = 24$ calls)—a call duration of 984 ± 197 ms (647–1,424 ms)—and silence between calls of 5.8–115.3 s (most commonly between 7 and 18 s) ($n = 24$ silence between calls). Notes are distinct, separated by silence intervals, with note duration of 11.7 ± 0.14 ms (9.6–14.8 ms), a silence between notes of 19.4 ± 0.2 ms (15.6–22.7 ms), and a note rate of 32.8 ± 2.2 s (28–36). Calls are emitted with a minimum frequency (LF) of $5,139 \pm 283$ Hz (4,699–5,860 Hz), a maximum frequency (HF) of $6,054 \pm 255$ Hz (5,545–6,600 Hz) and a dominant frequency (DF) of $5,633 \pm 289$ Hz (4,996–6,288 Hz) (Fig. 6).

Table 3. Acoustic variables of the advertisement call of 44 analyzed calls of seven males of *Ranitomeya aquamarina* sp. nov. Abbreviation: SD – standard deviation.

Variables	Mean	SD	Minimum	Maximum
CD – Call duration (ms)	984	197	647	1,424
SBC – Silence between calls (s)	19.3	20.6	5.8	115.3
NN – Number of notes per call	32.4	6.7	21	45
ND – Note duration (ms)	11.8	0.13	9.6	14.8
SBN – Silence between notes (ms)	19.4	0.19	15.6	22.7
NR – Note rate (notes per second)	32.4	2.4	28	36
LF – Minimum frequency (Hz)	5,132	272	4,699	5,860
HF – Maximum frequency (Hz)	6,059	244	5,545	6,600
DF – Dominant frequency (Hz)	5,640	277	4,996	6,288

Table 4. Morphometric measurements (mm) of three tadpoles of *Ranitomeya aquamarina* sp. nov. from Eirunepé municipality, Amazonas state, Brazil.

Measurements	Tadpole stages		
	26	29	39
TL – Total length	13.7	19.9	25.0
BL – Body length	5.1	7.3	9.1
TAL – Tail length	8.6	12.7	16.0
BH – Body height	2.4	4.0	4.5
BW – Body width	3.3	5.0	6.0
BHN – Body height at the nostril	1.3	1.7	2.0
BHE – Body height at the eyes	1.8	2.6	3.4
BWN – Body width at the nostril	2.2	2.6	3.0
BWE – Body width at the eyes	3.0	4.1	4.6
TMW – Tail muscle width at base	1.1	1.9	2.1
MTH – Maximum tail height	2.3	3.6	4.5
DF – Dorsal fin height	0.6	0.9	1.3
VF – Ventral fin height	0.6	0.9	1.2
TMH – Tail muscle height	1.2	1.6	2.3
IOD – Interorbital distance	1.3	1.6	2.8
IND – Internarial distance	0.8	1.2	1.5
RED – Rostro-eye distance	1.9	2.2	2.5
RND – Rostro-nostril distance	0.9	1.0	1.0
RSD – Rostro-spiracle distance	3.5	4.4	5.7
ED – Eye diameter	0.4	0.7	0.9
END – Eye-nostril distance	0.7	0.8	0.9
SL – Spiracle length	0.5	0.7	0.9
SW – Spiracle width	0.3	0.6	0.6
SH – Spiracle height	0.7	0.7	0.9
VL – Vent tube length	0.5	1.1	-
ODW – Oral disc width	1.4	1.8	2.1
AL – Anterior (upper) labium	0.1	0.3	0.3
PL – Posterior (lower) labium	0.1	0.2	0.3
A-1 – First anterior tooth row	1.1	1.3	1.4
A-2 – Second anterior tooth row	1.2	1.4	1.5
A-2 GAP – Medial gap in second anterior tooth row	0.5	0.5	0.6
P-1 – First posterior tooth row	0.9	1.2	1.4
P-2 – Second posterior tooth row	0.9	1.1	1.2
P-3 – Third posterior tooth row	0.8	1.0	1.1
P-1 GAP – Medial gap in the first posterior tooth row	0.1	0.3	0.1
LP – Lateral process of upper jaw sheath	0.1	0.1	0.1
LJ – Lower jaw sheath	0.5	0.8	0.8
UJ – Upper jaw sheath	0.7	0.9	0.9

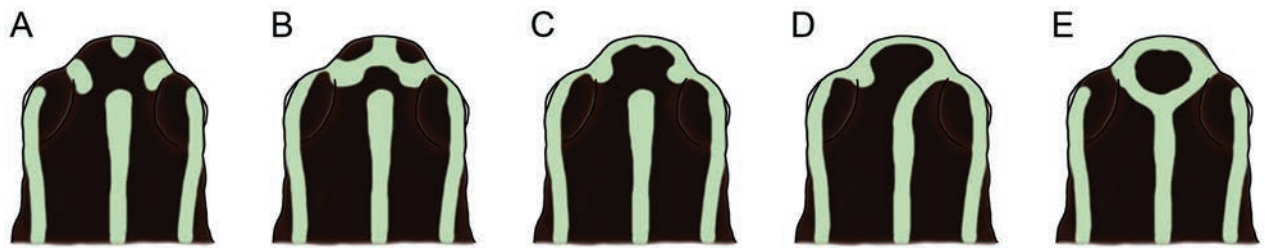


Figure 5. Schematic illustration of the head patterns in adult individuals of *Ranitomeya aquamarina* sp. nov.

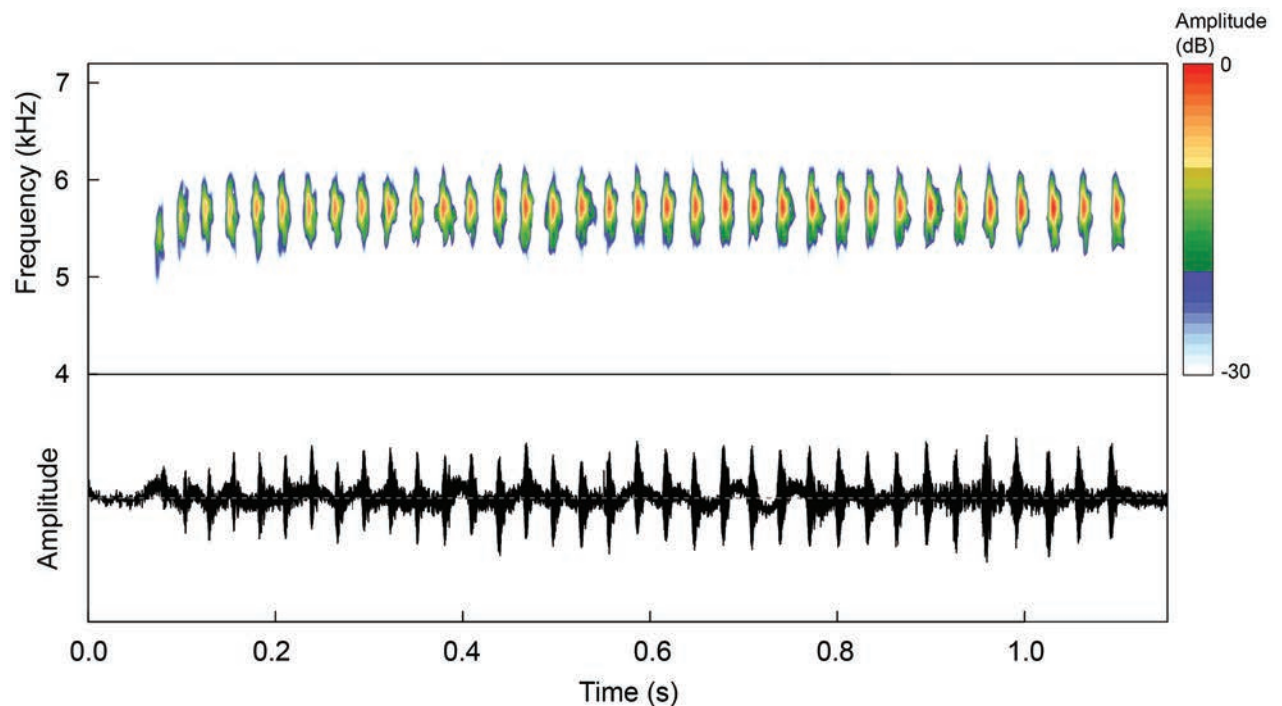


Figure 6. Advertisement call of the holotype (INPA-H 47568, FNJV 124337) of *Ranitomeya aquamarina* sp. nov. recorded at the Comunidade Santo Antônio, municipality of Eurinepé, Amazonas state, Brazil. Air temperature 25.2 °C.

However, the first note is emitted at approximately 300 Hz – a lower frequency compared to the subsequent notes (LF of $4,921 \pm 187$ Hz, HF of $5,683 \pm 211$ Hz and a DF of $5,340 \pm 202$ Hz). Temporal and spectral traits, summarized according to individual call arrangement, are presented in Table 3.

Tadpole morphology. Tadpole description is based on three specimens (vouchers INPA-H 47567) at Gosner (1960) stages 26, 29, and 39 (for measurements see Table 4). Since few tadpoles of *Ranitomeya* were described and each at a different stage, it is important to present the measurements for the three stages that were found (see Table 4).

Body shape in stage 26 ovoid in dorsal and lateral view (Fig. 7A). In stages 29 and 39, depressed, broadly rounded to truncate each end of body (Fig. 7B). Body length corresponds to 36.9%, 36.4%, and 36.3% of the total length, respectively. Tail length 63%, 64%, and 63% of the total length, respectively. Snout rounded in dorsal and lateral view in all stages (Fig. 7). Eyes positioned dorsally, directed dorsolaterally (Fig. 7), eye diameters stage 26 = 0.44 mm, stage 29 = 0.65 mm, and stage 39 = 0.88 mm (Table 4) correspond to 8.7%, 9.0%, and 9.6% of body length, respectively. Nostrils small and elliptical, with slightly elevated marginal

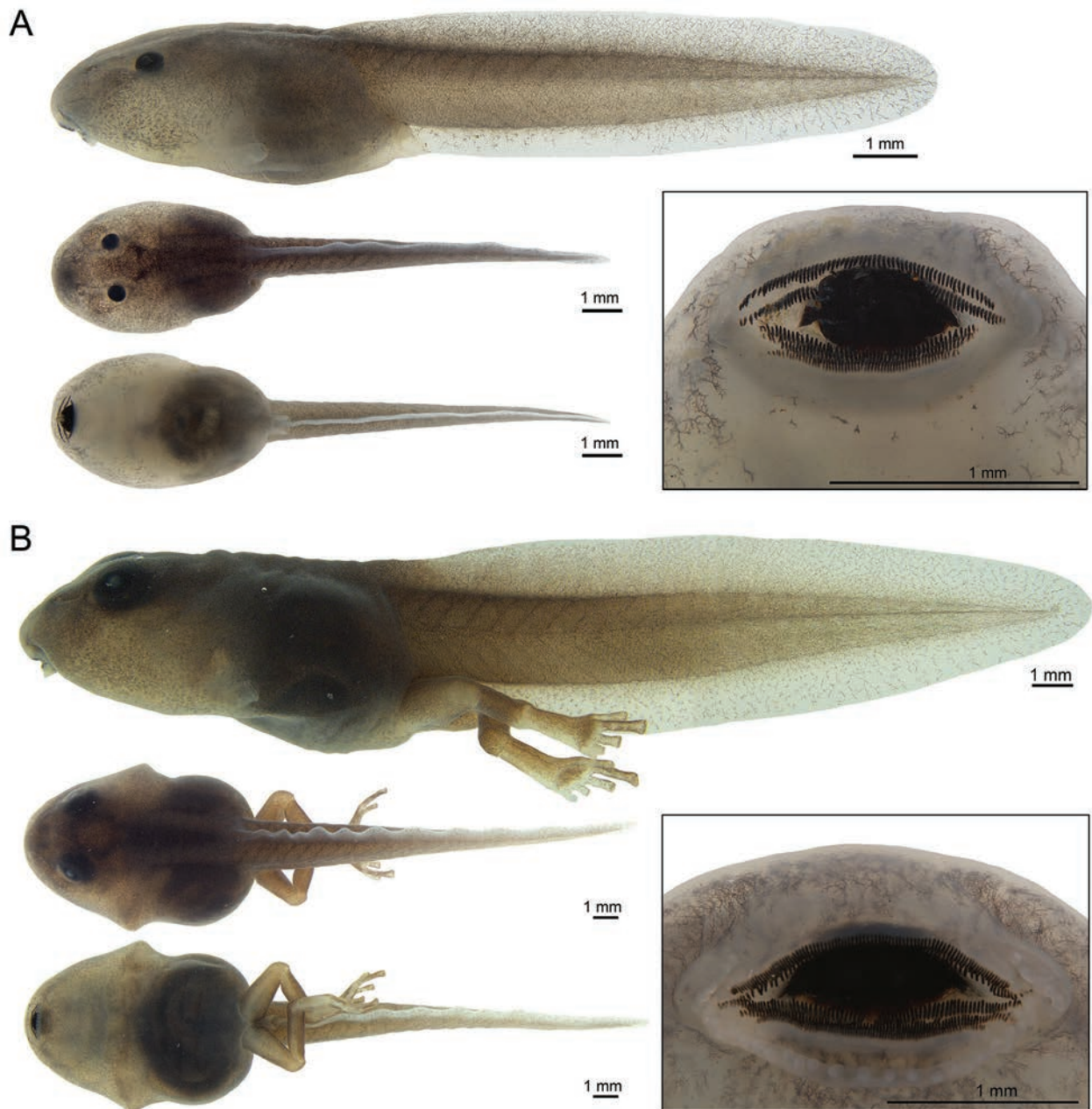


Figure 7. Preserved tadpoles of *Ranitomeya aquamarina* sp. nov. (INPA-H 47567). Lateral, dorsal and ventral views of the body, and ventral view of the oral disc, respectively. **A** Gosner stage 26 **B** gosner stage 39. Photographs ATM.

rim, located dorsally in the middle between the tip of snout and eyes, in all stages, directed antero-laterally, spiracle sinistral, opening dorsoposteriorly, located well below at the middle line of the body axis, length 10.2%, 9.1% and 8.9% of body length, respectively. In all stages, the spiracle is visible dorsally, ventrally, and laterally (Fig. 7). Digestive tract dark, folded, occupies half of the belly, without visible organs. Dextral vent tube measures 0.5 mm at stage 26, 1.1 mm at stage 29, and partially absorbed at stage 39. Caudal musculature robust, tapering gradually, width at body-tail junction of 1.1 mm at stage 26, 1.9 mm at stage 29 and 2.1 mm at stage 39), tail muscle height of 1.2 mm, 1.6 mm, and 2.3 mm, respectively, not reaching the tail tip. Dorsal fin slightly higher than ventral fin, 54.7% to 57.4% of the height of the tail muscles, originating at posterior end of the body. Ventral fin 24.3% to 26.4% of tail width (Table 4). Tail tip ovoid.



Figure 8. Tadpoles of *Ranitomeya aquamarina* sp. nov. in life. **A** Dorso-lateral view at Gosner stages 26, 29 and 39 respectively **B** ventral view at Gosner stage 29. Photographs APL.

Oral apparatus located antero-ventrally, not emarginated laterally. Transverse width of oral disc 42% of body width at stage 26, 36% at stage 29, and 35% at stage 39, respectively. Lower and lateral labium free from body wall. Anterior labium with groups of five or six short elliptical papillae, distributed in a single row on each side of the lateral margins and split by a medial gap. Posterior labium with a single row of marginal short elliptical papillae in all stages. Jaw sheaths oval, upper jaw sheath slightly wider than lower jaw sheath, edges of both jaw sheaths serrated along their entire length. Labial tooth row formula 2(2)/3(1) in all stages; tooth row A-1 complete; tooth row A-2 interrupted medially, consisting of two pieces of tooth of the same length, the medial gap broadly larger than tooth lines. Posterior tooth rows P-1 slightly longer than P-2, and P-2 longer than P-3 in all stages. P-1 with medial gap, 0.1 mm, 0.3 mm, and 0.1 mm, respectively (in each stage).

After four months preserved in 10% formalin, the tadpoles have a cream background color with brown reticulations on lateral, dorsal, anterior half of the belly, spiracles, tail muscle, and fins. Ventral fin less reticulated than dorsal fin (Fig. 7). The posterior half of the digestive tract is dark brown, iris black (Fig. 7).

In life, translucent head, eyes black, anterior portion of body gray in the middle and translucent on sides, posterior body portion gray. Tail musculature uniform gray, dorsal and ventral fins transparent. Abdomen mostly transparent, digestive tract gray, heart visible (Fig. 8).

Etymology. The specific epithet '*aquamarina*' is a Latin adjective that means "pale blue-green", referring to the coloration of the dorso-lateral stripes of the new species. Another aspect that led us to use this epithet was the metallic blue and greenish tones of the stripes, which resemble seawater. Additionally, aquamarine is a gemstone, which philosophically conveys the value of this discovery.

Distribution, habitat, natural history, and conservation. *Ranitomeya aquamarina* sp. nov. is only known from its type locality, in preserved forests on the Eiru River, a tributary of the Juruá River, near the Comunidade de Santo Antônio, municipality of Eirunepé, state of Amazonas, Brazil (Fig. 9). We sampled four RAPELD modules in the region, and the new species has only been recorded at one site. We did not find the new species living in sympatry with any other species of the genus. However, other Dendrobatoidea occur at the site: *Allobates femoralis*, *Allobates* sp. undescribed (A.P. Lima, unpublished data), *Ameerega hahneli* and *A. trivittata*.

Ranitomeya aquamarina sp. nov. is diurnal, showing greater activity in the early morning and late afternoon. On rainy days, activity lasts throughout the day. Most individuals were observed in clusters of '*banananeira brava*' (*Phenakospermum guyannense*, Strelitziaceae; Fig. 10A), but the species was

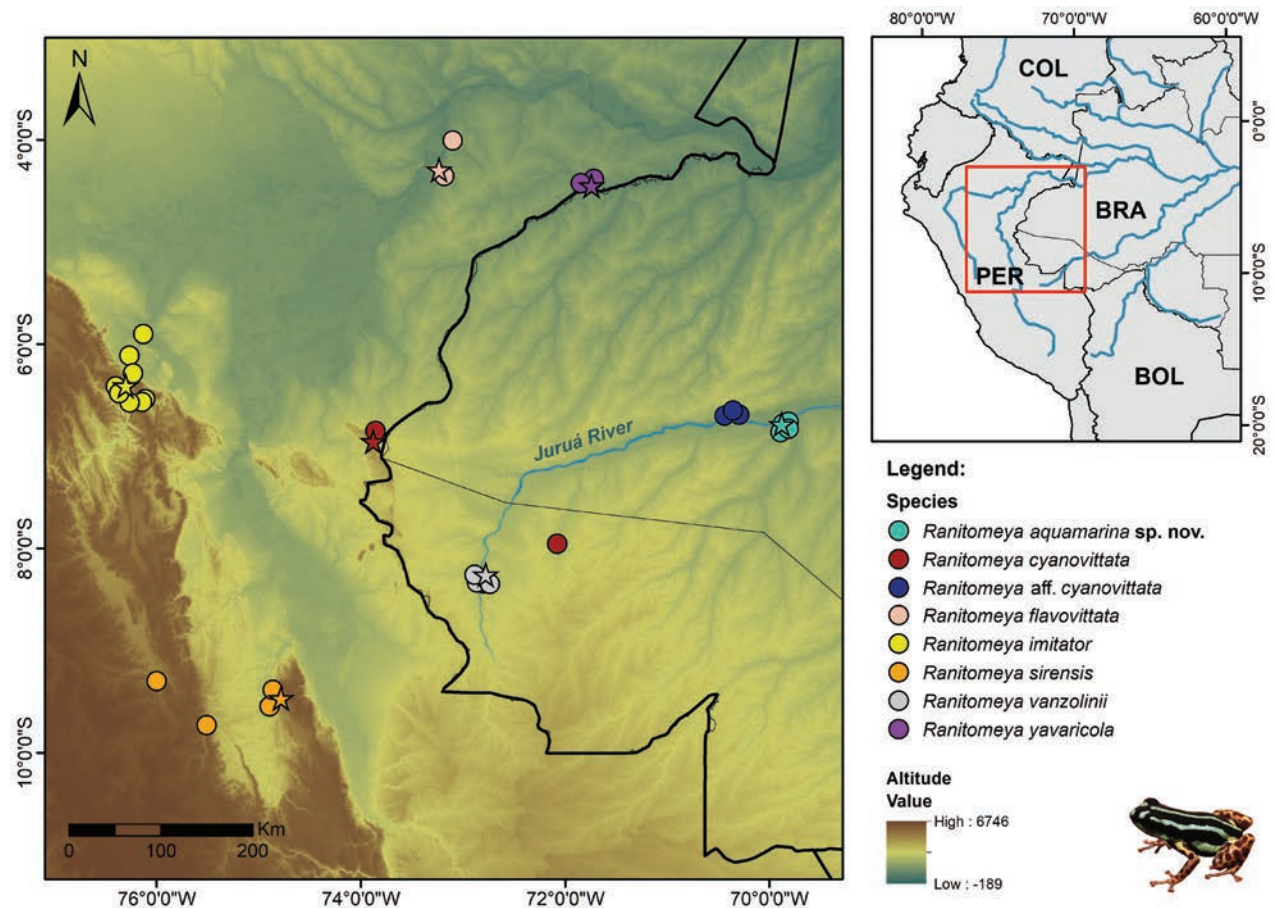


Figure 9. Geographic distribution of the *Ranitomeya aquamarina* sp. nov. and species of the *R. vanzolinii* clade. Stars indicate type localities of each species. Abbreviations: BRA – Brazil; PER – Peru; COL – Colombia; BOL – Bolivia.

also found in a phytotelma in the forest understory, ~ 3 m above the ground (Fig. 10B). Individuals climb vertically through vegetation (Fig. 10C) and are very agile.

Eggs are deposited in water accumulated in cavities in the vegetation. We found eggs (Fig. 10D) and tadpoles in the '*bananeira brava*' axils and in small holes in trees (Fig. 10B). The eggs are small and brown, wrapped in a thick transparent gelatinous layer. Furthermore, we found tadpoles at different stages of development and metamorphosing in the same area, which suggests that reproduction is prolonged, probably occurring during the entire rain season. Juveniles ($n = 5$; not collected) and adults ($n = 8$) were seen foraging among the dry leaves of the same plants. In juveniles, dorsolateral stripes are uniformly yellow and are not fully formed (Fig. 10E).

Males perform calling perched on vegetation (Fig. 10F). They start calling at dawn (~ 6 am) and remain active until ~ 9 am, with a peak between 7 am and 8 am. After that, their activity remains sporadic until ~ 11 am. They call again in the late afternoon, but with a lower intensity. Most of the time, we observed adults as couples ($n = 8$; Fig. 10G, H), which strongly suggests that the species is monogamous. Males appear to be territorial, responding to and approaching the playback. Additionally, when we captured the females, the respective males called incessantly.

The new species was found in only one of the four sampling sites (5 km RAPELD trails) and appears to be strongly associated with '*bananeira brava*' plants. Therefore, this species is not expected to be abundant nor



Figure 10. *Ranitomeya aquamarina* sp. nov. natural history and breeding aspects **A** example of the habitat used by the species **B** phytotelma used by a couple of the species for reproduction **C** adult male climbing (unvouchered) **D** eggs **E** juvenile **F** calling male (INPA-H 47563) **G** couple in cortege (male MPEG 45223 and female MPEG 45222) **H** couple who was in the cited phytotelma (male INPA-H 47568 and female INPA-H 47569). Photographs ATM (**A–E, H**) and APL (**F, G**).

homogeneously distributed throughout its range. Its known extent of occurrence and area of occupancy are restricted, suggesting that its conservation status deserves attention. Nevertheless, we currently do not have enough information to assign *Ranitomeya aquamarina* sp. nov. to any IUCN category, and here we classify it as Data Deficient (DD).

Discussion

All the species of the *Ranitomeya vanzolinii* species group are distributed across the southwestern Amazonia (Muell et al. 2022; Frost 2025), in the Andean foothills and forests of Peru and Brazil, and most of them are known to have narrow ranges of occurrence (see Fig. 9). The same applies to *Ranitomeya aquamarina* sp. nov., which is known only from the type locality, on the right bank of the Juruá River. However, the range of the new species is probably greater because, based on its molecular data, we believe that the lineage named as “*Ranitomeya* sp. Envira” (sensu Twomey et al. 2023), occurring ca 60 km to the south, is the same species. Additionally, we suspect that another record 330 km to the north, made through citizen science, corresponds to the new species based on its morphology (photography by Alex Less; iNaturalist 2024). We hope that more sampling in the region will take place soon, as this may provide a better overview of the distribution of the species.

Unlike other dendrobatids (e.g., *Ameerega*, *Dendrobates* and *Phylllobates*), *Ranitomeya* species are especially difficult to detect in fieldwork due to their diminutive body size, conspicuous habits, calls that cannot be heard over long distances, specific microhabitats, and because they are hardly ever seen during the night (Lötters et al. 2007; Brown et al. 2011). These factors contribute to the fact that *Ranitomeya* species are rarely listed in amphibian faunal inventories, even in areas where they occur. In Brazil, when found, the number of individuals observed is very low (e.g., Queiroz et al. 2011; Waldez et al. 2013). This is, for example, the case of *R. defleri*, which has only recently been confirmed in Brazil (Simões et al. 2019), although it was long assumed to be present in the country (Brown et al. 2011). Difficult detection of frogs of the genus *Ranitomeya* in the field resulted in many species being described using fewer than five individuals (e.g., *R. cyanovittata*, *R. defleri*, *R. fantastica*, *R. flavovittata*, *R. sirensis*, and *R. variabilis*).

The genus *Ranitomeya* was recovered to be monophyletic with a posterior probability of 1. Species relationships were found to be mostly consistent with the revisions of Grant et al. (2017) and Brown et al. (2011) but showed some differences from the genomic framework of Muell et al. (2022) and Twomey et al. (2023). This was expected as the first two studies use a multiple-loci approach similar to ours, while the last one uses a genomic approach (Ultraconserved Elements). For example, we recovered the same species groups as defined in Brown et al. (2011): *R. defleri*, *R. variabilis*, *R. reticulata* and *R. vanzolinii* group, which do not correspond to those in Muell et al. (2022). However, we found a low posterior probability between *R. defleri* and *R. toraro* indicating that there are incongruences in the relationships between these species, pointing to the findings of Muell et al. (2022) and Twomey et al. (2023) that their positions need further comparisons. Taken that, some of the interspecies relationships found here should be interpreted with caution. *Ranitomeya aquamarina* sp. nov. could be confirmed within the *R. flavovittata* clade sensu Muell et al. (2022, cit. *Ranitomeya* sp. Envira) but its relationships with its closest relatives, *R. imitator* (here) or *R. flavovittata* and *R. cyanovittata* (Twomey et al. 2023) need to be further evaluated. In addition, our DNA barcoding indicates that some populations (e.g. *R. aff. cyanovittata*) differentiate at species level.

Our species delimitation results also presented some incongruences to the current *Ranitomeya* taxonomy. While most valid species were correctly recovered as a single OTU, some species were merged within another OTU (*R. flavovittata*

and *R. vanzolinii*; *R. benedicta* and *R. fantastica*; *R. ventrimaculata* and *R. reticulata*) and others were split into multiple OTUs (*R. sirensis*, *R. variabilis* and *R. ventrimaculata*). Also, while the new species and others were congruent among all the delimitations, some incongruences were found, specially within the OTUs cited above. The diversity within *R. sirensis*, *R. variabilis* and *R. ventrimaculata* was already discussed before and some nominal taxa (e.g., *R. duellmani*, *R. biolat*, and *R. lamasi*) were already synonymized with the former species. The possible revalidation of *R. biolat* was already discussed in Muell et al. (2022). We also found that the species that clumped in one OTU have low genetic p-distances for 16S (*R. flavovittata* and *R. vanzolinii*, 1.66%; *R. benedicta* and *R. fantastica*, 1.55%; *R. ventrimaculata* and *R. reticulata*, 1.78%). Therefore, we should be cautious when interpreting molecular delimitation analysis, its results are of less significance unless included in an integrative background that includes morphology, ecology, calls, and other evidence that corroborates the results. The systematics and taxonomy of the *Ranitomeya* genus has proven to be complex, with many changes in the species placements and status through time. The use of genomic data helped to better understand its evolution and even stated the possibility of *Ranitomeya aquamarina* sp. nov. to be recognized as a full species (cit. *Ranitomeya* sp. Envira, Twomey et al. 2023). In any case, an integrative approach is essential for the continuous improvement of taxonomic knowledge within the genus *Ranitomeya*.

The last description of a species of *Ranitomeya* was published more than ten years ago (*R. toraro*; Brown et al. 2011), who presented relevant contribution that filled the knowledge gaps of previously described species, such as calls and tadpoles. However, now advances in integrative taxonomy have the potential to boost the study of *Ranitomeya* diversity. One of the important prerequisites for a thorough investigation of the taxonomy of the frogs of the genus *Ranitomeya* is the use of a wide range of easily comparable predetermined character definitions [for example, methodology of taking morphometric data might follow Randrianiaina et al. (2011) and bioacoustic analyzes should follow standards proposed by Köhler et al. (2017)]. Such an approach would prevent descriptions from being based almost exclusively on color patterns, which are generally highly variable (Brown et al. 2011; Lorigoux-Chevalier et al. 2023; Rubio et al. 2024).

Finally, it is generally accepted that the true diversity of frogs is still very poorly known in Amazonia (e.g., Vacher et al. 2020). This fact is doubly true for the region of lower and middle Juruá River. Although we are only taking the first steps to uncover the biodiversity of this area, we already have evidence of the extraordinary richness of the local fauna and we already identified many new candidate species (e.g., Moraes et al. 2022; Lima et al. 2024; Martins et al. 2024). We hope that our research will stimulate more interest in this region, shed more light on its enormous biological wealth and, last but not least, provide important information for its protection.

Acknowledgements

The authors would like to thank S. Dantas and A. Ferreira for their assistance with the fieldwork; Edgar Lehr and Alexandre Roland for their kind review and suggestions for improving the manuscript; Fernanda P. Werneck (INPA-H), Ariane Silva (INPA-H), Ana L.C. Prudente (MPEG), João F.M. Sarmiento (MPEG), Felipe Toledo (FNJV) and Simone Dena (FNJV) for allowing access to collec-

tions; Instituto Nacional de Pesquisas da Amazônia (INPA) for assistance with the logistics (especially Andresa Viana); Laboratório Temático de Biologia Molecular (LTBM) for supporting the molecular data acquisition; Programa de Pesquisa em Biodiversidade (PPBio: Grant CNPq 441260/2023-3) for facilitating the Data management; Instituto Chico Mendes de Conservação da Biodiversidade/Sistema de Autorização e Informação em Biodiversidade for issuing the sampling permit (Process No. 13777-1); and the Ethics Committee on the Use of Animals of the Instituto Nacional de Pesquisas da Amazônia (CEUA-INPA) for the permission for the study (Process No. 35/2020, SEI 01280.001134/2020-63); and Coleção Entomológica at INPA for assistance with photos of the lateral head, hand, and foot of the holotype.

Additional information

Conflict of interest

The authors have declared that no competing interests exist.

Ethical statement

No ethical statement was reported.

Funding

This study was funded by the Fundação de Amparo à Pesquisa do Estado do Amazonas (FAPEAM process No. 01.02.016301.03252/2021-67 from 007/2021 BIODIVERSA grant to A.P. Lima). ATM receives a post-doctorate fellowship from CNPq (process No. 174978/2023-5), EDK receives a PhD fellowship from FAPEAM, JSD received a AT/III fellowship from FAPEAM (process No. 01.02.016301.03252/2021-67 from 007/2021 BIODIVERSA) and AP Lima receives a productivity fellowship (CT&I Edital #013/2022) from FAPEAM. The work of JM was financially supported by the Ministry of Culture of the Czech Republic (DKRVO 2024–2028/6.I.b, National Museum of the Czech Republic, 00023272).

Author contributions

Conceptualization: ATM, EDK, APL. Data curation: ATM, JD, APL. Formal analysis: ATM, EDK, APL. Investigation: ATM, EDK, JM, APL. Resources: ATM, JM, APL. Visualization: ATM, EDK, JD, JM, APL. Writing – original draft: ATM, EDK, APL. Writing – review and editing: ATM, EDK, JM, APL.

Author ORCIDs

Alexander Tamanini Mônico  <https://orcid.org/0000-0002-2965-8020>

Esteban Diego Koch  <https://orcid.org/0000-0002-1181-403X>

Jussara Santos Dayrell  <https://orcid.org/0000-0003-4211-421X>

Jiří Moravec  <https://orcid.org/0000-0003-4114-7466>

Albertina Pimentel Lima  <https://orcid.org/0000-0003-4586-5633>

Data availability

All of the data that support the findings of this study are available in the main text or Supplementary Information.

The sequences are available at GenBank: PV190292–PV190301 (16S), PV197204–PV197209 (12S), PV189994–PV189997 (COI) and PV191292–PV191297 (cyt-b).

The call recordings are available at The Audiovisual Collection of the Museum of Biological Diversity (MDBio), Fonoteca Neotropical Jacques Vielliard (FNJV), UNICAMP (<https://www2.ib.unicamp.br/fnjv/>):

INPA-H 47561 - FNJV 124331 - <https://www2.ib.unicamp.br/fnjv/collection.php?fnjv=124331>

INPA-H 47563 - FNJV 124332 - <https://www2.ib.unicamp.br/fnjv/collection.php?fnjv=124332>

INPA-H 47563 - FNJV 124333 - <https://www2.ib.unicamp.br/fnjv/collection.php?fnjv=124333>

MPEG 45220 - FNJV 124334 - <https://www2.ib.unicamp.br/fnjv/collection.php?fnjv=124334>

MPEG 45220 - FNJV 124335 - <https://www2.ib.unicamp.br/fnjv/collection.php?fnjv=124335>

INPA-H 47566 - FNJV 124336 - <https://www2.ib.unicamp.br/fnjv/collection.php?fnjv=124336>

INPA-H 47568 - FNJV 124337 - <https://www2.ib.unicamp.br/fnjv/collection.php?fnjv=124337>

MPEG 45223 - FNJV 124338 - <https://www2.ib.unicamp.br/fnjv/collection.php?fnjv=124338>

INPA-H 47570 - FNJV 124339 - <https://www2.ib.unicamp.br/fnjv/collection.php?fnjv=124339>

References

- Aichinger M (1991) A new species of poison-dart frog (Anura: Dendrobatidae) from the Serranía de Sira, Peru. *Herpetologica* 47: 1–5.
- Altschul SF, Madden TL, Schäffer AA, Zhang J, Zhang Z, Miller W, Lipman DJ (1997) Gapped BLAST and PSI-BLAST: a new generation of protein database search programs. *Nucleic Acids Research* 25: 3389–3402. <https://doi.org/10.1093/nar/25.17.3389>
- Azevedo-Ramos C, Galatti U (2002) Patterns of amphibian diversity in Brazilian Amazonia: conservation implications. *Biological Conservation* 103.1(2002): 103–111. [https://doi.org/10.1016/S0006-3207\(01\)00129-X](https://doi.org/10.1016/S0006-3207(01)00129-X)
- Bernarde PS, Albuquerque S, Miranda DB, Turci LCB (2013) Herpetofauna da floresta do baixo rio Moa em Cruzeiro do Sul, Acre – Brasil. *Biota Neotropica* 13: 220–244. <https://doi.org/10.1590/S1676-06032013000100023>
- Bioacoustics Research Program (2014) Raven Pro: interactive sound analysis software. Version 1.5. Ithaca, New York: The Cornell Lab of Ornithology. <https://ravensound-software.com/software/raven-pro> [accessed 15 Jul 2024]
- Bouckaert R, Drummond A (2017) bModelTest: Bayesian phylogenetic site model averaging and model comparison. *BMC Evolutionary Biology* 17(1): 1–11. <https://doi.org/10.1186/s12862-017-0890-6>
- Bouckaert R, Heled J, Kühnert D, Vaughan T, Wu C-H, Xie D, Suchard MA, Rambaut A, Drummond AJ (2014) BEAST 2: A Software Platform for Bayesian Evolutionary Analysis. *PLOS Computational Biology* 10: e1003537. <https://doi.org/10.1371/journal.pcbi.1003537>
- Boulenger GA (1884) On a collection of frogs from Yurimaguas, Huallaga River, Northern Peru. *Proceedings of the Zoological Society of London* 1883: 635–638. <https://doi.org/10.1111/j.1469-7998.1883.tb06669.x>
- Brown JL, Schulte R, Summers K (2006) A new species of *Dendrobates* (Anura: Dendrobatidae) from the Amazonian lowlands of Perú. *Zootaxa* 1152: 45–58. <https://doi.org/10.11646/zootaxa.1152.1.2>
- Brown, JL, Twomey EM, Pepper M, Sanchez-Rodriguez, M (2008) Revision of the *Ranitomeya fantastica* species complex with description of two new species from central Peru (Anura: Dendrobatidae). *Zootaxa* 1823: 1–24. <https://doi.org/10.11646/zootaxa.1823.1.1>
- Brown JL, Twomey EM, Amézquita A, Souza MB, Caldwell JP, Lötters S, von May R, Melo-Sampaio PR, Mejía-Vargas D, Pérez-Peña, PE, Pepper, M, Poelman EH, Sanchez-Ro-

- driguez M, Summers K (2011) A taxonomic revision of the Neotropical poison frog genus *Ranitomeya* (Amphibia: Dendrobatidae). *Zootaxa* 3083: 1–120. <https://doi.org/10.11646/zootaxa.3083.1.1>
- Che J, Chen HM, Yang JX, Jin JQ, Jiang K, Yuan ZY, Murphy RW, Zhang YP (2012) Universal COI primers for DNA barcoding amphibians. *Molecular Ecology Resources* 12: 247–258. <https://doi.org/10.1111/j.1755-0998.2011.03090.x>
- Darst CR, Cannatella DC (2004) Novel relationships among hyloid frogs inferred from 12S and 16S mitochondrial DNA sequences. *Molecular Phylogenetics and Evolution* 31(2): 462–475. <https://doi.org/10.1016/j.ympev.2003.09.003>
- Del-Rio G, Mutchler MJ, Costa B, Hiller AE, Lima G, Matinata B, Salter JF, Silveira LF, Rego MA, Schmitt DC (2021) Birds of the Juruá River: Extensive várzea forest as a barrier to terra firme birds. *Journal of Ornithology* 162: 565–577. <https://doi.org/10.1007/s10336-020-01850-0>
- Feller AE, Hedges SB (1998) Molecular evidence for the early history of living amphibians. *Molecular Phylogenetics and Evolution* 9: 509–516. <https://doi.org/10.1006/mpev.1998.0500>
- Fonseca WL, Silva JD, Abegg AD, Rosa CM, Bernarde PS (2019) Herpetofauna of Porto Walter and surrounding areas, Southwest Amazonia, Brazil. *Herpetology Notes* 12: 91–107.
- Fouquet A, Gilles A, Vences M, Marty C, Blanc M, Gemmell NJ (2007) Underestimation of species richness in Neotropical frogs revealed by mtDNA analyses. *PLOS one* 2(10): e1109. <https://doi.org/10.1371/journal.pone.0001109>
- Frost DR (2025) Amphibian Species of the World: An Online Reference. <https://research.amnh.org/herpetology/amphibia/index.html> [accessed 03 February 2025]
- Gosner KL (1960) A Simplified table for staging anuran embryos and larvae with notes on identification. *Herpetologica* 16(3): 183–190.
- Grant T, Frost DR, Caldwell JP, Gagliardo RON, Haddad CF, Kok PJ, Means DB, Noonan BP, Schargel WE, Wheeler WC (2006) Phylogenetic systematics of dart-poison frogs and their relatives (Amphibia: Athesphatanura: Dendrobatidae). *Bulletin of the American Museum of Natural History* 2006(299): 1–262. [https://doi.org/10.1206/0003-0090\(2006\)299\[1:PSODFA\]2.0.CO;2](https://doi.org/10.1206/0003-0090(2006)299[1:PSODFA]2.0.CO;2)
- Grant T, Rada M, Anganoy-Criollo M, Batista A, Dias PH, Jeckel AM, Machado DJ, Rueda-Almonacid JV [2017] Phylogenetic systematics of dart-poison frogs and their relatives revisited (Anura: Dendrobatoidea). *South American Journal of Herpetology* 12(s1): S1–S90. <https://doi.org/10.2994/SAJH-D-17-00017.1>
- Haffer J (1997) Contact zones between birds of southern Amazonia. *Ornithology Monographs* 48: 281–305. <https://doi.org/10.2307/40157539>
- iNaturalist (2024) iNaturalist Research-grade Observations. [iNaturalist.org](https://www.inaturalist.org). Occurrence dataset. <https://doi.org/10.15468/ab3s5x> [accessed 08 October 2024]
- Kahn TR, La Marca E, Lotters S, Brown JL, Twomey E, Amézquita A (2016) Aposematic Poison Frogs (Dendrobatidae) of the Andean countries: Bolivia, Colombia, Ecuador, Perú and Venezuela. *Conservation International Tropical Field Guide Series*, Conservation International. Arlington, 588 pp.
- Katoh K, Rozewicki J, Yamada KD (2019) MAFFT online service: multiple sequence alignment, interactive sequence choice and visualization. *Briefings in Bioinformatics* 20: 1160–1166. <https://doi.org/10.1093/bib/bbx108>
- Kimura M (1980) A simple method for estimating evolutionary rate of base substitutions through comparative studies of nucleotide sequences. *Journal of Molecular Evolution* 16: 111–120. <https://doi.org/10.1007/BF01731581>

- Klein B, Regnet RA, Krings M, Rödder D (2020) Larval development and morphology of six Neotropical poison-dart frogs of the genus *Ranitomeya* (Anura: Dendrobatidae) based on captive-raised specimens. *Bonn Zoological Bulletin* 69: 191–223. <https://doi.org/10.20363/BZB-2020.69.2.191>
- Kocher TD, Thomas WK, Meyer A, Edwards SV, Paabo S, Villablanca FX, Wilson AC (1989) Dynamics of mitochondrial DNA evolution in Animals: amplification and sequencing with conserved primers *Proceedings of the National Academy of Science USA* 86: 6196–6200. <https://doi.org/10.1073/pnas.86.16.6196>
- Köhler G (2012) Color catalogue for field biologists. Offenback: Herpeton, Germany, 49 pp.
- Köhler J, Jansen M, Rodriguez A, Kok PJR, Toledo LF, Emmrich M, Glaw F, Haddad CFB, Rödel MO, Vences M (2017) The use of bioacoustics in anuran taxonomy: theory, terminology, methods and recommendations for best practice. *Zootaxa* 4251: 1–124. <https://doi.org/10.11646/zootaxa.4251.1.1>
- Kok PJR, Kalamandeen M (2008) Introduction to the taxonomy of the amphibians of Kaieteur National Park, Guyana. *Abc Taxa* 5: 1–278.
- Lima AP, Ferreira A, Dantas S, Ferrão M, Dayrell J (2024) Sapos de Eirunepé: Rios Eiru – Juruá – Gregório. 1ª Ed. Manaus, Brazil.
- Lorioux-Chevalier U, Tuanama-Valles M, Gallusser S, Mori Pezo R, Chouteau M (2023) Unexpected colour pattern variation in mimetic frogs: implication for the diversification of warning signals in the genus *Ranitomeya*. *Royal Society Open Science* 10(6): 230354. <https://doi.org/10.1098/rsos.230354>
- Lötters S, Jungfer KH, Henkel FW, Schmidt W (2007) Poison frogs: Biology, Species & Captive Husbandry. Chimaira, Frankfurt, 668 pp.
- Martins BC, Mônico AT, Mendonça C, Dantas SP, Souza JRD, Hanken J, Lima AP, Ferrão M (2024) A new species of terrestrial foam-nesting frog of the *Adenomera simon-stuarti* complex (Anura, Leptodactylidae) from white-sand forests of central Amazonia, Brazil. *Zoosystematics and Evolution* 100: 233–253. <https://doi.org/10.3897/zse.100.110133>
- Matocq MM, Patton JL, da Silva MNF (2000) Population genetic structure of two ecologically distinct Amazonian spiny rats: separating history and current ecology. *Evolution* 54(4): 1423–1432. <https://doi.org/10.1111/j.0014-3820.2000.tb00574.x>
- McDiarmid RW, Altig R (1999) Tadpoles: the biology of anuran larvae. University of Chicago Press.
- Monaghan MT, Wild R, Elliot M, Fujisawa T, Balke M, Inward DJG, Lees DC, Ranaivosolo R, Eggleton P, Barraclough TG, Vogler AP (2009) Accelerated species inventory on Madagascar using coalescent-based models of species delineation. *Systematic Biology* 58: 298–311. <https://doi.org/10.1093/sysbio/syp027>
- Moraes LJCL, Rainha RDN, Werneck FDP, Oliveira AFDS, Gascon C, Carvalho VTD (2022) Amphibians and reptiles from a protected area in western Brazilian Amazonia (Reserva Extrativista do Baixo Juruá). *Papéis Avulsos de Zoologia* 62: e202262054. <https://doi.org/10.11606/1807-0205/2022.62.054>
- Moritz C, Schneider CJ, Wake DB (1992) Evolutionary relationships within the *Ensatina eschscholtzii* complex confirm the ring species interpretation. *Systematic Biology* 41: 273–291. <https://doi.org/10.1093/sysbio/41.3.273>
- Muell MR, Chávez G, Prates I, Guillory WX, Kahn TR, Twomey EM, Rodrigues MT, Brown JL (2022) Phylogenomic analysis of evolutionary relationships in *Ranitomeya* poison frogs (Family Dendrobatidae) using ultraconserved elements. *Molecular Phylogenetics and Evolution* 168(107389): 1–10. <https://doi.org/10.1016/j.ympev.2022.107389>

- Myers CW (1982) Spotted poison frogs: Descriptions of three new *Dendrobates* from western Amazonia, and resurrection of a lost species from “Chiriqui”. *American Museum Novitates* 2721: 1–23.
- Noonan BP, Wray KP (2006) Neotropical diversification: the effects of a complex history on diversity within the poison frog genus *Dendrobates*. *Journal of Biogeography* 33(6): 1007–1020. <https://doi.org/10.1111/j.1365-2699.2006.01483.x>
- Palumbi SR (1996) Nucleic acids II: the polymerase chain reaction. In: Hillis DM, Moritz C, Mable BK (Eds) *Molecular Systematics*. Sinauer & Associates Inc., Sunderland, Massachusetts, 205–247.
- Pantoja DL, Fraga RD (2012) Herpetofauna of the Reserva Extrativista do Rio Gregório, Juruá Basin, southwest Amazonia, Brazil. *Check List* 8(3): 360–374. <https://doi.org/10.15560/8.3.360>
- Pérez-Peña PE, Chávez G, Twomey EM, Brown JL (2010) Two new species of *Ranitomeya* (Anura: Dendrobatidae) from eastern Amazonian Peru. *Zootaxa* 2439: 1–23. <https://doi.org/10.11646/zootaxa.2439.1.1>
- Pons J, Barraclough TG, Gomez-Zurita J, Cardoso A, Duran DP, Hazell S, Kamoun S, Sumlin WD, Vogler AP (2006) Sequence-Based Species Delimitation for the DNA Taxonomy of Undescribed Insects. *Systematic Biology* 55: 595–09. <https://doi.org/10.1080/10635150600852011>
- Puillandre N, Brouillet S, Achaz G (2021) ASAP: assemble species by automatic partitioning. *Molecular Ecology Resources* 21: 609–620. <https://doi.org/10.1111/1755-0998.13281>
- Queiroz SDS, da Silva AR, dos Reis FM, Lima JD, Ferreira Lima JR (2011) Anfíbios de uma área de castanhal da Reserva Extrativista do Rio Cajari, Amapá. *Biota Amazônia* 1(1): 1–18. <https://doi.org/10.18561/2179-5746/biotaamazonia.v1n1p1-18>
- R Core Team (2019) A language and environment for statistical computing. Vienna: R Foundation for Statistical Computing. www.r-project.org [accessed 11 August 2024]
- Randrianiaina RD, Strauß A, Glos J, Glaw F, Vences M (2011) Diversity, external morphology and ‘reverse taxonomy’ in the specialized tadpoles of Malagasy river bank frogs of the sugenus *Ochthomantis* (genus *Mantidactylus*). *Contributions to Zoology* 80(1): 17–65. <https://doi.org/10.1163/18759866-08001002>
- Roberts JL, Brown JL, Von May R, Arizabal W, Presar A, Symula R, Schulte R (2006) Phylogenetic relationships among poison frogs of the genus *Dendrobates* (Dendrobatidae): A molecular perspective from increased taxon sampling. *The Herpetological Journal* 16(4): 377–385.
- Rubio AO, Stuckert AM, Geraldts B, Nielsen R, MacManes MD, Summers K (2024) What makes a mimic? Orange, red, and black color production in the mimic poison frog (*Ranitomeya imitator*). *Genome Biology and Evolution* 16(7): 1–16. <https://doi.org/10.1093/gbe/evae123>
- Sambrook J, Russell DW (2001) *Molecular cloning: a laboratory manual*. 3rd edition. Cold Spring Harbor Laboratory Press, New York, 2344 pp.
- Santos JC, Cannatella DC (2011) Phenotypic integration emerges from aposematism and scale in poison frogs. *Proceedings of the National Academy of Sciences* 108(15): 6175–6180. <https://doi.org/10.1073/pnas.1010952108>
- Santos JC, Coloma LA, Summers K, Caldwell JP, Ree R, Cannatella DC (2009) Amazonian amphibian diversity is primarily derived from late Miocene Andean lineages. *PLOS Biology* 7(3): e1000056. <https://doi.org/10.1371/journal.pbio.1000056>
- Schulte R (1986) Eine neue *Dendrobates*-Art aus Ostperu (Amphibia: Salientia: Dendrobatidae). *Sauria* 8: 11–20.

- Schulte R (1999) Poison Dart Frogs / Pfeilgiftfrösche. "Artenteil—Peru". Waiblingen: Karl Hauck. Stuttgart, Germany, 292 pp.
- Segalla MV, Berneck BVM, Canedo C, Caramaschi U, Cruz CAG, Garcia PCA, Grant T, Haddad CFB, Lourenço ACC, Mângia S, Mott T, Nascimento LB, Toledo LF, Werneck FP, Langone JA (2021) List of Brazilian Amphibians. *Herpetologia Brasileira* 10(1): 121–216. <https://doi.org/10.5281/zenodo.4716176>
- Serrano-Rojas SJ, Whitworth A, Villacampa J, Von May R, Gutierrez RC, Padial JM, Chaparro, JC (2017) A new species of poison-dart frog (Anura: Dendrobatidae) from Manu province, Amazon region of southeastern Peru, with notes on its natural history, bioacoustics, phylogenetics, and recommended conservation status. *Zootaxa* 4221(1): 71–94. <https://doi.org/10.11646/zootaxa.4221.1.3>
- Shreve B (1935) On a new teiid and Amphibia from Panama, Ecuador, and Paraguay. *Occasional Papers of the Boston Society of Natural History* 8: 209–218.
- Simões PI, Rojas-Runjaic FJ, Gagliardi-Urrutia G, Fisher SJC (2019) Five new country records of Amazonian anurans for Brazil, with notes on morphology, advertisement calls, and natural history. *Herpetology Notes* 12: 211–219.
- Souza JRD, Ferrão M, Kaefer IL, Cunha-Machado AS, Melo-Sampaio PR, Hanken J, Lima AP (2023) A new pale-ventered Nurse Frog (Aromobatidae: *Allobates*) from southwestern Brazilian Amazonia. *Vertebrate Zoology* 73: 647–675. <https://doi.org/10.3897/vz.73.e103534>
- Sueur J, Aubin T, Simonis C (2008) Seewave, a free modular tool for sound analysis and synthesis. *Bioacoustics* 18: 213–226. <https://doi.org/10.1080/09524622.2008.9753600>
- Symula R, Schulte R, Summers K (2001) Molecular phylogenetic evidence for a mimetic radiation in Peruvian poison frogs supports a Müllerian mimicry hypothesis. *Proceedings of the Royal Society of London. Series B: Biological Sciences* 268(1484): 2415–2421. <https://doi.org/10.1098/rspb.2001.1812>
- Tamura K, Stecher G, Kumar S (2021) MEGA11: Molecular Evolutionary Genetics Analysis Version 11. *Molecular Biology and Evolution* 38(7): 3022–3027. <https://doi.org/10.1093/molbev/msab120>
- Titus TA, Larson A (1996) Molecular phylogenetics of desmognathine salamanders (Caudata: Plethodontidae): A reevaluation of evolution in ecology, life history, and morphology. *Systematic Biology* 45: 451–472. <https://doi.org/10.1093/sysbio/45.4.451>
- Tuomisto H, Van Doninck J, Ruokolainen K, Moulatlet GM, Figueiredo FO, Sirén A, Cárdenas G, Lehtonen S, Zuquim G (2019) Discovering floristic and geocological gradients across Amazonia. *Journal of Biogeography* 46(8): 1734–1748. <https://doi.org/10.1111/jbi.13627>
- Twomey EM, Brown JL (2008) Spotted poison frogs: rediscovery of a lost species and a new genus (Anura: Dendrobatidae) from northwestern Peru. *Herpetologica* 64(1): 121–137. <https://doi.org/10.1655/07-009.1>
- Twomey EM, Brown JL (2009) Another new species of *Ranitomeya* (Anura: Dendrobatidae) from Amazonian Colombia. *Zootaxa* 2302: 48–60. <https://doi.org/10.11646/zootaxa.2302.1.4>
- Twomey E, Melo-Sampaio P, Schulte LM, Bossuyt F, Brown JL, Castroviejo-Fisher S (2023) Multiple routes to color convergence in a radiation of neotropical poison frogs. *Systematic Biology* 72(6): 1247–1261. <https://doi.org/10.1093/sysbio/syad051>
- Vacher J-P, Chave J, Ficotola FG, Sommeria-Klein G, Tao S, Thébaud C, Blanc M, Camacho A, Cassimiro J, Colston TJ, Dewynter M, Ernst R, Gaucher P, Gomes JO, Jairam R, Kok PJR, Lima JD, Martinez Q, Marty C, Noonan BP, Nunes PMS, Ouboter P, Recoder R, Rodrigues MT, Snyder A, Marques-Souza S, Fouquet A (2020) Large scale DNA-based sur-

- vey of frogs in Amazonia suggests a vast underestimation of species richness and endemism. *Journal of Biogeography* 47: 1781–1791. <https://doi.org/10.1111/jbi.13847>
- Vences M, Kosuch J, Boistel R, Haddad CF, La Marca E, Lötters S, Veith M (2003) Convergent evolution of aposematic coloration in Neotropical poison frogs: a molecular phylogenetic perspective. *Organisms Diversity & Evolution* 3(3): 215–226. <https://doi.org/10.1078/1439-6092-00076>
- Waldez F, Menin M, Vogt RC (2013) Diversidade de anfíbios e répteis Squamata na região do baixo rio Purus, Amazônia Central, Brasil. *Biota Neotropica* 13(1): 300–316. <https://doi.org/10.1590/S1676-06032013000100029>
- Watters JL, Cummings ST, Flanagan RL, Siler CD (2016) Review of morphometric measurements used in anuran species descriptions and recommendations for a standardized approach. *Zootaxa* 4072(4): 477–495. <https://doi.org/10.11646/zootaxa.4072.4.6>
- Werner P, Elle O, Schulte LM, Lötters S (2010) Home range behaviour in male and female poison frogs in Amazonian Peru (Dendrobatidae: *Ranitomeya reticulata*). *Journal of Natural History* 45(1–2): 15–27. <https://doi.org/10.1080/00222933.2010.502257>
- Zhang J, Kapli P, Pavlidis P, Stamatakis A (2013) A general species delimitation method with applications to phylogenetic placements. *Bioinformatics* 29: 2869–2876. <https://doi.org/10.1093/bioinformatics/btt499>
- Zimmermann H, Zimmermann E (1988) Etho-Taxonomie und zoogeographische Artengruppenbildung bei Pfeilgiftfroschen (Anura: Dendrobatidae). *Salamandra* 24: 125–160.

Supplementary material 1

Morphometric measurements (in mm) of the type specimens of *Ranitomeya aquamarina* sp. nov.

Authors: Alexander Tamanini Mônico, Esteban Diego Koch, Jussara Santos Dayrell, Jiří Moravec, Albertina Pimentel Lima

Data type: docx

Copyright notice: This dataset is made available under the Open Database License (<http://opendatacommons.org/licenses/odbl/1.0/>). The Open Database License (ODbL) is a license agreement intended to allow users to freely share, modify, and use this Dataset while maintaining this same freedom for others, provided that the original source and author(s) are credited.

Link: <https://doi.org/10.3897/zookeys.1236.146533.suppl1>

Supplementary material 2

Acoustic parameters of advertisement call of *Ranitomeya aquamarina* sp. nov.

Authors: Alexander Tamanini Mônico, Esteban Diego Koch, Jussara Santos Dayrell, Jiří Moravec, Albertina Pimentel Lima

Data type: docx

Copyright notice: This dataset is made available under the Open Database License (<http://opendatacommons.org/licenses/odbl/1.0/>). The Open Database License (ODbL) is a license agreement intended to allow users to freely share, modify, and use this Dataset while maintaining this same freedom for others, provided that the original source and author(s) are credited.

Link: <https://doi.org/10.3897/zookeys.1236.146533.suppl2>

Supplementary material 3

Species of *Ranitomeya*, *Andinobates*, and *Excidobates* used in phylogenetic analyses, with respective voucher, Genbank accession numbers and references

Authors: Alexander Tamanini Mônico, Esteban Diego Koch, Jussara Santos Dayrell, Jiří Moravec, Albertina Pimentel Lima

Data type: docx

Copyright notice: This dataset is made available under the Open Database License (<http://opendatacommons.org/licenses/odbl/1.0/>). The Open Database License (ODbL) is a license agreement intended to allow users to freely share, modify, and use this Dataset while maintaining this same freedom for others, provided that the original source and author(s) are credited.

Link: <https://doi.org/10.3897/zookeys.1236.146533.suppl3>

Supplementary material 4

Species delimitation results of *Ranitomeya*

Authors: Alexander Tamanini Mônico, Esteban Diego Koch, Jussara Santos Dayrell, Jiří Moravec, Albertina Pimentel Lima

Data type: xlsx

Copyright notice: This dataset is made available under the Open Database License (<http://opendatacommons.org/licenses/odbl/1.0/>). The Open Database License (ODbL) is a license agreement intended to allow users to freely share, modify, and use this Dataset while maintaining this same freedom for others, provided that the original source and author(s) are credited.

Link: <https://doi.org/10.3897/zookeys.1236.146533.suppl4>

Supplementary material 5

Continuation of phylogenetic reconstruction showing the position of *Ranitomeya aquamarina* sp. nov.

Authors: Alexander Tamanini Mônico, Esteban Diego Koch, Jussara Santos Dayrell, Jiří Moravec, Albertina Pimentel Lima

Data type: tif

Explanation note: Bayesian inference tree inferred with 16S, 12S, COI, and *cyt-b*. Posterior probability is shown close to nodes (See Fig. 1).

Copyright notice: This dataset is made available under the Open Database License (<http://opendatacommons.org/licenses/odbl/1.0/>). The Open Database License (ODbL) is a license agreement intended to allow users to freely share, modify, and use this Dataset while maintaining this same freedom for others, provided that the original source and author(s) are credited.

Link: <https://doi.org/10.3897/zookeys.1236.146533.suppl5>

Two new species of larval Erythraeidae (Parasitengona) ectoparasites of leafhoppers from Southwestern China

Yan Jiang^{1,2}, Tian-Ci Yi¹, Si-Yuan Xu¹, Dao-Chao Jin¹

¹ Institute of Entomology, Guizhou University, Guizhou Provincial Key Laboratory for Plant Pest Management of the Mountainous Region, the Scientific Observing and Experimental Station of Crop Pest in Guiyang, Ministry of Agriculture and Rural Affairs of the P. R. China, Guiyang 550025, China

² Department of Pharmacy, Guizhou Provincial Engineering Research Center of Medical Resourceful Healthcare Products, Guiyang Healthcare Vocational University, Guiyang 550000, China

Corresponding authors: Si-Yuan Xu (syxusxy@163.com); Dao-Chao Jin (dcjin@gzu.edu.cn)

Abstract

In this study, three species were examined. Among them, two new species, *Caeculisoma taianensis* sp. nov. and *Iguatonia barboproxima* sp. nov. from Southwestern China, were described and illustrated based on larvae. The two new species can be distinguished from the known species by the following characteristics: the anterior sensilla are nude, and the gnathosoma has two pairs of nude hypostomatae in *C. taianensis* sp. nov.; the anterior sensilla and posterolateral scutalae are located in the posterior half of the scutum, and the posterior hypostomatae with barbs on the proximal half in *I. barboproxima* sp. nov. In addition, a new host and distribution range of *Abrolophus quadrapexicis* Xu & Jin, 2022 is reported.

Key words: Abrolophinae, Callidosomatinae, Chongqing, insect, new host, range extension, taxonomy, Yunnan



Academic editor: Mateusz Zmudzinski

Received: 14 October 2024

Accepted: 20 March 2025

Published: 25 April 2025

ZooBank: <https://zoobank.org/502F0F0F-85AC-439C-AC24-746A55EE51D2>

Citation: Jiang Y, Yi T-C, Xu S-Y, Jin D-C (2025) Two new species of larval Erythraeidae (Parasitengona) ectoparasites of leafhoppers from Southwestern China. ZooKeys 1236: 85–101. <https://doi.org/10.3897/zookeys.1236.139274>

Copyright: © Yan Jiang et al.
This is an open access article distributed under terms of the Creative Commons Attribution License (Attribution 4.0 International – CC BY 4.0).

Introduction

Southwestern China comprises three provinces (Sichuan, Guizhou, and Yunnan), one municipality (Chongqing), and one autonomous region (Xizang (Tibet)). This region is characterized by diverse topography with significant variations in elevation and numerous separated basins (Shi et al. 2018), including the Yunnan-Guizhou Plateau, the Qinghai-Tibetan Plateau, the Hengduan Mountains, and the Sichuan Basin. Simultaneously, the region exhibits diverse climatic conditions, including a subtropical monsoon climate, plateau mountain climate, mountain climate, tropical monsoon climate, dry-hot valley climate and a temperate monsoon climate. The variety of climates provides a wealth of environmental conditions, which play a pivotal role in fostering species diversity in the ecosystem. Therefore, Southwestern China is a key area for fauna-flora biodiversity research in China (Han et al. 2008; Shi et al. 2018).

To date, 13 species in eight genera (*Balaustium* von Heyden, 1826, *Caeculisoma* Berlese, 1888, *Charletonia* Oudemans, 1910, *Erythraeus* Latreille, 1806, *Grandjeanella* Southcott, 1961, *Leptus* Latreille, 1796, *Marantelophus* Haitlinger, 2011, and *Neoabrolophus* Khot, 1965) of five subfamilies

(Abrolophinae Witte, 1995, Balaustiinae Grandjean, 1947, Callidosomatinae Southcott, 1957, Erythraeinae Robineau-Desvoidy, 1828, and Leptinae Billberg, 1820) of Erythraeidae have been documented in Southwestern China (Xu et al. 2017, 2019a, b, 2020, 2022a, 2022b, 2023, 2025). Of them, three species were described based on post-larval forms, one species was recorded based on both larval and post-larval stages, and the remaining species were known only by larvae (Table 1).

Species of the genus *Abrolophus* Berlese, 1891 from China are distributed in the Macao Special Administrative Region, Hainan Province, Zhejiang Province, Shandong Province, Guangxi Zhuang Autonomous Region, Guangdong Province, and Hunan Province (Zheng 2002a; Haitlinger 2006; Xu et al. 2021, 2022a). However, there has been no report of *Abrolophus* in Southwestern China.

A total of 27 species of *Caeculisoma* have been reported worldwide, of which 14 were based on the post-larval stage, 12 were based on the larval stage, and only one species was based on both larval and post-larval instars (Maqol and Wohltmann 2012; Xu et al. 2019a, 2019b, 2020; Saboori et al. 2023; Kohansal et al. 2024; Noei et al. 2024). Among the 27 known *Caeculisoma* species, four were recorded in China based on the larval stage, with two (*C. penlineatus* Xu & Jin, 2019, *C. semispinus* Xu & Jin, 2019) collected from Southwestern China (Zheng 2002b; Xu et al. 2019a, 2019b, 2020).

Hitherto, only two species of the genus *Iguatonia* have been reported based on their larval stage worldwide (Haitlinger 2004; Xu et al. 2020; Noei et al. 2024): *I. barbilla* Haitlinger, 2004 from Brazil and *I. xinfengi* Xu & Jin, 2020 from Hainan Province (Island), China.

Table 1. Hosts and distribution of the known species of Erythraeidae from Southwestern China.

Species	Host	Distribution
<i>Balaustium allomedicagoense</i> Xu & Jin, 2025 [P]	Unknown	Yunnan
<i>Balaustium neomedicagoense</i> Xu & Jin, 2025 [P]	Unknown	Xizang
<i>Caeculisoma penlineatus</i> Xu & Jin, 2019 [L]	<i>Mileewa margheritae</i> (female) (Hemiptera, Cicadellidae, Mileewinae), <i>Neuterthron hamuliferum</i> (male) (Hemiptera, Delphacidae), unidentified Alebrini (Hemiptera, Cicadellidae, Typhlocybinae), unidentified Delphacinae (Hemiptera, Delphacidae), unidentified Issidae (Hemiptera, Auchenorrhyncha)	Chongqing, Guizhou
<i>Caeculisoma semispinus</i> Xu & Jin, 2019 [L]	<i>Shaddai</i> sp. (male) (Hemiptera, Cicadellidae), unidentified Zygineellini (female) (Cicadellidae)	Chongqing
<i>Charletonia rectangia</i> Xu & Jin, 2022 [L]	Unidentified Acrididae (Orthoptera), unidentified Tettigoniidae (Orthoptera), unknown Chrysomelidae (Coleoptera), unidentified mantis (Mantodea), unidentified moth (Lepidoptera), unidentified stick insect (Phasmatodea)	Yunnan
<i>Erythraeus (Zaracarus) mossesus</i> Xu & Jin, 2023 [P, L]	Unknown	Guizhou
<i>Grandjeanella dianensis</i> Xu & Jin, 2022 [L]	Unknown.	Yunnan
<i>Leptus (Leptus) bomiensis</i> Xu & Jin, 2022 [L]	Unidentified moth (Lepidoptera), unidentified Elateridae (Coleoptera), unidentified Pentatomidae (Hemiptera)	Xizang
<i>Leptus (Leptus) striatus</i> Xu & Jin, 2022 [L]	Unidentified Opiliones	Yunnan
<i>Leptus (Leptus) trisolenidionus</i> Xu & Jin, 2022 [L]	Unidentified Cicadellinae (Hemiptera, Cicadellidae)	Guizhou
<i>Marantelophus dubifurcatus</i> Xu, Yi & Jin, 2017 [L]	<i>Cacopsylla</i> sp. (Hemiptera, Psyllidae), unidentified Psocoptera.	Guizhou
<i>Marantelophus neodubifurcatus</i> Xu & Jin, 2023 [L]	Unknown	Guizhou
<i>Neoabrolophus guizhouensis</i> Xu & Jin, 2025 [P]	Unknown	Guizhou

In this checklist, host and distribution data were obtained from Xu et al. 2017, 2019a, b, 2020, 2022a, b, 2023, 2025. [P]: Post-larval form. [L]: Larva.

In this study, two new species, *C. taianensis* sp. nov. and *I. barboproxima* sp. nov., collected from Yunnan Province and Chongqing Municipality, respectively, are described and illustrated based on larvae. Additionally, new data for *A. quadrapexicis* Xu & Jin, 2022 is provided.

Material and methods

Erythraeid larvae were collected along with their insect hosts using 200 mesh insect nets, and subsequently preserved in small vials containing absolute ethanol. The larvae on the hosts were detached using a fine brush under a stereomicroscope (Nikon SMZ745) in the lab. Then, all larval specimens were cleared in Oudemans' fluid for about 12 h at 25 °C and slide-mounted in Hoyer's medium (Walter and Krantz 2009). Figures were drawn with the aid of a drawing tube attached to a Nikon Eclipse Ni-E compound microscope. Genus identification is based on the key to world genera of larval Callidosomatinae of Noei et al. (2024). Terminology and abbreviations are adapted from Noei et al. (2024), Wohltmann et al. (2007) and Xu et al. (2020). Measurements are expressed in micrometers (μm). The standard deviations (SD) are provided with two decimal places. All specimens were deposited at the Institute of Entomology, Guizhou University, Guiyang, China (GUGC).

Results

Abrolophinae Witte, 1995

Abrolophus Berlese, 1891

Abrolophus quadrapexicis Xu & Jin, 2022

Material examined. CHINA • one larva (2000–1600-GZ-yj); Guizhou Province, Fanjingshan National Nature Reserve; 27°59'27"N, 108°33'30"E; 673 m; 30 Jun. 2023; Si-Yuan Xu leg.; on an unidentified Psyllidae (Hemiptera).

Distribution. Guizhou Province (new distribution), Shandong Province, Zhejiang Province.

Note. This species was collected from plants without a host record in Zhejiang and Shandong (Xu et al. 2022b).

Callidosomatinae Southcott, 1957

Caeculisoma Berlese, 1888

Caeculisoma taianensis sp. nov.

<https://zoobank.org/F5C1A34A-2366-423A-B816-969D2202B854>

Figs 1–4

Diagnosis (larva). ASE nude and posterior to the level of ML, closer to ML than PL; PSE with barbs on the distal one-third; gnathosoma with two pairs of nude hypostomata; ISD 56–63; Ti I 188–207; Ti III 264–287.

Description. Dorsum. Idiosoma lateral cuticle of holotype used for drawing broken slide preparation, almost oval, with 30 (fD = 28–30 in paratypes) barbed setae, a pair of setae located between scutum and eyes (Fig. 1A).

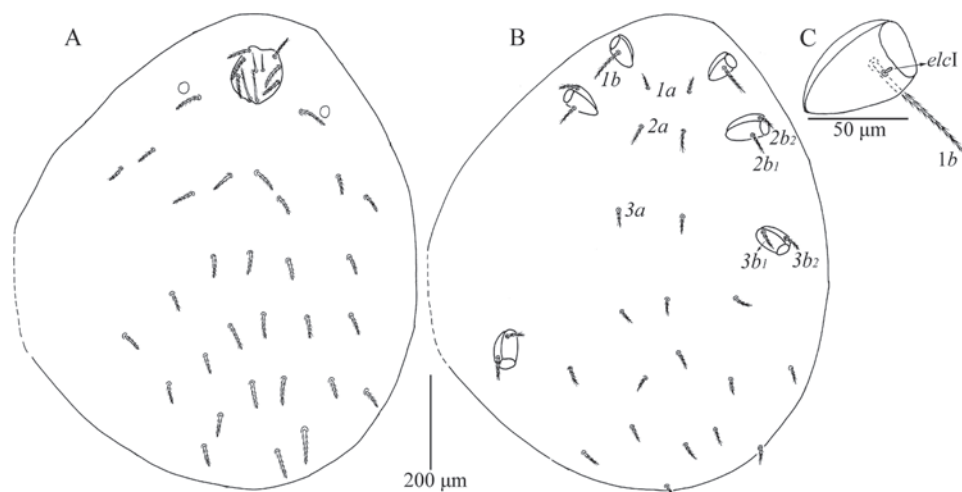


Figure 1. *Caeculisoma taianensis* sp. nov., larva **A** dorsal view of idiosoma **B** ventral view of idiosoma **C** dorsal view of coxa I, showing supracoxal seta.

Scutum outline pentagonal with rounded angles, length somewhat longer than width, anterior margin slightly concave, anterolateral and posterolateral margins slightly sinuous, posterior margin with small concavity between bases of PSE (Figs 1A, 2A, 3). Three pairs of normal setae (AL, ML and PL), and two pairs of sensilla (ASE and PSE) placed on scutum. AL, ML and PL completely barbed, ASE nude, PSE with fine barbs in distal about one-third. ASE placed between ML and PL, and closer to ML than PL, PSE near posterior margin of scutum. PSE much longer than ASE, ML slightly longer than AL and PL, AL slightly longer than PL, one paratype (c) AL equal to PL (Table 2).

Venter. All ventral setae, including coxalae, barbed and with pointed ends (Fig. 1B). Three pairs of intercoxal setae ($1a$, $2a$ and $3a$), $2a$ longer than $1a$ and $3a$, $3a$ slightly longer than $1a$ (Table 2), 14 setae behind coxae III (fV = 12–14 in paratypes). Five pairs of coxalae ($1b$, $2b_1$, $2b_2$, $3b_1$ and $3b_2$), $1b$ much longer than the other coxalae, $2b_1$ subequal $3b_1$, $2b_2$ and $3b_2$ subequal, $2b_1$ and $3b_1$ longer than $2b_2$ and $3b_2$, respectively (Table 2). Dorsum of coxa I with a peg-like supracoxal seta (*elc I*) (Fig. 1C).

Gnathosoma (Fig. 2B, C). Dorsal view of the cheliceral base punctated. One pair of galealae (*cs*) and two pairs of hypostomalae (*as* and *bs*) nude; *bs* longer than *cs* and much longer than *as* (Table 2). Hypostomal lip with fimbriation. Palpfemur and palpgenu each with one barbed, pointed dorsal seta (PaScFed and PaScGed). Palptibia with three barbed setae, one on ventral surface, odontus bifid. Palptarsus with seven setae, five nude, one solenidion (ω) and one eupathidium (ζ). fPp = 0-B-B-3B₂-5N ω ζ . Palpal supracoxal seta (*elcp*) peg-like.

Legs (Figs 1B, 3). With seven segments (femora divided). IP = 2533–2692 (Holotype and six paratypes). Claws hook-like and posterior claw with few cilia-tions, and empodium claw-like. Normal setae on legs barbed and pointed. Leg setal formula: leg I: Cx–1n; Tr–1n; Bfe–4n; Tfe–5n; Ge–1 σ , 1 κ , 12n; Ti–2 ϕ , 1 κ , 1Cp, 18n; Ta–1 ω , 1 ϵ , 2 ζ , 1Cp, 27n. leg II: Cx–2n; Tr–1n; Bfe–4n; Tfe–5n; Ge–1 κ , 12n; Ti–2 ϕ , 19n; Ta–1 ω , 1 ζ , 28n. leg III: Cx–2n; Tr–1n; Bfe–2n; Tfe–5n; Ge–12n; Ti–1 ϕ , 19n; Ta–1 ζ , 28n. The morphometric data of the legs is listed in Table 2.

Etymology. The new species' name is derived from Taian Town, where the holotype and paratype were collected.

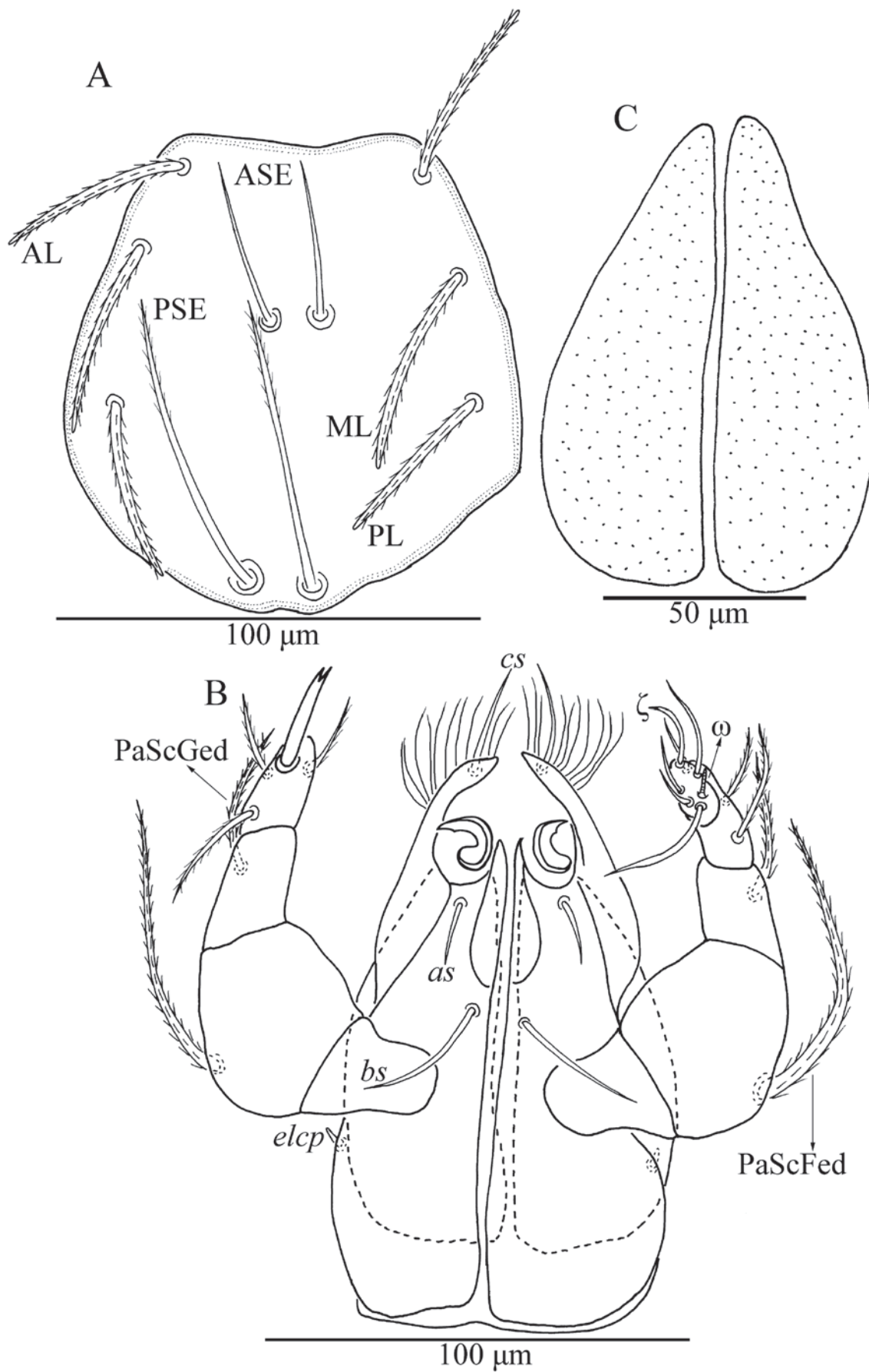


Figure 2. *Caeculisoma taianensis* sp. nov., larva **A** scutum **B** ventral view of gnathosoma **C** dorsal view of the cheliceral bases.

Table 2. Metric and some meristic data of *Caeculisoma taianensis* sp. nov. (larvae, a–f = paratypes; a: 1088–0275-YN-yl, b: 1082–0271-YN-yl, c: 1083–0271-YN-yl, d: 1084–0271-YN-yl, e: 1085–0272-YN-yl, f: 1086–0273-YN-yl).

Character	Holotype	a	b	c	d	e	f	SD	range
fD	30	28	30	30	28	30	28	0.99	28–30
fV	14	14	12	14	12	14	14	0.90	12–14
NDV	44	42	42	44	40	44	42	1.40	40–44
IL	999	689	1121	901	1069	1061	1543	240.10	689–1543
IW	843	415	840	608	720	678	1028	181.47	415–1028
DS	30–66	33–57	33–59	32–62	36–64	33–60	33–55	1.64–3.58	30–66
DS min.	30	33	33	32	36	33	33	1.64	30–36
DS max.	66	57	59	62	64	60	55	3.58	55–66
PDS	34–66	36–57	37–59	34–62	37–64	36–60	33–55	1.48–3.58	33–66
PDS min.	34	36	37	34	37	36	33	1.48	33–37
PDS max.	66	57	59	62	64	60	55	3.58	55–66
Oc	21	22	22	23	21	20	19	1.25	19–23
1a	35	30	32	27	21	25	24	4.53	21–35
2a	44	47	43	38	39	44	40	3.00	38–47
3a	38	36	38	32	34	35	33	2.17	32–38
1b	74	67	74	66	72	64	71	3.73	64–74
2b ₁	47	49	43	44	47	48	40	2.97	40–49
2b ₂	36	34	29	32	33	34	31	2.12	29–36
3b ₁	48	44	46	44	46	46	40	2.36	40–48
3b ₂	35	37	36	36	34	34	32	1.55	32–37
L	114	109	109	110	111	114	103	3.46	103–114
W	108	103	103	100	103	102	97	3.10	97–108
AW	57	60	57	53	55	61	56	2.56	53–61
MW	76	71	71	71	74	72	69	2.14	69–76
PW	85	78	79	77	79	80	76	2.70	76–85
MA	41	38	40	43	40	43	38	1.92	38–43
AA	13	12	12	13	12	13	11	0.70	11–13
SB	15	14	15	14	15	16	14	0.70	14–16
ISD	63	60	60	57	59	58	56	2.14	56–63
AP	56	52	54	55	54	53	54	1.20	52–56
AL	46	45	37	44	44	45	40	3.02	37–46
ML	50	50	49	48	46	51	47	1.67	46–51
PL	41	41	37	37	37	36	35	2.19	35–41
ASE	39	34	33	39	31	36	33	2.88	31–39
PSE	71	66	60	70	60	67	57	5.04	57–71
as	15	14	16	15	17	18	16	1.25	14–18
bs	34	27	30	36	35	33	34	2.91	27–36
cs	26	23	20	28	25	22	25	2.47	20–28
PaScFed	74	78	76	81	83	85	73	4.24	73–85
PaScGed	36	33	31	34	37	36	34	1.92	31–37
GL	136	141	132	135	136	140	138	2.85	132–141
Ta I (H)	22	19	22	20	18	18	15	2.29	15–22
Ta I (L)	152	153	160	159	152	160	157	3.44	152–160
Ti I	199	191	200	192	201	207	188	6.22	188–207
Ge I	162	155	166	151	151	162	152	5.76	151–166
TFe I	93	88	93	88	92	96	89	2.81	88–96
BFe I	105	96	100	94	97	101	95	3.61	94–105
Tr I	54	47	48	48	47	44	52	3.11	44–54
Cx I	56	51	57	58	63	64	62	4.27	51–64
Ta II (H)	18	20	19	21	22	17	17	1.81	17–22

Character	Holotype	a	b	c	d	e	f	SD	range
Ta II (L)	157	153	158	154	157	159	161	2.56	153–161
Ti II	215	198	214	204	211	216	194	8.17	194–216
Ge II	161	150	161	154	157	163	148	5.39	148–163
TFe II	95	86	85	85	91	90	84	3.78	84–95
BFe II	95	93	96	96	96	102	91	3.16	91–102
Tr II	58	54	50	53	48	51	54	3.02	48–58
Cx II	61	66	69	67	68	74	75	4.44	61–75
Ta III (H)	15	19	14	13	14	18	14	2.12	13–19
Ta III (L)	170	167	170	165	171	169	176	3.19	165–176
Ti III	287	266	277	264	271	277	273	7.17	264–287
Ge III	161	153	164	153	156	166	156	4.87	153–166
TFe III	136	124	132	133	128	131	126	3.89	124–136
BFe III	124	119	121	120	119	128	118	3.28	118–128
Tr III	66	57	57	53	53	54	51	4.61	51–66
Cx III	66	66	67	71	72	78	66	4.20	66–78
Leg I	821	781	824	790	803	834	795	18.28	781–834
Leg II	842	800	833	813	828	855	807	18.34	800–855
Leg III	1010	952	988	959	970	1003	966	20.68	952–1010
IP	2673	2533	2645	2562	2601	2692	2568	56.05	2533–2692

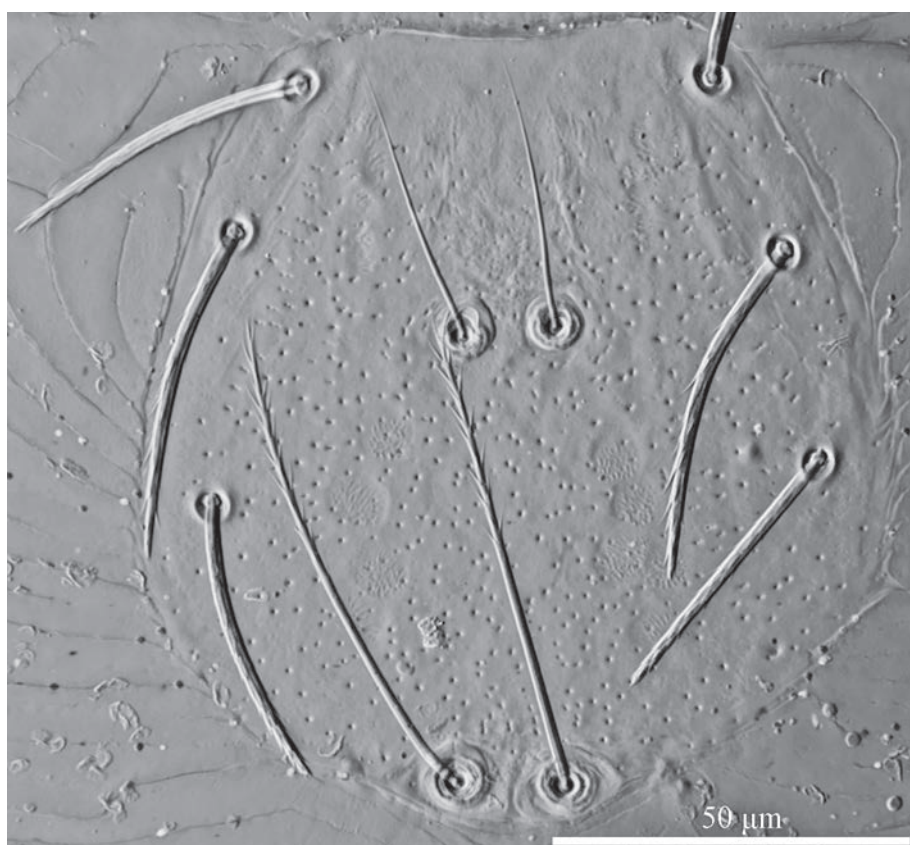


Figure 3. *Caeculisoma taianensis* sp. nov., larva photograph. Scutum, showing the shape of scutum, ASE and PSE.

Material examined. Holotype. CHINA • a larva (1087–0275-YN-yl); Yun-nan Province, Yulong County, Taian Town; 26°37'8"N, 100°02'9"E; 2502 m; 8 Aug. 2021; Yan Jiang leg.; from *Atkinsoniella* sp. (Hemiptera, Cicadellidae). **Paratypes** CHINA • one larva (1088–0275-YN-yl), same data as the holotype. China • three larvae (1082–0271-YN-yl, 1083–0271-YN-yl, 1084–0271-YN-yl);

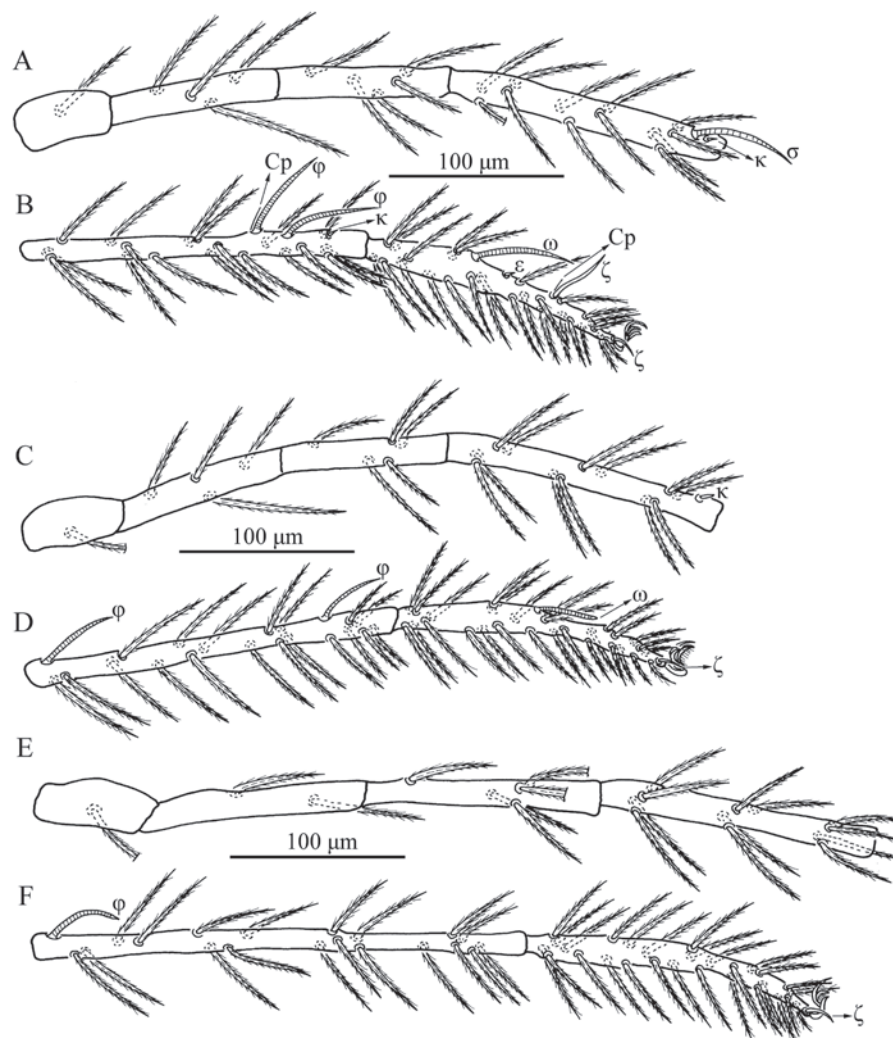


Figure 4. *Caeculisoma taianensis* sp. nov., larva. Leg I **A** trochanter–genu **B** tibia–tarsus; leg II **C** trochanter–genu **D** tibia–tarsus; leg III **E** trochanter–genu **F** tibia–tarsus.

Yunnan Province, Yulong County, Taian Town; 26°37'8"N, 100°02'9"E; 2502 m; 8 Aug. 2021; Yan Jiang leg.; from unidentified *Atkinsoniella* (Hemiptera: Cicadellidae). China • one larva (1085–0272-YN-yl); Yunnan Province, Yulong County, Taian Town; 26°37'8"N, 100°02'9"E; 2502 m; 8 Aug. 2021; Yan Jiang leg.; from an unknown nymph of Cicadellidae. China • one larva (1086–0273-YN-yl); Yunnan Province, Yulong County, Taian Town; 26°37'8"N, 100°02'9"E; 2502 m; 8 Aug. 2021; Yan Jiang leg.; from an unidentified nymph of Cicadellidae.

The holotype and paratypes are deposited in the Institute of Entomology, Guizhou University, Guiyang, China (GUGC).

Remarks. Based on the description of larvae, the genus *Caeculisoma* includes 13 species so far; of them, four species are from Australia and four from China, two species are from Brazil, while the remaining three species are found in Iran, the Republic of South Africa and New Zealand, respectively (Maqol and Wohltmann 2012; Xu et al. 2020; Kohansal et al. 2024; Noei et al. 2024).

Similar species to *C. taianensis* sp. nov. are currently known as *C. darwiniense* Southcott, 1961, *C. mouldsi* Southcott, 1988, *C. pouyani* Noei & Kohansal, 2024 and *C. sparnoni* Southcott, 1972 based on the key to species of *Caeculisoma* in Kohansal et al. (2024).

The new species differs from *C. darwiniense* by the shape of ASE (nude vs barbed), posterior hypostomatae (*bs*) (nude vs barbed), galealae (*cs*) (nude vs barbed), the number of normal setae on fn Ge I–III (12-12-12 vs 11-12-13), the number of normal setae on fn Ti I–III (18-19-19 vs 17-18-20), longer L (103–114 vs 87–88), Ti I (188–207 vs 102), and Ti III (264–287 vs 143); differs from *C. mouldsi* by the shape of ASE (nude vs barbed), shape of posterior hypostomatae (nude vs barbed), gnathosoma with two pairs hypostomatae (vs one pair hypostomatae), the number of normal setae on fn Ge I–III (12-12-12 vs 12-11-12), the number of normal setae on fn Ti I–III (18-19-19 vs 18-19-18), longer *1b* (64–74 vs 37–58), PaScFed (73–85 vs 42), leg II (800–855 vs 750), leg III (952–1010 vs 915), IP (2533–2692 vs 2455); differs from *C. pouyani* by the shape of ASE (nude vs barbed), galealae (nude vs barbed), hypostomatae (nude vs barbed), palp tarsus with five nude normal setae (vs with five barbed normal setae), longer W (97–108 vs 75–87), *1b* (64–74 vs 40–46), Ti I (188–207 vs 85–95), Ti II (194–216 vs 85–92), Ti III (264–287 vs 115–130), IP (2533–2692 vs 1360–1505) and differs from *C. sparnoni* by shape of ASE (nude vs barbed), cheliceral bases without striations (vs with lengthwise striations), longer L (103–114 vs 83), W (97–108 vs 85), *1b* (64–74 vs 28), Ta I (150–160 vs 77), Ti I (188–207 vs 83), Ta III (165–176 vs 79), Ti III (264–287 vs 100), IP (2533–2692 vs 1220).

The differences between the new species and the four present species of *Caeculisoma* found in China are as follows: *C. taianensis* sp. nov. differs from *C. alopenlineatus* by the positions of ASE (ASE closer to ML than PL vs ASE closer to PL than ML), shape of scutum (pentagonal vs oval), ASE (nude vs barbed), the longer Ti I (188–207 vs 164–170), Ti II (194–216 vs 151–161), Ti III (264–287 vs 227–239), IP (2533–2692 vs 2061–2115), the shorter ML (46–51 vs 114–120); differs from *C. hunanica* by the number of solenidia on Ti II (2 vs 1), the number of normal setae on TFe III (5 vs 4), the number of normal setae on fn Ti I–III (18-19-19 vs 16-16-18), longer leg I (781–834 vs 655), leg II (800–855 vs 621), leg III (952–1010 vs 728), IP (2533–2692 vs 2004); differs from *C. penlineatus* by ASE base location (closer to ML than PL vs in line with the level of PL), BFe I and II with four barbed setae (vs with three barbed setae and one nude seta), palptarsus with one eupathidium (vs with two eupathidia), longer Ti I (188–207 vs 143–167), Ti II (194–216 vs 150–179), Ti III (264–287 vs 213–239), leg I (781–834 vs 627–709), leg II (800–855 vs 645–724), leg III (952–1010 vs 768–878), IP (2533–2692 vs 2060–2298), data based on Xu et al. (2019b, 2020) and differs from *C. semispinus* by the shape of ASE (nude vs with barbs on distal halves), palptibia with three barbed setae (vs with one barbed seta and two nude setae), palptarsus with five nude setae (vs with two barbed setae and three nude setae), longer L (103–114 vs 78–84), W (97–108 vs 71–80), ISD (56–63 vs 41–44), Ti I (188–207 vs 149–163), Ti III (264–287 vs 213–227), IP (2533–2692 vs 2041–2100).

***Iguatonia* Haitlinger, 2004**

***Iguatonia barboproxima* sp. nov.**

<https://zoobank.org/B7AA6D5B-ADD7-4F98-9245-1789A345EFD3>

Figs 5–8

Diagnosis (larva). ASE and PL located in posterior half of scutum; ASE and PSE with fine barbs on distal halves; two pairs hypostomatae barbed; ISD 30–42.

Description. Idiosoma almost oval, with 32 (fD = 32–34 in paratypes) barbed setae, a pair of setae located between scutum and eyes at level with PSE bases (Fig. 5A). Scutum about trapezoid outline with rounded angles, wider than long, anterior margin concave, lateral margins arcuate obviously, posterior margin convex in median and with small concave between bases of PSE (Figs 6A, 7). Scutum with three pairs of normal setae (AL, ML and PL) and two pairs of sensilla (ASE and PSE). AL, ML and PL completely barbed, AL slightly shorter than PL, and ML longer than both, $PW > MW > AW$ (Table 3). ASE and PSE with setules in distal half, ASE bases posterior to PL bases, PL placed in posterior half of scutum, PSE near posterior border of scutum and longer than ASE (Fig. 6A, 7).

Venter. All ventral setae, including coxalae, barbed and with pointed ends (Fig. 5B). Dorsum of coxa I with a peg-like supracoxal seta (*elc* I) (Fig. 5C). Three pairs of intercoxal setae (*1a*, *2a* and *3a*), *1a* posterior to level of posterior edge of coxae I, *2a* between coxae II, and *3a* at a line with anterior edges of coxae III. *2a* and *3a* subequal and both slightly longer than *1a* (Table 3). Five pairs of coxalae (*1b*, *2b*₁, *2b*₂, *3b*₁ and *3b*₂), *1b* longest, *2b*₁, *3b*₁, and *2b*₂ subequal and all slightly longer than *3b*₂ (Table 3). 12 setae behind coxae III (fV = 12 in paratypes).

Gnathosoma (Fig. 6B) with a pair of nude galealae (*cs*), two barbed anterior hypostomalae (*as*) and two posterior hypostomalae with barbs on proximal half, *bs* slightly longer than *cs*, and both longer than *as* (Table 3). Hypostomal lip fimbriated. Cheliceral bases punctate on the dorsal surface (Fig. 6C). Palpfemur and palpgenu, each with one barbed, pointed dorsal seta. Palptibia with one nude ventral seta, one barbed ventral seta, and one barbed dorsal seta, odontus bifid. Palptarsus with seven setae, three barbed, two nude, one solenidion and one eupathidium. fPp = 0-B-B-2BN₂-3B2Nωζ. Palpal supracoxal seta (*elcp*) peg-like.

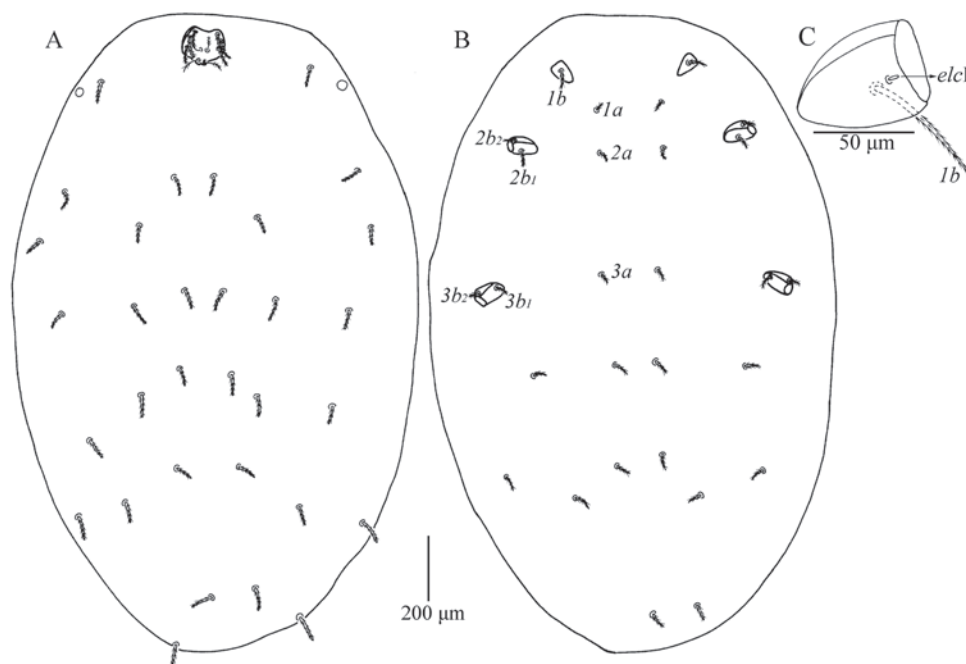


Figure 5. *Iguatonia barboproxima* sp. nov., larva **A** dorsal view of idiosoma **B** ventral view of idiosoma **C** dorsal view of coxa I, showing supracoxal seta.

Table 3. Metric and some meristic data of *Iguatonia barboproxima* sp. nov. (larvae, a–c = paratypes; a: 2024–1767-CQ-wx, b: 2025–1767-CQ-wx, c: 2026–1768-CQ-wx).

Character	Holotype	a	b	c	SD	range
fD	32	34	32	32	0.87	32–34
fV	12	12	12	12	0.00	12–12
NDV	44	46	44	44	0.87	44–46
IL	1928	1998	1672	1733	134.32	1672–1998
IW	1213	1320	1366	1276	56.45	1213–1366
DS	46–77	42–70	47–78	48–77	2.28–3.20	42–78
DS min.	46	42	47	48	2.28	42–48
DS max.	77	70	78	77	3.20	70–78
PDS	54–77	53–70	51–78	52–77	1.12–3.20	51–78
PDS min.	54	53	51	52	1.12	51–54
PDS max.	77	70	78	77	3.20	70–78
Oc	20	20	21	23	1.22	20–23
1a	24	28	25	26	1.48	24–28
2a	32	37	34	37	2.12	32–37
3a	33	31	34	34	1.22	31–34
1b	54	63	55	65	4.82	54–65
2b ₁	42	40	41	44	1.48	40–44
2b ₂	40	39	40	39	0.50	39–40
3b ₁	40	39	40	42	1.09	39–42
3b ₂	34	34	37	36	1.30	34–37
L	103	100	109	106	3.35	100–109
W	124	123	137	130	5.59	123–137
AW	72	70	81	77	4.30	70–81
MW	91	88	98	97	4.15	88–98
PW	99	98	109	104	4.39	98–109
MA	60	59	63	62	1.58	59–63
AA	14	15	16	16	0.83	14–16
SB	14	14	18	17	1.79	14–18
ISD	30	34	42	37	4.38	30–42
AP	47	47	56	60	5.68	47–60
AL	56	53	61	59	3.03	53–61
ML	70	68	76	71	2.95	68–76
PL	59	57	64	62	2.69	57–64
ASE	44	46	46	45	0.83	44–46
PSE	55	59	66	61	3.96	55–66
as	18	16	15	20	1.92	15–20
bs	37	35	37	41	2.18	35–41
cs	32	34	31	35	1.58	31–35
PaScFed	81	76	77	80	2.06	76–81
PaScGed	41	37	46	40	3.24	37–46
GL	136	146	137	141	3.94	136–146
Ta I (H)	18	19	19	19	0.43	18–19
Ta I (L)	159	154	147	157	4.55	147–159
Ti I	167	166	163	166	1.50	163–167
Ge I	135	133	131	135	1.66	131–135
TFe I	83	82	78	78	2.28	78–83
BFe I	89	90	89	91	0.83	89–91
Tr I	50	51	56	51	2.35	50–56
Cx I	73	66	67	63	3.63	63–73
Ta II (H)	19	16	18	18	1.09	16–19

Character	Holotype	a	b	c	SD	range
Ta II (L)	150	147	143	152	3.39	143–152
Ti II	178	169	165	174	4.92	165–178
Ge II	132	130	127	132	2.05	127–132
TFe II	74	74	72	79	2.59	72–79
BFe II	91	86	88	89	1.80	86–91
Tr II	60	56	57	57	1.50	56–60
Cx II	81	86	78	79	3.08	78–86
Ta III (H)	17	16	17	19	1.09	16–19
Ta III (L)	165	164	154	163	4.39	154–165
Ti III	252	251	246	254	2.95	246–254
Ge III	150	144	139	147	4.06	139–150
TFe III	115	117	118	111	2.68	111–118
BFe III	117	120	121	114	2.74	114–121
Tr III	67	61	56	54	5.02	54–67
Cx III	80	86	86	77	3.90	77–86
Leg I	756	742	731	741	8.90	731–756
Leg II	766	748	730	762	14.10	730–766
Leg III	946	943	920	920	12.30	920–946
IP	2468	2433	2381	2423	31.01	2381–2468

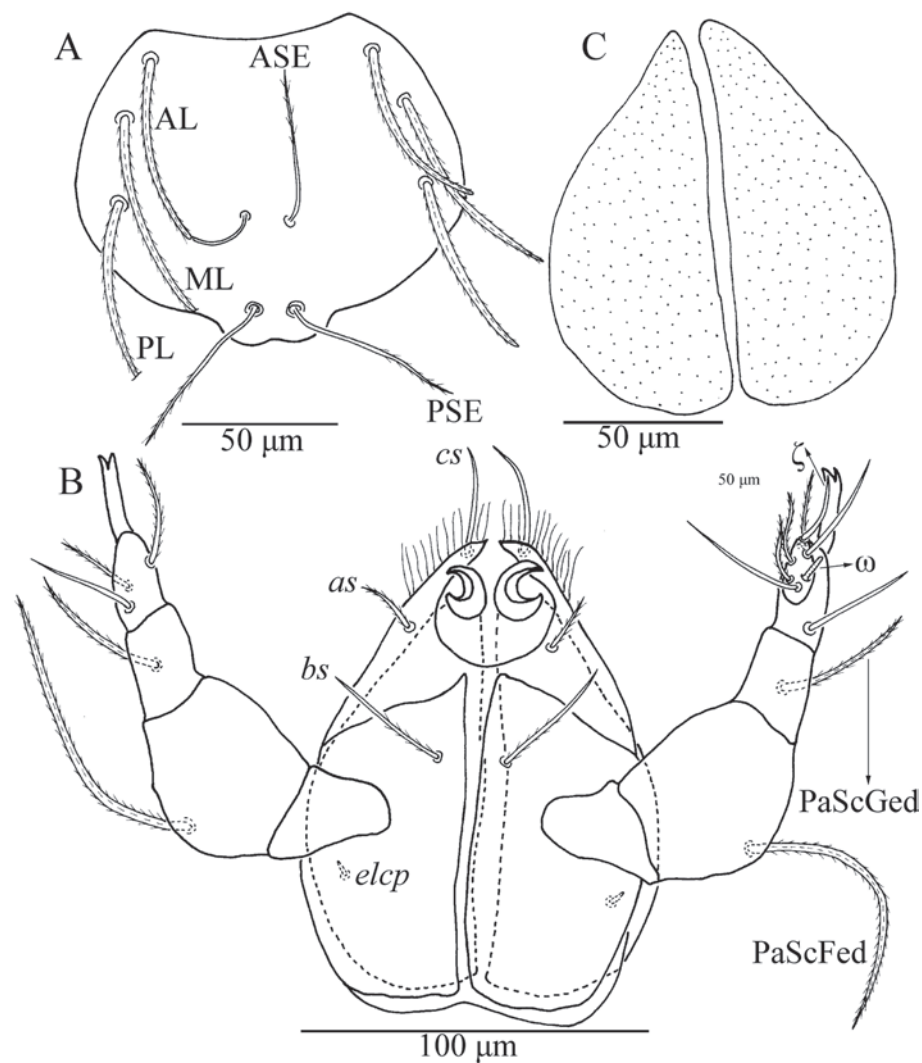


Figure 6. *Iguatonia barboproxima* sp. nov., larva **A** scutum **B** ventral view of gnathosoma **C** dorsal view of the cheliceral bases.



Figure 7. *Iguatonia barboproxima* sp. nov., larva photograph. Scutum, showing the shape of scutum, ASE and PSE.

Legs (Figs 5B, 8) with seven segments (femora divided). IP = 2381–2468 (Holotype and three paratypes) (Table 3). Anterior and posterior claws hook-like, subequal in length, and anterior claw with few ciliations. Claw-like empodium falciform, longer and slenderer than lateral claws. Normal setae on legs barbed and pointed. Leg setal formula: Leg I: Cx–1n; Tr–1n; Bfe–4n; Tfe–5n; Ge–1 σ , 1 κ , 12n; Ti–2 ϕ , 1 κ , 1Cp, 18n; Ta–1 ω , 1 ϵ , 2 ζ , 1Cp, 29n. leg II: Cx–2n; Tr–1n; Bfe–4n; Tfe–5n; Ge–1 κ , 12n; Ti–2 ϕ , 19n; Ta–1 ω , 1 ζ , 30n. leg III: Cx–2n; Tr–1n; Bfe–2n; Tfe–5n; Ge–12n; Ti–1 ϕ , 19n; Ta–1 ζ , 30n.

Etymology. The specific epithet of the new species refers to the posterior hypostomalae, which exhibit fine barbs on their proximal half.

Material examined. **Holotype** CHINA • a larva (2023–1767-CQ-wx); Chongqing Municipality, Wuxi County, Shuangyang Town; 31°31'29"N, 109°50'12"E; 1151 m; 30 Jun. 2022; Yan Jiang leg.; from an unidentified nymph of Cicadellidae (Hemiptera). **Paratypes** CHINA • two larvae (2024–1767-CQ-wx, 2025–1767-CQ-wx), the same data as the holotype. China • one larva (2026–1768-CQ-wx); Chongqing Municipality, Wuxi County, Shuangyang Town; 31°29'28"N, 109°49'44"E; 1132 m; 30 Jun. 2022; Xiao-Li Xu leg.; from an unidentified nymph of Cicadellidae (Hemiptera).

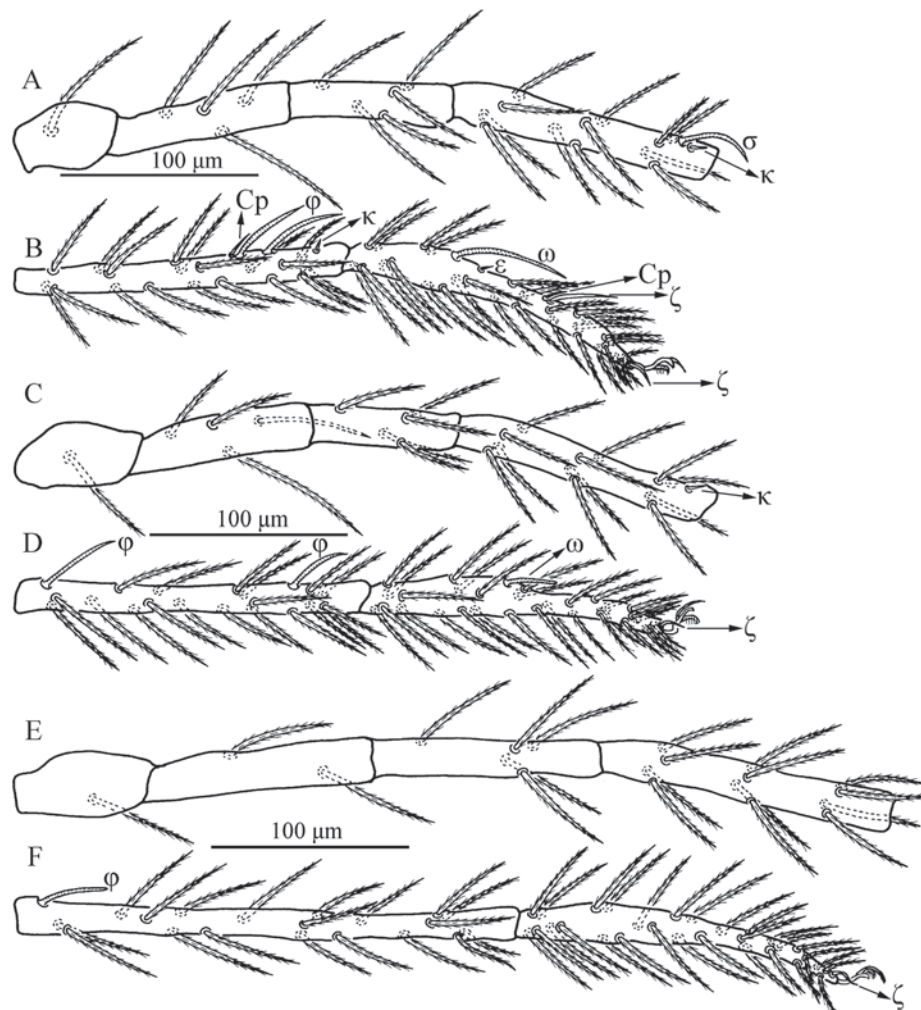


Figure 8. *Iguatonia barboproxima* sp. nov., larva. Leg I **A** trochanter—genus **B** tibia—tarsus; leg II **C** trochanter—gen **D** tibia—tarsus; leg III **E** trochanter—genus **F** tibia—tarsus.

The holotype and paratypes are deposited in the Institute of Entomology, Guizhou University, Guiyang, China (GUGC).

Remarks. To date, two species of *Iguatonia* have been documented based on larvae, one from Brazil and another one from China (Haitlinger 2004; Noei et al. 2024; Xu et al. 2020).

Iguatonia barboproxima sp. nov. differs from *I. barbillae* by the shape of scutum (about trapezoid vs quadrilateral), PL location (in posterior half of scutum vs in anterior half of scutum), ASE location (closer to PL than PSE vs far from PL and near PSE), longer ISD (30–42 vs 10), Ti I (163–167 vs 76–78), and Ti III (246–254 vs 116–126) and differs from *I. xinfengi* by the shape of scutum (about trapezoid vs sub-rounded), shape of hypostomatae (barbed vs nude), positions of ASE (far from PL and closer to PL than PSE vs almost at the same line with PL), longer ISD (30–42 vs 20–21), Ti I (163–167 vs 114–117), and Ti III (246–254 vs 194–197).

Discussion

Considering previously published data and the present study, 13 species of *Caeculisoma* have been documented based on the larval stage and one species was recorded based on both the larval and post-larval instars. Of them,

only five species (*C. brazilensis* Noei & Šundić, 2024; *C. carmenae* Haitlinger, 2008; *C. nestori* Haitlinger, 2004; *C. hunanica* Zheng, 2002; and *C. sparnoni* Southcott, 1972) are without host records (Southcott 1972; Zheng 2002b; Haitlinger 2004, 2008; Kohansal et al. 2024; Noei et al. 2024). The hosts of *Caeculisoma* larvae were recorded in Insecta, comprising three orders (Lepidoptera, Orthoptera, Hemiptera), and seven families (Acrididae, Cicadellidae, Cicadidae, Delphacidae, Geometridae, Issidae, Miridae) (Southcott 1961, 1972, 1988; Stroiński et al. 2013, Xu et al. 2019a, b, 2020; Kohansal et al. 2024). Only *C. pouyani* Noei & Kohansal, 2024 has a host distribution across three families (Acrididae, Cicadellidae, Miridae) in two orders (Hemiptera, Orthoptera); and *C. penlineatus* Xu & Jin, 2019 has a host distribution across three families (Cicadellidae, Delphacidae and Issidae). And the host of each of the remaining species was only recorded in a single family: three species (*C. allopenlineatus* Xu & Jin, 2020; *C. semispinus* Xu & Jin, 2019; *C. taianensis* sp. nov.) with hosts were recorded in Cicadellidae (Hemiptera), two species (*C. cooremani* Southcott, 1972; *C. darwiniense* Southcott, 1961) with hosts were recorded in Acrididae (Orthoptera), *C. mouldsi* Southcott, 1988 with a host was recorded in Cicadidae (Hemiptera), and *C. huxleyi* Southcott, 1972 with a host was recorded in Geometridae (Lepidoptera). According to the available data, there is a higher probability of finding larvae of the genus *Caeculisoma* ectoparasitic on Hemiptera compared to Orthoptera and Lepidoptera.

Iguatonia barbilla Haitlinger, 2004 from an unidentified Homoptera insect (Hemiptera), *I. xinfengi* Xu & Jin, 2020 from an unknown Delphacidae (Hemipteran) and *I. barboproxima* sp. nov. from an unidentified Cicadellidae species (Hemiptera) indicate that the host's spectrum of *Iguatonia* species is limited to the order Hemiptera.

Only three families of Hemiptera, including Cicadellidae, Delphacidae and Issidae were documented in China for *Caeculisoma* hosts. A similar situation occurs in the genus *Iguatonia*, whose hosts are from two families (Cicadellidae, Delphacidae) of Hemiptera.

According to the present information of these two genera the hosts are limited, which may be related to the locations, times, and methods of collection. Therefore, in future studies of their taxonomy, more attention should be paid to geographical ranges and the use of diverse collection methods at different periods in order to know more about the host.

Acknowledgments

We sincerely thank the editor and reviewers for their time, effort, and valuable suggestions during the review process. Their insightful comments and constructive suggestions greatly improved the quality and clarity of our manuscript.

Additional information

Conflict of interest

The authors have declared that no competing interests exist.

Ethical statement

No ethical statement was reported.

Funding

This work was supported by the National Natural Science Foundation of China (32300373, 32470478).

Author contributions

Data curation: TCY. Investigation: YJ. Resources: SYX. Supervision: DCJ. Writing - original draft: YJ. Writing - review and editing: SYX, DCJ.

Author ORCIDs

Yan Jiang  <https://orcid.org/0000-0002-8980-5344>

Tian-Ci Yi  <https://orcid.org/0000-0002-9953-3709>

Si-Yuan Xu  <https://orcid.org/0000-0001-6467-6120>

Dao-Chao Jin  <https://orcid.org/0000-0003-2727-5621>

Data availability

All of the data that support the findings of this study are available in the main text.

References

- Haitlinger R (2004) *Charletonia domawiti* n. sp., *Caeculisoma nestori* n. sp. and *Iguatonia barbilla* n. gen. and n. sp. from Brazil (Acari: Prostigmata: Erythraeidae). *Genus* 15(3): 435–444.
- Haitlinger R (2006) Eight new species and new records of mites (Acari: Prostigmata: Erythraeidae, Trombidiidae, Johnstonianidae) from China including Macao. *Systematic and Applied Acarology* 11: 83–105. <https://doi.org/10.11158/saa.11.1.11>
- Han B, Ouyang ZY, Xu WH, Xiao J, Jiang MK, Wang Z, Qin WH (2008) The effect of protecting species diversity in Southwest China. *Acta Ecologica Sinica* 28(9): 4589–4593. [In Chinese with English abstract]
- Kohansal M, Noei J, Ramroodi S, Rakhshani E (2024) First record of larval *Caeculisoma* (Acari: Erythraeidae) from Iran with description a new species. *Acarologia* 64(4): 1182–1190. <https://doi.org/10.24349/j8kk-8r4k>
- Mąkol J, Wohltmann A (2012) An annotated checklist of terrestrial Parasitengona (Actinotrichida: Prostigmata) of the world, excluding Trombiculidae and Walchiidae. *Annales Zoologici* 62 (3): 359–562. <https://doi.org/10.3161/000345412X656671>
- Noei J, Šundić M, Bernardi LFO (2024) A new species of larval *Caeculisoma* (Trombidiformes: Erythraeidae) from Brazil with a key to species. *Systematic and Applied Acarology* 29(10): 1437–1448. <https://doi.org/10.11158/saa.29.10.10>
- Saboori A, Starý J, Masoumi H, Cakmak I (2023) Two new species of *Caeculisoma* (Trombidiformes: Erythraeidae) from Madagascar. *Acarologia* 63(4): 1225–1259. <https://doi.org/10.24349/vqaa-42d1>
- Shi XW, Zhang L, Zhang JJ, Ouyang ZY, Xiao Y (2018) Priority area of biodiversity conservation in Southwest China. *Chinese Journal of Ecology* 37(12): 3721–3728. [In Chinese with English abstract]
- Southcott RV (1961) Notes on the genus *Caeculisoma* (Acarina: Erythraeidae) with comments on the biology of the Erythraeoidea. *Transactions of the Royal Society of South Australia* 84: 163–178.
- Southcott RV (1972) Revision of the larvae of the tribe Callidosomatini (Acarina: Erythraeidae) with observations on post-larval instars. *Australian Journal of Zoology* 20(13): 1–84. <https://doi.org/10.1071/AJZS013>

- Southcott RV (1988) Two new larval mites (Acarina: Erythraeidae) ectoparasitic on north Queensland Cicadas. *Records of the South Australian Museum* 22(2): 103–116.
- Stroiński A, Felska M, Mąkol J (2013) A review of host-parasite associations between terrestrial Parasitengona (Actinotrichida: Prostigmata) and bugs (Hemiptera). *Annales Zoologici* 63(2): 195–221. <https://doi.org/10.3161/000345413X669522>
- Walter DE, Krantz GW (2009) Collection, rearing and preparing specimens. In: Krantz GW, Walter DE (Eds) *A manual of Acarology* 3rd edn. Lubbock, Texas Tech University Press, 83–97.
- Wohltmann A, Gabrys G, Mąkol J (2007) Terrestrial Parasitengona inhabiting transient biotopes. In: Gerecke R (Ed.) *Süßwasserfauna Mitteleuropas*, Vol. 7/2-1, Chelicerata, Acari I. Spektrum Elsevier, München, 158–240. https://doi.org/10.1007/978-3-662-55958-1_6
- Xu SY, Yi TC, Jin DC (2017) A new species of larval *Marantelophus* (Acari: Prostigmata: Erythraeidae) parasitic on insects from China. *Systematic and Applied Acarology* 22(7): 1012–1021. <https://doi.org/10.11158/saa.22.7.9>
- Xu SY, Yi TC, Guo JJ, Jin DC (2019a) A new species of larval *Caeculisoma* (Acari: Erythraeidae: Callidosomatinae) ectoparasitic on insects from China and a revised generic diagnosis. *Zootaxa* 4604(3): 511–524. <https://doi.org/10.11646/zootaxa.4604.3.7>
- Xu SY, Yi TC, Guo JJ, Jin DC (2019b) A new species of larval *Caeculisoma* (Acari: Erythraeidae) parasitic on cicadas from China with detailed comparison of all larval members in the genus. *Systematic and Applied Acarology* 24(4): 560–571. <https://doi.org/10.11158/saa.24.4.3>
- Xu SY, Yi TC, Guo JJ, Jin DC (2020) Four new species of larval Callidosomatinae (Acari: Prostigmata: Erythraeidae) and a newly recorded genus *Iguatonia* from China with notes on generic concept. *Systematic and Applied Acarology* 25(2): 285–326. <https://doi.org/10.11158/saa.25.2.9>
- Xu SY, Yi TC, Guo JJ, Jin DC (2021) *Abrolophus diaoluensis* sp. nov. (Acari: Prostigmata: Erythraeidae) from a jungle of Hainan Island. *International Journal of Acarology* 47(1): 23–34. <https://doi.org/10.1080/01647954.2020.1866667>
- Xu SY, Jin DC, Guo JJ, Yi TC (2022a) Four new species of larval Erythraeoidea (Acari: Trombidiformes: Prostigmata) and three higher taxa new to China: Genus *Hirstiosoma* and subfamily Hirstiosomatinae (Smarididae), and genus *Grandjeanella* (Erythraeidae: Abrolophinae). *Systematic and Applied Acarology* 27(9): 1813–1840. <https://doi.org/10.11158/saa.27.9.10>
- Xu SY, Yi TC, Guo JJ, Jin DC (2022b) Four new species of larval *Charletonia* and *Leptus* (Acari: Trombidiformes: Erythraeidae), with a checklist of the two genera and their hosts from China. *Insects* 13(12): 1154. <https://doi.org/10.3390/insects13121154>
- Xu SY, Yi TC, Guo JJ, Jin DC (2023) Two new erythraeid mites (Acari: Trombidiformes Erythraeidae) from China: one based on larvae, another one based on larvae and adult. *Systematic and Applied Acarology* 28(6): 1056–1079. <https://doi.org/10.11158/saa.28.6.5>
- Xu SY, Yi TC, Guo JJ, Jin DC (2025) Contribution to Erythraeidae: the first finding of the genus *Balaustium* in Oriental realm and the genus *Neoabrolophus* in China based on adult mites (Acari: Trombidiformes) from Qinghai-Tibetan and Yunnan-Guizhou Plateaus, China. *Systematic and Applied Acarology* 30(1): 30–62. <https://doi.org/10.11158/saa.30.1.4>
- Zheng BY (2002a) A new species of the genus *Hauptmannia* Oudemans, 1910 from China (Acari: Erythraeidae). *Acta Zootaxonomica Sinica* 27: 89–92. [in Chinese with English abstract]
- Zheng BY (2002b) A new species of the genus *Caeculisoma* Berlese (Acari: Erythraeidae) in China. *Entomologia Sinica* 9: 61–64. <https://doi.org/10.1111/j.1744-7917.2002.tb00155.x>

Tetramorium sinensis sp. nov., a parabiotic ant from China, with a key to the *Tetramoriuminglebyi* group (Hymenoptera, Formicidae)

Benan Zhang^{1,2}, Congcong Du^{1,2}, Zhilin Chen^{1,2}

¹ Key Laboratory of Ecology of Rare and Endangered Species and Environmental Protection (Guangxi Normal University), Ministry of Education, Guilin 541006, China

² Guangxi Key Laboratory of Rare and Endangered Animal Ecology, Guangxi Normal University, Guilin 541006, China

Corresponding author: Zhilin Chen (chenzhilin35@163.com)

Abstract

In this paper, *Tetramorium sinensis* sp. nov., a parabiotic ant, is described. It was discovered within the nest of the queenless ant *Diacamma rugosum* (Le Guillou, 1842) in Fenghuang Mountain Park, Zhongshan, Guangdong Province, China. Additionally, a key to the *Tetramoriuminglebyi* group based on the worker caste is provided.

Key words: Identification key, Myrmicinae, new species, parabiosis, taxonomy

Introduction

Social Hymenoptera, including bees, wasps, and ants, exhibit a wide range of social behaviors and nesting habits. Among these are cases in which more than one species can be found in one nest. This phenomenon can be categorized into two primary types: mixed colonies and compound nests. Mixed colonies are a phenomenon where different species or populations of animals live and breed together in the same habitat, such as in social parasitism (Rabeling 2021). Compound nests are structures composed of multiple nests, which may belong to the same species or different species; the types have been classified as plesiobiosis, cleptobiosis, lestobiosis, xenobiosis, and parabiosis (Hölldobler and Wilson 1990).

The ant genus *Tetramorium* belongs to the subfamily Myrmicinae (Hymenoptera, Formicidae), and was initially proposed by Mayr in 1855, with *Formica caespitum* (Roger, 1862) designated as the type species through subsequent designation by Girard in 1879. Since that time, the classification of the various species within *Tetramorium* has become increasingly complex, with numerous junior and senior synonyms complicating the identification process (Bolton 2025).

The genus *Tetramorium* is the fourth largest within the Myrmicinae subfamily of Formicidae, encompassing 603 species that are extensively distributed across diverse biogeographic regions; notably, it lacks endemic species in the Neotropical region and is represented entirely by introduced species there (Bolton 2025). Taxonomic revision of this genus has been primarily conducted in specific regions (Bolton 1976, 1977, 1979, 1980; Radchenko 1992; Hita Garcia and Fisher 2014), and involves only certain species groups (Hita Garcia et



Academic editor: Matthew Prebus

Received: 18 September 2024

Accepted: 19 March 2025

Published: 25 April 2025

ZooBank: <https://zoobank.org/0984C28E-92BB-473C-8170-A81EE6F36072>

Citation: Zhang B, Du C, Chen Z (2025) *Tetramorium sinensis* sp. nov., a parabiotic ant from China, with a key to the *Tetramoriuminglebyi* group (Hymenoptera, Formicidae). ZooKeys 1236: 103–117. <https://doi.org/10.3897/zookeys.1236.137346>

Copyright: © Benan Zhang et al.
This is an open access article distributed under terms of the Creative Commons Attribution License (Attribution 4.0 International – CC BY 4.0).

al. 2010; Agavekar et al. 2017). Currently, *Tetramorium* is divided into 53 species groups, with most species featuring small eyes belonging to the *Tetramorium shiloense* group and the *Tetramorium inglebyi* group.

The *Tetramorium inglebyi* species group was initially recognized by Agavekar et al. (2017). This is a small species group, comprising only five species, all of which are from India. The main characteristics are small eyes and a strongly concave base of the first gastral tergite in dorsal view, which are crucial for distinguishing it from other species. The most significant characteristic of *Tetramorium sinensis* sp. nov. is its small eyes, which clearly distinguish it from other *Tetramorium* species in China. Due to the small eyes of the new species, we describe this new species as a member of the *T. inglebyi* group. A key to the *T. inglebyi* group based on the worker caste is provided.

Material and methods

Twenty-five specimens of *Tetramorium sinensis* sp. nov. were collected from Fenghuang Mountain Park, Shaxi Town, Zhongshan City, Guangdong Province, China. The type specimens of this new species have been deposited in the following repositories: (1) **GXNU** (Insect Collection, Guangxi Normal University, Guilin, Guangxi, China), (2) **SWFU** (Insect Collection, Southwest Forestry University, Kunming, Yunnan Province, China), and (3) **IZCAS** (Institute of Zoology, Chinese Academy of Sciences, Beijing, China). Morphological observations and identifications were conducted using a Nikon SMZ745 stereoscopic microscope, and photographs were taken and measurements obtained using a KEYENCE ultra-Depth of Field three-dimensional microscopy system (VHX-6000). The type specimen images of four species have been made available on the AntWeb (<http://www.antweb.org>) and *T. triangulatum* is available on the AntWiki (<http://www.antwiki.org>).

The measurement standard in this paper adheres to the definition provided by Hita Garcia and Fisher (2014). The unit of measurement is millimeters (mm), and the relevant measurement abbreviations are as follows:

- ED** (Eye diameter): Maximum diameter of eyes.
- HL** (Head length): Head in full-face view, the length from the midpoint of the anterior clypeal margin to the midpoint of the posterior margin of the head (when the midpoint of the anterior clypeal margin or the posterior margin of the head is depressed, the Central Line of the protruding part on both sides shall prevail).
- HW** (Head width): Head in full-face view, the maximum width of the head (excluding eyes).
- ML** (Mesosoma length): Mesosoma diagonal length (from the junction of the pronotum and neck to the lower end of the metapleural lobe).
- PH** (Pronotal height): Body in lateral view, the maximum height of the pronotum.
- PW** (Pronotal width): Body in dorsal view, the maximum width of the pronotum (excluding spines or denticles).
- PTL** (Petiolar node length): Maximum length of petiolar (in dorsal view).
- PTH** (Petiolar node height): Maximum height of the petiolar, excluding the subpetiolar process (in lateral view).
- PTW** (Petiolar node width): Maximum width of petiolar (in dorsal view).

- PPH** (Postpetiole height): In lateral view, the maximum height of the postpetiole.
PPL (Postpetiole length): In the dorsal view, the maximum length of the postpetiole.
PPW (Postpetiole width): In the dorsal view, the maximum width of the postpetiole.
SL (Scape length): Maximum length of antennal scape excluding globular base.
CI (Cephalic index): $HW \times 100 / HL$
DMI (Dorsal mesosoma index): $PW \times 100 / ML$
DPel (Dorsal petiole index): $PTW \times 100 / PTL$
DPpl (Dorsal postpetiole index): $PPW \times 100 / PPL$
LMI (Lateral mesosoma index): $PH \times 100 / ML$
LPel (Lateral petiole index): $PTL \times 100 / PTH$
LPpl (Lateral postpetiole index): $PPL \times 100 / PPH$
OI (Ocular index): $ED \times 100 / HW$
PeNI (Petiole node index): $PTW \times 100 / PW$
PpNI (Postpetiole node index): $PPW \times 100 / PW$
PPI (Postpetiole index): $PPW \times 100 / PTW$
SI (Scape index): $SL \times 100 / HW$

Results

List of the *Tetramorium inglebyi*-group species

- T. elisabethae* Forel, 1904
T. inglebyi Forel, 1902
T. jarawa Agavekar, Hita Garcia & Economo, 2017
T. myops Bolton, 1977
T. sinensis sp. nov.
T. triangulatum Bharti & Kumar, 2012

Description of new species

Tetramorium sinensis sp. nov.

<https://zoobank.org/420B95D7-C3EB-4FEF-A535-C343A263B327>

Figs 1, 2

Material examined. Holotype worker: CHINA • Guangdong Province, Zhongshan City, Fenghuang Mountain Park; 22°29'18"N, 113°18'32"E; elev. 35 m; in *D. rugosum* nest; 08–November–2021, Huasheng Huang leg.; No. GXNU2102704; (GXNU: GXNU2102704). **Paratype worker:** CHINA • 25 paratype workers from the same colony as the holotype (23 workers, GXNU; 1 worker, SWFU; 1 worker, IZCAS).

Diagnosis. Head in full-face view subrectangular, slightly longer than broad, long longitudinally striate from the anterior clypeal to the middle of head, lateral and posterior part of head slightly reticulate; eyes small, with 3–4 ommatidia in the greatest diameter. Mesosoma in dorsal view longitudinally sculptured, pronotum front slightly reticulate; in lateral view, distinctly dense transverse sculptured, propodeal spines short triangular and the tip straight. propodeal lobe angular. Petiole in dorsal view circular, as long as broad.

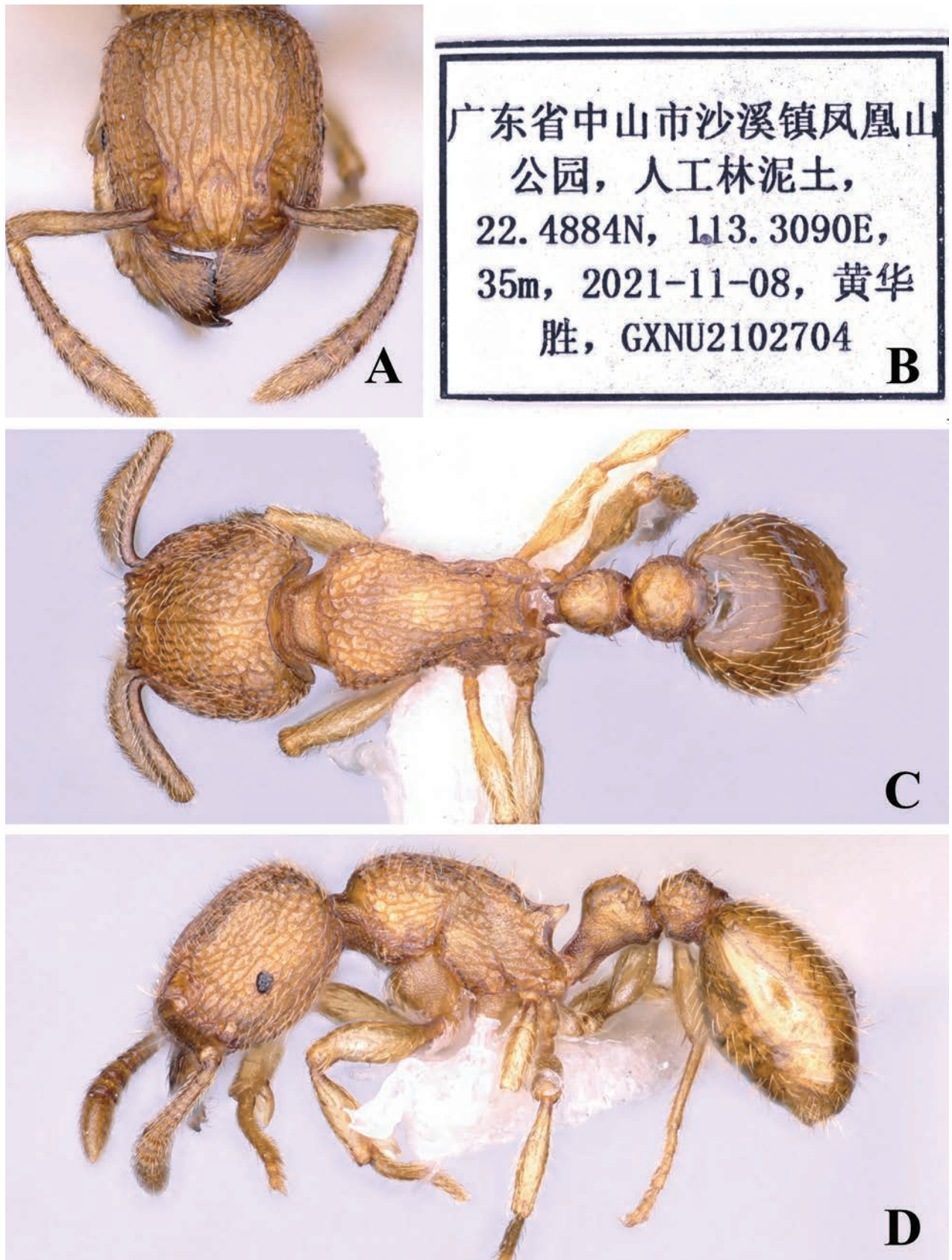


Figure 1. *Tetramorium sinensis* sp. nov., worker. Head in full-face view (A), label of holotype (B), body in dorsal view (C), body in lateral view (D).

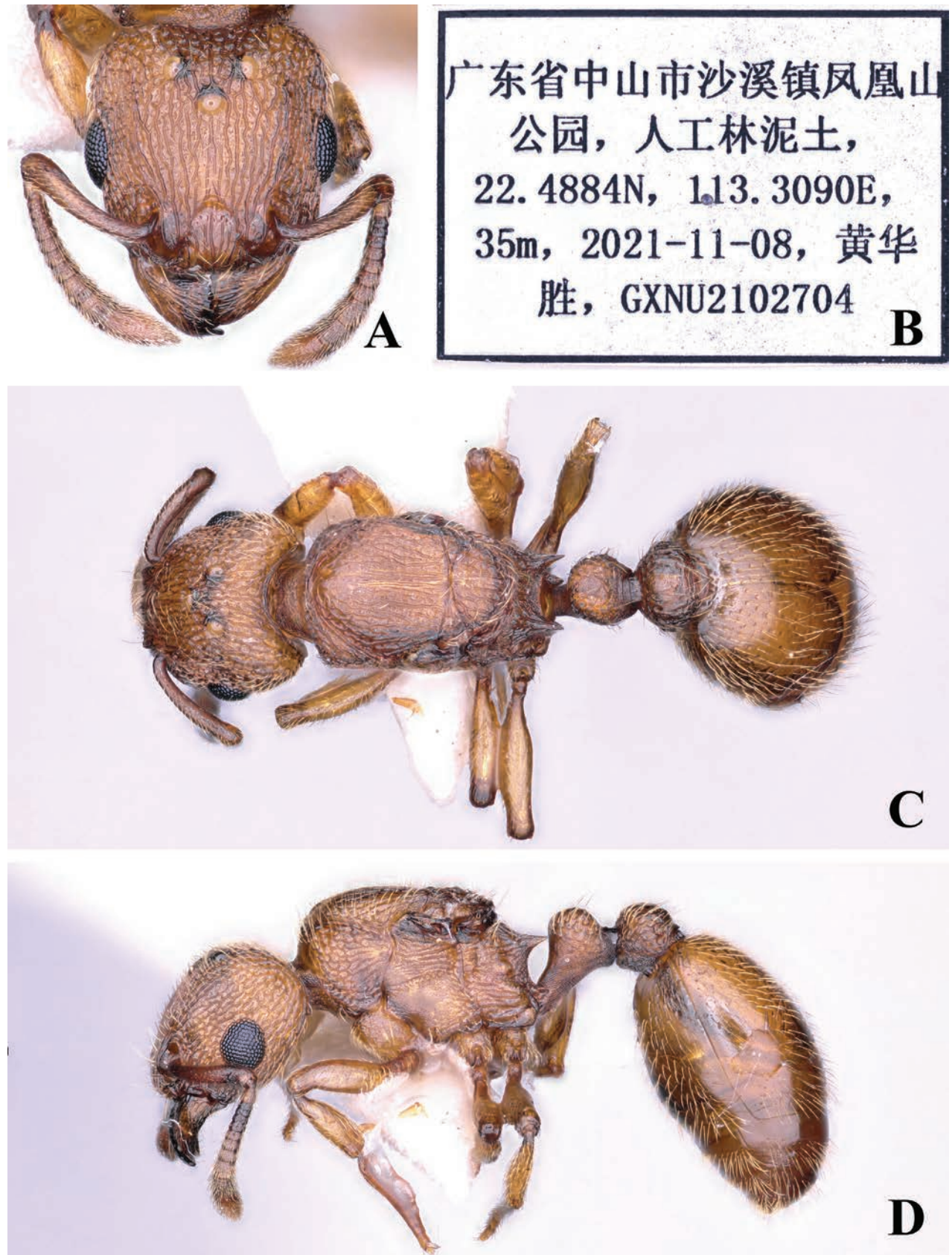


Figure 2. *Tetramorium sinensis* sp. nov., queen. Head in full-face view (A), label of holotype (B), body in dorsal view (C), body in lateral view (D).

Measurements and indices. Holotype worker ($N = 25$): **Measurements:** HL: 0.59–0.64; HW: 0.54–0.57; SL: 0.36–0.38; PH: 0.30–0.32; PW: 0.38–0.42; ML: 0.68–0.72; ED: 0.05–0.07; PTL: 0.20–0.21; PTH: 0.20–0.21; PTW: 0.19–0.20; PPH: 0.20–0.21; PPL: 0.17–0.19; PPW: 0.23–0.25. **Indices:** CI: 89.06–91.53; SI: 66.67; OI: 9.26–12.28; DMI: 55.88–58.33; LMI: 44.12–44.44; PeNI: 47.62–50.00; LPel: 100.00; Dpel: 95.00–95.24; PpNI: 59.52–60.53; LPpl: 85.00–90.48; DPpl: 131.58–135.29; PPI: 121.05–125.00.

Description. Head. Antennae with 12 segments; antennal scape slightly curved; scape reaching two-thirds of the length of the head. Head in full-face view subrectangular, slightly longer than broad, lateral margins convex, posterior margin slightly concave in middle, with posterolateral corner rounded, frontal carina short, only reaching to the middle of head. Anterior clypeus nearly straight, antennal scrobe obvious (Fig. 1A); in lateral view, the diameter of the eye less than half of the maximum diameter of the enlarged part of the antennal terminal segment (Fig. 1D).

Mesosoma. In dorsal view, lateral margins slightly convex, anterior margin convex (Fig. 1C); in lateral view, dorsal outline strongly convex, with transverse curve; promesonotal suture and metanotal groove inconspicuous; mesopleuron demarcated from pronotum by a distinct suture, but not demarcated from mesonotum and metapleuron; propodeal spines short triangular (Fig. 1D).

Metasoma. In dorsal view, petiole circular, as long as broad; lateral margins slightly convex; anterior margin convex and posterior margin slightly concave (Fig. 1C); in lateral view, petiolar node slightly convex dorsal outline, slightly higher than long, with bilateral edge sloped slightly (Fig. 1D). Postpetiole in dorsal view clearly larger than petiole, oval, lateral margins apparently convex, as long as broad (Fig. 1C); in lateral view, slightly convex dorsal outline (Fig. 1D). In dorsal view, anterior margin of gaster obviously concave (Fig. 1C).

Sculpture. Mandibles and clypeus longitudinally striate; antennal scape finely puncta; frontal area longitudinal striate, lateral and posterior part of head slightly reticulate (Fig. 1A). The pronotum reticulate, the mesonotum and metanotum longitudinally striate (Fig. 1C); the lateral sides of the mesosoma with transverse curve and sparsely puncta (Fig. 1D). Dorsum of petiole sparsely rugose (Fig. 1C). Coxa, peduncle, subpetiolar process with dense puncta (Fig. 1D). Gaster smooth and shining (Fig. 1C).

Pilosity. Body entirely covered with abundant decumbent, sub-erect, and erect hairs (Fig. 1A, C, D).

Coloration. Body brown. Antennae and legs slightly yellowish-brown (Fig. 1).

Etymology. The new species name is derived from the Latin word “Sina” (sinensis), a reference to the type locality.

Distribution. China (Guangdong).

Biology. The new species was collected multiple times from the nests of the queenless ant *Diacamma rugosum* (Le Guillou, 1842) in the soil of a plantation forest in Fenghuang Mountain Park, Shaxi Town, Zhongshan City, Guangdong Province, China. Consequently, in order to test the relationship between them, a detailed excavation of one of the nests was carried out by Huasheng Huang (Fig. 3A). Employing a hoe and pick to ascertain the direction of the ant without causing damage to the ant path whenever possible (Fig. 3C), small tools like tweezers and spoons were then used to trace the ant path (Fig. 3B). After an intensive 6-hour excavation, Huasheng Huang discovered both *D. rugosum* and

T. sinensis sp. nov. in the same nest area at a depth of 1.4 m (Fig. 4B, C). Once the shallow loose soil layer was removed, the main nest of *T. sinensis* sp. nov. became visible (Fig. 4A).

Based on observed facts, the two species share an ant canal and inhabit the same nest area; however, *T. sinensis* sp. nov. builds its own nest and broods its



Figure 3. Habitat (A), collection tools (B), and ant channels (C).

eggs, leading to the hypothesis that *T. sinensis* sp. nov. may exhibit parabiosis in the nest of *D. rugosum*. This assumption is primarily supported by the significant body type and population of *D. rugosum*, which suggests that *T. sinensis* sp. nov. is unlikely to provide sufficient food for *D. rugosum*. Therefore, we preliminarily believe that *T. sinensis* sp. nov. may feed on the food scraps left by *D. rugosum* and share the foraging trails. However, the method or pathway by which *T. sinensis* sp. nov. enters the nest of *D. rugosum* remains unclear, and long-term observation is needed to uncover this mystery.

Recognition. *Tetramorium sinensis* sp. nov. bears a resemblance to *T. jarawa* (Agavekar, Hita Garcia & Economo, 2017) due to the presence of similar longitudinal striae in the frontal area and posterior part of the head slightly reticulate in the full-face view of the head. However, it can be distinguished from the latter by the lateral sides of the mesosoma exhibiting transverse striae (while entirely reticulate punctate in *T. jarawa*), the propodeal spines short triangular, as long as broad basally and the tip straight (while the propodeal spines are long, significantly longer than broad basally and the tip upturned in *T. jarawa*). In dorsal view, the petiole of *T. sinensis* sp. nov. is as long as broad, distinguishing it from *T. jarawa* where the petiole is longer than broad.

Discussion

Tetramorium sinensis sp. nov. is found in Fenghuang Mountain Park in Guangdong Province, China. Similar to the type localities of the *T.inglebyi*-group species, this new species is situated within the Oriental Region (Holt et al. 2013). This indicates that the group extends significantly further east, beyond the confines of the Indian Subcontinent, and there remains a wealth of undiscovered species yet to be explored.

Parabiosis refers to the phenomenon where two (or more) different ant species use the same nest while keeping their broods separate (Jeanne 2021). Although this type of interaction is uncommon, a few case studies have been published. For example, *Strumigenys* (Smith, 1860) and *Diacamma* (Mayr, 1862) were found living together in a compound nest and they have a significant size difference (Kaufmann et al. 2003). Considering the distinguishing features mentioned above, the noticeable difference in body size between *T. sinensis* sp. nov. and *D. rugosum* suggests that the new species is significantly smaller than *D. rugosum*. As well as the two species inhabiting the same nest area, there is only one tunnel, and in contrast to most other species of the genus, *T. sinensis* sp. nov. has a marked vestigial eye. Therefore, our preliminary findings suggest that it is consistent with parabiotic characteristics (Vantaux et al. 2007; Emery and Tsutsui 2016). However, whether there is a parasitic relationship or some kind of ecological interaction between them and how the queen of *T. sinensis* sp. nov. infiltrates the host nest remains uncertain, which warrants detailed observation to unravel this question.

Key to members of the *Tetramoriuminglebyi*-group species based on the worker castes

- 1 Maximum diameter of the eyes longer than maximum diameter of the antennal scapes (Fig. 5A) ***T.inglebyi***
- Maximum diameter of the eyes shorter than maximum diameter of the antennal scapes **2**

- 2 In dorsal view, petiole broader than long (Fig. 8C)..... *T. elisabethae*
- In dorsal view, petiole longer than broad or as long as broad.....3
- 3 Anterior margin of clypeus concave in the middle.....4
- Anterior margin of clypeus flat or slightly convex.....5
- 4 In dorsal view, head reticulated rugose, petiole longer than broad (Fig. 6C)..... *T. myops*
- In dorsal view, head longitudinal rugose, petiole as long as broad (Fig. 7C)..... *T. triangulatum*
- 5 In lateral view, mesosoma very reticulate-punctate (Fig. 9D); in dorsal view, petiole longer than broad (Fig. 9C)..... *T. jarawa*
- In lateral view, mesosoma with a dense transverse striation (Fig. 1D); in dorsal view, petiole as long as broad (Fig. 1C)..... *T. sinensis* sp. nov.

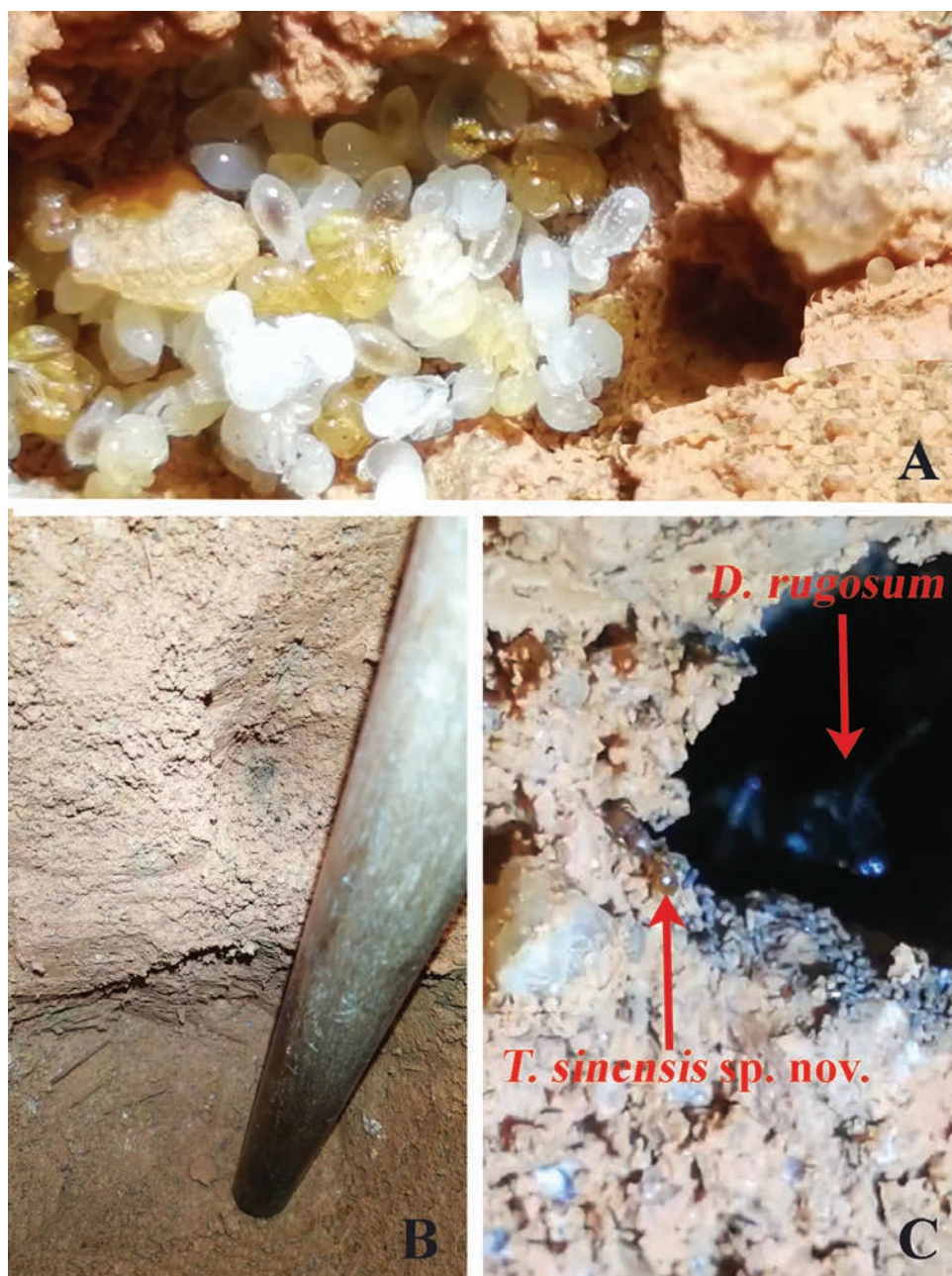


Figure 4. The nest of parabiotic ants (A), nest depth (B), *Tetramorium sinensis* sp. nov. and *Diacamma rugosum* (C).



Figure 5. *Tetramorium inglebyi*, worker. Head in full-face view (A), label of paratype (B), body in dorsal view (C), body in lateral view (D). Images sourced from AntWeb (2023) online at <https://www.antweb.org>.



Figure 6. *Tetramorium myops*, worker. Head in full-face view (A), label of paratype (B), body in dorsal view (C), body in lateral view (D). Images sourced from AntWeb (2023) online at <https://www.antweb.org>.



Figure 7. *Tetramorium triangulatum*, worker. Head in full-face view (A), body in lateral view (B), body in dorsal view (C). Images sourced from AntWiki (2023) online at <https://www.antwiki.org>.

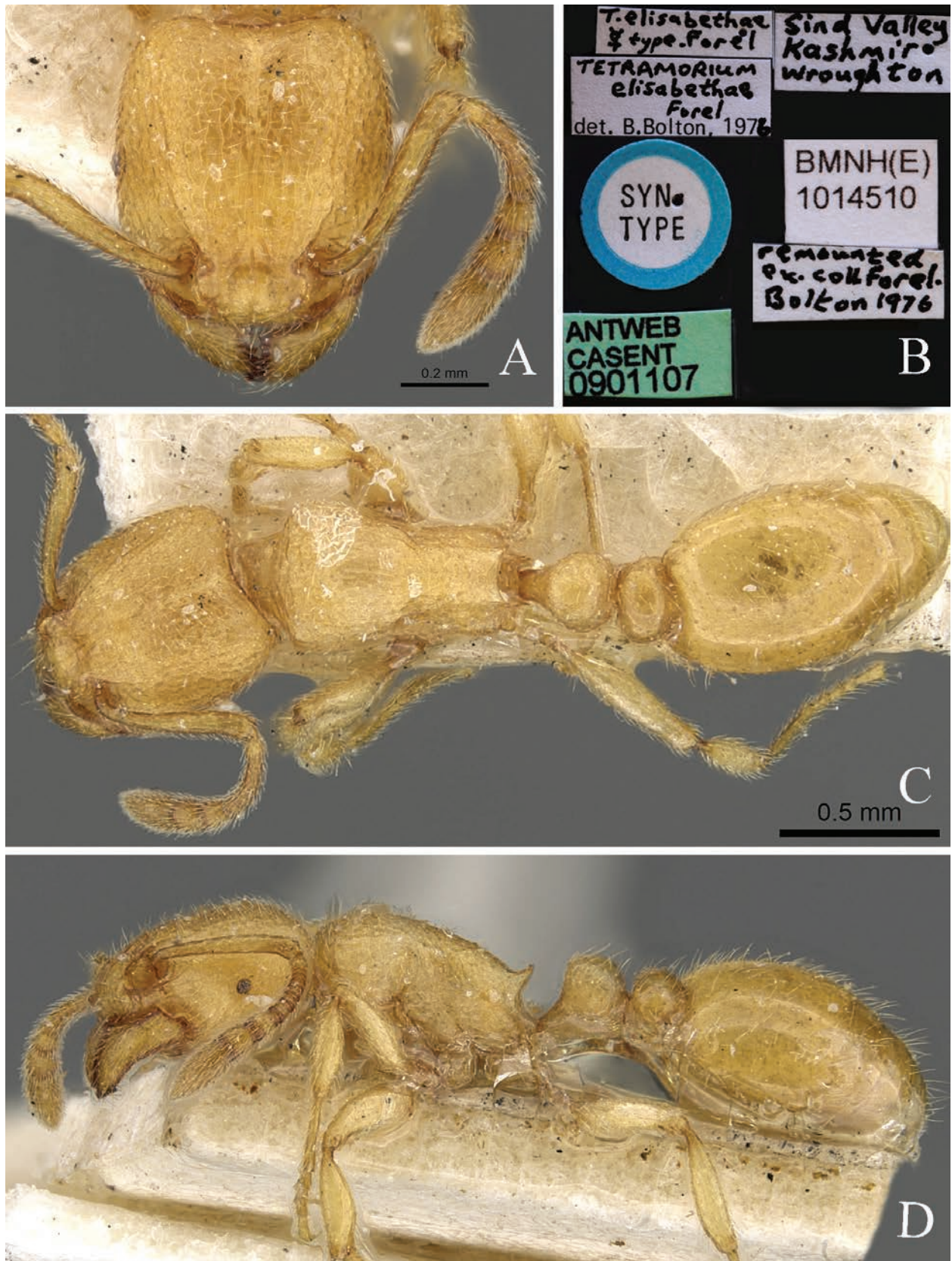


Figure 8. *Tetramorium elisabethae*, worker. Head in full-face view (A), label of syntype (B), body in dorsal view (C), body in lateral view (D). Images sourced from AntWeb (2023) online at <https://www.antweb.org>.



Figure 9. *Tetramorium jarawa*, worker. Head in full-face view (A), body in dorsal view (B), body in lateral view (C). Images sourced from AntWeb (2023) online at <https://www.antweb.org>.

Acknowledgments

We extend our gratitude to the California Academy of Sciences (San Francisco) for granting permission to use images of *Tetramorium* Mayr, 1855, from the AntWeb.

Additional information

Conflict of interest

The authors have declared that no competing interests exist.

Ethical statement

No ethical statement was reported.

Funding

This study received support from the National Natural Science Foundation of China (Grant No. 32360127), the Natural Science Foundation of Guangxi (2022GXNS-FAA035524), the National Animal Collection Resource Center of China, the Key Laboratory of Ecology of Rare and Endangered Species and Environmental Protection (Guangxi Normal University) under the Ministry of Education, and the Guangxi Key Laboratory of Rare and Endangered Animal Ecology (Guangxi Normal University).

Author contributions

All authors have contributed equally.

Author ORCIDs

Benan Zhang  <https://orcid.org/0000-0001-8427-7450>

Congcong Du  <https://orcid.org/0000-0002-8078-4751>

Zhilin Chen  <https://orcid.org/0000-0001-6564-1528>

Data availability

All of the data that support the findings of this study are available in the main text.

References

- Agavekar G, Hita Garcia F, Economo EP (2017) Taxonomic overview of the hyperdiverse ant genus *Tetramorium* Mayr (Hymenoptera, Formicidae) in India with descriptions and X-ray microtomography of two new species from the Andaman Islands. *PeerJ* 5: e3800 [50 pp.]. <https://doi.org/10.7717/peerj.3800>
- AntWeb (2024) Version 8.103.2. California Academy of Science. <https://www.antweb.org> [Accessed 13 Sep. 2024]
- AntWiki (2024) Electronic file. <https://www.antwiki.org> [Accessed 13 Sep. 2024]
- Bolton B (1976) The ant tribe Tetramoriini (Hymenoptera: Formicidae). Constituent genera, review of smaller genera and revision of *Triglyphothrix* Forel. *Bulletin of the British Museum (Natural History). Entomology* 34: 281–379.
- Bolton B (1977) The ant tribe Tetramoriini (Hymenoptera: Formicidae). The genus *Tetramorium* Mayr in the Oriental and Indo-Australian regions, and in Australia. *Bulletin of the British Museum (Natural History). Entomology* 36: 67–151.
- Bolton B (1979) The ant tribe Tetramoriini (Hymenoptera: Formicidae). The genus *Tetramorium* Mayr in the Malagasy region and in the New World. *Bulletin of the British Museum (Natural History). Entomology* 38: 129–181.
- Bolton B (1980) The ant tribe Tetramoriini (Hymenoptera: Formicidae). The genus *Tetramorium* Mayr in the Ethiopian zoogeographical region. *Bulletin of the British Museum (Natural History). Entomology* 40: 193–384.
- Bolton B (2025) An online catalog of the ants of the world. <https://antcat.org> [accessed 27 Feb. 2025]
- Emery VJ, Tsutsui ND (2016) Differential sharing of chemical cues by social parasites versus social mutualists in a three-species symbiosis. *Journal of Chemical Ecology* 42: 277–285. <https://doi.org/10.1007/s10886-016-0692-0>
- Forel A (1902) Myrmicinae nouveaux de l'Inde et de Ceylan. *Revue Suisse de Zoologie* 10:165–249. <https://doi.org/10.5962/bhl.part.13792>
- Forel A (1904) Miscellanea myrmécologiques. *Revue Suisse de Zoologie* 12: 1–52.
- Girard M (1879) *Traité élémentaire d'entomologie*. Vol. 2. Paris: Librairie J.-B. Baillière et Fils, 1028 pp.
- Hita Garcia F, Fisher BL (2014) The ant genus *Tetramorium* Mayr in the Afrotropical region (Hymenoptera, Formicidae, Myrmicinae): synonymisation of *Decamorium* Forel under *Tetramorium*, and taxonomic revision of the *T. decem* species group. *ZooKeys* 411: 67–103. <https://doi.org/10.3897/zookeys.411.7260>
- Hita Garcia F, Fischer G, Peters MK (2010) Taxonomy of the *Tetramorium weitzeckeri* species group (Hymenoptera: Formicidae) in the Afrotropical zoogeographical region. *Zootaxa* 2704: 1–90. <https://doi.org/10.11646/zootaxa.2704.1.1>
- Hölldobler B, Wilson EO (1990) *The ants*. Cambridge, Mass. Harvard University Press, [xii+]732 pp. <https://doi.org/10.1007/978-3-662-10306-7>

- Holt BG, Lessard JP, Borregaard KM, Fritz SA, Araújo MB, Dimitrov D, Fabre P, Graham CH, Graves GR, Jønsson KA, Nogués-Bravo D, Wang ZH, Whittaker RJ, Fjeldså J, Rahbek C (2013) An Update of Wallace's Zoogeographic Regions of the World. *Science* 339: 74–78. <https://doi.org/10.1126/science.1228282>
- Jeanne RL (2021) Nesting Associations Among Social Insects. In: Starr CK (Ed.) *Encyclopedia of Social Insects*. Springer, Cham. https://doi.org/10.1007/978-3-030-28102-1_86
- Kaufmann E, Malsch AKF, Erle M, Maschwitz U (2003) Compound nesting of *Strumigenys* sp. (Myrmicinae) and *Diacamma* sp. (Ponerinae), and other nesting symbioses of myrmicine and ponerine ants in southeast Asia. *Insectes Sociaux* 50: 88–97 <https://doi.org/10.1007/s000400300014>
- Mayr G (1855) *Formicina austriaca*. Beschreibung der bisher im österreichischen Kaiserstaate aufgefundenen Ameisen, nebst Hinzufügung jener in Deutschland, in der Schweiz und in Italien vorkommenden Arten. *Verhandlungen der Zoologisch-Botanischen Vereins in Wien* 5: 273–478.
- Rabeling C (2021) Social parasitism. *Encyclopedia of social insects*, 836–858. https://doi.org/10.1007/978-3-030-28102-1_175
- Radchenko AG (1992) Ants of the genus *Tetramorium* (Hymenoptera, Formicidae) of the USSR fauna. Report 1. *Zoologicheskii Zhurnal* 71(8): 39–49. [In Russian.]
- Roger J (1862) *Synonymische Bemerkungen*. 1. Ueber Formiciden. *Berliner Entomologische Zeitschrift* 6: 283–297. <https://doi.org/10.1002/mmnd.47918620122>
- Smith F (1860) Descriptions of new genera and species of exotic Hymenoptera. *Journal of Entomology* 1: 65–84.
- Vantaux A, Dejean A, Dor A, Orivel J (2007) Parasitism versus mutualism in the ant-garden parabiosis between *Camponotus femoratus* and *Crematogaster levior*. *Insectes Sociaux* 54: 95–99. <https://doi.org/10.1007/s00040-007-0914-0>

New data on the scale insect (Hemiptera, Coccoomorpha) fauna of Iceland, with description of a new species

Kornél Gerő¹, Matthías Alfreðsson², Éva Szita¹

¹ National Laboratory for Health Security, Plant Protection Institute, Centre for Agricultural Research, HUN-REN, H-2462 Martonvásár, Brunszvik u. 2, Budapest, Hungary

² Náttúrufræðistofnun, Natural Science Institute of Iceland, Urriðaholtstræti 6-8, 210 Garðabær, Iceland

Corresponding author: Éva Szita (szita.eva@atk.hun-ren.hu)

Abstract

This study adds seven species to the scale insect species list of Iceland, bringing the total number of recorded species to 15. Of these, 10 species can be considered as a part of the country checklist with breeding populations in Iceland (seven species can be found in outdoor conditions and three live indoors). An additional five species were recorded on imported fruits and most probably are not established in Iceland. A new species, *Trionymus icelandensis* Gerő & Szita, **sp. nov.** (Hemiptera: Pseudococcidae) is described from outdoor habitats, and the adult female is illustrated.

Key words: Adventive species, checklist, identification key, mealybug, new species, Pseudococcidae, Sternorrhyncha, taxonomy, *Trionymus*



Academic editor: Takumasa Kondo

Received: 19 February 2025

Accepted: 18 March 2025

Published: 29 April 2025

ZooBank: <https://zoobank.org/26BD9DBF-8F11-4040-8CD8-F81A921C396D>

Citation: Gerő K, Alfreðsson M, Szita É (2025) New data on the scale insect (Hemiptera, Coccoomorpha) fauna of Iceland, with description of a new species. ZooKeys 1236: 119–128. <https://doi.org/10.3897/zookeys.1236.150789>

Copyright: © Kornél Gerő et al.
This is an open access article distributed under terms of the Creative Commons Attribution License (Attribution 4.0 International – CC BY 4.0).

Introduction

Scale insects (Hemiptera: Sternorrhyncha: Coccoomorpha) are a substantial and diverse group, with over 8400 described species of small, obligate plant parasites (García Morales et al. 2016). The insects, often measuring less than 5 mm in length, are notorious as agricultural pests, posing a significant threat to a wide range of plant species (Kosztarab and Kozár 1988; Gullan and Martin 2009). Cryptic in their habits, scale insects are adept at evading detection at plant quarantine inspection, which enhances their potential for introduction to new regions globally (Watson 2002; Mazzeo et al. 2014). Their high adaptability enables them to establish populations in diverse environments, including urban parks, agricultural plantations, and tropical greenhouses (Williams and Pellizari 1997; Kozár 1998; Kondo and Watson 2022). Climate change, particularly increases in temperature, can facilitate the colonization and establishment of scale insects in new regions; this can have serious economic and ecological consequences (Kozár 2009; Kozár et al. 2013b; Gertsson 2023).

Iceland, a Nordic island country located on the Mid-Atlantic Ridge between North America and Europe, is the second largest island in Europe, covering an area of 103,000 km² (Thordarson and Höskuldsson 2014). The shortest distances to its nearest neighbours are approximately 280 km to Greenland, 400 km to the Faroe Islands, 800 km to Scotland, and 970 km to Norway (Denk et al.

2011). The climate ranges from Arctic in the far north to subarctic and temperate along the coastlines. This environmental heterogeneity contributes to a complex mosaic of ecosystems, including moss-covered lava fields, geothermal landscapes, glacial expanses, and coastal habitats. Iceland supports a rich biodiversity, with fauna and flora exhibiting unique adaptations to the island's specific ecological zones and variable weather conditions (Denk et al. 2011).

The scale insect fauna of Iceland is largely unexplored. The earliest mention of scale insects there dates back to 1772 (Olafsen and Povelsen 1772), when *Arcorthezia cataphracta* (Olafsen, 1772) (Hemiptera: Ortheziidae) was described. For the next 160 years, this remained the only recorded scale species in Iceland (Müller 1776; Mohr 1786; Staudinger 1857; Lindroth 1928). Green (1931) later described four new species from Iceland based on specimens collected by the Swedish entomologist Carl H. Lindroth. In a comprehensive study, Ossiannilsson (1955) re-described *Trionymus incertus* Green, 1931 (Hemiptera: Pseudococcidae), which originally was described from an immature female, reported several new locations of scale insect species, and referenced a few authors (Fristrup 1943; Gígja 1944; Björnsson 1951) who had previously investigated Iceland's scale insect fauna. Two greenhouse-inhabiting species were also reported by Gígja (1944) and Ossiannilsson (1955). Lindroth (1965) published the most recent scale insect data for Iceland, *Chionaspis salicis* (Linnaeus, 1758), an introduced outdoor species.

Our knowledge of cold-tolerant scale insect species is rather poor; to date, eight species of scale insects have been recorded from Iceland. The present work provides new data on the scale insect fauna of Iceland, including a description of a new *Trionymus* species adapted to the harsh outdoor conditions, a country checklist, and a list of adventive scale insect species in Iceland. Furthermore, an identification key is provided to the *Trionymus* species of Iceland.

Material and methods

During a brief survey in Iceland, 31 scale insect samples were collected between 15 and 30 September 2022 by the first author. Among these, 21 samples were collected from infested tropical and subtropical fruits in supermarkets and grocery stores in the towns of Reykjavík, Selfoss, and Vík í Mýrdal. Additionally, eight samples were collected from a greenhouse in the Reykjavík Botanical Garden. Moreover, ten soil samples were collected outdoors in Vík í Mýrdal, but only two of them provided scale insect specimens. The soil samples were processed in a Berlese funnel, which is a valuable tool for extracting arthropods and other small invertebrates from soil, leaf litter, and other organic matter (Southwood and Henderson 2000); it consists of a metal or plastic funnel, a heat and light source, and a collection container. The sample is placed in the funnel, and the heat source is positioned above. The heat creates temperature and humidity gradients within the funnel, with the warmest and driest conditions at the top and the coolest and moistest at the bottom. As the sample heats up, motile organisms move away from the heat and towards the cooler bottom of the funnel. They eventually fall into the collection container below, where they can be collected and identified (Southwood and Henderson 2000; Kaydan et al. 2016). All scale insects samples were stored in 96% ethyl alcohol before transport to the laboratory at HUN-REN Centre for Agricultural Research, Plant Protection Institute (PPI) in Hungary.

Specimens were prepared for light microscopy following the slide-mounting protocol described by Kosztarab and Kozár (1988). The slide-mounted specimens were examined using a phase-contrast light microscope (Olympus BX41) and identified using the published keys available in Borchsenius (1949), Tang (1992), Williams and Granara de Willink (1992), Danzig (1993), Hodgson (1994), Williams (2004), Miller and Davidson (2005), and Danzig and Gavrilov-Zimin (2014, 2015).

The type specimens of the new species are deposited in the Natural Science Institute of Iceland (NSII). For the holotype of the new species, the data on the label is listed with "/" indicating each line break. Voucher slides of the other species collected were deposited in the collections at PPI and NSII.

Results

A total of 31 scale insect samples were collected during the survey, representing seven species belonging to three families (Tables 1, 2).

A single species of soft scale insect (Coccidae), namely *Coccus hesperidum* Linnaeus, 1758, was collected from five different host-plant species from a greenhouse in Reykjavik Botanical Garden, and proved to be new to the Icelandic fauna.

Five armored scale insect species (Diaspididae) proved to be new records to Iceland. All the diaspidid specimens were collected from imported fruits, namely *Aonidiella aurantii* (Maskell, 1879), *Lepidosaphes gloverii* (Packard, 1869), *Lepidosaphes beckii* (Newman, 1869), *Parlatoria pergandii* Comstock, 1881, and *Pseudaulacaspis pentagona* (Targioni Tozzetti, 1886). These species are most probably not established and not breeding in Iceland, thus can't be considered as a part of the country's fauna, but as recorded in Iceland, belong to the scale insect species list of Iceland (Table 2).

An analysis of ten soil samples utilizing Berlese funnels, resulted in the detection of scale insects in two instances. This study led to the identification and description of a previously unknown species within the mealybug genus *Trionymus* (Pseudococcidae). A generic diagnosis of *Trionymus* can be found in Danzig and Gavrilov-Zimin (2015).

Trionymus icelandensis Gerő & Szita, sp. nov.

<https://zoobank.org/9B389D56-DBFB-44D6-9EF3-9B1B466E1260>

Fig. 1

Material examined. Holotype • 1 adult ♀ mounted singly on a slide; left label: NSII 113860 / PPI 13482 (work) / ICELAND / Vík í Mýrdal / 63°25'13"N, 18°59'58"W / 15 Sep. 2022 / *Festuca vivipara*; right label: *Trionymus icelandensis* / Gerő & Szita / 1 ♀, holotype / Leg. K. Gerő / Det. É. Szita. **Paratype** • 1 adult ♀ mounted singly on a slide; ICELAND, Vík í Mýrdal; 63°25'12"N, 19°00'06"W; 16 Sep. 2022; K. Gerő leg.; *Poa pratensis*; NSII code: 113859; PPI work code: 13481. (Both holotype and paratype are deposited in NSII)

Description. Unmounted adult female. Body elongate oval, light yellow, covered with fine powdery wax.

Slide-mounted adult female. Body elongate oval, 1.68–1.69 mm long, 0.83–0.86 mm wide. Eyes marginal, each 24–26 µm wide. Antennae each 6 segmented, 258–

264 µm long in total. Length of antennal segments: 1st 36–43.2 µm, 2nd 31.2–36 µm, 3rd 38.4–43.2 µm, 4th 19.2 µm, 5th 24–28.8 µm, 6th 72.8–79.2 µm, segments nearly parallel sided. Apical segment with 1 apical seta, 32–34 µm long; with 4 subapical setae, each 30–32 µm long, and with 5 fleshy setae, each 32–35 µm long. 5th segment with 1 fleshy seta, 32 µm long. Other setae throughout the segments hairlike, slightly curved with fine tip, 25–40 µm long. Clypeolabral shield not visible. Labium 3 segmented, 80–91 µm long, 81–82 µm wide, 5 or 6 setae each 12–20 µm long. Anterior spiracles each 36–38 µm long, and about 14 µm wide across atrium; posterior spiracles each 40–42 µm long, and about 15 µm wide across atrium. Legs well developed; hind leg without translucent pores, segment lengths (in µm): coxa 68–75; trochanter + femur 165–168; tibia + tarsus 207–210; claw 22–23. Ratio of lengths of tibia + tarsus to trochanter + femur 1: 1.23–1.27; ratio of lengths of tibia to tarsus 1: 1.14–1.27; ratio of lengths of hind trochanter + femur to greatest width of femur 1: 2.37–2.65. Tarsal digitules hairlike, each 27–30 µm long. Claw digitules capitate, 24–25 µm long. Both pairs of ostioles present, lips not sclerotized; anterior ostioles each with a total for both lips of 5–8 trilocular pores and no setae; posterior ostioles each with a total for both lips of 7 or 8 trilocular pores and no setae. Anal ring 74–75 µm wide, with two complete rows of pores, the outer row with spiculae, ring bearing 6 setae, each seta 110–130 µm long.

Dorsum. Derm membranous; with two pairs of cerarii on last abdominal segments. Setae flagellate, slightly curved, of 3 sizes: small setae each 12–15 µm long; mid-sized setae each 19–23 µm long; and longest setae each 27–30 µm long. Longest setae distributed mainly marginally, others scattered throughout. Trilocular pores numerous throughout, each about 3.2 µm in diameter. Oral collar tubular ducts of one size, outer ductule 4 µm wide, 6.5 µm long. Multilocular disc-pores absent.

Venter. Derm membranous; one small circulus, present on middle of abdominal segment III, 24 µm long and 26.4 µm wide. Apical seta on each anal lobe 130–132 µm long. Body setae flagellate, slightly curved, in 4 sizes: shortest setae each 11–14 µm long, present throughout; middle-sized setae each 25–26 µm long, present throughout; second longest setae each 40–43 µm long, situated on margins of abdomen and a few present in medial zone of abdomen; and longest setae each 66–80 µm long, situated medially on head. Trilocular pores numerous, each about 3.2 µm in diameter. Oral collar tubular ducts of one size, same as on dorsum. Multilocular disc-pores, each about 8 µm in diameter with 10 loculi, numbering 2–8, present on abdominal segments III–VIII and occasionally also on mesothorax.

Diagnosis. *Trionymus icelandensis* Gerő & Szita, sp. nov. can be recognised by possessing the following combination of features: (i) antennae each six segmented; (ii) eyes present; (iii) legs well developed, without translucent pores; (iv) one small circulus; (v) oral collar tubular ducts of one size present on both surfaces; (vi) multilocular disc-pores few, present on venter only, on abdominal segments III–VIII and occasionally on thoracic segment II; and (vii) body setae flagellate, in 3 sizes on dorsum, and in 4 sizes on venter, longest ones on venter of head.

Comments. *Trionymus icelandensis* is similar to three other species of *Trionymus*. It resembles *T. artemisiarum* (Borchsenius, 1949) in having two pairs of cerarii, lacking multilocular pores on dorsum, and in having 6-segmented antennae; however, it differs as follows (character states of *T. artemisiarum* are given in brackets): (i) having one circulus (circulus absent); (ii) oral collar tubular ducts of one size (two sizes); and (iii) hind coxa without translucent pores (translucent pores present).

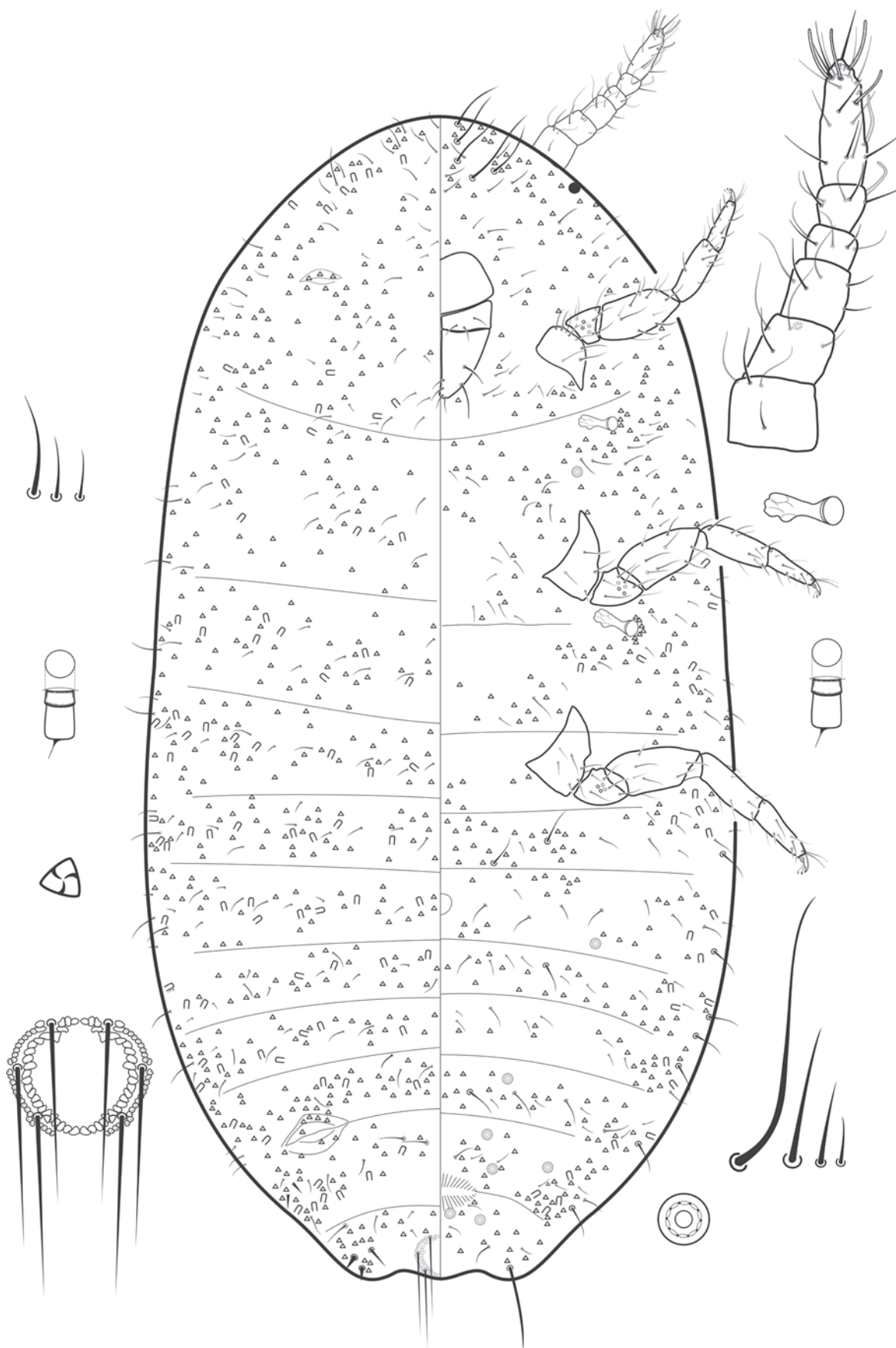


Figure 1. *Trionymus icelandensis* Gerő & Szita, sp. nov., holotype female. On antenna and legs, ventral setae are coloured grey, and dorsal setae are black.

Trionymus icelandensis resembles *T. massiliensis* (Goux, 1941) in lacking multilocular pores on dorsum; however, it differs as follows (character states of *T. massiliensis* are given in brackets): (i) having two pairs of cerarii (one pair); (ii) one circulus (circulus absent); (iii) oral collar tubular ducts of one size (two sizes); (iv) hind coxa without translucent pores (translucent pores present); and (v) antennae each with six segments (seven segments).

Trionymus icelandensis resembles *T. thulensis* Green, 1931 in having two pairs of cerarii, one circulus, and in lacking multilocular pores on dorsum; however, it differs as follows (character states of *T. thulensis* are given in brackets): (i) having oral collar tubular ducts of one size (two sizes); (ii) hind coxa without translucent pores (translucent pores present); and (iii) antennae each with six segments (seven or eight segments).

Etymology. The species is named in homage to the country of Iceland; the epithet is formed by the combination of the island name, Iceland, with the Latin suffix “-ensis”, meaning “originating from”.

Distribution. Iceland.

Host plants. Poaceae: *Festuca vivipara*, *Poa pratensis*.

Scale insect species list for Iceland

With this study, the total number of scale insect species with breeding populations recorded in Iceland was increased to ten species (Table 1). Of these, seven species can be found in outdoor conditions, three are indoor species. Five species were found exclusively on imported fruits and are not considered to be established in Iceland (Table 2).

Table 1. Country checklist of scale insect fauna (Hemiptera: Coccoomorpha) of Iceland, with comments on current collecting records and information on their occurrence in Iceland.

Taxon	Comments	Occurrence in Iceland
Diaspididae (2 genera)		
<i>Chionaspis salicis</i> (Linnaeus, 1758)	First recorded by Lindroth (1965)	Outdoors
<i>Pinnaspis aspidistrae</i> (Signoret, 1869)	Previously recorded as <i>Hemichionaspis aspidistrae</i> , first recorded by Ossiannilsson (1955).	Indoors
Coccidae (1 genus)		
<i>Coccus hesperidum</i> Linnaeus, 1758	New country record for Iceland. Reykjavík: From the greenhouse of the Reykjavík Botanical Garden on <i>Calycanthus Aphrodite</i> , <i>Clematis 'Jackmanii'</i> , <i>Libertia grandiflora</i> , <i>Magnolia grandiflora</i> , <i>Sarcococca confusa</i> , <i>Wisteria floribunda</i> .	Indoors
Pseudococcidae (3 genera)		
<i>Trionymus incertus</i> Green, 1931	First recorded by Green (1931).	Outdoors
<i>Trionymus icelandensis</i> Gerő & Szita, sp. nov.	New country record for Iceland. New to science. Vík í Mýrdal, samples from Berlese funnel: <i>Festuca vivipara</i> , <i>Poa pratensis</i> .	Outdoors
<i>Trionymus thulensis</i> Green, 1931	First recorded by Green (1931).	Outdoors
<i>Pelionella balteata</i> (Green, 1928)	Previously recorded as <i>Phenacoccus venustus</i> , first published by Green (1931).	Outdoors
<i>Pseudococcus maritimus</i> (Ehrhorn, 1900)	First recorded by Gíjja (1944).	Indoors
Ortheziidae (1 genus)		
<i>Arctorthezia cataphracta</i> (Olafsen, 1772)	First recorded by Olafsen and Povelsen (1772).	Outdoors
Acanthococcidae (1 genus)		
<i>Anophococcus granulatus</i> (Green, 1931)	First recorded by Green (1931).	Outdoors

Table 2. List of adventive scale insect species found on imported fruits in Iceland.

Taxon	Comments
Diaspididae (5 genera)	
<i>Aonidiella aurantii</i> (Maskell, 1879)	New record for Iceland. Reykjavík, Bónus supermarket, on <i>Citrus aurantiifolia</i> imported from Brazil. Vík í Mýrdal, Krónan supermarket, on <i>Citrus sinensis</i> and <i>Citrus × clementina</i> imported from Spain.
<i>Lepidosaphes beckii</i> (Newman, 1869)	New record for Iceland. Selfoss, Bónus supermarket, on <i>Citrus sinensis</i> imported from Spain. Vík í Mýrdal, Krónan supermarket on <i>Citrus sinensis</i> imported from Spain.
<i>Lepidosaphes gloverii</i> (Packard, 1869)	New record for Iceland. Vík í Mýrdal, Krónan supermarket on <i>Citrus sinensis</i> imported from Spain.
<i>Parlatoria pergandii</i> Comstock, 1881	New record for Iceland. Selfoss, Krónan supermarket on <i>Citrus sinensis</i> imported from Spain.
<i>Pseudaulacaspis pentagona</i> (Targioni Tozzetti, 1886)	New record for Iceland. Vík í Mýrdal, Krónan supermarket on <i>Actinidia deliciosa</i> .

Discussion

Ossiannilsson (1955) considered four species to be endemic to Iceland, namely *Anophococcus granulatus* (Green, 1931) (Hemiptera: Acanthococcidae), *Pelionella balteata* (Green, 1928), *Trionymus incertus* Green, 1931 and *T. thulensis* Green, 1931 (Hemiptera: Pseudococcidae). However, since the study by Ossiannilsson (1955), three of these species have also been found in other countries, meaning their endemic status is no longer confirmed. *Anophococcus granulatus* has been recorded in France (Foldi 2001) and in Hungary (Kozár et al. 2013a). *Pelionella balteata* was described under the name *P. venustus* by Green from Iceland in 1931, a synonymy discovered by Danzig (2001). *Pelionella balteata* seems to have a Holarctic distribution, as it has been found in 12 countries (García Morales et al. 2016). *Trionymus thulensis* has been reported from eight Palaearctic countries (García Morales et al. 2016) since its description from Iceland.

The redescription of *Trionymus incertus* Green, 1931 by Ossiannilsson (1955) was considered insufficient by Danzig and Gavrillov-Zimin (2015); but at the same time, it is accepted by ScaleNet (García Morales et al. 2016). In our opinion, the redescription made by Ossiannilsson can be used effectively in distinguishing the currently known *Trionymus* species in Iceland, although a redescription and redrawing of this species would be necessary to fulfil the requirements of modern taxonomy.

Identification key to *Trionymus* species found in Iceland

- 1 With 1 ventral circulus.....2
- With 2 ventral circuli..... ***Trionymus incertus* Green, 1931**
- 2 Abdominal segments VI–VIII with more than 15 ventral multilocular disc pores; antennae each eight segmented..... ***Trionymus thulensis* Green, 1931**
- Abdominal segments VI–VIII with fewer than 15 ventral multilocular disc pores; antennae each six segmented
..... ***Trionymus icelandensis* Gerő & Szita, sp. nov.**

To date, only eight species have been reported from Iceland, but with this study our knowledge of scale insects in Iceland has been improved significantly. The total number of scale insect species recorded on the territory of Iceland has been increased to 15. Of these, ten species can be considered as a part of the country checklist, with breeding populations in Iceland. Furthermore five

adventive species were also registered from imported fruits, which most probably are not established in Iceland.

For comparison, in nearby Greenland, nine species have been recorded (Morrison 1925; García Morales et al. 2016), and only one from Faeroe Islands (Anandale 1904). Among the subarctic countries in Europe, the scale insect fauna of Sweden is the most explored, with 108 recorded species (Gertsson 2001; García Morales et al. 2016), while Norway has 23, Scotland 32, and Finland 25 species (García Morales et al. 2016). These data suggest that it is worthwhile to make efforts to explore the scale insect fauna of Iceland in more detail in the future. The study of adventive species is also worth paying attention to, as they might become potential invaders indoors or outdoors, depending on the species.

Acknowledgements

We would like to express our sincere gratitude to Mr Hjörtur Þorbjörnsson (Director, Reykjavík Botanical Garden) for kindly providing us with an invitation letter and granting us permission to conduct research at the Botanical Garden in Reykjavík. Special thanks are due to Dr Takumasa Kondo (Colombian Agricultural Research Corporation (Agrosavia), Palmira, Colombia) for linguistic corrections. We are grateful to Gillian W. Watson (Natural History Museum, London, UK), M. Bora Kaydan (Imamoğlu Vocational School, Çukurova University, Adana, Türkiye) and an anonymous reviewer for their helpful suggestions to improve the manuscript.

Additional information

Conflict of interest

The authors have declared that no competing interests exist.

Ethical statement

No ethical statement was reported.

Funding

The study was financially supported by NKFIH (FK131550) and the National Laboratory for Health Security, Plant Protection Institute, HUN-REN Centre for Agricultural Research, Hungary (RRF-2.3.1-20-2022-00006).

Author contributions

KG: conceptualization, investigation, resources, visualization, funding acquisition; MSA: data curation, resources; ÉS: conceptualization, investigation, data curation, project administration, funding acquisition, methodology, supervision, visualization; All authors took part in writing, editing and revising the original draft.

Author ORCIDs

Kornél Geró  <https://orcid.org/0000-0002-0366-0050>

Matthías Alfreðsson  <https://orcid.org/0009-0006-5418-891X>

Éva Szita  <https://orcid.org/0000-0001-6335-5296>

Data availability

All of the data that support the findings of this study are available in the main text.

References

- Annandale N (1904) Contributions to the terrestrial zoology of the Faroes. Proceedings of the Royal Society of Edinburgh (Phys) 15: 153–160.
- Björnsson H (1951) Gróður og dýralíf í Esjufjöllum. Náttúrufræðingurinn 21: 109–112.
- Borchsenius NS (1949) Fauna of USSR (Homoptera, Pseudococcidae). [in Russian]. Akademii Nauk Zoologicheskogo Instituta Leningrad (n.s. 38), Leningrad, 383 pp.
- Danzig EM (1993) [Fauna of Russia and neighbouring countries. Rhynchota, Volume X: suborder scale insects (Coccinea): families Phoenicococcidae and Diaspididae.]. 'Nauka' Publishing House, St. Petersburg, 452 pp.
- Danzig EM (2001) Mealybugs of the genera *Peliococcus* and *Peliococcopsis* from Russia and neighbouring countries (Homoptera: Coccinea: Pseudococcidae). Zoosystematica Rossica 9: 123–154.
- Danzig EM, Gavrillov-Zimin IA (2014) Palaearctic mealybugs (Homoptera: Coccinea: Pseudococcidae), Part 1: Subfamily Phenacoccinae Russian Academy of Sciences, Zoological Institute, St. Petersburg, 678 pp.
- Danzig EM, Gavrillov-Zimin IA (2015) Palaearctic Mealybugs (Homoptera: Coccinea: Pseudococcidae) Part 2. Fauna of Russia and Neighbouring Countries, New series, No. 149. Zoological Institute, Russian Academy of Sciences, St. Petersburg, 619 pp.
- Denk T, Grimsson F, Zetter R, Simonarson LA (2011) Late Cainozoic Floras of Iceland. 15 Million Years of Vegetation and Climate History in the Northern North Atlantic. Springer, Dordrecht, 845 pp. <https://doi.org/10.1007/978-94-007-0372-8>
- Foldi I (2001) Liste des cochenilles de France (Hemiptera, Coccoidea). Bulletin de la Société entomologique de France 106: 303–308. <https://doi.org/10.3406/bsef.2001.16768>
- Fristrup B (1943) Contributions to the Fauna and Zoogeography of Northwest Iceland. Entomologiske Meddelelser 23: 148–173.
- García Morales M, Denno BD, Miller DR, Miller GL, Ben-Dov Y, Hardy NB (2016) ScaleNet: a literature-based model of scale insect biology and systematics. Database. [Date accessed: 26.03.2025]
- Gertsson CA (2001) An annotated checklist of the scale insects (Homoptera: Coccoidea) of Sweden. [Förteknung över Sveriges sköldlöss. In English; summary in Swedish]. Entomologisk Tidskrift Stockholm 122: 123–130.
- Gertsson CA (2023) Första fyndet av den invasiva sköldlusen *Pseudaulacaspis pentagona* (Tagioni Tozzetti, 1886) påfriland i Sverige (Hemiptera, Coccoomorpha, Diaspididae). [The first outdoor record of the invasive scale insect *Pseudaulacaspis pentagona* (Tagioni Tozzetti, 1886) in Sweden (Hemiptera, Coccoomorpha, Diaspididae). In Swedish]. FaZett 36: 20–26.
- Gígja G (1944) Meindýr í húsum og gróðri og varnir gegn beim. Jens Guðbjörnsson, Reykjavík, 235 pp.
- Green EE (1931) Notes on some Coccidae from Iceland. Entomologisk Tidskrift 52: 263–269.
- Gullan PJ, Martin JH (2009) Sternorrhyncha (jumping plant-lice, whiteflies, aphids, and scale insects). In: Resh VH, Cardé RT (Eds) Encyclopedia of Insects 2nd (Ed.) Elsevier, San Diego, 957–967. <https://doi.org/10.1016/B978-0-12-374144-8.00253-8>
- Hodgson CJ (1994) The scale insect family Coccidae: an identification manual to genera. CAB International, Wallingford, 639 pp.
- Kaydan MB, Konczné Benedicy Z, Kiss B, Szita É (2016) A survey of scale insects in soil samples from Europe (Hemiptera, Coccoomorpha). ZooKeys 565: 1–28. <https://doi.org/10.3897/zookeys.565.6877>

- Kondo T, Watson GW (Eds) (2022) Encyclopedia of scale insect pests. CAB International, Wallingford, UK, 640 pp. <https://doi.org/10.1079/9781800620643.0000>
- Kosztarab M, Kozár F (1988) Scale Insects of Central Europe. Akadémiai Kiadó, Budapest, 456 pp. <https://doi.org/10.1007/978-94-009-4045-1>
- Kozár F (1998) Éghajlatváltozás és a rovarvilág. Magyar Tudomány 9: 1069–1076.
- Kozár F (2009) Pajzstetű (Hemiptera: Coccoidea) fajok és a klímaváltozás: vizsgálatok Magyarországi autópályákon [Scale insect species (Hemiptera, Coccoidea) and climate change studies on Hungarian highways]. Növényvédelem 45: 577–588.
- Kozár F, Konczné Benedicty Z, Fetykó K, Kiss B, Szita É (2013a) An annotated update of the scale insect checklist of Hungary (Hemiptera, Coccoidea). ZooKeys 309: 49–66. <https://doi.org/10.3897/zookeys.309.5318>
- Kozár F, Szita É, Fetykó K, Neidert D, Konczné Benedicty Z, Kiss B (2013b) Pajzstetvek, sztrádák, klíma. MTA ATK Növényvédelmi Intézet, Budapest, 216 pp.
- Lindroth CH (1928) Zur Land-Evertebratenfauna Islands. Göteborgs Kungl. vetenskaps- och vitterhets- samhällens handlingar, 52 pp.
- Lindroth CH (1965) Skaftafell, Iceland, a living glacial refugium. Oikos Suppl. 6: 142 pp.
- Mazzeo G, Longo S, Pellizzari G, Porcelli F, Suma P, Russo A (2014) Exotic scale insects (Coccoidea) on ornamental plants in Italy: a never-ending story. Acta Zoologica Bulgarica suppl. 6: 55–61.
- Miller DR, Davidson JA (2005) Armored Scale Insect Pests of Trees and Shrubs. Cornell University Press, Ithaca, NY, 442 pp.
- Mohr N (1786) Forsøg til en Islandsk Naturhistorie. Trykt hos C. F. Holm, 413 pp.
- Morrison H (1925) Classification of scale insects of the subfamily Ortheziinae. Journal of Agricultural Research 30: 97–154.
- Müller OF (1776) Zoologiae Danicae prodromus, seu, Animalium Daniae et Norvegiae indigenarum characteres, nomina, et synonyma imprimis popularium. Typis Hallageriis, Havniae, 282 pp. <https://doi.org/10.5962/bhl.title.13268>
- Olafsen E, Povelsen B (1772) Reise igiennem Island. Soroe, 1042 pp.
- Ossiannilsson F (1955) Hemiptera 3. Coccina, Aleyrodina and Psyllina The Zoology of Iceland III: 1–12.
- Southwood TRE, Henderson PA (2000) Ecological methods. 3rd edn. Blackwell Science, Oxford, 593 pp.
- Staudinger O (1857) Reise nach Island zu entomologischen Zwecken unternommen. Entomologische Zeitung 18: 209–289.
- Tang FT (1992) The Pseudococcidae of China. Shanxi Agricultural University, Taigu, Shanxi, China, 768 pp.
- Thordarson T, Höskuldsson Á (2014) Iceland. Dunedin, 256 pp.
- Watson GW (2002) Arthropods of Economic Importance: Diaspididae of the World. World Biodiversity Database. ETI Information Services (Expert Center for Taxonomic Identification), Amsterdam, Netherlands. https://diaspididae.linnaeus.naturalis.nl/linnaeus_ng/app/views/introduction/topic.php?id=3377&epi=155
- Williams DJ (2004) Mealybugs of southern Asia. The Natural History Museum. Kuala Lumpur: Southdene SDN. BHD, 896 pp.
- Williams DJ, Granara de Willink MC (1992) Mealybugs of Central and South America. CAB International, Wallingford, 635 pp.
- Williams DJ, Pellizzari G (1997) Two species of mealybugs (Homoptera Pseudococcidae) on the roots of Aloaceae in greenhouses in England and Italy. Bollettino di Zoologia Agraria e di Bachicoltura (Milano) Ser II 29: 157–166.

Description of two new huntsman spiders from Vietnam (Araneae, Sparassidae)

He Zhang^{1,2,3}, Quang Duy Hoang⁴, Shuang Lei^{1,2,5}

1 Guo Shoujing Innovation College, Xingtai University, Xingtai City 054001, Hebei Province, China

2 Hebei Province Sweet Potato Breeding and Application Technology Innovation Center, Xingtai City 054001, Hebei Province, China

3 Arachnid Resource Centre of Hubei & Hubei Key Laboratory of Regional Development and Environmental Response, Faculty of Resources and Environmental Sciences, Hubei University, Wuhan City 430062, Hubei Province, China

4 Tay Nguyen University, 567 Le Duan, Buon Ma Thuot City 630000, Dak Lak Province, Vietnam

5 Shengzhou Agricultural Technology Extension Center, Shengzhou City 312400, Zhejiang Province, China

Corresponding authors: Shuang Lei (shuanglei857@163.com); Quang Duy Hoang (hqduy@ttn.edu.vn)

Abstract

Two new species of the sparassid genera *Heteropoda* Latreille, 1804 and *Pseudopoda* Jäger, 2000 are described from Vietnam: *Heteropoda taygiangensis* sp. nov. (♂) from Quang Nam Province and *Pseudopoda tadungensis* sp. nov. (♀) from Dak Nong Province. The new *Pseudopoda* species is described and diagnosed based on both morphological characteristics and DNA barcoding. DNA barcode data (COI) are provided for both new species.

Key words: Biodiversity, *Heteropoda*, huntsman spider, new species, *Pseudopoda*, sparassid systematics, taxonomy, Vietnam



Academic editor: Chris Hamilton

Received: 23 December 2024

Accepted: 24 March 2025

Published: 29 April 2025

ZooBank: <https://zoobank.org/58725738-EECC-4B66-A501-C7646919E13E>

Citation: Zhang H, Hoang QD, Lei S (2025) Description of two new huntsman spiders from Vietnam (Araneae, Sparassidae). ZooKeys 1236: 129–140. <https://doi.org/10.3897/zookeys.1236.145146>

Copyright: © He Zhang et al.
This is an open access article distributed under terms of the Creative Commons Attribution License (Attribution 4.0 International – CC BY 4.0).

Introduction

The family Sparassidae Bertkau, 1872, commonly known as huntsman spiders, is the tenth largest spider family globally, comprising 1531 valid species in 98 genera (World Spider Catalog 2025). Recently, several studies have focused on the family in Vietnam (Logunov and Jäger 2015; Zhang et al. 2023; Korai and Jäger 2024a). However, only 28 species of huntsman spiders have been documented, belonging to the following genera: *Heteropoda* Latreille, 1804 (11 species); *Pandercetes* L. Koch, 1875 (1 species); *Pseudopoda* Jäger, 2000 (9 species); *Rhitymna* Simon, 1897 (2 species); *Sinopoda* Jäger, 1999 (4 species); and *Thelcticopis* Karsch, 1884 (1 species) (World Spider Catalog 2025). Clearly, research on Vietnamese huntsman spiders remains limited, and the relatively low diversity reported may reflect an artifact due to insufficient taxonomic studies rather than reflecting the true species richness of the region.

This study aims to enhance the taxonomic understanding of the huntsman spiders in Vietnam by describing two new species: *Heteropoda taygiangensis* sp. nov. from central Vietnam and *Pseudopoda tadungensis* sp. nov. from the central highlands of Vietnam. These genera are among the most diverse in the region, and the new species described here will contribute to a more accurate representation of the huntsman spider fauna in Vietnam.

Material and methods

All specimens were collected by hand and examined with an Olympus SZX16 stereomicroscope; details were further investigated with an Olympus BX51 compound microscope. Colouration is described in all species from specimens in ethanol. Copulatory organs were examined and illustrated after dissection from the spider bodies; epigynes were cleared with Proteinase K. Habitus photos were obtained using a Leica M205 C digital microscope attached to a Leica DMC4500 digital camera. Coordinates are given in square brackets when retrieved secondarily from Google Earth.

Leg measurements are shown as: total length (femur, patella, tibia, metatarsus, tarsus). Number of spines is listed for each segment in the following order: prolateral, dorsal, retrolateral, ventral (in femora and patellae ventral spines are absent and the fourth digit is omitted in the spination formula). The terminology used in text and figure legends follows Li et al. (2013) and Quan et al. (2014). All measurements are given in millimetres. The map was produced using ArcMap ver. 10.8.1.

All specimens treated in the present paper were compared with individuals of described species within a certain distribution range to avoid describing synonyms.

Abbreviations used in text and figures: **AB**, anterior bands; **ALE**, anterior lateral eyes; **AME**, anterior median eyes; **C**, conductor; **CH**, clypeus height; **CO**, copulatory opening; **dRTA**, dorsal part of retrolateral tibial apophysis; **DS**, dorsal shield of prosoma; **E**, embolus; **FD**, fertilization duct; **Fe**, femur; **IDS**, internal duct system; **LL**, lateral lobes; **MHU**, Museum of Hubei University, Wuhan, China; **Mt**, metatarsus; **OL**, opisthosoma length; **OS**, opisthosoma; **OW**, opisthosoma width; **Pa**, patella; **PL**, prosoma length; **PLE**, posterior lateral eyes; **PME**, posterior median eyes; **Pp**, palp; **PW**, prosoma width; **RTA**, retrolateral tibial apophysis; **S**, spermophor; **Ti**, tibia; **TL**, total length; **vRTA**, ventral part of retrolateral tibial apophysis; **I, II, III, IV**, legs I to IV.

To obtain DNA barcodes, a mitochondrial gene (mitochondrial cytochrome c oxidase subunit I, COI) was amplified and sequenced from two specimens. DNA extraction, PCR amplification, and sequencing followed the protocols described by Zhang et al. (2021). The universal primers LCO1490 and HCO2198 (Folmer et al. 1994) were used for PCR amplification. GenBank accession numbers for the newly generated sequences are listed in Table 1.

For phylogenetic analysis, the newly obtained sequence of *Pseudopoda tadungensis* sp. nov. was incorporated into the COI dataset from Cao et al. (2016), while the sequence of *Heteropoda taygiangensis* sp. nov. was incorporated into a COI dataset retrieved from GenBank. Phylogenetic analyses were performed following the methodologies outlined in Cao et al. (2016) and Zhang et al. (2021).

Table 1. Information on newly sequenced *Heteropoda taygiangensis* sp. nov. (paratype) and *Pseudopoda tadungensis* sp. nov. (holotype) with specimen label and GenBank accession numbers.

Species name	Voucher code	Accession number
<i>Heteropoda taygiangensis</i> sp. nov.	LJ20240069	PV426987
<i>Pseudopoda tadungensis</i> sp. nov.	LJ20240005	PV426988

Result

Taxonomy

Family Sparassidae Bertkau, 1872

Subfamily Heteropodinae Thorell, 1873

Heteropoda taygiangensis sp. nov.

<https://zoobank.org/A6319416-85FF-430E-9ED3-7155AD8343A6>

Figs 1–3, 7

Type material. *Holotype* male: VIETNAM • Quang Nam Province: Tay Giang District, 15.8377°N, 107.3819°E, elevation 1353 m, 23 July 2019, Quang Duy Hoang leg. (MHU, LJ20240068). *Paratype*: • 1 male, same locality data as holotype, collected on 18 July 2024, Quang Duy Hoang leg. (MHU, LJ20240069).

Etymology. The specific name is derived from the type locality, the Tay Giang District; adjective.

Diagnosis. Males of *H. taygiangensis* sp. nov. resemble that of *H. hainanensis* Korai & Jäger, 2024 in having a similar shape of the tegulum and embolus, but can be distinguished from the latter by: (1) Conductor long, narrow, and distally curved in ventral view (Fig. 1A–C, E) (broader and slightly more rounded

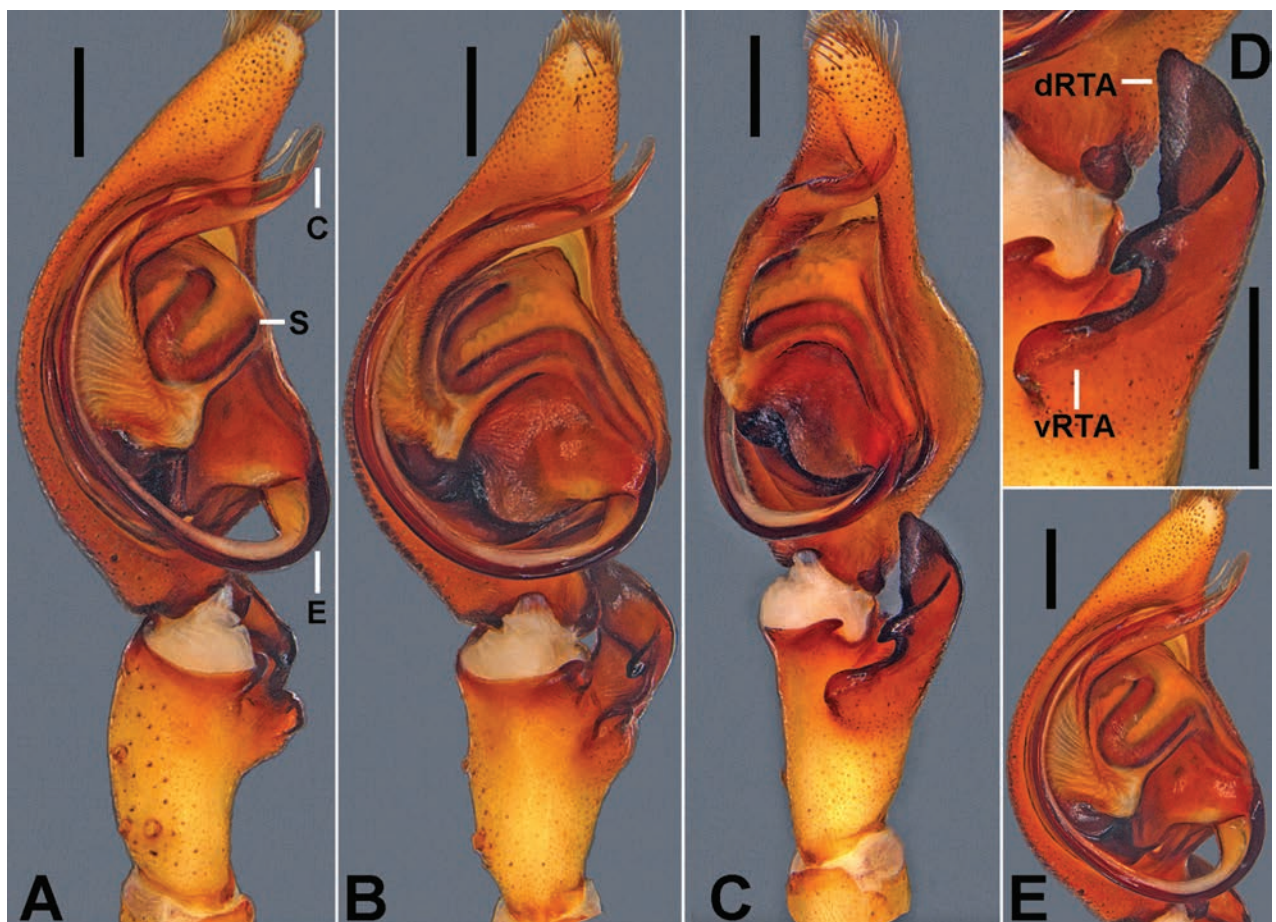


Figure 1. *Heteropoda taygiangensis* sp. nov., holotype, male **A–C** left male palp (**A** prolateral **B** ventral **C** retrolateral) **D** left male palpal tibia, retrolateral **E** left male palpal cymbium, retrolateral. Abbreviations: C, conductor; dRTA, dorsal retrolateral tibial apophysis; E, embolus; S, spermophor; vRTA, ventral retrolateral tibial apophysis. Scale bars: 0.5 mm.

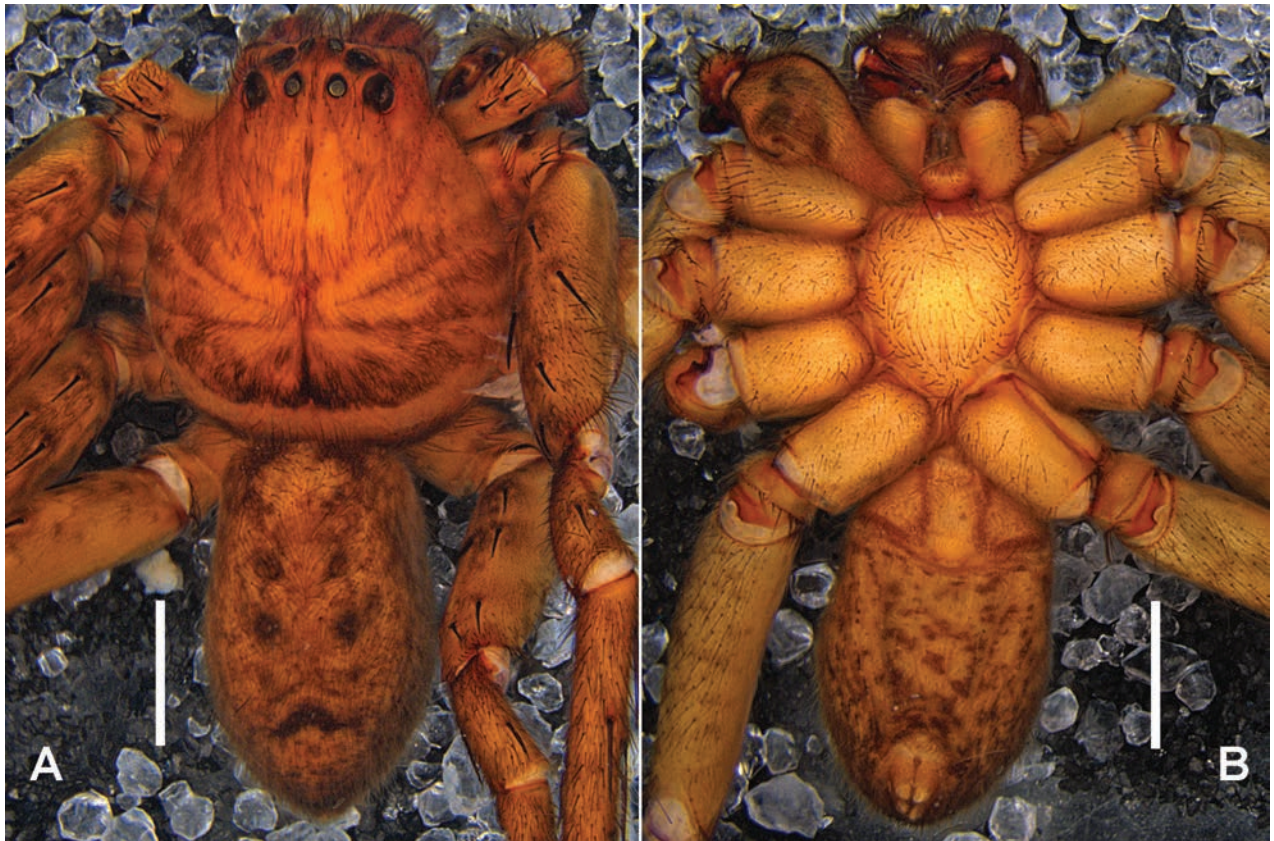


Figure 2. *Heteropoda taygiangensis* sp. nov. **A, B** male habitus (**A** dorsal **B** ventral). Scale bars: 2 mm.

distally in *H. hainanensis*, see fig. 5A in Korai and Jäger 2024b); (2) spermophor slightly curved in distal tegular half (Fig. 1B) (obviously bent in distal tegular half in *H. hainanensis*, see fig. 5A in Korai and Jäger 2024b); and (3) dRTA significantly wide, bent inward, and blunt-tipped, presenting a short and pointed projection, directed ventrally (Fig. 1B–D) (narrow, bent outward and pointed tip, without any projection in *H. hainanensis*, Korai and Jäger 2024b: figs 5A, 6B).

Description. Male (holotype): Measurements: Medium-sized. TL 10.4, PL 5.6, PW 5.2, OL 4.8, OW 3.2. Eyes: AME 0.25, ALE 0.45, PME 0.31, PLE 0.47, AME–AME 0.20, AME–ALE 0.14, PME–PME 0.37, PME–PLE 0.25, AME–PME 0.27, ALE–PLE 0.42, CH AME 0.44, CH ALE 0.33. Spination: Pp 131, 100, 2121; Fe I 123, II–III 323, IV 33(4)1; Pa I–II 101, III–IV 001; Ti I–IV 2226, III–IV 2126; Mt I–II 1014, III 2014, IV 3036. Measurements of palps and legs: Palp 7.5 (3.0, 1.6, 0.7, -, 2.2); I 22.5 (5.9, 2.4, 6.4, 5.8, 2.0); II 24.2 (6.5, 2.6, 7.3, 6.1, 1.7); III 18.5 (5.0, 2.2, 5.3, 4.8, 1.2); IV 20.2 (5.4, 1.8, 5.5, 5.6, 1.9). Leg formula: II-I-IV-III. Cheliceral furrow with 3 promarginal, 4 retromarginal teeth and ca. 42 denticles.

Palp (Fig. 1A–E): As in diagnosis. RTA arising distally on tibia, vRTA in retrolateral view with rounded hump. Cymbium almost two times as long as Ti. Conductor long, beyond cymbial margin. Spermophor strongly curved close to the base of conductor. Embolus arising from tegulum in 4:00 o’ clock position, filiform and almost forming a semicircular in ventral view.

Colouration (Fig. 2A, B): DS reddish brown, with dense black hairs in the posterior part. Fovea and radial marks distinct. OS dorsally with four dark round marks, regularly arranged in the median field, and with a dark transverse line in posterior part. OS ventrally yellow, with lots of reddish-brown spots, irregularly arranged.

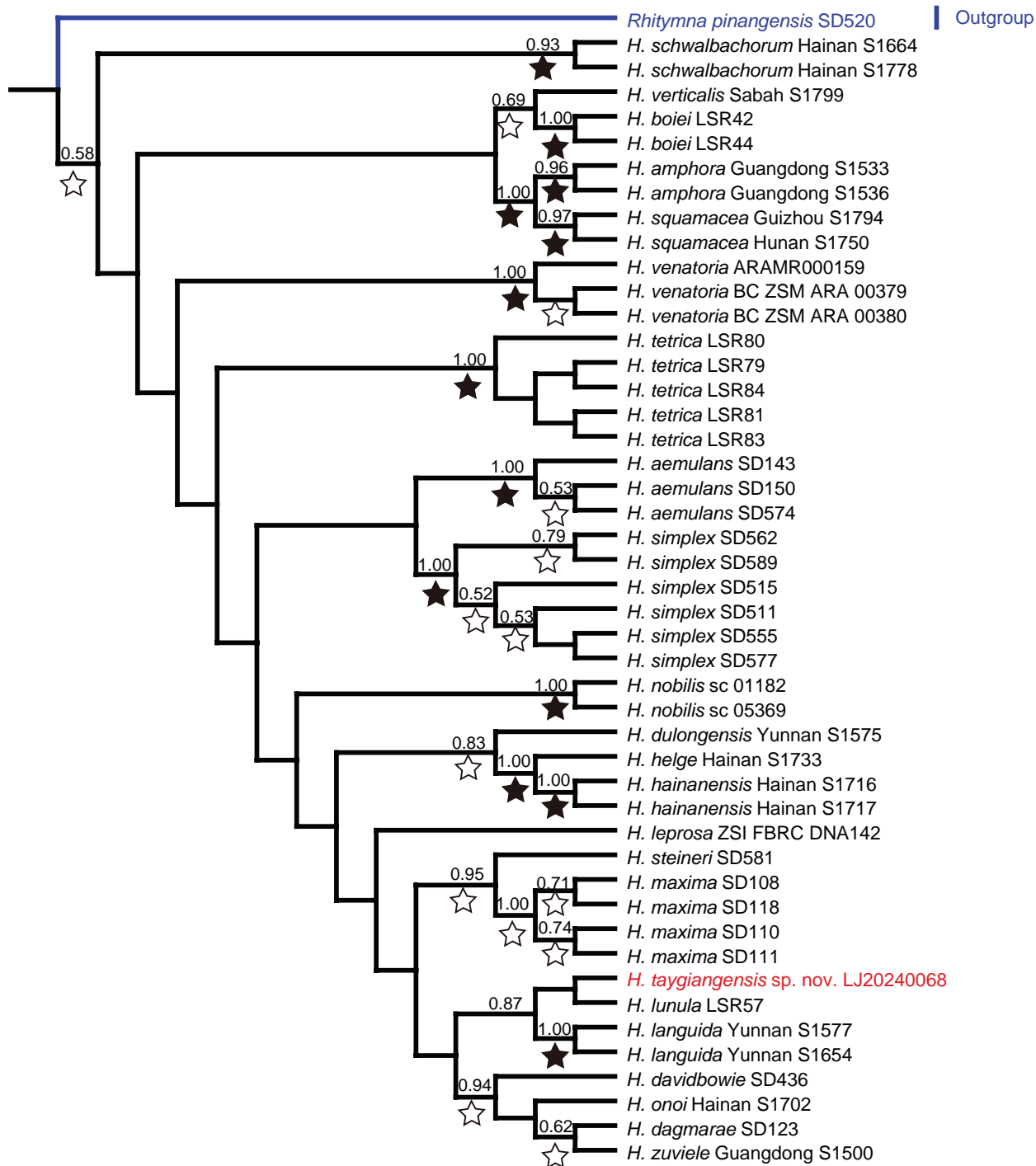


Figure 3. Bayesian tree based on the COI dataset including 46 *Heteropoda* individuals belonging to 23 species. Numbers on nodes are posterior probabilities; bootstrap support from ML analyses is indicated as solid stars for values > 95%, open stars > 50–95%. Red font indicates *H. taygiangensis* sp. nov., blue line indicates the outgroup.

Female: Unknown.

Distribution. Known only from the type locality (Fig. 7).

Notes. To date, four *Heteropoda* species from Vietnam are known only from females: *H. altmannae* Jäger, 2008 from Ca Mau Province in southern Vietnam; *H. ignichelis* (Simon, 1880) from Sai Gon, southern Vietnam; *H. pressula* Simon, 1886 from Bachiou (=Ba Chieu?), Sai Gon, Vietnam; and *H. zuviele* Jäger, 2008 from northern Vietnam (Simon 1880, 1886; Jäger

2008). The newly described species, *H. taygiangensis* sp. nov., is represented by male specimens and could potentially be conspecific with one of these species, which are known only from females. However, *H. taygiangensis* sp. nov. is found more than 500 km away from the known localities of *H. altmannae*, *H. ignichelis*, and *H. zuviele*. *Heteropoda altmannae* and *H. ignichelis* have only been recorded from their original localities, with no further records available. Although *H. zuviele* has been documented beyond its type locality, all known records are restricted to the north of the type locality. The type locality of *H. pressula*, “Bachiou,” remains uncertain. Simon (1886) repeatedly referred to it as a locality in Cambodia, but its exact location has not been verified. Because “Bachiou” cannot be confidently located in Cambodia, some subsequent authors (Ono et al. 2012; Yamasaki et al. 2018; Seyfulina and Kartsev 2022) have suggested it may correspond to Ba Chieu, Sai Gon, Vietnam. Determining whether “Bachiou” lies in Vietnam or Cambodia requires further investigation, particularly through re-examination of the *H. pressula* type specimen. Therefore, we consider the new species, *H. taygiangensis* sp. nov. to be a separate species in the present study. To support future efforts to resolve this taxonomic ambiguity, we provide COI sequence data. Additionally, we constructed the first phylogenetic tree of the genus *Heteropoda* based on all currently available COI sequences (Fig. 3).

***Pseudopoda tadungensis* sp. nov.**

<https://zoobank.org/EB77EE59-7A7C-4A9F-8342-CFED94C2AAA1>

Figs 4–7

Type material. Holotype female: VIETNAM • Dak Nong Province: Dak Glong District, Ta Dung National Park, 11.8616°N, 107.9923°E, elevation 953 m, 1 February 2024, Quang Duy Hoang leg. (MHU, LJ20240005).

Etymology. The specific name is derived from the type locality, the Ta Dung National Park; adjective.

Diagnosis. The female of *P. tadungensis* sp. nov. can be distinguished from all congeners by the medially incompletely fused lateral lobes in ventral view, and the internal duct system twisted into a wing shape.

Description. Female (holotype): Measurements: Medium-sized. TL 10.1, PL 4.4, PW 4.0, OL 5.7, OW 2.7. Eyes: AME 0.14, ALE 0.24, PME 0.17, PLE 0.23, AME–AME 0.16, AME–ALE 0.09, PME–PME 0.20, PME–PLE 0.35, AME–PME 0.27, ALE–PLE 0.25, CH AME 0.37, CH ALE 0.30. Spination: Pp 131, 101, 2101, 1014; Fe I 323, II–III 322, IV 331; Pa I–III 101, IV 000; Ti I–II 2228, III 2226, IV 2126; Mt I–II 3034, III–IV 3036. Measurements of palps and legs: Pp 7.6 (1.6, 0.7, 1.4, –, 2.3); I 19.3 (5.5, 1.9, 5.5, 5.0, 1.4); II 22.0 (6.1, 2.2, 6.4, 5.6, 1.7); III 16.0 (4.9, 1.7, 4.4, 4.0, 1.0); IV 18.8 (5.6, 1.1, 5.1, 5.5, 1.5). Leg formula: II-I-IV-III. Cheliceral furrow with ca. 20 denticles.

Epigyne (Fig. 4A–C): As in diagnosis. Epigynal field wider than long. Anterior bands short. Anterior margins of lateral lobes slightly curved, posterior margins of lateral lobes with median indentation. Posterior part of internal duct system with loops. Fertilization duct long and narrow, situated postero-laterally.

Colouration (Fig. 5A, B): DS reddish brown, with dark spots. Fovea and radial marks distinct. OS dorsally with reddish-brown patches, arranged symmetrically

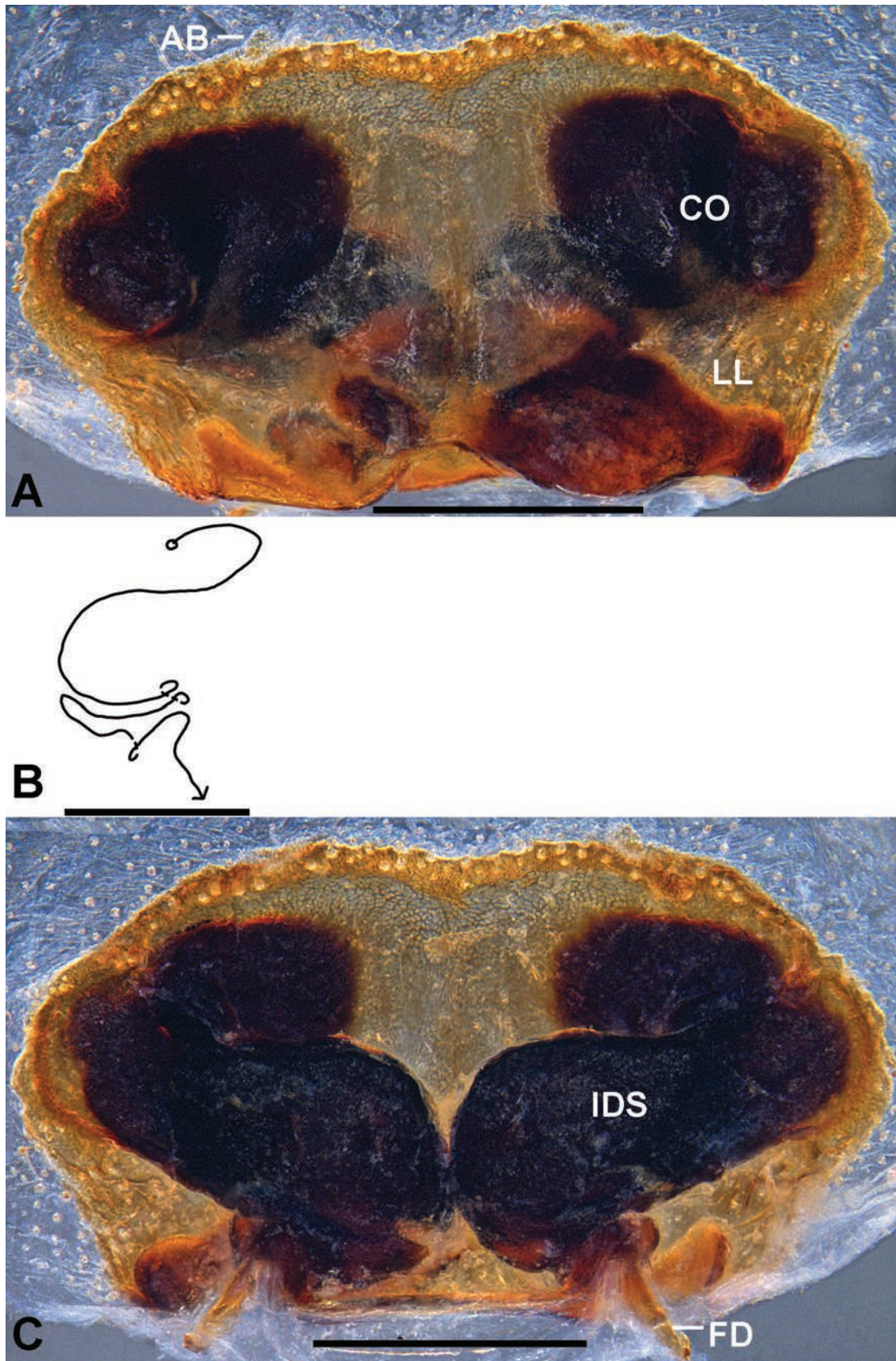


Figure 4. *Pseudopoda tadungensis* sp. nov., holotype, female **A** epigyne, ventral **B** schematic course of IDS, dorsal **C** vulva, dorsal. Abbreviations: AB, anterior bands; CO, copulatory opening; FD, fertilization duct; IDS, internal duct system; LL, lateral lobes. Scale bars: 0.5 mm.



Figure 5. *Pseudopoda tadungensis* sp. nov. **A, B** female habitus (**A** dorsal **B** ventral). Scale bars: 2 mm.

in two longitudinal lines. OS ventrally yellow with a longitudinal brown region, margins with few small marks.

Male: Unknown.

Distribution. Known only from the type locality (Fig. 7).

Note. *Pseudopoda tadungensis* sp. nov. exhibits subtle differences in genital morphology compared to most other species of the genus. To confirm its generic placement, we amplified the COI sequence of the holotype and conducted a phylogenetic analysis based on currently available COI sequences of the genus. The resulting tree supports the placement of *P. tadungensis* sp. nov. within *Pseudopoda* (Fig. 6). These molecular data provide an additional line of evidence for the validity and generic assignment of the new species.

Up to now, four *Pseudopoda* species from Vietnam are known only from males. The collection sites of these four species are located at a considerable distance from *P. tadungensis* sp. nov. (all exceeding 200 km, outside the endemic range of most *Pseudopoda* species; personal observation, Zhang et al. 2023), and their size and patterns do not match. Therefore, *P. tadungensis* sp. nov. is currently regarded as a distinct species. Further studies are required to address this ambiguity conclusively.

Discussion

The genera *Pseudopoda* Jäger, 2000 and *Heteropoda* Latreille, 1804 are among the most species-rich lineages within Sparassidae. However, the faunal diversity of both genera in Vietnam remains poorly documented, and recent surveys continue to uncover new taxa through targeted fieldwork and integrative taxonomic approaches.

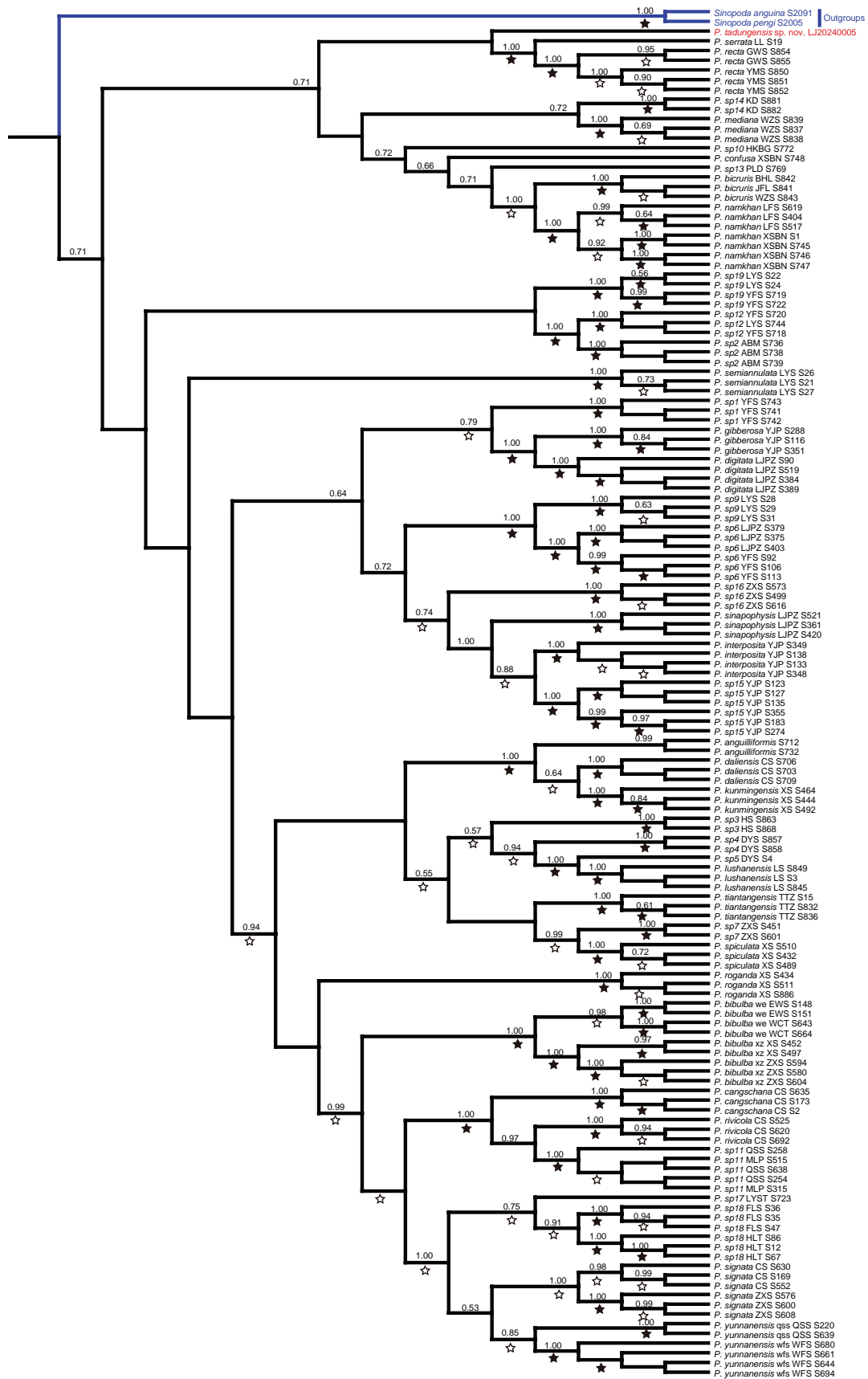


Figure 6. Bayesian tree based on the COI dataset including 139 *Pseudopoda* individuals belonging to 42 species. Numbers on nodes are posterior probabilities; bootstrap support from ML analyses is indicated as solid stars for values > 95%, open stars > 50–95%. Red font indicates *P. tadungensis* sp. nov., blue lines indicate the outgroup clade.



Figure 7. Records of the new *Heteropoda* and *Pseudopoda* species in Vietnam. 1 *H. taygiangensis* sp. nov. 2 *P. tadungensis* sp. nov.

In the present study, two new species, *P. tadungensis* sp. nov. and *H. taygiangensis* sp. nov., are described based on detailed morphological examinations. To further validate their taxonomic placements, COI barcoding and phylogenetic analyses were conducted as independent molecular evidence.

In the *Heteropoda* phylogeny (Fig. 3), *H. taygiangensis* sp. nov. clusters with other representatives of the genus, including *H. languida* and *H. lunula*, with strong support (posterior probability = 0.87). This finding agrees with the observed morphological characteristics and further supports placing it in the genus *Heteropoda*.

Similarly, in the COI-based phylogenetic tree (Fig. 6), *P. tadungensis* sp. nov. is recovered within the *Pseudopoda* clade and forms a well-supported monophyletic

group (posterior probability = 0.73), confirming its placement in the genus. Although the species differs from most congeners by having fused lateral lobes (LL), this feature has also been documented in several other *Pseudopoda* species (e.g., *P. exigua* (Fox, 1938)), and therefore does not conflict with its generic assignment.

Overall, the COI phylogenetic analyses provide robust molecular support for the generic placements of *P. tadungensis* sp. nov. and *H. taygiangensis* sp. nov., reinforcing the morphological diagnoses and underscoring the utility of integrative taxonomy in sparassid systematics.

Acknowledgments

We thank Prof. Zhisheng Zhang (School of Life Sciences, Southwest University, Chongqing, China) for providing sparassid specimens.

Additional information

Conflict of interest

The authors have declared that no competing interests exist.

Ethical statement

No ethical statement was reported.

Funding

This study was supported in part by grant from National Natural Sciences Foundation of China (NSFC-32300378).

Author contributions

Writing – original draft: HZ, SL. Writing – review and editing: HZ, QDH, SL.

Author ORCIDs

He Zhang  <https://orcid.org/0000-0002-1478-9837>

Quang Duy Hoang  <https://orcid.org/0000-0003-1672-7960>

Shuang Lei  <https://orcid.org/0000-0002-5732-5231>

Data availability

All of the data that support the findings of this study are available in the main text.

References

- Cao XW, Liu J, Chen J, Zheng G, Kuntner M, Agnarsson I (2016) Rapid dissemination of taxonomic discoveries based on DNA barcoding and morphology. *Scientific Reports* 6(1): 37066. <https://doi.org/10.1038/srep37066>
- Folmer O, Black M, Hoeh W, Lutz R, Vrijenhoek R (1994) DNA primers for amplification of mitochondrial cytochrome c oxidase subunit I from diverse metazoan invertebrates. *Molecular Marine Biology and Biotechnology* 3: 294–299.
- Jäger P (2008) Revision of the huntsman spider genus *Heteropoda* Latreille 1804: species with exceptional male palpal conformations from Southeast Asia and Australia (Arachnida, Araneae: Sparassidae: Heteropodinae). *Senckenbergiana Biologica* 88: 239–310. <https://doi.org/10.11646/zootaxa.5352.1.1>

- Korai SK, Jäger P (2024a) Five new species of *Heteropoda* Latreille, 1804 spiders (Araneae: Sparassidae) from Southeast Asia. *Zootaxa* 5481(2): 241–259. <https://doi.org/10.11646/zootaxa.5481.2.4>.
- Korai SK, Jäger P (2024b) Five new species of the spider genus *Heteropoda* Latreille, 1804 (Araneae: Sparassidae) from China. *European Journal of Taxonomy* 947: 109–129. <https://doi.org/10.5852/ejt.2024.947.2623>
- Li JL, Jäger P, Liu J (2013) The female of *Heteropoda schwalbachorum* Jäger, 2008 (Araneae: Sparassidae). *Zootaxa* 3750(2): 185–188. <https://doi.org/10.11646/zootaxa.3750.2.6>
- Logunov DV, Jäger P (2015) Spiders from Vietnam (Arachnida: Aranei): new species and records. *Russian Entomological Journal* 24(4): 343–363. <https://doi.org/10.15298/rusentj.24.4.09>
- Ono H, Thinh TH, Sac PD (2012) Spiders (Arachnida, Araneae) recorded from Vietnam, 1837–2011. *Memoirs of the National Museum of Nature and Science Tokyo* 48: 1–37.
- Quan D, Zhong Y, Liu J (2014) Four *Pseudopoda* species (Araneae: Sparassidae) from southern China. *Zootaxa* 3754(5): 555–571. <https://doi.org/10.11646/zootaxa.3754.5.2>
- Seyfulina RR, Kartsev VM (2022) On the spider fauna of the Oriental Region: new data from Thailand (Arachnida: Aranei). *Arthropoda Selecta* 31(1): 115–128. <https://doi.org/10.15298/arthsel.31.1.14>
- Simon E (1880) Révision de la famille des Sparassidae (Arachnides). *Actes de la Société Linnéenne de Bordeaux* 34(2/3/4): 223–351.
- Simon E (1886) Arachnides recueillis par M. A. Pavie (sous chef du service des postes au Cambodge) dans le royaume de Siam, au Cambodge et en Cochinchine. *Actes de la Société Linnéenne de Bordeaux* 40: 137–166.
- Sterling EJ, Hurley MM (2005) Conserving Biodiversity in Vietnam: Applying Biogeography to Conservation Research. *Proceedings of the California Academy of Sciences* 56(9): 98–114.
- World Spider Catalog (2025) World Spider Catalog. Version 26. Natural History Museum Bern. <http://wsc.nmbe.ch> [accessed on 1 April 2025]
- Yamasaki T, Henriques S, Phung LTH, Hoang QD (2018) Redescription of the sole species of the enigmatic solifuge genus *Dinorhax* Simon, 1879 (Solifugae: Melanoblosiidae) in Southeast Asia. *The Journal of Arachnology* 46(3): 498–506. <https://doi.org/10.1636/JoA-S-17-090.1>
- Zhang H, Zhong Y, Zhu Y, Agnarsson I, Liu J (2021) A molecular phylogeny of the Chinese *Sinopoda* spiders (Sparassidae, Heteropodinae): implications for taxonomy. *PeerJ* 9: e11775. <https://doi.org/10.7717/peerj.11775>
- Zhang H, Zhu Y, Zhong Y, Jäger P, Liu J (2023) A taxonomic revision of the spider genus *Pseudopoda* Jäger, 2000 (Araneae: Sparassidae) from East, South and Southeast Asia. *Megataxa* 9(1): 1–304. <https://doi.org/10.11646/megataxa.9.1.1>

Genera *Colastes* Haliday, *Colastinus* Belokobylskij, and *Xenarcha* Foerster (Hymenoptera, Braconidae, Exothecinae) from the Korean Peninsula with a discussion on the Exothecinae genus and subgenus composition

Sergey A. Belokobylskij¹, Deokseo Ku²

¹ Zoological Institute of the Russian Academy of Sciences, St. Petersburg 199034, Russia

² The Science Museum of Natural Enemies, Geochang 50147, Republic of Korea

Corresponding author: Sergey A. Belokobylskij (doryctes@gmail.com)

Abstract

The Exothecinae genera *Colastes* Haliday, 1833, *Colastinus* Belokobylskij, 1984, and *Xenarcha* Foerster, 1863 of the Korean peninsula are reviewed. The names *Pseudophanomeris* Belokobylskij, 1984 and *Shawiana* van Achterberg, 1983 are synonymised with the genus *Xenarcha* Foerster and treated as subgenera. The two new species of *Colastes* and one new species and subspecies of *Xenarcha* are described and illustrated. *Exothecus effectus* Papp, 1972 is included in *Xenarcha* Foerster, **comb. nov.** The composition and distribution of the world-known Exothecinae genera are discussed and an illustrated key to its genera and subgenera is presented. A key to the Korean species of the genera *Colastes*, *Xenarcha*, and *Colastinus* is also provided.

Key words: Asia, descriptions, Ichneumonoidea, keys, *Pseudophanomeris*, parasitoid, *Shawiana*



Academic editor: Kees van Achterberg

Received: 6 February 2025

Accepted: 24 February 2025

Published: 29 April 2025

ZooBank: <https://zoobank.org/56D57FC2-75BC-488B-B68D-C92D2D6ADDD1>

Citation: Belokobylskij SA, Ku D (2025) Genera *Colastes* Haliday, *Colastinus* Belokobylskij, and *Xenarcha* Foerster (Hymenoptera, Braconidae, Exothecinae) from the Korean Peninsula with a discussion on the Exothecinae genus and subgenus composition. ZooKeys 1236: 141–183. <https://doi.org/10.3897/zookeys.1236.148928>

Copyright: ©

Sergey A. Belokobylskij & Deokseo Ku.

This is an open access article distributed under

terms of the Creative Commons Attribution

License (Attribution 4.0 International – CC BY 4.0).

Introduction

The subfamily Exothecinae is one of the small taxonomical groups of the cyclostome phylogenetic clade of the family Braconidae with reduced number of the genera in the World fauna. Previous to the current publication, seven genera were included in this subfamily, namely *Colastes* Haliday, 1833, *Colastinus* Belokobylskij, 1984, *Hormiopi* Blanchard, 1962, *Orientocolastes* Belokobylskij, 1999, *Shawiana* van Achterberg, 1983, *Vietcolastes* Belokobylskij, 1992, and *Xenarcha* Foerster, 1863 (Yu et al. 2016). However, the name *Hormiopi* Blanchard was recently synonymized under *Heterospilus* Haliday, 1836, a member of subfamily Doryctinae (Martínez and Diez 2024). The status of *Shawiana* and *Xenarcha* has also changed and they have been treated only as subgenera of *Colastes* (Belokobylskij 1998).

The Palaearctic fauna of this subfamily includes only three genera *Colastes*, *Colastinus* and *Xenarcha*. *Shawiana* and *Pseudophanomeris* Belokobylskij, 1984 are treated here only as subgenera of *Xenarcha* (syn. nov.). On the other hand,

the species diversity of *Colastes* and *Xenarcha* in this realm is relatively large and includes 23 and 28 already known species respectively. The information on the species of subfamily Exothecinae from the Korean peninsula is sparse and scattered (Papp 1987, 1992, 2003; Belokobylskij 1998; Ku et al. 2001).

In this paper we include illustrated descriptions of the two new species of *Colastes*, and the new species and subspecies of *Xenarcha*, a key to all species recorded on the Korean peninsula, and the original key to all known Exothecinae genera and subgenera.

Materials and methods

The terminology employed for the morphological features, sculpture, and body measurements follows Belokobylskij and Maetô (2009) and Belokobylskij et al. (2024). The wing venation nomenclature follows Belokobylskij and Maetô (2009) and Belokobylskij et al. (2024), with the terminology of van Achterberg (1993) shown in parentheses. The new distribution records presented in this paper are marked with an asterisk (*). In the key, additional features useful for separating taxa are listed after a dash (-). The specimens were examined using an Olympus SZ51 microscope. Photographs were taken with an Olympus OM-D E-M1 digital camera mounted on an Olympus SZX10 microscope (Zoological Institute of the Russian Academy of Sciences, St Petersburg, Russia). Image stacking was performed using Helicon Focus 8.0. The figures were produced using Adobe Photoshop CS6. The specimens examined in this study are deposited in the collections of the National Institute of Biological Resources (Incheon, Republic of Korea; **NIBR**), the Science Museum of Natural Enemies (Geochang, Republic of Korea; **SMNE**), and the Zoological Institute of the Russian Academy of Sciences (St Petersburg, Russia; **ZISP**). Abbreviations of Korean provinces used in this paper as follows: **CB** – Chungcheongbuk-do, **CN** – Chungcheongnam-do, **GB** – Gyeongsangbuk-do, **GG** – Gyeonggi-do, **GN** – Gyeongsangnam-do, **GW** – Gangwon-do, **JB** – Jeollabuk-do, **JJ** – Jeju-do, **JN** – Jeollanam-do.

Taxonomy

Class Insecta Linnaeus, 1758

Order Hymenoptera Linnaeus, 1758

Family Braconidae Nees, 1811

Subfamily Exothecinae Foerster, 1863

Genus *Colastes* Haliday, 1833

Type species. *Colastes braconius* Haliday, 1833.

***Colastes (Colastes) braconius* Haliday, 1833**

Fig. 13

Colastes braconius Haliday, 1833: 266; Shenefelt 1975: 1117; Belokobylskij and Tobias 1986: 57; Belokobylskij 1998: 143; Ku et al. 2001: 153; Yu et al. 2016; Belokobylskij et al. 2019: 281.

Exothecus debilis Wesmael, 1838: 75; Shenefelt 1975: 1118.

Colastes gracilis Papp, 1975: 411; Belokobylskij 1994: 69 (as synonym); 1998: 143.

Material examined. SOUTH KOREA: [GW] • Goseong-gun, Ganseong-eup, Jinbu-ri, Hyangrobong-peak (DMZ), 13.VI.1992 (J.-W. Lee), 4 females, 1 male (SMNE, ZISP) • Hyangrobong, Gangwondo, 13.VI.1992 (J.-W. Lee), 1 female (SMNE).

Hosts. Polyphagous species, its hosts include the larval stages of flies (Diptera) of the family Agromyzidae, moths (Lepidoptera) of the families Coleophoridae, Cosmopterigidae, Elachistidae, Eriocraniidae, Gracillariidae, Heliozelidae, Lycaenidae, Lyonetiidae, Momphidae, Nepticulidae, Pyralidae, Tischeriidae, Tortricidae, and Ypsolophidae, beetles (Coleoptera) of the family Curculionidae, and sawflies (Hymenoptera) of the family Tenthredinidae (Yu et al. 2016; Belokobylskij et al. 2019).

Distribution. Korean peninsula; Tunisia, Europe (widely), Caucasus, Turkey, Iran, Kazakhstan, Russia (European part, Urals, Siberia, Far East), Japan.

***Colastes (Colastes) dersu* Belokobylskij, 1998**

Colastes (Colastes) dersu Belokobylskij, 1998: 142; Ku et al. 2001: 155; Yu et al. 2016; Belokobylskij et al. 2019: 281.

Material examined. SOUTH KOREA [GN] • Hamyang-gun, Macheon-myeon, Samjeong-Byeoksoryeong, Mt. Jiri, 29.VII.1992 (Deokseo Ku), 1 male (SMNE) • Changyeong-gun, Yueo-myeon, Daedae-ri, Upo-swamp, 3.VII.2015 (E. Tselikh), 1 female (ZISP).

[GW] • Goseong-gun, Ganseong-eup, Jinbu-ri, Hyangrobong-peak (DMZ), 13.VI.1992 (J.-W. Lee), 1 female (SMNE) • Yanggu-gun, Dong-myeon, Panlrang-ri, Mt. Daeamsan (DMZ), 30.V.1992 (collector unknown), 1 female (SMNE) • Taebaek-shi, Mt. Taebaek, 13.VIII.1989 (S.M. Ryu), 1 female, 1 male (paratypes) (SMNE).

Host. Unknown.

Distribution. Korean Peninsula; Russia (southern Far East).

***Colastes (Colastes) fragiloides* Belokobylskij & Ku, sp. nov.**

<https://zoobank.org/B8A7CB58-FCCF-49C8-9641-DAC0D711CF42>

Figs 1, 2

Type material. **Holotype** • female, "Korea (GN) Namhae-gun, Seo-myeon, Noguri, Temple Mangunsa 15.X–14.XI.2022 (Malaise trap), Deokseo Ku, Jaehyeon Lee, Hyojin Jeong," (NIBR). **Paratypes** • 3 females, with same label as in holotype (SMNE, ZISP).

Description. Female. **Body** length 2.1–2.5 mm; fore wing length 2.2–2.8 mm. **Head** width 1.7–1.8× its medial length (dorsal view), 1.2× wider than mesoscutum. Temple behind eye weakly convex in anterior 1/2 and distinctly curvedly narrowed in posterior 1/2. Transverse diameter of eye 1.1–1.3× longer than temple (dorsal view). Ocelli small, arranged almost in equilateral triangle. POL approximately equal to Od, 0.3–0.4× OOL. Eye oval, glabrous, 1.25–1.30× as high as broad (lateral view). Malar space ~ 0.4× height of eye, 1.0–1.2× basal width of mandible. Malar



Figure 1. *Colastes (Colastes) fragiloides* sp. nov., female, holotype **A** habitus, lateral view **B** head, front view **C** head and anterior part of mesosoma, dorsal view **D** basal segments of antenna **E** apical segments of antenna **F** head and mesosoma, lateral view **G** mesosoma, dorsal view **H** hind leg.

suture indistinct or very shallow. Face width 1.1–1.2× height of face and clypeus combined, almost equal to height of eye. Hypoclypeal depression suboval, its width 1.0–1.1× distance from edge of depression to eye, ~ 0.4× width of face. Head distinctly and almost linearly narrowed below eyes. **Antenna** rather slender, filiform, 28–29-segmented, 1.2–1.3× longer than body. First flagellar segment 4.0–4.5× longer than its apical width, 1.05–1.15× longer than second segment. Penultimate segment 2.8–3.0× longer than wide, ~ 0.6× as long as first segment, 0.9–1.0× as long as apical segment; the latter acuminate apically and without spine.

Mesosoma 1.9–2.0× longer than its height. Pronotum dorsally with wide, lens-shaped shallow sculptured transverse groove, with distinct and curved medially transverse carina. Mesoscutum distinctly and curvedly elevated above prothorax. Notauli distinct in anterior 0.6, shallow to almost partly absent in posterior 0.4, entirely smooth. Prescutellar depression distinctly rugulose-crenulate, 0.3–0.4× as long as scutellum. Scutellum without transverse furrow and smooth posteriorly. Precoxal sulcus absent. **Wings.** Fore wing 2.6–2.8× longer than its maximum width. Pterostigma narrow, 6.0–7.0× its maximum width, 0.8–0.9× as long as metacarp (1-R1). Radial vein (r) arising before middle of pterostigma, from its basal 0.3. Second radial abscissa (3-SR) 2.0–2.7× longer than first abscissa (r) and forming obtuse angle with it, 0.45–0.50× as long as the straight third abscissa (SR1), 1.3–1.4× longer than first radiomedial vein (2-SR). Recurrent vein (m-cu) weakly antefurcal. Second radiomedial (submarginal) cell weakly or very weakly narrowed distally, its length 2.4–2.6× maximum width, 1.7–1.8× longer than brachial (subdiscal) cell. First abscissa of medial vein (1-SR+M) weakly sinuate. Distance (1-CU1) from nervulus (cu-a) to basal vein (1-M) 2.0–2.3× nervulus (cu-a) length. Parallel vein (CU1a) arising from posterior 0.3 of distal margin (3-CU1) of brachial (subdiscal) cell. In hind wing, first abscissa of mediocubital vein (M+CU) ~ 0.8× as long as second abscissa (1-M). First abscissa of costal vein (C+SC+R) 0.5× as long as second abscissa (1-SC+R). Recurrent vein (m-cu) short or very short, sclerotised, weakly antefurcal. **Legs.** Hind femur 5.2–5.5× longer than wide. Inner spur of hind tibia ~ 0.2× as long as hind basitarsus. Hind tarsus as long as hind tibia. Hind basitarsus 0.6× as long as combined length of second to fifth segments. Second tarsal segment of hind leg 0.5× as long as basitarsus, 1.5–1.7× as long as fifth segment (without pretarsus).

Metasoma as long as head and mesosoma combined. First tergite slender, evenly and linearly widened from base to apex, with weak spiracular tubercles, with dorsal carinae fused in basal quarter. Length of first tergite 1.2–1.3× its anterior width, anterior width 2.0–2.2× its posterior width. Second suture very fine, weakly curved, smooth. Medial length of second tergite 0.80–0.85× its anterior width, 1.2–1.3× length of third tergite. Setose part of ovipositor sheath 0.3–0.4× as long as metasoma, 1.2–1.6× longer than first tergite, 1.1–1.6× hind basitarsus, 0.15–0.20× as long as fore wing.

Sculpture and pubescence. Vertex and temple smooth; face smooth in upper half and densely reticulate-granulate in lower half or in lower lateral 0.7. Mesoscutum entirely smooth, without medio-posterior sculptured area; scutellum and mesopleuron smooth. Metapleuron almost entirely smooth, weakly rugulose anteriorly and posteriorly. Propodeum with medial carina in anterior 1/2, without delineated areas, smooth to almost smooth in anterior 0.3–0.4, densely reticulate-striate posteriorly. Legs smooth. First metasomal tergite entirely and densely rugose-striate; second tergite mostly or entirely smooth, rarely obliquely striate basally in short

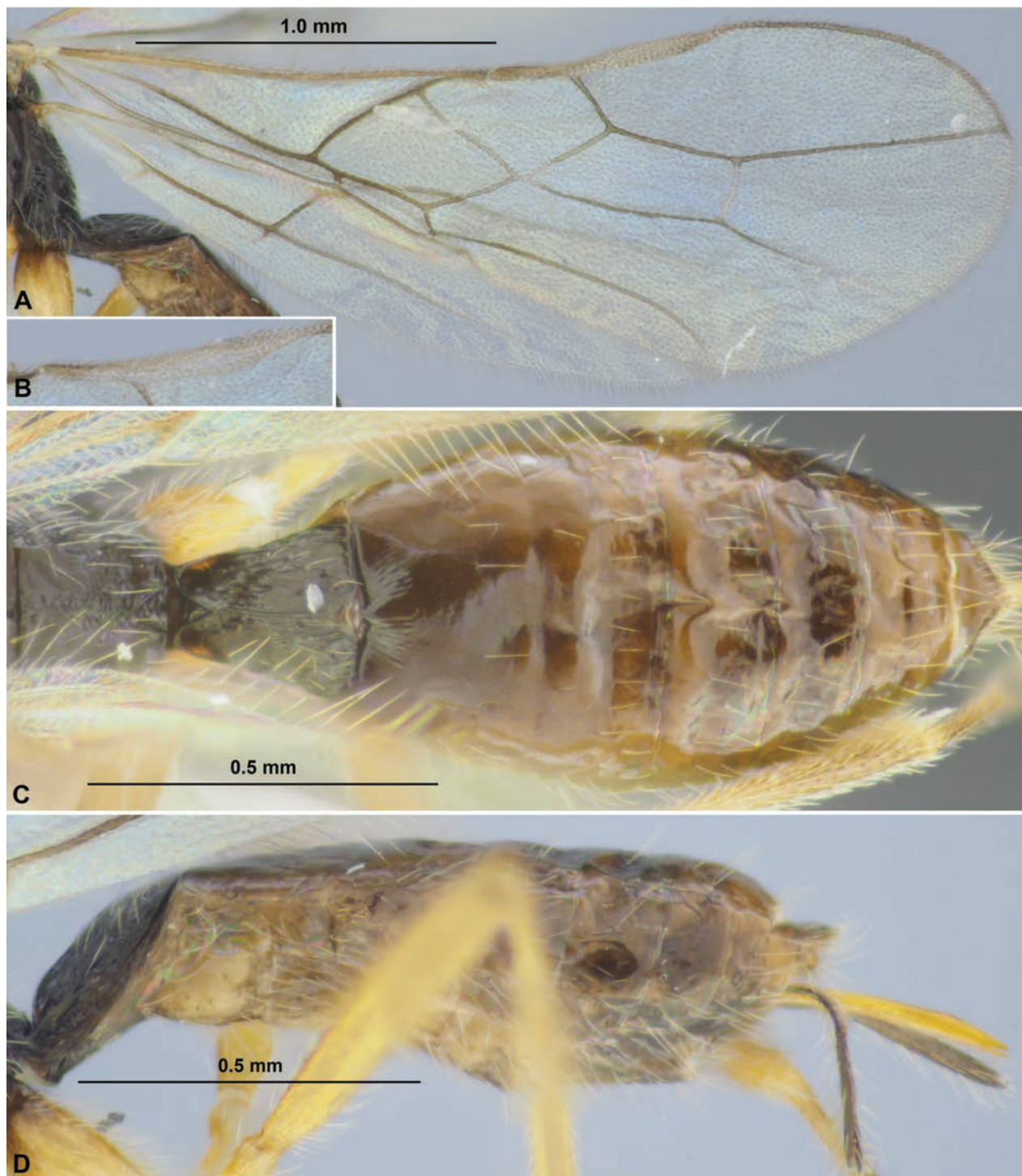


Figure 2. *Colastes (Colastes) fragiloides* sp. nov., female, holotype **A** wings **B** pterostigma **C** propodeum and metasoma, dorsal view **D** metasoma and ovipositor, lateral view.

area. Remaining tergites smooth. Mesoscutum with sparse, semi-erect and long pale setae along notauli. Hind tibia dorsally with short, dense and semi-erect pale setae, length of these setae $\sim 0.5\times$ as long as maximum width of hind tibia.

Colour. Body mainly black; metasoma behind first tergite brown to dark brown. Antennae mainly dark brown to black, four or five basal segments reddish brown. Palpi yellow. Legs mainly yellow, hind coxa basally brown. Wings hyaline. Pterostigma pale yellow.

Male. Unknown.

Discussion. This new species is very similar to *Colastes (Colastes) fragilis* (Haliday, 1836), but differs from later by having the first metasomal tergite longer, 1.2–1.3× longer than its apical width (shorter, not longer than its apical width in *C. fragilis*), the pronotum dorsally with lens-shaped shallow depression (without depression in *C. fragilis*), the propodeum mostly smooth in basal areas and with distinct basal carina (entirely rugose-reticulate or smooth only on small anterior areas and without basal carina in *C. fragilis*), fore wing first abscissa of radial vein (r) long and situated distinctly oblique to pterostigma (short and subvertical or only weakly oblique in *C. fragilis*), upper part of pronotum side and metapleuron mainly smooth (mainly rugose-reticulate in *C. fragilis*), and the second tergite sometimes striate medio-basally (entirely smooth in *C. fragilis*).

Etymology. Named from a combination of the species name *fragilis* and the Latin suffix *-oides* (resembling) because the new species is similar to *Colastes fragilis*.

Distribution. Korean peninsula.

***Colastes (Colastes) interdictus* Belokobylskij, 1998**

Colastes (Colastes) interdictus Belokobylskij, 1998: 143; Ku et al. 2001: 155; Papp 2003: 118; Yu et al. 2016; Belokobylskij et al. 2019: 281.

Material examined. SOUTH KOREA: [GB] • Bonghwa-gun, Myeongho-myeon, Gwanjang-ri, Mt. Cheongryang, 14.VII.2015 (E. Tselikh), 1 female (ZISP).

[GG] • Inchen-si, Jung-gu, Muui-dong, 37°23'46.09"N, 126°24'36.38"E, Malaise trap, 14–27.IX.2017 (Hyung-Keun Lee), 1 male (SMNE).

[GN] • Sancheong-gun, Chahwang-myeon, Mt. Hwangmae, (30 km NNW Jinju, forest, h = 800 m), 12.VI.2002 (S. Belokobylskij) (SMNE) • same locality, 29.VI.2002 (S. Belokobylskij), 1 female (ZISP) • Namhae-gun, Namhae-eup, Asan-ri, 34°51'06.7"N, 127°51'31"E, 19.VI.2022 (S. Belokobylskij), 1 female (ZISP).

[GW] • Jeongseon-gun, Imgye-myeon, Jikwon-ri, Mt. Seokbyeong, Malaise trap, 3.VIII–19.IX.2002 (Deokseo Ku), 1 male (SMNE) • Goseong-gun, Ganseong-eup, Jinbu-ri, Hyangrobong-peak, (DMZ), 13.VI.1992 (J.-W. Lee), 1 female, 2 males (SMNE) • Inje-gun, Girin-myeon, Jindong-ri, Mt. Jeombong, (Gombaeryeong), 38°1'58.52"N, 128°27'54.19"E, 14.IX–16.X.2017 (Hyung-Keun Lee), 1 female (SMNE) • Taebaek-shi, Mt. Taebaek, 13.VIII.1989 (S.-M. Ryu), 1 female (paratype) (SMNE); Mt. Taebaek, 23.VI.1989 (Deokseo Ku), 1 male (SMNE).

[JN] • Gurye-gun, Toji-myeon, Bangok-gil, Mt. Jiri, Nogodan, 35°17'37.2"N, 127°31'55.6"E, Malaise trap, 10.VII–11.IX.2001 (Deokseo Ku), 5 females (SMNE, ZISP).

Hosts. Unknown.

Distribution. Korean peninsula; Russia (southern Far East), Japan.

Remarks. J. Papp (1987) recorded the species *Colastes (Colastes) affinis* (Wesmael, 1838) in the fauna of the Korean peninsula. However, during visit to the Hungarian Natural History Museum in 2000, the first author studied and determined that the Korean specimens belong actually to the East Palaearctic *C.(C.) interdictus* Belokobylskij, 1998. These corrections and new information were later published by Papp (2003: 118). Thus, the species *C. (C.) affinis* is here excluded from the fauna of the Korean peninsula.

***Colastes (Colastes) pubicornis* (Thomson, 1892)**

Exothecus pubicornis Thomson, 1892: 1699.

Colastes pubicornis: Shenefelt 1975: 1122; Belokobylskij and Tobias 1986: 53; Papp 2003: 118.

Xenarcha (Xenarcha) pubicornis: Papp 1987: 161.

Colastes (Colastes) pubicornis: Belokobylskij, 1998: 139; Ku et al. 2001: 154; Yu et al. 2016; Belokobylskij et al. 2019: 281.

Material examined. SOUTH KOREA: [GW] • Jeongseon-gun, Nam-myeon, Mungok-ri, Jamiwon (Doowibong-peak), 2.IX.2000 (collector unknown), 1 female (SMNE).

[GG] • Mt. Yumyeong, Okcheon-myeon, Yangpyeonggun, Gyeonggi-do, 14. VI. 1992 (collector unknown), 1 male (SMNE).

Hosts. Diptera: *Chirosia histricina* (Rondani, 1886) (Anthomyiidae).

Distribution. Korean peninsula; Europe (rarely), Russia (European part, Siberia, Far East), China (Taiwan), Japan.

Remarks. This species was also recorded from North Korea as *Colastes flavitarsis* Thomson (Papp, 1992). Papp (2003: 118) used later the correct determination of this species.

***Colastes (Colastes) semiflavus* Belokobylskij & Ku, sp. nov.**

<https://zoobank.org/70A45341-B4D4-4E33-BEFF-A03F2234AF97>

Figs 3, 4

Type material. Holotype • female, "Korea (GN) [= Gyeongsangnam-do]. Namhae-gun, Seo-myeon, Nogu-ri, Temple Mangunsa, 15.X–14.XI.2022 (Malaise trap), Deokseo Ku, Jaehyeon Lee, Hyojin Jeong (NIBR).

Description. Female. Body length 2.8 mm; fore wing length 2.9 mm. **Head** width 1.8× its medial length (dorsal view), 1.2× wider than mesoscutum. Temple behind eye weakly convex in anterior 1/2 and distinctly curvedly narrowed in posterior 1/2. Transverse diameter of eye 1.6× longer than temple (dorsal view). Ocelli small, arranged in triangle with base 1.2× its sides. POL 1.5× Od, 0.8× OOL. Eye oval, glabrous, 1.25× as high as broad (lateral view). Malar space ~ 0.4× height of eye, almost equal to basal width of mandible. Malar suture indistinct. Face width 1.4× height of face and clypeus combined, equal to height of eye. Hypoclypeal depression circular, its width 1.1× distance from edge of depression to eye, 0.4× width of face. Head distinctly and almost linearly narrowed below eyes. **Antenna** weakly thickened, almost filiform, 28-segmented, ~ 1.2× longer than body. First flagellar segment 3.3× longer than its apical width, 1.2× longer than second segment. Penultimate segment 2.3× longer than wide, ~ 0.6× as long as first segment, 0.9× as long as apical segment; the latter acuminate apically and with short 'spine'.

Mesosoma 1.9× longer than its height. Pronotum dorsally with shallow and sculptured transverse groove, with weak transverse pronotal carina. Mesoscutum highly and curvedly elevated above prothorax. Notauli complete, deep in anterior 0.6, shallow in posterior 0.4, crenulate anteriorly. Prescutellar depression

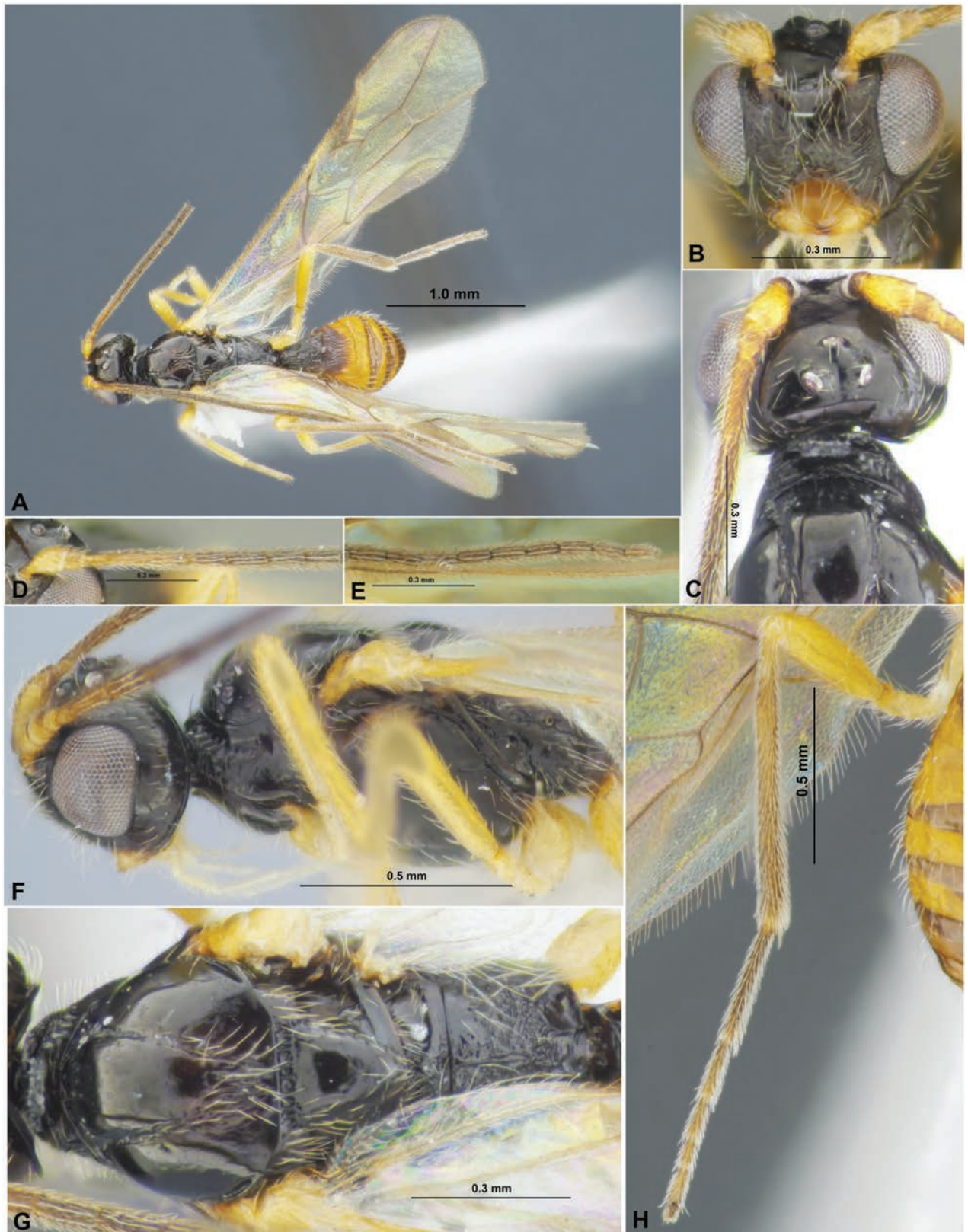


Figure 3. *Colastes (Colastes) semiflavus* sp. nov., female, holotype **A** habitus, dorsal view **B** head, front view **C** head and anterior part of mesosoma, dorsal view **D** basal segments of antenna **E** apical segments of antenna **F** head and mesosoma, lateral view **G** mesosoma, dorsal view **H** hind leg.

short, distinctly crenulate, $\sim 0.2\times$ as long as scutellum. Scutellum without transverse furrow and smooth posteriorly. Precoxal sulcus absent. **Wings.** Fore wing $2.7\times$ longer than maximum width. Pterostigma relatively wide, $4.2\times$ its maximum width, $0.8\times$ as long as metacarp (1-R1). Radial vein (r) arising weakly before middle of pterostigma, from its basal ~ 0.45 . Second radial abscissa (3-SR) $2.8\times$ longer than first abscissa (r) and forming very obtuse angle with it, $0.5\times$ as long as the straight third abscissa (SR1), $1.3\times$ longer than first radiomedial vein (2-SR). Recurrent vein (m-cu) distinctly antefurcal. Second radiomedial (submarginal) cell not narrowed distally, its length $2.6\times$ maximum width, $1.9\times$ longer than brachial (subdiscal) cell. First abscissa of medial vein (1-SR+M) weakly sinuate. Distance (1-CU1) from nervulus (cu-a) to basal vein (1-M) $0.6\times$ nervulus (cu-a) length. Parallel vein (CU1a) arising from posterior 0.4 of distal margin (3-CU1) of brachial (subdiscal) cell. Brachial (subdiscal) cell distinctly widened distally. In hind wing, first abscissa of mediocubital vein (M+CU) $\sim 0.9\times$ as long as second abscissa (1-M). First abscissa of costal vein (C+SC+R) approx. as long as second abscissa (1-SC+R). Recurrent vein (m-cu) long, unsclerotised, weakly antefurcal, weakly curved. **Legs.** Hind femur $5.0\times$ longer than wide. Inner spur of hind tibia $\sim 0.2\times$ as long as hind basitarsus. Hind tarsus as long as hind tibia. Hind basitarsus $0.7\times$ as long as combined length of second to fifth segments. Second tarsal segment of hind leg $0.45\times$ as long as basitarsus, $1.7\times$ as long as fifth segment (without pretarsus).

Metasoma $\sim 0.9\times$ as long as head and mesosoma combined. First tergite comparatively slender, evenly and almost linearly widened from base to apex, with very weak spiracular tubercles, with dorsal carinae distinct in anterior 0.3 and connected subbasally by additional transverse carina. Length of first tergite $1.25\times$ its anterior width, anterior width $1.7\times$ its posterior width. Second suture distinct, wide, almost straight, rugulose. Medial length of second tergite $0.8\times$ its anterior width, $1.3\times$ length of third tergite. Setose part of ovipositor sheath $0.2\times$ as long as metasoma, almost as long as first tergite, almost equal to hind basitarsus, $\sim 0.1\times$ as long as fore wing.

Sculpture and pubescence. Vertex and temple smooth; face densely granulate in lateral lower 0.6, smooth or almost smooth on remaining part. Mesoscutum mainly smooth, with striation in medio-posterior 0.4; scutellum and mesopleuron smooth. Metapleuron widely smooth in anterior 0.5–0.6, rugulose-reticulate on remaining posterior part. Propodeum mainly rugose-reticulate, smooth in narrow anterior part, with distinct medial carina in anterior 1/2, areola small and weakly delineated by carinae. Legs (including hind coxa) entirely smooth. First metasomal tergite entirely and densely rugose-striate; second tergite entirely distinctly striate, almost without reticulation; third tergite rugose-reticulate in anterior 0.3–0.4, remaining part smooth. Remaining tergites smooth. Mesoscutum mainly glabrous, with sparse, semi-erect, short and pale setae arranged along notauli and in medio-posterior area. Hind tibia dorsally with short, dense and semi-erect brownish setae, length of these setae $\sim 0.5\times$ as long as maximum width of hind tibia.

Colour. Head, mesosoma, first and anterior 1/2 of second metasomal tergites black; remaining part of metasoma yellow to brownish yellow. Antenna mainly dark brown to black, two basal segments yellowish brown with faint infuscation. Palpi pale yellow. Legs mainly yellow, hind tibia in distal 1/2 and hind tarsus brown. Wings hyaline. Pterostigma pale brown.

Male. Unknown.

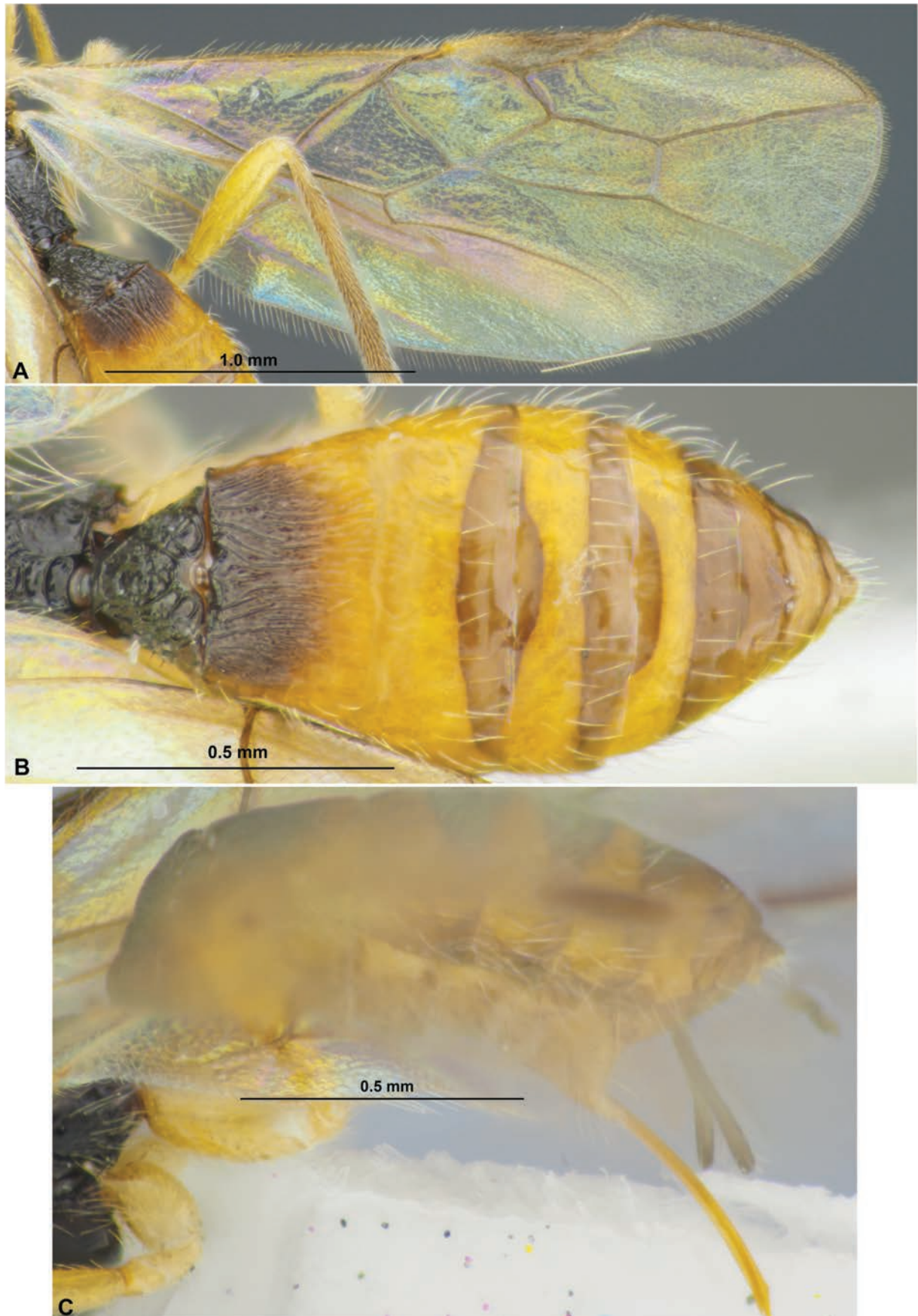


Figure 4. *Colastes (Colastes) semiflavus* sp. nov., female, holotype **A** wings **B** metasoma, dorsal view **C** metasoma and ovipositor, lateral view.

Discussion. This new species is very similar to *C. (C.) ussuricus* Belokobylskij, 1996, but differs from later by having the face width 1.4× height of face and clypeus combined (1.1–1.2× in *C. ussuricus*), antenna 28-segmented (32–35-segmented in *C. ussuricus*), tergites behind third tergite entirely smooth (fourth in basal 1/2 and fifth basally striate in *C. ussuricus*), metasoma in posterior 1/2 yellow to brownish yellow (metasoma black or sometimes partly dark reddish brown in *C. ussuricus*).

Colastes (C.) semiflavus sp. nov. is also close to *C. (C.) interdictus* Belokobylskij, 1998, but differs from later by having the face densely granulate in lower 0.6 (in lower 0.3 in *C. interdictus*), the first flagellar segment 3.3× longer than its apical width (4.0–5.0× in *C. interdictus*), penultimate segment of antenna 2.3× longer than wide (3.0× in *C. interdictus*), prescutellar depression short (relatively long in *C. interdictus*), radial vein (r) of fore wing arising from basal 0.45 of pterostigma (from basal 0.3 of pterostigma in *C. interdictus*), third metasomal tergite rugose-reticulate in anterior 0.3–0.4 (third tergite entirely smooth or only sometimes with short striae basally in *C. interdictus*), metasoma yellow to brownish yellow in posterior 0.5–0.6 (pale reddish brown behind first tergite in *C. interdictus*), and hind tibia in distal 1/2 and hind tarsus brown (hind legs entirely yellow in *C. interdictus*).

Etymology. Named from the combination of the Latin words *semi* (half) and *flavus* (yellow) because metasoma is yellow in its posterior half.

Distribution. Korean peninsula.

****Colastes (Colastes) sylvicola* Belokobylskij, 1998**

Colastes (Colastes) sylvicola Belokobylskij, 1998: 141; Yu et al. 2016; Belokobylskij et al. 2019: 281.

Material examined. SOUTH KOREA: [GB] • Ulreung-gun, Buk-myeon, Nari-ri, Nariryong, sweeping, 29.VII.2001 (collector unknown), 1 female (NIBR).

Hosts. Unknown.

Distribution. *Korean peninsula; Russia (southern Far East), Japan (Kyushu).

****Colastes (Colastes) ussuricus* Belokobylskij, 1996**

Colastes (Colastes) ussuricus Belokobylskij, 1996: 1667; 1998: 141; Yu et al. 2016; Belokobylskij et al. 2019: 281.

Material examined. SOUTH KOREA: [GB] • Uljin-gun, Buk-myeon, Deokgu-ri, Huinmoki, 6.V.2000 (collector unknown), 1 female (NIBR).

Hosts. Unknown.

Distribution. *Korean peninsula; Russia (southern Far East), Japan (Kyushu).

Genus *Colastinus* Belokobylskij, 1984

Type species. *Colastinus crustatus* Belokobylskij, 1984.

****Colastinus crustatus* Belokobylskij, 1984**

Fig. 9

Colastinus crustatus Belokobylskij, 1984: 1022; 1994: 73; 1998: 159; Yu et al. 2016; Belokobylskij et al. 2019: 282.

Material examined. SOUTH KOREA: [GB] • Yeongyang-gun, Ilwol-myeon, Mt. Ilwolsan, 36°48'29"N, 129°05'25"E, 7.VII.2015 (E. Tselikh), 1 female (NIBR).

Hosts. Unknown.

Distribution. *Korean peninsula; Russia (southern Far East).

Genus *Xenarcha* Foerster, 1863

Type species. *Rogas (Colastes) lustrator* Haliday, 1836.

Subgenus *Pseudophanomeris* Belokobylskij, 1984, syn. nov.

Type species. *Colastes (Pseudophanomeris) unicolor* Belokobylskij, 1984.

****Xenarcha (Pseudophanomeris) insularis* (Belokobylskij, 1984), comb. nov.**

Colastes (Pseudophanomeris) insularis Belokobylskij, 1984: 1024; 1994: 70; 1998: 145; Yu et al. 2016; Belokobylskij et al. 2019: 281.

Material examined. SOUTH KOREA: [GG] • Gwangju-si, Toechon-myeon, Gwaneum-ri, 37°26'43.6"N, 127°19'55.26"E, Malaise trap, 24.V–6.VI.2017 (Hyung-Keun Lee), 1 female (SMNE).

[GB] • Cheongsong-gun, Budong-myeon, Sangui-ri, Mt. Juwang, sweeping, 20.VII.1999 (Jungsuk Park), 1 male (NIBR).

Hosts. Unknown.

Distribution. *Korean peninsula; Russia (southern Far East), Japan.

***Xenarcha (Pseudophanomeris) pilosa* (Belokobylskij, 1984), comb. nov.**

Colastes (Pseudophanomeris) pilosa Belokobylskij, 1984: 1024; 1994: 70; 1998: 145; Yu et al. 2016; Belokobylskij et al. 2019: 281.

Xenarcha (Pseudophanomeris) pilosa: Papp 1987: 160.

Material recorded. This species was previously recorded from North Korea (Papp 1987) • "Kangwon Province, Kum-gang-san, 12.X.1978, No 488", 2 females (HNHM).

Hosts. Unknown.

Distribution. Korean peninsula; Czech Republic, Ukraine, Russia (European part, southern Far East), Japan.

Subgenus *Shawiana* van Achterberg, 1983

Type species. *Exothecus laevis* Thomson, 1892.

Xenarcha (Shawiana) attonita (Papp, 1987), comb. nov.

Shawiana attonita Papp, 1987: 173; Yu et al. 2016.

Colastes (Shawiana) attonitus: Belokobylskij 1998: 148.

Material recorded. NORTH KOREA • “Korea, Prov. North Pyongan, Mt. Myohyang-san (first label). “Hotel. 14 VIII 1982, leg. Beron et Porov, No. 11” (second label), 1 female (holotype) (HNHM, N^o.7077) (examined).

Hosts. Unknown.

Distribution. Korean peninsula.

* *Xenarcha (Shawiana) catenator* (Haliday, 1836), comb. nov.

Rhogas (Colastes) catenator Haliday, 1836: 93.

Phanomeris catenator: Shenefelt 1975: 1130; van Achterberg 1983: 345.

Shawiana catenator: van Achterberg 1983: 345; Yu et al. 2016.

Colastes catenator: Belokobylskij and Tobias 1986: 52; Belokobylskij 1994: 71; 1998: 152.

Colastes (Shawiana) catenator: Belokobylskij et al. 2019: 282.

Material examined. SOUTH KOREA: [GN] • Sancheong-gun, Chahwang-myeon, Mt. Hwangmae, (30 km NNW Jinju, forest, h = 800 m), 12.VI.2002 (S. Belokobylskij), 1 female (NIBR).

Hosts. Hymenoptera: *Fenella nigrita* (Westwood), *Fenusa dohrnii* (Tischbein), *F. pumila* Leach, *F. pusilla* Leach, *F. rubi* Boie, *F. ulmi* Sundevall, *Heterarthrus aceris* (Kaltenbach), *H. vagans* Fallen, *Messa hortulana* (Klug), *M. nana* (Klug), *Metallus albipes* (Cameron), *M. pumilus* (Klug), *Parna tenella* (Klug), *Profenusa pygmaea* (Klug), *Scolioneura betuleti* (Klug) (Tenthredinidae). **Lepidoptera:** *Eriocrania semipurpurella* (Stephens) (Eriocraniidae); *Phyllonorycter quercifoliella* (Zeller) (Gracillariidae).

Distribution. *Korean peninsula; Western Europe, Georgia, Russia (European part, Siberia, Far East), Mongolia, Japan.

* *Xenarcha (Shawiana) foveolator* (Thomson, 1892), comb. nov.

Exothecus foveolator Thomson, 1892: 1698.

Colastes foveolator: Shenefelt 1975: 1119; Belokobylskij and Tobias 1986: 57.

Shawiana foveolator: van Achterberg 1983: 348; Yu et al. 2016.

Colastes (Shawiana) foveolator: Belokobylskij 1998: 145; Belokobylskij et al. 2019: 282.

Material examined. SOUTH KOREA: [GN] • Goseong-gun, Hail-myeon, Suyang-ri, 34°58'34.8"N, 128°12'08.3"E, 18.VI.2022 (E. Tselikh), 1 female (NIBR).

Hosts. Hymenoptera: *Blasticotoma filiceti* Klug (Blasticotomidae). **Lepidoptera:** *Phyllonorycter alpina* (Fray), *Ph. coryli* (Nicelli) (Gracillariidae)

Distribution. *Korean peninsula; Germany, Sweden, Finland, Russia (European part, Siberia, Far East), Japan.

***Xenarcha (Shawiana) laevis* (Thomson, 1892), comb. nov.**

Fig. 11

Exothecus laevis Thomson, 1892: 1699.

Colastes laevis: Shenefelt 1975: 1120 Belokobylskij and Tobias 1986: 53.

Shawiana laevis: van Achterberg 1983: 343; Papp 1987: 160; 1992: 66; Yu et al. 2016.

Colastes (Shawiana) laevis: Belokobylskij 1998: 147; Belokobylskij et al. 2019: 282.

Material examined. SOUTH KOREA: [JN] • Gurye-gun, Toji-myeon, Bangok-gil, Mt. Jiri, Nogodan, 35°17'37.2"N, 127°31'55.6"E, Malaise trap, 10.VII–11.IX.2001 (Deokseo Ku), 1 female (SMNE).

Hosts. Hymenoptera: *Euura mucronata* (Hartig), *Fenusa dohrnii* (Tischbein), *Heterarthrus aceris* (Kaltenbach), *H. microcephalus* (Klug), *H. vagans* Fallen, *H. wuestneii* (Konow), *Pontania glaucae* Kopelke, *P. lapponicola* Kopelke, *P. nigricantis* Kopelke, *P. vesicator* Bremi, *Scolioneura betuleti* (Klug), *S. vicina* Konow (Tenthredinidae).

Distribution. Korean peninsula; Europe (widely), Russia (European part, Far East), Turkey, Iran, Mongolia.

***Xenarcha (Shawiana) nupta* (Papp, 1983), comb. nov.**

Colastes nuptus Papp, 1983: 447.

Shawiana nupta: Papp 1987: 160; Yu et al. 2016.

Colastes (Shawiana) nuptus: Belokobylskij 1998: 152; Belokobylskij et al. 2019: 282.

Material examined. SOUTH KOREA: [GN] • Geochang-gun, Sinwon-myeon, Waryong-ri, Malaise trap, 2–16.VII.2022 (Deokseo Ku, Jaehyeon Lee, Hyojin Jeong), 1 female (SMNE).

Hosts. Unknown.

Distribution. Korean peninsula; Mongolia, Russia (southern Far East).

***Xenarcha (Shawiana) orientalis* (Belokobylskij, 1998), comb. nov.**

Colastes (Shawiana) orientalis Belokobylskij, 1998: 152; Ku et al. 2001: 155; Belokobylskij et al. 2019: 282.

Shawiana orientalis: Yu et al. 2016.

Material examined. SOUTH KOREA: [GB] • Andong-si, Bukhu-myeon, Daehyeon-ri, Malaise trap, 3–18.V.2022.(Gi-Myon Kwon), 1 female (SMNE) • Sonsan-gun, Suryun, Bongyang-ri, 9.VI.1992 (Deokseo Ku), 1 female (paratype) (SMNE).

[GN] • Namhae-gun, Namhae-eup, Simcheon-ri, Simcheon, light trap, 26–27.IX.1998 (Jesik Jeon), 1 female (SMNE).

[GW] • Sokcho-si, Seolak-dong, 12.VI.1992 (Deokseo Ku), 1 female (SMNE).

Hosts. Unknown.

Distribution. Korean peninsula; Russia (Siberia, southern Far East).

* *Xenarcha (Shawiana) rupicola* (Belokobylskij, 1998), **comb. nov.**

Colastes (Shawiana) rupicola Belokobylskij, 1998: 147; Belokobylskij et al. 2019: 282.

Shawiana rupicola: Yu et al. 2016.

Material examined. SOUTH KOREA: [JN] • Gurye-gun, Toji-myeon, Bangok-gil, Mt. Jiri, Nogodan, 35°17'37.2"N, 127°31'55.6"E, Malaise trap, 10.VIII–11.IX.2001 (Deokseo Ku), 1 female (NIBR).

Hosts. Unknown.

Distribution. *Korean peninsula; Russia (southern Far East).

Subgenus *Xenarcha* s. str.

Xenarcha (Xenarcha) effecta (Papp, 1972), **comb. nov.**

Exothecus effectus Papp, 1972: 323.

Colastes effectus: Shenefelt 1975: 1119.

Xenarcha effecta: van Achterberg 1983: 349.

Colastes (Shawiana) effectus: Belokobylskij 1990: 37; 1994: 71.

Colastes (Xenarcha) effectus: Belokobylskij 1998: 154; Ku et al. 2001: 154.

Colastes (Fungivenator) effectus: van Achterberg and Shaw 2008: 1854; Yu et al. 2016; Belokobylskij et al. 2019: 281.

Material examined. SOUTH KOREA: [GN] • Jinju, Gajwa, 28.IX.1993 (Deokseo Ku), 1 female (SMNE); • Sancheong-gun, Chahwang-myeon, Mt. Hwangmae, (30 km NNW Jinju, forest, h = 800 m), 16.VI.2002 (S. Belokobylskij), 1 female (ZISP).

[GB] • Yeongcheon-si, Hyeonseo-myeon, Galjeon-ri, Mt. Bohyeon, sweeping, 4.IX.1998 (Jungsuk Park), 1 female (SMNE).

Hosts. Unknown.

Distribution. Korean peninsula; Russia (European part, southern Far East), China, Japan.

Remarks. This species was included in the subgenus *Fungivenator* van Achterberg & Shaw, 2008 of the genus *Colastes* Haliday (van Achterberg and Shaw 2008). However the material of our study from China, Korea, and the Russian Far East distinctly shows that the members of this species have a distinct and deep round pronope, which together with some other characters (complete no-tauli, radial vein (r) of the fore wing arising almost from middle of pterostigma) demonstrate that it belongs to *Xenarcha* (subgenus *Xenarcha*).

* *Xenarcha (Xenarcha) ivani* (Belokobylskij, 1986), comb. nov.

Colastes ivani Belokobylskij, 1996: 68.

Colastes (Shawiana) ivani: Belokobylskij 1994: 72; 1998: 156.

Xenarcha ivani: Yu et al. 2016.

Colastes (Xenarcha) ivani: Belokobylskij et al. 2019: 282.

Material examined. SOUTH KOREA: [GN] • Namhae-gun, Seo-myeon, Nogu-ri, Temple Mangunsa, Malaise trap, 27.VII–13.VIII.2022 (Deokseo Ku, Jaehyeon Lee, Hyojin Jeong), 1 female (NIBR) • Namhae-gun, Namhae-eup, Asan-ri, 34°51'06.7"N, 127°51'31"E, 19.VI.2022 (S. Belokobylskij), 1 male (SMNE) • Sancheong-gun, Chahwang-myeon, Mt. Hwangmae, (30 km NNW Jinju, forest, h = 800 m), 10.VII.2002 (S. Belokobylskij), 1 male (ZISP).

Hosts. Unknown.

Distribution. *Korean peninsula; Russia (southern Far East).

Xenarcha (Xenarcha) pacificoformis Belokobylskij & Ku, sp. nov.

<https://zoobank.org/583B493F-ACE4-4D6E-A534-A1FB1BD580AC>

Figs 5, 6

Type material. Holotype • female, SOUTH KOREA, Gyeonggi-do [GG], Yangpyeong-gun, Okcheon-myeon, Mt. Yumyeong, 14.VI.1992 (collector unknown) (NIBR). **Paratypes:** SOUTH KOREA. [GG] • Yangpyeong-gun, Okcheon-myeon, Yongcheon-ri, Mt. Yongmun, sweeping, 28.VII.2000 (Tae-Ho An), 1 female (SMNE) • Suwon-si, Gwonseon-gu, Seodun-dong, Mt. Yeogi, 5.VIII.1997 (June-Yeol Choi), 1 female (SMNE) • Yangpyeong-gun, Okcheon-myeon, Yongcheon-ri, Mt. Yongmun, sweeping, 28.VII.2000 (Tae-Ho An), 1 male (SMNE). [GW] • Cheolwon-gun, Galmal-eup, Naedae-ri, 14.VI.1992 (collector unknown), 1 female (SMNE) • Sokcho-si, Seolak-dong, 12.VI.1992 (Deokseo Ku), 1 female (SMNE) • Gangreung-si, Yeongok-myeon, Sinwang-ri Sogum River (Mt. Odae), 3.VIII.1998 (collector unknown), 1 male (SMNE). [GB] • Yeongyang-gun, Inwol-myeon, Mt. Inwol, 36°48'29"N, 129°05'25"E, 14.VII.2023 (E. Tselikh), 1 female (ZISP) • Seongju-gun, Suryun-myeon, Baekun-ri, Baekunbunso, Mt. Gaya, sweeping, 22.VIII.2000 (Tae-Ho An), 1 female (SMNE) • Ulleung-gun, Ulleung-eup, Sadong-ri, San35 Nari-Seonginbong No.15, sweeping, 10.IX.2017, (Deokseo Ku), 1 male (SMNE) • Cheongsong-gun, Budong-myeon, Sangui-ri, Mt. Juwang, 20.VII.1999 (Juhwan Son, Gyeongryeon Han), 2 males (SMNE) • Cheongsong-gun, Budong-myeon, Sangui-ri, Mt. Juwang, 20.VII.1999 (Juhwan Son, Gyeongryeon Han), 2 males (SMNE, ZISP). [GN] • Geochang-gun, Wicheon-myeon, Janggi-ri, Malaise trap, 16.X–30.XI.2015 (Tae-Ho An), 1 female (SMNE) • Goseong-gun, Gaechon-myeon, Bukpyeong-ri, Mt. Yeonhwa, Temple Okcheon, sweeping, 22.V.1999 (Seongnam Kim), 1 female (SMNE) • Sancheong-gun, Chahwang-myeon, Mt. Hwangmae, (30 km NNW Jinju, forest, meadow, h = 800 m), 12.VI.2002 (S. Belokobylskij), 1 female (ZISP) • same label, but 16.VI.2002, 2 females (SMNE, ZISP) • same label, but 29.VI.2002, 1 male (ZISP) • same label, but 10.VII.2002, 1 male (ZISP).

Description. Female. Body length 3.1–4.1 mm; fore wing length 3.0–4.1 mm. **Head** width 1.8–1.9× its medial length (dorsal view), ~ 1.3× wider than me-



Figure 5. *Xenarcha (Xenarcha) pacificoformis* sp. nov., female, holotype **A** habitus, lateral view **B** head, front view **C** head and anterior part of mesosoma, dorsal view **D** basal segments of antenna **E** apical segments of antenna **F** head and mesosoma, lateral view **G** mesosoma and first metasomal tergite, dorsal view **H** hind leg.

soscutum. Temple strongly curvedly narrowed behind eye. Transverse diameter of eye 1.5–1.6× longer than temple (dorsal view). Ocelli small, arranged almost in equilateral triangle. POL 1.0–1.2× Od, 0.45–0.50× OOL. Eye oval, glabrous, 1.3× as high as broad (lateral view). Malar space 0.3–0.4× height of eye,

1.0–1.3× basal width of mandible. Malar suture absent or almost absent. Face width 1.2–1.3× height of face and clypeus combined, almost equal to height of eye. Hypoclypeal depression circular, its width 0.8–1.0× distance from edge of depression to eye, ~ 0.4× width of face. Head distinctly and almost linearly narrowed below eyes. **Antenna** rather slender, filiform or weakly setiform, 34–36-segmented, ~ 1.2× longer than body. First flagellar segment 3.3–3.7× longer than its apical width, 1.2–1.3× longer than second segment. Penultimate segment 2.7–2.8× longer than wide, ~ 0.5× as long as first segment, ~ 0.8× as long as apical segment; the latter acuminate apically and with short 'spine'.

Mesosoma 1.8–2.0× longer than its height. Pronotum dorsally with large, deep, smooth round pit (pronope), with high and strongly curved medially transverse carina. Mesoscutum distinctly and curvedly elevated above prothorax. Notauli complete, rather deep, finely and sparsely crenulate. Prescutellar depression distinctly rugulose-crenulate, 0.25–0.30× as long as scutellum. Scutellum without transverse furrow and smooth posteriorly. Precoxal sulcus absent.

Wings. Fore wing 2.8–3.0× longer than maximum width. Pterostigma narrow, 5.0–5.6× its maximum width, 0.8–0.9× as long as metacarp (1-R1). Radial vein (r) arising before middle of pterostigma, from its basal ~ 0.4. Second radial abscissa (3-SR) 2.5–3.0× longer than first abscissa (r) and forming obtuse angle with it, ~ 0.5× as long as the almost straight third abscissa (SR1), 1.2–1.4× longer than first radiomedial vein (2-SR). Recurrent vein (m-cu) distinctly antefurcal. Second radiomedial (submarginal) cell weakly narrowed distally, its length 2.5–2.7× maximum width, 1.7–2.0× longer than brachial (subdiscal) cell. First abscissa of medial vein (1-SR+M) weakly sinuate. Distance (1-CU1) from nervulus (cu-a) to basal vein (1-M) 1.2–1.3× nervulus (cu-a) length. Parallel vein (CU1a) arising from posterior 0.3 of distal margin (3-CU1) of brachial (subdiscal) cell. In hind wing, first abscissa of mediocubital vein (M+CU) 1.0–1.1× as long as second abscissa (1-M). First abscissa of costal vein (C+SC+R) 0.8–0.9× as long as second abscissa (1-SC+R). Recurrent vein (m-cu) long, unsclerotised, infuscate, antefurcal. **Legs.** Hind femur 4.6–5.3× longer than wide. Inner spur of hind tibia ~ 0.2× as long as hind basitarsus. Hind tarsus approximately as long as hind tibia. Hind basitarsus 0.7–0.8× as long as combined length of second to fifth segments. Second tarsal segment of hind leg 0.45–0.50× as long as basitarsus, 1.4–1.7× as long as fifth segment (without pretarsus).

Metasoma 0.9–1.1× longer than head and mesosoma combined. First tergite comparatively slender, evenly and linearly widened from base to apex, with very weak spiracular tubercles, with distinct dorsal carinae fused in basal one-third. Length of first tergite 1.2–1.3× its anterior width, anterior width 2.3–2.5× its posterior width. Second suture distinct, rather deep, almost straight, shortly crenulate or smooth. Medial length of second tergite ~ 0.7× its anterior width, 1.2–1.3× length of third tergite. Setose part of ovipositor sheath ~ 0.3× as long as metasoma, 1.0–1.1× as long as first tergite, 1.0–1.1× as long as hind basitarsus, 0.15–0.17× as long as fore wing.

Sculpture and pubescence. Vertex, frons and temple smooth; face almost smooth in upper 1/2 and densely reticulate-granulate in lower 0.4–0.5. Mesoscutum mainly smooth, with striation in narrow area in medioposterior quarter; scutellum and mesopleuron smooth. Metapleuron widely smooth, rugulose-reticulate in posterior 0.2. Propodeum with or without medial carina in basal 1/2; without delineated areas, mainly rugulose-reticulate, smooth or almost smooth in anterior

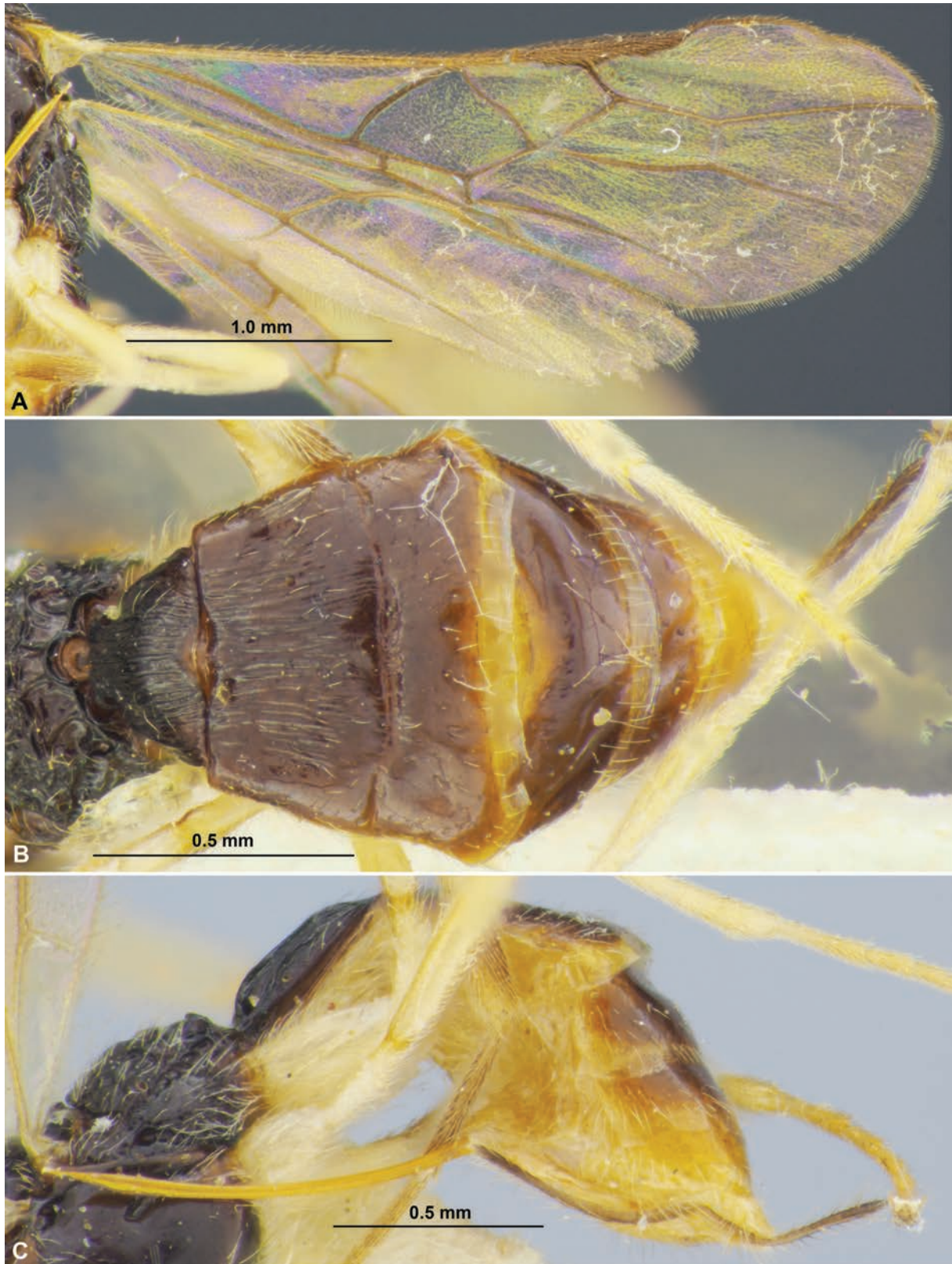


Figure 6. *Xenarcha (Xenarcha) pacificoformis* sp. nov., female, holotype **A** wings **B** metasoma, dorsal view **C** propodeum, metasoma and ovipositor, lateral view.

0.2–0.4. Legs smooth. First metasomal tergite entirely and densely striate, without reticulation between striae; second tergite mainly striate, smooth or almost smooth laterally and in posterior 0.2–0.3; second suture smooth or with short

crenulae; remaining tergites smooth. Mesoscutum mainly glabrous, with sparse, semi-erect or erect and long pale setae arranged along notauli and in medio-posterior area. Hind tibia dorsally with short, very dense and semi-erect pale setae.

Colour. Body mainly black; metasoma behind first or second tergite dark reddish brown. Antenna mainly black, 2–3 basal segments brownish yellow with infuscation. Palpi pale yellow. Legs mainly yellow, hind tibia in distal 0.3 and hind tarsus more or less distinctly infuscate. Wings hyaline. Pterostigma brown.

Male. Body length 3.2–3.5 mm; fore wing length 2.9–3.4 mm. Antenna 34–37-segmented. Pterostigma of fore wing distinctly sclerotised, wide, dark brown, 3.8–4.5× its maximum width. Length of first tergite 1.2–1.4× its anterior width. Second suture usually crenulate. Medial length of second tergite 0.8–0.9× its anterior width, 1.3–1.5× length of third tergite. Hind leg sometimes darkened. Otherwise similar to female.

Discussion. This new species is very similar to *Xenarcha (Xenarcha) pacifica* (Belokobylskij, 1998), comb. nov. (Fig. 8), but differs from later by having the strongly curved temple (less strongly curved in *X. pacifica*), the penultimate segment of antenna 2.7–2.8× longer than wide (2.0–2.3× in *X. pacifica*), pronotum dorsally with wide pronope and high curved transverse carina (with narrow pronope and without visible carina in *X. pacifica*), and the first metasomal tergite 1.2–1.3× longer than its anterior width (1.0–1.1× in *X. pacifica*).

Etymology. Named after the related species *Xenarcha pacifica* and the Latin word *formis* (form) because it is similar to this species.

Distribution. Korean peninsula.

***Xenarcha (Xenarcha) pacifica* (Belokobylskij, 1998) ssp. *brevisculpta*
Belokobylskij & Ku, ssp. nov.**

<https://zoobank.org/426F409D-8863-4ACF-8953-869A98ED32F5>

Fig. 7

Type material. *Holotype* • female, SOUTH KOREA, [GW], Taebaek-si, Mt. Taebaek, 13.VIII.1989 (Seungman Ryu) (NIBR). *Paratypes* • Same label as holotype. 5 females, 1 male (SMNE, ZISP) • same label, but 13.VIII.1989 (Wonyeong Choi), 1 female (SMNE).

Description. *Female.* **Body** length 3.0–3.5 mm; fore wing length 3.4–3.8 mm. **Head** width 1.8–1.9× its medial length (dorsal view), ~ 1.2× wider than mesoscutum. Temple distinctly and convex-curvedly narrowed behind eye. Transverse diameter of eye 1.2–1.3× longer than temple (dorsal view). Ocelli small, arranged almost in equilateral triangle. POL 1.0–1.2× Od, 0.3–0.4× OOL. Eye oval, glabrous, 1.25–1.30× as high as broad (lateral view). Malar space 0.4–0.5× height of eye, 0.9–1.3× basal width of mandible. Malar suture very fine. Face width 1.1–1.2× height of face and clypeus combined, 1.0–1.1× height of eye. Hypoclypeal depression circular, its width almost equal to distance from edge of depression to eye, ~ 0.4× width of face. Head distinctly and almost linearly narrowed below eyes. **Antenna** rather slender, weakly setiform, 37–38-segmented, ~ 1.3× longer than body. First flagellar segment 3.5–3.8× longer than its apical width, 1.2–1.3× longer than second segment. Penultimate segment 2.3–2.6× longer than wide, ~ 0.5× as long as first segment, 0.8–0.9× as long as apical segment; the latter acuminate apically and with short ‘spine’.

Mesosoma 1.7–1.8× longer than its height. Pronotum dorsally with distinct, deep and smooth round pit (pronope), without transverse pronotal carina. Mesoscutum distinctly and curvedly elevated above prothorax. Notauli complete, rather deep, but more shallow posteriorly, smooth. Prescutellar depression short, coarsely rugulose-crenulate, 0.25× as long as scutellum. Scutellum without transverse furrow and smooth posteriorly. Precoxal sulcus completely absent. **Wings.** Fore wing 2.8–3.0× longer than maximum width. Pterostigma narrow, 5.0–5.3× its maximum width, 0.7–0.8× as long as metacarp (1-R1). Radial vein (r) arising distinctly before middle of pterostigma, from its basal ~ 0.3. Second radial abscissa (3-SR) 2.7–3.0× longer than first abscissa (r) and forming very obtuse angle with it, 0.5–0.6× as long as the straight third abscissa (SR1), 1.6–1.8× longer than first radiomedial vein (2-SR). Recurrent vein (m-cu) weakly antefurcal. Second radiomedial (submarginal) cell not narrowed distally, its length 2.6–2.8× maximum width, 1.7–1.9× longer than brachial (subdiscal) cell. Brachial (subdiscal) cell distinctly widened distally. First abscissa of medial vein (1-SR+M) sinuate. Distance (1-CU1) from nervulus (cu-a) to basal vein (1-M) 1.2–1.3× nervulus (cu-a) length. Parallel vein (CU1a) arising from posterior 0.4 of distal margin (3-CU1) of brachial (subdiscal) cell. In hind wing, first abscissa of mediocubital vein (M+CU) 1.0–1.1× as long as second abscissa (1-M). First abscissa of costal vein (C+SC+R) 0.6–0.7× as long as second abscissa (1-SC+R). Recurrent vein (m-cu) not long, mainly unsclerotised, infusate basally, weakly antefurcal and weakly curved. **Legs.** Hind femur 5.5–5.6× longer than wide. Inner spur of hind tibia ~ 0.2× as long as hind basitarsus. Hind tarsus approximately as long as hind tibia. Hind basitarsus ~ 0.6× as long as combined length of second to fifth segments. Second tarsal segment of hind leg 0.5–0.6× as long as basitarsus, 1.5–1.7× as long as fifth segment (without pretarsus).

Metasoma 1.0–1.1× longer than head and mesosoma combined. First tergite comparatively slender, evenly and linearly widened from base to apex, with very weak spiracular tubercles, with distinct dorsal carinae fused in basal one-third by additional transverse carina. Length of first tergite 1.0–1.1 (rarely 1.15)× its anterior width, anterior width 2.0–2.3× its posterior width. Second suture weak, shallow, weakly curved, smooth. Medial length of second tergite 0.8–0.9× its anterior width, 1.6–1.7× length of third tergite. Setose part of ovipositor sheath ~ 0.2× as long as metasoma, usually as long as first tergite, 0.7–1.0× as long as hind basitarsus, ~ 0.1× as long as fore wing.

Sculpture and pubescence. Vertex, frons and temple smooth; face mainly densely granulate, smooth or almost smooth medially in upper 0.3. Mesoscutum mainly smooth, with striation in narrow area in medioposterior quarter; scutellum and mesopleuron smooth. Metapleuron mainly coarsely transverse striate with rugosity, almost smooth in anterior 0.3. Propodeum entirely or almost entirely coarsely rugose-reticulate, with distinct medial carina in basal 0.6–0.7; without delineated areas. Legs mainly smooth, but hind coxa almost entirely rugose-reticulate. First metasomal tergite entirely and densely curvedly striate, with dense and coarse reticulation between striae; second tergite finely striate in anterior 0.3–0.5, smooth on remaining posterior part; remaining tergites entirely smooth. Mesoscutum mainly glabrous, with short, sparse and semi-erect pale setae arranged along notauli and in medio-posterior area. Hind tibia dorsally with short, very dense and semi-erect pale setae.

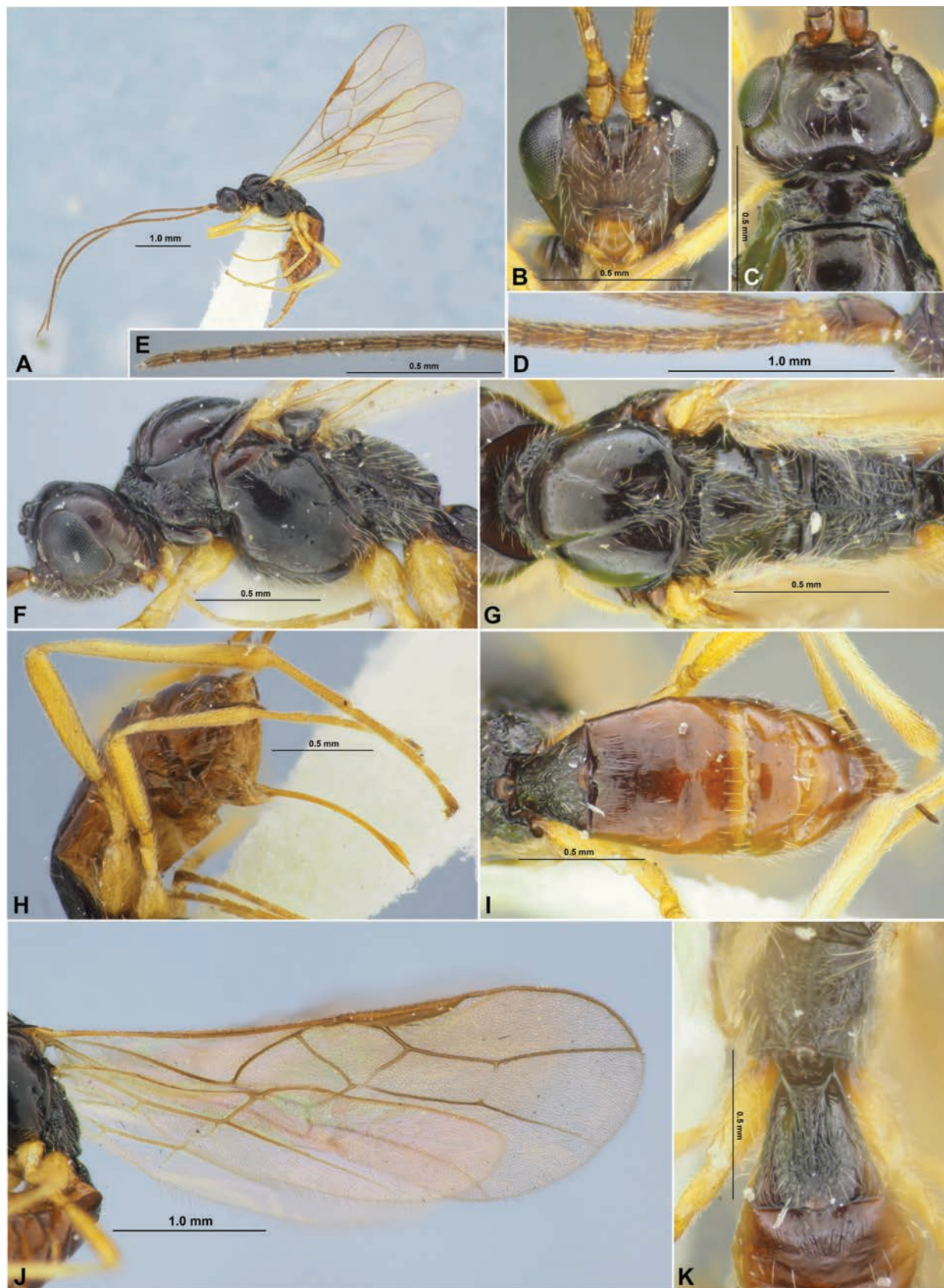


Figure 7. *Xenarcha (Xenarcha) pacifica* ssp. *brevisculpta* ssp. nov., female, holotype **A** habitus, lateral view **B** head, front view **C** head and anterior part of mesosoma, dorsal view **D** basal segments of antenna **E** apical segments of antenna **F** head and mesosoma, lateral view **G** mesosoma, dorsal view **H** metasoma and hind leg, lateral view **I** metasoma, dorsal view **J** wings **K** propodeum and anterior part of metasoma, dorsal view.

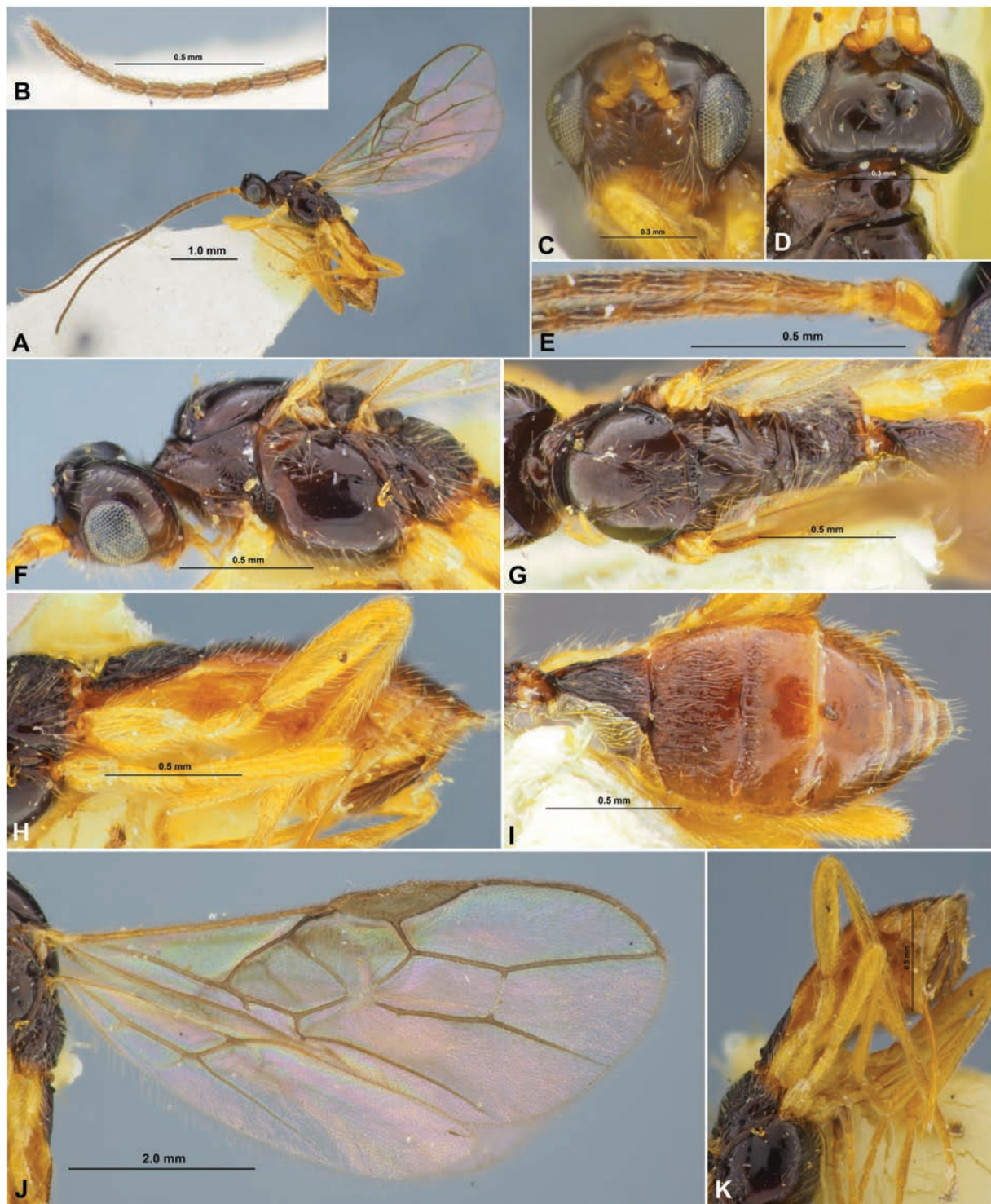


Figure 8. *Xenarcha (Xenarcha) pacifica* (Belokobylskij), comb. nov., female, holotype **A** habitus, lateral view **B** apical segments of antenna **C** head, front view **D** head and anterior part of mesosoma, dorsal view **E** basal segments of antenna **F** head and mesosoma, lateral view **G** mesosoma and first metasomal tergite, dorsal view **H** metasoma and ovipositor, lateral view **I** metasoma, dorsal view **J** wings **K** metasoma and hind leg, lateral view.

Colour. Body mainly black; metasoma behind first tergite reddish brown or dark reddish brown. Antenna mainly dark brown or black, 2–3 basal segments faintly paler. Palpi pale yellow. Legs mainly yellow, hind tarsus faintly infusate. Wings hyaline. Pterostigma brown.

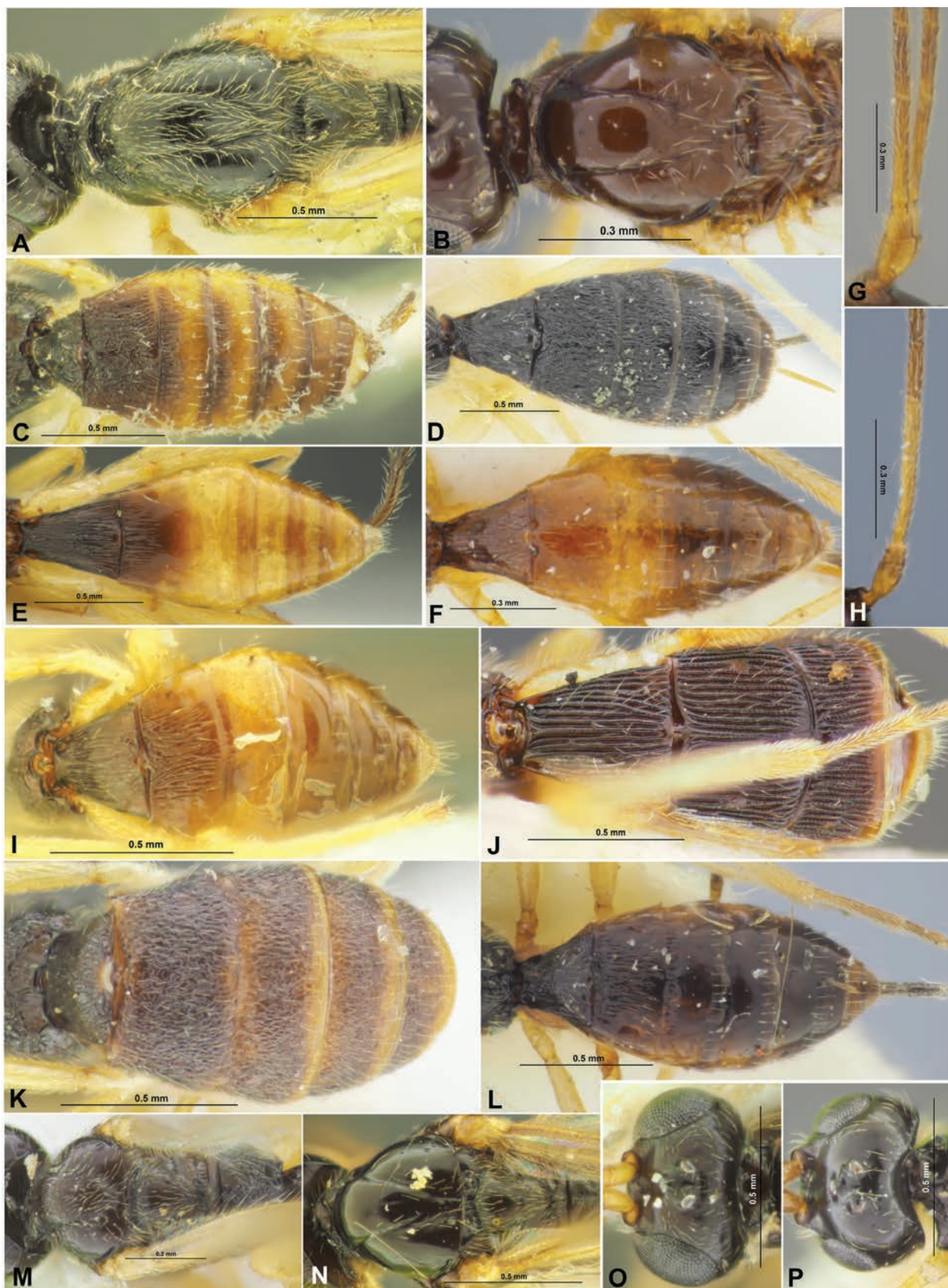


Figure 9. Morphological details of *Colastes (Colastes) pubicornis* (A), *C. (C.) braconius* (B, F, H), *C. (C.) sylvicola* (C), *C. (C.) ussuricus* (D), *C. (C.) dersu* (E, G), *C. (C.) interdictus* (I), *Colastinus crustatus* (J), *Xenarcha (Pseudophanomeris) pilosa* (K, M, O), *X. (Shawiana) catenator* (L), *X. (Ps.) insularis* (N, P). A, B, M, N Mesoscutum and scutellum, dorsal view C–F, I–L metasoma, dorsal view G, H basal segments of antenna O, P head, dorsal view.

Male. Body length 3.4 mm; fore wing length 3.2 mm. Antenna 36-segmented. Pterostigma of fore wing additionally sclerotised, dark brown, 3.2× its maximum width. Length of first tergite 1.4× its anterior width. Second suture finely and shortly crenulate. Second tergite striate-rugulose in anterior 0.7, its medial length 0.9× anterior width, 1.2× length of third tergite. Otherwise similar to female.

Discussion. This new subspecies is very similar to *Xenarcha* (*Xenarcha*) *pacifica* ssp. *pacifica* (Belokobylskij, 1998) (Fig. 8), but differs from later by having the second metasomal tergite striate-rugulose only in anterior 0.3–0.4 (entirely or basically striate-rugulose in *X. pacifica* ssp. *pacifica*).

Etymology. Named from the combination of the Latin words “brevis” (= short) and “sculpta” (= sculptural) because its second tergite of metasoma is sculptured only in the basal 1/2.

Distribution. Korean peninsula.

Key to the genera, subgenera, and species of the subfamily Exothecinae of Korean peninsula

- 1 Pronotum dorsally without deep round smooth pit (pronope), sometimes only with more or less distinct sculptured transverse groove (Figs 1C, 3C) (Genus *Colastes* Haliday, 1833).....**2**
- Pronotum dorsally with distinct and deep round smooth pit (pronope) (Figs 5C, 7C, 8D).....**9**
- 2 Medial lobe of mesoscutum entirely and usually densely setose (Fig. 9A). Body length 2.1–3.3 mm **C. (*Colastes*) *pubicornis* (Thomson, 1892)**
- Medial lobe of mesoscutum mainly glabrous, setae present only along notauli and in its medio-posterior area (Fig. 9B).....**3**
- 3 Second tergite of metasoma entirely, third tergite mainly, often fourth tergite in basal 0.3–0.5, and rarely fifth tergite basally striate-rugulose (Figs 9C, D). – Notauli complete. Pterostigma yellow or pale brown.....**4**
- Usually only second tergite entirely or at least basally sculptured, but sometimes entirely smooth, following tergites smooth, rarely also only third tergite sculptured in basal 0.2–0.3 (Figs 2C, 9E, F, I)**5**
- 4 First metasomal tergite 0.9–1.0× as long as its maximum posterior width. Metasoma posterior to second tergite (pale) reddish brown (Fig. 9C). Transverse diameter of eye 1.4–1.6× longer than temple (dorsal view). First flagellar segment of antenna 1.0–1.1× as long as second segment. Body length 2.7–3.2 mm **C. (*Colastes*) *syvicola* Belokobylskij, 1998**
- First metasomal tergite 1.1–1.2× longer than its maximum posterior width. Metasoma entirely dark brown to black (Fig. 9D). Transverse diameter of eye 1.8–2.0× longer than temple (dorsal view). First flagellar segment of antenna 1.2–1.3× longer than second segment. Body length 3.0–3.4 mm**C. (*Colastes*) *ussuricus* Belokobylskij, 1996**
- 5 Notauli incomplete, distinct in anterior 0.6, very shallow to partly absent in posterior 0.4 (Fig. 1G). Mesoscutum medio-posteriorly entirely smooth (Fig. 1G). Body length 2.1–2.5 mm **C. (*Colastes*) *fragiloides* sp. nov.**
- Notauli complete, distinct and reaching posterior margin of mesoscutum (Fig. 3G). Mesoscutum medio-posteriorly striate or striate-rugulose at least medially (Fig. 3G)**6**

- 6 First flagellar segment of antenna 7.0–8.0× longer than its apical width; penultimate segment 3.5–4.0× longer than its width (Fig. 9G). First tergite of metasoma of female 1.3–1.5× longer than its posterior width (Fig. 9E). Third abscissa of medial vein (2-M) of fore wing in male not widened. Body length 2.2–3.4 mm **C. (*Colastes*) *dersu* Belokobylskij, 1998**
- First flagellar segment of antenna 3.5–6.0× longer than its apical width; penultimate segment 2.3–3.0× longer than its width (Fig. 9H). First tergite of metasoma of female 1.0–1.1× (rarely 1.20–1.25×) longer than its posterior width (Fig. 9F). Third abscissa of medial vein (2-M) of fore wing in male sometimes widened..... **7**
- 7 Third metasomal tergite rugose-reticulate in its basal 0.3–0.4 (Fig. 4B). Metasoma yellowish brown or yellow in posterior 0.6 (Fig. 4B). First tergite of metasoma of female 1.25× its posterior width. Tibia of hind leg in distal 1/2 and hind tarsus distinctly infuscate (Fig. 3H). Body length 2.8 mm **C. (*Colastes*) *semiflavus* sp. nov.**
- Third metasomal tergite usually smooth, very rarely anteriorly rugose at short area (Figs 9F, I). Metasoma in posterior 0.6–0.7 reddish brown or dark reddish brown (Figs 9F, I). First tergite of metasoma of female 1.00–1.15× as long as its posterior width (Figs 9F, I). Tibia and tarsus of hind leg yellow **8**
- 8 Second metasomal tergite entirely smooth (Fig. 9F). Second metasomal suture very fine (Fig. 9F). Third abscissa of medial vein (2-M) of fore wing in male distinctly widened. Recurrent vein (m-cu) of fore wing subinterstitial or weakly antefurcal to first radiomedial vein (2-SR). Body length 2.5–4.0 mm **C. (*Colastes*) *braconius* Haliday, 1833**
- Second metasomal tergite entirely or mostly striate with reticulation (Fig. 9I). Second metasomal suture distinct (Fig. 9I). Third abscissa of medial vein (2-M) of fore wing in male not widened. Recurrent vein (m-cu) of fore wing distinctly antefurcal to first radiomedial vein (2-SR). Body length 2.4–3.3 mm **C. (*Colastes*) *interdictus* Belokobylskij, 1998**
- 9 Second and third metasomal tergites enlarged, forming a subcarapace, posterior segments entirely or almost entirely covered by third tergite (Figs 9J) (Genus *Colastinus* Belokobylskij, 1984). Body length 2.5–3.0 mm **C. *crustatus* Belokobylskij, 1984**
- Second and third metasomal tergites not enlarged, not forming a subcarapace, posterior segments distinctly protruding beyond third tergite (Figs 9K, L) (Genus *Xenarcha* Foerster, 1863)..... **10**
- 10 Fifth metasomal tergite enlarged and usually completely covering posterior segments (Fig. 9K). First to fifth tergites entirely or almost entirely sculptured (Fig. 9K) (Subgenus *Pseudophanomeris* Belokobylskij, 1984) **11**
- Fifth metasomal tergite not enlarged and never covered posterior segments (Figs 9L, 10C–F, K, P, Q). Posterior tergites (fourth and fifth) rarely and only partly (basally) sculptured, often entirely smooth (Figs 9L, 10C–F, K, P, Q) **12**
- 11 Medial lobe of mesoscutum entirely covered by dense setae (Fig. 9M). Mesoscutum short, 0.8× as long as its maximum width (Fig. 9M). Transverse diameter of eye ~ 2.0× longer than temple (dorsal view) (Fig. 9O).

- Face narrow, 1.1–1.2× wider than height of face with clypeus. Body length 2.6–3.0 mm **X. (P.) pilosa (Belokobylskij, 1984)**
- Medial lobe of mesoscutum mostly glabrous (Fig. 9N). Mesoscutum long, approx. as long as its maximum width (Fig. 9N). Transverse diameter of eye 1.3–1.5× longer than temple (dorsal view) (Fig. 9P). Face wide, 1.4–1.5× wider than height of face with clypeus. Body length 2.7–3.2 mm.....
..... **X. (P.) insularis (Belokobylskij, 1984)**
- 12 Notauli distinct in anterior 1/2 of mesoscutum, absent in its posterior 1/2; mesoscutum smooth medio-posteriorly (Fig. 10A) (Subgenus *Shawiana* van Achterberg, 1983)..... **13**
- Notauli complete and entirely distinct on mesoscutum; mesoscutum striate or striate-rugose medio-posteriorly (Figs 5G, 7G, 10B) (Subgenus *Xenarcha* s. str.) **19**
- 13 Second metasomal tergite entirely smooth (Figs 10C, D)..... **14**
- Second metasomal tergite at least partly (Fig. 10K) or entirely sculptured (Figs 10E, F) **15**
- 14 Ovipositor long, its sheath 0.8–1.1× as long as hind tibia, 2.3–2.7× longer than first metasomal tergite (Fig. 10C). Hind tibia distally and hind tarsus entirely yellow or greyish-yellow (Fig. 10G). Body length 2.4–4.5 mm.....
..... **X. (Sh.) foveolator (Thomson, 1892)**
- Ovipositor short, its sheath 0.4–0.5× as long as hind tibia, approx. as long as first metasomal tergite (Fig. 10D). Hind tibia distally and hind tarsus almost entirely distinctly infusate (Fig. 10H). Body length 2.2–3.5 mm ...
..... **X. (Sh.) laevis (Thomson, 1892)**
- 15 Medial lobe of mesoscutum entirely setose (Fig. 10I). First metasomal tergite narrow, its length 1.2× posterior width (Fig. 10J). Body length 2.4–2.9 mm **X. (Sh.) rupicola (Belokobylskij, 1998)**
- Medial lobe of mesoscutum mostly glabrous, setae present only along notauli and in medioposterior area. First metasomal tergite wider, its length usually not larger than posterior width **16**
- 16 Basal flagellar segments of antenna longer; first flagellar segment 2.8–4.0× longer than maximum width. – Frons entirely smooth. Second tergite entirely and third at least basally striate with reticulation. Second metasomal tergite 0.6–0.7× as long as its anterior width. Body length 4.1 mm.....
..... **X. (Sh.) attonita Papp, 1987**
- Basal flagellar segments of antenna shorter; first flagellar segment 2.0–2.5× longer than its maximum width (Figs 10L, M)..... **17**
- 17 Second metasomal tergite only partly sculptured, its sides and posterior margin (sometimes entirely in posterior 1/2) smooth (Fig. 10K). Antenna reddish brown basally (Fig. 10L). Body length 2.3–3.3 mm.....
..... **X. (Sh.) nupta (Papp, 1983)**
- Second metasomal tergite entirely sculptured (Fig. 10F). Antenna usually pale reddish brown basally (Fig. 10M) **18**
- 18 Third metasomal tergite rugose-striate in anterior 0.2–0.5; fourth tergite entirely smooth (Fig. 9L). Body length 3.0–5.0 mm.....
..... **X. (Sh.) catenator (Haliday, 1836)**
- Third metasomal tergite mainly or entirely rugose-striate; fourth tergite sculptured basally (Fig. 10F). Body length 2.5–3.3 mm.....
..... **X. (Sh.) orientalis (Belokobylskij, 1998)**

- 19 Ovipositor long, its sheath 1.0–1.5× as long as hind tibia, 2.1–2.7× longer than first metasomal tergite (Fig. 10O). Precoxal sulcus weakly present (Fig. 10N). – Second tergite of metasoma striate only in antero-medial part (Fig. 10P). Body length 2.7–3.4 mm**X. (X.) *effecta* (Papp, 1972)**
- Ovipositor short, its sheath 0.5–0.7× as long as hind tibia, approx. as long as first metasomal tergite (Fig. 10Q). Precoxal sulcus always absent ...**20**
- 20 Third metasomal tergite entirely striate, with more or less distinct oblique antero-lateral furrows (Fig. 10Q). Temple short, transverse diameter of eye 2.0–2.5× longer than temple (dorsal view) (Fig. 10R). Body length 1.6–2.7 mm**X. (X.) *ivani* (Belokobylskij, 1986)**
- Third metasomal tergite usually entirely smooth, rarely with short basal striae, without oblique antero-lateral furrows (Figs 6B, 7I). Temple long, transverse diameter of eye 1.3–1.7× longer than temple (dorsal view) (Figs 5C, 7C)**21**
- 21 Temple (dorsal view) strongly curvedly narrowed behind eye (Fig. 5C). Penultimate segment of antenna 2.7–2.8× longer than its width (Fig. 5D). Pronotum dorsally with wide pronope and high, medially curved pronotal carina (Fig. 5C). First metasomal tergite 1.2–1.3× longer than its anterior width (Fig. 6B). Body length 3.1–4.1 mm **X. (X.) *pacificiformis* sp. nov.**
- Temple (dorsal view) not strongly and convex-curvedly narrowed behind eye (Fig. 7C). Penultimate segment of antenna 2.0–2.3× longer than its width (Fig. 7D). Pronotum dorsally with narrow pronope and without pronotal carina (Fig. 7C). First metasomal tergite 1.0–1.1× longer than its anterior width (Fig. 7K). Body length 3.0–3.5 mm
..... **X. (X.) *pacifica* (Blkb) ssp. *brevisculpta* ssp. nov.**

Discussion

The generic composition of the subfamily Exothecinae s. str. has been changed several times during its modern history (van Achterberg 1995). The tribe Exothecini (sensu Belokobylskij 1993) included the following genera: *Colastes* (with subgenera *Pseudophanomeris* and *Shawiana*), *Colastinus*, *Vietcolastes* and *Xenarcha*. On the other hand, *Shawiana* was treated as a separate valid genus for a long time (van Achterberg 1983; Whitfield and Wharton 1997; Yu et al. 2016), but Belokobylskij (1998) included this name (as well as *Xenarcha*) as a subgenus of the genus *Colastes* sensu lato. However, the eastern Asian genera *Colastinus* Belokobylskij, 1984, *Orientocolastes* Belokobylskij, 1999 and *Vietcolastes* Belokobylskij, 1992 described later (Belokobylskij 1984, 1992, 1999) maintained their status without changing until now.

The first molecular-phylogenetic study using the 28S and COI genes for more than single Exothecinae supraspecies taxa (genera or subgenera) (*Colastes*, *Pseudophanomeris*, *Shawiana*, and *Xenarcha*) was provided by Zaldivar-Riverón et al. (2006). This study revealed the separate position of *Colastes* from the other three taxa which were united in a separate clade. Overall, the member of Exothecinae was showed a distinct phylogenetic relation with the subfamilies Alysiinae and Opiinae. Similar results were obtained in other analyses of the cyclostome braconids however with using only single gene 28S (D2-D3) (Ranjith et al. 2017), but the two studied here *Colastes* species (*C. braconius* Haliday and *C. incertus* (Wesmael, 1838)) were separated in different but related clades. Finally, a large mitochondrial



Figure 10. Morphological details of *Xenarcha (Shawiana) foveolator* (A, C, G), *X. (Xenarcha) ivani* (B, Q, R), *X. (Sh.) laevis* (D, H), *X. (Sh.) rupicola* (E, I, J), *X. (Sh.) orientalis* (F), *X. (Sh.) nupta* (K, L), *X. (Sh.) catenator* (M), *X. (X.) effecta* (N, O, P). A Mesosoma, dorsal view B head and mesosoma, dorsal view C–F, K, P, Q metasoma and ovipositor, dorsal view G, H tibia and tarsus of hind leg I mesoscutum and scutellum, dorsal view J propodeum and first tergite of metasoma, dorsal view L, M basal segments of antenna N mesosoma, lateral view O metasoma and ovipositor, lateral view R head, dorsal view.

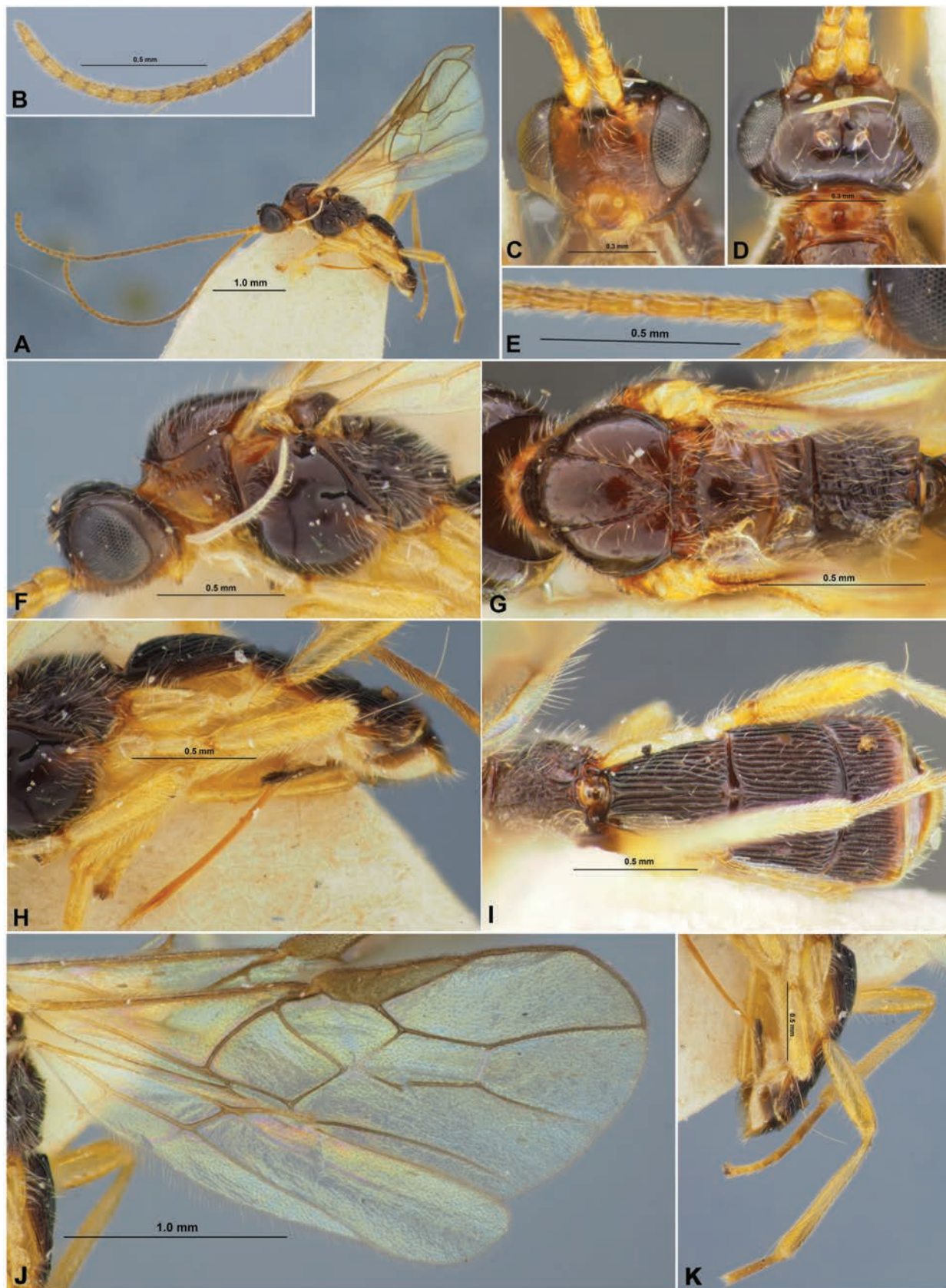


Figure 11. *Colastinus crustatus* Belokobylskij, female, holotype **A** habitus, lateral view **B** apical segments of antenna **C** head, front view **D** head and anterior part of mesosoma, dorsal view **E** basal segments of antenna **F** head and mesosoma, lateral view **G** mesosoma, dorsal view **H** metasoma and ovipositor, lateral view **I** propodeum and metasoma, dorsal view **J** wings **K** metasoma and hind leg, lateral view.

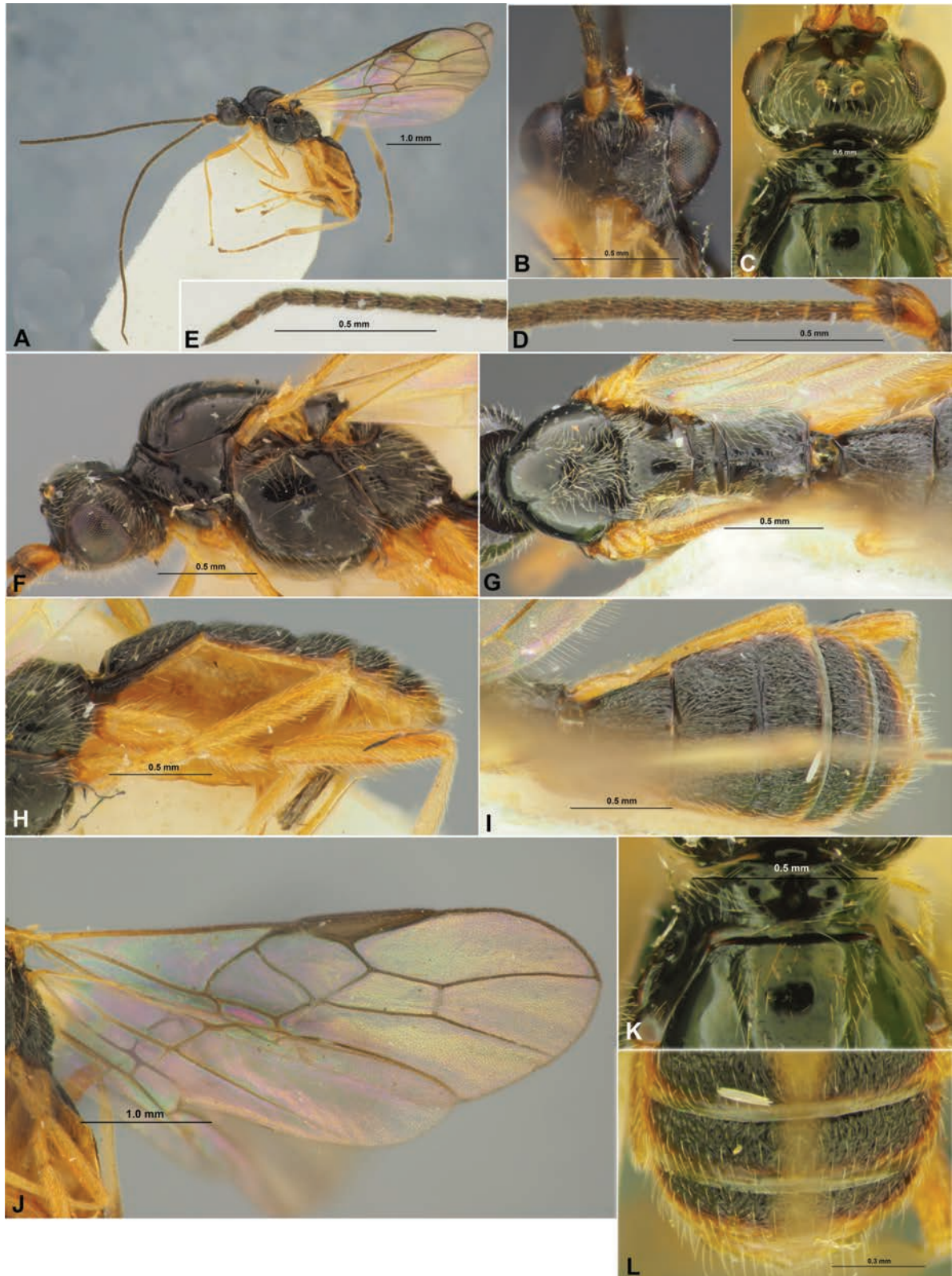


Figure 12. *Xenarcha (Pseudophanomeris) unicolor* (Belokobylskij), female, holotype **A** habitus, lateral view **B** head, front view **C** head and anterior part of mesosoma, dorsal view **D** basal segments of antenna **E** apical segments of antenna **F** head and mesosoma, lateral view **G** mesosoma and first metasomal tergite, dorsal view **H** propodeum, metasoma and ovipositor, lateral view **I** propodeum and metasoma, dorsal view **J** wings **K** anterior part of mesosoma, dorsal view **L** posterior part of metasoma, dorsal view.

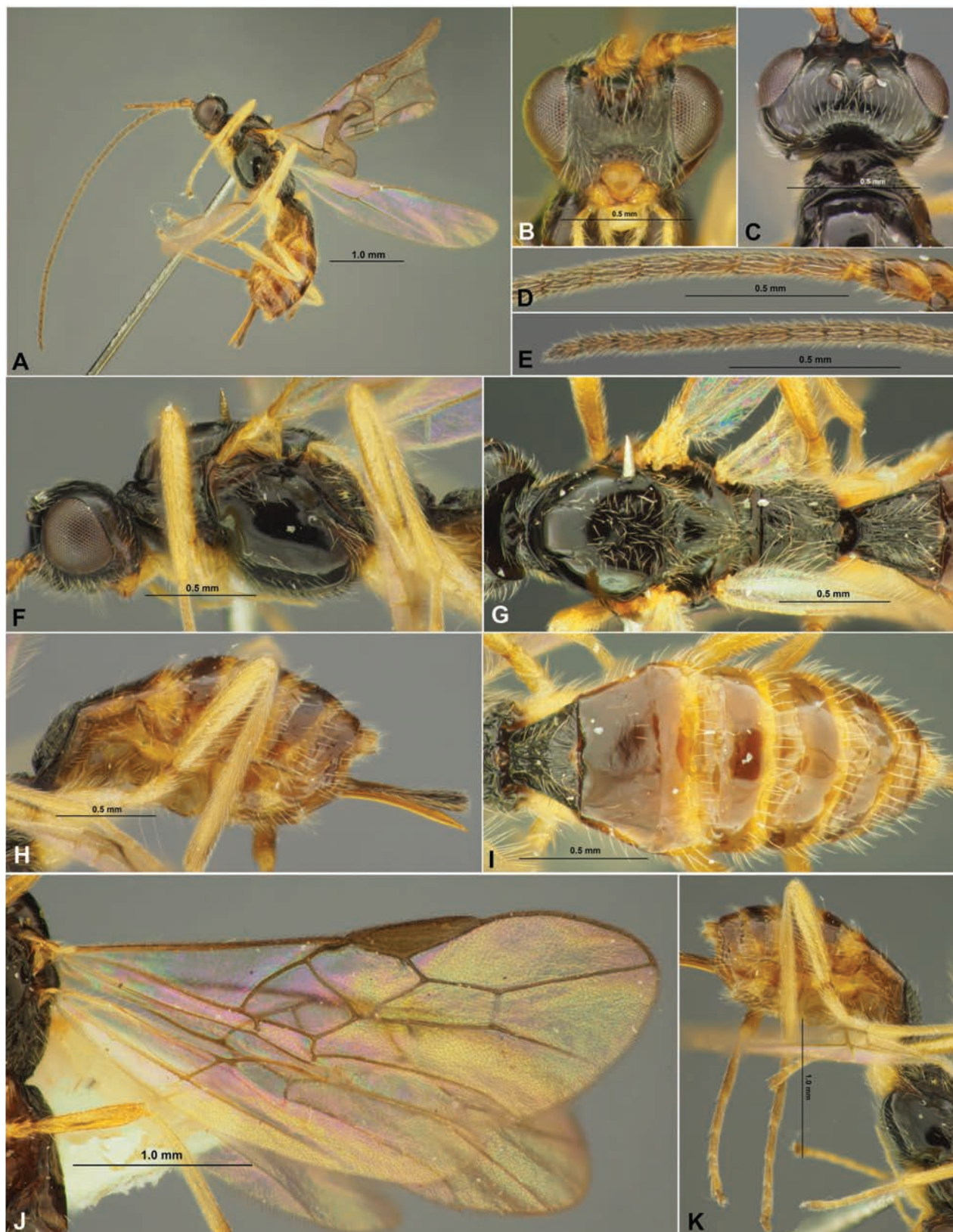


Figure 13. *Xenarcha (Shawiana) laevis* (Thomson), female **A** habitus, lateral view **B** head, front view **C** head and anterior part of mesosoma, dorsal view **D** basal segments of antenna **E** apical segments of antenna **F** head and mesosoma, lateral view **G** mesosoma and first metasomal tergite, dorsal view **H** metasoma and ovipositor, lateral view **I** metasoma, dorsal view **J** wings **K** metasoma and hind leg, lateral view.

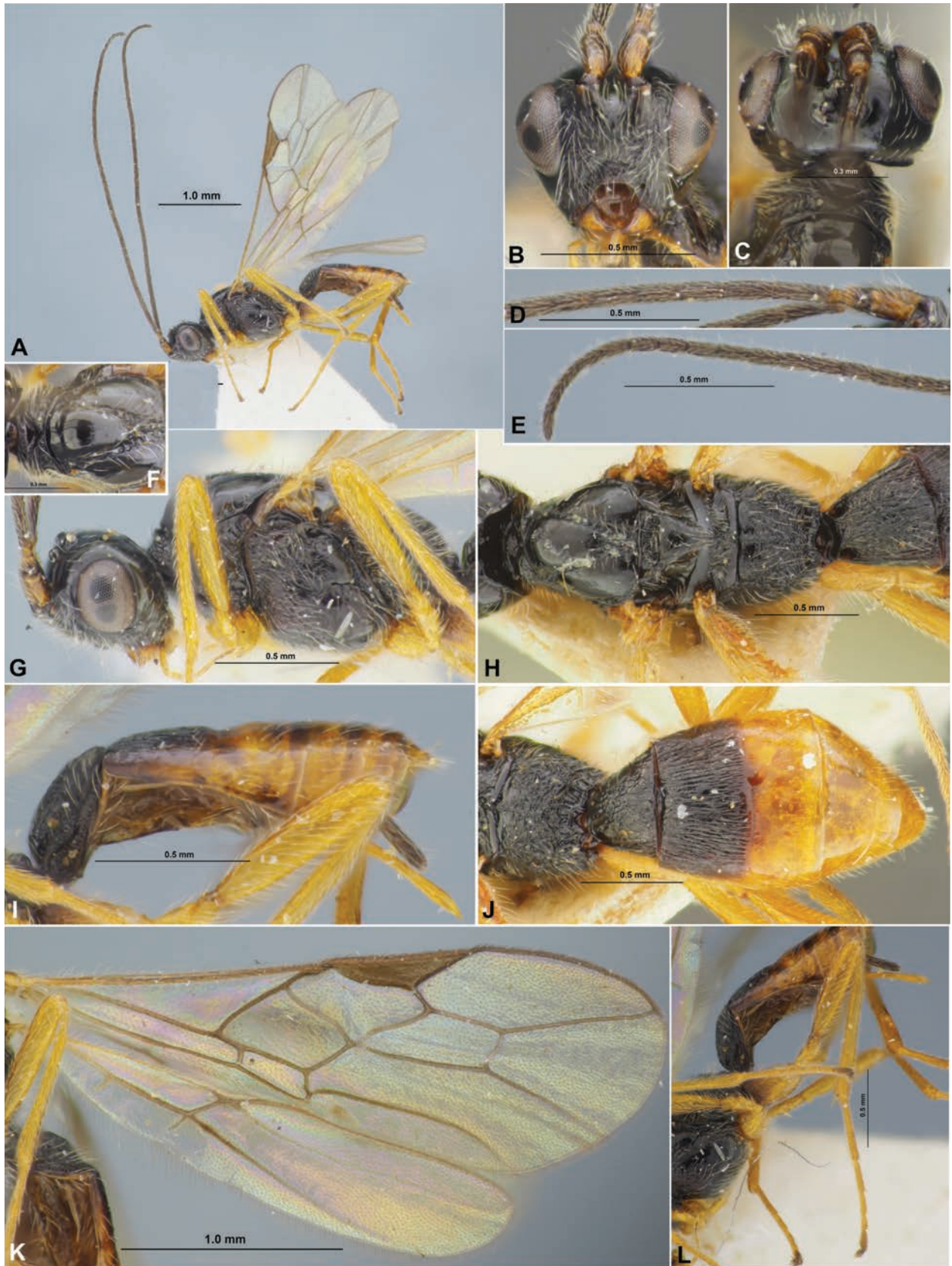


Figure 14. *Xenarcha (Xenarcha) lustrator* (Haliday), female **A** habitus, lateral view **B** head, front view **C** head and anterior part of mesosoma, dorsal view **D** basal segments of antenna **E** apical segments of antenna **F** anterior half of mesosoma **G** head and mesosoma, lateral view **H** mesosoma and first metasomal tergite, dorsal view **I** metasoma and ovipositor, lateral view **J** propodeum and metasoma, dorsal view **K** wings **L** metasoma and hind leg, lateral view.

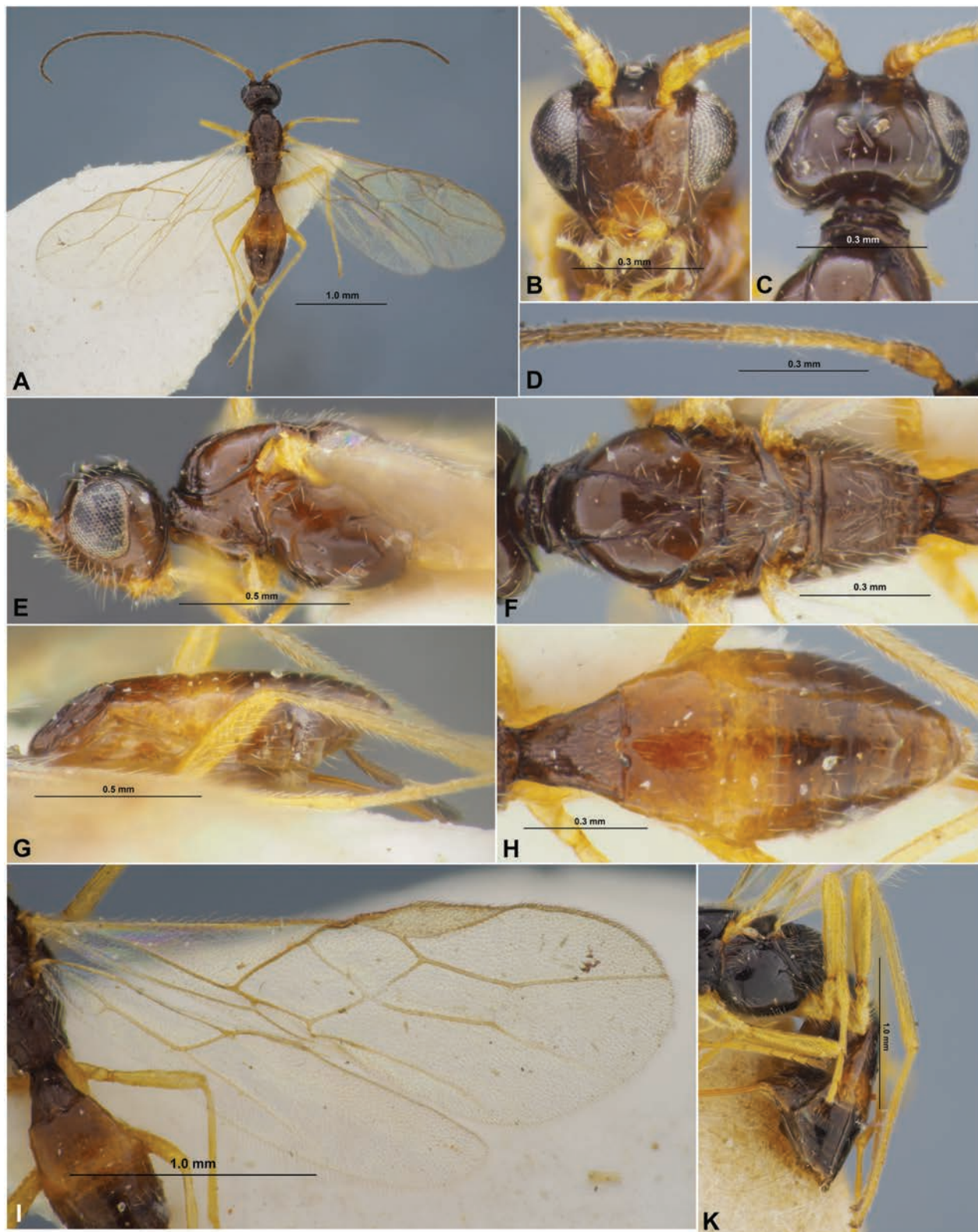


Figure 15. *Colastes (Colastes) braconius* Haliday, female **A** habitus, dorsal view **B** head, front view **C** head and anterior part of mesosoma, dorsal view **D** basal segments of antenna **E** head and mesosoma, lateral view **F** mesosoma, dorsal view **G** metasoma and ovipositor, lateral view **H** metasoma, dorsal view **I** wings **K** metasoma and hind leg, lateral view.

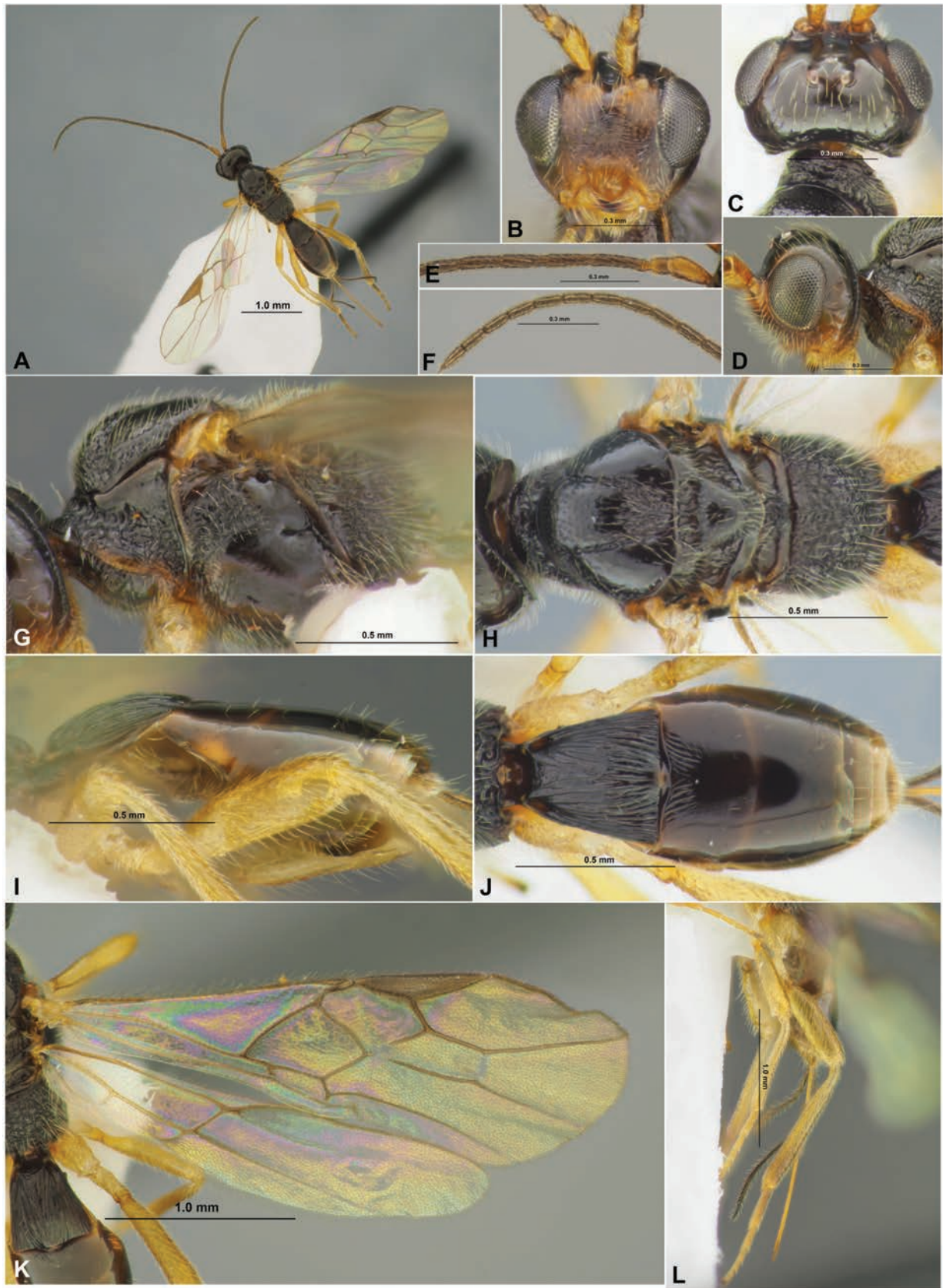


Figure 16. *Colastes (Fungivenator) fritzeni* van Achterberg & Shaw, female **A** habitus, dorsal view **B** head, front view **C** head and anterior part of mesosoma, dorsal view **D** head and anterior part of mesosoma, lateral view **E** basal segments of antenna **F** apical segments of antenna **G** mesosoma, lateral view **H** mesosoma, dorsal view **I** metasoma, lateral view **J** metasoma, dorsal view **K** wings **L** hind leg, lateral view.

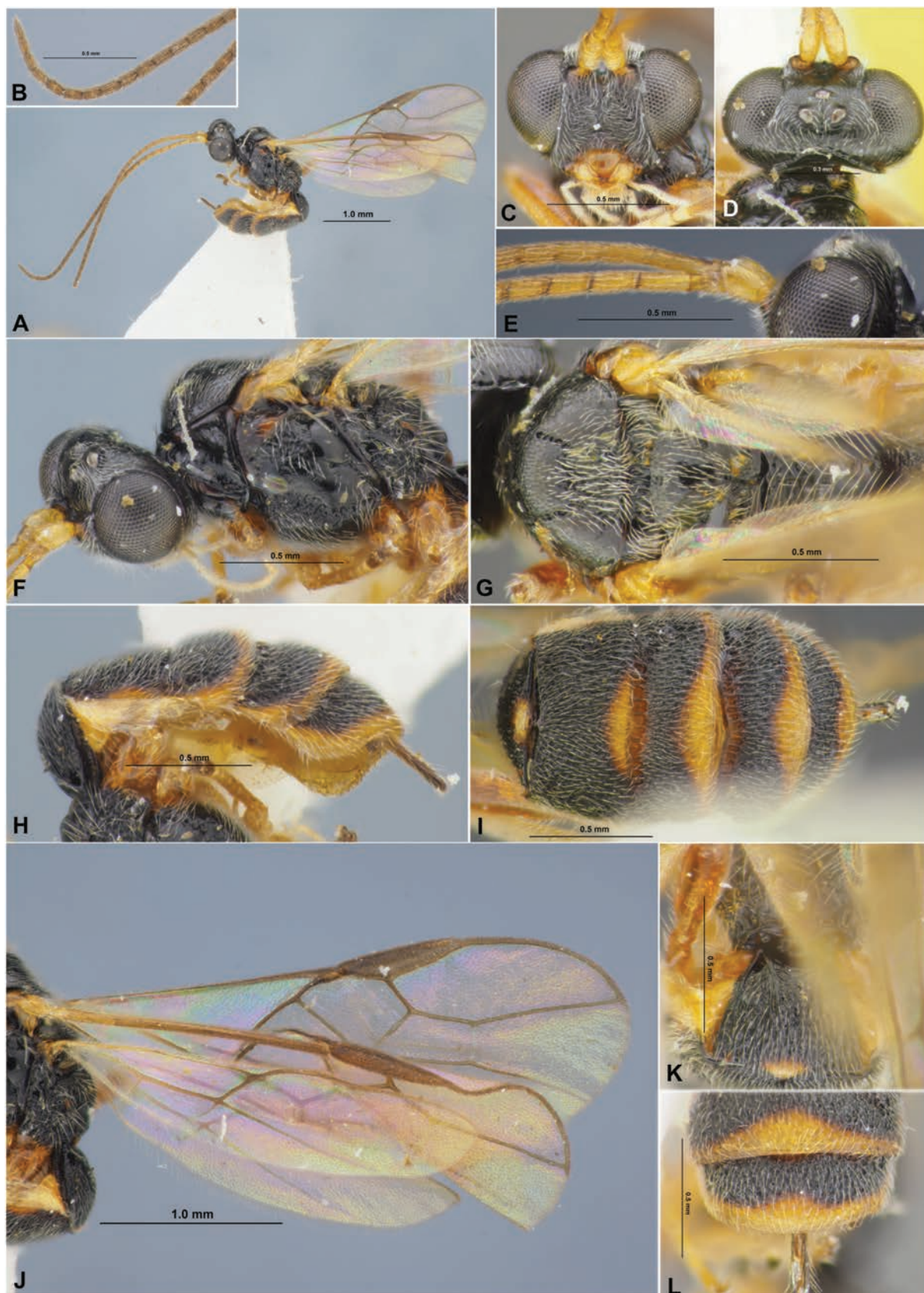


Figure 17. *Orientocolastes io* Belokobylskij, female **A** habitus, lateral view **B** apical segments of antenna **C** head, front view **D** head and anterior part of mesosoma, dorsal view **E** basal segments of antenna **F** head and mesosoma, lateral view **G** mesosoma, dorsal view **H** metasoma and ovipositor, lateral view **I** metasoma, dorsal view **J** wings **K** propodeum and first metasomal tergite, dorsal view **L** posterior part of metasoma, dorsal view.



Figure 18. *Vietcolastes rhaconotus* Belokobylskij, female, holotype (A, C–L), and male, paratype (B) A habitus, lateral view B head, dorsal view C head, front view D head and anterior part of mesosoma, dorsal view E basal segments of antenna F apical segments of antenna G head and mesosoma, lateral view H mesosoma, dorsal view I propodeum, metasoma and ovipositor, lateral view J propodeum and metasoma, dorsal view K wings L posterior part of metasoma, dorsal view.

phylogenomic study of the Braconidae subfamilies (Jasso-Martínez et al. 2022) have been also showed a distinct relation between the taxa *Pseudophanomeris*, *Xenarcha*, and *Shawiana* (with very high bootstrap values), but they were nested separately in the same clade together with *Vietcolastes* and *Colastinus*.

Our morphological study of Exothecinae taxa showed that the genera of this subfamily are divided into two morphological groups based on pronotal structure: dorsally with distinct, wide, deep and mainly smooth round pit (pronope) or without pronope (however rarely with a distinct transverse sculptured groove). The genera *Colastinus* (Fig. 11) and *Xenarcha* [including subgenera *Pseudophanomeris* (Fig. 12), *Shawiana* (Fig. 13) and *Xenarcha* s. str. (Fig. 14)] belong to the first group (with pronope). The second morphological group (without pronope) includes *Colastes* [with subgenera *Colastes* s. str. (Fig. 15), *Discolastes* Belokobylskij, 2000 and *Fungivenator* van Achterberg & Shaw, 2008 (Fig. 16)], *Orientocolastes* (Fig. 17), and *Vietcolastes* (Fig. 18). A key for determination of Exothecinae genera and subgenera is provided below.

Key to the world Exothecinae genera and subgenera

- 1 Pronotum dorsally with distinct, deep and rather wide round and usually smooth pit (pronope) (Figs 11D, 12C, 13C, 14C).....**2**
 - Pronotum dorsally without deep round pit (pronope), sometimes only with transverse sculptured groove (Figs 15C, 16C, 17D, 18D).....**5**
- 2 Second and third metasomal tergites forming a carapace, covering or almost covering the following segments. Third tergite with flange on posterior margin (Fig. 11I). Oriental, Palaearctic regions**Colastinus Belokobylskij, 1984**
 - Second and third metasomal tergites not forming a carapace, following segments (at least till fifth one) distinctly protruding behind third one. Third tergite without flange on posterior margin (Figs 12I, 13I, 14J). Afrotropical, Oriental, Palaearctic regions (*Xenarcha* Foerster, 1863)**3**
- 3 Fifth metasomal tergite enlarged and usually covered posterior segments (Fig. 12I). First to fifth tergites entirely sculptured (Fig. 12I). Afrotropical, Oriental, Palaearctic regions.....**Xenarcha (Pseudophanomeris Belokobylskij, 1984)**
 - Fifth metasomal tergite not enlarged and never covering posterior segments (Figs 13I, 14J). Posterior tergites (fourth and fifth) rarely and only partly (anteriorly) sculptured, often entirely or mostly smooth (Figs 13I, 14J)**4**
- 4 Notauli incomplete, absent in posterior 0.3–0.5 of mesoscutum; mesoscutum predominantly smooth in medioposterior part (Fig. 13G). Radial vein (r) of fore wing usually arising from basal 0.3–0.4 of pterostigma (Fig. 13J). Nearctic, Oriental, Palaearctic regions.....**Xenarcha (Shawiana van Achterberg, 1983)**
 - Notauli complete, reaching posterior margin of mesoscutum; mesoscutum always sculptured in its medioposterior part (Fig. 14H). Radial vein (r) of fore wing usually arising from basal 0.4–0.5 of pterostigma (Fig. 14K). Nearctic, Oriental, Palaearctic regions.....**Xenarcha (Xenarcha s. str.)**
- 5 Occipital carina present dorsally (Fig. 17D). Frons with sculptured longitudinal furrow. Precoxal sulcus present and distinct (Fig. 17F). Prepectal

- carina present laterally (Fig. 17F). Oriental region
 **Orientocolastes Belokobylskij, 1999**
- Occipital carina widely interrupted dorsally (Figs 15C, 16C, 18D). Frons without sculptured longitudinal furrow (Figs 15C, 16C, 18D). Precoxal sulcus usually absent (Figs 15E, 16G, 18G), if rarely present then very shallow. Prepectal carina completely absent (Figs 15E, 16G, 18G)..... **6**
- 6** Fifth metasomal tergite enlarged and covering posterior segments (Figs 18J, L). First to fifth tergite entirely sculptured (Fig. 18J). In male, occipital carinae absent; temple with distinct lateral vertical occipital lumps (Fig. 18B). Oriental region **Vietcolastes Belokobylskij, 1992**
- Fifth metasomal tergite not enlarged and never covering posterior segments (Figs 15H, 16J). Posterior tergites (fourth and fifth) rarely only partly (basally) sculptured, often entirely or mostly smooth (Figs 15H, 16J). In male, occipital carinae always present laterally; temple without lateral vertical occipital lumps. Nearctic, Neotropical, Oriental, Palaearctic regions (*Colastes* Haliday, 1833) **7**
- 7** Notauli complete and widely separated in posterior margin of mesoscutum. Propodeum smooth, with areola delineated by distinct carinae. Precoxal sulcus present, but fine, with distinct longitudinal carina on its posterior margin. Oriental region.....
 **Colastes (Discolastes) Belokobylskij, 2000**
- Notauli complete or incomplete, if complete, than always fused near posterior margin of mesoscutum (Figs 15F, 16H). Propodeum usually mostly sculptured and often without areola, if sometimes areola present, than delineated (often only partly) by weak carinae. Precoxal sulcus predominantly absent, longitudinal carina on lower margin of mesopleuron absent.... **8**
- 8** Ventral rim of clypeus thick, situated at same level as that of face and apex of mandible (lateral view) (Fig. 15E). Scutellum smooth medio-posteriorly (Fig. 15F). Parasitoid of leaf-mining larvae and of larvae in leaf-galls. Australasian, Nearctic, Neotropical, Oriental, Palaearctic regions.....
 **Colastes (Colastes s. str.)**
- Ventral rim of clypeus thin, protruding beyond level of face and apex of mandible (lateral view) (Fig. 16D). Scutellum often rugulose medio-posteriorly (Fig. 16H). Parasitoids of larvae in bracket fungi. – Notauli posteriorly meeting in rugose-striate medio-posterior area (Fig. 16H). Nearctic, Palaearctic regions..... **Colastes (Fungivenator) van Achterberg & Shaw, 2008**

Acknowledgements

The authors are very thankful to Dr Michael J. Sharkey (Redlands, USA) and Prof. Cornelis van Achterberg (Leiden, the Netherlands) for their very useful suggestions and comments on this manuscript. We are grateful to Mrs. Kyongim Kim (Geochang, SMNE) for the preparation of braconid specimens.

Additional information

Conflict of interest

The authors have declared that no competing interests exist.

Ethical statement

No ethical statement was reported.

Funding

This work was supported by a grant from the National Institute of Biological Resources (NIBR), funded by the Ministry of Environment (MOE) of the Republic of Korea (project numbers: NIBR201801201, NIBR202402202, NIBR202502202) for DSK, and was funded in part by the Russian State Research Project No 125012901042-9 for SAB.

Author contributions

Conceptualisation: SAB, DK. Data curation: SAB. Investigation: SAB, DK. Methodology: SAB. Writing – original draft: SAB. Writing – review and editing: DK.

Author ORCIDs

Sergey A. Belokobylskij  <https://orcid.org/0000-0002-3646-3459>

Deokseo Ku  <https://orcid.org/0000-0002-6274-6479>

Data availability

All of the data that support the findings of this study are available in the main text.

References

- Belokobylskij SA (1984) On the division of the tribe Exothecini s.l. (Hymenoptera, Braconidae) in two with the description of a new genus and subgenus. *Zoologicheskij Zhurnal* 63: 1019–1026. [In Russian]
- Belokobylskij SA (1986) A new braconid species of the supertribe Exothecidii (Hymenoptera, Braconidae) from south of the USSR Far East. In: Lehr PA (Ed.) *Systematika i Ekologiya Nasekomykh Dalinego Vostoka*. [Systematics and ecology of the insects from the Far East.] Vladivostok: 58–69. [In Russian]
- Belokobylskij SA (1990) A contribution to the braconid fauna (Hymenoptera) of the Far East. *Vestnik Zoologii* 1990(6): 32–39. [In Russian]
- Belokobylskij SA (1992) Contribution to the fauna of the Indo-Malayan braconid wasps of the tribe Exothecini, Pambolini and Pentatermini (Hymenoptera, Braconidae). *Proceedings of the Zoological Institute* 245: 125–173. [In Russian]
- Belokobylskij SA (1993) On the classification and phylogeny of the braconid wasps subfamilies Doryctinae and Exothecinae (Hymenoptera, Braconidae). Part 1. On the classification, 2. *Entomologicheskoe Obozrenie* 72(1): 143–164. [In Russian]
- Belokobylskij SA (1994) A review of parasitic wasps of the subfamilies Doryctinae and Exothecinae (Hymenoptera, Braconidae) of the Far East, eastern Siberia and neighbouring territories. In: Kotenko AG (Ed.) *Hymenopteran insects of Siberia and Far East*. *Memoirs of the Dauriskiy Nature Reserve* 3: 5–77. [In Russian]
- Belokobylskij SA (1996) Nine new species of Braconidae (Hymenoptera) from the Russian Far East. *Journal of Natural History* 30(11): 1661–1681. <https://doi.org/10.1080/00222939600770981>
- Belokobylskij SA (1998) Subfam. Exothecinae. In: Lehr PA (Ed.) *Key to insects of the Russian Far East*. Vol. 4. Neuropteroidea, Mecoptera, Hymenoptera. Pt 3. *Dal'nauka*, Vladivostok: 111–159. [In Russian]

- Belokobylskij SA (1999) New genera of the subfamilies Rhyssalinae, Exothecinae and Gnaptodontinae from the Old World (Hymenoptera: Braconidae). *Zoosystematica Rossica* 8(1): 155–169.
- Belokobylskij SA, Maetô K (2009) Doryctinae (Hymenoptera, Braconidae) of Japan. *Fauna mundi*. Vol. 1. Warszawska Drukarnia Naukowa, Warszawa, 806 pp.
- Belokobylskij SA, Tobias VI (1986) Subfam. Doryctinae. In: Medvedev GS (Ed.) *Keys to insects of the USSR European part*. Vol. 4. Hymenoptera. Pt. 4. Nauka, Leningrad: 21–72. [In Russian]
- Belokobylskij SA, Samartsev KG, Il'inskaya AS [Eds] (2019) Annotated catalogue of the Hymenoptera of Russia. Volume II. Apocrita: Parasitica. *Proceedings of the Zoological Institute Russian Academy of Sciences. Supplement 8*. St Petersburg, 594 pp. <https://doi.org/10.31610/trudyzin/2019.supl.8.5>
- Belokobylskij SA, Ku D-S, Lee H-R, Kwon G-M (2024) Braconidae: Rhyssalinae and Doryctinae. *Arthropoda: Insecta: Hymenoptera. Insect Fauna of Korea* 13 (16): 1–513.
- Haliday AH (1833) An essay on the classification of the parasitic Hymenoptera of Britain, which correspond with the *Ichneumonones minuti* of Linnaeus. *Entomological Magazine* 1(iii): 259–276, 333–350.
- Haliday AH (1836) Essay on parasitic Hymenoptera. *Entomological Magazine* 4(ii): 92–106.
- Jasso-Martínez JM, Quicke DLJ, Belokobylskij SA, Santos BF, Fernández-Triana JL, Kula RR, Zaldivar-Riverón A (2022) Mitochondrial phylogenomics and mitogenome organization in the parasitoid wasp family Braconidae (Hymenoptera: Ichneumonoidea). *BMC Ecology and Evolution* 22: 46. <https://doi.org/10.1186/s12862-022-01983-1>
- Ku DS, Belokobylskij SA, Cha JY (2001) Hymenoptera (Braconidae). *Economic Insects of Korea* 16. *Insecta Koreana. Supplement 23*: 1–283.
- Martínez JJ, Diez F (2024) Taxonomic notes on some neglected doryctine wasps (Hymenoptera: Braconidae) from Argentina described by J. Brèthes and E. Blanchard. *Zootaxa* 5406 (1): 190–200. <https://doi.org/10.11646/zootaxa.5406.1.11>
- Papp J (1972) *Exothecus effectus* sp. n., a new braconid species from N.E. China (Hym.). *Acta Zoologica Academiae Scientiarum Hungaricae* 18: 323–325.
- Papp J (1975) Three new European species of *Colastes* Hal. with taxonomic remarks (Hym., Braconidae, Exothecinae). *Acta Zoologica Academiae Scientiarum Hungaricae* 21: 411–423.
- Papp J (1983) Braconidae (Hymenoptera) from Mongolia. IX. *Acta Zoologica Academiae Scientiarum Hungaricae* 29: 441–449.
- Papp J (1987) Braconidae (Hymenoptera) from Korea. VIII. *Acta Zoologica Academiae Scientiarum Hungaricae* 33: 157–175.
- Papp J (1992) Braconidae (Hymenoptera) from Korea. XIV. *Acta Zoologica Academiae Scientiarum Hungaricae* 38: 63–73.
- Papp J (2003) Braconidae (Hymenoptera) from Korea, XXI. Species of fifteen subfamilies. *Acta Zoologica Academiae Scientiarum Hungaricae* 49: 115–152.
- Ranjith AP, Belokobylskij SA, Quicke DLJ, Kittel RN, Butcher BA, Nasser M (2017) An enigmatic new genus of Hormiinae (Hymenoptera: Braconidae) from South India. *Zootaxa* 4272(3): 371–385. <https://doi.org/10.11646/zootaxa.4272.3.3>
- Shenefelt RD (1975) Braconidae 8. Exothecinae, Rogadinae. *Hymenopterorum Catalogus, Nova Editio, Pars* 12: 1115–1262.
- Thomson CG (1892) XLIV. Bidrag till Braconidernas kannedom. *Opuscula Entomologica* 16: 1659–1751.

- van Achterberg C (1983) Revisionary notes on the Palaearctic genera and species of the tribe Exothecini Foerster (Hymenoptera: Braconidae). *Zoologische Mededelingen* 57(26): 339–355.
- van Achterberg C (1993) Illustrated key to the subfamilies of the Braconidae (Hymenoptera: Ichneumonoidea). *Zoologische Verhandelingen* 283: 1–189.
- van Achterberg C (1995) Generic revision of the subfamily Betylobraconinae (Hymenoptera: Braconidae) and other groups with modified fore tarsus. *Zoologische Verhandelingen* 298: 1–242.
- van Achterberg C, Shaw MR (2008) A new subgenus of the genus *Colastes* Haliday (Hymenoptera: Braconidae: Exothecinae) for species reared from bracket fungi, with description of two new species from Europe. *Journal of Natural History* 42(27–28): 1849–1860. <https://doi.org/10.1080/00222930802114280>
- Wesmael C (1838) Monographie des Braconides de Belgique. 4. Nouveaux Mémoires de l'Académie Royale des Sciences et Belles-lettres de Bruxelles 11: 1–166. <https://doi.org/10.3406/marb.1837.2702>
- Whitfield JB, Wharton RA (1997) Hormiinae. In: Wharton RA, Marsh PM, Sharkey MJ (Eds) *Manual of the New World genera of the family Braconidae (Hymenoptera)*. International Society of Hymenopterists. Special Publication No. 1: 285–301.
- Yu DS, van Achterberg C, Horstmann K (2016) Taxapad 2016. Ichneumonoidea 2015. Nepean, Ottawa, Ontario. [Database on flash-drive]
- Zaldivar-Riverón A, Mori M, Quicke DLJ (2006) Systematics of the cyclostome subfamilies of braconid parasitic wasps (Hymenoptera: Ichneumonoidea): a simultaneous molecular and morphological Bayesian approach. *Molecular Phylogenetics and Evolution* 38(1): 130–145. <https://doi.org/10.1016/j.ympev.2005.08.006>

Three new species of the genus *Weintrauboa* Hormiga, 2003 (Araneae, Linyphiidae) from China

Zhizhong Gao¹, Muhammad Irfan^{2,3}, Lu-Yu Wang²

¹ Department of Biology, Xinzhou Normal University, Xinzhou, Shanxi 034000, China

² Key Laboratory of Eco-environments in Three Gorges Reservoir Region (Ministry of Education), School of Life Sciences, Southwest University, Chongqing 400715, China

³ College of Plant Protection, Southwest University, Chongqing 400715, China

Corresponding author: Lu-Yu Wang (wangluyu1989@163.com)

Abstract

Three new species of the genus *Weintrauboa* Hormiga, 2003 are described here as: *W. denticulata* **sp. nov.** (Hunan, ♂), *W. shenwu* **sp. nov.** (Hubei and Chongqing, ♂♀), and *W. wanglangensis* **sp. nov.** (Sichuan, ♂♀). Detailed descriptions, photographs of genital characters, somatic features, and a distribution map are provided.

Key words: Description, distribution, morphology, sheet-web spiders, taxonomy

Introduction

Linyphiidae is one of the most diverse spider families worldwide, comprising 640 extant genera and 4947 species globally, including 11 fossil genera and 62 species (WSC 2025). In China, approximately 608 species across 182 genera have been documented (Tanasevitch 2025). The genus *Weintrauboa* Hormiga, 2003 includes eight species found in China (Guizhou, Sichuan, Yunnan), Japan, and Russia (Far East, Sakhalin) (WSC 2025). Initially classified within the family Pimoidae Wunderlich, 1986, the genus was transferred to Linyphiidae based on a molecular analysis and reinterpretation of its morphology (Hormiga et al. 2021).

Recent studies of linyphiid spiders have mainly focused on the southern regions of the country: Yunnan Province (Zhao and Li 2014; Irfan and Peng 2018, 2019a, 2019b; Zhou et al. 2018, 2021, 2023; Irfan et al. 2019, 2020, 2021, 2022a, 2022b, 2023a, 2023b, 2024, 2025; Zhang et al. 2022; Yang et al. 2023) and Chongqing Region (Irfan et al. 2023a, 2023b). These studies have not only substantially increased the known diversity of Linyphiidae in Yunnan and Chongqing but also suggest that a significant number of species remain undiscovered in southern China. Future extensive research in this region is likely to reveal more species, further enriching our understanding of this complex and diverse spider family. While examining specimens collected from south China, three new species of the genus *Weintrauboa* were identified and are described here.



Academic editor: Francesco Ballarin

Received: 9 January 2025

Accepted: 17 March 2025

Published: 29 April 2025

ZooBank: <https://zoobank.org/51D33FA7-0F4B-44B5-88AB-BE70484D7ACA>

Citation: Gao Z, Irfan M, Wang L-Y (2025) Three new species of the genus *Weintrauboa* Hormiga, 2003 (Araneae, Linyphiidae) from China. ZooKeys 1236: 185–196. <https://doi.org/10.3897/zookeys.1236.146324>

Copyright: © Zhizhong Gao et al.
This is an open access article distributed under terms of the Creative Commons Attribution License (Attribution 4.0 International – CC BY 4.0).

Material and methods

Specimens were collected by hand picking and sieving leaf litter, and were kept in 75% ethanol. The left male palps were used for photography. After dissection, epigynes were cleared in trypsin enzyme solution before examination and photography. All specimens were examined, photographed and measured using a Leica M205A stereomicroscope and LAS00 software (ver. 4.6). Left male palps and epigynes were examined and photographed after dissection. Compound focus images were generated using Helicon Focus ver. 6.7.1 software. Eye sizes were measured at the maximum dorsal diameter. Legs measurements are shown as total length (femur, patella, tibia, metatarsus, tarsus). All measurements are in millimeters. Specimens are deposited in the School of Life Sciences, Southwest University, Chongqing (SWUC), China. The map was created using the online mapping software SimpleMappr (Shorthouse 2010) (Fig. 7). The terminology used in the text and figure legends follows Hormiga et al. (2021). In the text, “Fig.” and “Figs” refer to figures herein, while “fig.” and “figs” refer to figures published elsewhere.

The following abbreviations are used in the text and figures: **a.s.l.** = above sea level; **AER** = anterior eye row; **ALE** = anterior lateral eyes; **AME** = anterior median eyes; **AME–ALE** = the distance between AME and ALE; **AME–AME** = the distance between AMEs; **ARP** = anterior radical process; **CD** = copulatory ducts; **CO** = copulatory openings; **CP** = cymbial process (CDP in Hormiga 1994); **DP** = dorsal plate; **E** = embolus; **EF** = embolus flap; **FD** = fertilization ducts; **PC** = paracymbium; **PER** = posterior eye row; **PLE** = posterior lateral eyes; **PME** = posterior median eyes; **PME–PLE** = distance between PME and PLE; **PME–PME** = distance between PMEs; **S** = spermatheca; **SPT** = suprategulum; **ST** = subtegulum; **T** = tegulum; **Tml** = position of trichobothrium on metatarsus I; **VP** = ventral plate.

Taxonomy

Family Linyphiidae Blackwall, 1859

Genus *Weintrauboa* Hormiga, 2003

(文蛛属)

Type species. *Labulla contortipes* Karsch, 1881; gender feminine.

Weintrauboa denticulata sp. nov.

<https://zoobank.org/131F061C-4553-4D40-9306-4741C5DEF9D2>

Figs 1, 6A, 7

(齿文蛛)

Type material. *Holotype* ♂ (SWUC-T-LIN-38-01); CHINA, Hunan Province, Changsha City, Yuelu District, Yuelu Mountain, 28°11'33.9"N, 112°56'17.52"E, a.s.l. 208 m, 27.IX.2017, Wang Luyu leg.

Etymology. The specific epithet is derived from Latin adjective “*denticulatus*” meaning “toothed”, referring to the tegulum apically toothed in the male palp.

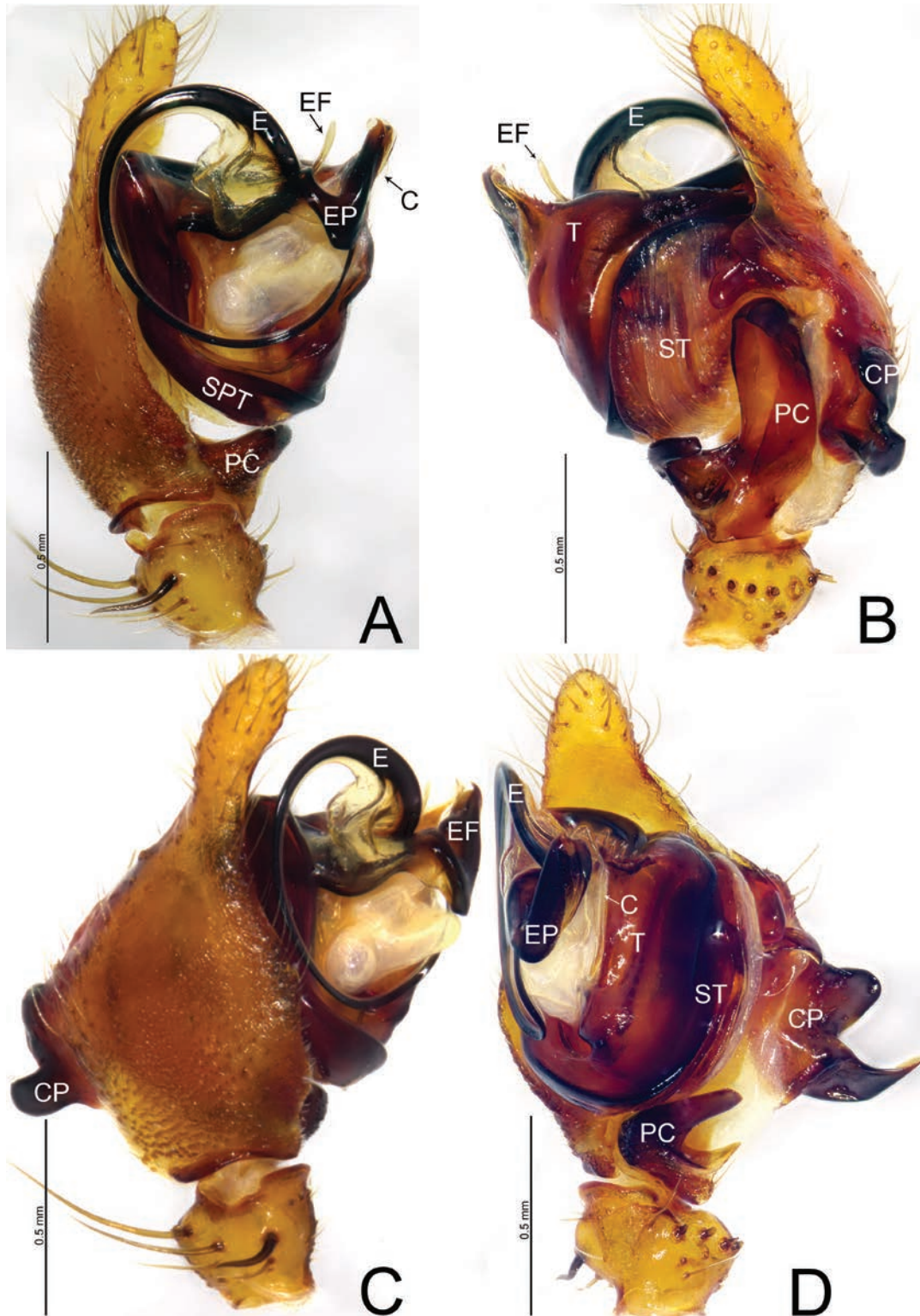


Figure 1. *Weintrauboa denticulata* sp. nov., male holotype **A** palp, prolateral view **B** palp, retrolateral view **C** palp, dorsal view **D** palp, ventral view. Abbreviations: CP = cymbial process; E = embolus; EF = embolus flap; EP = embolus process; PC = paracymbium; SPT = suprategulum; ST = subtegulum; T = tegulum.

Diagnosis. This new species resembles *Weintrauboa yele* Hormiga, 2008 in having similar embolus in male palp (Fig. 1A–D; Hormiga 2008, figs 2A–C, 3A–C; Hormiga et al. 2021, fig. 6A, B), but can be differentiated by the tegular apophysis with teeth in *W. denticulata* sp. nov. (Fig. 1B, D; vs teeth absent); embolic process

tip grooved in ventral view in *W. denticulata* sp. nov. (Fig. 1D; vs hook-shaped); embolic flap like in retrolateral view in *W. denticulata* sp. nov. (Fig. 1B; vs almost wing-shaped); proximal ramus of cymbial process two times longer than distal one in *W. denticulata* sp. nov. (Fig. 1D; vs both rami almost same in length).

Description. Male (holotype, Fig. 6A) total length 5.63. Carapace 2.86 long, 2.23 wide; opisthosoma 2.77 long, 2.13 wide. Eye sizes and interdistances: AME 0.17, ALE 0.16, PME 0.17, PLE 0.14; AME–AME 0.10, AME–ALE 0.09, PME–PME 0.14, PME–PLE 0.16, ALE–PLE contiguous. MOA 0.91 long, front width 0.62, back width 0.51. Clypeus height 0.27. Chelicerae brown, with three promarginal and three retromarginal teeth. Leg measurements: I 11.6 (3.08, 1.11, 2.58, 3.23, 1.60); II 10.96 (2.95, 1.02, 2.53, 3.12, 1.34); III 8.41 (2.47, 0.79, 1.84, 2.32, 0.99); IV 10.26 (2.88, 0.88, 2.45, 2.88, 1.17). Leg formula: 1243.

Palp (Fig. 1A–D). Patella as long as tibia, ventrally grooved, dorsally with long thick spine. Tibia cone-shaped, with one retrolateral trichobothrium, retrolateral margin with seven thick spines. Cymbium with an ectal process wider than long, with bifurcated tip, proximal ramus hook-shaped, two times longer than distal one with pointed end, distal ramus tongue-shaped with blunt end; retrolateral margin of cymbium with tongue-shaped projection extending ventrally with blunt tip. Paracymbium bowl-shaped, apically hook-shaped, with median margin edge curved inward. Tegulum large, apically with long tegular apophysis with seven teeth, tip membranous. Conductor membranous, as long as patella, present on apical end of tegulum. Embolus circular with fine tip, embolic flap rod-like slightly curved with blunt tip, embolic process sclerotized, apically tip grooved, parallel to tegular apophysis.

Female. Unknown.

Distribution. Known only from the type locality, Hunan, China (Fig. 7).

***Weintrauboa shenwu* sp. nov.**

<https://zoobank.org/9A89FD67-41A6-4424-8CE9-CD19A91DF5DE>

Figs 2, 3, 6A, B, 7

(神巫文蛛)

Type material. Holotype ♂ (SWUC-T-LIN-39-01): CHINA, Hubei Province, Shennongjia, Yazikou, 31°30'55.0008"N, 110°19'58.0008"E, 1817 m a.s.l., 24.X.2020, L.Y. Wang, Y. Zhang, J.X. Zhao and J.S. Luo leg. **Paratypes:** 1♀ (SWUC-T-LIN-39-02), with same data as holotype • 2♂2♀ (SWUC-T-LIN-39-03~06), Hubei Province, Shennongjia, Hongping Town, 31°31'27.9957"N, 110°20'9.0416"E, 1711 m a.s.l., 14.VI.2023, Z.S. Zhang, X.L. Chen and Q.L. Lu leg. • **Chongqing Municipality:** 1♀ (SWUC-T-LIN-39-07), Wushan County, Dangyang Town, Xiejia-cao, 31°26'57.00"N, 109°58'45.57"E, a.s.l. 1449 m, 02.X.2021, L.Y. Wang, T.Y. Ren, J.X. Zhao, L. Xiao and X.W. Zhou leg. • 5♂8♀ (SWUC-T-LIN-39-08~20), Wushan County, Guanyang Town, Pingqian, 31°22'22.75"N, 109°56'17.25"E, a.s.l. 1832 m, 04.X.2021, L.Y. Wang, T.Y. Ren, J.X. Zhao, L. Xiao and X.W. Zhou leg.

Etymology. The specific name is derived from the Chinese word 'shen' and 'wu'; Shen is the first name for Shennongjia and Wu is an abbreviated name for Wushan; noun in apposition.

Diagnosis. *Weintrauboa shenwu* resembles those of *W. wanglangensis* and *W. yele* Hormiga, 2008 in having a similar embolus and embolic process in male

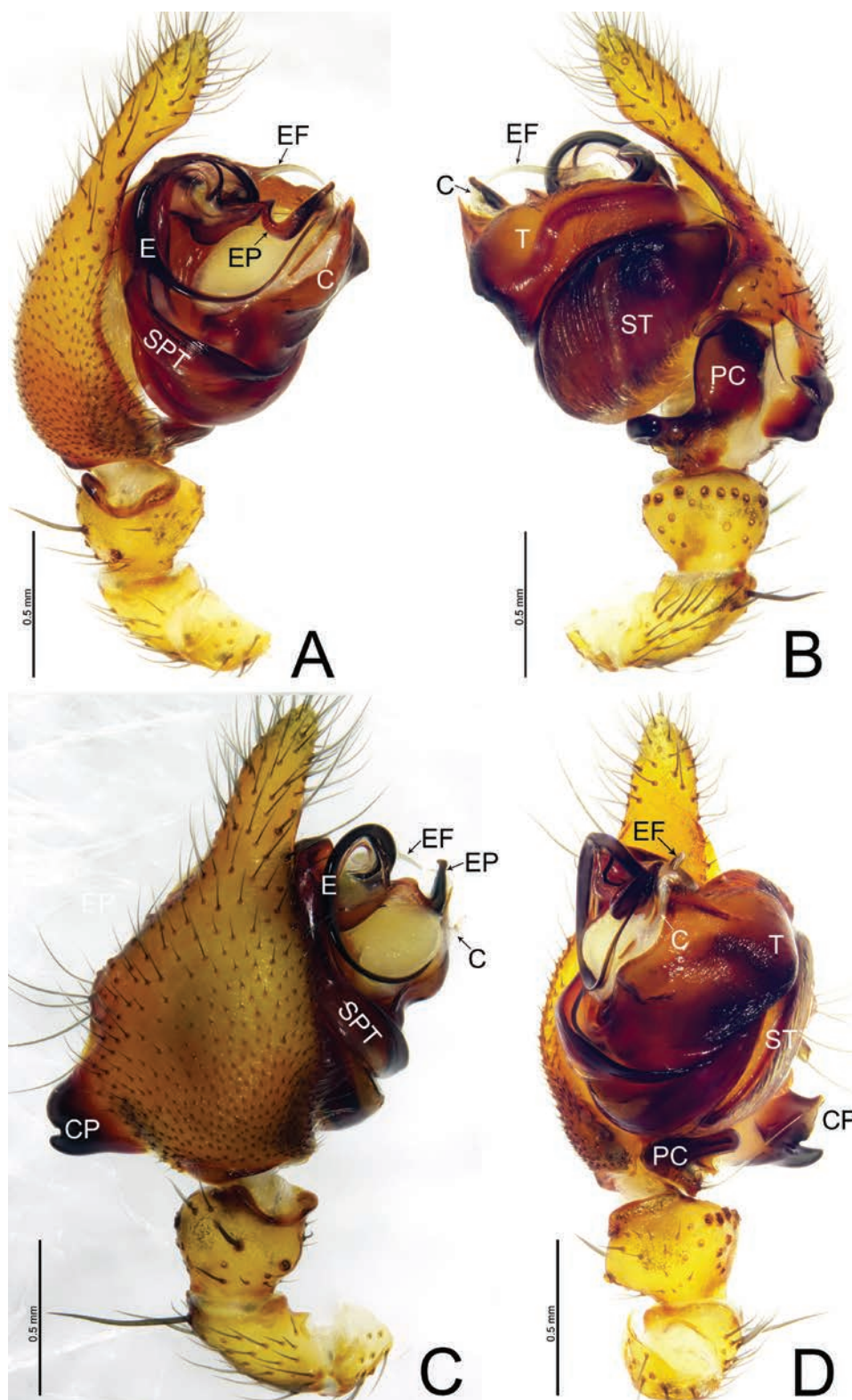


Figure 2. *Weintrauboa shennongjiaensis* sp. nov., male holotype **A** palp, prolateral view **B** palp, retrolateral view **C** palp, dorsal view **D** palp, ventral view. Abbreviations: CP = cymbial process; E = embolus; EF = embolus flap; EP = embolus process; PC = paracymbium; SPT = suprategulum; ST = subtegulum; T = tegulum.

palp (Figs 2A–D, 4A–D; Hormiga 2008, figs 2A–C, 3A–C; Hormiga et al. 2021, fig. 6A–B) and can be distinguished by the embolic flap needle-shaped in *W. shenwu* (Fig. 2A, B; vs horn-shaped in *W. wanglangensis* and wing-shaped in *W. yele*); distal

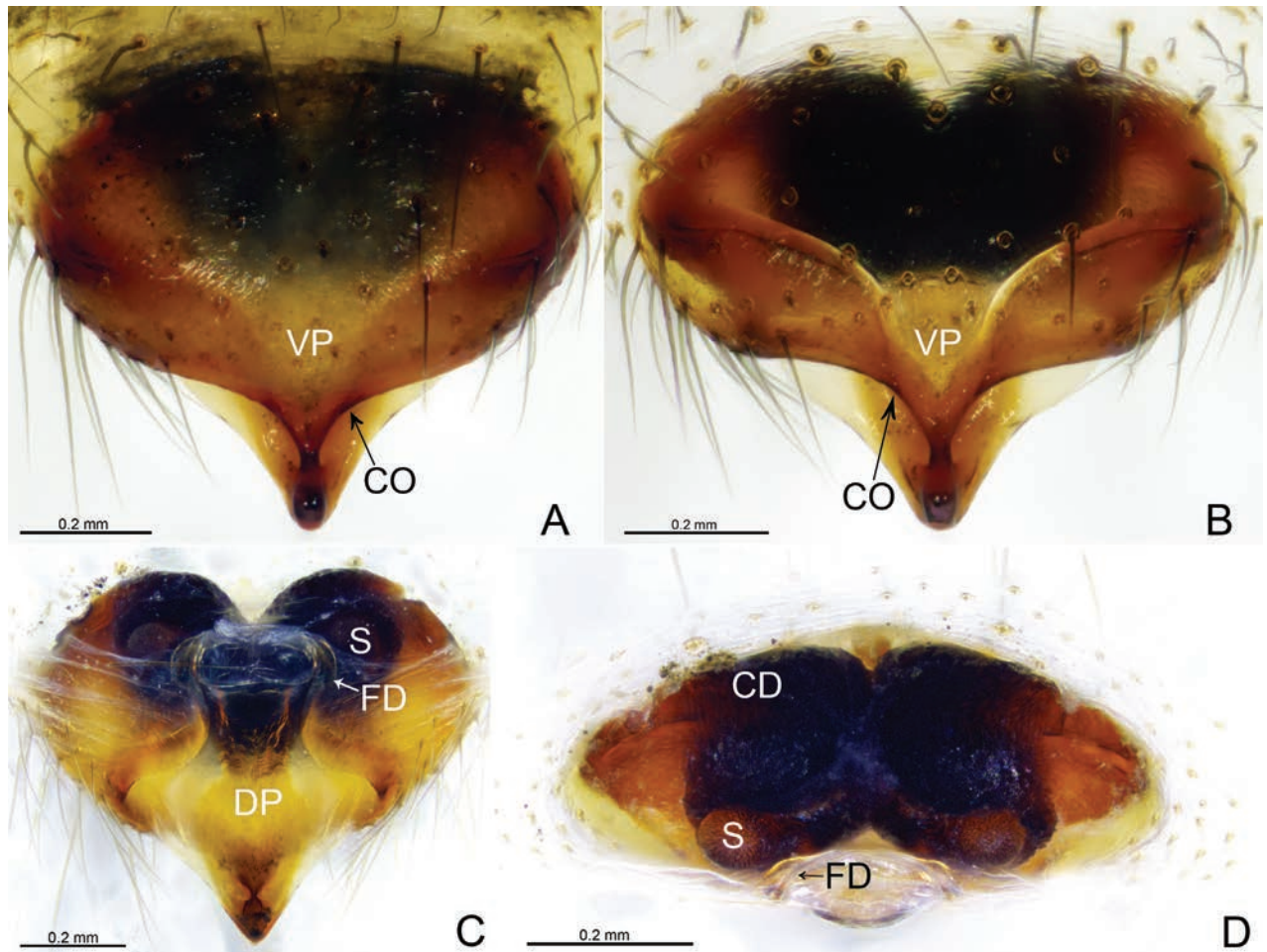


Figure 3. *Weintrauboa shennongjiaensis* sp. nov., female paratype **A, B** epigyne, ventral view **C** vulva, dorsal view **D** vulva, anterior view. Abbreviations: CD = copulatory duct; CO = copulatory opening; DP = dorsal plate; FD = fertilization duct; S = spermathecae; VP = ventral plate.

ramus of cymbial process somewhat rectangular in ventral view in *W. shenwu* (Fig. 2A, B; vs somewhat thumb-shaped both in *W. wanglangensis* and *W. yele*). Females of *W. shenwu* resemble *W. wanglangensis* in having similar morphology of epigyne (Figs 3A–D, 5A–D), but can be distinguished by the copulatory duct comma-shaped in *W. shenwu* (Fig. 3A–C; vs sinuous with three loops before entering spermathecae in *W. wanglangensis*, Fig. 5A–D); dorsal plate posteriorly triangular in *W. shenwu* (Fig. 3A–C; vs trapezoid in *W. wanglangensis*, Fig. 5A–D).

Description. Male (holotype, Fig. 6B) total length 7.01. Carapace 3.42 long, 2.39 wide; opisthosoma 3.81 long, 2.55 wide. Eye sizes and interdistances: AME 0.18, ALE 0.22, PME 0.18, PLE 0.18; AME–AME 0.09, AME–ALE 0.11, PME–PME 0.12, PME–PLE 0.17, ALE–PLE 0.02. MOA 0.49 long, front width 0.47, back width 0.49. Clypeus height 0.46. Chelicerae brown, with four pro-marginal and three retromarginal teeth. Leg measurements: I 21.41 (5.55, 7.19, 6.08, 2.59); II 16.96 (4.63, 5.37, 4.79, 2.17); III 11.15 (3.27, 3.46, 2.93, 1.49); IV 13.44 (3.72, 4.07, 3.69, 1.96). Leg formula: 1243.

Palp (Fig. 2A–D). Patella as long as tibia, ventrally grooved, dorsally with long thick spine. Tibia cone-shaped, with one retrolateral and one dorsal trichobothrium, retrolateral margin with eight thick spines. Cymbium with an ectal process wider than long, half the length of tibia, with bifurcated tip, proximal ramus

thumb-shaped and distal ramus somewhat rectangular; retrolateral margin of cymbium with thumb-shaped projection extending ventrally with blunt tip. Paracymbium bowl-shaped, apically hook-shaped, with median margin edge curved inward. Tegulum large, pointed apically. Distal suprategular apophysis sclerotized reduced. Conductor small, membranous, present on apical end of tegulum. Embolus circular with fine tip, embolic flap needle-shaped, slightly curved with pointed tip, embolic process sclerotized, apically expanded with blunt tip, extending towards ventral side of tegulum.

Female (paratype, Fig. 6C) total length 7.62. Prosoma 3.32 long, 2.63 wide; opisthosoma 5.05 long, 3.64 wide. Eye sizes and interdistances: AME 0.21, ALE 0.23, PME 0.19, PLE 0.20; AME–AME 0.05, AME–ALE 0.09, PME–PME 0.10, PME–PLE 0.16. ALE–PLE 0.03. MOA 0.56 long, front width 0.44, back width 0.49. Clypeus height 0.38. Leg measurements: I 13.60 (3.67, 4.34, 3.52, 2.07); II 12.12 (3.41, 3.89, 3.03, 1.79); III 9.54 (2.83, 2.87, 2.43, 1.41); IV 11.68 (3.40, 3.69, 3.05, 1.54). Leg formula: 1243.

Epigyne (Fig. 3A–D). Epigynal plate 1.5 times wider than long. Most of the atrium divided by septum. Ventral plate oval, anteriorly grooved, posterior margin convex. Copulatory openings present within atrium. Dorsal plate somewhat triangular extending posteriorly. Copulatory ducts elongated, V-shaped in ventral view, forming broad loop extending anteriorly before entering spermathecae. Spermathecae round, separated by distance equal to four times their diameter. Fertilization ducts present mesally.

Variation. Males ($N = 2$) total length 5.85–7.01; females ($N = 2$) total length 7.06–8.03.

Distribution. China (Hubei, Chongqing) (Fig. 7).

***Weintrauboa wanglangensis* sp. nov.**

<https://zoobank.org/8B70618A-53F1-4657-8B3D-EFBAF3966CE8>

Figs 4–6D, E, 7

(王朗文蛛)

Type material. **Holotype** ♂ (SWUC-T-LIN-40-01): CHINA, Sichuan Province, Pingwu County, Wanglang National Nature Reserve, Wuyangchang, 32°58'3.8388"N, 104°6'17.9388"E, a.s.l. 2503 m, 24.IX.2019, L.Y. Wang, P. Liu, T. Yuan, Z. Fan, Y. Zhang and M. Zhang leg. **Paratypes:** 22♂15♀, same data as holotype (SWUC-T-LIN-40-02~38).

Etymology. The specific epithet is derived from the type locality; adjective.

Diagnosis. See diagnosis of *Weintrauboa shenwu* sp. nov.

Description. **Male** (holotype, Fig. 6D) total length 7.64. Carapace 3.53 long, 2.65 wide; opisthosoma 4.21 long, 2.68 wide. Eye sizes and interdistances: AME 0.22, ALE 0.22, PME 0.18, PLE 0.20; AME–AME 0.10, AME–ALE 0.11, PME–PME 0.13, PME–PLE 0.21, ALE–PLE 0.03. MOA 0.57 long, front width 0.49, back width 0.51. Clypeus height 0.32. Chelicerae brown, with three promarginal and three retromarginal teeth. Leg measurements: I 18.62 (4.84, 6.42, 5.21, 2.15); II 16.57 (4.46, 5.55, 4.62, 1.94); III 10.97 (3.35, 3.50, 2.86, 1.56); IV 13.24 (3.94, 3.99, 3.67, 1.64). Leg formula: 1243.

Palp (Figs 4A–D). Patella as long as tibia, ventrally grooved, dorsally with long thick spine. Tibia cone-shaped, with two retrolateral and one dorsal

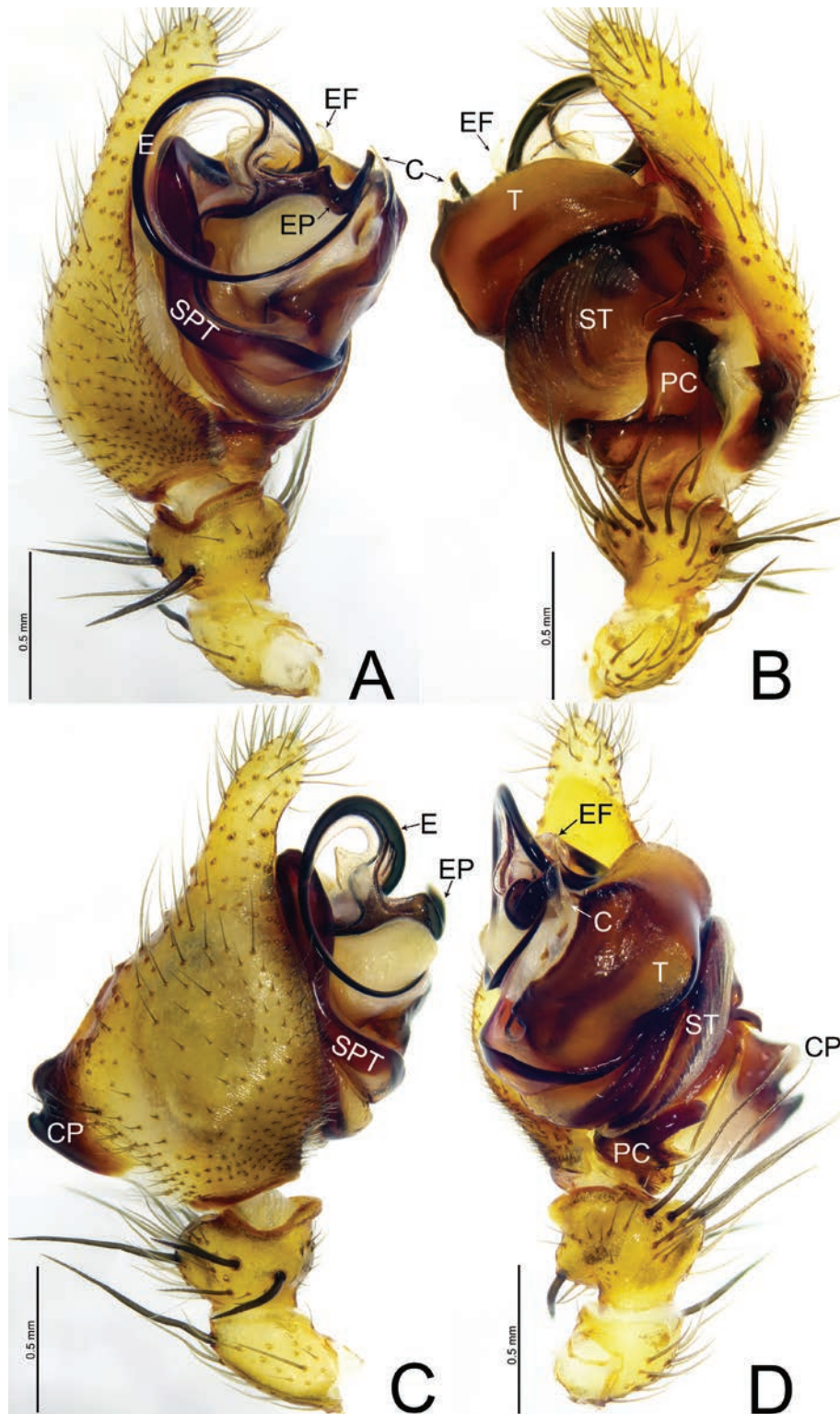


Figure 4. *Weintrauboa wanglangensis* sp. nov., male holotype **A** palp, prolateral view **B** palp, retrolateral view **C** palp, dorsal view **D** palp, ventral view. Abbreviations: CP = cymbial process; E = embolus; EF = embolus flap; EP = embolus process; PC = paracymbium; SPT = suprategulum; ST = subtegulum; T = tegulum.

trichobothria, retrolateral margin with nine thick spines. Cymbium with an ectal process wider than long, half the length of tibia, with bifurcated tip, both rami are almost equal in size and shape with blunt end; retrolateral margin of cymbium with thumb-shaped projection extending ventrally with blunt tip. Paracymbium

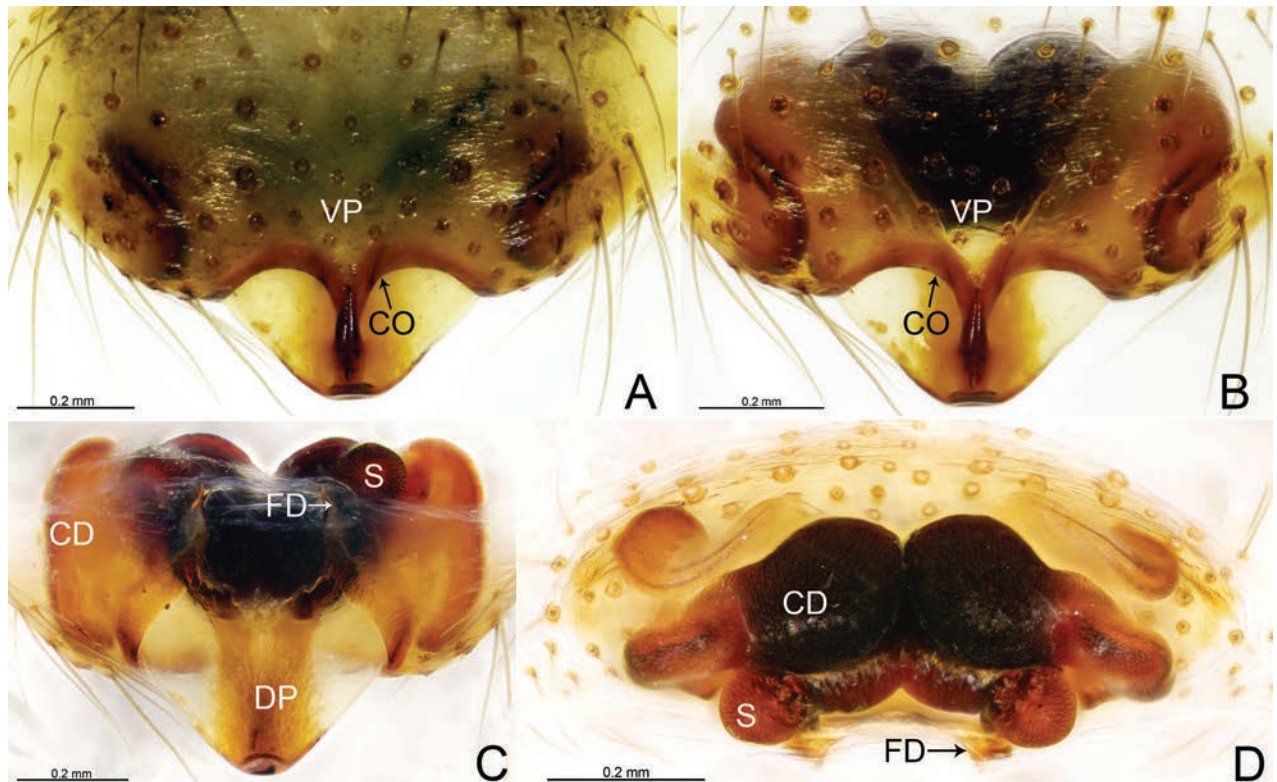


Figure 5. *Weintrauboa wanglangensis* sp. nov., female paratype **A, B** epigyne, ventral view **C** vulva, dorsal view **D** vulva, anterior view. Abbreviations: CD = copulatory duct; CO = copulatory opening; DP = dorsal plate; FD = fertilization duct; S = spermathecae; VP = ventral plate.

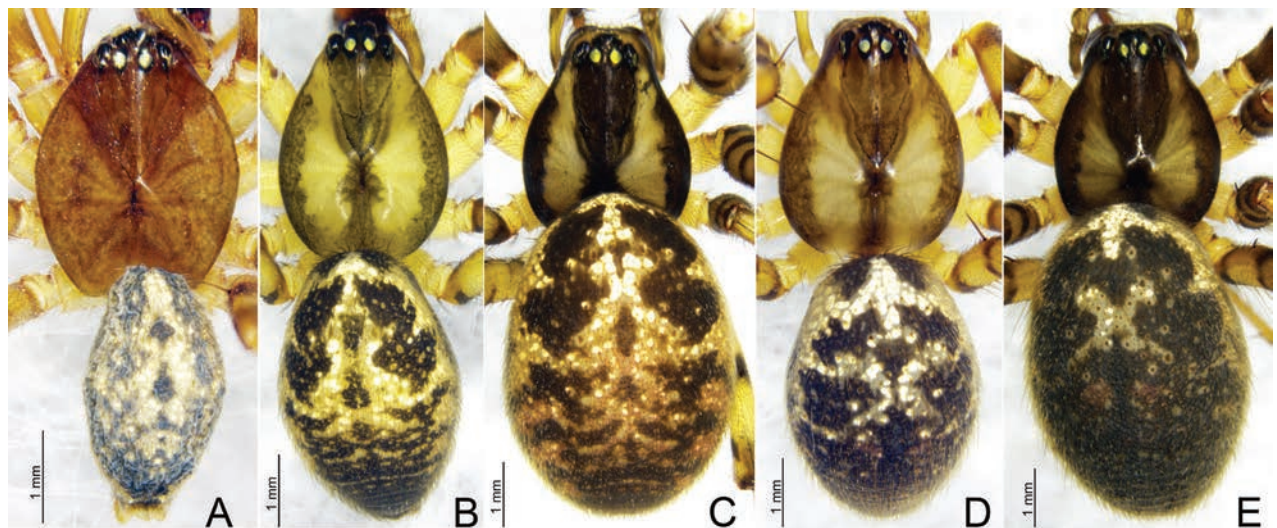


Figure 6. *Weintrauboa* species habitus, dorsal view **A** *W. denticulata* sp. nov. male holotype **B, C** *W. shennongjiaensis* sp. nov., male holotype (**B**), female paratype (**C**) **D, E** *W. wanglangensis* sp. nov., male holotype (**D**) female paratype (**E**).

bowl-shaped, apically hook-shaped, with median margin edge curved inward. Tegulum large, apically tapering. Conductor membranous, almost half the length of patella, present on apical end of tegulum. Embolus circular with fine tip, embolic flap horn-shaped, curved with pointed tip, embolic process sclerotized, apically with pointed tip, extending towards ventral side of tegulum.

Female (paratype, Fig. 6E) total length 9.64. Prosoma 3.66 long, 2.94 wide; opisthosoma 6.09 long, 4.88 wide. Eye sizes and interdistances: AME 0.23, ALE

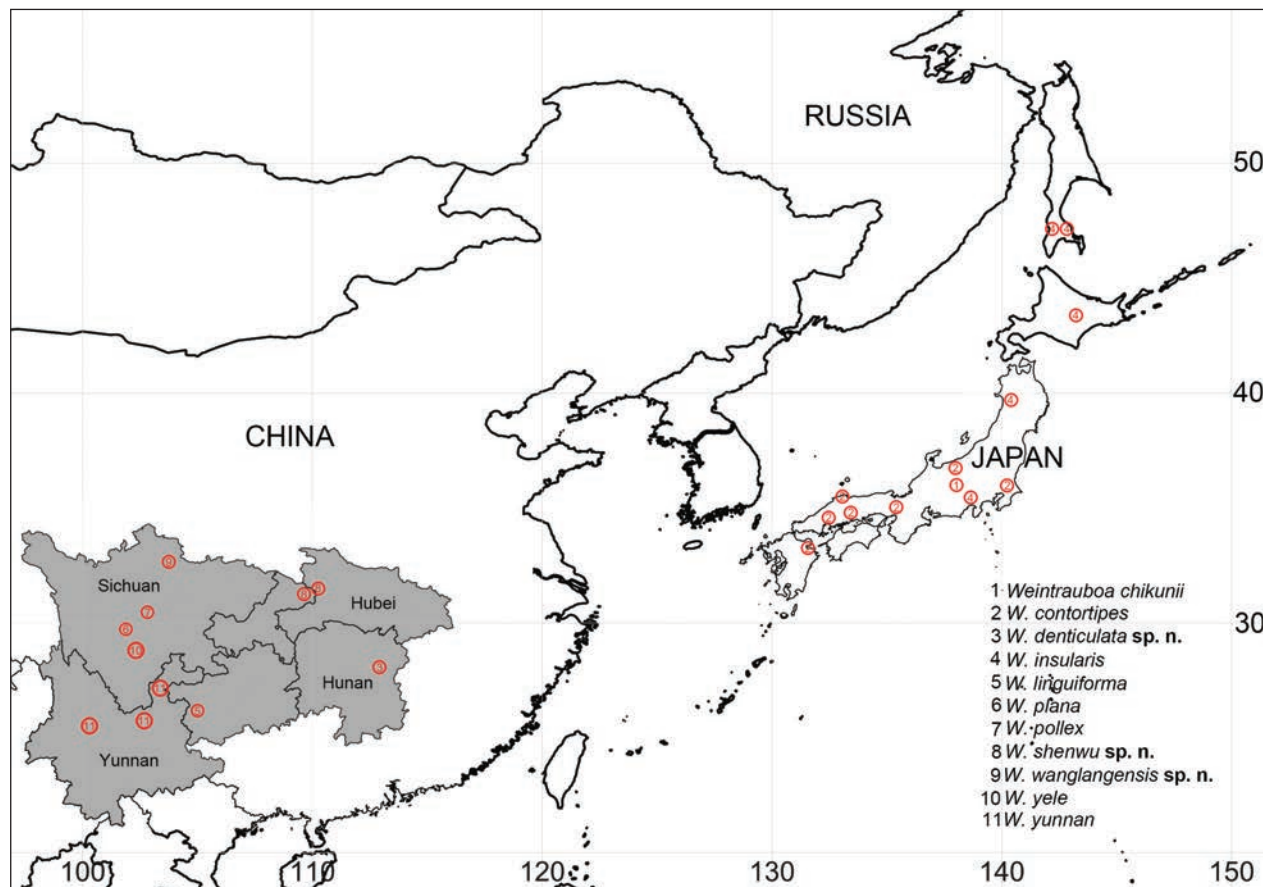


Figure 7. Distribution of *Weintrauboa* species (WSC 2025).

0.25, PME 0.23, PLE 0.23; AME–AME 0.08, AME–ALE 0.16, PME–PME 0.16, PME–PLE 0.20. ALE–PLE 0.02. MOA 0.65 long, front width 0.50, back width 0.60. Clypeus height 0.32. Leg measurements: I 15.87 (442, 5.34, 4.04, 2.07); II 14.46 (4.09, 4.76, 3.70, 1.91); III 10.96 (325, 3.53, 2.77, 1.41); IV 13.62 (3.92, 4.37, 3.42, 1.91). Leg formula: 1243.

Epigyne (Fig. 5A–D). Epigynal plate wider than long. Most of the atrium divided by septum. Ventral plate oval, anteriorly grooved, posterior margin wavy. Copulatory openings present within atrium. Dorsal plate somewhat triangular, with broad tip posteriorly. Copulatory ducts sinuous, forming three curved loops before entering spermathecae. Spermathecae round, separated by distance equal to three times their diameter. Fertilization ducts present mesally.

Variation. Males ($N = 23$) total length 6.26–7.87; females ($N = 15$) total length 7.37–9.64.

Distribution. Known only from the type locality, Sichuan, China (Fig. 7).

Acknowledgements

We are grateful to the subject editor, Francesco Ballarin, and two reviewers, Andrei Tanasevitch and an anonymous one for their helpful comments. We are thankful to Wanglang National Nature Reserve administration for helping us during fieldwork and collection.

Additional information

Conflict of interest

The authors have declared that no competing interests exist.

Ethical statement

No ethical statement was reported.

Funding

This work was supported, by the Fundamental Research Program of Shanxi Province (202403021211040) to ZG, by the Project of Background Resources Survey in Shennongjia National Park (SNJNP2022009) and Open Project Fund of Hubei Provincial Key Laboratory on Conservation Biology of the Shennongjia Golden Snub-nosed Monkey (SNJGKL2022009).

Author contributions

Data curation: MI. Writing – original draft: ZG. Writing – review and editing: LYW.

Author ORCIDs

Zhizhong Gao  <https://orcid.org/0000-0002-6666-8746>

Muhammad Irfan  <https://orcid.org/0000-0003-0445-9612>

Lu-Yu Wang  <https://orcid.org/0000-0002-5250-3473>

Data availability

All of the data that support the findings of this study are available in the main text.

References

- Hormiga G (1994) Cladistics and the comparative morphology of linyphiid spiders and their relatives (Araneae, Araneoidea, Linyphiidae). *Zoological Journal of the Linnean Society* 111: 1–71. <https://doi.org/10.1111/j.1096-3642.1994.tb01491.x>
- Hormiga G (2008) On the spider genus *Weintrauboa* (Araneae, Pimoidae), with a description of a new species from China and comments on its phylogenetic relationships. *Zootaxa* 1814: 1–20. <https://doi.org/10.11646/zootaxa.1814.1.1>
- Hormiga G, Kulkarni S, da Silva Moreira T, Dimitrov D (2021) Molecular phylogeny of pimoid spiders and the limits of Linyphiidae, with a reassessment of male palpal homologies (Araneae, Pimoidae). *Zootaxa* 5026(1): 71–101. <https://doi.org/10.11646/zootaxa.5026.1.3>
- Irfan M, Peng XJ (2018) Three new species of Linyphiidae (Arachnida: Araneae) from Yunnan, China. *Oriental Insects* 52(3): 229–244. <https://doi.org/10.1080/00305316.2017.1398115>
- Irfan M, Peng XJ (2019a) *Herbiphantes* Tanasevitch, 1992 and *Labullinyphia* van Helsdingen, 1985 (Araneae, Linyphiidae), two newly recorded spider genera from the Gaoligong Mountains in China with the description of two new species. *Zootaxa* 4638(4): 547–561. <https://doi.org/10.11646/zootaxa.4638.4.5>
- Irfan M, Peng XJ (2019b) The genus *Parbatthorax* Tanasevitch, 2019 (Araneae, Linyphiidae) new to China, with a new species from the Gaoligong Mountains. *European Journal of Taxonomy* 555: 1–19. <https://doi.org/10.5852/ejt.2019.555>

- Irfan M, Zhou GC, Peng XJ (2019) *Zhezhoulinyphia* gen. nov. (Araneae, Linyphiidae) from Yunnan, China. *ZooKeys* 862: 43–60. <https://doi.org/10.3897/zookeys.862.31406>
- Irfan M, Zhou GC, Bashir S, Mukhtar MK, Peng XJ (2020) *Yuelushannus* gen. nov. (Araneae, Linyphiidae) from China. *European Journal of Taxonomy* 642: 1–17. <https://doi.org/10.5852/ejt.2020.642>
- Irfan M, Bashir S, Peng XJ (2021) *Acroterius* gen. nov. (Araneae: Linyphiidae: Linyphiinae) with twelve new species from Yunnan, China. *European Journal of Taxonomy* 743: 1–53. <https://doi.org/10.5852/ejt.2021.743.1293>
- Irfan M, Wang LY, Zhang ZS (2022a) Two new species of Micronetinae Hull, 1920 spiders (Araneae: Linyphiidae) from Yintiaoling Nature Reserve, Chongqing, China. *Acta Arachnologica Sinica* 31(1): 17–26. <https://doi.org/10.3969/j.issn.1005-9628.2022.01.003>
- Irfan M, Zhang ZS, Peng XJ (2022b) Survey of Linyphiidae (Arachnida: Araneae) spiders from Yunnan, China. *Megataxa* 8(1): 1–292. <https://doi.org/10.11646/megataxa.8.1.1>
- Irfan M, Wang LY, Zhang ZS (2023a) One new genus and nine new species of Linyphiidae spiders from Yintiaoling Nature Reserve, Chongqing of China. *Zootaxa* 5257(1): 82–114. [incl. Erratum: *Zootaxa* 5263(4): 575–600.] <https://doi.org/10.11646/zootaxa.5257.1.7>
- Irfan M, Wang LY, Zhang ZS (2023b) Survey of Linyphiidae spiders (Arachnida: Araneae) from Wulipo National Nature Reserve, Chongqing, China. *European Journal of Taxonomy* 871: 1–85. <https://doi.org/10.5852/ejt.2023.871.2129>
- Irfan M, Dai Y, Wang LY, Zhang ZS (2024) Four new species of *Tapinocyba* Simon, 1884 (Araneae, Linyphiidae) from Jiangjin District of Chongqing, China. *ZooKeys* 1219: 195–214. <https://doi.org/10.3897/zookeys.1219.133899>
- Irfan M, Zhou GC, Peng XJ, Zhang ZS (2025) Survey of Linyphiidae spiders (Arachnida: Araneae) from some oriental regions of China. *Megataxa* 15(1): 1–248. <https://doi.org/10.11646/megataxa.15.1.1>
- Shorthouse DP (2010) SimpleMappr, an online tool to produce publication-quality point maps. <https://www.simplemappr.net> [Accessed on 07 January 2025]
- Tanasevitch AV (2025) Linyphiidae Spiders of the World. <http://old.cepl.rssi.ru/bio/tan/linyphiidae/> [Accessed on, 05 January 2025]
- WSC (2025) World Spider Catalog. Version 25.5. Natural History Museum Bern, online at <http://wsc.nmbe.ch> accessed on 07 January 2025. <https://doi.org/10.24436/2>
- Yang L, Yao ZY, Irfan M, He QQ (2023) A newly recorded genus with description of a new cave-dwelling species of *Flagelliphantes* (Araneae, Linyphiidae) from northeastern China. *Biodiversity Data Journal* 11: e105488. [1–7] <https://doi.org/10.3897/BDJ.11.e105488>
- Zhang MT, Liu P, Irfan M, Peng XJ (2022) A survey of the genus *Himalaphantes* Tanasevitch, 1992 (Araneae, Linyphiidae) with description of three new species from Yunnan, China. *ZooKeys* 1123: 47–62. <https://doi.org/10.3897/zookeys.1123.86261>
- Zhao QY, Li SQ (2014) A survey of linyphiid spiders from Xishuangbanna, Yunnan Province, China (Araneae, Linyphiidae). *ZooKeys* 460: 1–181. <https://doi.org/10.3897/zookeys.460.7799>
- Zhou GC, Irfan M, Peng XJ (2018) Redescription of *Ketambea nigripectoris* (Oi, 1960) comb. nov. (Araneae: Linyphiidae). *Turkish Journal of Zoology* 42(4): 488–494. <https://doi.org/10.3906/zoo-1803-29>
- Zhou GC, Irfan M, Peng XJ (2021) A new species of *Denisiphantes* Tu, Li & Rollard, 2005 (Araneae, Linyphiidae) from Yunnan, China. *ZooKeys* 1023: 1–12.
- Zhou GC, Du WF, Xu CX, Irfan M (2023) A new species of *Floronia* Simon, 1887 from Baiyan Cave in Guizhou Province, China (Araneae, Linyphiidae). *ZooKeys* 1185: 309–319. <https://doi.org/10.3897/zookeys.1185.109285>

Review of the genus *Ageleradix* Xu & Li, 2007 (Araneae, Agelenidae), with descriptions of three new species

Yan-Nan Mu¹, Lu-Yu Wang¹, Tian-Yu Ren¹, Yuan Tian², Zhi-Sheng Zhang¹

¹ Key Laboratory of Eco-environments in Three Gorges Reservoir Region (Ministry of Education), School of Life Sciences, Southwest University, Chongqing 400715, China

² Yunnan Nangunhe National Nature Reserve Management and Protection Bureau, Lincang, China

Corresponding author: Zhi-Sheng Zhang (zhangzs327@qq.com)

Abstract

The spider genus *Ageleradix* Xu & Li, 2007 is reviewed. Three new species are described: *A. dulong* Mu, Wang & Zhang, **sp. nov.** (♂♀, Yunnan), *A. jinshoshan* Mu, Wang & Zhang, **sp. nov.** (♀, Chongqing) and *A. nangunhe* Mu, Wang & Zhang, **sp. nov.** (♂♀, Yunnan). A key to all nine species of *Ageleradix* is provided, and the genus is split into three species-groups.

Key words: Ageleninae, Asia, funnel weavers, identification key, morphology, taxonomy

Introduction

Agelenidae C.L. Koch, 1837 comprises 1427 species in 98 genera (including 1 extinct genus and 7 species) and is distributed almost worldwide. In China, the family is represented by 490 species, belonging to 39 genera in four subfamilies (Zhu et al. 2017; WSC 2024). *Ageleradix* Xu & Li, 2007 described based on *A. sichuanensis* Xu & Li, 2007, and placed in the subfamily Ageleninae C.L. Koch, 1837 (Zhu et al. 2017) currently comprising six species, all reviewed by Zhu et al. (2017). The genus is distributed in Guangxi, Guizhou, Sichuan, Xizang and Yunnan provinces of China.

While examining specimens collected from Yunnan and Chongqing, three new species of *Ageleradix* were recognized. This paper aims to describe these new species, provide a comprehensive review of the genus, and present an identification key for all its known species and notes on species grouping.

Material and methods

All specimens were preserved in 75% ethanol and examined, illustrated, photographed, and measured using a Leica M205A stereomicroscope equipped with a drawing tube, a Leica DFC450 Camera, and LAS v. 4.6 software. Male palps and epigynes were examined and illustrated after they were dissected. Epigynes were cleared by immersing them in pancreatin for about an hour (Álvarez-Padilla and Hormiga 2007). Eye sizes were measured as the maximum diameter. Leg measurements are shown as: total length (femur, patella



Academic editor: Yuri Marusik
Received: 5 December 2024
Accepted: 25 March 2025
Published: 2 May 2025

ZooBank: <https://zoobank.org/87186858-6A30-4403-8B3A-D2D86D7C61EA>

Citation: Mu Y-N, Wang L-Y, Ren T-Y, Tian Y, Zhang Z-S (2025) Review of the genus *Ageleradix* Xu & Li, 2007 (Araneae, Agelenidae), with descriptions of three new species. ZooKeys 1236: 197–208. <https://doi.org/10.3897/zookeys.1236.143650>

Copyright: © Yan-Nan Mu et al.
This is an open access article distributed under terms of the Creative Commons Attribution License (Attribution 4.0 International – CC BY 4.0).

and tibia, metatarsus, tarsus). All measurements are in millimeters. Specimens examined here are deposited in the Collection of Spiders, School of Life Sciences, Southwest University, Chongqing, China (SWUC).

Terminology follows Xu and Li (2007) and Zhang et al. (2008). Abbreviations used in the text: **ALE** = anterior lateral eye; **AME** = anterior median eye; **PLE** = posterior-lateral eye; **PME** = posterior median eye.

Taxonomy

Family Agelenidae C. L. Koch, 1837

Subfamily Ageleninae C. L. Koch, 1837

***Ageleradix* Xu & Li, 2007**

Type species. *Ageleradix sichuanensis* Xu & Li, 2007 (by original designation).

Diagnosis. This genus is similar to *Allagelena* Zhang, Zhu & Song, 2006 in having centrally originated, extending distally and proximally and sclerotized conductor (C), but can be separated from it by: palpal patella lacking apophysis (vs. with apophysis), retrolateral tibial apophysis (RTA) not well developed (vs. well developed), embolus (E) slender (vs. thick), tegular apophysis (TA) well developed (vs. not well developed); scape (Sc) extending to middle part of epigynal plate (vs. absent or not extending to middle part), and atrium shallow (vs. deep).

Composition. *A. cymbiforma* (Wang, 1991) (♀), *A. otiforma* (Wang, 1991) (♀♂), *A. schwendingeri* Zhang, Li & Xu, 2008 (♀♂), *A. sichuanensis* Xu & Li, 2007 (♀♂), *A. sternseptum* Zhang, Li & Xu, 2008 (♀) and *A. zhishengi* Zhang, Li & Xu, 2008 (♀♂), *A. dulong* Mu, Wang & Zhang sp. nov. (♀♂), *A. jinfoshan* Mu, Wang & Zhang sp. nov. (♀) and *A. nangunhe* Mu, Wang & Zhang sp. nov. (♀♂).

Distribution. Known only from China (Yunnan, Sichuan, Xizang, Guangxi, Guizhou).

***Ageleradix dulong* Mu, Wang & Zhang, sp. nov.**

<https://zoobank.org/65098D5D-3675-4B82-8C02-EE84112EAFAD>

Chinese name: 独龙盾漏斗蛛

Figs 1, 2

Type material. **Holotype** • ♂, CHINA, Yunnan Prov., Nujiang Lisu Auton. Pref., Gongshan Dulong and Nu Auton. Co., Dulong River, dangbanglaka; 27°49'38.85"N, 98°19'35.52"E, elev. 1430 m, 20.04.2024, leg. L.Y. Wang, et al. **Paratypes**: • 2♂1♀, with same data as holotype. • 1♀, Hapang waterfall; 27°40'43.66"N, 98°16'13.25"E, elev. 1156 m, leg. L.Y. Wang.

Etymology. The specific name is derived from the Dulong River; noun in apposition.

Diagnosis. The new species resembles *A. schwendingeri* in having similar median apophysis (MA) and retrolateral tibial apophysis (RTA) (cf. Fig. 1D–F, Fig. 5E–G, and figs 10–11 in Zhang et al. 2008), but can be differentiated from by: 1) palpal tibia long, about 2/3 length of cymbium (Fig. 1D–F) (vs. short, about 1/4 length of cymbium, Fig. 5G and fig. 10–12 in Zhang et al. 2008); 2) embolus

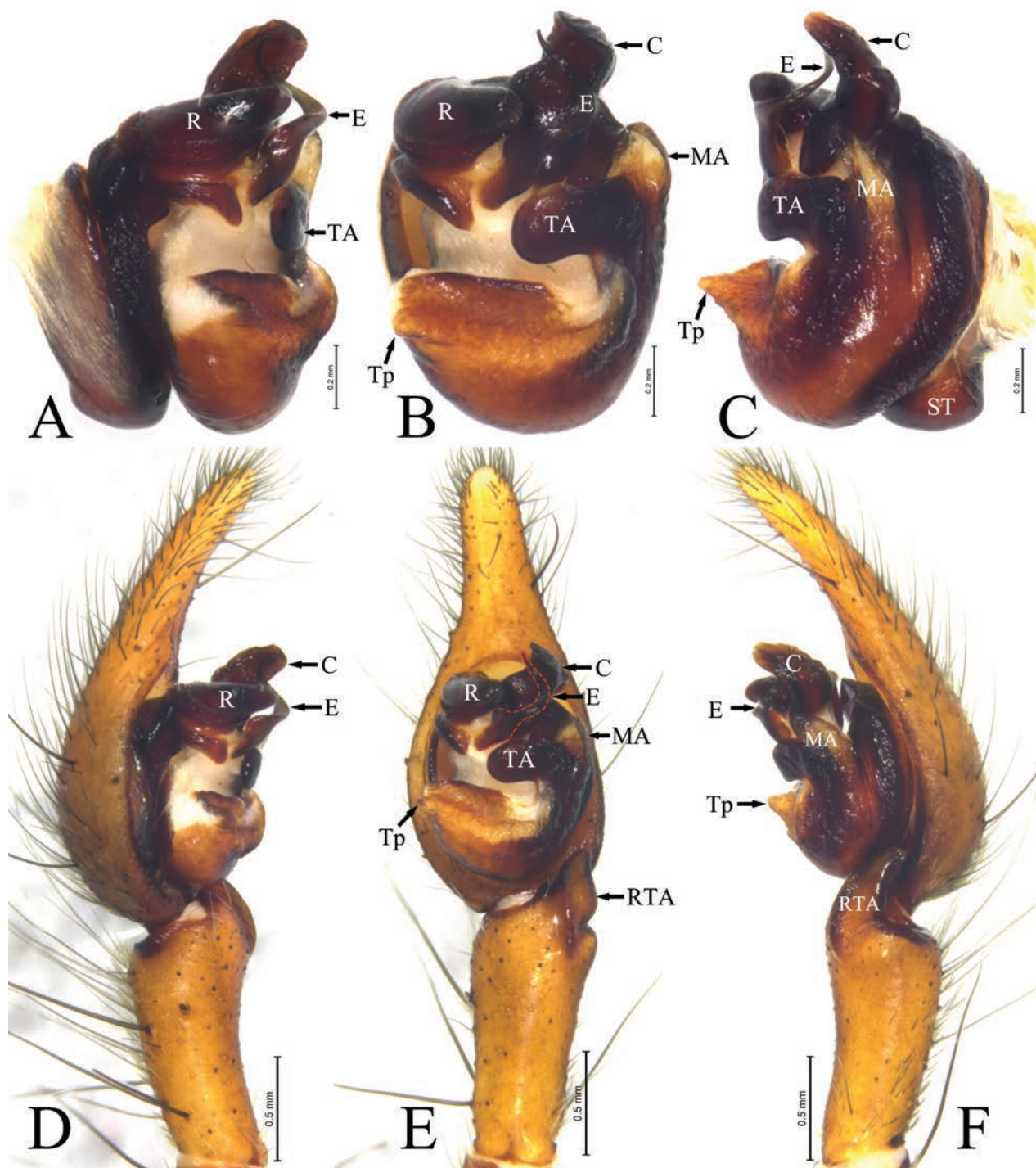


Figure 1. *Ageleradix dulong* Mu, Wang & Zhang, sp. nov., male left palp **A** bulb, prolateral view **B** same, ventral view **C** same, retrolateral view **D** prolateral view **E** ventral view **F** retrolateral view. Abbreviations: **C**—conductor; **E**—embolus; **MA**—median apophysis; **R**—radix; **RTA**—retrolateral tibial apophysis; **TA**—tegular apophysis; **Tp**—tegular process; **ST**—subtegulum.

(E) with wide base and curved tip (Fig. 1D–F) (vs. thin base and straight tip, Fig. 5F and fig. 11 in Zhang et al. 2008); 3) conductor (C) tongue-shaped with narrow tip (Fig. 1D–F) (vs. not tongue-shaped, with wider tip, Fig. 5F, G and fig. 12 in Zhang et al. 2008); 4) scape (Sc) extending posteriorly to the center of atrium (Fig. 2C) (vs. scape extending to posterior edge of atrium, Fig. 5C and fig. 14 in Zhang et al. 2008); and 5) spermathecae (S) kidney-shaped (Fig. 2D) (vs. spherical, Fig. 5D fig. 16 in Zhang et al. 2008).

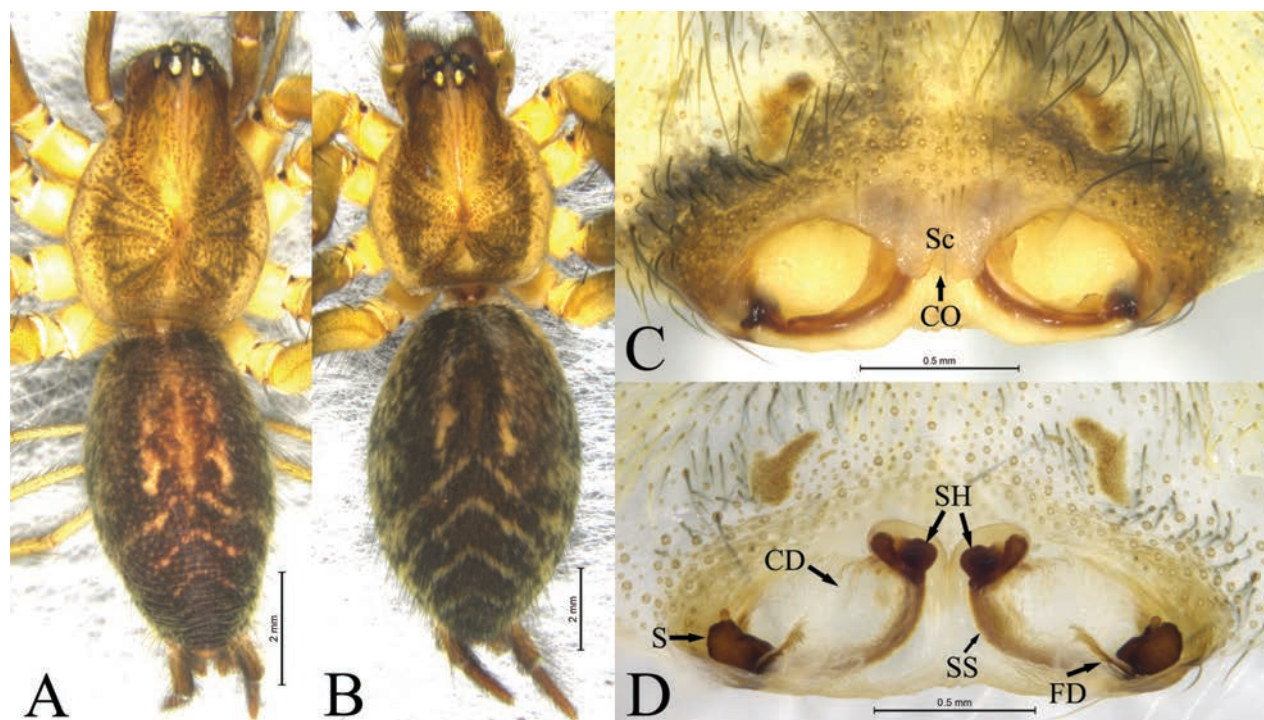


Figure 2. *Ageleradix dulong* Mu, Wang & Zhang, sp. nov. Male holotype (A) and female paratype (B–D) A, B habitus, dorsal view C epigyne, ventral view D same, dorsal view. Abbreviations: CD—copulatory duct; CO—copulatory opening; FD—fertilization duct; S—spermathecae; Sc—scape; SH—spermathecal head; SS—spermathecal stalk.

Description. Male (holotype, Fig. 2A). Total length 10.91. Carapace: 4.94 long, 3.60 wide. Abdomen: 5.83 long, 3.28 wide. Eye sizes and interdistances: AME 0.28, ALE 0.32, PME 0.25, PLE 0.30, AME–AME 0.09, AME–ALE 0.07, PME–PME 0.17, PME–PLE 0.16, ALE–PLE 0.07. MOA: anterior width 0.59, posterior width 0.67, 0.70 long. Clypeus 0.37 long. Chelicerae with 3 promarginal and 3 retromarginal teeth. Leg measurements: I 28.48 (7.65, 9.13, 8.04, 3.66), II 24.64 (6.81, 7.61, 6.78, 3.44), III 21.29 (5.89, 6.23, 6.18, 2.99), IV 25.88 (6.67, 7.60, 8.03, 3.58). Carapace yellow, with U-shaped brown pattern. Cervical groove and radial groove distinct. Fovea short, slightly depressed. Abdomen ovoid, gray; cardiac mark red-brown; posterodorsal part of abdomen with 3 distinct chevrons. Anterior spinnerets shorter than basal segment of posterior-lateral spinnerets.

Palp (Fig. 1A–F). Tibia about 2/3 length of cymbium, tibial apophysis (RTA) nubbly, extending towards dorsal part of cymbium. Cymbial tip long, about half length of cymbium. Bulb oval, about half length of cymbium. Tegulum with cuspides process (Tp) at middle of prolateral margin. Tegular apophysis (TA) transverse, tip round. Conductor (C) lamellar, heavily sclerotized, tongue-shaped, tip curved toward prolateral, with several sclerites at retro-surface. Radix (R) strongly sclerotized, tip blunt. Median apophysis (MA) straight, formed concavity in ventral view, with blunt end. Embolus (E) originating from anterior part of tegulum, hook-shaped in ventral view and S-shaped in prolateral view, tapering from base to tip.

Female (paratype, Fig. 2B). Total length 14.34. Carapace: 5.74 long, 4.46 wide. Abdomen: 8.29 long, 5.22 wide. Eye sizes and interdistances: AME 0.34, ALE 0.37, PME 0.31, PLE 0.36, AME–AME 0.12, AME–ALE 0.09, PME–PME 0.24, PME–PLE 0.21, ALE–PLE 0.10. MOA: anterior width 0.72, poste-

rior width 0.82, 0.87 long. Clypeus 0.49 long. Leg measurements: I 23.52 (6.47, 7.69, 5.93, 3.43), II 20.65 (5.83, 6.58, 5.19, 3.05), III 18.55 (5.43, 5.61, 4.98, 2.53), IV 23.91 (6.65, 7.51, 6.73, 3.02). All other somatic characters same as in male.

Epigyne (Fig. 2C, D). Atrium oval, located posteriorly, binocular-shaped, anterior edge of atrium with kind of scape (Sc). Copulatory openings (CO) located anteromesally. Copulatory ducts (CD) transparent, membranous, “八” shaped. Spermathecae (S) kidney-shaped, located at posterior-lateral edge epigynal plate, spermathecal stalk (SS) tube-like, spermathecal head (SH) oval, anteriorly located in dorsal view. Fertilization ducts (FD) extending anteromesally.

Distribution. Known only from the type locality.

***Ageleradix jinfoshan* Mu, Wang & Zhang, sp. nov.**

<https://zoobank.org/025747BE-8F6A-40DB-89A3-875AFC819008>

Chinese name: 金佛山漏斗蛛

Fig. 3

Type material. Holotype • ♀, CHINA, Chongqing Mun., Nanchuan Dist., Jinfo Mt Reserve (Gufo Cave); 29°2'6.93"N, 107°11'32.14"E, elev. 2043 m, 4.09.2024, leg. Z.S. Zhang.

Etymology. The specific name is derived from the type locality (jinfoshan = Jinfo mountain); noun in apposition.

Diagnosis. The new species resembles *A. zhishengi* in having similar-shaped anterior part of atrium (cf. Fig. 3B, C, and fig. 29A, B in Zhu et al. 2017), but can be differentiated from it by: 1) septum (Se) reaching posterior edge of epigyne (Fig. 3B) (vs. epigyne with scape, fig. 29A in Zhu et al. 2017), and 2) copulatory duct (CD) nearly straight (Fig. 3C) (vs. strongly curved, fig. 29B in Zhu et al. 2017).

Description. Female. Total length 7.94. Carapace: 3.68 long, 2.91 wide. Abdomen: 4.70 long, 2.95 wide. Eye sizes and interdistances: AME 0.22, ALE 0.24, PME 0.20, PLE 0.21, AME–AME 0.07, AME–ALE 0.06, PME–PME 0.19, PME–PLE 0.12, ALE–PLE 0.07. MOA: anterior width 0.44, posterior width 0.55, 0.48 long. Clypeus 0.10 long. Chelicerae with 3 promarginal and 3 retromarginal teeth. Leg measurements: I 11.84 (3.18, 4.07, 2.73, 1.86), II 10.26 (3.00, 3.29, 2.33, 1.64), III 10.19 (2.79, 3.29, 2.57, 1.54), IV 13.96 (3.83, 4.32, 3.81, 2.00). Carapace white-yellow, with U-shaped dark brown pattern. Cervical groove and radial grooves distinct. Fovea short, slightly depressed. Abdomen ovoid, gray; cardiac mark nearly as long as abdomen, red-brown. Anterior spinnerets shorter than basal segment of posterior-lateral spinnerets.

Epigyne as in Fig. 3B, C. Atrium balloon-shaped, membranous, with distinct septum (Se) reaching posterior margin, more than 3 times longer than wide, with parallel margins. Copulatory opening (CO) located posteriorly. Copulatory ducts (CD) curved. Spermathecal head (SH) clavate. Spermathecae (S) fist-shaped, posteriorly located spaced by about 2 times diameter of spermathecae. Fertilization ducts (FD) extending antero-laterally.

Male. Unknown.

Distribution. Known only from the type locality.

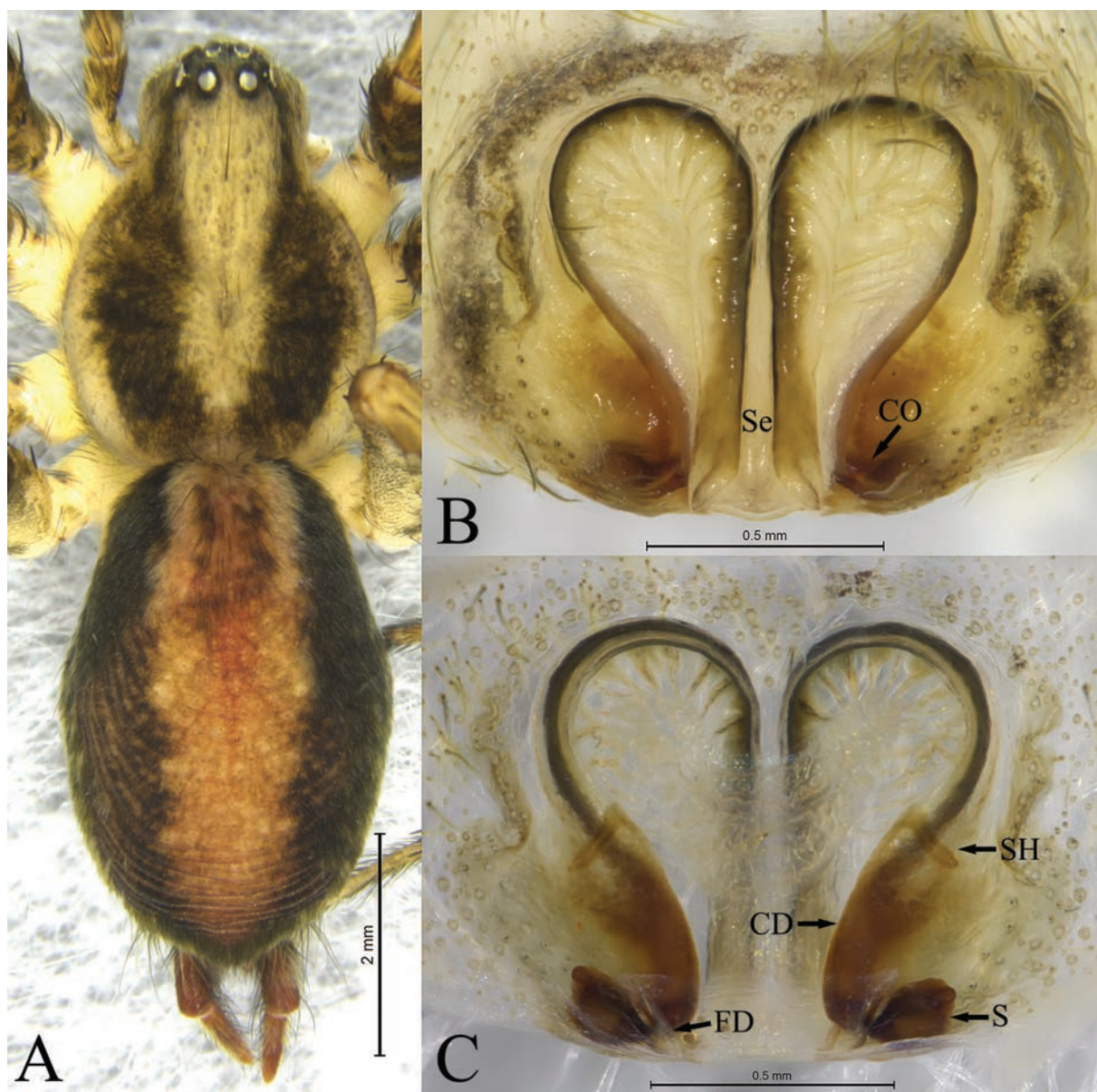


Figure 3. *Ageleradix jinshoshan* Mu, Wang & Zhang, sp. nov., female holotype **A** dorsal view **B** epigyne, ventral view **C** same, dorsal view. Abbreviations: **CD**—copulatory duct; **CO**—copulatory opening; **FD**—fertilization duct; **S**—spermathecae; **Se**—septum; **SH**—spermathecal head.

***Ageleradix nangunhe* Mu, Wang & Zhang, sp. nov.**

<https://zoobank.org/0CD4166C-E283-4EF3-B3E4-181EE2084F2F>

Chinese name: 南滚河盾漏斗蛛

Fig. 4

Type material. *Holotype* • ♂, CHINA, Yunnan Prov., Lincang City, Cangyuan Co., Nangunhe National Nature Reserve, Mengjiao station; 23°16'36.01"N, 99°11'24.13"E, elev. 1747 m, 29.09.2024, leg. Y.J. Cai and L.X. Cheng. *Paratypes*: • 2♀, with same data as holotype.

Etymology. The specific name is derived from the type locality; noun in apposition.

Diagnosis. The male of this new species resembles those of *A. schwendingeri* in having similarly shaped retrolateral tibial apophysis (RTA) and short tibia

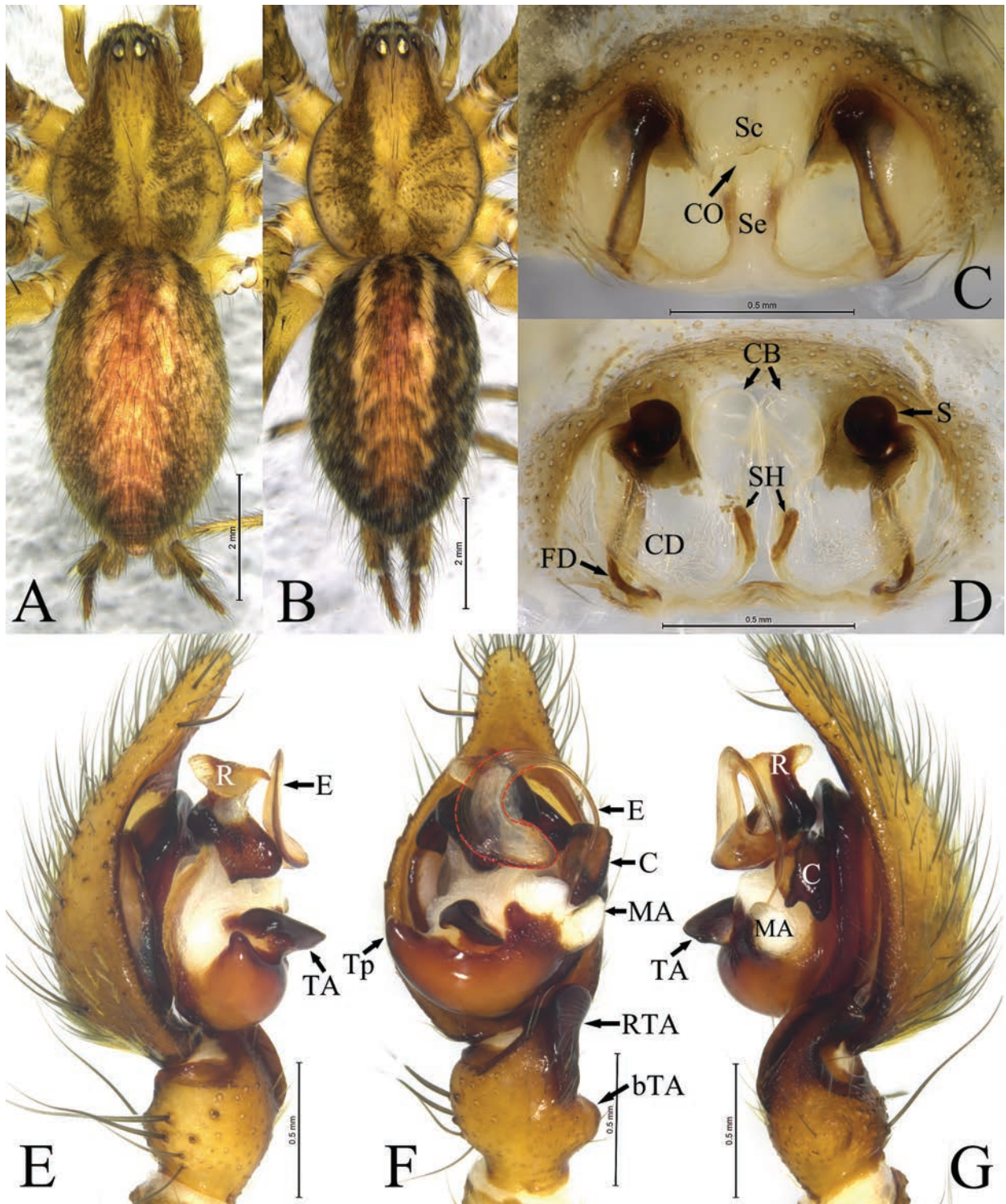


Figure 4. Mu, Wang & Zhang, sp. nov., male holotype and female paratype **A** male, dorsal view **B** female, dorsal view **C** epigyne, ventral view **D** same, dorsal view **E** left palp, prolateral view **F** same, ventral view **G** same, retrolateral view. Abbreviations: **bTA**—basal tibial apophysis; **C**—conductor; **CB**—copulatory bursa; **CD**—copulatory duct; **CO**—copulatory opening; **E**—embolus; **FD**—fertilization duct; **MA**—median apophysis; **R**—radix; **RTA**—retrolateral tibial apophysis; **S**—spermathecae; **Sc**—scape; **Se**—septum; **SH**—spermathecal head; **TA**—tegular apophysis; **Tp**—tegular process.

(cf. Fig. 4E–G and Fig. 5E–G, fig. 26D in Zhu et al. 2017), but can be differentiated from it by: 1) embolus (E) long, filiform (Fig. 4E–G) (vs. short, hooked, fig. 26D in Zhu et al. 2017); and 2) conductor (C) membranous, with rounded tip (Fig. 4E–G)

(vs. strongly sclerotized, tip winding, Fig. 4E–G and Fig. 5E–G). The female of the new species resembles those of *A. cymbiforma* in having similarly shaped atrium located posteriorly (cf. Fig. 4C and fig. 24A in Zhu et al. 2017), but can be differentiated from it by: 1) septum (Sp) 2 times longer than wide (Fig. 4C) (vs. narrow, more than 4 times longer than wide, fig. 24A in Zhu et al. 2017); and 2) copulatory bursae (CB) balloon-shaped (Fig. 4D) (vs. clavate, fig. 24B in Zhu et al. 2017).

Description. Male (holotype, Fig. 4A). Total length 8.40. Carapace: 3.90 long, 2.82 wide. Abdomen: 4.90 long, 2.86 wide. Eye sizes and interdistances: AME 0.23, ALE 0.25, PME 0.19, PLE 0.25, AME–AME 0.08, AME–ALE 0.09, PME–PME 0.16, PME–PLE 0.13, ALE–PLE 0.11. MOA: anterior width 0.49, posterior width 0.56, 0.58 long. Clypeus 0.19 long. Chelicerae with 3 promarginal and 5 retromarginal teeth. Leg measurements: I 16.77 (4.37, 5.35, 4.42, 2.63), II 13.74 (3.80, 4.20, 3.50, 2.24), III 12.68 (3.46, 3.66, 3.64, 1.92), IV 17.07 (4.55, 5.08, 5.20, 2.24). Carapace yellow, with 2 rows of brown stripe. Cervical groove and radial groove distinct. Fovea short, slightly depressed. Abdomen ovoid, gray; cardiac mark red-brown. Anterior spinnerets shorter than basal segment of posterior-lateral spinnerets.

Palp (Fig. 4E–G). Tibia shorter than cymbium, about 1/3 length of cymbium, with small retrolateral lump (bTA). Retrolateral tibial apophysis (RTA) nearly as long as tibia, nubbly, roundly bent dorsally. Cymbial tip about 1/5 width of median part of cymbium. Bulb oval. Tegulum with horseshoe-shaped apophysis (TA) located almost medially, retrolateral margin with subconical baso-prolateral process (Tp). Conductor (C) nubbly, extending posteriorly, bifurcated at tip. Radix (R) with sclerotized base and membranous, tongue-shaped tip. Median apophysis (MA) membranous, thumb-shaped. Embolus (E), with wide base, gradually tapering into filamentous embolus proper, roundly clockwise bent embolus proper as long as half of bulb, tip resting on 3'clock position.

Female (paratype Fig. 4B). Total length 9.18. Carapace: 4.29 long, 3.17 wide. Abdomen: 5.28 long, 2.96 wide. Eye sizes and interdistances: AME 0.26, ALE 0.26, PME 0.23, PLE 0.25, AME–AME 0.09, AME–ALE 0.10, PME–PME 0.18, PME–PLE 0.14, ALE–PLE 0.11. MOA: anterior width 0.51, posterior width 0.59, 0.62 long. Clypeus 0.15 long. Chelicerae with 3 promarginal and 4 retromarginal teeth. Leg measurements: I 15.19 (4.06, 4.92, 3.74, 2.47), II 12.98 (3.66, 4.15, 3.21, 1.96), III 12.83 (3.56, 4.08, 3.34, 1.85), IV 17.42 (4.81, 5.21, 5.11, 2.29). Color darker than male, appearance of body similar as male.

Epigyne (Fig. 4C–D). Atrium large, posteriorly located, with distinct scape (Sc) and septum (Se). Copulatory openings (CO) located anteromesally. Copulatory ducts (CD) transparent, membranous, sclerotized part encircling spermathecae. Copulatory bursae (CB) balloon-shaped, transparent. Spermathecae (S) spherical, located anteriorly. Spermathecal head (SH) clavate. Fertilization ducts (FD) long, well sclerotized extending to posterior of epigynal plate.

Distribution. Known only from the type locality.

***Ageleradix schwendingeri* Zhang, Li & Xu, 2008**

Fig. 5

Material examined. CHINA, Xizang • 2♂3♀, Chayu Co., Xiachayu Town, Xiachayu Bridge, scrub-grassland near river, 28°27'24.72"N, 97°02'40.68"E, elev. 1464 m, 26.06.2018, leg. L.Y. Wang et al. • 1♀, Chayu Co., 28°39'35.88"N, 97°27'57.84"E,

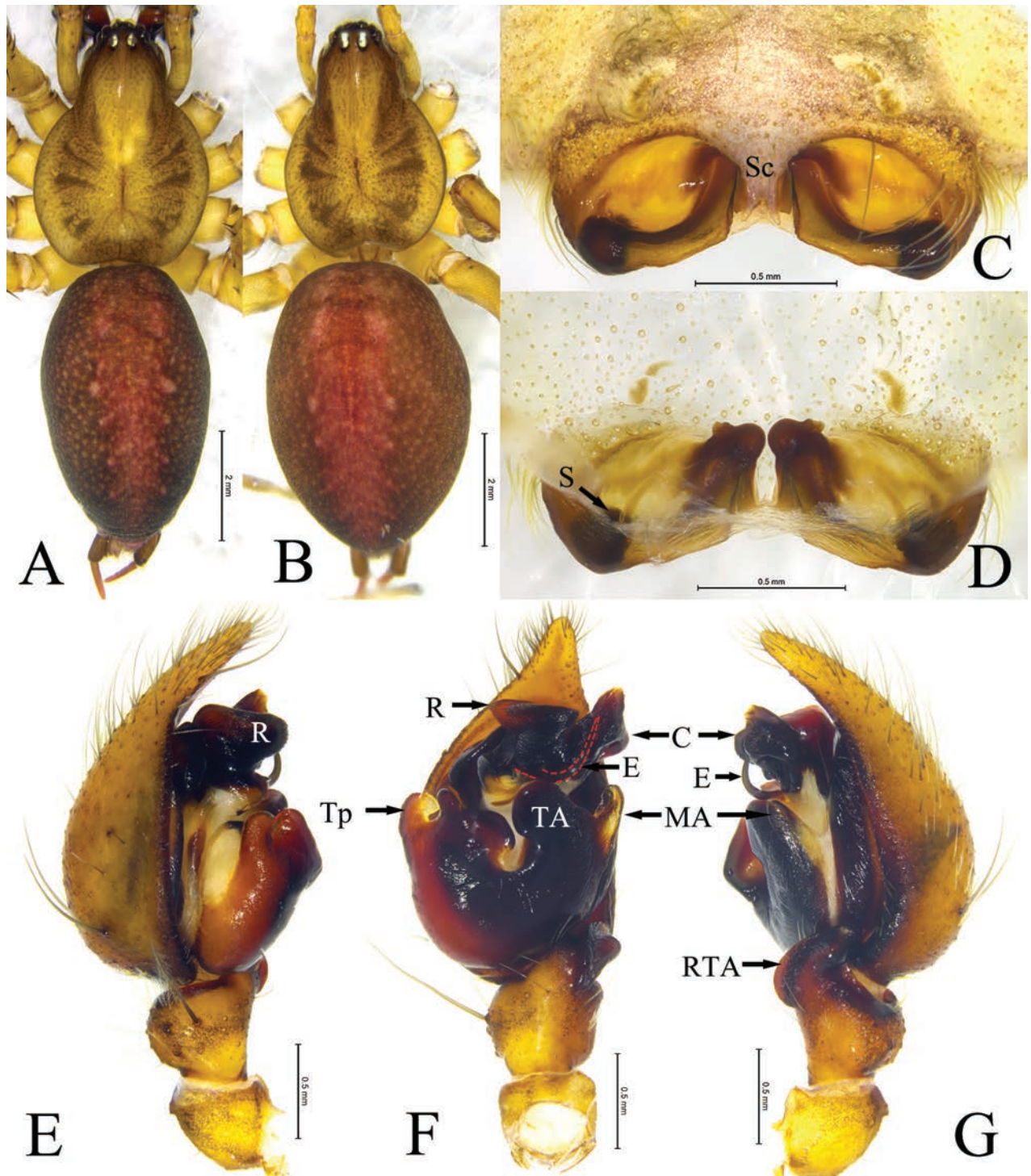


Figure 5. Habitus of *Ageleradix schwendingeri* Zhang, Li & Xu, 2008 **A** male, dorsal view **B** female, dorsal view **C** epigyne, ventral view **D** same, dorsal view **E** male left palp, prolateral view **F** same, ventral view **G** same, retrolateral view. Abbreviations: **C**—conductor; **E**—embolus; **MA**—median apophysis; **R**—radix; **RTA**—retrolateral tibial apophysis; **TA**—tegular apophysis; **Tp**—tegular process; **S**—spermathecae; **Sc**—scape.

elev. 2323 m, 25.06.2018, leg. L.Y. Wang. • 1♂1♀, Chayu Co., 28°39'35.88"N, 97°27'57.84"E, elev. 2323 m, 25.05.2019, leg. L.Y. Wang and P. Liu. • 1♂, Chayu Co., 28°39'35.88"N, 97°27'57.84"E, elev. 2323 m, 27.05.2019, leg. L.Y. Wang.

Diagnosis and description. See Zhu et al. (2017).

Distribution. China (Xizang, Sichuan).

Key to species of *Ageleradix*

1	Female.....	2
–	Male.....	10
2	Atrium posteriorly located	3
–	Atrium anteriorly located	6
3.	Spermathecae (S) anteriorly located	4
–	Spermathecae (S) posteriorly located	5
4	Copulatory bursa (CB) oval.....	<i>A. nangunhe</i> sp. nov.
–	Copulatory bursa (CB) clavate.....	<i>A. cymbiforma</i>
5	Scape (Sc), bifurcated with blunt tips wider than long.....	<i>A. dulong</i> sp. nov.
–	Scape (Sc), bifurcated with pointed tips longer than wide....	<i>A. schwendingeri</i>
6	Scape (Sc) lacking.....	7
–	Scape (Sc) present.....	8
7	Atrium divided.....	<i>A. sternseptum</i>
–	Atrium undivided	<i>A. otiforma</i>
8	Spermathecae (S) round.....	<i>A. sichuanensis</i>
–	Spermathecae (S) oval.....	9
9	Septum (Se) lacking.....	<i>A. zhishengi</i>
–	Septum (Se) as long as atrium, with parallel margins	<i>A. jinfoshan</i> sp. nov.
10	RTA developed, large; conductor (C) tongue-shaped.....	11
–	RTA strongly reduced or absent; conductor (C) not tongue-shaped.....	13
11	Embolus (E) reach mid part of bulb, filiform.....	<i>A. nangunhe</i> sp. nov.
–	Embolus (E) extending anteriorly	12
12	Tibia about 2/3 length of cymbium, embolus (E) S-shaped in retrolateral view	<i>A. dulong</i> sp. nov.
–	Tibia about 1/4 length of cymbium, embolus (E) C-shaped in retrolateral view	<i>A. schwendingeri</i>
13	Embolus (E) long, filiform bent anticlockwise.....	<i>A. otiforma</i>
–	Embolus (E) short.....	14
14	Conductor (C) longer than bulb, tibia wider than long	<i>A. zhishengi</i>
–	Conductor (C) about 1/2 of bulb length, tibia longer than wide.....	<i>A. sichuanensis</i>

Discussion

The genus *Ageleradix* now comprises nine species, all distributed in southwest China. Although species within this genus appear similar in general appearance, they exhibit significant differences in copulatory organs. For instance, in *A. zhishengi*, the conductor is longer than the bulb, whereas in other species, it is shorter than the bulb. In addition, *A. otiforma* also display notable differences compared to the type species *A. sichuanensis*. For example, *A. otiforma* exhibits a filiform embolus, a conductor with a membranous tip, and the scape absent in the epigyne, while in contrast, *A. sichuanensis* has a short embolus, sclerotized conductor, and the scape extends to the middle part of the epigynal plate.

In summary, we propose that *Ageleradix* can be divided into three species-groups based on the shape of copulatory organs: the *A. cymbiforma*-group, the *A. otiforma*-group, and the *A. sichuanensis*-group. The diagnosis and composition of each species group are provided in Table 1.

Table 1. Characteristics of the *Ageleradix* species-groups and list of species in each.

Species group name	Diagnostic character	Species
<i>A. cymbiforma</i> -group	RTA well developed, nubbly	<i>A. cymbiforma</i> ; <i>A. dulong</i> sp. nov.; <i>A. nangunhe</i> sp. nov.; <i>A. schwendingeri</i>
	conductor tongue-shaped	
	atrium posteriorly located; with scape	
<i>A. otiforma</i> -group	RTA with sharp tip	<i>A. otiforma</i> (Wang, 1991); <i>A. sternseptum</i> Zhang, Li & Xu, 2008
	conductor long, with narrow and membranous tip	
	atrium anteriorly located; scape absent	
<i>A. sichuanensis</i> -group	RTA inconspicuous	<i>A. sichuanensis</i> Xu & Li, 2007; <i>A. zhishengi</i> Zhang, Li & Xu, 2008; <i>A. jinfoshan</i> sp. nov.
	conductor strong sclerotized, nubbly	
	atrium large, anteriorly located; scape present	

Acknowledgements

Many thanks to the anonymous reviewers and editor (Yuri Marusik) for their valuable comments that greatly improved the manuscript. Thanks also to Yujun Cai, Lingxin Cheng, Huiyi Chen and Qianle Lu (Southwest University) for helping collect specimens.

Additional information

Conflict of interest

The authors have declared that no competing interests exist.

Ethical statement

No ethical statement was reported.

Funding

This research is also supported by the Science Foundation of School of Life Sciences SWU (20232008071901 and 20212020110501).

Author contributions

All authors have contributed equally.

Author ORCIDs

Yan-Nan Mu  <https://orcid.org/0000-0002-2504-673X>

Luyu Wang  <https://orcid.org/0000-0002-5250-3473>

Yuan Tian  <https://orcid.org/0009-0007-5358-271X>

Zhi-Sheng Zhang  <https://orcid.org/0000-0002-9304-1789>

Data availability

All of the data that support the findings of this study are available in the main text.

Reference

Álvarez-Padilla F, Hormiga G (2007) A protocol for digesting internal soft tissues and mounting spiders for scanning electron microscopy. *Journal of Arachnology* 35: 538–542. <https://doi.org/10.1636/Sh06-55.1>

- Wang JF (1991) Six new species of the genus *Agelena* from China (Araneae: Agelenidae). *Acta Zootaxonomica Sinica* 16: 407–416.
- World Spider Catalog (2024) World Spider Catalog. Version 25.0. Natural History Museum Bern, online at <http://wsc.nmbe.ch> [Accessed on 2 December 2024]. <https://doi.org/10.24436/2>
- Xu X, Li SQ (2007) A new genus and species of the spider family Agelenidae from western Sichuan Province, China (Arachnida: Araneae). *Revue Suisse de Zoologie* 114: 59–64. <https://doi.org/10.5962/bhl.part.80388>
- Zhang XF, Li SQ, Xu X (2008) A further study on the species of the spider family Agelenidae from China (Arachnida: Araneae). *Revue Suisse de Zoologie* 115: 95–106. <https://doi.org/10.5962/bhl.part.80422>
- Zhu MS, Wang XP, Zhang ZS (2017) *Fauna Sinica: Invertebrata Vol. 59: Arachnida: Araneae: Agelenidae and Amaurobiidae*. Science Press, Beijing, 727 pp.

A new species of a rarely encountered genus *Sclerobregma* Hartman, 1965 (Annelida, Scalibregmatidae) from the deep South China Sea

Jun-Hui Lin¹, Ya-Qin Huang¹, Qian-Yong Liang^{2,3}, Xue-Bao He¹

¹ Third Institute of Oceanography, Ministry of Natural Resources, 178 Daxue Road, Xiamen 361005, China

² National Engineering Research Center of Gas Hydrate Exploration and Development, Guangzhou, 511458, China

³ Guangzhou Marine Geological Survey, China Geological Survey, Guangzhou 511458, China

Corresponding author: Xue-Bao He (hexuebao@tio.org.cn)

Abstract

In the present study, a new species of a rarely encountered genus *Sclerobregma* Hartman, 1965, *Sclerobregma nanhaiensis* sp. nov., is described based on specimens collected from slope depths of the northern South China Sea. It is characterized by the presence of branched branchiae and heavy acicular spines in the anterior chaetigers, and is morphologically distinct from the other species of the genus in the shape of the anterior margin of the prostomium, the number of neuropodia with nipple-like projections distally, and the segment annulation. Four gene fragments of the new species were sequenced, comprising 16S rRNA, 18S rRNA, 28S rRNA, and histone H3. This study represents the first report of *Sclerobregma* in the South China Sea.

Key words: Continental slope, deep sea, molecular sequences, morphology, Polychaeta, taxonomy



Academic editor: Greg Rouse

Received: 13 February 2025

Accepted: 30 March 2025

Published: 2 May 2025

ZooBank: <https://zoobank.org/ABAAB7C5-F10C-45D0-9991-85D6D5C18C83>

Citation: Lin J-H, Huang Y-Q, Liang Q-Y, He X-B (2025) A new species of a rarely encountered genus *Sclerobregma* Hartman, 1965 (Annelida, Scalibregmatidae) from the deep South China Sea. ZooKeys 1236: 209–218. <https://doi.org/10.3897/zookeys.1236.149576>

Copyright: © Jun-Hui Lin et al.
This is an open access article distributed under terms of the Creative Commons Attribution License (Attribution 4.0 International – CC BY 4.0).

Introduction

Annelids of the family Scalibregmatidae are widespread in the world's oceans, with a broad depth range from the intertidal to the deep sea (Blake 2023). Scalibregmatids mainly feed on organic matter in marine sediment and are generally considered subsurface deposit feeders (Jumars et al. 2015). Compared to many annelid families, Scalibregmatidae is less species-rich, including 88 valid species distributed in 15 genera (Read and Fauchald 2025). The majority of scalibregmatid species prefer to occupy sediment depth greater than 100 m, and knowledge of their diversity in the deep sea is continuously increasing, as evidenced by the numerous species discovered from the lower continental slope or abyssal plains over the past 25 years (Blake 2023), chiefly from the Southern Ocean (Schüller and Hilbig 2007; Schüller 2008), eastern Pacific (Wiklund et al. 2019), southwest Atlantic (Mendes et al. 2023; Mendes et al. 2024a; Mendes et al. 2024b; Mendes et al. 2024c) and off eastern Australian (Blake 2023).

The phylogenetic position of Scalibregmatidae and relationships among its genera remain unclear (Parapar et al. 2021). In a phylogenetic study aiming to resolve the systematic position of *Travisia* (Paul et al. 2010), *Travisia* and scalibregmatids were identified as sister groups to one another, but the inclusion of *Travisia* within Scalibregmatidae was opposed by Blake (2020) due to the great morphological differences. Taxonomically, four scalibregmatid genera possess dorsal and ventral cirri on posterior segments (Blake 2015), i.e., *Oligobregma* Kudenov & Blake, 1978, *Pseudoscalibregma* Ashworth, 1901, *Scalibregma* Rathke, 1843, and *Sclerobregma* Hartman, 1965, and thus are distinguished from the remaining genera. Of these four genera, *Sclerobregma* is unique in that it bears both branched branchiae and heavy acicular spines in anterior chaetigers. The genus *Sclerobregma* was initially erected by Hartman (1965) for the type species *Scl. branchiatum* collected at a depth of 400–2500 m off New England, northwestern Atlantic. The second described species *Sclerobregma stenocerum*, established by Bertelsen and Weston (1980), was later transferred to *Scalibregma* because this species bears short spinous chaetae instead of heavy acicular spines in the anterior body (Mackie 1991), the former chaetae considered to be homologous with lyrate chaetae. Therefore, *Sclerobregma* is a monospecific genus to date. There are few reports of *Sclerobregma* worldwide. Prior to this study, a record of an undescribed species of this genus was reported from the deep eastern Pacific (11.0722°N, 119.655°E); however, it lacked a morphological description (Bonifacio et al. 2020).

The South China Sea (SCS) is the largest semi-enclosed marginal sea in the West Pacific Ocean, with a maximum depth of 5560 m (Wang et al. 2024). Currently, little is known about the diversity of Scalibregmatidae in this region. In the list of annelid species compiled by Glasby et al. (2016), only one scalibregmatid species was recorded, namely *Scalibregma inflatum*, which might be a misidentification based on our findings of molecular identification of the *Scalibregma* specimens from China's coasts (unpublished data). During several cruises to the continental slope of the northern SCS in recent years, several specimens of *Sclerobregma* were collected from deep-sea sediments. Detailed examination of the available collections determined that they belonged to a new species, which is described and illustrated herein. Four gene fragments were obtained from ethanol-fixed specimen, comprising 16S, 18S, 28S rRNA and histone H3. To the best of our knowledge, this study represents the first report of *Sclerobregma* in the SCS, and even in the Indo-west Pacific.

Material and methods

Field collection

The specimens examined in this study were collected from the continental slope of the northern South China Sea (Fig. 1) during several cruises organized by the Guangzhou Marine Geological Survey (Guangzhou, China) in recent years. Sediment samples for the analysis of benthic fauna were obtained with a 0.25 m² box corer. Each sample was washed through a 0.25 mm mesh sieve with chilled, filtered seawater (4 °C) on board. The fauna retained by the sieve were fixed in either 95% ethanol or 8% formalin. The tissue of the ethanol-fixed specimen was used for DNA extraction.

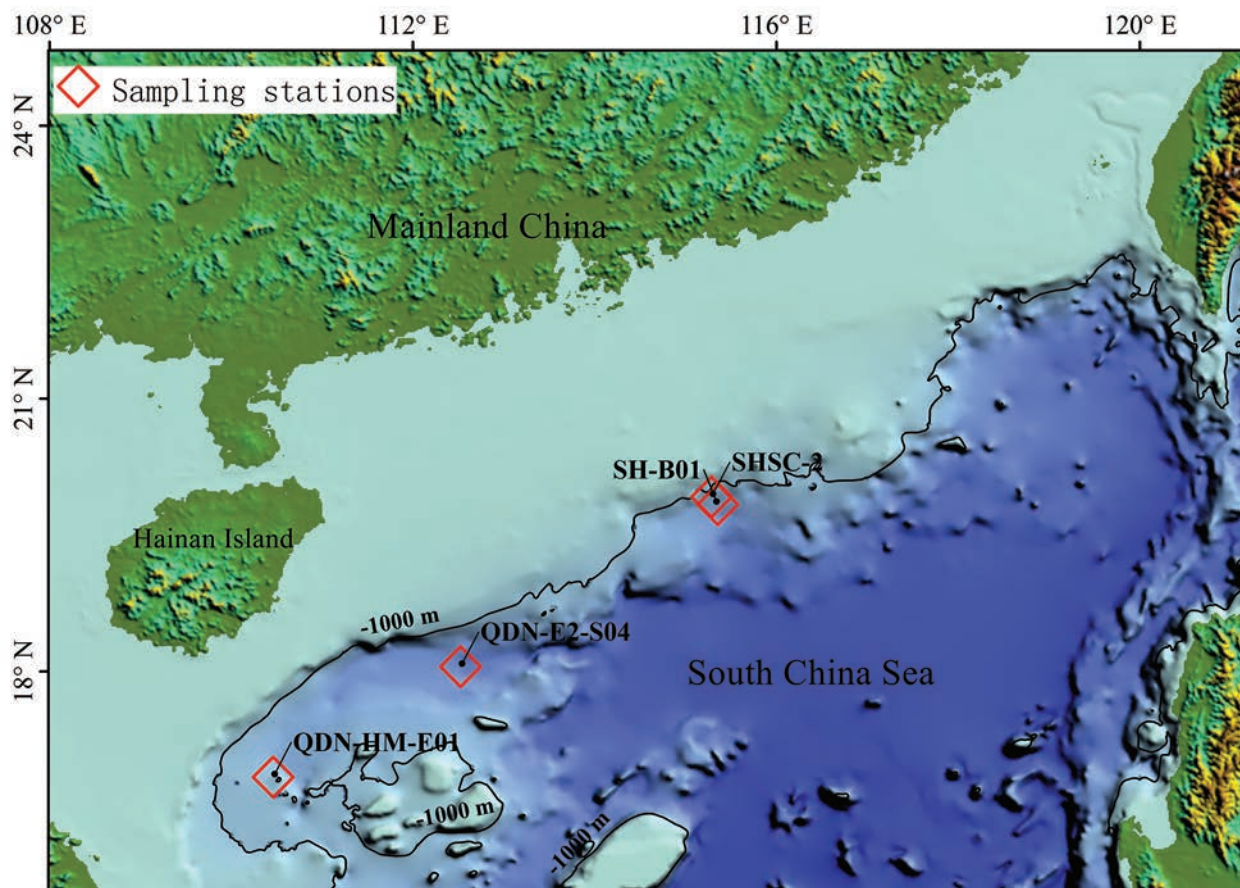


Figure 1. Map of collection localities (squares) of *Sclerobregma nanhaiensis* sp. nov.

Morphological observation

In the laboratory, the type and additional specimens were observed using a Leica MZ95 optical stereoscope and a Leica DM6B compound microscope. Parapodia from anterior and posterior segments were dissected and mounted on slides for observation. Light microscope photographs were obtained using a Leica M205A stereoscope equipped with a DFC 550 digital camera. The shape of the chaetae was photographed under a Leica compound microscope (DM6B) with a DFC170 digital camera. SEM observations were not conducted given the paucity of specimens. Plates were prepared using the software Adobe Photoshop CS5. The type material and additional material examined in this study were deposited at the Third Institute of Oceanography, Ministry of Natural Resources, Xiamen, China (TIO, MNR).

DNA extraction, PCR amplification and sequencing

The total genomic DNA was extracted from the ethanol-fixed specimen using a TransGen Micro Genomic DNA EE 181 Kit (TransGen Biotech, Beijing, China) following the protocol provided by the manufacturer. One mitochondrial (16S) and three nuclear gene markers (18S, 28S, H3) were amplified using primer sets and thermal cycling conditions as delineated by Lin et al. (2023). Then, the 5- μ L PCR products were subsequently checked using 1% agarose gel electrophoresis. Sequencing of the successful products was performed in both directions

at Sangon (Shanghai, China). Both forward and reverse strands of sequences were manually assembled into a consensus sequence using DNAMAN software (Lynnon Biosoft, Quebec, Canada), then checked for potential contamination using BLAST in GenBank.

Data analysis

The partial sequences of the 16S, 18S and 28S rRNA were aligned with those of other *Sclerobregma* species available in GenBank using MAFFT (Kato et al. 2002) with default settings. The interspecific genetic distances were calculated based on Kimura's 2-parameter (K2P) model (Kimura 1980) implemented in MEGA X (Kumar et al. 2018).

Systematics

Class Polychaeta Grube, 1850

Family Scalibregmatidae Malmgren, 1867

Genus *Sclerobregma* Hartman, 1965

Type species. *Sclerobregma branchiatum* Hartman, 1965.

Generic diagnosis. (after Blake 2020) Body elongate and arenicoliform, ventral groove with elevated pads present from chaetiger 1 along entire body. Prostomium T-shaped with a pair of narrow frontal horns; eyes absent. Peristomium a single inflated ring, encompassing the prostomium dorsally; nuchal organs narrow slits posteriorly between prostomium and peristomium. Parapodia of posterior segments with dorsal and ventral cirri; each cirrus inflated, with numerous internal tubular glands with external openings visible as minute pores using SEM; interramal sense organ present as distinct papilla. Branched pectinate-like branchiae present on chaetigers 2–5. Chaetae include capillaries throughout, lyrate chaetae from chaetiger 3, large acicular spines present on notopodia of chaetigers 1 and 2 and neuropodia of chaetiger 1; few very small blunt-tipped spinous chaetae anterior to acicular spines on chaetigers 1 to 2, representing homologues of lyrate chaetae found on following chaetigers. Pygidium with five anal cirri.

***Sclerobregma nanhaiensis* sp. nov.**

<https://zoobank.org/22D4D1A4-FB82-4D8A-BB21-526BF49CC7D7>

Figs 2A–I, 3A–E

Material examined. Holotype. CHINA • TIO-Poly-149, incomplete; northern South China Sea; sta. 2016SH-B01; 19°50'N, 115°21'E; depth 1601 m; 3 Apr. 2016; Xue-Bao He leg. **Paratype.** CHINA • TIO-Poly-150, 1 spec., incomplete; northern South China Sea; sta. 2018SHSC-2; 19°55'N, 115°17'E; depth 1277 m; 11 Apr. 2018; Xue-Bao He leg.

Additional material. CHINA • TIO-Poly-151, 2 specs, incomplete; northern South China Sea; sta. QDN-E2-S04; 18°3'N, 112°31'E; depth 2352 m; 21 Jun. 2019; Jun-Hui Lin leg. • TIO-Poly-152, 1 spec., incomplete; northern South China Sea; sta. QDN-HM-E01; 16°50'N, 110°28'E; depth 1464 m; 3 Jul. 2023; Zhi-Zhong Huang leg.

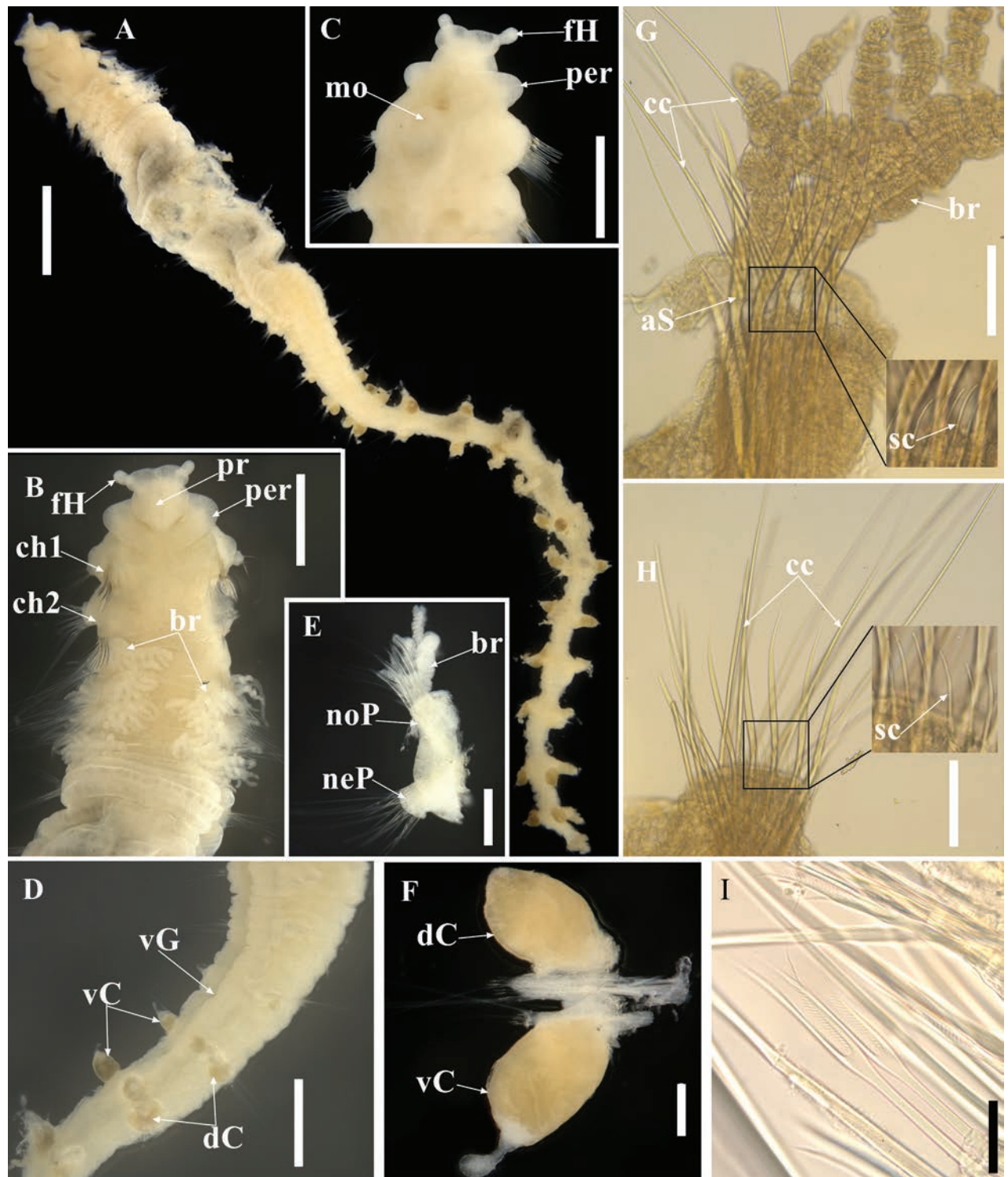


Figure 2. *Sclerobregma nanhaiensis* sp. nov. holotype (TIO-Poly-149) **A** entire specimen in dorsal view **B** anterior end in dorsal view (right parapodium of chaetiger 2 dissected) **C** anterior end in ventro-lateral view **D** middle segments in lateral view **E** chaetiger 2 in anterior view **F** chaetiger 28 in anterior view **G** notopodium of chaetiger 2 in anterior view **H** neuropodium of chaetiger 2 in anterior view **I** lirate chaetae. Abbreviations: aS, acicular spine; br, branchiae; cc, capillary chaetae; ch, chaetiger; dC, dorsal cirrus; fh, frontal horn; mo, mouth; neP, neuropodium; noP, notopodium; per, peristomium; pr, prostomium; sc, spinous chaetae; vC, ventral cirrus; vG, ventral groove. Scale bars: 1 mm (**A**); 500 µm (**B–D**); 200 µm (**E**); 100 µm (**F–H**); 20 µm (**I**).

Description. Holotype incomplete, measuring 12.6 mm long by 1.1 mm wide for 29 chaetigers; paratype incomplete, broken into two fragments with 7 chaetigers (2.7 mm long) and 12 chaetigers (4.8 mm long). Body arenicoliform (Fig. 2A), with weakly expanded thoracic region (chaetigers 6–10), narrowing to posterior end. Color in alcohol light tan, without pigmentation. Chaetigers 1–5 smooth (Fig. 2B), without distinct annulation; chaetigers 6–15 quadriannulate; posterior segments with 6 annuli. Chaetigers 6–10 with transverse rows of weakly elevated pads on dorsum (Figs 2A, 3A), closely spaced. Venter with prominent ventral groove bearing elevated pads from chaetiger 3 (Fig. 3B). Four pairs of branched branchiae located on chaetigers 2–5 (Fig. 2B), arising posterior to notochaetae, first branchia smaller than others. Pygidium absent on both specimens.

Prostomium bell-shaped, with anterior margin broadly rounded, medially incised (Fig. 2B, C); posterior part dorsally narrowing into V-shape (Fig. 2B); a pair of nearly spherical frontal horns emerging subapically from anterior margin (Fig. 2B, C), directed laterally or anterolaterally. Eyes absent. Nuchal organs present as slits on posterolateral side of prostomium (Figs 2B, 3A). Proboscis slightly everted in holotype (Fig. 2C). Peristomium a smooth, single-lobed ring around prostomium dorso-laterally, interrupted mid-dorsally, ventrally forming upper lips of mouth. Structure of mouth obscured.

Parapodia biramous with squared parapodial lobes anteriorly (Fig. 2E), becoming conical from midbody to posterior end; parapodial lobes always shorter than cirri. Dorsal and ventral cirri present from chaetiger 14 in holotype, relatively small at first, becoming well developed on subsequent segments, inflated and bright brick-red (Fig. 2D, F). Dorsal cirri ellipsoid, broad basally, tapering to rounded tips; ventral cirri asymmetrical with broad basal attachment and terminated in nipple-like tips. Interramal papillae present between noto- and neuropodia in midbody, obscured in posterior segment.

Heavy recurved acicular spines (Figs 2E, G, 3C) present in notopodia of chaetigers 1 and 2, anterior to capillaries, numbering 9 spines arranged in one row at chaetiger 1 and 6 spines in one row at chaetiger 2; spines tapering to pointed tip bearing arista. Long and thin capillary chaetae (Fig. 2G, H) present in both rami throughout the body. Lyrate chaetae (Figs 2I, 3D) present from chaetiger 3, positioned anteriorly to capillaries, numbering 3–4 per noto- and neuropodium on anterior segments and increasing to 9–10 on posterior ones. Lyrate chaetae short, with unequal tynes bearing short bristles between tynes. A row of 15–20 short, blunt-tipped spinous chaetae per noto- and neuropodia present in chaetigers 1 and 2 (Figs 2G, H, 3F), anterior to all other chaetae. Transitional chaetae, broader but shorter than capillaries (Fig. 3E), occurred in neuropodia of chaetiger 2.

Morphological variations. Individual variability was observed with respect to the shape of the prostomium and the distribution of branchiae. Specifically, the anterior margin of the prostomium was medially incised in the holotype (TIO-Poly-149) and an additional specimen (TIO-Poly-152), whereas it was truncated in the paratype (TIO-Poly-150). Regarding the branchiae, some may be lost during field collection. The holotype exhibited four complete pairs of branchiae. In contrast, the paratype (TIO-Poly-150) had lost the first branchia on the right side of chaetiger 2.

Remarks. The genus *Sclerobregma* was initially established by Hartman (1965) for the type species *Scl. branchiatum* collected from the northwestern Atlantic, which was characterized by the presence of heavy acicular spines and

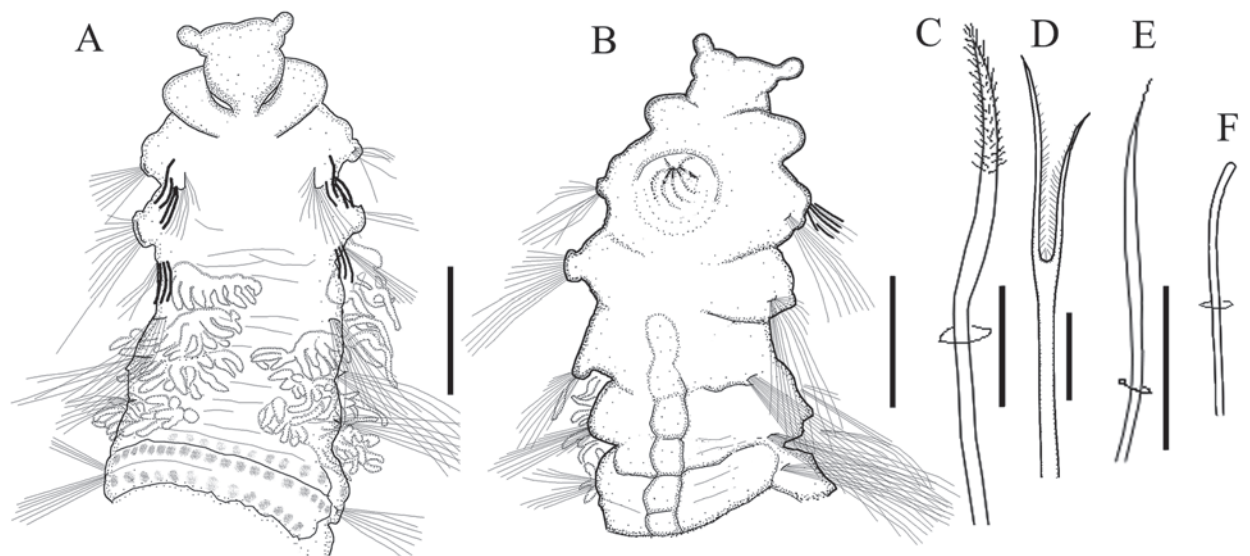


Figure 3. *Sclerobregma nanhaiensis* sp. nov. holotype **A** anterior 6 chaetigers in dorsal view **B** anterior 5 chaetigers in ventral view **C** acicular spine on notopodium of chaetiger 2 **D** lyrate chaetae **E** transitional chaetae from neuropodium of chaetiger 2 **F** spinous chaetae from chaetiger 2. Scale bars: 500 µm (**A**, **B**); 100 µm (**C**, **E**); 20 µm (**D**); 25 µm (**F**).

branched branchiae in anterior chaetigers. Subsequently, Bertelsen and Weston (1980) and Mackie (1991) made some corrections to the original description after careful re-examination of type and additional material. As a result, *Scl. branchiatum* is mainly characterized by the following characters: (1) four pairs of branchiae located on chaetigers 2–5; (2) heavy acicular spines occurring in notopodia of chaetigers 1 and 2 rather than only in chaetiger 1 (also occur in neuropodia of chaetiger 1 as noted by Blake, 2020); (3) posterior segments bearing inflated dorsal and ventral cirri, with nipple-like projections at the tip of the six anteriormost ventral cirri; and (4) short spinous chaetae, homologous with lyrate chaetae, are located on chaetigers 1 and 2, which is not mentioned in the original description by Hartman (1965).

Sclerobregma nanhaiensis sp. nov. resembles *Scl. branchiatum* with both species sharing many morphological characters, i.e. four pairs of branchiae on chaetigers 2–5, heavy acicular spines in the notopodia of chaetigers 1 and 2, short spinous chaetae in chaetigers 1 and 2, and lyrate chaetae present from chaetiger 3. Besides, they lack eyes on the prostomium. However, both species differ in the following respects:

1. Shape of anterior margin of prostomium. In *Scl. branchiatum*, the anterior margin of the prostomium was broadly curved and smooth, whereas it is medially incised in *Scl. nanhaiensis* sp. nov.;
2. Number of ventral cirri with nipple-like tips on the posterior segments. Nipple-like tips are present in the six anteriormost ventral cirri of *Scl. branchiatum*, while they are present throughout the posterior segments in *Scl. nanhaiensis* sp. nov.;
3. Body annulation. According to the generic diagnosis provided by Blake (2020), a segment of *Scl. branchiatum* possesses up to four annulations along the body while that of *Scl. nanhaiensis* has six annulations on the posterior segments.

Etymology. The specific name “*nanhaiensis*” is derived from Nánhǎi (南海), the Chinese name for the South China Sea, where the specimens were collected.

Distribution. Currently known from the continental slope of the northern South China Sea at water depth between 1277–2352 m.

Gene sequences. In this study, 452 bp of 16S (accession number PV102047), 1665 bp of 18S (PV102048), 976 bp of 28S (PV102046), and 353 bp of H3 (PV102951) were successfully amplified. Currently, there are genetic data available in GenBank for two congeneric species, i.e., *Sclerobregma branchiatum* (with sequences for 18S rRNA and 28S rRNA) and an undescribed *Sclerobregma* species (with sequences for COI and 16S rRNA). The 18S rRNA and 28S rRNA were highly conserved with the K2P distances of 0% and 0.5% between *Sclerobregma nanhaiensis* sp. nov. and *Scl. branchiatum*, respectively. However, the K2P distance was significantly higher for 16S rRNA between the new species and *Sclerobregma* sp.339PB (Accession number MK971015), at 43.4%.

Acknowledgments

We extend our sincere gratitude to the captains and crews for their invaluable assistance in collecting deep-sea samples during the cruises organized by the Guangzhou Marine Geological Survey (Guangzhou, China). We also thank Dr James A. Blake for providing essential references.

Additional information

Conflict of interest

The authors have declared that no competing interests exist.

Ethical statement

No ethical statement was reported.

Funding

This study was supported by the National Natural Science Foundation of China (Grant No. 42006127), the Scientific Research Foundation of Third Institute of Oceanography, MNR (Project No. 2016043), and the Marine Geological Survey Program of the China Geological Survey (Project No. DD20221706).

Author contributions

Conceptualization: JHL, XBH. Funding acquisition: YQH, QYL. Writing original draft: JHL. Review and editing: XBH.

Data availability

All of the data that support the findings of this study are available in the main text.

References

Ashworth JH (1901) The anatomy of *Scalibregma inflatum* Rathke. Quarterly Journal of Microscopical Science 45: 237–309. <https://doi.org/10.1242/jcs.s2-45.178.237>

- Bertelsen RD, Weston DP (1980) A new species of *Sclerobregma* (Polychaeta: Scalibregmatidae) from off the southeastern United States. *Proceedings of the Biological Society of Washington* 93(3): 708–713.
- Blake JA (2015) New species of Scalibregmatidae (Annelida, Polychaeta) from the East Antarctic Peninsula including a description of the ecology and post-larval development of species of *Scalibregma* and *Oligobregma*. *Zootaxa* 4033(1): 57–93. <https://doi.org/10.11646/zootaxa.4033.1.3>
- Blake JA (2020) 7.6.3 Scalibregmatidae Malmgren, 1867. In: Purschke G, Böggemann M, Westheide W (Eds) *Handbook of Zoology. Annelida Vol. 2 (Pleistoannelida, Sedentaria II)*. De Gruyter, Berlin, 312–349. <https://doi.org/10.1515/9783110291681-010>
- Blake JA (2023) New species of Scalibregmatidae (Annelida) from slope and abyssal depths off eastern Australia. *Records of the Australian Museum* 75(3): 271–298. <https://doi.org/10.3853/j.2201-4349.75.2023.1827>
- Bonifacio P, Martinez-Arbizu P, Menot L (2020) Alpha and beta diversity patterns of polychaete assemblages across the nodule province of the eastern Clarion-Cliperton Fracture Zone (equatorial Pacific). *Biogeosciences* 17: 865–886. <https://doi.org/10.5194/bg-17-865-2020>
- Glasby CJ, Lee Y-L, Hsueh P-W (2016) Marine Annelida (excluding clitellates and siboglinids) from the South China Sea. *The Raffles Bulletin of Zoology Supplement* 34: 178–234.
- Hartman O (1965) Deep-water benthic polychaetous annelids off New England to Bermuda and other North Atlantic areas. Allan Hancock Foundation Publications, Occasional Paper 28: 1–378. <http://digitalibrary.usc.edu/digital/collection/p15799coll82/id/20299>
- Jumars PA, Dorgan KM, Lindsey SM (2015) Diet of worms emended: an update of polychaete feeding guilds. *Annual Review of Marine Science* 7: 497–520. Supplemental Appendix A. Family-by-Family Updates: A1-A350+Supplemental Table of Guild Characteristics: 1–14. <https://doi.org/10.1146/annurev-marine-010814-020007>
- Katoh K, Misawa K, Kuma K, Miyata T (2002) MAFFT: A novel method for rapid multiple sequence alignment based on fast Fourier transform. *Nucleic Acids Research* 30(14): 3059–3066. <https://doi.org/10.1093/nar/gkf436>
- Kimura M (1980) A simple method for estimating evolutionary rates of base substitutions through comparative studies of nucleotide sequences. *Journal of Molecular Evolution* 16(2): 111–120. <https://doi.org/10.1007/BF01731581>
- Kudenov JD, Blake JA (1978) A review of the genera and species of the Scalibregmatidae (Polychaeta) with descriptions of one new genus and three new species from Australia. *Journal of Natural History* 12: 427–444. <https://doi.org/10.1080/00222937800770291>
- Kumar S, Stecher G, Li M, Knyaz C, Tamura K (2018) MEGA X: Molecular evolutionary genetics analysis across computing platforms. *Molecular Biology and Evolution* 35(6): 1547–1549. <https://doi.org/10.1093/molbev/msy096>
- Lin J-H, García-Garza ME, Mou J-F, Lin H-S (2023) Description of a new *Promastobranchnus* species (Annelida, Capitellidae) from Chinese coasts, with molecular evidence for intraspecific variation in the number of thoracic chaetigers. *ZooKeys* 1174: 1–14. <https://doi.org/10.3897/zookeys.1174.106624>
- Mackie ASY (1991) *Scalibregma celticum* new species (Polychaeta: Scalibregmatidae) from Europe, with a redescription of *Scalibregma inflatum* Rathke, 1843 and comments on the genus *Sclerobregma* Hartman, 1965. *Bulletin of Marine Science* 48(2): 268–276.

- Mendes SLSD, Rizzo AE, Paiva PC (2023) Unravelling the diversity of *Scalibregma* Rathke, 1843 (Annelida: 'Polychaeta': Scalibregmatidae) from southeast Brazilian coast. *Zootaxa* 5353 (5): 441–454. <https://doi.org/10.11646/zootaxa.5353.5.3>
- Mendes SLSD, De Paiva PC, Rizzo AE (2024a) On species of *Asclerocheilus* Ashworth, 1901 (Annelida: Scalibregmatidae) from Brazil. *European Journal of Taxonomy* 947: 88–108. <https://doi.org/10.5852/ejt.2024.947.2621>
- Mendes SLSD, Paiva PC, Rizzo AE (2024b) First record of *Oligobregma* Kudenov & Blake, 1978 (Annelida: Polychaeta: Scalibregmatidae Malmgren, 1867) from Brazil with the description of three new species. *Zootaxa* 5424(1): 80–98. <https://doi.org/10.11646/zootaxa.5424.1.4>
- Mendes SLSD, Paiva PC, Rizzo AE (2024c) New species of *Pseudoscalibregma* Ashworth, 1901 (Annelida: Scalibregmatidae Malmgren, 1867) from Brazil. *Zootaxa* 5399(1): 19–36. <https://doi.org/10.11646/zootaxa.5399.1.2>
- Parapar J, Martínez A, Moreira J (2021) On the Systematics and Biodiversity of the Opheliidae and Scalibregmatidae. *Diversity* 13(2): 1–34. <https://doi.org/10.3390/d13020087>
- Paul C, Halanych KM, Tiedemann R, Bleidorn C (2010) Molecules reject an opheliid affinity for *Travisia*. *Systematics and Biodiversity* 8(4): 507–512. <https://doi.org/10.1080/14772000.2010.517810>
- Rathke H (1843) Beiträge zur Fauna Norwegens. *Verhandlungen Kaiserlichen Leopoldinisch-Carolinischen Akademie Naturforscher* 20: 1–264. [Breslau] <https://doi.org/10.5962/bhl.title.120119>
- Read G, Fauchald K [Ed.] (2025) World Polychaeta Database. Scalibregmatidae Malmgren, 1867. through: World Register of Marine Species. <https://www.marinespecies.org/aphia.php?p=taxdetails&id=925> [Accessed on 2025-02-10]
- Schüller M (2008) New polychaete species collected during the expeditions ANDEEP I, II, and III to the deep Atlantic sector of the Southern Ocean in the austral summers 2002 and 2005 – Ampharetidae, Opheliidae, and Scalibregmatidae. *Zootaxa* 1705: 51–68. <https://doi.org/10.11646/zootaxa.1705.1.4>
- Schüller M, Hilbig B (2007) Three new species of the genus *Oligobregma* (Polychaeta, Scalibregmatidae) from the Scotia and Weddell Seas (Antarctica). *Zootaxa* 1391: 35–45. <https://doi.org/10.11646/zootaxa.1391.2>
- Wang X, Sun Q, Wang H, Yin S, Wan X, Chen J, Hernández-Molina FJ (2024) Flow conditions of the Quaternary Deep-water Current reconstructed by sediment waves in the northeastern South China Sea. *Marine Geology* 477: 107414. <https://doi.org/10.1016/j.margeo.2024.107414>
- Wiklund H, Neal L, Glover AG, Drennan R, Rabone M, Dahlgren TG (2019) Abyssal fauna of polymetallic nodule exploration areas, eastern Clarion-Clipperton Zone, central Pacific Ocean: Annelida: Capitellidae, Opheliidae, Scalibregmatidae, and Traviidae. *Zookeys* 883: 1–82. <https://doi.org/10.3897/zookeys.883.36193>

A survey of *Belisana* spiders (Araneae, Pholcidae) from eastern Sichuan, China

Bing Wang¹, Ying Wang¹, Shuqiang Li², Pengfeng Wu¹, Zhiyuan Yao¹

¹ College of Life Science, Shenyang Normal University, Shenyang 110034, Liaoning, China

² Institute of Zoology, Chinese Academy of Sciences, Beijing 100101, China

Corresponding authors: Zhiyuan Yao (yaozy@synu.edu.cn); Pengfeng Wu (xiaowu8181@126.com)

Abstract

China exhibits remarkable diversity of the spider genus *Belisana* Thorell, 1898, while Sichuan Province has recorded only one species, *Belisana maoer* Yao & Li, 2020. In this study, four species were collected in eastern Sichuan by canopy fogging. These comprise two new species, *Belisana miyi* Wang, Li & Yao, **sp. nov.** and *B. tongjiang* Wang, Li & Yao, **sp. nov.**, as well as two known species, *B. tongji* Zhang, Li & Yao, 2024 and *B. yanhe* Chen, Zhang & Zhu, 2009, which are reported from Sichuan for the first time. A distribution map of all five species is provided.

Key words: Biodiversity, cellar spider, fogging, invertebrate, new record, new species, taxonomy



Academic editor: Cristina Rheims

Received: 11 January 2025

Accepted: 24 March 2025

Published: 2 May 2025

ZooBank: <https://zoobank.org/1418A533-D021-4823-A947-EE2CA2013C35>

Citation: Wang B, Wang Y, Li S, Wu P, Yao Z (2025) A survey of *Belisana* spiders (Araneae, Pholcidae) from eastern Sichuan, China. ZooKeys 1236: 219–231. <https://doi.org/10.3897/zookeys.1236.146511>

Copyright: © Bing Wang et al.
This is an open access article distributed under terms of the Creative Commons Attribution License (Attribution 4.0 International – CC BY 4.0).

Introduction

The family Pholcidae C.L. Koch, 1850 is one of the most species-rich spider families, with 2037 extant species in 97 genera (WSC 2025). *Belisana* Thorell, 1898, the second largest genus in Pholcidae, comprises 169 species (WSC 2025). They are mainly distributed in southern China, and the Indo-Malayan and Australasian regions (Huber 2005; Yao and Li 2013; Yao et al. 2018; Zhu et al. 2020). The former exhibits the highest diversity with 83 described species and represents 49% of the genus (Wang et al. 2024; WSC 2025). Recently, numerous expeditions of pholcid spiders have been conducted in China, resulting in the discovery and description of a large number of new species. These efforts have primarily focused on two genera: *Pholcus* Walckenaer, 1805 in northern and central China (e.g., Yao et al. 2021; Lu et al. 2022; Zhao et al. 2023b; Yang et al. 2024a, b; Li et al. 2025; Yao and Li 2025) and *Belisana* in southern China (e.g., Zhao et al. 2023a; Wang et al. 2024; Zhang et al. 2024a, b). Nevertheless, the distribution of these two genera in China is still conspicuously patchy. For instance, Sichuan Province, located in the southwest of China, has recorded only one species of *Belisana*: *B. maoer* Yao & Li, 2020 (Zhu et al. 2020). Sichuan is situated in the transitional zone between the Tibetan Plateau (often considered the first step of China's geographical terrain) and the middle and lower reaches of the Yangtze River (typically classified as the third step), within the framework of China's three major geographical steps.

Furthermore, eastern Sichuan boasts a subtropical humid climate (Wang et al. 2020). Therefore, its species diversity deserves further investigation. We recently conducted a field survey targeting *Belisana* in eastern Sichuan by canopy fogging and discovered two new species. Additionally, two known species were reported from Sichuan for the first time (Fig. 1).

Material and methods

All specimens were collected by canopy fogging. Specimens were examined and measured with a Leica M205 C stereomicroscope. Left male palps were photographed. The ventral views of epigyna were photographed before dissection. Vulvae were photographed after treating them in a 10% warm solution of potassium hydroxide (KOH) to dissolve soft tissues. Images were captured with a Canon EOS 750D wide zoom digital camera (24.2 megapixels) mounted on the stereomicroscope mentioned above and assembled using Helicon Focus v. 3.10.3 image stacking software (Khmelik et al. 2005). For each sample, ~100 individual photos were stacked together. Using Procreate v. 5.0.2 (Savage Interactive Pty Ltd), the drawings were done based on the photos, with further modifications made according to direct observations of the samples. All measurements are given in millimeters (mm). Leg measurements are shown as: total length (femur, patella, tibia, metatarsus, tarsus). Leg segments were measured on their dorsal sides. The distribution map was generated with ArcGIS v. 10.2 (ESRI Inc.). The specimens studied are preserved in 75% ethanol and deposited in the College of Life Science, Shenyang Normal University (SYNU) in Liaoning, China.

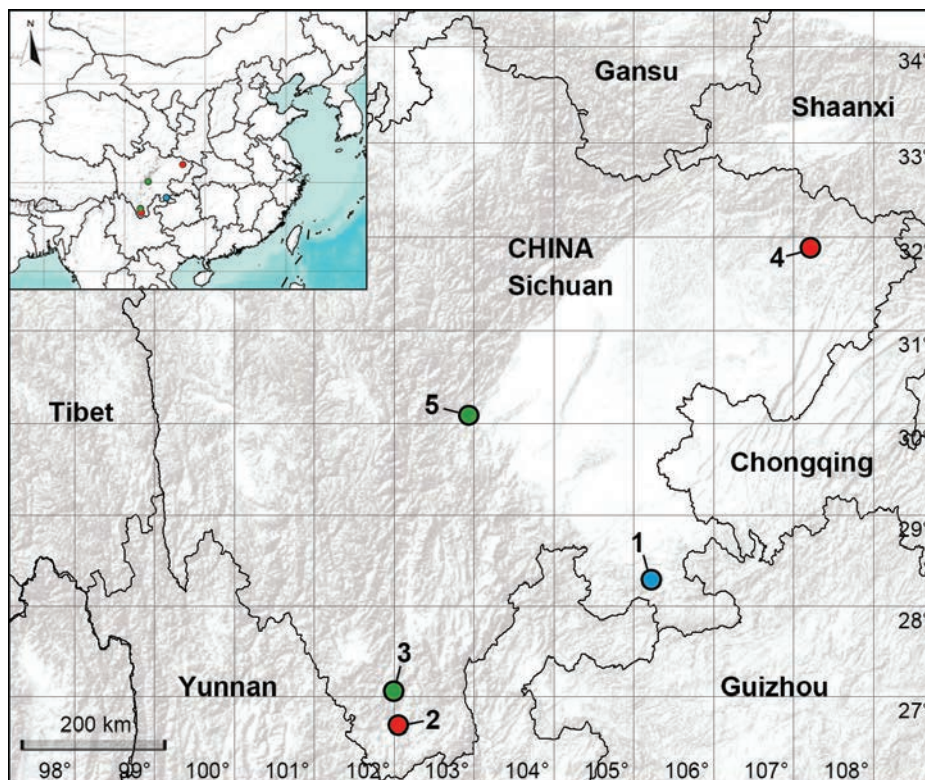


Figure 1. Distribution records of the *Belisana* species from eastern Sichuan, China **1** *Belisana maoer* Yao & Li, 2020 **2** *B. miyi* sp. nov. **3** *B. tongji* Zhang, Li & Yao, 2024 **4** *B. tongjiang* sp. nov. **5** *B. yanhe* Chen, Zhang & Zhu, 2009. Blue, green and red circles indicate previously recorded species, newly recorded species, and new species, respectively.

Terminology and taxonomic descriptions follow Huber (2005) and Yao et al. (2015). The following abbreviations are used: **aa** = anterior arch, **ALE** = anterior lateral eye, **b** = bulb, **ba** = bulbal apophysis, **da** = distal apophysis, **e** = embolus, **ep** = epigynal pocket, **f** = flap, **L/d** = length/diameter, **pa** = proximo-lateral apophysis, **PME** = posterior median eye, **pp** = pore plate, **pr** = procurus.

Taxonomy

Family Pholcidae C.L. Koch, 1850

Subfamily Pholcinae C.L. Koch, 1850

Genus *Belisana* Thorell, 1898

Type species. *Belisana tauricornis* Thorell, 1898.

***Belisana miyi* Wang, Li & Yao, sp. nov.**

<https://zoobank.org/EF9C76D6-1612-4301-87FF-3ACEAE8F7B0F>

Figs 2, 3, 6A, B, 7A, B

Type material. Holotype: CHINA • ♂; Sichuan, Panzhihua, Miyi County, Binggu Town, Maidichong Village; 26.679384°N, 102.062562°E; alt. 2235 m; 7 Jun. 2024; X. Zhang, Y. Wang & Q. Meng leg.; SYNU-Ar00453. **Paratypes:** CHINA • 3 ♂; same data as for holotype; SYNU-Ar00454–56 • 1 ♀; same data as for holotype; SYNU-Ar00457.

Etymology. The specific name refers to the type locality; noun in apposition.

Diagnosis. The new species resembles *B. erromena* Zhang & Peng, 2011 (Zhang and Peng 2011: 58, fig. 7A–G) by having similar bulbal apophysis (distally hooked; Fig. 3C) and vulval pore plates (strongly curved, with several teeth; Figs 3B, 7B), but can be distinguished by procurus with prolatero-distal sclerite (arrow 1 in Figs 2C, 6A vs membranous lamella bearing comb-shaped apophyses, fig. 7D in Zhang and Peng 2011), by male cheliceral distal apophyses on distal part of chelicerae (da in Fig. 3D vs on submedian part, fig. 7B in Zhang and Peng 2011), and by epigynal pockets on postero-median part of epigynal plate and close to each other (ep in Figs 3A, B, 7A, B vs on anterior part of epigynal plate and widely separated, ep in fig. 7F in Zhang and Peng 2011).

Description. Male (holotype): Total length 2.00 (2.10 with clypeus), carapace 0.72 long, 0.73 wide, opisthosoma 1.28 long, 0.89 wide. Leg I: 12.56 (3.28, 0.32, 3.13, 4.55, 1.28), leg II missing, leg III: 5.29 (1.51, 0.22, 1.25, 1.72, 0.59), leg IV: 7.19 (2.13, 0.25, 1.82, 2.30, 0.69); tibia I L/d: 41. Eye interdistances and diameters: PME–PME 0.14, PME 0.13, PME–ALE 0.02. Sternum width/length: 0.50/0.45. Habitus as in Fig. 3E, F. Carapace yellowish, without marks; clypeus and sternum yellowish. Legs whitish, without darker rings. Opisthosoma yellowish, without spots. Thoracic furrow absent. Clypeus frontally projected. Chelicerae with a pair of proximo-lateral apophyses (pa in Fig. 3D) and a pair of distal, prolaterally curved apophyses (distance between tips: 0.05; da in Fig. 3D). Palp as in Fig. 2A, B; trochanter with ventral apophysis (2× longer than wide; arrow 1 in Fig. 2B) and retrolateral apophysis (as long as wide; arrow 2 in Fig. 2B); femur with retrolateral protrusion (arrow 3 in Fig. 2B); procurus with fan-shaped prolatero-distal

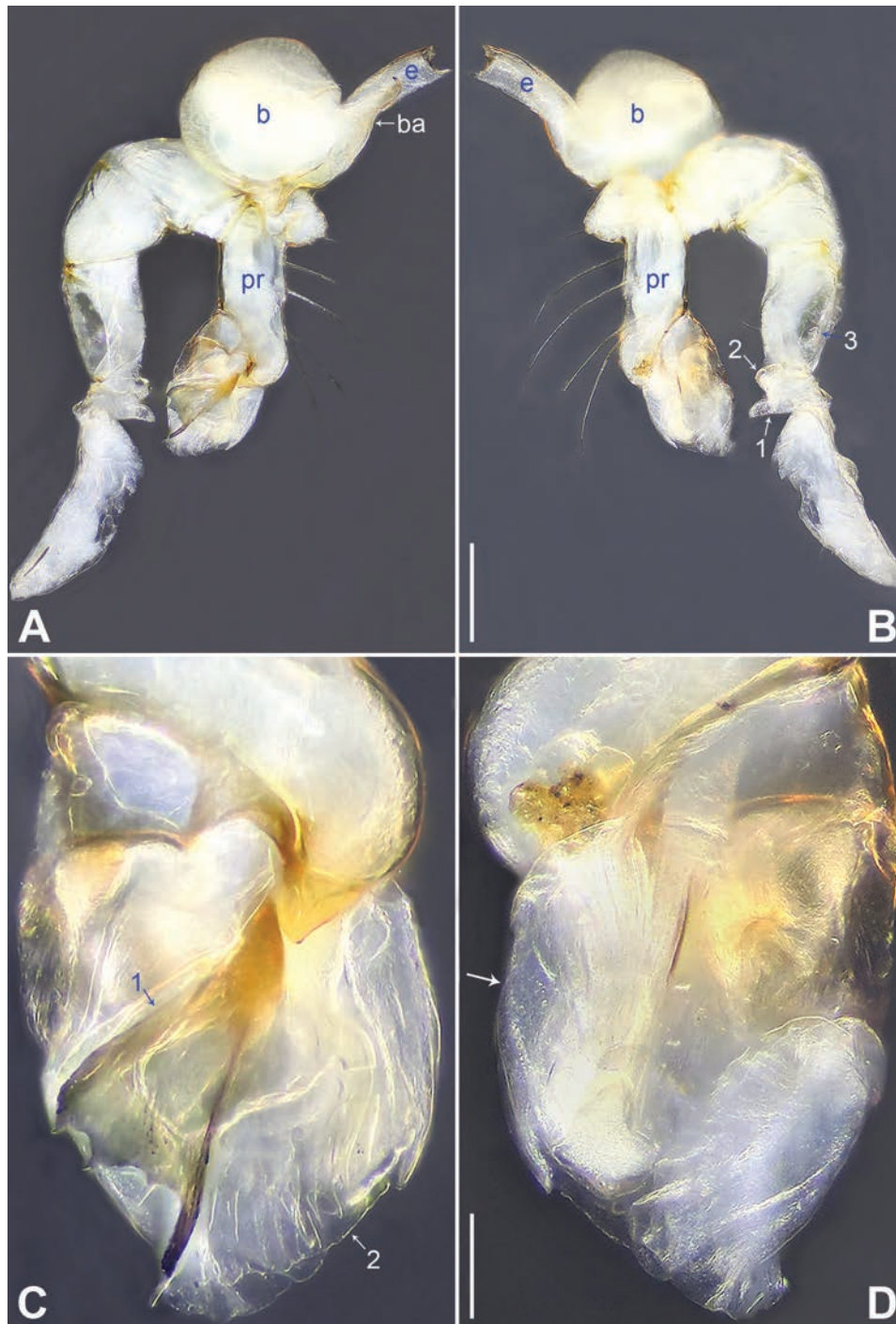


Figure 2. *Belisana miyi* sp. nov., holotype male **A, B** palp (**A** prolateral view **B** retrolateral view, arrow 1 points at ventral apophysis, arrow 2 points at retrolateral apophysis, arrow 3 points at retrolateral protrusion) **C, D** distal part of procurus (**C** prolateral view, arrow 1 points at prolatero-distal sclerite, arrow 2 points at distal membranous lamella **D** retrolateral view, arrow points at retrolatero-subdistal membranous lamella). Abbreviations: b = bulb, ba = bulbal apophysis, e = embolus, pr = procurus. Scale bars: 0.20 (**A, B**); 0.05 (**C, D**).

sclerite (arrow 1 in Figs 2C, 6A), distal membranous lamella (arrow 2 in Figs 2C, 6A), and retrolatero-subdistal membranous lamella (arrow in Figs 2D, 6B); bulb with hooked apophysis (ba in Fig. 3C) and distally bifurcated embolus (e in Fig. 3C). Retrolateral trichobothrium on tibia I at 5% proximally; legs with short vertical setae on metatarsi; tarsus I with 16 distinct pseudosegments.

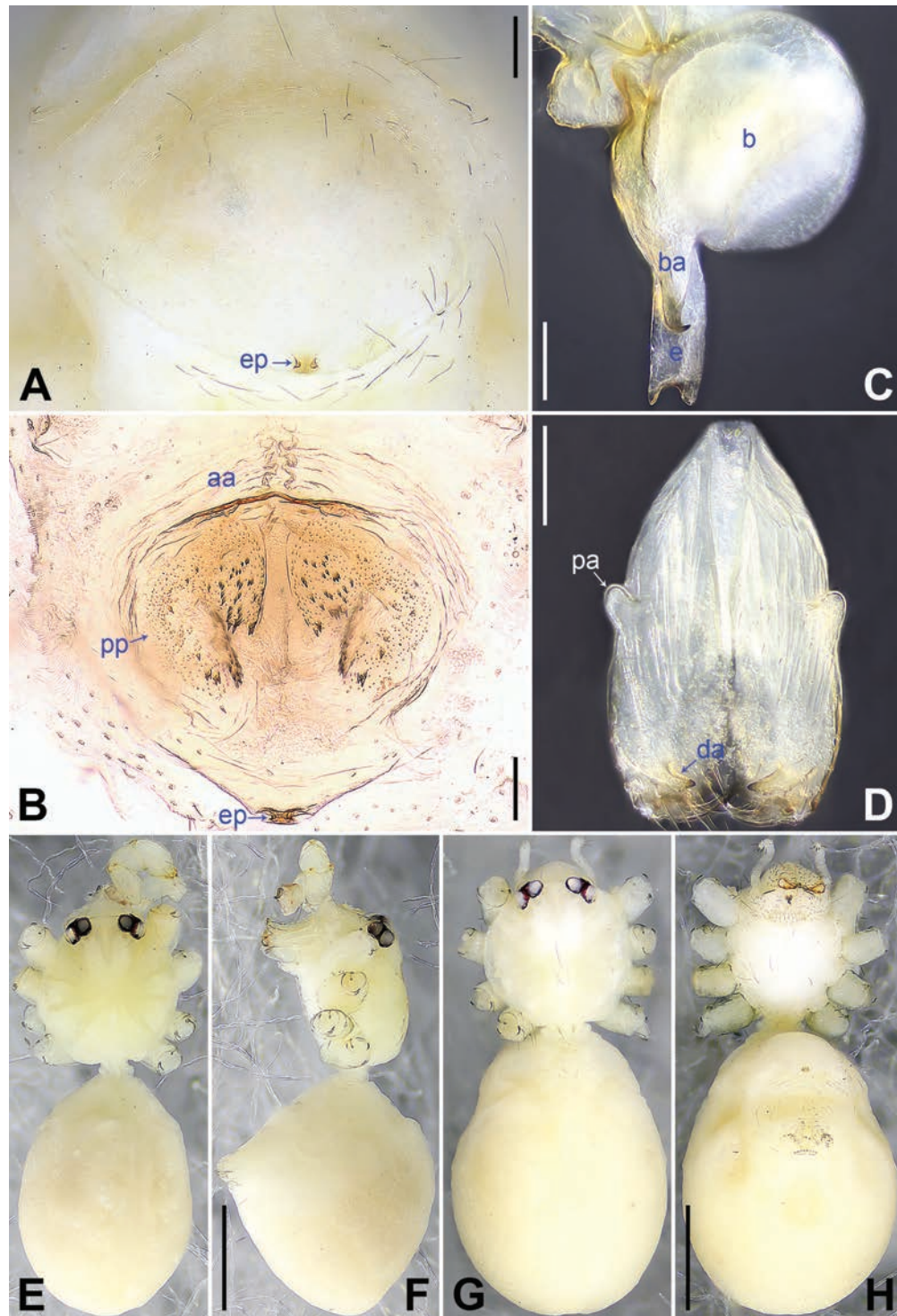


Figure 3. *Belisana miyi* sp. nov., holotype male (C–F) and paratype female (A, B, G, H) A epigynum, ventral view B vulva, dorsal view C bulb, prolateral view D chelicerae, frontal view E–H habitus (E, G dorsal view F lateral view H ventral view). Abbreviations: aa = anterior arch, b = bulb, ba = bulbal apophysis, da = distal apophysis, e = embolus, ep = epigynal pocket, pa = proximo-lateral apophysis, pp = pore plate. Scale bars: 0.10 (A–D); 0.50 (E–H).

Female (paratype, SYNU-Ar00457): Similar to male, habitus as in Fig. 3G, H. Total length 2.22 (2.32 with clypeus), carapace 0.70 long, 0.72 wide, opisthosoma 1.52 long, 1.10 wide. Leg I missing. Eye interdistances and diameters: PME–PME 0.12, PME 0.10, PME–ALE 0.02. Sternum width/length:

0.58/0.55. Clypeus unmodified. Epigynum oval, posteriorly curved, with postero-median pockets 0.03 apart (ep in Figs 3A, 7A). Vulva with anterior arch (aa in Figs 3B, 7B) and a pair of strongly curved pore plates with several teeth (pp in Figs 3B, 7B).

Variation. Tibia I in two male paratypes (SYNU-Ar00454–55): 2.30, 3.00 (Leg I missing in SYNU-Ar00456).

Distribution. China (Sichuan, type locality; Fig. 1).

***Belisana tongjiang* Wang, Li & Yao, sp. nov.**

<https://zoobank.org/CFA56021-48BF-4FC0-9FD8-5F5D22D3BAF6>

Figs 4, 5, 6C, D, 7C, D

Type material. Holotype: CHINA • ♂; Sichuan, Bazhong, Tongjiang County, Nuojiang Town, Mulingzui Village; 31.892294°N, 107.217638°E; alt. 583 m; 21 Jun. 2024; X. Zhang, Y. Wang & Q. Meng leg.; SYNU-Ar00463. **Paratypes:** CHINA • 5 ♀; same data as for holotype; SYNU-Ar00464–68.

Etymology. The specific name refers to the type locality; noun in apposition.

Diagnosis. The new species resembles *B. honghe* Zhang, Li & Yao, 2024 (Zhang et al. 2024b: 257, figs 2A–D, 3A–H, 18A, B, 20A, B) by having similar bulbal apophysis (distally hooked; Fig. 5C) and epigynum (epigynal pockets on postero-lateral part of epigynal plate; Figs 5A, B, 7C, D), but can be distinguished by procurus with distal membranous process (arrow 2 in Figs 4C, 6C vs sclerotized apophysis, arrow 2 in figs 2C, 18A in Zhang et al. 2024b), prolatero-distal membranous process (arrow 4 in Figs 4C, 6C vs absent, figs 2C, 18A in Zhang et al. 2024b) and retrolateral membranous flap (4× wider than long, f in Figs 4D, 6D vs 2× wider than long, f in figs 2D, 18B in Zhang et al. 2024b), by male cheliceral distal apophyses distally blunt (da in Fig. 5D vs distally pointed, da in fig. 3D in Zhang et al. 2024b), and by vulval pore plates nearly rectangular (pp in Figs 5B, 7D vs anteriorly pointed and posteriorly wide, pp in figs 3B, 20B in Zhang et al. 2024b).

Description. Male (holotype): Total length 1.27 (1.38 with clypeus), carapace 0.45 long, 0.40 wide, opisthosoma 0.82 long, 0.50 wide. Legs I, II and IV missing, leg III: 4.42 (1.27, 0.18, 1.04, 1.44, 0.49). Eye interdistances and diameters: PME–PME 0.10, PME 0.07, PME–ALE 0.02. Sternum width/length: 0.43/0.40. Habitus as in Fig. 5E, F. Carapace yellowish, without marks; clypeus and sternum yellowish. Legs whitish, without darker rings. Opisthosoma yellowish, without spots. Thoracic furrow absent. Clypeus unmodified. Chelicerae with a pair of proximo-lateral apophyses (pa in Fig. 5D) and a pair of distal apophyses pointing downwards (distance between tips: 0.14; da in Fig. 5D). Palp as in Fig. 4A, B; trochanter with ventral apophysis (2× longer than wide; arrow in Fig. 4B); procurus with ventro-distal membranous process (arrow 1 in Figs 4C, 6C), distal membranous process (arrow 2 in Figs 4C, 6C), sclerotized distal apophysis (arrow 3 in Figs 4C, 6C), prolatero-distal membranous process (arrow 4 in Figs 4C, 6C), dorso-distal membranous process (arrow 5 in Figs 4C, 6C), and retrolateral membranous flap (f in Figs 4D, 6D); bulb with hooked apophysis (ba in Fig. 5C) and distally pointed embolus (e in Fig. 5C).

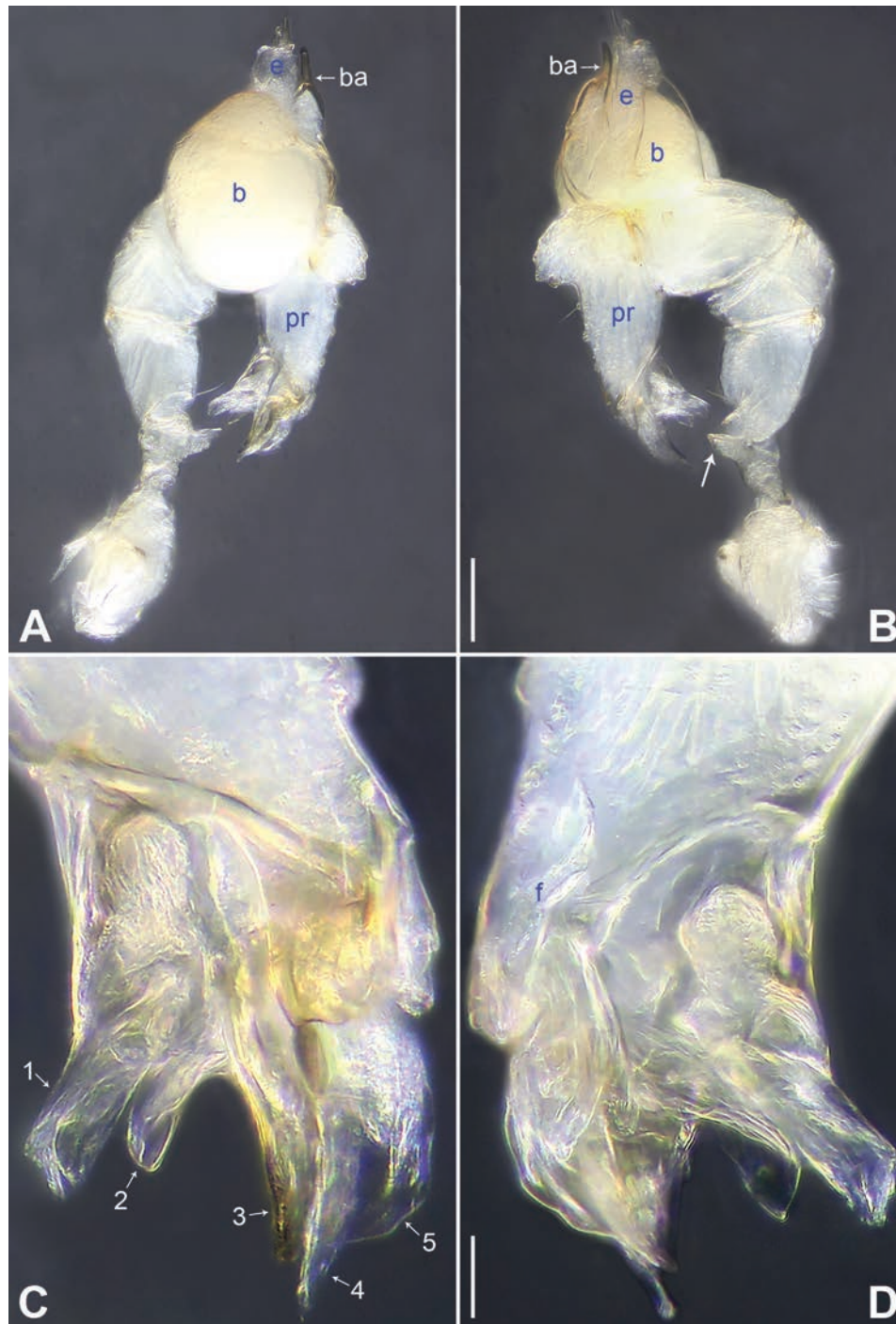


Figure 4. *Belisana tongjiang* sp. nov., holotype male **A, B** palp (**A** prolateral view **B** retrolateral view, arrow points at ventral apophysis) **C, D** distal part of procurus (**C** prolateral view, arrow 1 points at ventro-distal membranous process, arrow 2 points at distal membranous process, arrow 3 points at sclerotized distal apophysis, arrow 4 points at prolatero-distal membranous process, arrow 5 points at dorso-distal membranous process **D** retrolateral view). Abbreviations: b = bulb, ba = bulbal apophysis, e = embolus, f = flap, pr = procurus. Scale bars: 0.10 (**A, B**); 0.02 (**C, D**).

Female (paratype, SYNU-Ar00464): Similar to male, habitus as in Fig. 5G, H. Total length 1.48 (1.60 with clypeus), carapace 0.53 long, 0.56 wide, opisthosoma 0.95 long, 0.63 wide. Tibia I: 1.70; tibia I L/d: 22. Eye interdistances and diameters: PME–PME 0.12, PME 0.06, PME–ALE 0.02. Sternum width/length: 0.44/0.40.

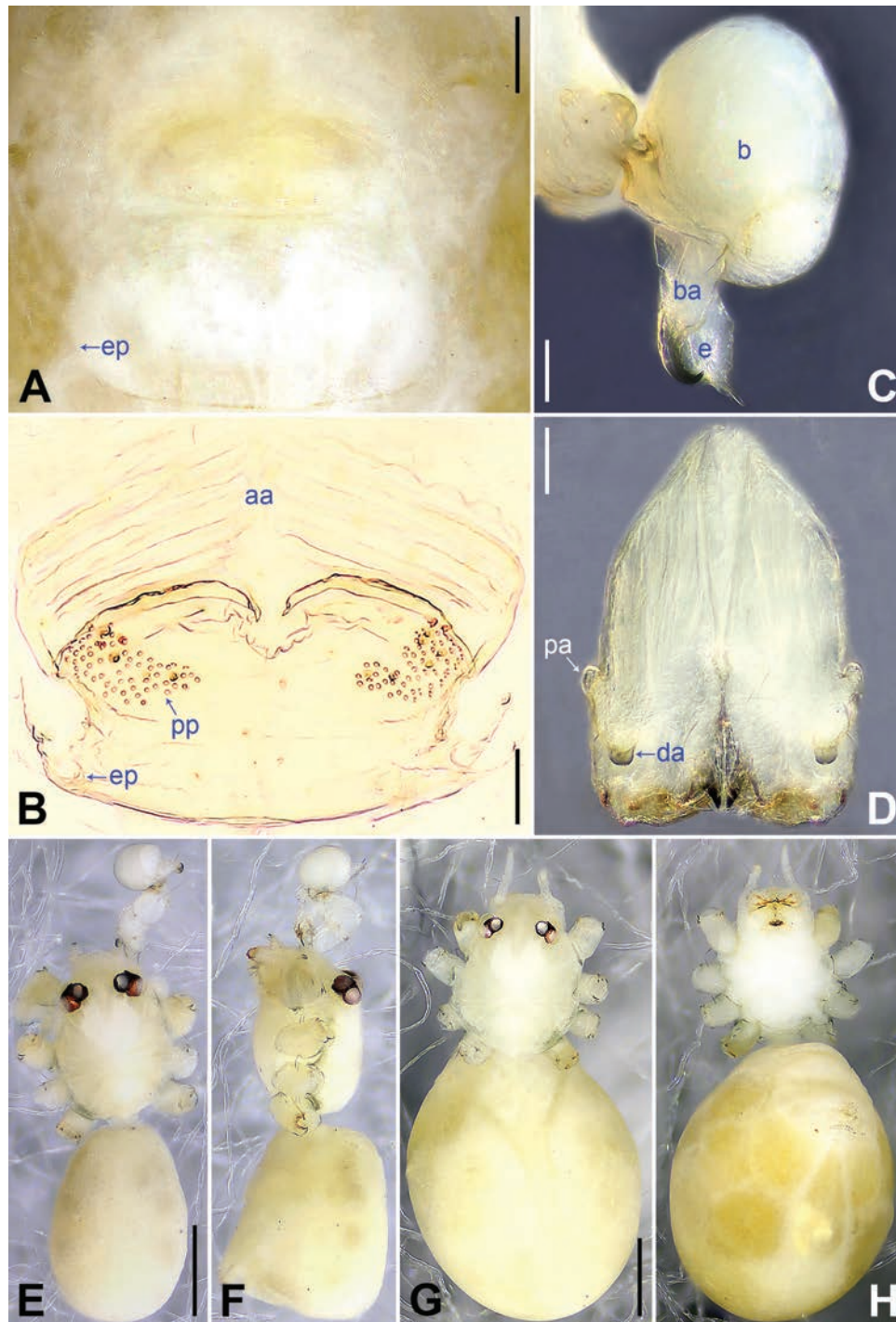


Figure 5. *Belisana tongjiang* sp. nov., holotype male (C–F) and paratype female (A, B, G, H) **A** epigynum, ventral view **B** vulva, dorsal view **C** bulb, prolateral view **D** chelicerae, frontal view **E–H** habitus (**E, G** dorsal view **F** lateral view **H** ventral view). Abbreviations: aa = anterior arch, b = bulb, ba = bulbal apophysis, da = distal apophysis, e = embolus, ep = epigynal pocket, pa = proximo-lateral apophysis, pp = pore plate. Scale bars: 0.05 (A–D); 0.30 (E–H).

Epigynum nearly triangular, posteriorly straight, with postero-lateral pockets 0.25 apart (ep in Figs 5A, 7C). Vulva with anterior arch (aa in Figs 5B, 7D) and a pair of nearly rectangular pore plates (2× longer than wide; pp in Figs 5B, 7D).

Variation. Tibia I in another female paratype (SYNU-Ar00465): 1.44 (Leg I missing in SYNU-Ar00466–68).

Distribution. China (Sichuan, type locality; Fig. 1).

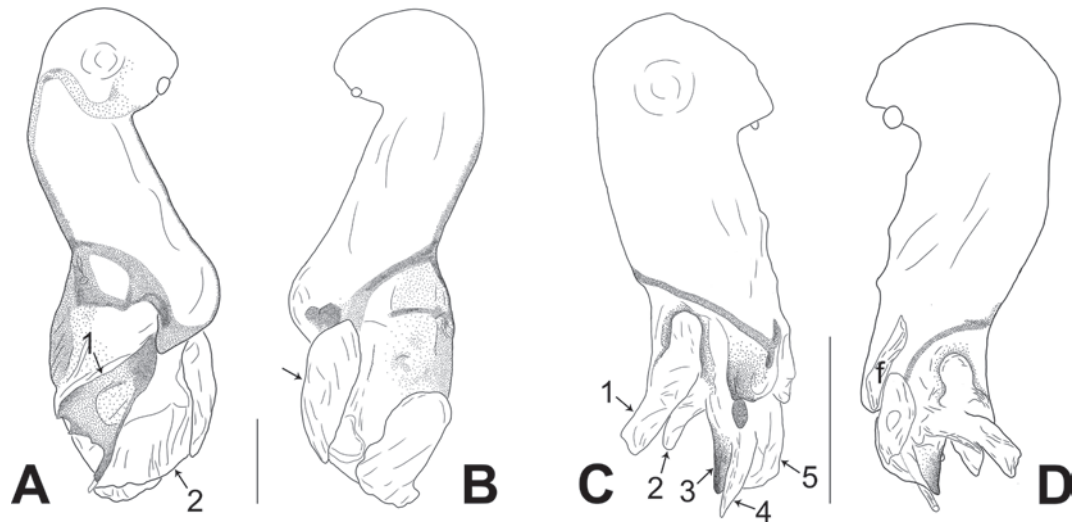


Figure 6. Procurus in prolateral and retrolateral views (arrows point at the same structures as those shown in the photos of each species) **A, B** *Belisana miyi* sp. nov. **C, D** *B. tongjiang* sp. nov. Abbreviation: f = flap. Scale bars: 0.10.

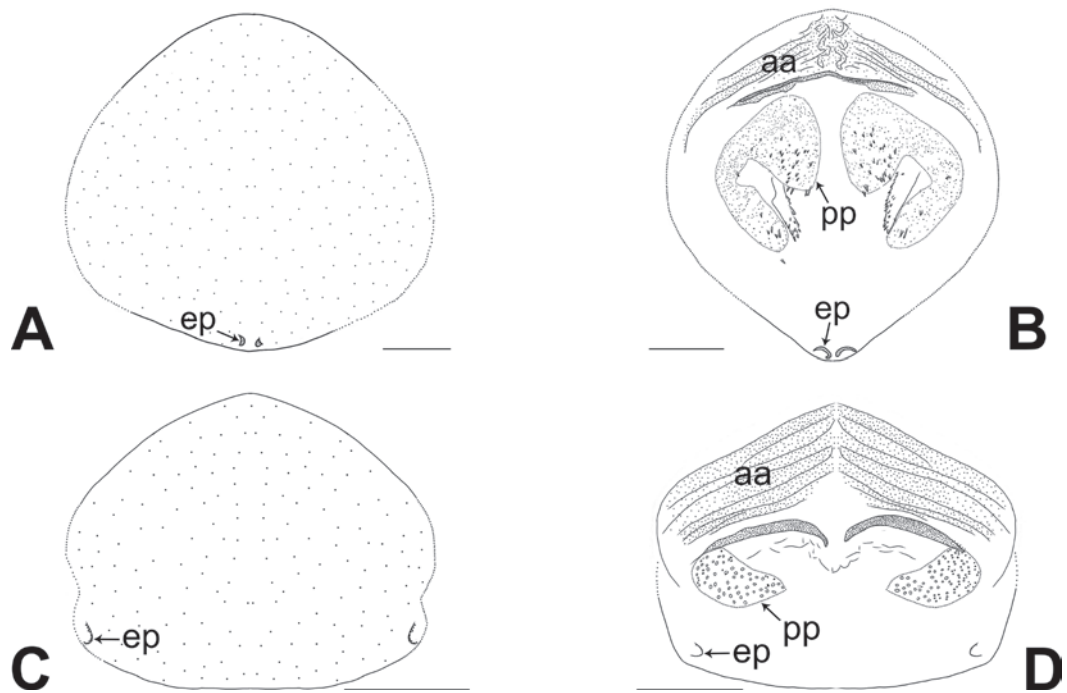


Figure 7. Female genitalia in ventral and dorsal views **A, B** *Belisana miyi* sp. nov. **C, D** *B. tongjiang* sp. nov. Abbreviations: aa = anterior arch, ep = epigynal pocket, pp = pore plate. Scale bars: 0.10.

***Belisana tongi* Zhang, Li & Yao, 2024**

Fig. 8

Belisana tongi Zhang et al. 2024b: 273, figs 12A–D, 13A–H, 18K, L, 21C, D.

Material examined. CHINA • 2 ♂; Sichuan, Panzhihua, Miyi County, Puwei Town, Pengjiayakou Village; 27.060020°N, 102.000282°E; alt. 2464 m; 5 Jun. 2024; X. Zhang, Y. Wang & Q. Meng leg.; SYNU-Ar00458–59 • 3 ♀; same data as for preceding; SYNU-Ar00460–62.

Distribution. China (Sichuan, Fig. 1; Yunnan, type locality).

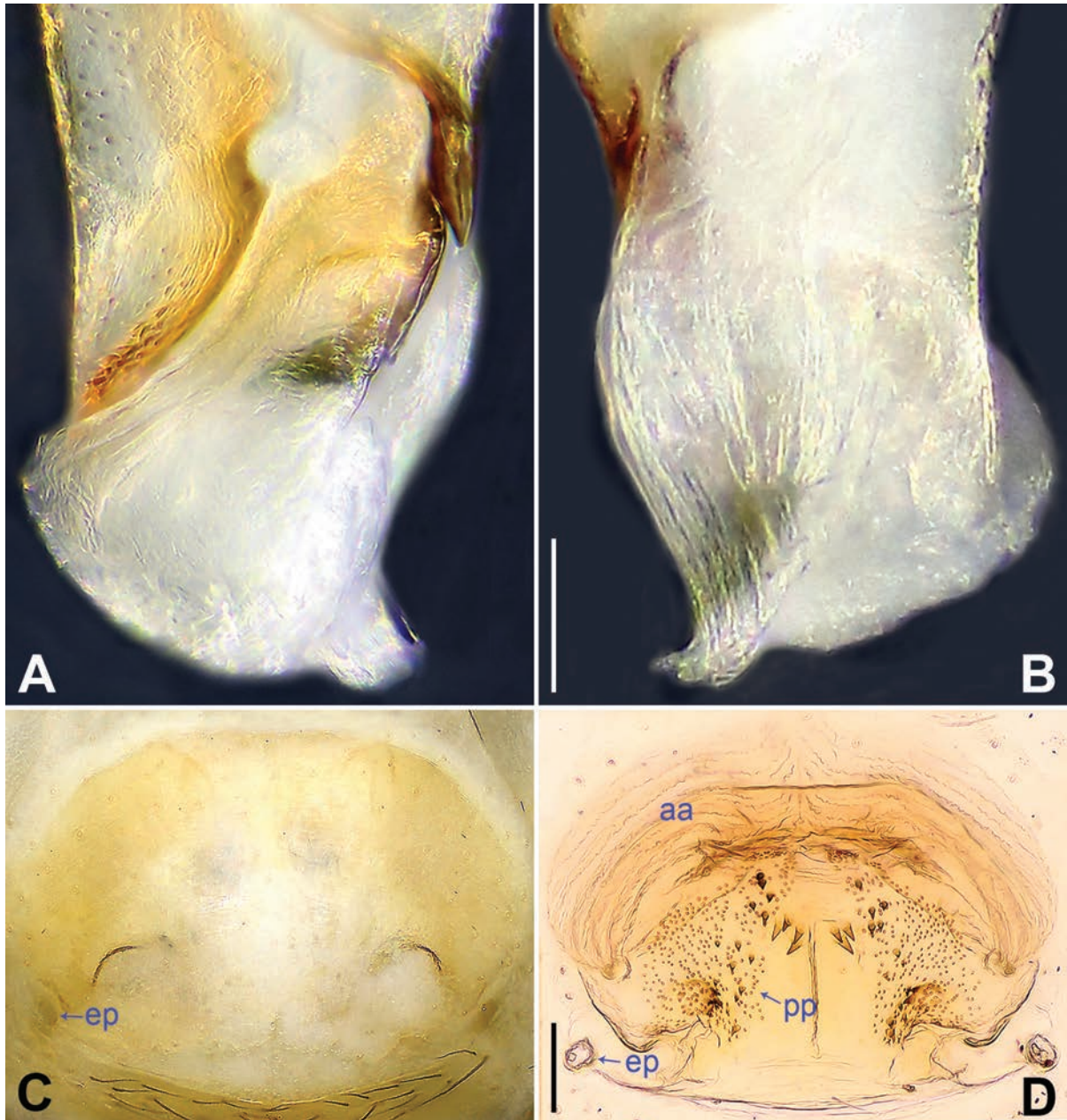


Figure 8. *Belisana tongi* Zhang, Li & Yao, 2024, male (**A, B**) and female (**C, D**) **A, B** distal part of procurus (**A** prolateral view **B** retrolateral view) **C** epigynum, ventral view **D** vulva, dorsal view. Abbreviations: aa = anterior arch, ep = epigynal pocket, pp = pore plate. Scale bars: 0.05 (**A, B**); 0.10 (**C, D**).

***Belisana yanhe* Chen, Zhang & Zhu, 2009**

Fig. 9

Belisana yanhe Chen et al. 2009: 65, figs 31–38.

Material examined. CHINA • 1 ♂; Sichuan, Yaan, Lushan County, Feixianguan Town, Longdongpo; 30.090000°N, 102.930556°E; alt. 905 m; 24 May 2024; X. Zhang, Y. Wang & Q. Meng leg.; SYNU-Ar00469 • 1 ♀; same data as for preceding; SYNU-Ar00470.

Distribution. China (Sichuan, Fig. 1; Guizhou, type locality).

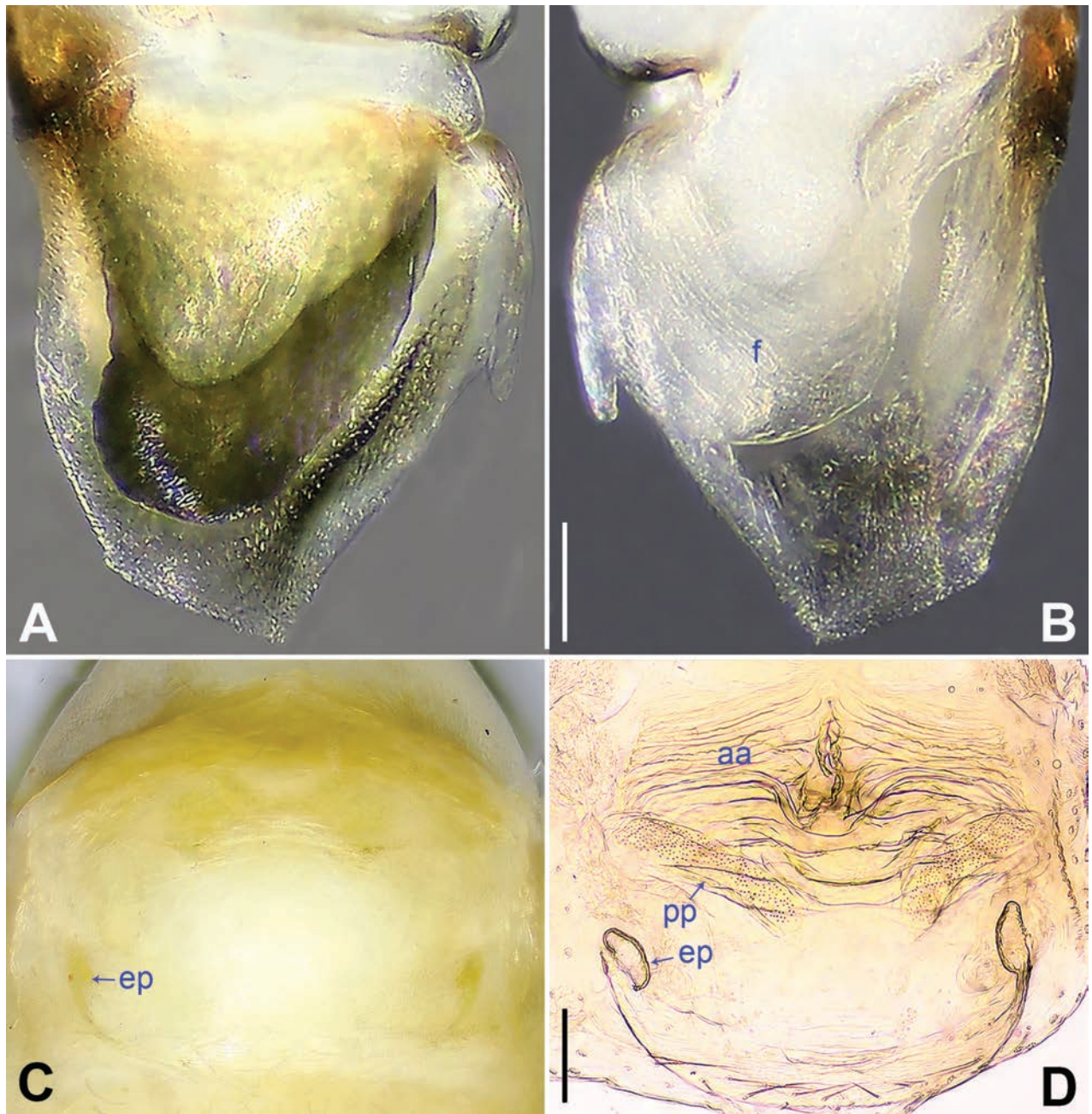


Figure 9. *Belisana yanhe* Chen, Zhang & Zhu, 2009, male (**A, B**) and female (**C, D**) **A, B** distal part of procurus (**A** prolateral view **B** retrolateral view) **C** epigynum, ventral view **D** vulva, dorsal view. Abbreviations: aa = anterior arch, ep = epigynal pocket, f = flap, pp = pore plate. Scale bars: 0.05 (**A, B**); 0.10 (**C, D**).

Acknowledgements

The manuscript benefited greatly from comments by Cristina Rheims, Éwerton Machado, Alexander Sánchez-Ruiz, and two anonymous reviewers.

Additional information

Conflict of interest

The authors have declared that no competing interests exist.

Ethical statement

No ethical statement was reported.

Funding

This study was supported by the Science & Technology Fundamental Resources Investigation Program of China (2023FY100200) and the National Natural Science Foundation of China (NSFC-32170461, 31872193).

Author contributions

ZY and PW designed the study. BW, SL, and ZY performed morphological species identification. BW and YW finished the descriptions and took the photos and drawings. ZY, BW, PW, and SL drafted and revised the manuscript.

Author ORCIDs

Bing Wang  <https://orcid.org/0009-0009-7047-4395>

Ying Wang  <https://orcid.org/0009-0007-9173-4438>

Shuqiang Li  <https://orcid.org/0000-0002-3290-5416>

Pengfeng Wu  <https://orcid.org/0000-0001-5617-6708>

Zhiyuan Yao  <https://orcid.org/0000-0002-1631-0949>

Data availability

All of the data that support the findings of this study are available in the main text.

References

- Chen H, Zhang F, Zhu M (2009) Four new troglomorphic species of the genus *Belisana* Thorell, 1898 (Araneae, Pholcidae) from Guizhou Province, China. *Zootaxa* 2092(1): 58–68. <https://doi.org/10.11646/zootaxa.2092.1.5>
- Huber BA (2005) High species diversity, male-female coevolution, and metaphyly in Southeast Asian pholcid spiders: The case of *Belisana* Thorell 1898 (Araneae, Pholcidae). *Zoologica* 155: 1–126.
- Khmelik VV, Kozub D, Glazunov A (2005) Helicon Focus 3.10.3. <https://www.heliconsoft.com/heliconsoft-products/helicon-focus/> [Accessed 6 July 2024]
- Li J, He Q, Li S, Yao Z (2025) Filling a zoogeographical gap in China: Taxonomic descriptions of six new spider species of the *Pholcus phungiformes* species group (Araneae, Pholcidae). *ZooKeys* 1232: 285–310. <https://doi.org/10.3897/zookeys.1232.145622>
- Lu Y, Chu C, Zhang X, Li S, Yao Z (2022) Europe vs China: *Pholcus* (Araneae, Pholcidae) from Yanshan-Taihang Mountains confirms uneven distribution of spiders in Eurasia. *Zoological Research* 43(4): 532–534. [& Suppl. 1–78] <https://doi.org/10.24272/j.issn.2095-8137.2022.4.dwxj202204005>
- Wang N, Cheng W, Wang B, Liu Q, Zhou C (2020) Geomorphological regionalization theory system and division methodology of China. *Journal of Geographical Sciences* 30(2): 212–232. <https://doi.org/10.1007/s11442-020-1724-9>
- Wang B, Li J, Li S, Yao Z (2024) Nine new spider species of *Belisana* Thorell, 1898 (Araneae, Pholcidae) from karst caves, with a list of species of the genus from Guizhou, southwestern China. *ZooKeys* 1216: 265–302. <https://doi.org/10.3897/zookeys.1216.132561>
- WSC (2025) World Spider Catalog, Version 26. Natural History Museum Bern. <https://wsc.nmbe.ch> [Accessed 25 March 2025]

- Yang L, Fu C, Zhang Y, He Q, Yao Z (2024a) A survey of *Pholcus* spiders (Araneae, Pholcidae) from the Qinling Mountains of central China, with descriptions of seven new species. *Zoosystematics and Evolution* 100(1): 199–221. <https://doi.org/10.3897/zse.100.116759>
- Yang L, He Q, Yao Z (2024b) Taxonomic study of four closely-related species of the *Pholcus yichengicus* species group (Araneae, Pholcidae) from China's Qinling Mountains: An integrated morphological and molecular approach. *Zoosystematics and Evolution* 100(1): 279–289. <https://doi.org/10.3897/zse.100.115633>
- Yao Z, Li S (2013) New and little known pholcid spiders (Araneae: Pholcidae) from Laos. *Zootaxa* 3709(1): 1–51. <https://doi.org/10.11646/zootaxa.3709.1.1>
- Yao Z, Li S (2025) Evolutionary history of Old World cellar spiders in the context of Neo-Tethyan sea-land transformations. *Zoological Research* [in press]. <https://doi.org/10.24272/j.issn.2095-8137.2024.395>
- Yao Z, Pham DS, Li S (2015) Pholcid spiders (Araneae: Pholcidae) from northern Vietnam, with descriptions of nineteen new species. *Zootaxa* 3909(1): 1–82. <https://doi.org/10.11646/zootaxa.3909.1.1>
- Yao Z, Zhu K, Du Z, Li S (2018) The *Belisana* spiders (Araneae: Pholcidae) from Xishuangbanna Tropical Botanical Garden, Yunnan, China. *Zootaxa* 4425(2): 243–262. <https://doi.org/10.11646/zootaxa.4425.2.3>
- Yao Z, Wang X, Li S (2021) Tip of the iceberg: species diversity of *Pholcus* spiders (Araneae, Pholcidae) in the Changbai Mountains, Northeast China. *Zoological Research* 42(3): 267–271. [& Suppl. 1–60] <https://doi.org/10.24272/j.issn.2095-8137.2021.037>
- Zhang F, Peng Y (2011) Eleven new species of the genus *Belisana* Thorell (Araneae: Pholcidae) from South China. *Zootaxa* 2989(1): 51–68. <https://doi.org/10.11646/zootaxa.2989.1.2>
- Zhang L, Wang Y, Li S, Zhang X, Yao Z (2024a) Three new spider species of *Belisana* Thorell, 1898 (Araneae, Pholcidae) from karst caves, with a list of *Belisana* species from Guangxi, China. *ZooKeys* 1209: 315–330. <https://doi.org/10.3897/zookeys.1209.127951>
- Zhang L, Wu Z, Li S, Yao Z (2024b) Eight new spider species of *Belisana* Thorell, 1898 (Araneae, Pholcidae), with an updated overview of *Belisana* species from Yunnan, China. *ZooKeys* 1202: 255–286. <https://doi.org/10.3897/zookeys.1202.121633>
- Zhao F, Yang L, Li S, Zheng G, Yao Z (2023a) A further study on the *Belisana* spiders (Araneae: Pholcidae) from Xishuangbanna, Yunnan, China. *Zootaxa* 5351(5): 543–558. <https://doi.org/10.11646/zootaxa.5351.5.3>
- Zhao F, Yang L, Zou Q, Ali A, Li S, Yao Z (2023b) Diversity of *Pholcus* spiders (Araneae: Pholcidae) in China's Lüliang Mountains: an integrated morphological and molecular approach. *Insects* 14(4): 364. [1–34] <https://doi.org/10.3390/insects14040364>
- Zhu W, Yao Z, Zheng G, Li S (2020) Six new species of the spider genus *Belisana* Thorell, 1898 (Araneae: Pholcidae) from southern China. *Zootaxa* 4810(1): 175–197. <https://doi.org/10.11646/zootaxa.4810.1.12>

Assessing the effect of local heterogeneity on anuran diversity in the Serra da Capivara National Park, Piauí State, Brazil

Kássio de Castro Araújo¹, Nayla Letícia Rodrigues Assunção², Mirco Solé^{3,4},
Etielle Barroso de Andrade¹

1 Grupo de Pesquisa em Biodiversidade e Biotecnologia do Centro-Norte Piauiense, Instituto Federal de Educação, Ciência e Tecnologia do Piauí, Campus Pedro II, 64255-000, Pedro II, Piauí, Brasil

2 Programa de Pós-graduação em Ecologia e Conservação da Biodiversidade, Departamento de Ciências Biológicas, Universidade Estadual de Santa Cruz, Rodovia Jorge Amado km 16, 45662-900, Ilhéus, Bahia, Brasil

3 Departamento de Ciências Biológicas, Universidade Estadual de Santa Cruz, Rodovia Ilhéus-Itabuna, km 16, 45662-900, Ilhéus, Bahia, Brasil

4 Museum Koenig Bonn (ZFMK), Leibniz Institute for the Analysis of Biodiversity Change, Adenauerallee 160, 53113 Bonn, North Rhine-Westphalia, Germany
Corresponding author: Kássio de Castro Araújo (kassio.ufpi@gmail.com)

Abstract

Anurans are among the most diverse groups of vertebrates globally, and environmental heterogeneity plays a key role in shaping their diversity patterns. This study aimed to update the anuran checklist of the Serra da Capivara National Park, Piauí State, northeastern Brazil, and investigate the influence of local heterogeneity on anuran abundance and richness. We recorded 16 anuran species across five families – Bufonidae, Hylidae, Leptodactylidae, Microhylidae, and Phyllomedusidae – most of which are typical Caatinga species or widely distributed taxa. Our results indicate that local heterogeneity did not significantly affect species richness; however, it had a notable impact on anuran abundance. We highlight the importance of heterogeneous habitats in supporting larger anuran populations and enhancing population stability. This study contributes to the understanding of biodiversity patterns and the primary environmental factors affecting anuran communities in Serra da Capivara National Park, offering insights to inform current and future conservation strategies.

Key words: Abundance, amphibians, biodiversity patterns, Caatinga, checklist, conservation unit, semiarid, species richness



Academic editor: Uri García-Vázquez

Received: 8 October 2024

Accepted: 31 December 2024

Published: 5 May 2025

ZooBank: <https://zoobank.org/DFCB2E97-AFB2-4F96-8912-B4F50605E17F>

Citation: Araújo KdeC, Assunção NLR, Solé M, de Andrade EB (2025) Assessing the effect of local heterogeneity on anuran diversity in the Serra da Capivara National Park, Piauí State, Brazil. ZooKeys 1236: 233–248. <https://doi.org/10.3897/zookeys.1236.138858>

Copyright: © Kássio de Castro Araújo et al. This is an open access article distributed under terms of the Creative Commons Attribution License (Attribution 4.0 International – CC BY 4.0).

Introduction

Amphibians are among the most diverse vertebrate groups, with 8827 species registered worldwide (Frost 2024). They were the first vertebrates to colonize terrestrial environments in the Devonian period, approximately 300 million years ago (Bray and Lawson 1985). Morphophysiological adaptations enabled amphibians to occupy a wide range of habitats, including aquatic, terrestrial, and arboreal environments (Vitt and Caldwell 2013), and their varied reproductive strategies (Crump 2015) have contributed significantly to the group's diversification. Most amphibian species are found in Neotropical regions (Duellman and Trueb 1994), with Brazil hosting the highest amphibian diversity worldwide, where anurans dominate in terms of species richness (Segalla et al. 2021).

Anurans play vital ecological roles, participating in various trophic interactions (Toledo et al. 2007; Ceron et al. 2019) and serving as bioindicators of environmental quality (Lebboroni et al. 2006; Calderon et al. 2019). As such, they contribute to maintaining ecosystem stability and functions (Hocking and Babbitt 2014). Anurans are present in all Brazilian biomes, including the semi-arid Caatinga biome (Garda et al. 2017) in northeastern Brazil, which, despite being historically understudied, harbors a high diversity of species. To date, 116 anuran species have been cataloged in the Caatinga, including several endemic taxa (Silva 2022).

Among the states within the Caatinga biome, Piauí is one of the few to have an anuran checklist with 54 species registered (Roberto et al. 2013). The last decade has seen a surge in herpetofaunal research in the state, primarily conducted within Conservation Units (UCs) such as National Parks (e.g., Dal-Vecchio et al. 2016; Araújo et al. 2020a; Marques et al. 2023) and Environmental Protection Areas (e.g., Andrade et al. 2016; Araújo et al. 2020b). Nevertheless, unprotected areas outside these UCs also harbor a rich anuran fauna (Benício et al. 2014, 2015). Of the 44 UCs in Piauí, herpetological studies have been conducted in only eight (Pantoja et al. 2022), and some of these are still considered under-sampled, as is the case with Serra da Capivara National Park, where only seven anuran species have been documented so far (Calvacanti et al. 2014).

Understanding the main drivers of anuran diversity is a complex task, as these animals are highly sensitive to environmental conditions (Hopkins 2007). Local habitat heterogeneity has been identified as a key factor influencing anuran diversity in otherwise homogeneous landscapes (e.g., Afonso and Eterovick 2007; Silva et al. 2011; Andrade et al. 2019; Mausberg et al. 2023), including in Piauí State (Andrade et al. 2016; Araújo et al. 2018). According to this hypothesis, more heterogeneous areas tend to support greater species diversity (MacArthur and MacArthur 1961). However, it remains unclear which specific environmental variables play the most significant role in shaping anuran diversity patterns. To address this knowledge gap, we (i) characterized the anuran fauna of Serra da Capivara National Park (SCNP), Piauí State, Brazil, and (ii) tested how local habitat heterogeneity influences anuran abundance and species richness.

Material and methods

Study area

This study was conducted in the Serra da Capivara National Park (SCNP), located in the state of Piauí, northeastern Brazil (Fig. 1). The park, established by Federal Decree No. 83.548 on June 5, 1979, spans a total area of 130,000 hectares (BRASIL 1990). Although SCNP is situated within the Caatinga biome (IBGE 2019), it is characterized by a mosaic of vegetation types with high species richness. The area includes a variety of vegetation forms, such as tall and dense shrublands, arboreal communities, medium-density woodlands, low shrublands, and mixed shrub-arboreal habitats (Lemos 2004). Rainfall is concentrated primarily between November and April, with an average annual precipitation exceeding 600 mm and a mean temperature of 26 °C (Lemos and Rodal 2002; Aquino and Oliveira 2017).

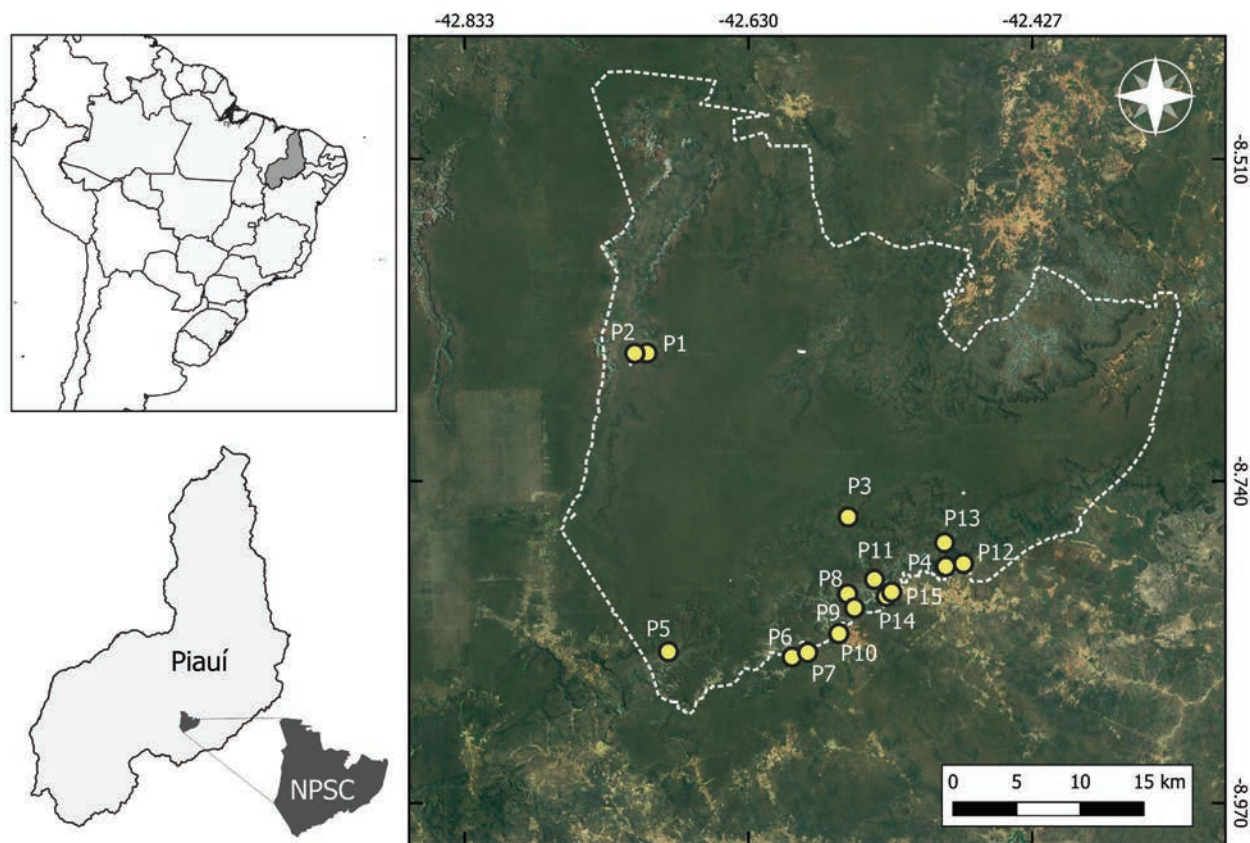


Figure 1. Geographical location of the Serra da Capivara National Park (SCNP), Piauí State, northeastern Brazil, with the distribution of the 15 sampling points.

Sampling

We conducted four expeditions, each lasting five consecutive days, from December 2023 to April 2024 in SNCP, totaling 20 sampling days. We used visual and auditory searches (Heyer et al. 1994) in different environments used by anurans within the park. A total of 15 sampling points were randomly chosen according to the vocalization activities of the anurans (Table 1). Fieldwork was carried out by five researchers, beginning at 18:00 h and concluding at 00:00 h each night. We surveyed three points per night, spending approximately 1.5 hours at each site. This resulted in a total sampling effort of 600 hours (5 researchers × 120 hours). A single voucher specimen for each species was collected and deposited in the Coleção Biológica of the Instituto Federal de Ciência e Tecnologia do Piauí, Campus Pedro II (CBPII), Piauí State, northeastern Brazil.

Environmental variables of sampling points

We measured a set of nine abiotic and biotic variables at each of the 15 sampling points (Table 2). These variables were selected as they are considered strong indicators of local heterogeneity in anuran communities (e.g., Silva et al. 2011; Araújo et al. 2018; Mausberg et al. 2023). The sampling points were distributed across different habitats: three in natural ponds, three in artificial ponds, and eight in modified ponds (Fig. 2). To minimize observer bias, all variables were consistently measured by the same researcher (NLRA).

Table 1. Environmental description of the 15 sampling points in the Serra da Capivara National Park, Piauí State, north-eastern Brazil.

Sampling points	Geographic coordinates	Description
P1	8°38.92'S, 42°42.15'W	Artificial drinking fountain surrounded by shrubs and trees
P2	8°38.93'S, 42°42.68'W	Artificial drinking fountain surrounded by shrubs and trees
P3	8°45.97'S, 42°33.52'W	Temporary pond with shrub and tree vegetation inside and on the edge of the pond
P4	8°48.07'S, 42°36.55'W	Temporary pond with shrub and tree vegetation inside and on the edge of the pond
P5	8°51.72'S, 42°41.24'W	Rocky outcrop modified to accumulate water for longer, presence of thorny shrub and tree vegetation
P6	8°51.94'S, 42°35.93'W	Artificial drinking fountain surrounded by shrubs and trees
P7	8°51.75'S, 42°35.26'W	Modified passage that accumulates water surrounded by shrubs and trees
P8	8°49.24'S, 42°33.54'W	Modified pond located inside the cave
P9	8°49.85'S, 42°33.25'W	Modified passage that accumulates water surrounded by shrubs and trees
P10	8°50.94'S, 42°33.92'W	Modified pond located inside the cave
P11	8°48.62'S, 42°32.40'W	Artificial drinking fountain surrounded by shrubs and trees
P12	8°47.94'S, 42°28.57'W	Temporary pond with shrub and tree vegetation inside and on the edge of the pond
P13	8°47.05'S, 42°29.39'W	Modified passage that accumulates water surrounded by shrubs and trees
P14	8°49.34'S, 42°31.89'W	Permanent reservoir with shrub and tree vegetation inside and on the edge of the pond
P15	8°49.16'S, 42°31.65'W	Temporary pond with shrub and tree vegetation inside and on the edge of the pond

Table 2. List of variables recorded at each sampling point within the Serra da Capivara National Park, Piauí State, north-eastern Brazil, including unit, detailed nomenclature and method.

Variable name	Definition	Unit	Method
Margin type	Pond edge characteristic	Three categories: plan (1), inclined (2) or both (3)	Visual characterization
Vegetation within the pond	Approximate percentual vegetation on pond surface	Four categories: No vegetation (0), < or = 20% (1), < or = 50% (2), > 50% (3)	Visual estimation
Types of vegetation within the pond	Characteristics of the vegetation (herbaceous, shrubby and arboreal) present in the water body	Four categories: no vegetation (0), one type of vegetation (1), two types (2), three types (3)	Visual characterization
Types of marginal vegetation	Characteristics of marginal vegetation (herbaceous, shrubby and arboreal) on the margin of the water body	Four categories: no vegetation (0), one type of vegetation (1), two types (2), three types (3)	Visual characterization
Pond localization	Characteristics of where the pond is located	Two categories: inside the cave (1), outside the cave (2)	Visual characterization
Pond number	Number of ponds present within a 200m radius of the largest pond	Three categories: one (1), two (2), more than two (3)	Visual characterization
Pond size	Surface area of the pond (m ²) when full (if there is more than one pond, it will be considered the largest)	Four categories: < or = 3 m ² (1), < or = 5 m ² (2), < or = 10 m ² (3), > 10 m ² (4)	Measured using length, width and shape
Maximum pond depth	Maximum depth (m) when full (if there is more than one pond, it will be considered the largest)	Three categories: < or = 1 m (1), < or = 2 m (2), > 2 m (3)	Measured at deepest point of water body.
Pond type	Characterized based on the level of anthropic action	artificial (1), modified (2), natural (3)	Visual characterization



Figure 2. Sampled environments in the Serra da Capivara National Park, Piauí State, northeastern Brazil **A–C** represent, respectively, artificial, modified, and natural ponds.

Statistical analyses

We used sample-based accumulation curves (Gotelli and Colwell 2001) with 1000 randomizations based on an incidence matrix to evaluate our sampling efficiency. To estimate expected species richness in SCNP, we applied the non-parametric estimators CHAO 2 and JACKKNIFE 1 (Magurran and McGill 2011), each with 100 randomizations. To compile abundance data and avoid biases in interpretation, we used the highest abundance value recorded among the four expeditions (Andrade et al. 2019).

Considering the SCNP is a UC located in the Caatinga biome, we compared the diversity of anurans registered in the present study with 13 other localities within this biome characterized by the Caatinga *sensu stricto* as the predominant plant physiognomy: Picos municipality (PICOS), Piauí State (Benício et al. 2015); Seridó Ecological Station (SERID), Rio Grande do Norte State (Caldas et al. 2016); Catimbau National Park (CATNP) and Serrita municipality (SERR), Pernambuco State (Pedrosa et al. 2014; Pereira et al. 2015); São João do Cariri (SJCA) and Cabaceiras (CABAC) municipalities, Paraíba State (Vieira et al. 2009; Leite-Filho et al. 2015; Protázio et al. 2015; Cascon and Langguth 2016); Aiuaba Ecological Station (AIUAB), Rio Salgado Basin (BHRS), Middle Jaguaribe River (JAGUA), and the municipalities of Farias Brito (FBRIT) and Itapipoca (ITAP), Ceará State (Santana et al. 2015; Ávila et al. 2017; Costa et al. 2018; Castro et al. 2018; Silva-Neta et al. 2018; Oliveira et al. 2021); and Raso da Catarina Ecological Station (RCAT) and Nordestina municipality (NORD), Bahia State (Garda et al. 2013; Leite et al. 2019). For this analysis, we constructed a matrix with presence and absence data for 43 anuran species, excluding species having an uncertain specific identification (“gr.” – group, “aff.” – affinity with a known species, and “sp.” – exact species is unknown) and considering only species with an identification to be confirmed (“cf.”). Thereafter, we performed a cluster analysis by Unweighted Pair Group Average Method (UPGAM) to illustrate the similarity between the anuran composition of the SCNP and other Caatinga areas.

We first tested the normality of the variables using the SHAPIRO-WILK test and log-transformed those that did not meet normality assumptions (Shapiro-Wilk $p < 0.05$), which applied only to species abundance data. To detect col-

linearity among the variables, we calculated the Variance Inflation Factors (VIF) and excluded any variable with a $VIF \geq 10$ (James et al. 2013), resulting in the removal of pond size from the analysis. We then constructed Generalized Linear Models (GLMs) to assess the effect of predictor variables – pond margin profile, percentage of vegetation within the pond, vegetation types within the pond, types of marginal vegetation, pond location, number of ponds at the sampling point, depth of the largest pond, and pond type – on response variables (anuran richness and abundance). Our general model was defined as: Response variable (richness or abundance) \sim predictor variables, family = poisson (link = “log”).

We then used Akaike’s Information Criterion with second-order bias correction for small samples (AICc) to compare models for each response variable alone or in combination (Burnham and Anderson 2002). We considered both $\Delta AICc$ and Akaike’s weight (w) of each model. Models with $\Delta AICc$ lower than 2 were interpreted as having the strongest support (Burnham and Anderson 2002). Statistical analyses were performed using the R packages *vegan* (Oksanen et al. 2019), *bbmle* (Bolker 2020), *dendextend* (Leonnardi et al. 2018), *factoextra* (Kassam et al. 2020), *ggplot2* (Wickham 2016), and *usdm* (Naimi 2015).

Results

We recorded a total of 551 individuals representing 16 anuran species across five families: Bufonidae ($N = 2$), Hylidae ($N = 4$), Leptodactylidae ($N = 8$), Microhylidae ($N = 1$), and Phyllomedusidae ($N = 1$) (Table 3, Fig. 3). The most abundant species were *Leptodactylus troglodytes* ($N = 77$), *Scinax x-signatus* ($N = 72$), and *Pithecopus gonzagai* ($N = 65$), while *Trachycephalus* cf. *nigromaculatus* ($N = 7$) and *Pleurodema diplolister* ($N = 1$) were the least abundant. All species are classified as “Least Concern” (LC) according to the IUCN Red List Categories and Criteria (IUCN, 2024).

The species accumulation curve indicated a strong tendency toward stabilization (Fig. 4), with observed species richness accounting for approximately 90% of the richness estimated by the non-parametric JACKKNIFE 1 estimator (17.9 ± 1.34) and about 95% of that estimated by CHAO 2 (16.9 ± 2.19). Consequently, we anticipate the discovery of at least two additional species in the study area.

We observed the formation of four clusters regarding the anuran composition of the Caatinga sensu stricto areas analyzed: the first one was formed by São João do Cariri and the Cabaceiras municipalities, Paraíba State, and the Itapipoca municipality, Ceará State. The second one is the largest cluster with seven areas within Ceará, Pernambuco, Piauí, and Rio Grande do Norte states. The anuran composition of the SCNP was more similar to those registered in the Catimbau National Park, Pernambuco State, and Nordestina municipality, Bahia State. The Raso da Catarina Ecological Station was isolated in the cluster analysis (Fig. 5).

Regarding the variables analyzed, we found that local habitat heterogeneity did not significantly influence anuran richness in SCNP ($P > 0.05$); however, it played a crucial role in explaining anuran abundance. Specifically, significant variables included margins profile (z-value = 2.907, $P = 0.003$), types of marginal vegetation (z-value = 2.304, $P = 0.021$), percentage of vegetation cover within ponds (z-value = 4.070, $P < 0.001$), number of ponds at the sampling point (z-value = 5.600, $P < 0.001$), depth of the largest pond at the sampling point (z-value = 2.991, $P = 0.002$), and type of ponds at the sampling point (z-value = -3.211, $P = 0.001$);

Table 3. Anurans registered in the Serra da Capivara National Park, Piauí State, northeastern Brazil, including voucher, occurrence in the SCNP, and distribution in the Brazilian biomes.

Taxa	Voucher	Occurrence	Biome
BUFONIDAE			
<i>Rhinella diptycha</i> (Cope, 1862)	CBP11 534	1–3, 5–11, 13–15	WD
<i>Rhinella granulosa</i> (Spix, 1824)	CBP11 536	2, 3, 5, 6, 8–12, 14, 15	WD
HYLIDAE			
<i>Corythomantis greeningi</i> Boulenger, 1896	CBP11 567	1, 6, 9, 10, 12	AT, CA, CE
<i>Dendropsophus soaresi</i> (Caramaschi & Jim, 1983)	CBP11 537	1–7, 9, 10	AT, CA, CE
<i>Scinax x-signatus</i> (Spix, 1824)	CBP11 528	1–6, 9–12, 14, 15	WD
<i>Trachycephalus cf. nigromaculatus</i> Tschudi, 1838	CBP11 558	3	AT, CA, CE
LEPTODACTYLIDAE			
<i>Leptodactylus fuscus</i> (Schneider, 1799)	CBP11 590	10, 12, 14, 15	WD
<i>Leptodactylus macrosternum</i> Miranda-Ribeiro, 1926	CBP11 583	10, 11, 13–15	WD
<i>Leptodactylus siphax</i> Bokermann, 1969	CBP11 569	2, 6, 8–11, 13	WD
<i>Leptodactylus troglodytes</i> Lutz, 1926	CBP11 526	1–15	WD
<i>Leptodactylus vastus</i> Lutz, 1930	CBP11 587	1, 3–11, 13–15	WD
<i>Physalaemus cicada</i> Bokermann, 1966	CBP11 585	11, 12, 15	–
<i>Physalaemus cuvieri</i> Fitzinger, 1826	CBP11 531	1, 3–9, 13, 14, 15	WD
<i>Pleurodema dipolister</i> (Peters, 1870)	CBP11 769	11	AT, CA, CE
MICROHYLIDAE			
<i>Dermatonotus muelleri</i> (Boettger, 1885)	CBP11 555	3, 4, 6, 7, 9, 11, 12, 15	WD
PHYLLOMEDUSIDAE			
<i>Pithecopus gonzagai</i> Andrade, Haga, Ferreira, Recco-Pimentel, Toledo & Bruschi, 2020	CBP11 548	1–6, 9–14	CA, CE

Legends: Biome distribution: Caatinga (CA), Cerrado (CE), Atlantic Forest (AT), and widely distributed (WD). See Table 1 for sampling points characterization.

Suppl. material 1: appendix S1). Furthermore, based on Akaike's Information Criterion, the model incorporating all significant variables together provided a better explanation of anuran abundance in SCNP than models considering each variable in isolation (Suppl. material 1: appendix S2).

Discussion

We identified 16 anuran species in the Serra da Capivara National Park (SCNP), which accounts for approximately 30% of the anurans known from Piauí State (Roberto et al. 2013). In addition, we recorded more than double the number of anuran species previously documented for the SCNP (Calvacanti et al. 2014). This level of species richness is considered moderate when compared to other studies conducted in areas of Caatinga sensu stricto (e.g., Pedrosa et al. 2014; Benício et al. 2015). It is interesting to highlight that the anuran composition of the SCNP was more similar to those recorded in the Catimbau National Park, Pernambuco State (Pedrosa et al. 2014) and Nordestina municipality, Bahia State (Leite et al. 2019). It is unclear why these locations are more similar, given their geographical distances. Thus, Brazilian state divisions did not seem to be predominant regarding differences in the composition of anurans in the Caatinga biome. In addition,

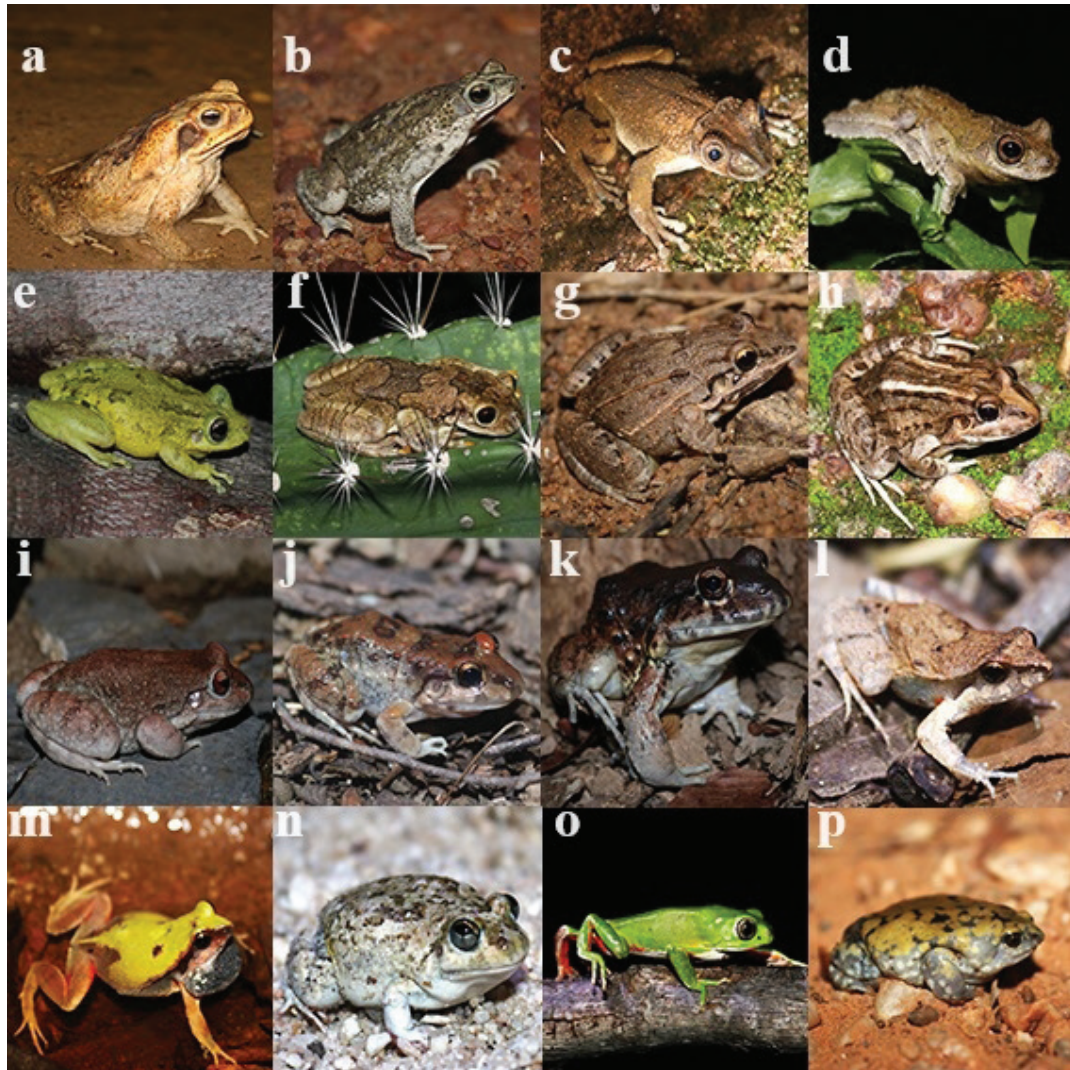


Figure 3. Anurans registered in the Serra da Capivara National Park, Piauí State, northeastern Brazil: **a** *Rhinella diptycha* **b** *Rhinella granulosa* **c** *Corythomantis greeningi* **d** *Dendropsophus soaresi* **e** *Scinax x-signatus* **f** *Trachycephalus* cf. *nigromaculatus* **g** *Leptodactylus fuscus* **h** *Leptodactylus macrosternum* **i** *Leptodactylus syphax* **j** *Leptodactylus troglodytes* **k** *Leptodactylus vastus* **l** *Physalaemus cicada* **m** *Physalaemus cuvieri* **n** *Pleurodema diplolister* **o** *Pithecopus gonzagai* **p** *Dermatoneotus muelleri*.

we suggest further studies aiming to investigate the main factors filters driving the anuran composition dissimilarity in different localities of this biome.

When focusing solely on conservation units in Piauí State, the number of species in SCNP is lower than in other protected areas, such as Uruçuí–Una Ecological Station (Dal-Vechio et al. 2013; 26 species), Sete Cidades National Park (Araújo et al. 2020a; 30 species), Serra das Confusões National Park (Marques et al. 2023; 29 species), and the Environmental Protection Area Delta do Parnaíba (Araújo et al. 2020b; 33 species). Notably, except for SCNP and Uruçuí–Una Ecological Station, all other conservation units are situated within ecotonal regions of the Caatinga and Cerrado biomes. Ecotones are typically characterized by high biodiversity (Kark 2013), which may help explain the observed variation in species richness.

In terms of anuran species composition, most species identified are considered widespread across Brazilian biomes, including *Rhinella diptycha*, *Scinax x-signatus*, *Leptodactylus fuscus*, *L. macrosternum*, *L. syphax*, *L. vastus*, *Physalaemus cuvieri*,

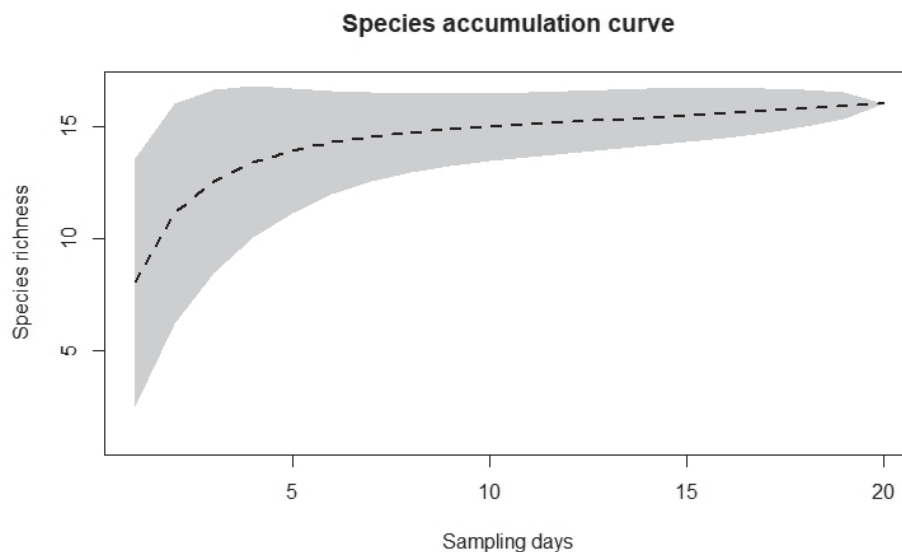


Figure 4. Accumulation curve for anurans sampled in the Serra da Capivara National Park, Piauí State, northeastern Brazil, based on the number of samples, constructed from 1000 randomizations.

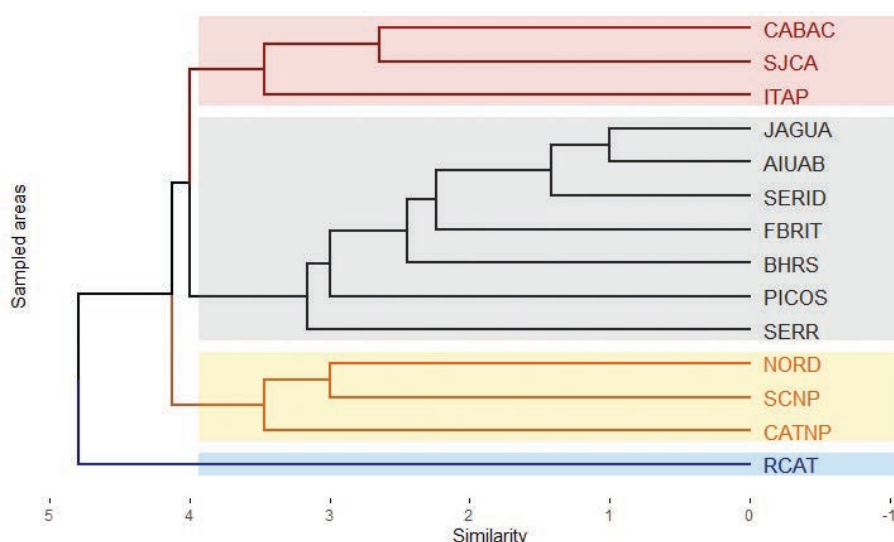


Figure 5. Similarity (Jaccard index and clustering method “UPGMA”) among the anuran species composition in areas of Caatinga sensu stricto.

and *Dermatonotus muelleri* (Frost 2024). Although we did not document any endemic species, we did encounter several species commonly associated with the Caatinga biome, such as *Corythomantis greeningi*, *Pleurodema diplolister*, *Pithecopus gonzagai*, *Physalaemus cicada*, and *Rhinella granulosa* (Garda et al. 2017).

Overall, the families Leptodactylidae and Hylidae exhibited the highest diversity within the SCNP, a pattern that is frequently observed in the Neotropical region (Duellman 1978). Similar findings have been reported in the Caatinga biome (Arzabe 1999; Vieira et al. 2007; Pedrosa et al. 2014), including various conservation units in Piauí State (e.g., Araújo et al. 2020a; Marques et al. 2023). Due to the spatial segregation between leptodactylids and hylids (Protázio et al. 2015; Leite-Filho et al. 2017; Caldas et al. 2019), anurans from these families typically coexist habitually and stably in diverse environments.

We found that anuran richness in the Serra da Capivara National Park (SCNP) was not significantly influenced by local heterogeneity, regardless of whether the sampling ponds were natural, modified, or artificial. While some studies have similarly reported a lack of support for this relationship (e.g., Vasconcelos et al. 2009; Gouveia and Faria 2015), such a pattern is atypical since more heterogeneous environments generally support higher species richness (e.g., Tews et al. 2004; Andrade et al. 2016; Lorenzón et al. 2016; Araújo et al. 2018; Piña et al. 2019), particularly among anuran communities (e.g., Silva et al. 2011; Couto et al. 2017; Andrade et al. 2016, 2019; Figueiredo et al. 2019). The absence of a relationship between richness and local heterogeneity may be attributed to the prevalence of habitat-generalist species that are typical of Caatinga environments, which are present across all sampling points. These species are adapted to explore a variety of ponds within these landscapes due to their strategies for surviving in semiarid conditions. This finding aligns with Gouveia and Faria (2015), who suggested that anurans in the Caatinga exhibit stochastic usage patterns of available water bodies.

In contrast, we observed that sampling points with a higher percentage of vegetation within the ponds and a greater diversity of marginal vegetation tended to support greater anuran abundance. Additionally, the characteristics of the ponds played a significant role in influencing anuran abundance. Other studies have similarly highlighted the impact of vegetation and pond characteristics on anuran populations (e.g., Bickford et al. 2010; Dória et al. 2015; Agostini et al. 2021). Generally, more heterogeneous areas provide greater resources (MacArthur and MacArthur 1961), which can reduce both intraspecific and interspecific competition (Morin 2011). Consequently, more heterogeneous sampling areas within the SCNP facilitate the coexistence of a higher number of individuals.

This study enhances the understanding of biodiversity in the Serra da Capivara National Park by presenting an updated anuran checklist, which may inform current and future conservation strategies. Furthermore, we found that local heterogeneity influences population sizes, emphasizing the importance of heterogeneous environments in promoting stable anuran populations. Notably, artificial drinking fountains designed to support vertebrate populations during the dry season also contribute to anuran diversity, as some species utilize these structures for reproduction and establish nearby populations. Although our study is pioneering in exploring the primary drivers of anuran diversity in the SCNP, further research is essential to deepen our understanding of the ecological processes shaping these anuran communities.

Acknowledgements

We are grateful to ICMBio for the collection license (Permit: ICMBio 87498-1). We thank the Federal Institute of Piauí for the logistical support in the field and for the use of the laboratory.

Additional information

Conflict of interest

The authors have declared that no competing interests exist.

Ethical statement

This study was approved by the Ethics Committee on the Use of Animals of the Instituto Federal do Piauí (CEUA/IFPI – 02/2024).

Funding

We are grateful to CNPq/CAPES/FAPEPI for financial support (Finance Code 001; 150013/2023-0). NLAR thanks CAPES for granting a research grant (8888.7827305/2023-00) and Programa de Pós-graduação em Ecologia e Conservação da Biodiversidade, da Universidade Estadual de Santa Cruz (PPGECB UESC) for financial support. MS acknowledges funding by CNPq through a research scholarship (309365/2019-8).

Author contributions

Conceptualization: KCA, EBA, NLRA. Data curation: EBA. Formal analysis: NLRA, MS, EBA, KCA. Investigation: KCA, NLRA, MS. Methodology: KCA, NLRA. Project administration: EBA, MS. Resources: MS. Supervision: EBA, MS. Visualization: EBA. Writing – original draft: NLRA, KCA. Writing – review and editing: EBA, KCA, MS.

Author ORCIDs

Kássio de Castro Araújo  <https://orcid.org/0000-0003-4091-8521>

Nayla Letícia Rodrigues Assunção  <https://orcid.org/0000-0002-6847-1269>

Mirco Solé  <https://orcid.org/0000-0001-7881-6227>

Etielle Barroso de Andrade  <https://orcid.org/0000-0002-5030-1675>

Data availability

All of the data that support the findings of this study are available in the main text or Supplementary Information.

References

- Afonso LG, Eterovick PC (2007) Spatial and temporal distribution of breeding anurans in streams in southeastern Brazil. *Journal of Natural History* 41(13–16): 949–963. <https://doi.org/10.1080/00222930701311680>
- Agostini G, Deutsch C, Bilenca DN (2021) Differential responses of anuran assemblages to land use in agroecosystems of central Argentina. *Agriculture, Ecosystems & Environment* 311: 107323. <https://doi.org/10.1016/j.agee.2021.107323>
- Andrade EB, Leite JRSA, Andrade GV (2016) Diversity and distribution of anuran in two islands of Parnaíba River Delta, Northeastern Brazil. *Journal of Biodiversity and Environmental Sciences* 8: 74–86.
- Andrade EB, Leite JRSA, Weber LN (2019) Composition, phenology, and habitat use of anurans in a Cerrado remnant in Northeastern Brazil. *Herpetological Conservation and Biology* 14(2): 546–559.
- Aquino CMS, Oliveira JGB (2017) Balanço hídrico climatológico e erosividade do parque nacional da serra da capivara e entorno, Piauí, Brasil. *Geoambiente* 29: 36–55. <https://doi.org/10.5216/revgeoamb.v0i29.48493>
- Araújo KC, Guzzi A, Ávila RW (2018) Influence of habitat heterogeneity on anuran diversity in Restinga landscapes of the Parnaíba River delta, northeastern Brazil. *ZooKeys* 757: 69–83. <https://doi.org/10.3897/zookeys.757.21900>
- Araújo KC, Andrade EB, Brasileiro AC, Benício RA, Sena FP, Silva RA, Santos AJS, Costa CA, Ávila RW (2020a) Anurans of Sete Cidades National Park, Piauí state, north-

- eastern Brazil. *Biota Neotropica* 20: e20201061. <https://doi.org/10.1590/1676-0611-bn-2020-1061>
- Araújo KC, Ribeiro AS, Andrade EB, Pereira AO, Guzzi A, Ávila RW (2020b) Herpetofauna of the Environmental Protection Area Delta do Parnaíba, Northeastern Brazil. *Cuadernos de Herpetología* 34: 185–199.
- Arzabe C (1999) Reproductive activity patterns of anurans in two different altitudinal sites within the Brazilian Caatinga. *Revista brasileira de Zoologia* 16: 851–864. <https://doi.org/10.1590/S0101-81751999000300022>
- Ávila RW, Almeida WDO, Ferreira FS, Gaiotti MG, Lima SMQ, Morais DH, Silva MJ (2017) Fauna da estação ecológica de Aiubá: integração de informações para subsídio de planos de conservação eo uso sustentável. *Pesquisas em Unidades de Conservação no domínio da Caatinga: subsídios a gestão*, 1st edn. Edições UFC, Fortaleza, 405–437.
- Benício RA, Silva GR, Fonseca MG (2014) Comunidade de anuros em uma área de ecótono no nordeste do Brasil. *Boletim do Museu Paraense Emílio Goeldi-Ciências Naturais* 9(3): 511–517. <https://doi.org/10.46357/bcnaturais.v9i3.507>
- Benício RA, Silva GR, Fonseca MG (2015) Anurans from a Caatinga area in state of Piauí, northeastern Brazil. *Boletim do Museu de Biologia Mello Leitão* 37(2): 207–217.
- Bickford D, Ng TH, Qie L, Kudavidanage EP, Bradshaw CJ (2010) Forest fragment and breeding habitat characteristics explain frog diversity and abundance in Singapore. *Biotropica* 42(1): 119–125. <https://doi.org/10.1111/j.1744-7429.2009.00542.x>
- Bolker BM (2020). *bbmle: Tools for general maximum likelihood estimation*. R package version 1.0.24. <https://CRAN.R-project.org/package=bbmle>
- BRASIL (1990) Decreto nº 99.143, de 12 de Março de 1990. Declara de preservação permanente a vegetação natural das áreas que descreve. *Diário Oficial da União, Brasília, DF*, 12 March, 1990. https://www.planalto.gov.br/ccivil_03/decreto/1990-1994/d99143.htm
- Bray AA, Lawson JD (1985) The evolution of the terrestrial vertebrates: environmental and physiological considerations. *Philosophical Transactions of the Royal Society of London B, Biological Sciences* 309(1138): 289–322. <https://doi.org/10.1098/rstb.1985.0088>
- Burnham KP, Anderson DR (2002) *Model selection and multimodel inference: A practical information-theoretic approach* (2nd ed.). Springer-Verlag, New York, 488 pp.
- Caldas FL, Costa TB, Laranjeiras DO, Mesquita DO, Garda AA (2016). Herpetofauna of protected areas in the Caatinga V: Seridó ecological station (Rio Grande do Norte, Brazil). *Check list* 12(4): 1–14. <https://doi.org/10.15560/12.4.1929>
- Caldas FL, Garda AA, Cavalcanti LB, Leite-Filho E, Faria RG, Mesquita DO (2019) Spatial and trophic structure of anuran assemblages in environments with different seasonal regimes in the Brazilian Northeast Region. *Copeia* 107(3): 567–584. <https://doi.org/10.1643/CH-18-109>
- Calderon MR, Almeida CA, González P, Jofré MB (2019) Influence of water quality and habitat conditions on amphibian community metrics in rivers affected by urban activity. *Urban Ecosystems* 22: 743–755. <https://doi.org/10.1007/s11252-019-00862-w>
- Calvacanti LBDQ, Borges Costa T, Colli GR, Corrêa Costa G, Rodrigues França FG, Mesquita DO, Palmeira CNS, Pelegrin NI, Soares AHB, Tucker DB, Garda AA (2014) Herpetofauna of protected areas in the Caatinga II: Serra da Capivara National Park, Piauí, Brazil. *Check List* 10(1): 18–27. <https://doi.org/10.15560/10.1.18>
- Cascon P, Langguth A (2016) Composition, reproduction, and ecological aspects of a Caatinga anurofauna in Paraíba State, Brazil. *Revista Nordestina de Zoologia* 24: 23–26.

- Castro DP, Rodrigues JFM, Lima DC, Borges-Nojosa DM (2018) Composition and diversity of anurans from rock outcrops in the Caatinga Biome, Brazil. *Herpetology Notes* 11: 189–195.
- Ceron K, Oliveira-Santos LGR, Souza CS, Mesquita DO, Caldas FL, Araujo AC, Santana DJ (2019) Global patterns in anuran–prey networks: structure mediated by latitude. *Oikos*, 128(11): 1537–1548. <https://doi.org/10.1111/oik.06621>
- Costa TB, Laranjeiras DO, Caldas FLS, Santana DO, Silva CF, Alcântara EP, Garda AA (2018) Herpetofauna of protected areas in the Caatinga VII: Aiuaba Ecological Station (Ceará, Brazil). *Herpetology Notes* 11: 929–941.
- Couto AP, Ferreira E, Torres RT, Fonseca C (2017) Local and landscape drivers of pond-breeding amphibian diversity at the northern edge of the Mediterranean. *Herpetologica* 73(1): 10–17. <https://doi.org/10.1655/HERPETOLOGICA-D-16-00020.1>
- Crump ML (2015) Anuran reproductive modes: evolving perspectives. *Journal of Herpetology* 49(1): 1–16. <https://doi.org/10.1670/14-097>
- Dal-Vechio F, Recoder R, Rodrigues MT, Zaher H (2013) The herpetofauna of the estação ecológica de uruçuí-una, state of Piauí, Brazil. *Papéis Avulsos de Zoologia* 53: 225–243. <https://doi.org/10.1590/S0031-10492013001600001>
- Dal-Vechio F, Teixeira Jr M, Recoder RS, Rodrigues MT, Zaher H (2016) The herpetofauna of Parque Nacional da Serra das Confusões, state of Piauí, Brazil, with a regional species list from an ecotonal area of Cerrado and Caatinga. *Biota Neotropica* 16: e20150105. <https://doi.org/10.1590/1676-0611-BN-2015-0105>
- Dória TA, Klein W, de Abreu RO, Santos DC, Cordeiro MC, Silva LM, Bonfim VM, Napoli MF (2015) Environmental variables influence the composition of frog communities in riparian and semi-deciduous forests of the Brazilian Cerrado. *South American Journal of Herpetology* 10(2): 90–103. <https://doi.org/10.2994/SAJH-D-14-00029.1>
- Duellman WE (1978) *The biology of an equatorial herpetofauna in Amazonian Ecuador*. University of Kansas, Lawrence, 352 pp.
- Duellman WE, Trueb L (1994) *Biology of Amphibians*. Baltimore and London, John Hopkins University Press 670 pp. <https://doi.org/10.56021/9780801847806>
- Figueiredo GDT, Storti LF, Lourenco-De-Moraes R, Shibatta OA, Anjos LD (2019) Influence of microhabitat on the richness of anuran species: a case study of different landscapes in the Atlantic Forest of southern Brazil. *Anais da Academia Brasileira de Ciências* 91(02): e20171023. <https://doi.org/10.1590/0001-3765201920171023>
- Frost DR (2024) *Amphibian Species of the World: an Online Reference*. Version 6.2 (accessed on 15 May 2024). American Museum of Natural History, New York, USA. Retrieved from <https://amphibiansoftheworld.amnh.org/index.php>
- Garda AA, Costa TB, Santos-Silva CR, Mesquita DO, Faria RG, Conceição BM, Soares da Silva IR, Ferreira AS, Rocha SM, Palmeira CNS, Rodrigues R, Ferrari SF, Torquato S (2013) Herpetofauna of protected areas in the caatinga I: Raso da Catarina Ecological Station (Bahia, Brazil). *Check list* 9(2): 405–414. <https://doi.org/10.15560/9.2.405>
- Garda AA, Stein MG, Machado RB, Lion MB, Juncá FA, Napoli MF (2017) Ecology, biogeography, and conservation of amphibians of the Caatinga. In: Cardoso da Silva JM, Leal IR, Tabarelli M (Eds) *Caatinga: The largest tropical dry forest region in South America*, Springer, Cham, 133–150. https://doi.org/10.1007/978-3-319-68339-3_5
- Gotelli NJ, Colwell RK (2001) Quantifying biodiversity: procedures and pitfalls in the measurement and comparison of species richness. *Ecology Letters* 4: 379–391. <https://doi.org/10.1046/j.1461-0248.2001.00230.x>

- Gouveia SF, Faria RG (2015) Effects of habitat size and heterogeneity on anuran breeding assemblages in the Brazilian Dry Forest. *Journal of Herpetology* 49(3): 442–446. <https://doi.org/10.1670/13-220>
- Heyer R, Donnelly MA, Foster M, McDiarmid R (1994) Measuring and monitoring biological diversity: standard methods for amphibians. Smithsonian Institution, Washington, 364 pp.
- Hocking DJ, Babbitt KJ (2014) Amphibian contributions to ecosystem services. *Herpetological conservation and biology*. 9(1): 1–17. <https://doi.org/10.1093/ilar.48.3.270>
- Hopkins WA (2007) Amphibians as models for studying environmental change. *ILAR Journal* 48(3): 270–277. <https://doi.org/10.1093/ilar.48.3.270>
- IBGE [Instituto Brasileiro de Geografia e Estatística] (2019) *Biomass e Sistema Costeiro-Marinho do Brasil. Coordenação de Recursos Naturais e Estudos Ambientais*, Rio de Janeiro, 168 pp.
- IUCN (2024) The IUCN Red List of Threatened Species. Version 2024-1. <https://www.iucnredlist.org>
- James G, Witten D, Hastie T, Tibshirani R (2013) *An introduction to statistical learning: With applications in R*. Springer. <https://doi.org/10.1007/978-1-4614-7138-7>
- Kark S (2013) Effects of ecotones on biodiversity. *Encyclopedia of biodiversity* 142: 148–149. <https://doi.org/10.1016/B978-0-12-384719-5.00234-3>
- Kassam K, Lê S, Husson F (2020) factoextra: Extract and visualize the results of multivariate data analyses. <https://cran.r-project.org/web/packages/factoextra/index.html>
- Lebboroni M, Ricchiardino G, Bellavita M, Chelazzi G (2006) Potential use of anurans as indicators of biological quality in upstreams of central Italy. *Amphibia-Reptilia* 27(1): 73–79. <https://doi.org/10.1163/156853806776052164>
- Leite AK, Oliveira MLT, Dias MA, Tinôco MS (2019) Species composition and richness of the herpetofauna of the semiarid environment of Nordestina, in northeastern Bahia, Brazil. *Biotemas* 32(4): 63–78. <https://doi.org/10.5007/2175-7925.2019v32n4p63>
- Leite-Filho E, Silva-Vieira WL, Santana GG, Eloi FJ, Mesquita DO (2015) Structure of a Caatinga anuran assemblage in Northeastern Brazil. *Neotropical Biology and Conservation* 10(2): 63–73. <https://doi.org/10.4013/nbc.2015.102.02>
- Leite-Filho E, Oliveira FA, Eloi FJ, Liberal CN, Lopes AO, Mesquita DO (2017) Evolutionary and ecological factors influencing an anuran community structure in an Atlantic Rainforest urban fragment. *Copeia*: 105(1): 64–74. <https://doi.org/10.1643/CH-15-298>
- Lemos JR (2004) Composição florística do parque nacional Serra da Capivara, Piauí, Brasil. *Rodriguésia* 55: 55–66. <https://doi.org/10.1590/2175-78602004558503>
- Lemos JR, Rodal MJN (2002) Fitossociologia do componente lenhoso de um trecho da vegetação de caatinga no Parque Nacional Serra da Capivara, Piauí, Brasil. *Acta Botanica Brasilica* 16: 23–42. <https://doi.org/10.1590/S0102-33062002000100005>
- Leonnardi N, Lê S, Husson F (2018) dendextend: an R package for visualizing, manipulating, and comparing trees of hierarchical clustering. <https://cran.r-project.org/web/packages/dendextend/index.html>
- Lorenzón RE, Beltzer AH, Olguin PF, Ronchi-Virgolini AL (2016) Habitat heterogeneity drives bird species richness, nestedness and habitat selection by individual species in fluvial wetlands of the Paraná River, Argentina. *Austral Ecology* 41(7): 829–841. <https://doi.org/10.1111/aec.12375>
- MacArthur RH, MacArthur JW (1961) On bird species diversity. *Ecology* 42(3): 594–598. <https://doi.org/10.2307/1932254>
- Magurran AE, McGill BJ (2011) *Biological diversity: frontiers in measurement and assessment*. Oxford University Press, Oxford, 384 pp.

- Marques R, Garda AA, Furtado AP, Bruinjé AC, Protázio ADS, Carvalho BF, Vieira CR, Gomes D, Pantoja DL, Figueiredo DS, Shepard DB, Camurugi F, Coelho FEA, Magalhães FM, Caetano GHO, Guarino R, Colli GR, Paulino HM, Graciene J, Alvarenga JM, Clay NA, Albuquerque RL, Furtado AP, Carvalho ITS, Bosque RJ, Faria R, Silveira-Filho RR, Mângia S, Cavalcante VHGL, Vieira WLS, Silva WP, Soares YFFS, Mesquita DO (2023) Herpetofauna of protected areas in the Caatinga VIII: An updated checklist for the Serra das Confusões region with new data from Serra Vermelha, Piauí, Brazil. *Biota Neotropica* 23: e20231520. <https://doi.org/10.1590/1676-0611-bn-2023-1520>
- Mausberg N, Dausmann KH, Glos J (2023) In search of suitable breeding sites: Habitat heterogeneity and environmental filters determine anuran diversity of western Madagascar. *Animals* 13(23): 3744. <https://doi.org/10.3390/ani13233744>
- Morin PJ (2011) *Community ecology*. Wiley-Blackwell, Hoboken, 407 pp. <https://doi.org/10.1002/9781444341966>
- Naimi B. (2015) Uncertainty analysis for species distribution models. R Package (Version 1.1-18).
- Oksanen J, Blanchet FG, Friendly M, Kindt R, Legendre P, McGlenn D, Minchin PR, O'Hara RB, Simpson GL, Solymos P, Henry M, Stevens H, Szoecs E, Wagner H (2019) *Vegan: Community Ecology Package*. R package version 2.5-6. <https://CRAN.R-project.org/package=vegan>
- Oliveira CR, Araujo KC, Oliveira HF, Ávila RW (2021) Herpetofauna from a Caatinga area at Farias Brito municipality, Ceará State, Northeastern Brazil. *Herpetology Notes* 14: 135–146.
- Pantoja DL, Andrade EB, Avila RW, Cavalcante VHGL, Colli GR, Garda AA, Mesquita DO, Rocha WA, Santana GL, Silva GF, Silva JS, Silva MB (2022) Herpetofauna das Unidades de Conservação do estado do Piauí, nordeste do Brasil. In: Ivanov MMM, Lemos JR (Eds) *Unidades de conservação do Estado do Piauí, Teresina*, 144–188.
- Pedrosa IMMDC, Costa TB, Faria RG, França FGR, Laranjeiras DO, Oliveira TCSPD, Palmeira CNS, Torquato S, Mott T, Vieira GHC, Garda AA (2014) Herpetofauna of protected areas in the Caatinga III: The Catimbau National Park, Pernambuco, Brazil. *Biota Neotropica* 14: e20140046. <https://doi.org/10.1590/1676-06032014004614>
- Pereira, EN, Teles MJL, Santos EM (2015) Herpetofauna em remanescente de Caatinga no Sertão de Pernambuco, Brasil. *Boletim do Museu de Biologia Mello Leitão* 37: 37–51.
- Piña TE, Carvalho WD, Rosalino LMC, Hilário RR (2019) Drivers of mammal richness, diversity and occurrence in heterogeneous landscapes composed by plantation forests and natural environments. *Forest Ecology and Management* 449: 117467. <https://doi.org/10.1016/j.foreco.2019.117467>
- Protázio AS, Albuquerque RL, Falkenberg LM, Mesquita DO (2015) Niche differentiation of an anuran assemblage in temporary ponds in the Brazilian semiarid Caatinga: influence of ecological and historical factors. *The Herpetological Journal* 25(2): 109–121.
- Roberto IJ, Ribeiro SC, Loebmann D (2013) Amphibians of the state of Piauí, Northeastern Brazil: a preliminary assessment. *Biota Neotropica* 13: 322–330. <https://doi.org/10.1590/S1676-06032013000100031>
- Santana DJ, Mângia S, Silveira-Filho RRD, Silva-Barros LCD, Andrade I, Napoli MF, Juncá F, Garda AA (2015) Anurans from the middle Jaguaribe River region, Ceará state, northeastern Brazil. *Biota Neotropica* 15(3), e20150017. <https://doi.org/10.1590/1676-06032015001715>
- Segalla MV, Berneck B, Canedo C, Caramaschi U, Cruz CG, Garcia PDA, ... , Langone JA (2021) List of Brazilian amphibians. *Herpetologia Brasileira* 10(1): 121–216.

- Silva JPSD (2022) Distribuição geográfica dos anfíbios na Caatinga, Nordeste do Brasil. Master's thesis, Universidade Federal do Rio Grande do Norte.
- Silva RA, Martins IA, Rossa-Feres DDC (2011) Environmental heterogeneity: Anuran diversity in homogeneous environments. *Zoologia (Curitiba)* 28: 610–618. <https://doi.org/10.1590/S1984-46702011000500009>
- Silva-Neta AF, Silva MC, Ávila RW (2018) Herpetofauna da Bacia Hidrográfica do Rio Salgado, Estado do Ceará, Nordeste do Brasil. *Boletim do Museu de Biologia Mello Leitão* 40: 23–48.
- Tews J, Brose U, Grimm V, Tielbörger K, Wichmann MC, Schwager M, Jeltsch F (2004) Animal species diversity driven by habitat heterogeneity/diversity: the importance of keystone structures. *Journal of Biogeography* 31(1): 79–92. <https://doi.org/10.1046/j.0305-0270.2003.00994.x>
- Toledo LF, Ribeiro RS, Haddad CFB (2007) Anurans as prey: an exploratory analysis and size relationships between predators and their prey. *Journal of Zoology* 271: 170–177. <https://doi.org/10.1111/j.1469-7998.2006.00195.x>
- Vasconcelos TS, Santos TD, Rossa-Feres DDC, Haddad CFB (2009) Influence of the environmental heterogeneity of breeding ponds on anuran assemblages from southeastern Brazil. *Canadian Journal of Zoology* 87(8): 699–707. <https://doi.org/10.1139/Z09-058>
- Vieira WLS, Arzabe C, Santana GG (2007) Composição e distribuição espaço-temporal de anuros no Cariri paraibano, Nordeste do Brasil. *Oecologia Brasiliensis* 11(3): 383–396. <https://doi.org/10.4257/oeco.2007.1103.08>
- Vieira WLS, Santana GG, Arzabe C (2009). Diversity of reproductive modes in anurans communities in the Caatinga (dryland) of northeastern Brazil. *Biodiversity and Conservation* 18: 55–66. <https://doi.org/10.1007/s10531-008-9434-0>
- Vitt LJ, Caldwell JP (2013) *Herpetology: an introductory biology of amphibians and reptiles*. Academic Press, San Diego, 757 pp. <https://doi.org/10.1016/B978-0-12-386919-7.00002-2>
- Wickham H (2016) *ggplot2: Elegant graphics for data analysis*. 3rd ed. New York, Springer-Verlag, 2016. <https://doi.org/10.1007/978-3-319-24277-4>

Supplementary material 1

Supplementary data

Authors: Kássio de Castro Araújo, Nayla Leticia Rodrigues Assunção, Mirco Solé, Etielle Barroso de Andrade

Data type: docx

Copyright notice: This dataset is made available under the Open Database License (<http://opendatacommons.org/licenses/odbl/1.0/>). The Open Database License (ODbL) is a license agreement intended to allow users to freely share, modify, and use this Dataset while maintaining this same freedom for others, provided that the original source and author(s) are credited.

Link: <https://doi.org/10.3897/zookeys.1236.138858.suppl1>

Mitochondrial phylogenomics of pygmy grasshoppers (Orthoptera, Tetrigidae, Metrodorinae): descriptions of a new genus, two new species, and new synonyms from China

Yuemei Li^{1,2,3}, Shixiong Leng⁴, Jiasong He⁴, Weian Deng^{1,2,3,5}, Delong Guan^{5,6}

1 Key Laboratory of Ecology of Rare and Endangered Species and Environmental Protection, Guangxi Normal University, Ministry of Education, Guilin 541006, China

2 Guangxi Key Laboratory of Rare and Endangered Animal Ecology, Guangxi Normal University, Guilin 541006, China

3 College of Life Sciences, Guangxi Normal University, Guilin 541006, China

4 Guangxi Daguishan Crocodile Lizard National Nature Reserve, Hezhou, Guangxi 542824, China

5 Guangxi Key Laboratory of Sericulture ecology and Applied intelligent technology, Hechi University, Hechi, China

6 School of Chemistry and Bioengineering, Hechi University, Yizhou, Guangxi 546300, China

Corresponding authors: Weian Deng (dengweian5899@163.com); Delong Guan (2023660006@hcnu.edu.cn)

Abstract

The Chinese wingless brachypronotal pygmy grasshoppers of the subfamily Metrodorinae have often been classified within the genus *Macromotettixoides*. In this study, two undescribed species of wingless brachypronotal pygmy grasshoppers belonging to Metrodorinae were collected. To elucidate their taxonomic positions, the complete mitochondrial genomes of these two species were sequenced and analyzed. Phylogenetic analyses were conducted using 13 protein-coding genes (PCGs) from 28 tetrigid mitogenomes. Genetic distances and divergence times were estimated. Our results indicate that one species represents a new genus within Metrodorinae, while the other is a new species of *Macromotettixoides*. Consequently, a new genus and two new species of Metrodorinae from China are described and illustrated: *Edentatettix* Deng, **gen. nov.** containing *Edentatettix leyeensis* Deng, **sp. nov.**, and *Macromotettixoides yaana* Deng, **sp. nov.** Additionally, five new synonyms are proposed: *Hainantettix angustivertex* (Zha & Peng, 2021), **syn. nov.** and *Macromotettixoides angustivertex* Zha & Peng, 2021, **syn. nov.** of *Hainantettix strictivertex* Deng, 2020; *Hyboella badagongshanensis* Zheng, 2013, **syn. nov.**, *Macromotettixoides badagongshanensis* (Zheng, 2013), **syn. nov.**, and *Macromotettixoides wuyishana* Zheng, 2013, **syn. nov.** of *Macromotettixoides jiuwan-shanensis* Zheng, Wei & Jiang, 2005. For the first time, edentate ovipositors constituting an important taxonomic character within Tetrigidae is reported and discussed.

Key words: *Macromotettixoides*, Metrodoridae, mitochondrial genome, new taxa, ovipositor, phylogeny, taxonomy

Introduction

In the highly diverse orthopteran insects, tetrigids (Orthoptera: Tetrigidae) represent a relatively ancient group of orthopteran insects. Among them, Metrodorinae Bolívar, [1887] is one of the three largest subfamilies in Tetrigidae and currently includes 105 genera containing more than 648 species distributed



Academic editor: Zhu-Qing He

Received: 4 January 2025

Accepted: 7 March 2025

Published: 5 May 2025

ZooBank: <https://zoobank.org/7B675E54-601E-42D2-8B31-91C009B6A80F>

Citation: Li Y, Leng S, He J, Deng W, Guan D (2025) Mitochondrial phylogenomics of pygmy grasshoppers (Orthoptera, Tetrigidae, Metrodorinae): descriptions of a new genus, two new species, and new synonyms from China. ZooKeys 1236: 249–281. <https://doi.org/10.3897/zookeys.1236.145914>

Copyright: © Yuemei Li et al.
This is an open access article distributed under terms of the Creative Commons Attribution License (Attribution 4.0 International – CC BY 4.0).

around the world (Deng 2016; Cigliano et al. 2024), with 16 genera (including the new genus *Edentatettix* Deng, gen. nov.) found in China. Although Metrodorinae has a wide distribution in the world, there are still many species with classification disputes due to the similarity and diversity of morphological characteristics. Since the establishment of Metrodorinae, numerous species within it have undergone transfers between genera, and the genera within the subfamily have been revised frequently (Storozhenko 2014; Tumbrinck and Telnov 2014; Tumbrinck 2019; Skejo et al. 2019; Peng et al. 2021; Kasalo 2022; Kasalo et al. 2023b).

Pygmy grasshoppers (Tetrigidae) is a taxonomic challenging group, exhibiting striking polymorphism in various morphological traits such as body color, patterns, wing lengths, and pronotum size and shape. Long et al. (2023) systematically scrutinized type specimens of pygmy grasshoppers stored in China, revealing 23 new synonyms of *Tetrix japonica* (Bolívar, 1887), indicating notable morphological diversity. Concurrently, Zhang et al. (2023) found similar variability in *Tetrix japonica* morphology throughout their life cycles. Given the complexity and variability of morphological features within Tetrigidae, relying solely on these traits often leads to recurrent classification errors, hindering the achievement of the rigorous accuracy standards required in contemporary species classification. Consequently, it is necessary to utilize molecular data as an auxiliary verification tool to ensure the accuracy of classification. In recent years, with the rapid development of high-throughput sequencing, especially the progress of whole mitochondrial genome sequencing, insect mitochondrial genomes have been widely used as a molecular marker to investigate phylogenetic relationships, biological identification, and the genetic structure of populations (Boore 1999; Cameron 2014; Song et al. 2019; Nie et al. 2021; Li et al. 2021b). Mitogenomes have greatly improved our understanding of the phylogenetics of Tetrigidae, and some scholars have begun to use these methods to answer questions about the taxonomy and phylogeny of tetrigids (Fang et al. 2010; Pavón-Gozalo et al. 2012; Lin et al. 2015; Chen et al. 2018; Adžić et al. 2020; Huang et al. 2022; Kasalo et al. 2023a).

In this study, we obtained two unknown species of wingless pygmy grasshoppers of Metrodorinae. To determine their taxonomic positions, we sequenced their mitochondrial genomes, constructed molecular phylogenetic relationships, and estimated genetic distances and divergence times. Finally, it was determined that one of them belongs to a new genus of Metrodorinae, while the other belongs to a new species of the genus *Macromotettixoides*. We establish a new genus *Edentatettix* Deng, gen. nov., characterized by the absence or degeneration of the unique saw-like teeth in the female ovipositor. *Edentatettix leyeensis* Deng, sp. nov. is described as type species. Meanwhile, *Macromotettixoides yaana* Deng, sp. nov., is described as new to science. Based on a re-examination of type specimens, we propose five critical taxonomic revisions as follows: 1) synonymization of *Hainantettix strictivertex* Deng, 2020 with *H. angustivertex* (Zha & Peng, 2021); 2) reclassification of *Macromotettixoides angustivertex* Zha & Peng, 2021 under *Hainantettix*; 3) consolidation of *Macromotettixoides jiuwanshanensis* Zheng, Wei & Jiang, 2005 with *Hyboella badagongshanensis* Zheng, 2013, *M. badagongshanensis* (Zheng, 2013), and *M. wuyishana* Zheng, 2013 based on overlapping diagnostic characters. In addition, the taxonomic significance of toothless ovipositors in Tetrigidae is discussed.

Materials and methods

Mitogenome sequencing, assembly, annotation and analysis

Total genomic DNA was extracted from muscle tissues of the hind femur using TIANamp Genomic DNA Kit (TIANGEN) and sent to Berry Genomics (Beijing, China) for genomic sequencing using Next Generation Sequencing (NGS) method. Separate 350-bp insert libraries were created from the whole genomic DNA and sequenced using the Illumina HiSeq X Ten sequencing platform. A total of 5 Gb of 150-bp paired-end (PE) reads were generated in total for each sample.

The mitochondrial genome was assembled by NOVOPlasty 4.2.1 and annotated using the MITOS2 Web Server (<http://mitos2.bioinf.uni-leipzig.de/index.py>, accessed on 17 May 2024; Donath et al. 2019). The annotated mitogenome sequences were checked in CLC Genomics Workbench 12.0.1, MEGA 11.0.13, and Geneious Prime 11.0.18. The maps of the mitogenomes were generated using the Proksee website (<https://proksee.ca>, accessed on 10 August 2024, Grant et al. 2023). The nucleotide composition of the mitogenome, PCGs, three codon positions of PCGs, tRNA genes, rRNA genes, and the control regions (CR) was computed in PhyloSuite v.1.2.3 and MEGA 11.0.13. The AT and GC skews were calculated using the formula: $AT\text{-skew} = (A - T) / (A + T)$ and $GC\text{-skew} = (G - C) / (G + C)$.

Phylogenetic analysis

To determine the phylogenetic positions of two new species in Metrodoridae, a total of 30 mitogenomes, including 28 downloaded from NCBI and two from this study were employed. *Mirhipipteryx andensis* (Ripipterygidae: Ripipteryginae) and *Ellipes minuta* (Tridactylidae: Tridactylinae) were selected as outgroups (Table 1). The analysis was performed using PhyloSuite v. 1.2.3. Redundant sequences were removed, and PCGs in the mitochondrial genome were extracted, aligned in batches, and concatenated with MAFFT (Katoh and Standley 2013). Thirteen PCGs were aligned and concatenated through the MAFFT v. 7.505 (Katoh and Standley 2013) plugin in PhyloSuite v. 1.2.3. ModelFinder v. 2.2.0 (Kalyanamoorthy et al. 2017) was used to select the best-fit model using AICc and BICc standards. The phylogenetic tree was assessed with the maximum likelihood method and the bayesian inference method. The maximum likelihood estimations with IQ-TREE v. 2.2.0 (Nguyen et al. 2015) under the Edge-linked partition model with 15,000 ultrafast bootstrap replicates (Minh et al. 2013) and Bayesian inference used MrBayes v. 3.2.7a under the GTR+F+I+G4 model (with two parallel runs, 2,000,000 generations). Genetic distances were calculated using the Tajima-Nei model based on the sequence of 13 PCGs with the bootstrap method of 1000 replications using MEGA 11.0.13.

Divergence time analysis

The divergence times were estimated using BEAST v. 1.8.4 (Drummond and Rambaut 2007; Drummond et al. 2012), and the calibration times estimated from previous studies were queried from the timetree.org website (<http://timetree.org/>, accessed on 9 December 2024; Kumar et al. 2022). The nodes of *Tetrix* and *Alulatettix* (4.35~7.98 MYA) was selected for calibration (Song et al. 2015). The parameters, including time priors and prior distributions, were set as "Yule Process" and "Normal". The range was strictly set according to the

Table 1. Accession numbers and references of the mitogenomes of Tetrigidae included in this study.

Subfamily	Species	Accession number	Reference
Batrachideinae	<i>Saussurella borneensis</i>	MZ169555	Deng et al. 2021
Tripetalocerinae	<i>Tripetaloceroides tonkinensis</i>	MW770353	Zhang et al. 2021
Scelimeninae	<i>Eucriotettix oculatus</i>	MT162546	Li et al. 2021a
	<i>Loxilobus prominenculus</i>	MT162545	Li et al. 2021b
Metrodorinae	<i>Bolivaritettix sikkinensis</i>	KY123120	Yang et al. 2017b
	<i>Bolivaritettix yuanbaoshanensis</i>	KY123121	Yang et al. 2017b
	<i>Bolivaritettix lativertex</i>	MN083173	Chang et al. 2020
	<i>Macromotettixoides maoershanensis</i>	OR030790	Luo et al. 2024
	<i>Macromotettixoides brachycorna</i>	OR003899	Luo et al. 2024
	<i>Macromotettixoides orthomargina</i>	OR030789	Luo et al. 2024
	<i>Macromotettixoides yaana</i> Deng, sp. nov.	PQ826485	This study
	<i>Edentatettix leyeensis</i> Deng, sp. nov.	PQ826484	This study
	<i>Systolederus spicupennis</i>	MH791445	Yang 2017a
	<i>Teredorus bashanensis</i> = <i>Systolederus bashanensis</i> (Devriese & Husemann, 2023)	MZ041208	Li et al. 2021c
	<i>Teredorus anhuiensis</i> = <i>Systolederus anhuiensis</i> (Devriese & Husemann, 2023)	NC_071822	Unpublished
	<i>Teredorus guangxiensis</i> = <i>Systolederus zhengi</i> (Devriese & Husemann, 2023)	NC_082935	Guan et al. 2024
	<i>Teredorus hainanensis</i> = <i>Systolederus hainanensis</i> (Devriese & Husemann, 2023)	NC_063117	Li et al. 2021c
	<i>Teredorus nigropennis</i> = <i>Systolederus nigropennis</i> (Devriese & Husemann, 2023)	MN938922	Li et al. 2020b
Tetriginae	<i>Coptotettix longtanensis</i>	OK540319	Unpublished
	<i>Coptotettix longjiangensis</i>	KY798413	Lin et al. 2017
	<i>Euparatettix tridentatus</i>	NC_082933	Guan et al. 2024
	<i>Euparatettix variabilis</i>	NC_046542	Chang et al. 2020
	<i>Euparatettix bimaculatus</i>	NC_046541	Chang et al. 2020
	<i>Exothotettix guangxiensis</i>	NC_082934	Guan et al. 2024
	<i>Formosatettix qinlingensis</i>	KY798412	Lin et al. 2017
	<i>Alulatettix yunnanensis</i>	NC_018542	Xiao et al. 2012a
	<i>Tetrix japonica</i>	NC_018543	Xiao et al. 2012b
	<i>Tetrix ruyuanensis</i> = <i>Tetrix japonica</i> (Long et al., 2023)	NC_046412	Chang et al. 2020
	Outgroup	<i>Mirhipipteryx andensis</i>	NC_028065
<i>Ellipes minuta</i>		NC_014488	Sheffield et al. 2010

queried calibration times. The uncorrelated relaxed clock model was selected with the relaxed distribution set as lognormal, and the same partition generated from the IQ-TREE was adopted. Finally, the MCMC generations and burn-ins were set as 10 million and 10%, respectively. The generated trees were imported into the Treeannotator to yield a consensus tree. The resulting phylogenetic tree was viewed and edited in ChiPlot (v. 2.6.1) (<https://www.chiplot.online/>, accessed on 10 December 2024; Xie et al. 2023).

Taxonomy, nomenclature, terminology, and measurements

Taxonomy follows the Orthoptera Species File [OSF] (Cigliano et al. 2024), a database of Orthoptera taxonomy. Nomenclature follows the International Code of the Zoological Nomenclature (ICZN 1999). Morphological terminology and landmark-based measurement methods followed those used by Zheng (2005a), Deng et al. (2007), Tumbrinck and Telnov (2014), Tumbrinck (2019),

Tan and Artchawakom (2015), Muhammad et al. (2018), and Zha et al. (2017). Measurements are given in millimeters (mm). Grasshopper specimens were examined using a Motic-SMZ-168 stereo-microscope and photographed using a KEYENCE VHX-600 Digital Microscope (Keyence Corporation, Osaka, Japan). All images were processed with Adobe Photoshop 24.0.0. The distribution map was prepared by ArcMap 10.8.1 and edited in Adobe Photoshop 24.0.0.

The species of *E. leyeensis* Deng, sp. nov. was collected from Wutaishan Forest Park, Leye County, Guangxi Province, China (24°51'11"N, 106°32'17"E) on 23 August 2021 by Wei-An Deng. Specimens of *M. yaana* Deng, sp. nov. were collected from Longdong (Ganyanggou), Baoxing County, Yaan City, Sichuan Province, China (30°24'19"N, 102°35'45"E) on 2 August 2016 by Wei-An Deng. The collected specimens were preserved in 100% anhydrous ethanol and stored in the refrigerator at -20 °C at the College of Life Science, Guangxi Normal University, Guilin, China (CLSGNU).

Type specimen depositories

The specimens examined in this study, including all holotypes and paratypes, have been deposited in the following institutions:

- CLSGNU** College of Life Science, Guangxi Normal University, Guilin, China;
EMHU Entomological Museum of Hechi University, Hechi, China;
IZSNU Institute of Zoology, Shaanxi Normal University, Xi'an, China;
HNU Huaibei Normal University, Huaibei, Anhui, China.

Results

Mitogenome characteristics of *E. leyeensis* Deng, sp. nov. and *M. yaana* Deng, sp. nov.

Genome organization and nucleotide composition

The mitogenomes of *E. leyeensis* Deng, sp. nov. and *M. yaana* Deng, sp. nov. are circularized, with sizes of 15,813 bp and 16,379 bp, respectively (Fig. 1). Both mitogenomes contain 13 PCGs, 22 tRNAs, 2 rRNA (*rrnS* and *rrnL*), and a control region. Most genes (9 PCGs and 14 tRNA genes) were encoded on the majority strand (J-strand), and the rest of the genes (4 PCGs, 8 tRNAs, and 2 rRNAs) were located on the minority strand (N-strand) (Table 2).

The AT-skew and nucleotide composition of the mitogenomes of *E. leyeensis* Deng, sp. nov. and *M. yaana* Deng, sp. nov. are shown in Table 3. With asymmetric nucleotide composition (*E. leyeensis* Deng, sp. nov.: 42.4% A, 30.2% T, 17.7% C, and 9.8% G; *M. yaana* Deng, sp. nov.: 44.3% A, 30.2% T, 16.5% C, and 9.3% G) and A+T-biased (*E. leyeensis* Deng, sp. nov.: 72.6%; *M. yaana* Deng, sp. nov.: 74.2%). This nucleotide composition pattern is consistent with other species of Tetrigidae (Xiao et al 2012a; Zhang et al 2021). The AT skews of *E. leyeensis* Deng, sp. nov. and *M. yaana* Deng, sp. nov. are 0.169 and 0.194, respectively, and the CG skews are -0.287 and -0.276, respectively. The AT-skew is positive, and the CG skew is negative. This shows that the content of bases C is higher than that of G, and A is higher than T in the whole (Table 3).

Table 2. Mitochondrial genome organization of *E. leyeensis* Deng, sp. nov. and *M. yaana* Deng, sp. nov.

Genes	Strand	Anticodon	Location	Length (bp)	Intergenic nucleotides	Start codon	Stop codon
<i>trnI</i>	J	GAT	1–64/1–65	64/65	0/.	–	–
<i>trnQ</i>	N	TTG	66–134/.	69/.	1/.	–	–
<i>trnM</i>	J	CAT	134–201/134–205	68/72	-1/.	–	–
<i>nad2</i>	J	–	202–1209/221–1216	1008/996	0/15	ATG/ATT	TAA/.
<i>trnW</i>	J	TCA	1208–1272/1215–1282	65/68	-2/.	–	–
<i>trnC</i>	N	GCA	1265–1326/1275–1338	62/64	-8/.	–	–
<i>trnY</i>	N	GTA	1327–1389/1339–1402	63/64	0/.	–	–
<i>cox1</i>	J	–	1387–2925/1400–2938	1539/.	-3/.	ATC/.	TAA/.
<i>trnL2</i>	J	TAA	2921–2983/2934–2997	63/64	0/-5	–	–
<i>cox2</i>	J	–	2985–3662/2999–3682	678/684	1/.	ATG/.	TAA/.
<i>trnD</i>	J	GTC	3666–3728/3682–3744	63/.	3/-1	–	–
<i>trnK</i>	J	CTT	3732–3797/3746–3811	67/66	2/1	–	–
<i>atp8</i>	J	–	3797–3958/3815–3973	162/159	-1/3	ATA/ATG	TAA/.
<i>atp6</i>	J	–	3952–4623/3967–4638	672/.	-7/.	ATG/.	TAA/.
<i>cox3</i>	J	–	4623–5411/4638–5444	789/807	-1/.	ATG/.	TAA/.
<i>trnG</i>	J	TCC	5411–5473/5428–5489	63/62	-1/-17	–	–
<i>nad3</i>	J	–	5474–5827/5490–5843	354/.	0/.	ATT/.	TAG/.
<i>trnA</i>	J	TGC	5826–5892/5842–5906	67/65	-2/.	–	–
<i>trnR</i>	J	TCG	5892–5953/5906–5965	62/60	-1/.	–	–
<i>trnN</i>	J	GTT	5954–6017/5966–6032	64/67	0/.	–	–
<i>trnS1</i>	J	GCT	6018–6081/6033–6099	64/67	0/.	–	–
<i>trnE</i>	J	TTC	6082–6145/6100–6163	64/.	0/.	–	–
<i>trnF</i>	N	GAA	6144–6207/6162–6223	64/62	-2/.	–	–
<i>nad5</i>	N	–	6208–7930/6224–7946	1723/.	0/.	ATG/.	T(AA)/.
<i>trnH</i>	N	GTG	7933–7996/7951–8015	64/65	2/4	–	–
<i>nad4</i>	N	–	7996–9315/8015–9340	1320/1326	-1/.	ATA/ATG	TAG/.
<i>nad4l</i>	N	–	9315–9602/9334–9624	288/291	-1/-7	ATT/.	TAA/.
<i>trnT</i>	J	TGT	9605–9666/9627–9688	62/.	2/.	–	–
<i>trnP</i>	N	TGG	9667–9729/9689–9755	63/67	0/.	–	–
<i>nad6</i>	J	–	9740–10225/9769–10248	486/480	10/13	ATT/ATA	TAA/.
<i>cob</i>	J	–	10225–11361/10248–11387	1137/1140	-1/.	ATG/.	TAA/.
<i>trnS2</i>	J	TGA	11370–11434/11386–11452	65/67	8/-2	–	–
<i>nad1</i>	N	–	11450–12491/11811–12749	942/945	115/358	ATT/.	TAA/.
<i>trnL1</i>	N	TAG	12492–12555/12750–12813	64/.	0/.	–	–
<i>rrnL</i>	N	–	12560–13852/12815–14099	1293/1285	4/1	–	–
<i>trnV</i>	N	TAC	13857–13924/14103–14170	68/.	4/3	–	–
<i>rrnS</i>	N	–	13923–14657/14170–14913	735/744	-2/-1	–	–
CR	–	–	14658–15813/14914–16379	1156/1466	–	–	–

Note: “H” indicates the majority strand and “L” indicates the minority strand.

Protein-coding genes and codon usage

The mitogenomes of both *E. leyeensis* Deng, sp. nov. and *M. yaana* Deng, sp. nov. contain 13 PCGs, with *nad5* being the longest and *atp8* being the shortest. The total length of the 13 PCGs in *E. leyeensis* Deng, sp. nov. and *M. yaana* Deng, sp. nov. are 11,098 bp and 11,116bp, respectively, approximately accounting for 70.18% and 67.87% of the whole mitogenome, respectively (Table 2). Nine of the 13 PCGs are encoded on the J-strand (*cox1*, *cox2*, *cox3*, *cytb*, *nad2*, *nad3*, *nad6*, *atp6*, *atp8*),

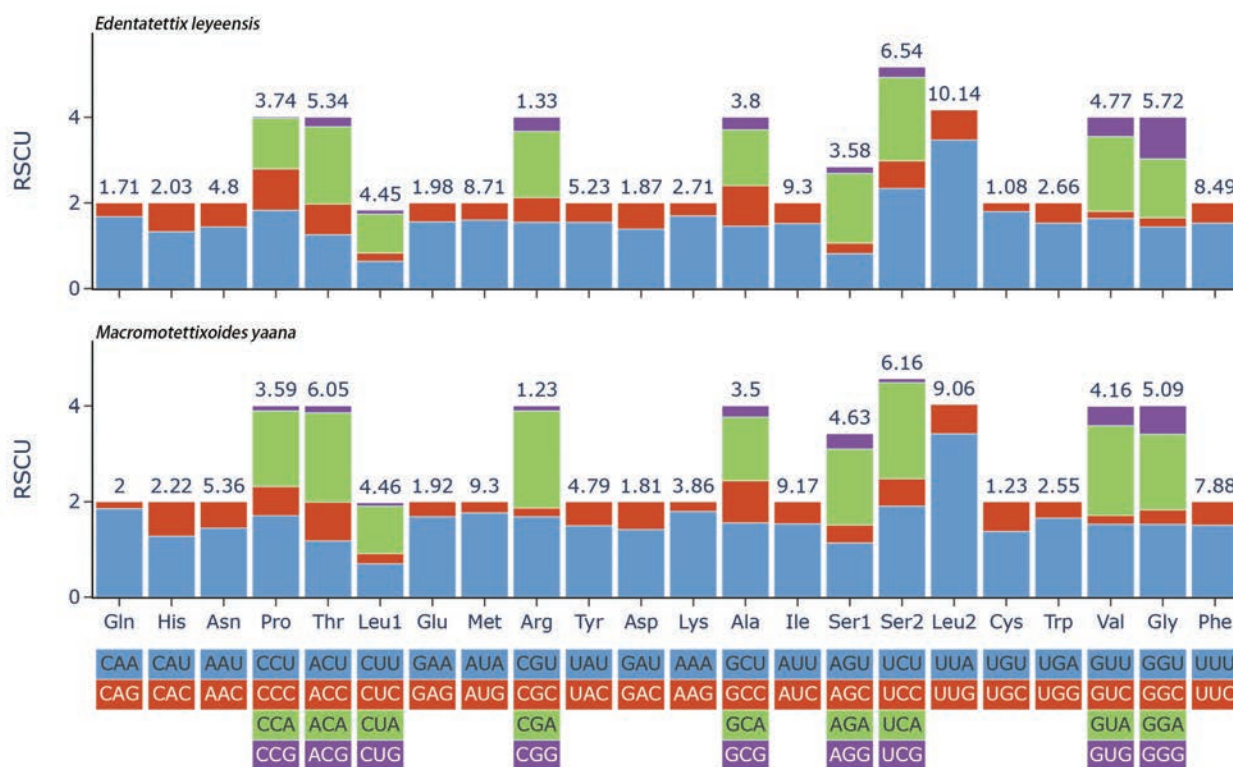


Figure 2. Relative synonymous codon usage (RSCU) in the mitogenomes of *E. leyeensis* Deng, sp. nov. and *M. yaana* Deng, sp. nov.

and A+T-rich region. The total AT-skew of *E. leyeensis* Deng, sp. nov. and *M. yaana* Deng, sp. nov. in rRNA are -0.220 and 0.272, respectively. The total GC-skew of *E. leyeensis* Deng, sp. nov. and *M. yaana* Deng, sp. nov. in rRNA are 0.319 and -0.332, respectively. All tRNA genes could be folded into the typical clover-leaf structure, except *trnS1* and *trnV*, which lacked the dihydrouridine (DHU) arm (Fig. 3).

Phylogenetic analysis

We constructed maximum likelihood (ML) and Bayesian inference (BI) trees based on the sequences of 13 PCGs from the mitochondrial genomes of 28 species from five subfamilies (Tetriginae, Metrodorinae, Scelimeninae, Tripetalocerinae, and Batrachideinae) of Tetrigidae and two outgroup species with the best partition schemes (Table 1). All phylogenetic analyses used the same data matrices, yet different methods yielded the same topology. Similar topologies were obtained from BI and ML trees (Fig. 4).

In this study, ML and BI trees had the same topological structures, and both phylogenies revealed the non-monophyletic relationships among species of the subfamily Metrodorinae. Tetrigidae was retrieved as monophyletic with strong support (posterior probability, PP = 1). However, only one species' datum was available for Batrachideinae, and Tripetalocerina, making it impossible to determine their monophyly.

The results of phylogeny analysis conducted by ML and BI methods are as follows: (Batrachideinae + (Tripetalocerinae + ((Scelimeninae + Metrodorinae) + (Metrodorinae + (Metrodorinae + Tetriginae))))). *Saussurella borneensis*

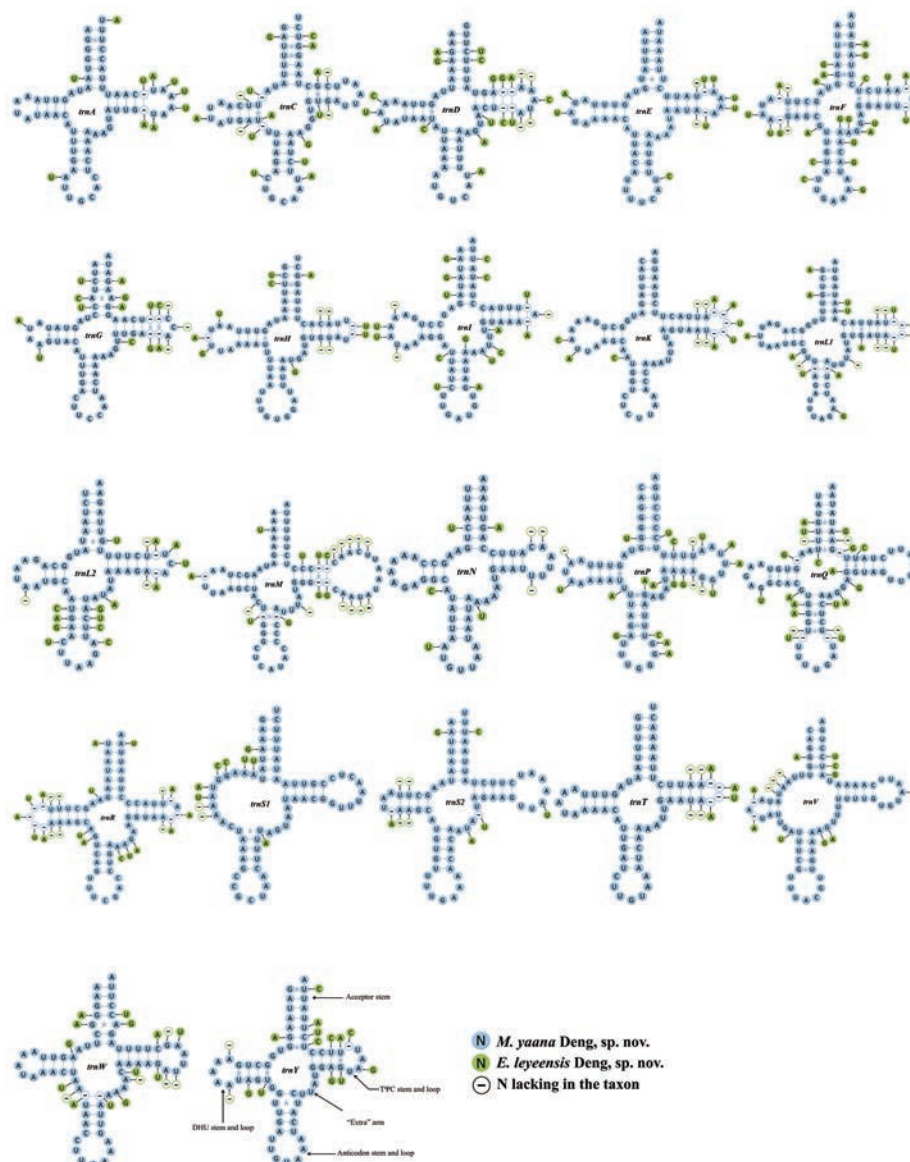


Figure 3. The secondary structures for 22 tRNA genes of *E. leyeensis* Deng, sp. nov. and *M. yaana* Deng, sp. nov. Watson-Crick base pairings and mismatches are represented by dashes (–) and stars, respectively.

Hancock, 1912 (Batrachideinae) split off earliest from the other taxa, suggesting that it is the earliest species within Tetrigidae. The subfamily Tetriginae represented the most evolutionarily advanced group within Tetrigidae, while the subfamily Metrodorinae occupied an intermediate position. These findings are consistent with previous studies (Chen 2005; Lin et al. 2015; Wang 2022). Although *E. leyeensis* Deng, sp. nov. bears a striking morphological similarity to species of *Macromotettixoides*, both belonging to wingless pygmy grasshoppers of the Metrodorinae, phylogenetic evidence does not justify classifying *E. leyeensis* within *Macromotettixoides*. Instead, it constitutes a separate new genus, namely *Edentatettix* Deng, gen. nov. Furthermore, another new species *M. yaana* Deng, sp. nov. forms a sister-group relationship with *Macromotettixoides orthomargina* Wei & Deng, 2023, which is strongly supported (PP = 1), confirming that *M. yaana* Deng, sp. nov. belongs to *Macromotettixoides*.

to 0.200, which were greater than the interspecific distance (0.004), confirming that *M. yaana* Deng, sp. nov. is a separate species. Furthermore, the genetic distances between *E. leyeensis* Deng, sp. nov. and the other 27 species ranged from 0.403 to 0.582, which is significantly greater than the intergeneric genetic distances observed in *Systolederus* (0.018–0.360), *Bolivaritettix* (0.053–0.096), *Euparatettix* (0.133–0.227), and *Macromotettixoides* (0.087–0.228). Therefore, despite morphological similarities to species like *Macromotettixoides*, the genetic distances indicate that *E. leyeensis* Deng, sp. nov. warrants classification in a new genus.

Divergence time analysis

Divergence time analysis shows that Metrodorinae appeared around 120.52 Mya (Fig. 6). This analysis also identifies considerable variability in the timings of differentiation across diverse genera within this subfamily. For example, the new genus *Edentatettix* Deng, gen. nov. can be traced back to approximately 112.23 Mya, which is close to the estimated split time of Metrodorinae. The early divergence of this genus may indicate distinct adaptive shifts in its evolutionary history, leading to the development of unique ecological niches and morphological characteristics. Additionally, *Tetrix japonica*, with a divergence timescale of approximately 0.71 Mya, represents one of the most recently evolved species in Tetrigidae. It also exhibits the broadest global distribution among its relatives, reflecting its remarkable adaptability and ecological success.

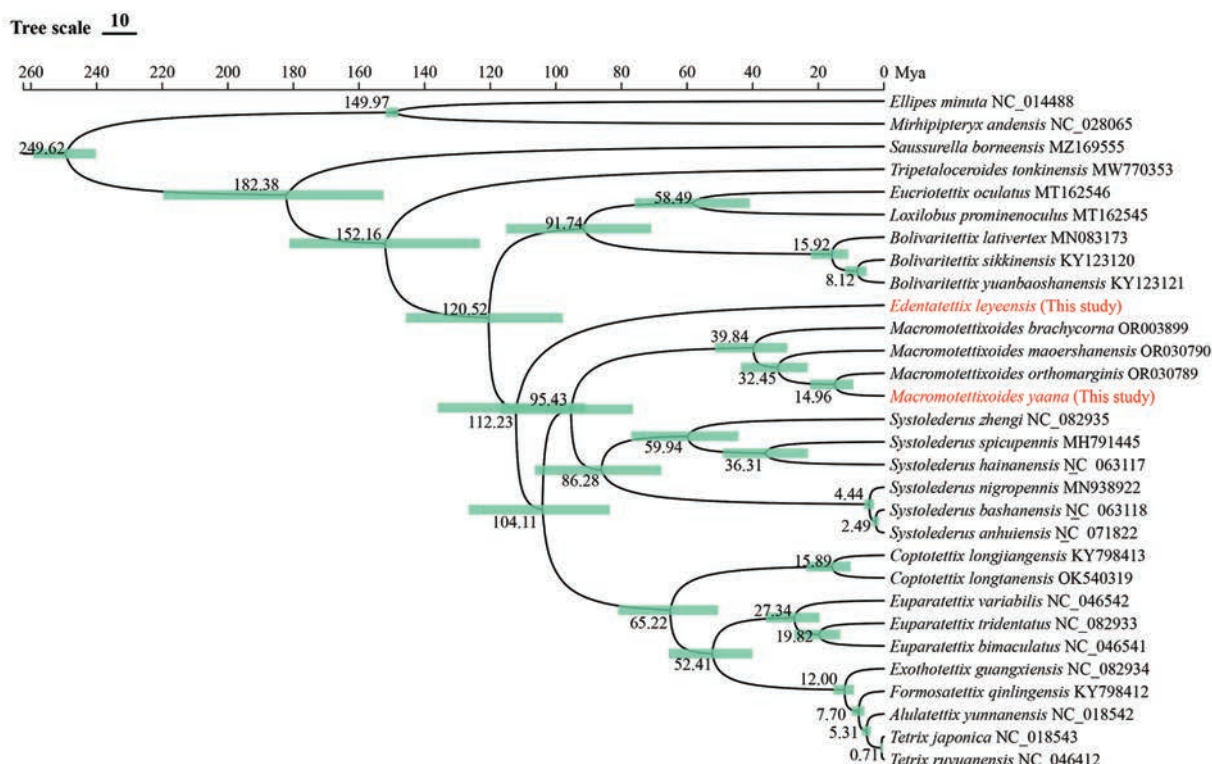


Figure 6. Dated phylogenetic tree of Tetrigidae based on the PCGs dataset. A time scale is provided. Mya refers to one million years ago.

Taxonomy of the subfamily Metrodorinae Bolívar, 1887

Key to the Chinese genera of Metrodorinae Bolívar, 1887

Modified from Lu and Deng (2021), Metrodorinae currently includes 16 genera in China (including the new genus *Edentatettix* Deng, gen. nov.).

- 1 Fastigium of the vertex distinctly projecting before anterior margin of compound eyes.....**2**
 - Fastigium of the vertex not or slightly projecting before anterior margin of compound eyes **4**
- 2 Fastigium of the vertex calyptriform protruding before anterior margin of compound eyes ***Calyptraeus* Wang, 2001**
 - Fastigium of the vertex angular projecting or square projecting **3**
- 3 Fastigium of the vertex angular projecting; antennal grooves inserted between inferior margin of compound eyes ***Rhopalotettix* Hancock, 1910**
 - Fastigium of the vertex square projecting; antennal grooves inserted at lowest third of compound eyes height..... ***Miriatoroides* Zheng & Jiang, 2002**
- 4 Saw-like teeth of female ovipositor absent or degenerate ***Edentatettix* Deng, gen. nov.**
 - Saw-like teeth of female ovipositor present **5**
- 5 With a distinct obtuse projection under each lateral carina of prozona; pronotum platy, in dorsal view, dorsum of pronotum with irregular concavities ***Concavetettix* Deng, 2021**
 - Without obtuse projection under each lateral carina of prozona; pronotum tectiform..... **6**
- 6 Vertex narrow, still narrower towards front, eyes drawn to each other in front and elevated..... ***Systolederus* Bolívar, 1887**
 - Vertex not as above..... **7**
- 7 Posterior margins of each lateral lobes of pronotum only with ventral sinus ***Macromotettixoides* Zheng, Wei & Jiang, 2005**
 - Posterior margins of each lateral lobe of pronotum with ventral sinus and tegminal (upper) sinus **8**
- 8 Humeral apex ridge and lower margin of pronotum connected in the middle or behind middle of lower margin of pronotum..... ***Macromotettix* Günther, 1939**
 - Humeral apex ridge and lower margin of pronotum connected before middle of lower margin of pronotum..... **9**
- 9 Tegmina present and hind wings absent ***Paramphinotus* Zheng, 2004**
 - Tegmina and hind wings present **10**
- 10 Ventral margins of fore femora and middle femora with two big teeth..... ***Orthotettixoides* Zheng, 1998**
 - Ventral margins of fore femora and middle femora without big teeth **11**
- 11 Head and eyes not exerted above pronotal surface **12**
 - Head and eyes distinctly exerted above pronotal surface..... **13**
- 12 Anterior part of pronotum strongly widened, arched and uplifted ***Hyboella* Hancock, 1915**
 - Anterior part of pronotum normal and strongly widened ***Bolivaritettix* Günther, 1939**

- 13 Antennal grooves inserted far below inferior margin of compound eyes **14**
– Antennal grooves inserted at lowest third of compound eye height or between inferior margin of compound eyes **15**
- 14 The vertex horn is distinctly raised above the dorsal margin of eyes and the vertex is deeply depressed between eyes in frontal view; pronotum between the shoulders is not elevated to an obtuse gibbosity ***Xistra* Bolívar, 1887**
– In frontal view, the vertex horn slightly raised above the dorsal margin of eyes (or not) and the vertex is slightly depressed (or not depressed) between eyes; pronotum between the shoulders generally strongly elevated to an obtuse gibbosity ***Xistrella* Bolívar, 1909**
- 15 Antennal grooves inserted at lowest third of compound eye height; median carina of pronotum with a series of projections
..... ***Cotysoides* Zheng & Jiang, 2000**
– Antennal grooves inserted between inferior margin of compound eyes; median carina of pronotum generally straight or undulated ... ***Mazarredia* Bolívar, 1887**

Descriptions

Genus *Edentatettix* Deng, gen. nov.

<https://zoobank.org/A21EDA29-0040-4AF1-B899-87A4DB4D19DF>

Type species. *Edentatettix leyeensis* Deng, sp. nov., here designated.

Diagnosis. The new genus can be easily distinguished from other genera of Metrodorinae by the saw-like teeth of the female ovipositor absent (Fig. 8G). *Edentatettix* is allied to *Macromotettixoides* Zheng, Wei & Jiang, 2005, but differs as follows: head and eyes slightly exserted above pronotal surface (not exserted in *Macromotettixoides*), dorsal surface of pronotum low and flat and tectiform is not obvious (distinctly tectiform in *Macromotettixoides*), saw-like teeth of female ovipositor absent (present in *Macromotettixoides*). *Edentatettix* is also similar to *Concavetettix* Deng, 2021 but differs from the latter by the obtuse projection under each lateral carina of the prozona absent (present in *Concavetettix*), dorsum of pronotum flat and slightly depressed in the middle part between the shoulders (dorsum of pronotum with irregular concavities in *Concavetettix*), saw-like teeth of female ovipositor absent (present in *Concavetettix*).

Description. General characters and coloration. Size small, brachypronotal. Coloration uniformly brown, antennae and face dark brown, middle of the dorsal surface of pronotum with a dark spot. Body surface is interspersed with sparse carinae and notches.

Head. Head and eyes slightly exserted above pronotal surface. Fastigium of vertex short; in dorsal view, width of vertex between eyes 1.5–1.6× width of compound eye. In lateral view, frontal ridge and vertex forming a rounded-angle shape and slightly projected inferior margin of the compound eye, frontal costa distinctly concave between lateral ocelli. In frontal view, frontal costa bifurcated above lateral ocelli, the bifurcation of the frontal costa in the middle of the compound eye height; width of longitudinal furrow of frontal ridge narrower than antennal groove diameter. Antennae short, filiform, antennal grooves inserted below inferior margin of compound eyes. Eyes globose, lateral (paired) ocelli located lowest third of compound eye height.

Thorax. Dorsal surface of pronotum low and flat and tectiform is not obvious; pronotal surface interspersed with sparse carinae and notches between shoulders and behind the middle, slightly depressed in the middle part between the shoulders. Pronotum with truncate anterior margin, median carina entire and nearly straight in profile; lateral carinae of prozona parallel; humeral angle obtuse; with interhumeral carina; hind pronotal process narrow, nearly reaching apex of hind femur and its apex narrowly rounded. Posterior angles of lateral lobes produced outwards, end of posterior angles truncate, posterior margins of lateral lobes of pronotum only with ventral sinus. Tegmina and hind wings invisible.

Legs. Fore and middle femora slightly compressed, margins finely serrated and carinate and ventral margins slightly undulated. Hind femora robust and short, 2.8× as long as wide; with carinated. Length of first segment of posterior tarsi equal to third.

Abdomen. Female ovipositor narrow and long, dorsal margins of upper valvulae and ventral margins of lower valvulae without saw-like tooth or saw-like teeth indistinct (Fig. 8G).

Etymology. The generic epithet is derived from *edent*, referring to the absent saw-like teeth of female ovipositor (Fig. 8G).

***Edentatettix leyeensis* Deng, sp. nov.**

<https://zoobank.org/8DCD114B-F272-41D3-9C83-0426CD226421>

Figs 7–9

Type material. Holotype • ♀, CHINA, Guangxi Prov., Leye county (Wutaishan Forest Park), 24°51'11"N, 106°32'17"E, 1200 m alt., 23 August 2021, collected by Wei-An Deng, CLSGNU. **Paratypes** • 2♂, 5♀, same data, CLSGNU • 3♂, 6♀, same data, 18 August 2022, collected by Wei-An Deng and Yue-Mei Li, CLSGNU.

Diagnosis. As there is only one species in the genus, see the generic diagnosis.

Description. Female. Small size, short, body surface interspersed with sparse carinae and notches.

Head. Head and eyes slightly exserted above pronotal surface. Fastigium of vertex short; in dorsal view, width of vertex between eyes 1.5–1.6× width of compound eye; anterior margin of fastigium arched and not surpassing anterior margin of eye; median carina visible; lateral margins turned backward; vertex uneven with paired fossulae. In lateral view, frontal ridge and vertex forming a rounded-angle shape and slightly projected inferior margin of the compound eye, frontal costa distinctly concave between lateral ocelli, protruding anteriorly and broadly rounded between antennal grooves. In frontal view, frontal costa bifurcated above lateral ocelli, the bifurcation of the frontal costa in the middle of the compound eye height; longitudinal furrow widely divergent between antennae, width of longitudinal furrow of frontal ridge narrower than antennal groove diameter. Antennae short, filiform, antennal grooves inserted below inferior margin of compound eyes, 15-segmented; the 10th and 11th segment are the longest, ~ 7.0–8.0× longer than its width. Eyes globose, lateral (paired) ocelli located lowest third of compound eye height.

Thorax. Brachypronotal. Dorsal surface of pronotum low and flat and tectiform is not obvious; pronotal surface interspersed with sparse carinae and notches between shoulders and behind the middle, slightly depressed in the middle part between the shoulders. Pronotum with truncate anterior margin,

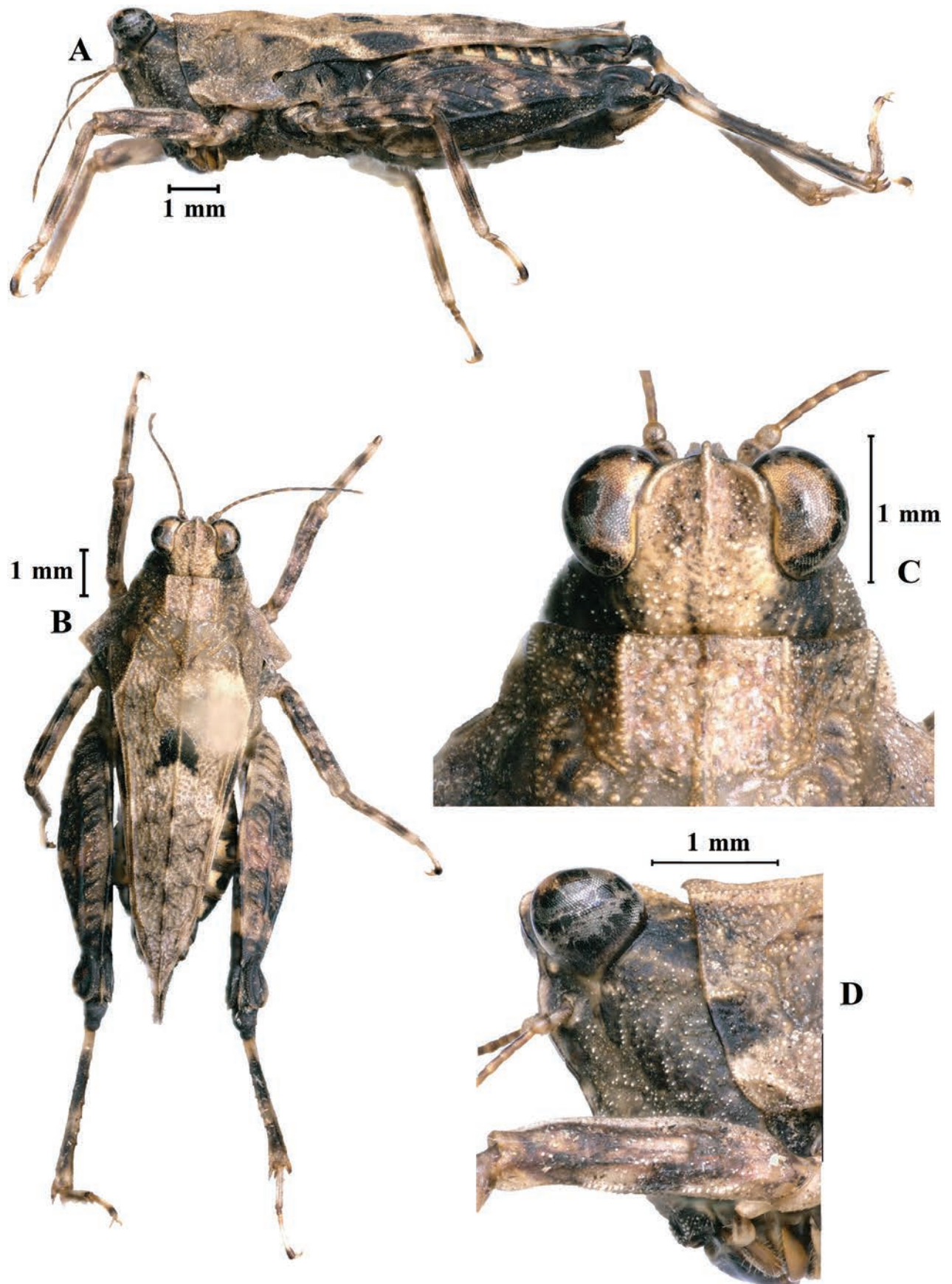


Figure 7. *E. leyeensis* Deng, sp. nov., holotype female **A** body, lateral view **B** the same, dorsal view **C** head and anterior part of pronotum, dorsal view **D** the same, lateral view.

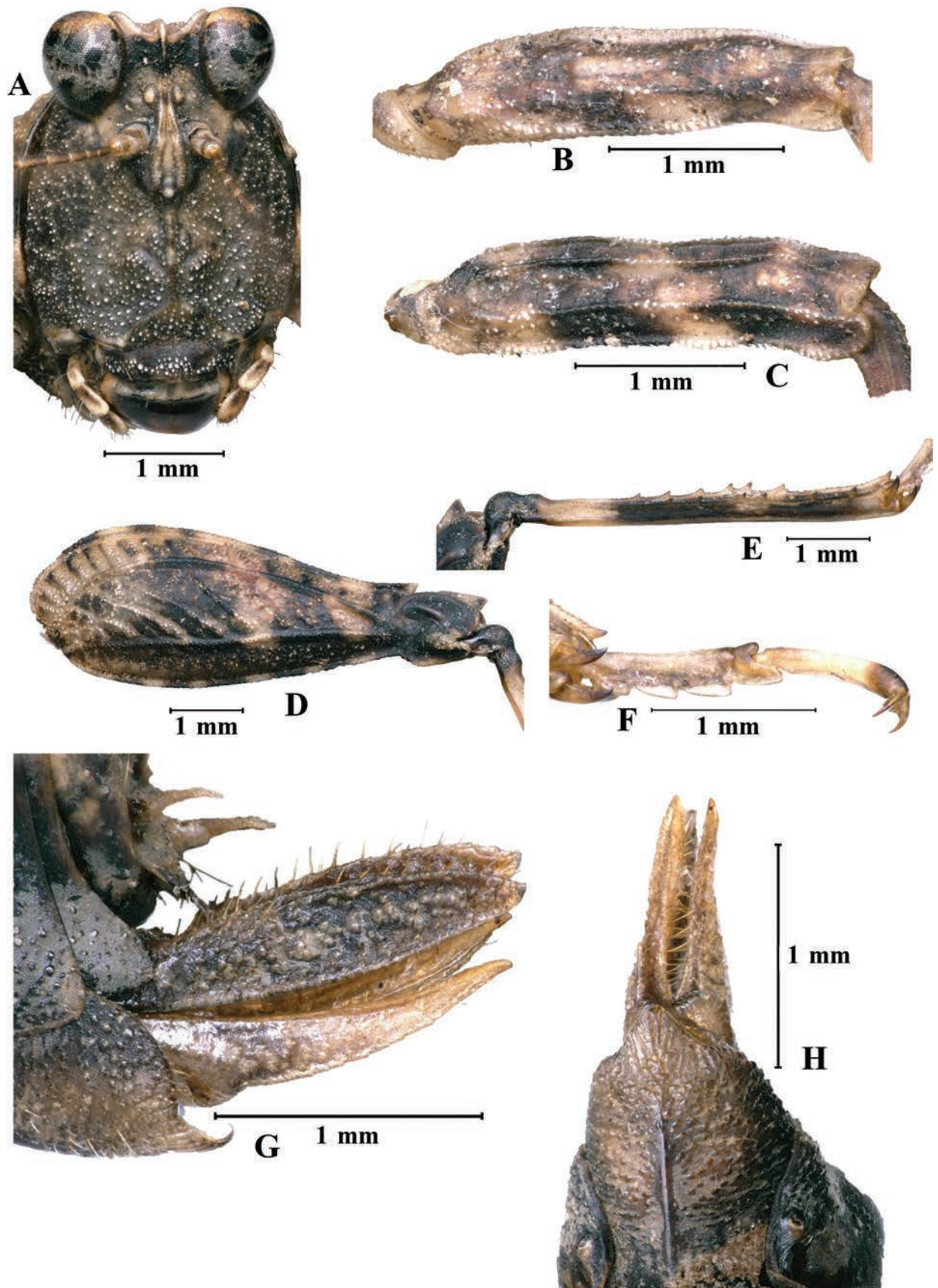


Figure 8. *E. Ieyeensis* Deng, sp. nov., holotype female **A** head, frontal view **B** left fore femur, lateral view **C** left mid femur, lateral view **D** left hind femur, lateral view **E** left hind tibia, lateral view **F** left posterior tarsus, lateral view **G** ovipositor of female, lateral view **H** subgenital plate of female, ventral view.

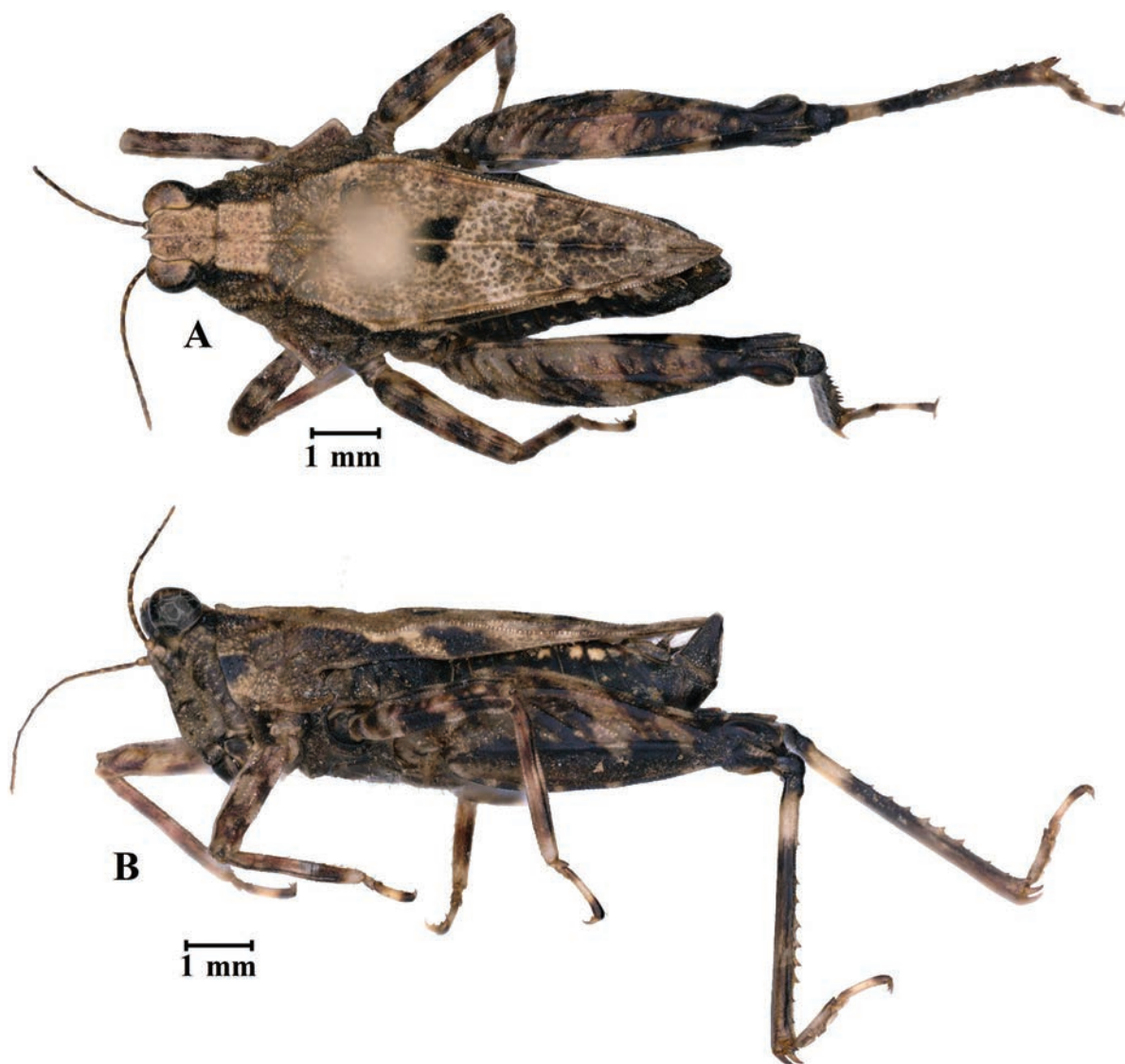


Figure 9. *Edentatettix leyeensis* Deng, sp. nov., paratype male **A** body in dorsal view **B** body in lateral view.

median carina entire and nearly straight in profile; lateral carinae of prozona parallel; humeral angle obtuse; with interhumeral carina; hind pronotal process narrow, nearly reaching apex of hind femur and its apex narrowly rounded. Lower margin of hind process nearly straight, lateral carinae of metazona slightly curved, width of infrascapular area is 0.7 mm. Posterior angles of lateral lobes produced outwards, end of posterior angles truncate, posterior margins of lateral lobes of pronotum only with ventral sinus. Tegmina and hind wings invisible.

Legs. Fore and middle femora slightly compressed, margins finely serrated and carinate and ventral margins slightly undulated. Hind femora robust and short, 2.8× as long as wide; with carinated, dorsal margins smooth and ventral margins finely serrated; antegenicular denticles and genicular denticles acute. Outer and inner side of hind tibia with five or six spines. Length of first segment of posterior tarsi equal to third, three pulvilli of first segment of posterior tarsi: first small, second and third large; apices of all pulvilli obtuse.

Abdomen. Ovipositor narrow and long, length of upper valvulae 3.8× its width, dorsal margins of upper valvulae and ventral margins of lower valvulae without saw-like tooth or saw-like teeth indistinct (Fig. 8G). Length of subgeni-

tal plate slightly longer than its width, middle of posterior margin of subgenital plate triangular projecting.

Coloration. Body brown; antennae and face dark brown. Middle of dorsal surface of pronotum with a dark spot. Fore and middle femora and tibia brown, with two dark brown transverse spots. Hind femora dark brown, outer side with two pale stripes. Hind tibia black, with two pale rings in the middle.

Male. Similar to female, but smaller and narrower. Width of vertex between eyes 1.3–1.5× width of compound eye. Ventral margins of middle femora undulated. Subgenital plate short, cone-shaped, apex bifurcated.

Measurements (mm). Length of body: ♂ 9.0–9.5, ♀ 11.5–12.0; length of pronotum: ♂ 8.0–8.5, ♀ 9.5–10.0; length of hind femur: ♂ 5.5–5.8, ♀ 6.5–7.0.

Etymology. The specific name refers to the type locality: Leye, Guangxi, China; adjective.

Distribution. P. R. China.

***Macromotettixoides yaana* Deng, sp. nov.**

<https://zoobank.org/63C2CA79-9127-44CB-A783-4E2F135833CB>

Figs 11–13

Type material. *Holotype* • ♀, CHINA, Sichuan Prov., Yaan City, Baoxing county, Longdong (Ganyanggou), 30°24'19"N, 102°35'45"E, 1400 m alt., 02 August 2016, collected by Wei-An Deng, CLSGNU. *Paratypes* • 8♂, 7♀, same data, CLSGNU.

Diagnosis. This new species is similar to *Macromotettixoides convexa* Deng, 2020, from which it differs in that the pronotal surface is without a tuberculiform convex between shoulders (pronotal surface with a distinctly tuberculiform convexity between shoulders in *M. convexa*); lower margin of hind pronotal process straight (lower margin of hind pronotal process curved in *M. convexa*); median carina of pronotum undulated in profile (median carina of pronotum distinctly arch-like before shoulders and undulated behind shoulders in profile in *M. convexa*); lower outer carina of hind femora without projections (postmedian of lower outer carina of hind femora with two inconspicuous projections in *M. convexa*).

Description. Female. Small size, short, body surface interspersed with coarse protuberances.

Head. Head and eyes not exserted above pronotal surface. Fastigium of vertex short; in dorsal view, width of vertex between eyes 1.4–1.6× width of compound eye; anterior margin of fastigium slightly concave in the middle, slightly surpassing anterior margin of eye; median carina visible anteriorly; lateral margins turned backward; vertex uneven with paired fossulae. In lateral view, frontal ridge and vertex forming a rounded-angle shape, frontal costa distinctly concave between eyes, protruding anteriorly and broadly rounded between antennal grooves. In frontal view, frontal costa bifurcated above lateral ocelli, the bifurcation of the frontal costa in the middle of the compound eye height; longitudinal furrow widely divergent between antennae, width of longitudinal furrow of frontal ridge narrower than antennal groove diameter. Antennae short, filiform, antennal grooves inserted below inferior margin of compound eyes, 14-segmented, the 10th and 11th segment are the longest, ~ 2.5–3.0× longer than its width. Eyes globose, lateral (paired) ocelli located lowest third of compound eye height.

Thorax. Brachypronotal. Pronotum with distinctly tectiform, pronotal surface interspersed with dense protuberances of variable sizes and notches. Pronotum with truncate anterior margin, median carina slightly lamellar and entire and undulated in profile; lateral carinae of prozona slightly lamellar and parallel; humeral angle obtuse; hind pronotal process narrow, nearly reaching apex of hind femur and its apex narrowly rounded. Lower margin of hind process straight, lateral carinae of metazona curved, width of infrascapular area is 0.9 mm. Posterior angles of lateral lobes slightly produced outwards, end of posterior angles truncate, posterior margins of lateral lobes of pronotum with distinctly ventral sinus and very weakly tegminal sinus. Tegmina and hind wings strongly reduced and covered by infrascapular area and invisible or slightly visible.

Legs. Fore and middle femora slightly compressed, margins finely serrated and carinate and ventral margins with two inconspicuous projections and undulated. Hind femora robust and short, 2.8× as long as wide; with carinated and margins finely serrated; antegenicular denticles and genicular denticles acute. Outer side of hind tibia with 6–8 spines, inner side with six or seven spines. Length of first segment of posterior tarsi slightly longer than third, three pulvilli of first segment of posterior tarsi: first and second small and apices acute, third large and apex a right angle.

Abdomen. Ovipositor narrow and long, length of upper valvulae 3.5× its width, upper and lower valvulae with slender saw-like teeth. Length of subgenital plate slightly longer than its width, middle of posterior margin of subgenital plate slightly triangular projecting.

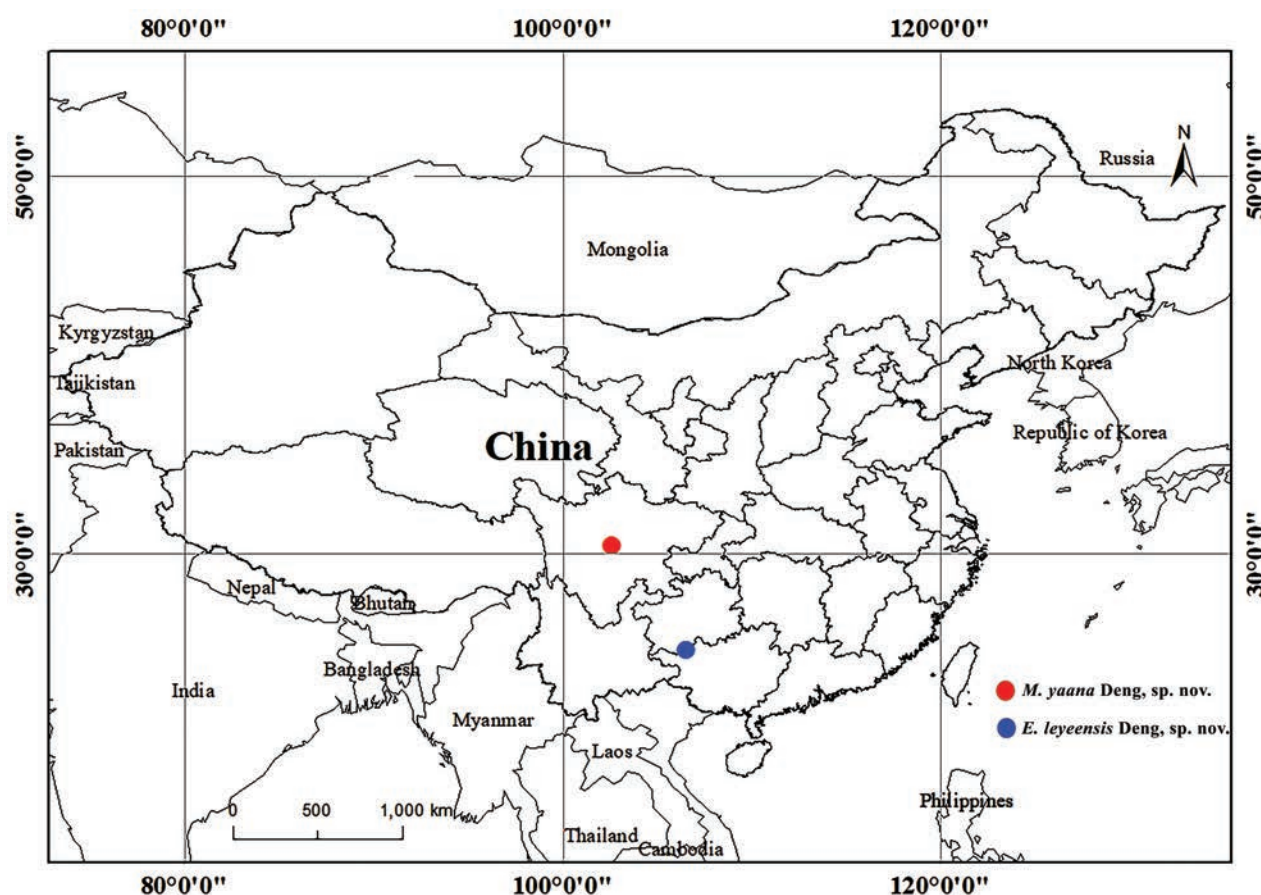


Figure 10. Distribution map of *E. leyeensis* Deng, sp. nov. and *M. yaana* Deng, sp. nov.

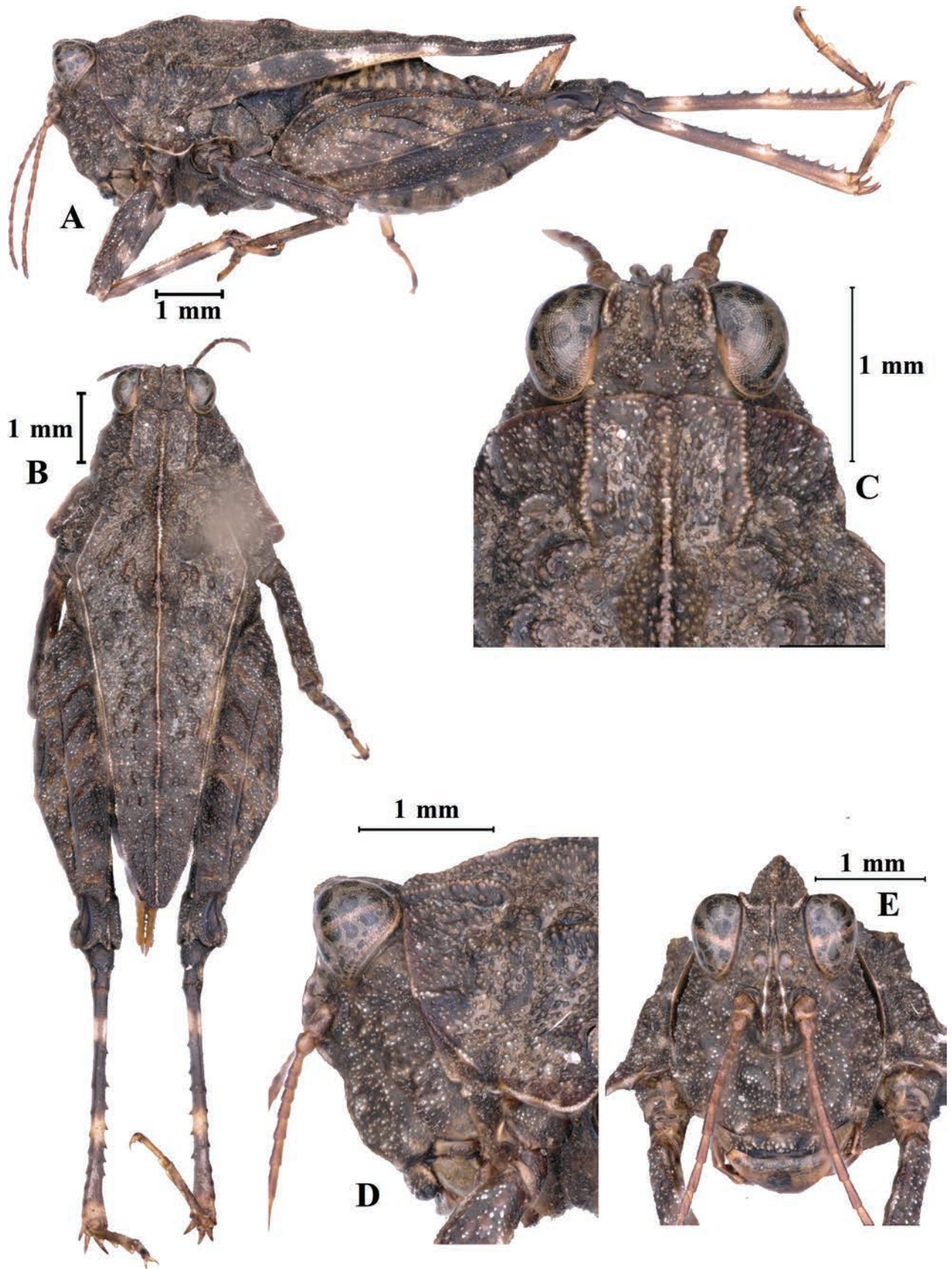


Figure 11. *Macromotettixoides yaana* Deng, sp. nov., holotype female **A** body, lateral view **B** the same, dorsal view **C** head and anterior part of pronotum, dorsal view **D** the same, lateral view **E** head, frontal view.

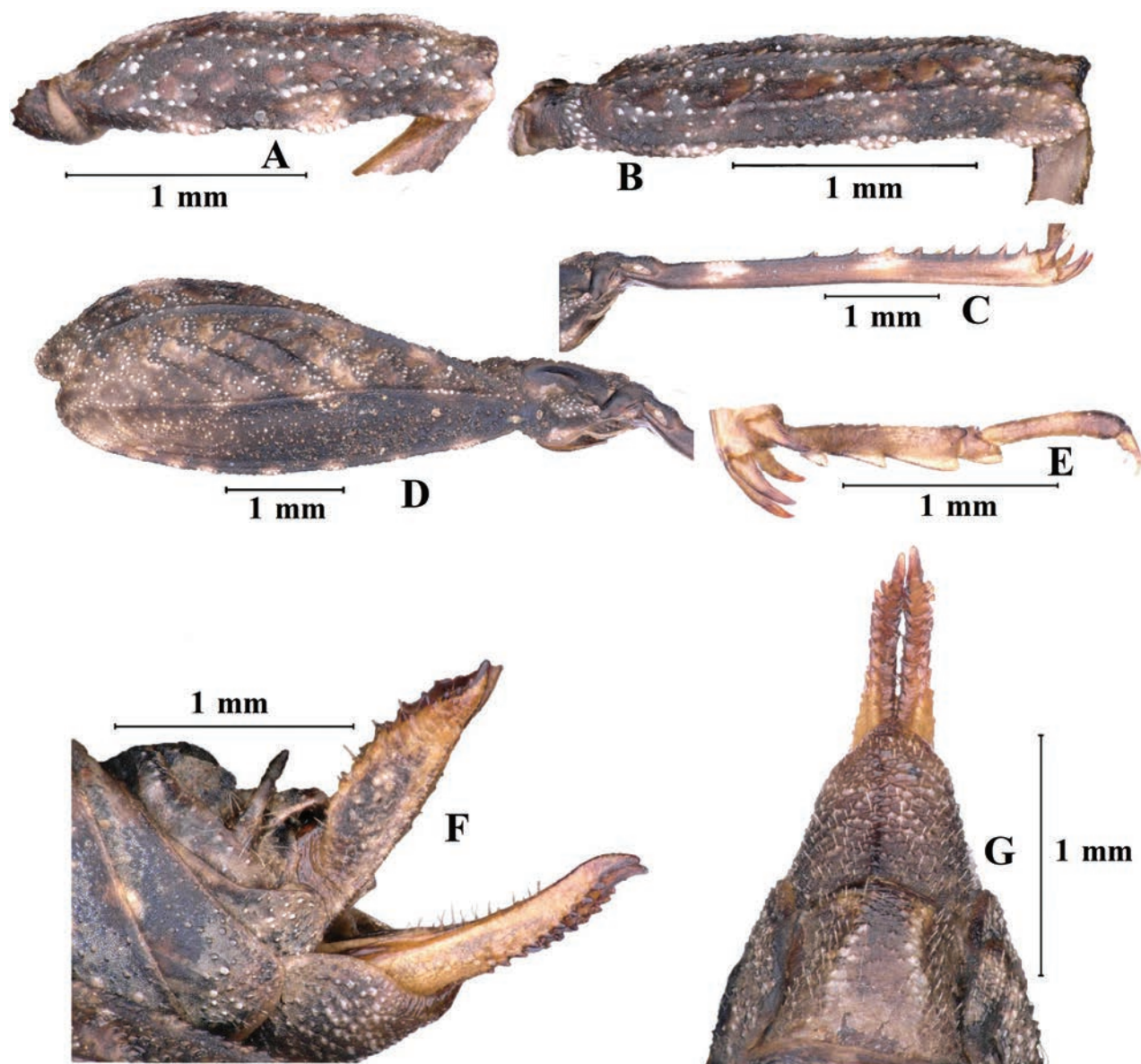


Figure 12. *Macromotettixoides yaana* Deng, sp. nov., holotype female **A** left fore femur, lateral view **B** left mid femur, lateral view **C** left hind femur, lateral view **D** left hind tibia, lateral view **E** left posterior tarsus, lateral view **F** subgenital plate of female, lateral view **G** subgenital plate of female, ventral view.

Coloration. Body dark brown or brown; antennae dark brown. Hind tibia dark brown, with two pale rings in the middle.

Male. Similar to female, but smaller and narrower. Width of vertex between eyes 1.4–1.5× width of compound eye. Ventral margins of fore and middle femora slightly undulated. Subgenital plate short, cone-shaped, apex bifurcated.

Measurements (mm). Length of body: ♂ 6.5–7.0, ♀ 8.5–9.0; length of pronotum: ♂ 5.2–5.6, ♀ 7.0–7.5; length of hind femur: ♂ 4.0–4.5, ♀ 5.0–5.5.

Etymology. The specific name refers to the type locality: Yaan, Jinxiu, Sichuan, China; adjective.

Distribution. P. R. China: Sichuan (Fig. 10).

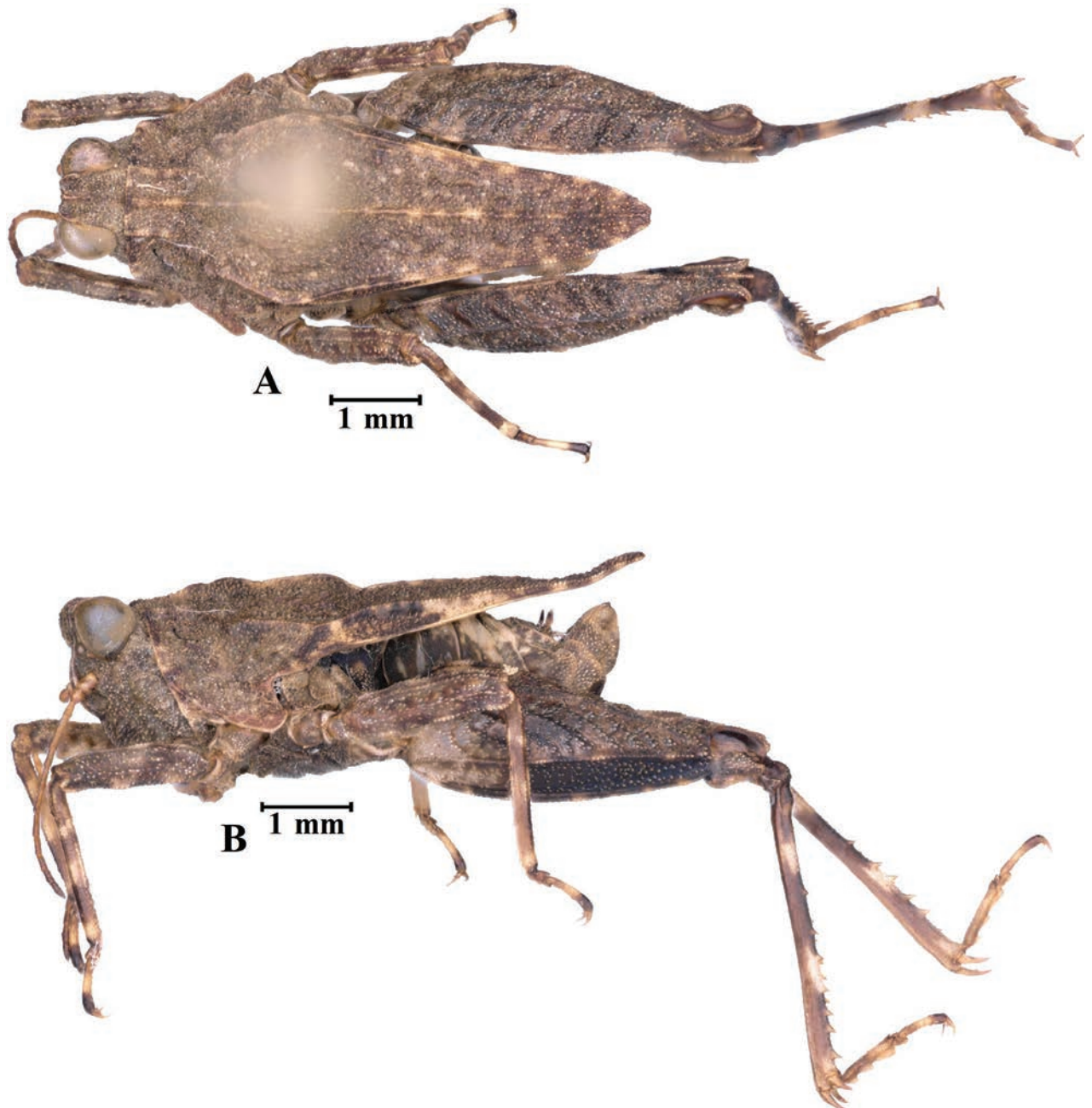


Figure 13. *Macromotettixoides yaana* Deng, sp. nov., paratype male **A** body in dorsal view **B** body in lateral view.

New synonyms

Hainantettix strictivertex Deng, 2020

Fig. 14

Hainantettix strictivertex Deng in Zhang, Zhao, Wu & Deng, 2020: 552 [description] (holotype – ♀, China: Hainan Prov., Qiongzong, Limushan; paratypes – 4♀, China: Hainan Prov., Wuzhishan; in EMHU; examined).

Macromotettixoides angustivertex Zha & Peng in Peng, Shi, Ding & Zha, 2021: 48 [description] (holotype – ♀, China: Hainan Prov., Wuzhishan, in HNU, not examined).

Hainantettix angustivertex (Zha & Peng): Subedi 2022: 40; syn. nov.

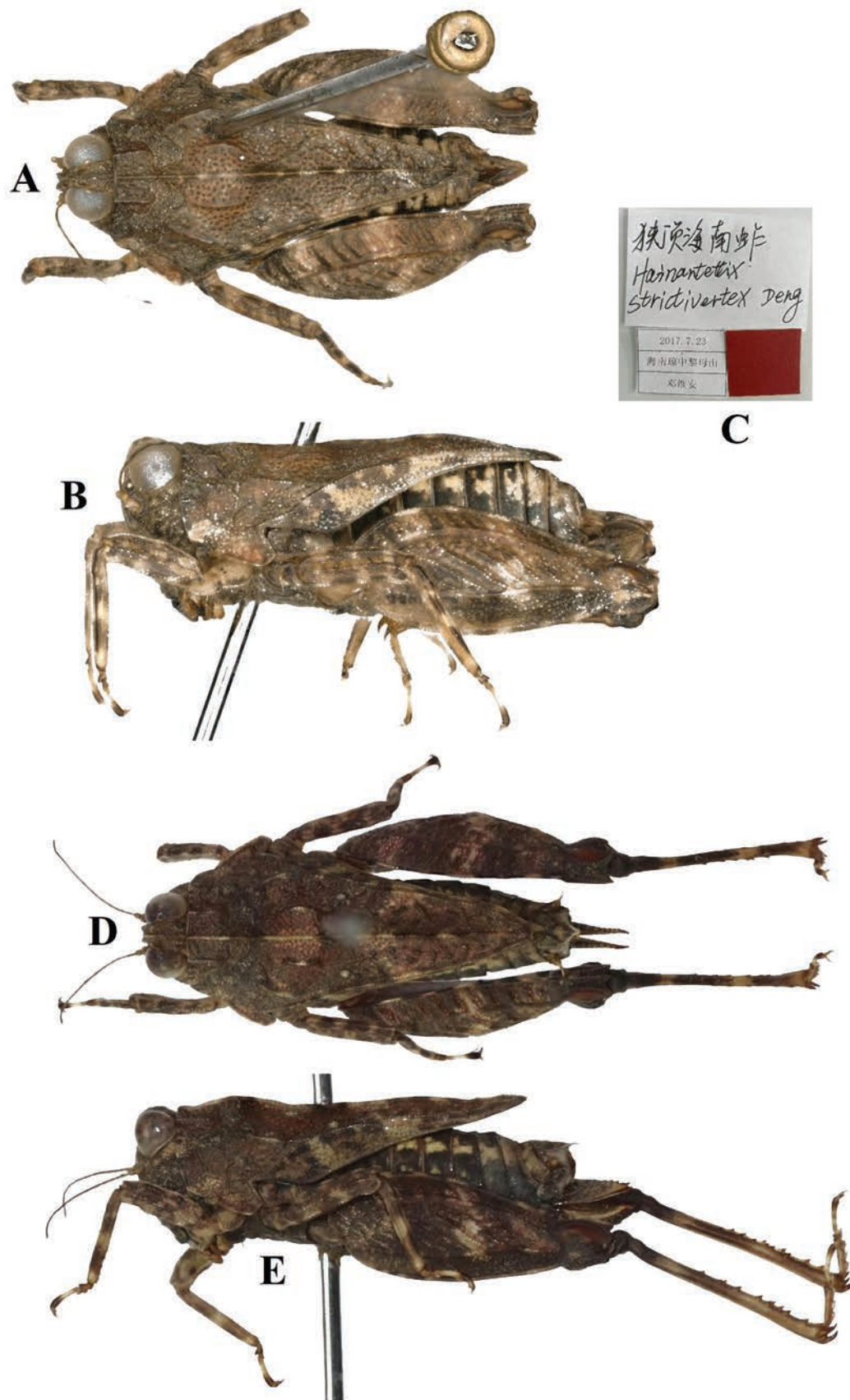


Figure 14. **A–C** Holotype of *Hainantettix strictivertex* Deng, 2020 **A** body in dorsal view **B** body in lateral view **C** labels **D**, **E** holotype of *Macromotettixoides angustivertex* Zha & Peng, 2021, syn. nov. **D** body in dorsal view **E** body in lateral view (photographs from Peng et al.).

Remarks. *Macromotettixoides angustivertex* Zha & Peng was described by Peng et al. (2021) and was later transferred to the genus *Hainantettix* by Subedi (2022). We examined the type specimen of *Hainantettix strictivertex* Deng, 2020. Although we did not examine the type material of *M. angustivertex* from Hainan, according to the original description and photographs of the type specimens in Peng et al. (2021), we found that the two species share identical morphological structures, type locality, and coloration. These two taxa are conspecific and characterized by the vertex very strongly narrowed towards the front drawing the eyes together; antennal grooves inserted below inferior margin of compound eyes; rami strongly divergent, width of longitudinal furrow of frontal ridge is distinctly wider than antennal groove diameter.

***Macromotettixoides jiuwanshanensis* Zheng, Wei & Jiang, 2005**

Figs 15, 16

Macromotettixoides jiuwanshanensis Zheng, Wei & Jiang, 2005: 366 [description] (holotype – ♀, China: Guangxi Prov., Luocheng (jiuwanshan), in IZSNU, examined). Zheng et al. 2005b: 176; Zheng et al. 2006: 604; Deng et al. 2007: 160; Zheng and Shi 2009: 572; Deng 2011: 544; Zheng 2013a: 242; Deng et al. 2014: 548; Deng et al. 2015: 165; Deng 2016: 156; Zha et al. 2017: 16; Han et al. 2020: 563; Li et al. 2020a: 110; Fan et al. 2023: 128.

Hyboella badagongshanensis Zheng, 2013b: 11 (holotype – ♀, China: Hunan Prov., Sangzhi (Badagongshan), in IZSNU, examined); Deng 2016: 150; syn. nov.

Macromotettixoides badagongshanensis (Zheng, 2013b): Zha, Yu, Boonmee, Eungwanichayapant, Wen, 2017: 23; Han et al. 2020: 564; Li et al. 2020a: 112; Fan et al. 2023: 129; syn. nov.

Macromotettixoides wuyishana Zheng, 2013: 242 [description] (holotype – ♀, China: Fujian Prov., Wuyishan, in IZSNU, examined); Deng 2016: 156; Zha et al. 2017: 15; Han et al. 2020: 563; Li et al. 2020a: 111; Fan et al. 2023: 128; syn. nov.

Remarks. *Hyboella badagongshanensis* was described by Zheng (2013b) but was later transferred to the genus *Macromotettixoides* by Zha et al. (2017). We examined the type specimens of *M. jiuwanshanensis*, *M. badagongshanensis*, and *M. wuyishana* and found that the structures and coloration of the body are the same in these three taxa. Therefore, we consider *M. badagongshanensis*, and *M. wuyishana* as synonyms of *M. jiuwanshanensis*. These three taxa are conspecific and characterized by the width of the vertex between the eyes being 2.1–2.2× the width of the compound eye; anterior margin of fastigium arched and surpassing anterior margin of eye; the anterior margin of pronotum is slightly obtuse protruding; and the lower carinae of fore and mid femora is straight.

Discussion

In this study, we describe two new pygmy grasshoppers of Metrodorinae found in China, *E. leyeensis* Deng, sp. nov. and *M. yaana* Deng, sp. nov. Through detailed morphological description and mitochondrial genome sequencing, we conducted a comprehensive analysis of the two new species. We have discovered

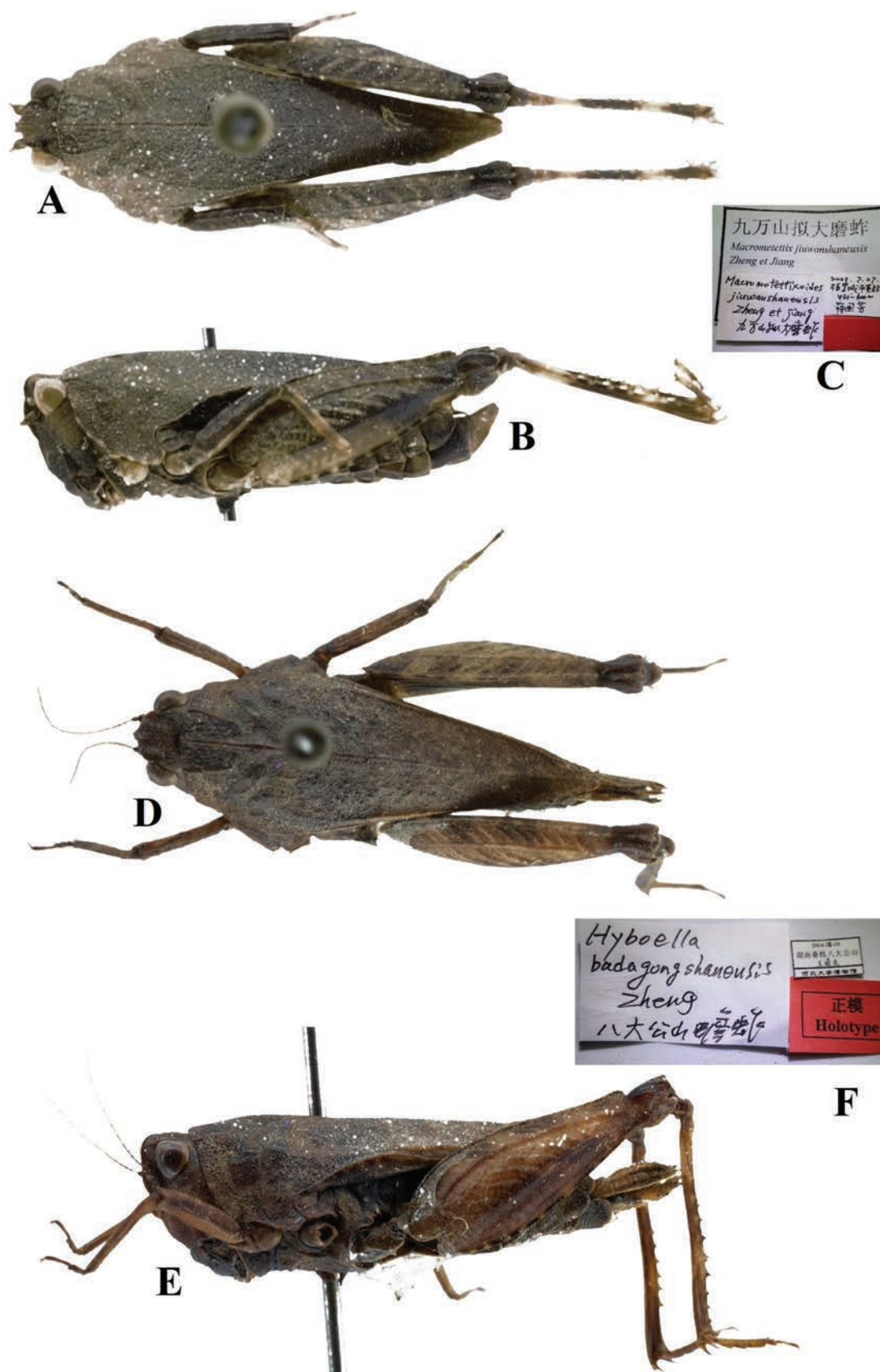


Figure 15. A–C Holotype of *Macrometettixoides jiuwanshanensis* Zheng, Wei & Jiang, 2005 A body in dorsal view B body in lateral view C labels D–F holotype of *Hyboella badagongshanensis* Zheng, 2013, syn. nov. D body in dorsal view E body in lateral view F labels.

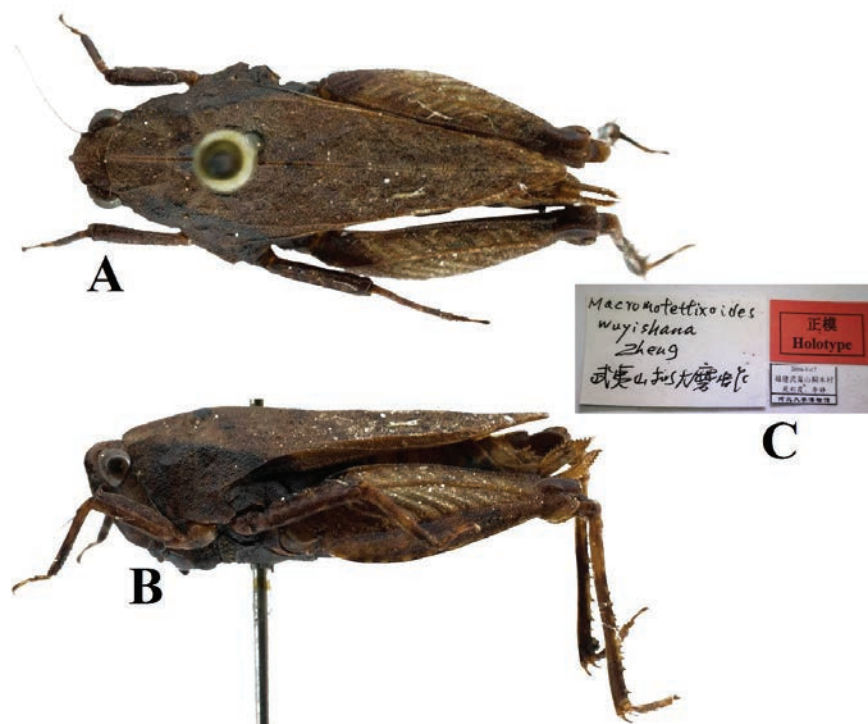


Figure 16. *Macromotettixoides jiuwanshanensis* Zheng, Wei & Jiang, 2005. Holotype of *Macromotettixoides wuyishana* Zheng, 2013, syn. nov. **A** body in dorsal view **B** lateral view **C** body in labels.

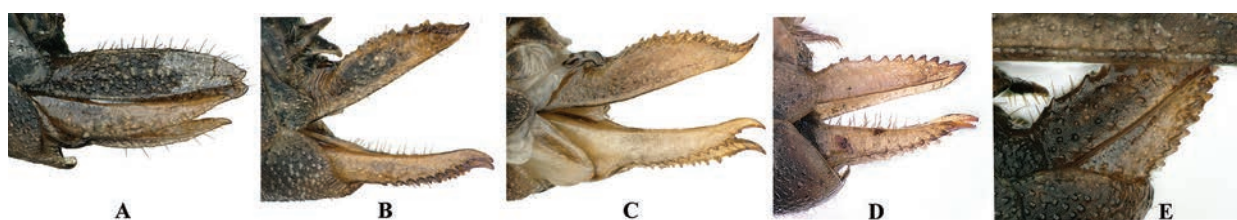


Figure 17. ovipositor of female, lateral view **A** *E. leyeensis* Deng, sp. nov. **B** *M. yaana* Deng, sp. nov. **C** *M. orthomargina* **D** *M. brachycorna* **E** *M. maoershanensis*.

something quite intriguing. Although *E. leyeensis* Deng, sp. nov. morphologically resembles the genus *Macromotettixoides*, its uniqueness lies in the absence of serrated teeth on the female ovipositor (Fig. 17), which is extremely rare among Tetrigidae. Based on morphological characteristics, phylogeny, and divergence time analysis, *E. leyeensis* Deng, sp. nov. is set apart in classification, leading us to classify it under the new genus *Edentatettix* Deng, gen. nov.

The existence of an ovipositor serves as a shared derived characteristic (synapomorphy) among Insecta (Barbosa and Fianco 2024). Across this expansive class, a diverse array of morphological and functional characteristics can be observed in the ovipositors among different orders, and the varied structures of ovipositors in Orthoptera are no exception, vividly mirroring their unique adaptations to diverse ecological niches (Austin and Browning 1981; Kluge 2016). For instance, the sword-like or spear-shaped ovipositors of katydids and crickets exemplify their high adaptability for laying eggs in plant tissues or soil, ensuring both egg safety and enhanced larval survival rates (Kluge 2016; Chen et al. 2021). Conversely, the ovipositors of locusts and pygmy grasshoppers (Tetrigidae) are geared more towards excavating functionality, with the former having

a conical shape facilitating efficient soil digging (Kalogianni 1995; Zhao et al. 2022). The latter, while also adept at digging, may further enhance oviposition precision and efficiency by having fine teeth along the dorsal and ventral edges of their ovipositors (Kluge 2016). These varied oviposition strategies typify Orthopteran responses to environmental pressures, embodying a co-evolutionary mechanism between form and function.

The emergence of *E. leyeensis* Deng, sp. nov. with a toothless ovipositor provides not only morphological evidence for early Tetrigidae diversification but also insights into the ancient origins of complex reproductive structure transformations. The toothless ovipositor may represent a unique adaptive strategy, potentially associated with specific oviposition habitats or behaviors, meriting further investigation.

Importantly, we note for the first time that toothless ovipositors are an important taxonomic feature. This distinctive feature intimates the likelihood of diverse morphological variations in reproductive organs that may have emerged throughout the evolutionary journey of this group. Such variations are plausibly influenced by a multitude of factors, encompassing genetics, environmental conditions, and reproductive strategies (Hornig et al. 2018; Chen et al. 2021; Barbosa and Fianco 2024). Moreover, the timing of the emergence of this toothless characteristic (*E. leyeensis* Deng, sp. nov.), paralleling the divergence period of Tetrigidae, implies that it is an ancient character. This finding reinforces the hypothesis that Tetrigidae insects have undergone intricate morphological transformations, implicating their reproductive structures, over the course of their evolutionary progression.

Fossil records from the Early Miocene and Middle Eocene epochs affirm that the ovipositors of female Tetrigidae were adorned with saw-like teeth (Heads et al. 2014; Skejo et al. 2024), congruent with observations in contemporary species. The ancient divergence time of *E. leyeensis* Deng, sp. nov., given the constraints posed by the fossil record, accentuates that our current paleontological evidence likely constitutes merely a fraction of the extensive and diverse history of life. Some species, especially those inhabiting environments unfavorable to fossil preservation, may have irretrievably lost their historical footprint. Consequently, integrating insights from molecular biology, morphology, and paleontology becomes indispensable for elucidating the profound evolutionary mechanisms underlying global biodiversity.

Additional information

Conflict of interest

The authors have declared that no competing interests exist.

Ethical statement

No ethical statement was reported.

Funding

This study was supported by the Science & Technology Fundamental Resources Investigation Program of China (2023FY100200), the National Natural Science Foundation of China (32360124), and the Guangxi Natural Science Foundation under Grant No. 2023GXNSFDA026037.

Author contributions

Conceptualization: Wei-An Deng. Investigation: Wei-An Deng, Shi-Xiong Leng, Jia-Song He. Species identification: Wei-An Deng. Software: Yue-Mei Li, De-Long Guan. Analysed the data: Yue-Mei Li, De-Long Guan. Original draft writing: Yue-Mei Li, Wei-An Deng. Review and editing: Wei-An Deng. Funding acquisition: Wei-An Deng.

Author ORCIDs

Yuemei Li  <https://orcid.org/0009-0001-7327-5334>

Shixiong Leng  <https://orcid.org/0009-0002-3422-3862>

Jiasong He  <https://orcid.org/0009-0002-7224-594X>

Weian Deng  <https://orcid.org/0000-0002-8023-2498>

Delong Guan  <https://orcid.org/0000-0001-6866-0943>

Data availability

All of the data that support the findings of this study are available in the main text.

References

- Adžić K, Deranja M, Franjević D, Skejo J (2020) Are Scelimeninae (Orthoptera: Tetrigidae) monophyletic and why it remains a question? *Entomological News* 129(2): 128–146. <https://doi.org/10.3157/021.129.0202>
- Austin AD, Browning TO (1981) A mechanism for movement of eggs along insect ovipositors. *International Journal of Insect Morphology and Embryology* 10(2): 93–108. [https://doi.org/10.1016/S0020-7322\(81\)80015-3](https://doi.org/10.1016/S0020-7322(81)80015-3)
- Barbosa DN, Fianco M (2024) A Tale's blade: Understanding evolutionary features of oviposition behavior based on Tettigoniidae (Insecta, Orthoptera, Ensifera) ovipositor morphology. *Arthropod Structure and Development* 79: 101332. <https://doi.org/10.1016/j.asd.2024.101332>
- Bolívar I (1887) Essai sur les Acridiens de la tribu des Tettigidae. *Annales de la Societe Entomologique de Belgique* 31: 173–313.
- Bolívar I (1909) Nouvelles espèces d'Acridiens du Musée de Genève. *Boletín de la Real Sociedad Española de Historia Natural* 9: 399–400.
- Boore JL (1999) Animal mitochondrial genomes. *Nucleic Acids Research* 27(8): 1767–1780. <https://doi.org/10.1093/nar/27.8.1767>
- Cameron SL (2014) Insect mitochondrial genomics: implications for evolution and phylogeny. *Annual Review of Entomology* 59(1): 95–117. <https://doi.org/10.1146/annurev-ento-011613-162007>
- Chang HH, Nie YM, Zhang N, Zhang X, Sun HM, Mao Y, Qiu ZY, Huang Y (2020) MtOrt: an empirical mitochondrial amino acid substitution model for evolutionary studies of Orthoptera insects. *BMC Evolutionary Biology* 20: 1–5. <https://doi.org/10.1186/s12862-020-01623-6>
- Chen AH (2005) Phylogenetic Relationship Research of Tetrigoidea in China. Nanjing Normal University, M.Sc. thesis, 52 pp.
- Chen YZ, Deng WA, Wang JM, Lin LL, Zhou SY (2018) Phylogenetic relationships of Scelimeninae genera (Orthoptera: Tetrigoidea) based on COI, 16S rRNA and 18S rRNA gene sequences. *Zootaxa* 4482(2): 392–400. <https://doi.org/10.11646/zootaxa.4482.2.11>

- Chen L, Gu JJ, Yang Q, Ren D, Blanke A, Béthoux O (2021) Ovipositor and mouthparts in a fossil insect support a novel ecological role for early orthopterans in 300 million years old forests. *Elife* 10: e71006. <https://doi.org/10.7554/eLife.71006>
- Cigliano MM, Braun H, Eades DC, Otte D (2024) Orthoptera Species File Online. Version 5.0/5.0. 2024 <http://Orthoptera.SpeciesFile.org> [Accessed 13 December 2023]
- Deng WA (2011) A taxonomic study on the genus *Macromotettixoides* Zheng (Orthoptera, Tetrigoidea, Metrodorinae). *Acta Zootaxonomica Sinica* 36(3): 543–546.
- Deng WA (2016) Taxonomic Study of Tetrigoidea from China. Huazhong Agricultural University, Ph.D. Dissertation, 341 pp.
- Deng WA, Zheng ZM, Wei SZ (2007) Fauna of Tetrigoidea from Yunnan and Guangxi. Science and Technology Press, Nanning, 458 pp.
- Deng WA, Lei CL, Zheng ZM, Li XD, Lin LL, Lin MP (2014) Description of a new species of the genus *Macromotettixoides* Zheng (Orthoptera: Tetrigoidea: Metrodorinae) from China. *Neotropical Entomology* 43: 547–554. <https://doi.org/10.1007/s13744-014-0237-6>
- Deng WA, Zheng ZM, Li XD, Lin MP, Wei SZ, Yuan BD, Lin LL (2015) The groundhopper fauna (Orthoptera: Tetrigidae) of Shiwanshan (Guangxi, China) with description of three new species. *Zootaxa* 3925(2): 151–178. <https://doi.org/10.11646/zootaxa.3925.2.1>
- Deng WA, Zhang RJ, Li XD, Xin L (2021) The complete chloroplast genome of *Saussurella borneensis* (Orthoptera: Tetrigoidea) from China and its phylogenetic analysis. *Mitochondrial DNA Part B* 6(9): 2739–2740. <https://doi.org/10.1080/23802359.2021.1966336>
- Devriese H, Husemann M (2023) *Afrosystolederus garmsi* (Orthoptera, Tetrigidae), a new genus and species from Mount Gibi (Liberia) with remarks on *Systolederus*, *Pseudosystolederus* and *Teredorus*. *Zootaxa* 5258(3): 331–341. <https://doi.org/10.11646/zootaxa.5258.3.6>.
- Donath A, Jühling F, Al-Arab M, Bernhart SH, Reinhardt F, Stadler PF, Middendorf M, Bern M (2019) Improved annotation of protein-coding genes boundaries in metazoan mitochondrial genomes. *Nucleic Acids Research* 47(20): 10543–10552. <https://doi.org/10.1093/nar/gkz833>
- Drummond AJ, Rambaut A (2007) BEAST: Bayesian evolutionary analysis by sampling trees. *BMC Evolutionary Biology* 7: 1–8. <https://doi.org/10.1186/1471-2148-7-214>
- Drummond AJ, Suchard MA, Xie D, Rambaut A (2012) Bayesian phylogenetics with BEAUti and the BEAST 1.7. *Molecular Biology and Evolution* 29(8): 1969–1973. <https://doi.org/10.1093/molbev/mss075>
- Fan CM, Li M, Mao BY (2023) Descriptions of two new species of the genus *Macromotettixoides* (Orthoptera: Tetrigidae: Metrodorinae) from China. *Zootaxa* 5306(1): 127–134. <https://doi.org/10.11646/zootaxa.5306.1.6>
- Fang N, Xuan WJ, Zhang YY, Jiang GF (2010) Molecular phylogeny of Chinese Tetrigoids (Orthoptera, Tetrigoidea) based on the mitochondrial cytochrome C oxidase I gene. *Acta Zootaxonomica Sinica* 35: 696–702.
- Grant JR, Enns E, Marinier E, Mandal A, Herman EK, Chen C, Graham M, Van Domselaar G, Stothard P (2023) Proksee: In-depth characterization and visualization of bacterial genomes. *Nucleic Acids Research* 51(W1): W484–492. <https://doi.org/10.1093/nar/gkad326>
- Guan DL, Huang CM, Deng WA (2024) Reassessment of the phylogenetics of two pygmy grasshopper generic groups *Tetrix* and *Systolederus* through mitochondrial phylogenomics using four new mitochondrial genome assemblies. *Insects* 15(3): 174. <https://doi.org/10.3390/insects15030174>

- Günther K (1939) Revision der Acrydiinae (Orthoptera), III. Sectio Amorphopi (Metrodorae Bol. 1887 auct.). Abhandlungen und Berichte der Museum für Tierkunde und Volkerkunde zu Dresden (Ser. A: Zool.) (N.F.) 20: 16–335.
- Han YA, Li M, Mao BY (2020) A taxonomic study of the genus *Macromotettixoides* (Tetrigidae, Metrodorinae) with descriptions of two new species and two newly discovered males. *Zootaxa* 4718(4): 562–572. <https://doi.org/10.11646/zootaxa.4718.4.9>
- Hancock JL (1910) Third paper on the Tetriginae (Orthoptera) in the Oxford University Museum. *Transactions of the Entomological Society of London* 58(3): 346–365. <https://doi.org/10.1111/j.1365-2311.1910.tb01173.x>
- Hancock JL (1915) Indian Tetriginae (Acrydiinae). *Records of the Indian Museum* 11(1): 55–137. <https://doi.org/10.26515/rzsi/v11/i1/1915/163610>
- Heads SW, Thomas MJ, Wang Y (2014) A remarkable new pygmy grasshopper (Orthoptera, Tetrigidae) in Miocene amber from the Dominican Republic. *ZooKeys* 30(429): 87–100. <https://doi.org/10.3897/zookeys.429.8020>
- Hornig MK, Haug C, Schneider JW, Haug JT (2018) Evolution of reproductive strategies in dictyopteran insects—clues from ovipositor morphology of extinct roachoids. *Acta Palaeontologica Polonica* 63(1): 1–24. <https://doi.org/10.4202/app.00324.2016>
- Huang CM, Deng WA, Zhang RJ, He CX (2022) The molecular phylogenetic analysis of some species of Tetriginae based on *COI*, 16S rRNA & 18S rRNA genes. *Genomics and Applied Biology* 41(5): 970–980.
- Kalogianni E (1995) Physiological properties of wind-sensitive and tactile trichoid sensilla on the ovipositor and their role during oviposition in the locust. *Journal of Experimental Biology* 198(6): 1359–1369. <https://doi.org/10.1242/jeb.198.6.1359>
- Kalyaanamoorthy S, Minh BQ, Wong TK, Von Haeseler A, Jermini LS (2017) ModelFinder: fast model selection for accurate phylogenetic estimates. *Nature Methods* 14(6): 587–589. <https://doi.org/10.1038/nmeth.4285>
- Kasalo N (2022) *Metamazarredia* is *Rosacris* is *Mazarredia* (Orthoptera: Tetrigidae) – a long-awaited sequel to a taxonomic dilemma. *Zootaxa* 5200(2): 495–500. <https://doi.org/10.11646/zootaxa.5200.5.7>
- Kasalo N, Skejo J, Husemann M (2023a) DNA barcoding of pygmy hoppers – the first comprehensive overview of the BOLD Systems' Data Shows Promise for Species Identification. *Diversity* 15(6): 696. <https://doi.org/10.3390/d15060696>
- Kasalo N, Yong S, Rebrina F, Skejo J (2023b) Definition of the tribe Metrodorini (Orthoptera: Tetrigidae) with notes on biogeography and evolution of Metrodorinae and Cladonotinae. *Acta Entomologica Musei Nationalis Pragae* 63(1): 187–193. <https://doi.org/10.37520/aemnp.2023.010>
- Katoh K, Standley DM (2013) MAFFT multiple sequence alignment software version 7: improvements in performance and usability. *Molecular Biology and Evolution* 30(4): 772–780. <https://doi.org/10.1093/molbev/mst010>
- Kluge NJ (2016) Structure of ovipositors and Cladoendosis of Saltatoria, or Orchesopia. *Entomological Review* 96: 1015–1040. <https://doi.org/10.1134/S0013873816080078>
- Kumar S, Suleski M, Craig JM, Kasprówicz AE, Sanderford M, Li M, Stecher G, Hedges SB (2022) TimeTree 5: an expanded resource for species divergence times. *Molecular Biology and Evolution* 39(8): msac174. <https://doi.org/10.1093/molbev/msac174>
- Li M, Deng Y, Yin FX, Mao BY (2020a) A new species of *Macromotettixoides* (Orthoptera: Tetrigidae: Metrodorinae) from Yunnan, China. *Entomotaxonomia* 42(2): 110–115.
- Li XD, Wang YQ, Deng WA, Rong WT, Li R (2020b) First record of mitochondrial genome of *Teredorus nigropennis* (Orthoptera: Tetrigidae) and phylogenetic analysis. *Mitochondrial DNA B Resour* 5(2): 1145–1146. <https://doi.org/10.1080/23802359.2020.1730259>

- Li RR, Li M, Yan J, Bai M, Zhang HF (2021a) Five mitochondrial genomes of the genus *Eysarcoris* Hahn, 1834 with phylogenetic implications for the Pentatominae (Hemiptera: Pentatomidae). *Insects* 12(7): 597. <https://doi.org/10.3390/insects12070597>
- Li R, Ying XL, Deng WA, Rong WT, Li XD (2021b) Mitochondrial genomes of eight Scelimeninae species (Orthoptera) and their phylogenetic implications within Tetrigoidea. *PeerJ* 9: e10523. <https://doi.org/10.7717/peerj.10523>
- Li XJ, Liu YX, Lin LL (2021c) Comparative mitogenomes and phylogenetic analysis reveal taxonomic relationship of genera *Teredorus* and *Systolederus* (Orthoptera, Tetrigoidea). *Zootaxa* 5027(1): 127–135. <https://doi.org/10.11646/zootaxa.5027.1.7>
- Lin LL (2014) Mitochondrial Genome Analysis and Phylogenetic Relationship of Three Species of Tetrigoidea. Shaanxi Normal University, Ph.D. Dissertation, 140 pp.
- Lin MP, Li XD, Wei SZ, Deng WA (2015) Mitochondrial *COI* gene partial sequences and phylogenetic relationship of some groups of Tetrigoidea. *Journal of Huazhong Agricultural University* 34(6): 40–48.
- Lin LL, Li XJ, Zhang HL, Zheng ZM (2017) Mitochondrial genomes of three Tetrigoidea species and phylogeny of Tetrigoidea. *PeerJ* 5: e4002. <https://doi.org/10.7717/peerj.4002>
- Long Y, Teng CL, Huang CM, Zhang RJ, Deng WA, Lin LL (2023) Twenty-three new synonyms of the Eastern common groundhopper, *Tetrix japonica* (Bolívar, 1887) (Orthoptera, Tetrigidae). *ZooKeys* 1187: 135–167. <https://doi.org/10.3897/zookeys.1187.110067>
- Lu XY, Deng WA (2021) New genus and new species of the subfamily Metrodorinae from China (Orthoptera: Tetrigidae). *Zootaxa* 4964(2): 345–362. <https://doi.org/10.11646/zootaxa.4964.2.6>
- Luo JL, Zhang RJ, Deng WA (2024) First mitogenomic characterization of *Macromotettixoides* (Orthoptera, Tetrigidae), with the descriptions of two new species. *ZooKeys* 1195: 95–120. <https://doi.org/10.3897/zookeys.1195.112623>
- Minh BQ, Nguyen MA, Von Haeseler A (2013) Ultrafast approximation for phylogenetic bootstrap. *Molecular Biology and Evolution* 30(5): 1188–1195. <https://doi.org/10.1093/molbev/mst024>.
- Muhammad AA, Tan MK, Abdullah NA, Azirun MS, Bhaskar D, Skejo J (2018) An annotated catalogue of the pygmy grasshoppers of the tribe Scelimenini Bolívar, 1887 (Orthoptera: Tetrigidae) with two new *Scelimena* species from the Malay Peninsula and Sumatra. *Zootaxa* 4485(1): 1–70. <https://doi.org/10.11646/zootaxa.4485.1.1>
- Nguyen LT, Schmidt HA, Von Haeseler A, Minh BQ (2015) IQ-TREE: a fast and effective stochastic algorithm for estimating maximum-likelihood phylogenies. *Molecular Biology and Evolution* 32(1): 268–274. <https://doi.org/10.1093/molbev/msu300>
- Nie R, Vogler AP, Yang XK, Lin M (2021) Higher-level phylogeny of longhorn beetles (Coleoptera: Chrysomeloidea) inferred from mitochondrial genomes. *Systematic Entomology* 46(1): 56–70. <https://doi.org/10.1111/syen.12447>
- Pavón-Gozalo P, Manzanilla J, García-Paris M (2012) Taxonomy and morphological characterization of *Allotettix simony* (Bolívar, 1890) and implications for the systematics of Metrodorinae (Orthoptera: Tetrigidae). *Zoological Journal of the Linnean Society* 164(1): 52–70. <https://doi.org/10.1111/j.1096-3642.2011.00764.x>
- Peng T, Shi TZ, Ding JH, Zha LS (2021) Two *Macromotettixoides* species from Hainan Island, PR China, with taxonomic notes for the genus (Metrodorinae, Tetrigidae). *Entomological News* 130(1): 47–60. <https://doi.org/10.3157/021.130.0104>
- Sheffield NC, Hiatt KD, Valentine MC, Song H (2010) Mitochondrial genomics in Orthoptera using MOSAS. *Mitochondrial DNA* 21(3–4): 87–104. <https://doi.org/10.3109/19401736.2010.500812>

- Skejo J, Gupta SK, Chandra K, Panhwar WA, Franjevic D (2019) Oriental macropterous leaf-mimic pygmy grasshoppers – genera *Oxyphyllum* and *Paraphyllum* (Orthoptera: Tetrigidae) and their taxonomic assignment. *Zootaxa* 4590(5): 546–560. <https://doi.org/10.11646/zootaxa.4590.5.3>
- Skejo J, Kasalo N, Thomas MJ, Heads SW (2024) A new long-winged pygmy grasshopper in Eocene Baltic amber raises questions about the evolution of reduced tegmenula in Tetrigidae (Orthoptera). *Journal of Orthoptera Research* 33(1): 1–26. <https://doi.org/10.3897/jor.33.105144>
- Song H, Amédégnato C, Cigliano MM, Desutter-Grandcolas L, Heads SW, Huang Y, Otte D (2015) 300 million years of diversification: elucidating the patterns of orthopteran evolution based on comprehensive taxon and gene sampling. *Cladistics* 31(6): 621–651. <https://doi.org/10.1111/cla.12116>
- Song N, Li XX, Yin XM, Li X, Yin J, Pan P (2019) The mitochondrial genomes of palaeopteran insects and insights into the early insect relationships. *Scientific Reports* 9(1): 17765. <https://doi.org/10.1038/s41598-019-54391-9>
- Storozhenko SY (2014) To synonymy of the genus *Xistrella* Bolívar, 1909 (Orthoptera: Tetrigidae, Metrodorinae). *Far Eastern Entomologist* 277: 47–48.
- Subedi M (2022) A new genus and a new groundhopper species from Nepal (Orthoptera: Tetriginae: *Skejotettix netrajyoti* gen. et sp. nov.). *Zootaxa* 5205(1): 35–54. <https://doi.org/10.11646/zootaxa.5205.1.3>
- Tan MK, Artchawakom T (2015) A new species from the genus *Gorochovitettix* (Tetrigidae: Metrodorinae) from Thailand. *Zootaxa* 3990(3): 444–450. <https://doi.org/10.11646/zootaxa.3990.3.9>
- Tumbrinck J, Telnov D (2014) Taxonomic revision of the Cladonotinae (Orthoptera: Tetrigidae) from the islands of South-East Asia and from Australia, with general remarks to the classification and morphology of the Tetrigidae and descriptions of new genera and species from New Guinea and New Caledonia. *Biodiversity, Biogeography and Nature Conservation in Wallacea and New Guinea*. 2: 345–396.
- Tumbrinck J (2019) Taxonomic and biogeographic revision of the genus *Lamellitettigodes* (Orthoptera: Tetrigidae) with description of two new species and additional notes on *Lamellitettix*, *Probolotettix*, and *Scelimena*. *Journal of Orthoptera Research* 28(2): 167–180. <https://doi.org/10.3897/jor.28.34605>
- Wang YZ (2001) A new genus and new species of Metrodoridae (Orthoptera: Tetrigidae) recorded in Yunnan, China. *Journal of Southwest Agricultural University* 23: 147–148.
- Wang MQ (2022) Phylogenetic Analyses of Metrodorinae (Orthoptera: Tetrigidae) based on the Mitochondrial Genome. Dali University, M.Sc. thesis, 116 pp.
- Xiao B, Chen W, Hu CC, Jiang GF (2012a) Complete mitochondrial genome of the groundhopper *Alulatettix yunnanensis* (Insecta: Orthoptera: Tetrigoidea). *Mitochondrial DNA* 23(4): 286–287. <https://doi.org/10.3109/19401736.2012.674122>
- Xiao B, Feng X, Miao WJ, Jiang GF (2012b) The complete mitochondrial genome of grouse locust *Tetrix japonica* (Insecta: Orthoptera: Tetrigoidea). *Mitochondrial DNA* 23(4): 288–289. <https://doi.org/10.3109/19401736.2012.674123>
- Xie JM, Chen YR, Cai GJ, Cai RL, Hu Z, Wang H (2023) Tree Visualization By One Table (tvBOT): a web application for visualizing, modifying and annotating phylogenetic trees. *Nucleic Acids Research* 51(W1): W587–592. <https://doi.org/10.1093/nar/gkad359>
- Yang J (2017a) Mitochondrial genome sequencing of three Tetrigoidea and comparative analysis of mitochondrial genome of Acrididae. Shaanxi Normal University, Master thesis, 87 pp.

- Yang J, Lu C, Zhang ZB, Huang Y, Lin LL (2017b) Mitochondrial genomes of two pygmy grasshoppers (Orthoptera: Tetrigoidea) and a comparative analysis of Caelifera mitogenomes. *Zoological Science* 34(4): 287–294. <https://doi.org/10.2108/zs160217>
- Zha LS, Yu FM, Boonmee S, Eungwanichayapant PD, Wen TC (2017) Taxonomy of *Macromotettixoides* with the description of a new species (Tetrigidae, Metrodorinae). *ZooKeys* (645): 13–25. <https://doi.org/10.3897/zookeys.645.9055>
- Zhang RJ, Zhao CL, Wu FP, Deng WA (2020) Molecular data provide new insights into the phylogeny of Cladonotinae (Orthoptera: Tetrigoidea) from China with the description of a new genus and species. *Zootaxa* 4809(3): 547–559. <https://doi.org/10.11646/zootaxa.4809.3.8>
- Zhang RJ, Xin L, Deng WA (2021) Characterization of the complete mitochondrial genome of *Tripetaloceroides tonkinensis* (Orthoptera: Tetrigoidea) from China and its phylogenetic analysis. *Mitochondrial DNA Part B* 6(7): 1990–1991. <https://doi.org/10.1080/23802359.2021.1938724>
- Zhang RJ, Wang JG, Huang DL, Deng WA (2023) Life cycle and other biological characteristics of *Tetrix japonica*. *Journal of Environmental Entomology* 45(4): 965–973.
- Zhao XM, Su YZ, Shao T, Fan ZY, Cao LL, Liu WM, Zhang JZ (2022) Cuticle protein gene *LmCP8* is involved in the structural development of the ovipositor in the migratory locust *Locusta migratoria*. *Insect Molecular Biology* 31(6): 747–759. <https://doi.org/10.1111/imb.12801>
- Zheng ZM (1998) A study of Tetrigoidea from Xishuangbanna (Orthoptera). *Acta Zootaxonomica Sinica* 23(2): 161–180.
- Zheng ZM (2005a) Fauna of the Tetrigoidea from Western China. Science Press, Beijing, 501 pp.
- Zheng ZM (2013a) A new species of the genus *Macromotettixoides* Zheng (Orthoptera: Metrodorida) from Fujian Province. *Entomotaxonomia* 35(4): 241–244.
- Zheng ZM (2013b) Key to the species of *Systolederus*, *Hyboella*, *Bolivaritettix* (Orthoptera: Tetrigoidea: Metrodoridae) from China with descriptions of three new species. *Journal of Shangqiu Normal University* 29(12): 1–13.
- Zheng ZM, Jiang GF (2000) New genus and new species of Metrodoridae from Guangxi (Orthoptera: Tetrigoidea). *Acta Zootaxonomica Sinica* 25(4): 402–405.
- Zheng ZM, Jiang GF (2002) One new genus and seven new species of Tetrigoidea from southern region of Guangxi. *Zoological Research* 23(5): 409–416.
- Zheng ZM, Ou XH (2004) Three new species of the genus *Formosatettix* Tinkham from Hengduan Mountain region of western Yunnan (Orthoptera, Tetrigidae). *Acta Zootaxonomica Sinica* 29(1): 107–109.
- Zheng ZM, Shi FM (2009) Five new species of Tetrigoidea from Jiangxi Province of China (Orthoptera). *Acta Zootaxonomica Sinica* 34(3): 572–577.
- Zheng ZM, Wei ZM, Jiang GF (2005b) A new genus and a new species of Metrodoridae (Orthoptera) from China. *Acta Zootaxonomica Sinica* 30(2): 366–367.
- Zheng ZM, Li P, Wan B (2006) A revision of *Macromotettixoides* Zheng from China (Orthoptera: Metrodoridae). *Journal of Huazhong Agricultural University* 25(6): 603–605.

Chaomyia, a new monotypic genus of Tachininae from the Qinghai-Tibet Plateau, China (Arthropoda, Insecta, Diptera, Tachinidae)

Xusheng Liu^{1*}, Jiayi Ji^{2*}, Youpeng Lai², Dong Zhang³, Pierfilippo Cerretti⁴, Chuntian Zhang¹

1 Liaoning Key Laboratory of Biological Evolution and Biodiversity, College of Life Science, Shenyang Normal University, Shenyang 110034, China

2 Institute of Plant Protection, Academy of Agriculture and Forestry Sciences, Qinghai University, Xining 810016, China

3 School of Ecology and Nature Conservation, Beijing Forestry University, Beijing 100083, China

4 Department of Biology and Biotechnology 'Charles Darwin', University of Rome 'Sapienza', Rome, Italy

Corresponding authors: Chuntian Zhang (chuntianzhang@aliyun.com); Youpeng Lai (yplai@126.com); Dong Zhang (ernest8445@163.com);

Pierfilippo Cerretti (pierfilippo.cerretti@uniroma1.it)

Abstract

We erected a new genus of Tachinidae in the subfamily Tachininae, *Chaomyia* **gen. nov.** for the new species *C. qinghaiensis* **sp. nov.** from grasslands of Haiyan County, Qinghai Province, Qinghai-Tibet Plateau, China. *Chaomyia* **gen. nov.** is distinguishable from all other genera of Tachininae (Diptera: Tachinidae) based on morphological evidence. Key morphological characters include: small size (ca. 4–5 mm); eye nearly bare; lower facial margin strongly protruding forward in front of vibrissal angle; occiput with only black setulae; lower occiput bulging; bare prosternum; two postpronotal setae; 2 presutural and 3 postsutural dorsocentral setae; 3 pairs of strong marginal scutellar setae, apical setae strong and crossed; wing membrane around crossveins r-m and dm-cu darkened; male fore claws and pulvilli shorter than 5th tarsomere; and mid-dorsal depression of abdominal syntergite 1+2 not reaching hind margin of syntergite, sternites well exposed. A possible affiliation with the tribes Polideini or Ernestiini has been discussed using morphological evidence.

Key words: *Chaomyia*, new taxa, Palaearctic, systematics, tachinids



Academic editor: Filippo Di Giovanni

Received: 6 November 2024

Accepted: 24 March 2025

Published: 5 May 2025

ZooBank: <https://zoobank.org/6DACD34C-34F4-45E9-8D78-477281136FD5>

Citation: Liu X, Ji J, Lai Y, Zhang D, Cerretti P, Zhang C (2025)

Chaomyia, a new monotypic genus of Tachininae from the Qinghai-Tibet Plateau, China (Arthropoda, Insecta, Diptera, Tachinidae). ZooKeys 1236: 283–295. <https://doi.org/10.3897/zookeys.1236.141122>

Copyright: © Xusheng Liu et al.

This is an open access article distributed under terms of the Creative Commons Attribution License (Attribution 4.0 International – CC BY 4.0).

Introduction

Despite previous research efforts (O'Hara et al. 2009), the tachinid fauna of China remains significantly understudied (1109 species, 257 genera), especially in the more remote and inaccessible regions of the country, such as the Himalayas and the tropical forests of southern China.

Tachinidae (Diptera) are an important group of insect parasitoids (Stireman et al. 2006); most of them attack lepidopteran larvae, including many pest species (Tschorsnig 2017). In recent years, several initiatives have been undertaken to study the diversity of this group in China. These include expeditions (Chao and Zhou 1996), species cataloguing (O'Hara et al. 2020),

* These authors contributed equally to this work.

and sampling with Malaise traps in China (e.g., Pei et al. 2021; 2024a). The primary aim of these studies is to address ecological questions, such as whether and how parasitoid communities respond to environmental variables (Pei et al. 2024b).

In this context, a Malaise trap was placed in 2023 on the Qinghai-Tibet Plateau at an altitude of 3178 m a.s.l., a region that has been little explored. The Qinghai Province of China is located in the northeastern part of the Qinghai-Tibet Plateau, from the Hoh Xil region in the west (Chao and Zhou 1996) to the Aemye Ma-chhen Range in the east (about 1200 km), and from the southern edge of the Tanggula Mountains in the south to the Kunlun and northern Qilian Mountains in the north (800 km), with the average elevation of Qinghai being over 3000 m a.s.l. The collected material is currently being studied in detail using morphological techniques. As part of our results, we have found nine specimens of an unidentified species that share several characters with members of the tribe Polideini and Ernestiini of Tachininae but apparently cannot be assigned to any known genera. The aim of this study is to describe the new species, establish a new monotypic genus for it and provide explicit arguments for the placement of this new taxon within the tribe Polideini sensu O'Hara, 2002 or Ernestiini Townsend, 1912.

Material and methods

Taxon sampling and terminology

The specimens were collected in northern Qinghai, on the Qinghai-Tibet Plateau, China (Fig. 1). Specifically, the collection site was Halejing Mongolian Village (37°2'3"N, 100°59'52"E; elevation: 3178.7 m), located in Haiyan County, Haibei Tibetan Autonomous Prefecture. The sampling was conducted on September 5, 2023, using a Malaise trap by Jiayi Ji. Qinghai Province spans an area of 721,200 km² and is situated between 89°35'–103°04'E and 31°40'–39°19'N.

Morphological terminology and measurements used follow Tschorsnig and Richter (1998) and Cumming and Wood (2017). Preliminary identifications were made using the key of Tschorsnig and Richter (1998) and the matrix-based interactive key of Cerretti et al. (2012).

Specimens were examined using a Leica M205 C stereomicroscope. Digital images of the heads, bodies of male and female were taken with a Canon EOS 60D camera and the images were combined using Helicon Focus v. 8.1.0. Dissections of male and female terminalia were carried out following the method described by O'Hara (2002), digital images were taken with Leica M205 A stereomicroscope and images were combined using Leica Application Suiter v. 4.12.0. Dissected terminalia were placed in glycerin in a small plastic tube and pinned together with the source specimen. The species distribution map was generated with ArcGIS v. 10.2 (ESRI Inc.). The tachinid specimens of this study were deposited in the Insect Collection of Shenyang Normal University (**SYNU**), Shenyang and the Institute of Plant Protection, Academy of Agriculture and Forestry Sciences, Qinghai University (**QHU**), Xining, China.

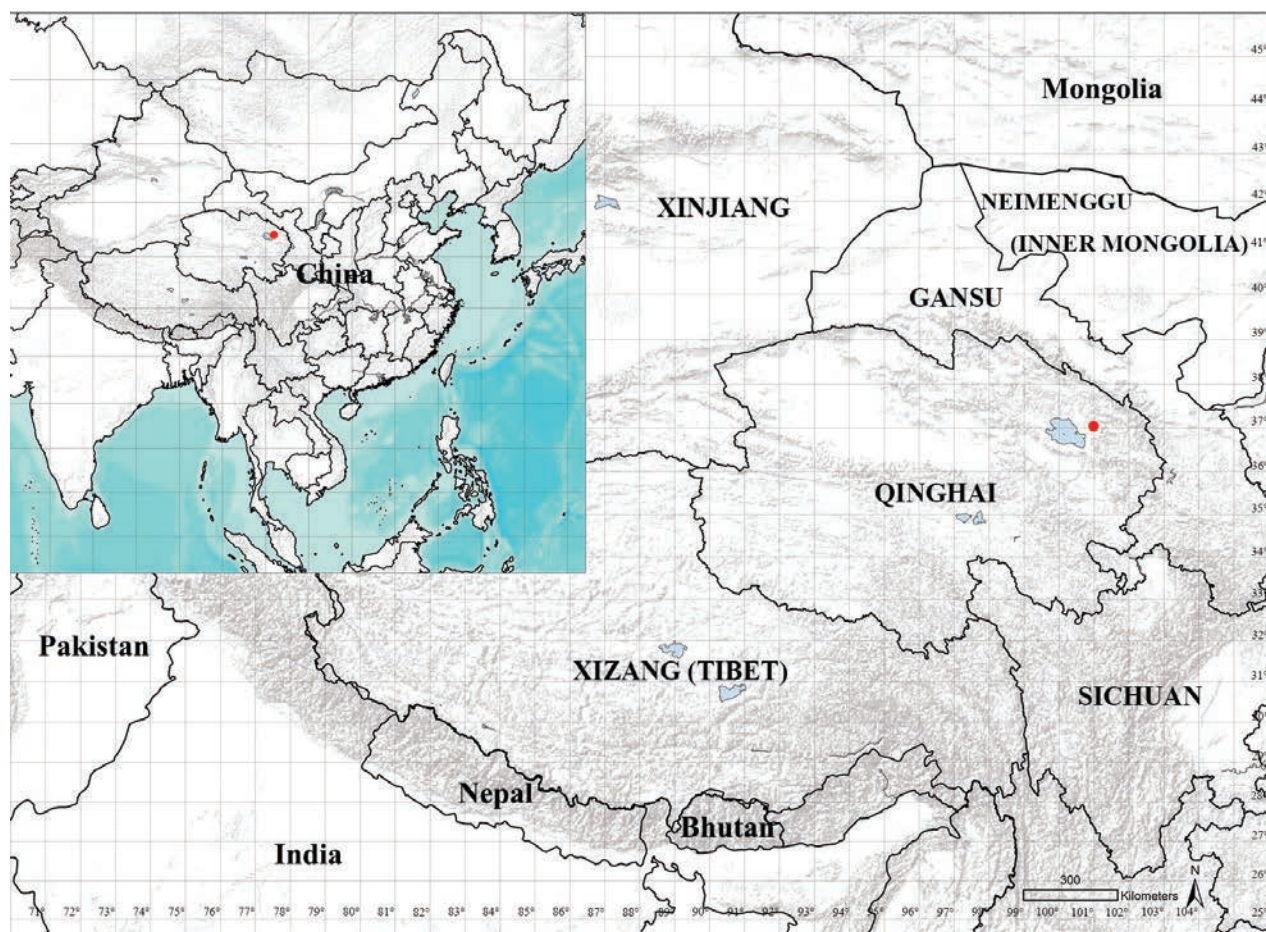


Figure 1. Type locality (Halejing, 3178.7 m, Haiyan County, Haibei Prefecture) of *Chaomyia qinghaiensis* sp. nov. from Qinghai, China.

Systematics

Subfamily Tachininae Rondani, 1859

Tribe Polideini sensu O'Hara, 2002 or Ernestiini Townsend, 1912

Chaomyia C. Zhang & Cerretti, gen. nov.

<https://zoobank.org/FEC2D23C-9C66-4491-84E9-F48DA6D8B414>

Figs 2–4

Type species. *Chaomyia qinghaiensis* C. Zhang & Cerretti, sp. nov., by present designation.

Remarks. Tribe Affiliation. *Chaomyia qinghaiensis* gen. & sp. nov. exhibits several characteristic morphological features, including a strongly protruding lower facial margin, which is well visible in front of vibrissal angle, a bare prosternum, and preapical anterodorsal seta of the fore tibia only slightly shorter than the preapical dorsal seta. Moreover, its male terminalia display a tergite 6 that is not longitudinally divided into hemitergites, a weakly sclerotized lateroventral area of distiphallus, and basiphallus that runs nearly parallel to distiphallus. This combination of likely derived character states is consistent with the assignment of the genus to the subfamily Tachininae (Tschorsnig and Herting 1994; Cerretti et al. 2014).

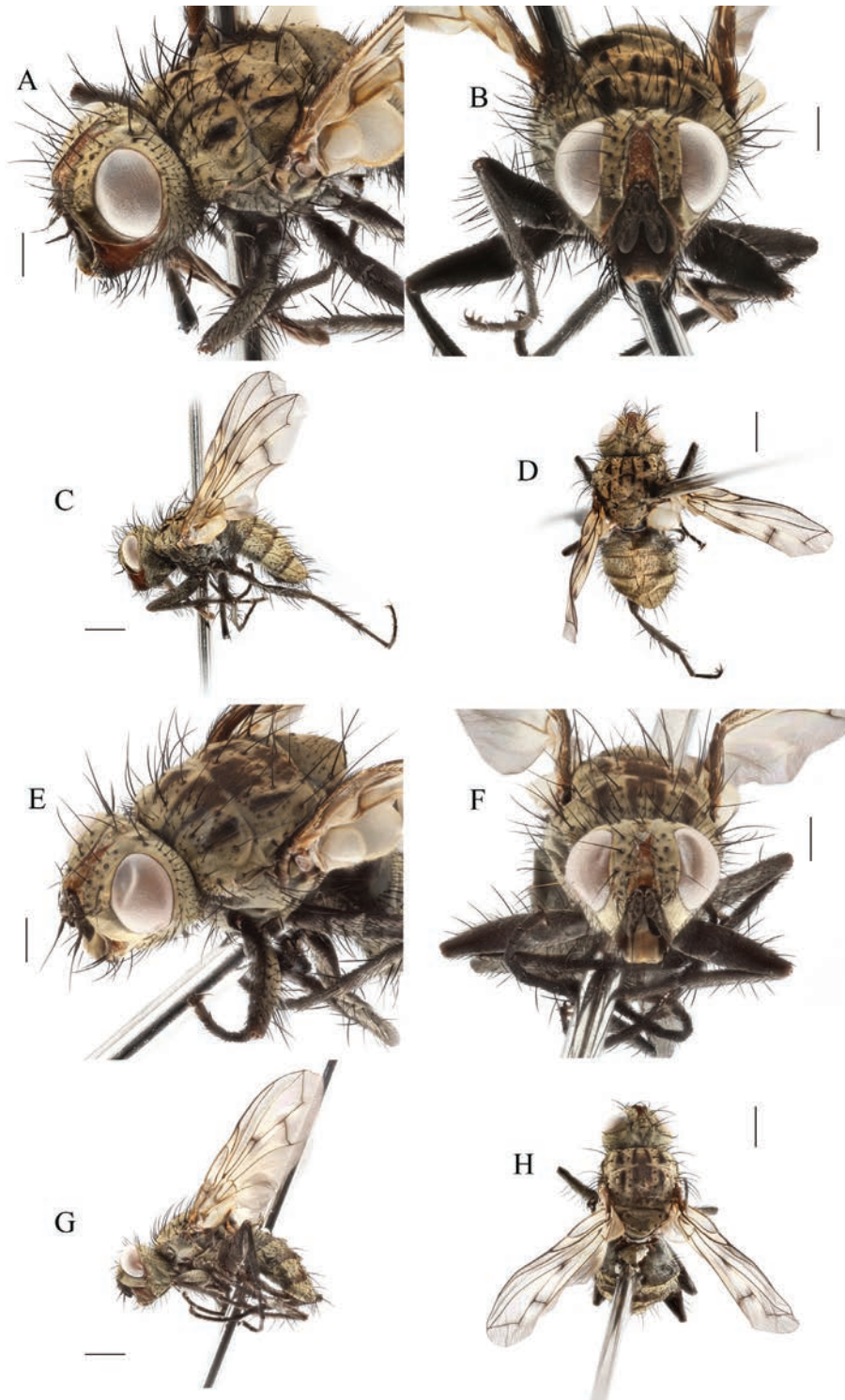


Figure 2. *Chaomyia qinghaiensis* sp. nov. **A–D**, ♂; **E–H**, ♀. **A, E, C, G** head and body in lateral view **B, F** head in anterior view **D, H** body in dorsal views. Scale bars 0.5 mm (**A, B, E, F**); 1.0 mm (**C, D, G, H**).

Recent phylogenetic reconstructions based on molecular data support Tachininae as a monophyletic group, with the exclusion of Macquartiini and Myiophasiini, a clade of parasitoids of beetle larvae that is widely distributed globally (Stireman et al. 2019). Adult Macquartiini and Myiophasiini share having males with strongly narrow frons, a body ground color which is mostly black and, although very variable, a male phallus lacking a sclerotize medioventral

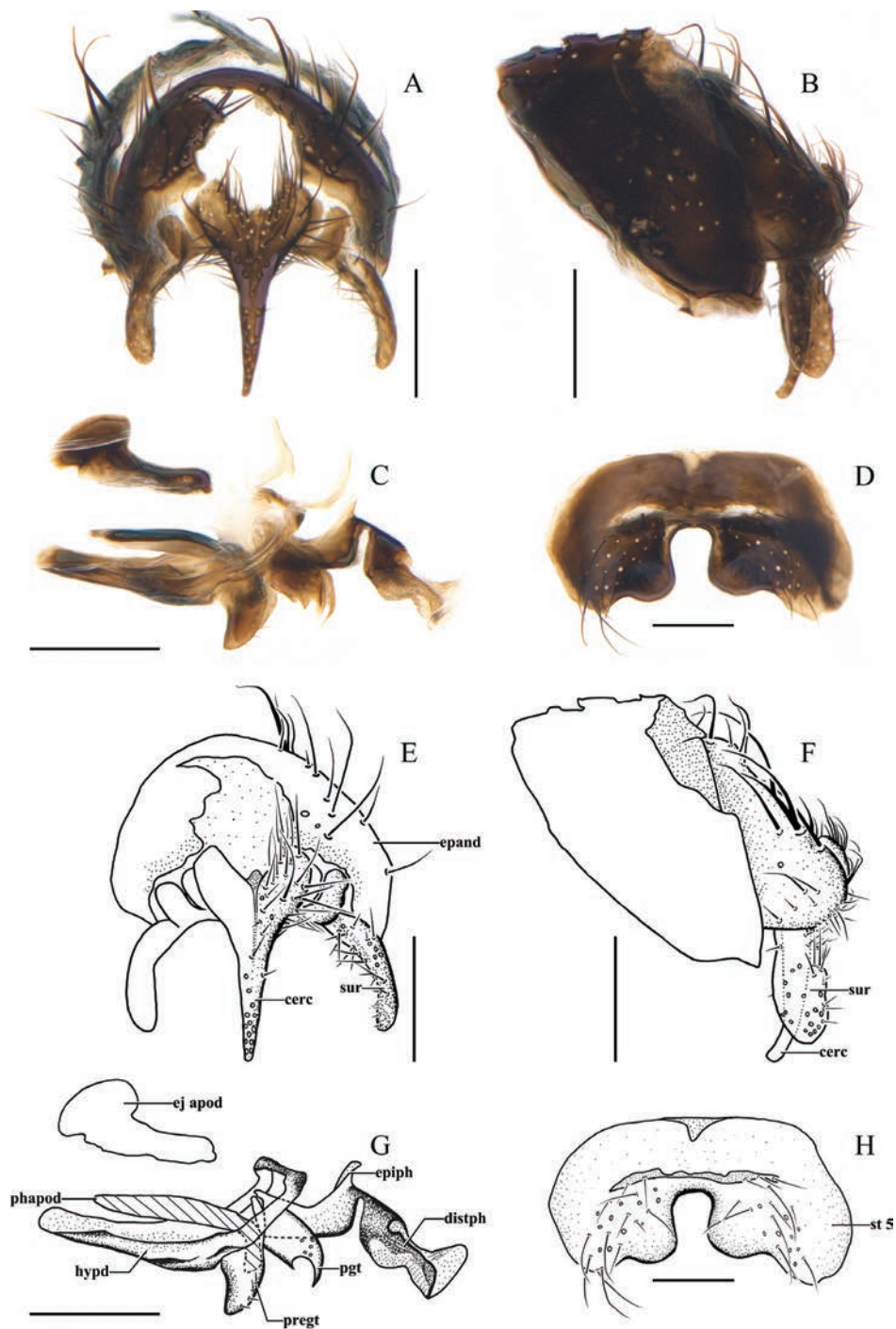


Figure 3. *Chaomyia qinghaiensis* sp. nov. **A–H**, ♂, **A, E**; **B, F** cerci, surstyli and epandrium of male in caudal and lateral views **C, G** phallus (aedeagal apodeme, ejaculatory apodeme, hypandrium, epiphallus, pregonite, postgonite, basiphallus and distiphallus) of male in lateral view **D, H** sternite 5 in ventral view. Scale bars: 0.1 mm.

sclerite, and cerci not fused into a syncercus. *Chaomyia* has male cerci fused into a syncercus, membranous posterior sclerite of distiphallus, well-developed anepimeral seta, male hypandrial arms that are posteromedially fused and completely encircle the base of the phallus, male epandrium with setae dorsally, and a distinctly shaped medioventral sclerite of the distiphallus (see O'Hara 2002, who described this as the anterior sclerite of the distiphallus). For these reasons, we think *Chaomyia* cannot be assigned to either of these two tribes.

Chaomyia shares most of the putative synapomorphies identified by O'Hara (2002) supporting the monophyly of the tachinine tribe Polideini. However, it lacks certain diagnostic features: the male surstylus in *Chaomyia* is nearly bare apically, rather than bearing spine-like setae; male sternite 5 possesses micro-pubescent along the inner margin of the posteromedian cleft, rather than distinct microspines; and the posterior thoracic spiracle is not uniformly haired on both sides but instead is covered by flap-like setulae originating only from its posterior margin. We interpret these morphological differences as evidence that *Chaomyia* could represent a member of the Polideini, pending confirmation of its phylogenetic position through molecular data.

In the key to Palearctic genera by Tschorsnig and Richter (1998: 756, 772, 777), our specimens key out to *Synactia* Villeneuve of the tribe Ernestiini. However, *Synactia* differs from *Chaomyia* in several respects, including: densely hairy eyes, facial ridge with setae on lower 2/5 to 2/3, lower facial margin not protruding forward, arista thickened on basal 1/2 or more, R_{4+5} with setulae at the base, and median excavation of syntergite 1+2 reaching to hind margin. Given these differences, *Chaomyia* cannot be confidently placed within *Synactia* or most other members of Ernestiini. Nevertheless, the available morphological evidence provisionally supports the assignment of *Chaomyia* to either the tribe Polideini or Ernestiini, pending further study.

Evidence supporting *Chaomyia* as new genus. Following a thorough examination and comparison of *C. qinghaiensis* sp. nov. with both collection material and scientific literature (Crosskey 1976; Wood 1987; Tschorsnig and Richter 1998; Wood and Zumbado 2010; Cerretti et al. 2012), we conclude that it exhibits a unique combination of morphological traits among Tachininae. This combination of characters is considered apomorphic, providing a strong justification for the establishment of a new genus to accommodate the species from Halejing.

Description. Male and female. Small-sized tachinid flies.

Head (Fig. 2A, B, E, F). Eyes nearly bare, with sparse very short ommatrichia. Frons 1.26–1.41 (male) and 1.33–1.60 (female) of eye width. Frontal vitta slightly narrower than fronto-orbital plate in front of ocellar triangle. Parafacial bare, at most as wide as postpedicel in anterior view. Face without facial carina; lower margin of face distinctly protruding forward in front of vibrissal angle and visible in lateral view. Gena 0.5–0.6 of eye height. Fronto-orbital plate with 5–7 inclinate frontal setae; 4–5 outer orbital setae, anterior one or two proclinate, posterior two or three latero-clinate in male; 4 outer orbital setae, anterior one proclinate and posterior three latero-clinate in female. Occiput with only black hairs behind postocular row, ventral part bulging. Arista bare, thickened at basal 1/3 to 2/5. Palpus about 3/4 as long as postpedicel, with 2–3 apical setae. Prementum 7–8 times as long as wide. Labellum small.

Thorax (Fig. 2C, D, G, H). Body densely covered with yellowish pruinosity. Prosternum bare. Postpronotal lobe with two setae and some hairs; first postsutural supra-alar seta about as long as the first postsutural intra-alar seta; one anepimeral seta extending to posterior margin of upper calypter. Scutellum entirely black, with 3 pairs of marginal setae, subapical scutellar seta not extending back to apices of strong crossed apical scutellar setae. Spiracles dark and small; posterior spiracle posterior fringe visibly larger than anterior fringe, proepimeral setae directed upward. Base of vein R_{4+5} with 2–4 small setulae dorsally and ventrally.

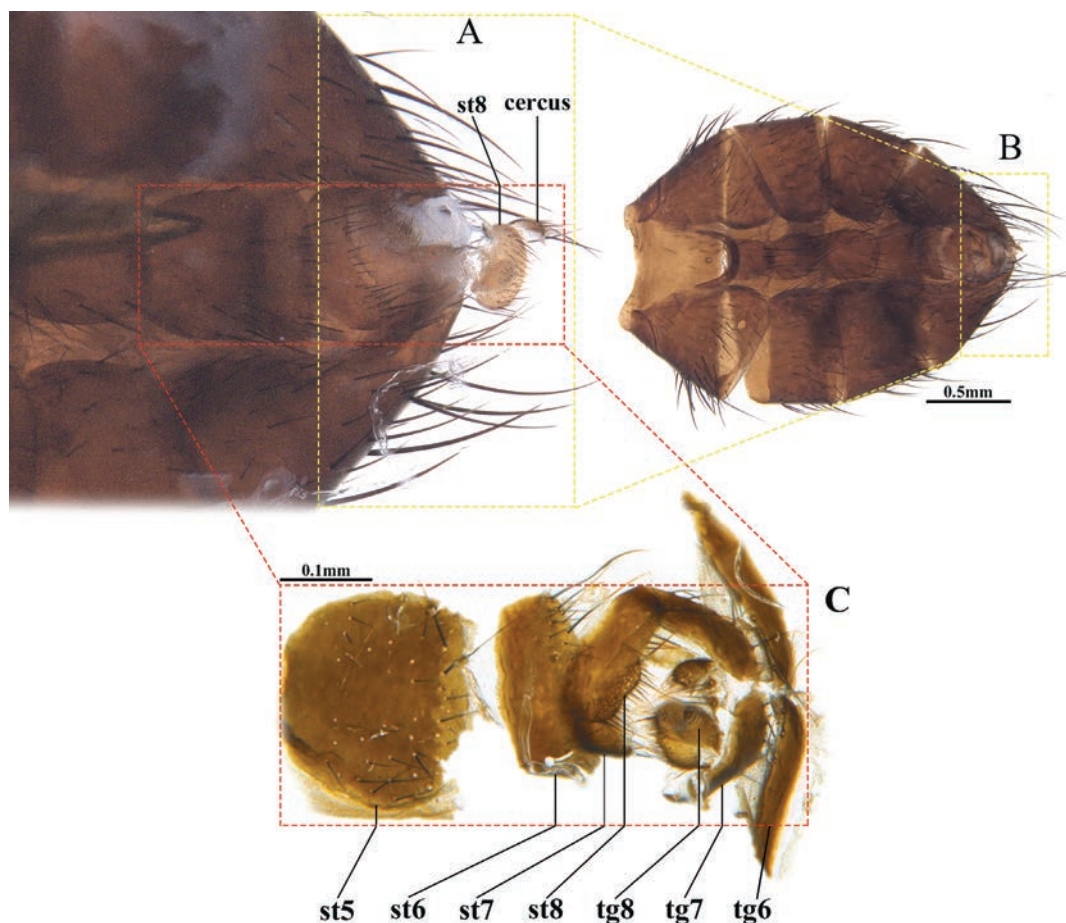


Figure 4. *Chaomyia qinghaiensis* sp. nov. ♀ Female abdomen in ventral view **A** postabdomen **B** abdomen **C** postabdomen in detail, st = sternite, tg = tergite, sternites 5, 6, 7, 8 and tergites 6, 7, 8.

Wing membrane around crossveins r-m and dm-cu darkened. Vein M evenly bent, bluntly angled, extending to wing margin making cell r_{4+5} closed at wing margin or merged to vein R_{4+5} to form a very short petiole.

Leg. Fore claws and pulvilli shorter than 5th tarsomere. Fore tibia with 2–3 short anterodorsal, 2 posterior and 1 posterodorsal setae, preapical anterodorsal seta approximately as long as preapical dorsal seta or just slightly shorter. Hind tibia with 2 preapical dorsal setae, preapical anteroventral seta about as long as preapical posteroventral seta.

Abdomen. Mid-dorsal depression on abdominal syntergite 1+2 not reaching to hind margin. Syntergites 1+2 to tergite 4 each with dark transverse band only on lateral posterior 1/4–1/5. Sternite 1 hairy; the other sternites exposed.

Male terminalia (Fig. 3A–H). Tergite 6 not divided medially into two hemitergites. In ventral view, sternite 5 nearly square with a deep, U-shaped median cleft which is approximately 1/2 length of the sternite; lateral lobe of sternite 5 with an inner protrusion bluntly rounded apically. In caudal view, cerci fused to form a syncercus, narrowed on apical 2/3 and pointed, not separated apically; surstylus narrowed and bent inwardly and blunt apically. In lateral view, syncercus longer than surstylus, bent backward apically; surstylus thick, bluntly round apically, without teeth or spines apically. Hypandrium broadly expanded posteriorly on both sides, hypandrial arms narrowly fused dorsally; pregonite broad, lobe-like; postgonite pointed apically; phallus well developed, basiphallus with a weakly sclero-

tized epiphallus in distal position; medioventral ridge of distiphallus present and well developed; lateroventral region of the distiphallus membranous, ejaculatory apodeme large and process fan-shaped.

Female terminalia (Fig. 4). Sternite 5 nearly square, with median and posterior setae; tergites 6–8 not divided into 2 hemiterigites, with a row of strong setulae; sternites 6–8 with posterior setulae.

Distribution. China: Halejing, 3178.7 m, Haiyan County, Haibei Prefecture, Qinghai Province (Fig. 1).

Etymology. The genus name is formed by the name of Chao Cheiming (= Zhao Jianming), a late Chinese dipterologist, plus the Greek *myia*, meaning “fly”, in memory of Chao’s great contributions to Tachinidae taxonomy of China. *Chaomyia* is treated as feminine.

***Chaomyia qinghaiensis* C. Zhang & Cerretti, sp. nov.**

<https://zoobank.org/F2E04888-2975-4ED7-AFFA-D9D639849793>

Figs 2–4

Material examined. Holotype: CHINA • ♂ (SYNU-QH 230001); Qinghai Province; Haiyan County, Haibei Tibetan Autonomous Prefecture, Halejing Mongolian Village; 37.0342°N, 100.9977°E; 3178.7 m elev., 5.IX.2023; Malaise trap-Jiayi Ji (SYNU). **Paratypes:** • 4 ♂ 4 ♀ (SYNU-QH 230002-9), same data as holotype (Fig. 1).

Diagnosis. Eyes nearly bare. Head and body densely covered with yellowish pruinosity. Frons more than eye width in both sexes, fronto-orbital plate of male with 5 to 7 inclinate frontal setae, 1~2 proclinate outer orbital setae and 2~3 latero-clinate outer orbital setae, gena height 0.5–0.6 of eye height, lower facial margin distinctly protruding forward, occiput with only black setulae. Wing with dark clouded at crossveins r-m and dm-cu. Male fore claws and pulvilli shorter than 5th tarsomere. Mid-dorsal depression of abdominal syntergite 1+2 extending on basal half, sternites well exposed.

Description. Male. Body length 4.5–5.2 mm.

Head (Fig. 2A, B). Eyes nearly bare, with only sparsely whitish short ommatrichia. Frontal vitta reddish brown. Frontal-orbital plate and parafacial covered with yellow pruinosity. Gena reddish brown. Antenna and arista black. Palpus dark brown. Prementum gleaming black. Frons 1.26–1.41 times of eye width. Frontal vitta slightly narrower than fronto-orbital plate in front of ocellar triangle. Parafacial bare, at most as wide as postpedicel in frontal view, as wide as postpedicel in lateral view. Median facial carina absent, lower facial margin distinctly protruding forward in front of vibrissal angle. Gena height about as long as postpedicel, 0.5–0.6 of eye height; genal dilation well developed. Fronto-orbital plate wide, with 2 rows of setae, 5 to 7 inclinate frontal setae, reaching on parafacial, the middle of pedicel; 1–2 proclinate outer orbital setae and 2–3 latero-clinate outer orbital setae; 2 ocellar setae situated between the anterior and posterior ocelli, proclinate, well developed, nearly as long as frontal setae close to ocellar triangle. Inner vertical seta about 0.7 of eye height; outer vertical seta 2/3–3/4 as long as inner vertical seta. Facial ridge more or less straight, with more or less erect short setae on lower 1/3. Vibrissa inserted level with lower facial margin or below, slightly longer than subvibrissal setae; subvibrissal ridge with 4–5 strong subvibrissal setae mixed with some fine setulae. Postpedicel

2.0–2.3 times as long as pedicel; pedicel with 1 long seta on dorsal surface, which is slightly longer than pedicel. Arista thickened on basal 1/3 to 2/5, about as long as antenna, 2nd aristomere 2.0–2.5 times as long as wide. Palpus filiform, not apically enlarged, about 3/4 as long as postpedicel, with 2–3 apical setae. Prementum 7–8 times as long as its diameter. Labellum small.

Thorax (Fig. 2C, D). Scutum covered with yellow pruinosity and four dark longitudinal vittae on dorsum, presutural inner vitta about 1/4 as wide as pruinose portion between inner and outer vittae, presutural outer vittae approximately triangular; inner vittae only on anterior 1/3 of postsutural scutum. Two presutural and 2 postsutural acrostichal setae; 2 presutural and 3 postsutural dorsocentral setae; 2 postsutural intra-alar setae separated by a distance greater than the distance between the first seta and the suture; first postsutural supra-alar seta slightly longer than notopleural setae, about as long as the first postsutural intra-alar seta. Scutellum with 3 pairs of marginal setae, subapical scutellar seta not extending back to level of apices of strong crossed apical scutellar setae and tilted upwards by 30–60°. Prosternum bare; postpronotal lobe with two setae; proepisternum bare; anepisternum with two antero-upper weak setae and a row of 4–6 posterior setae. Anepimeron with 1 seta extending to anterior 1/2 of lower calypter; katepisternum with 3 setae (2 anterior and 1 posterior, anterior-lower one weaker) with 3 seta-like hairs between anterior and posterior setae. Katepimeron bare. Anatergite below calypter and katatergite bare. Posterior spiracle small and posterior fringe visibly larger than anterior fringe. Postmetacoxal area membranous.

Wing long and narrow, hyaline, brownish. Tegula and basicosta dark brown. Second costal section bare ventrally, costal spine short or absent. Base of R_{4+5} with 2–4 small setulae dorsally and ventrally. Relative lengths of 2nd, 3rd and 4th costal sectors approximately 1:4:2. Vein M evenly bent, bluntly angled, extending to wing margin, making cell r_{4+5} closed or short petiolate. Costal sector 4 distinctly longer than costal sector 6. Section of vein M between r-m and dm-cu about as long as section between dm-cu and bend of M. Crossvein dm-cu nearly straight and not exceptionally oblique. Section of vein M between dm-cu and bend at least 2 times distance between the bend and wing posterior margin. Vein CuA_1 bare. Lower calypters milky white with yellowish, bare on dorsal surface, inner edge of lower calypters close to outer edge of scutellum, its outer margin not strongly convex. Halter brownish yellow, only darker at apex and larger than posterior spiracle.

Leg dark brown. Fore claws and pulvilli shorter than 5th tarsomere. Fore tibia with 2–3 short anterodorsal, 2 posterior and 1 posterodorsal setae, preapical anterodorsal seta slightly shorter or approximately as long as preapical dorsal seta or just slightly shorter. Mid femur with 1 anterior, 1 preapical dorsal seta and a row of posteroventral setae on basal half; mid tibia with 2 anterodorsal, 2–3 posterior and 1 ventral setae. Hind coxa bare on posterodorsal surface; hind femur separately with a row of anteroventral, posteroventral setae and anterodorsal setae, 2 posterodorsal setae on apical 1/3; hind tibia with 3–4 anterodorsal, 3 posterodorsal and 2 ventral setae, 2 preapical dorsal setae, preapical anteroventral seta about as long as preapical posteroventral seta.

Abdomen long ovate, almost covered with grayish-yellow pruinosity, tergites not fused dorsally, syntergite 1+2 to tergite 4 each with dark transverse band on lateral posterior 1/5. Mid-dorsal depression of syntergite 1+2 extending on the proximal half, syntergite 1+2 with 2 median marginal and 1–3 lateral marginal setae. Tergite 3 with 2 median marginal and 2 weak median discal setae, 1 pair

of lateral marginal and 2 pairs of lateral discal setae. Tergite 4 with a row of marginal setae, 2 median discal and 2 pairs of lateral discal setae. Tergite 5 inverted trapezoid-like, approximately the same length as tergite 4, with a row of a marginal setae, 2 median discal setae, 2–3 pairs of lateral discal setae. Ventral surface of tergites 4 and 5 covered with thin decumbent hairs on a shiny, non-pruinose cuticle. Sternite 1 hairy, the other sternites exposed; sternites 2 to 4 each with 3–4 setae on posterior portion. Sternite 5 and male terminalia are the same as generic descriptions as shown in Fig. 3A–H.

Female (Figs 2E–H; 4). Frons 1.33–1.60 of eye width. Parafacial equal or slightly wider than postpedicel in frontal view, wider than postpedicel in lateral view. Gena higher than antennal length in lateral view. Six pairs of frontal setae. Postpedicel 1.5–2.0 times as long as pedicel. Mid tibia with 4–5 posterodorsal setae. Hind tibia with 2–3 ventral setae. Abdominal syntergite 1+2 without median marginal seta; tergite 5 inverted cone-like. Other features are same as in male.

Distribution. China: Halejing, 3178.7 m, Haiyan County, Haibei Prefecture, Qinghai Province (Fig. 1).

Etymology. The species name is taken from the type locality, Qinghai Province, China. Adjective.

Discussion

This study is yet another example, among many now available in the global scientific literature, of how environments increasingly threatened by anthropogenic activities risk erasing the traces of species whose identity and functions within the ecosystem are still unknown (Wilson 2017). Parasitoids are key organisms in the functioning of all terrestrial ecosystems, and we cannot predict the impact of their extinction or population reduction if we do not even know how many species exist. This is particularly true at a time when human-induced climate change will also affect human activities to such an extent that many populations will be forced to migrate (Kaczan and Orgill-Meyer 2020), possibly to higher altitudes. Parasitoid communities regulate the population dynamics of their hosts, which are often primary consumers. Any imbalance in these dynamics could lead to instability, with potentially dramatic consequences for local economies and human health (Di Marco et al. 2023). Describing biodiversity is only the first but essential step, and it is up to taxonomists to accelerate the pace of this description.

The *Chaomyia qinghaiensis* gen. & sp. nov. specimens were found on a plateau at high altitudes where anthropogenic impact, although still limited, is mainly characterized by pastoralism and some cultivations. This habitat and region have been rarely explored previously and what we found is remarkable. The specimens display a unique combination of morphological features not shared by any other tachinid genus described from the Palaearctic (Tschorsnig and Richter 1998; Cerretti et al. 2012) and Oriental (Crosskey 1976) regions. For this reason, we propose to establish a new genus for them.

Acknowledgements

We are thankful to Filippo Di Giovanni, the editor, Hiroshi Shima (Kyushu University, Fukuoka, Japan), and James E. O'Hara (Agriculture and Agri-Food Canada, Ottawa, Ontario), who kindly proofread the manuscript, carefully checked the

references, and gave much help and critical comments throughout our work on the final text. Our special thanks are extended to two anonymous referees, for their critical reviews and suggestions. We are grateful to Hans-Peter Tschorsnig (Staatliches Museum für Naturkunde, Stuttgart), Ziegler J. (Museum für Naturkunde, Berlin) and Hui Yang (Shenyang Normal University) for their assistance to Z-CT.

Additional information

Conflict of interest

The authors have declared that no competing interests exist.

Ethical statement

No ethical statement was reported.

Funding

This study was supported by the National Natural Science Foundation of China to Z-CT (32470459, 31970443) and Key Research and Development and Transformation Projects (No. 2023NK152) from Qinghai Provincial Science and Technology Department and Qinghai innovation platform construction project: Qinghai Provincial Key Laboratory of Restoration Ecology of Cold Area to L-YP (2017-ZJ-Y20).

Author contributions

Conceptualization: Z-CT, L-YP, P-C, Z-D. Data curation: Z-CT, L-YP, J-JY, L-XS. Formal analysis: P-C, Z-CT. Investigation and material: L-YP, J-JY. Writing-original draft: Z-CT, L-XS and P-C, J-JY. Visualization: L-XS. Funding acquisition and Supervision: Z-CT and L-YP. Writing - review and discussion: Z-CT, P-C, Z-D.

Author ORCIDs

Xusheng Liu  <https://orcid.org/0009-0001-3758-1465>

Jiayi Ji  <https://orcid.org/0009-0001-7402-8239>

Youpeng Lai  <https://orcid.org/0000-0001-9188-9906>

Dong Zhang  <https://orcid.org/0000-0001-6427-7867>

Pierfilippo Cerretti  <https://orcid.org/0000-0002-9204-3352>

Chuntian Zhang  <https://orcid.org/0000-0002-9514-0502>

Data availability

All of the data that support the findings of this study are available in the main text or Supplementary Information.

References

- Cerretti P, Tschorsnig HP, Lopresti M, Di Giovanni F (2012) MOSCHweb – a matrix-based interactive key to the genera of the Palaearctic Tachinidae (Insecta, Diptera). *ZooKeys* 205: 5–18. <https://doi.org/10.3897/zookeys.205.3409>
- Cerretti P, O'Hara J, Wood DM, Shima H, Inclan DJ, Stireman JO III (2014) Signal through the noise? Phylogeny of the Tachinidae (Diptera) as inferred from morphological evidence. *Systematic Entomology* 39: 335–353. <https://doi.org/10.1111/syen.12062>
- Chao CM, Zhou SX (1996) Diptera Tachinidae. In: Wu SG, Feng ZJ (Eds) *The biology and human physiology in the Hoh Xil Region. The Series of the Comprehensive Scientific*

- Expedition to the Hoh Xil Region. Science Press, Beijing, 217–224. [In Chinese with English summary]
- Crosskey RW (1976) A taxonomic conspectus of the Tachinidae (Diptera) of the Oriental Region. *Bulletin of the British Museum (Natural History) Entomology. Supplement* 26: 1–357. <https://doi.org/10.5962/p.78194>
- Cumming JM, Wood DM (2017) Adult morphology and terminology. In: Kirk-Spriggs AH, Sinclair BJ (Eds) *Manual of Afrotropical Diptera: Vol. 1, Suricata 4*. SANBI Publications, Pretoria, 89–133.
- Di Marco M, Santini L, Corcos D, Tschorsnig HP, Cerretti P (2023) Elevational homogenization of mountain parasitoids across six decades. *Proceedings of the National Academy of Sciences of the United States of America* 120(46): e2308273120. <https://doi.org/10.1073/pnas.2308273120>
- Kaczan DJ, Orgill-Meyer J (2020) The impact of climate change on migration: a synthesis of recent empirical insights. *Climatic Change* 158: 281–300. <https://doi.org/10.1007/s10584-019-02560-0>
- O’Hara JE (2002) Revision of the Polideini (Tachinidae) of America north of Mexico. *Studia Dipterologica. Supplement* 10: 1–170.
- O’Hara JE, Shima H, Zhang CT (2009) Annotated Catalogue of the Tachinidae (Insecta: Diptera) of China. *Zootaxa* 2190(1): 1–236. <https://doi.org/10.11646/zootaxa.2190.1.1>
- O’Hara JE, Zhang CT, Shima H (2020) Tachinidae. In: Yang D, Wang MQ, Li WL et al. (Eds) *Species Catalogue of China, Vol. 2. Animals, Insecta (VII), Diptera (3): Cyclorhaphous Brachycera*. Science Press, Beijing, 841–963. [In Chinese]
- Pei WY, Yan LP, Pape T, Wang QK, Zhang CT, Yang N, Du FX, Zhang D (2021) High species richness of tachinid parasitoids (Diptera: Calyptratae) sampled with a Malaise trap in Baihua Mountain Reserve, Beijing, China. *Scientific Reports* 11: 22193. <https://doi.org/10.1038/s41598-021-01659-8>
- Pei WY, Feng V, Hansen AH, Yan LP, Srivathsan A, Xu W, Sun HR, Yang J, Zhang XC, Yang N, Yuan QY, Zhang D, Meier R (2024a) Megabarcoding reveals a tale of two very different dark taxa along the same elevational gradient. *bioRxiv*. <https://doi.org/10.1101/2024.04.29.591578>
- Pei WY, Xu WT, Li HN, Yan LP, Gai Y, Yang N, Yang J, Chen JL, Peng HL, Pape T, Zhang D, Zhang CT (2024b) Unusual rearrangements of mitogenomes in Diptera revealed by comparative analysis of 135 tachinid species (Insecta, Diptera, Tachinidae). *International Journal of Biological Macromolecules* 258: 128997. <https://doi.org/10.1016/j.ijbiomac.2023.128997>
- Stireman JO III, O’Hara JE, Wood DM (2006) Tachinidae: evolution, behavior, and ecology. *Annual Review of Entomology* 51: 525–555. <https://doi.org/10.1146/annurev.ento.51.110104.151133>
- Stireman JO III, Cerretti P, O’Hara JE, Blaschke JD, Moulton JK (2019) Molecular phylogeny and evolution of world Tachinidae (Diptera). *Molecular Phylogenetics and Evolution* 139: 106358. <https://doi.org/10.1016/j.ympev.2018.12.002>
- Tschorsnig H-P (2017) Preliminary host catalogue of Palaearctic Tachinidae (Diptera). Version 1. PDF document, 480 pp. <http://www.nadsdiptera.org/Tach/WorldTachs/CatPalHosts/Home.html>
- Tschorsnig H-P, Herting B (1994) Die Raupenfliegen (Diptera: Tachinidae) Mitteleuropas: Bestimmungstabellen und Angaben zur Verbreitung und Ökologie der einzelnen Arten. *Stuttgarter Beiträge zur Naturkunde Serie A (Biologie)* 506: 1–170.

- Tschorsnig HP, Richter VA (1998) Family Tachinidae. In: Papp L, Darvas B (Eds) Contributions to a Manual of Palaearctic Diptera (with special reference to flies of economic importance). Vol. 3. Higher Brachycera. Science Herald, Budapest, 691–827.
- Wilson EO (2017) Biodiversity research requires more boots on the ground: Comment. *Nature Ecology & Evolution* 1(11): 1590–1591. <https://doi.org/10.1038/s41559-017-0360-y>
- Wood DM (1987) Tachinidae. In: McAlpine JF, Peterson BV, Shewell GE, Teskey HJ, Vockeroth JR, Wood DM (Eds) Manual of Nearctic Diptera. Vol. 2. Agriculture Canada Monograph 28, 1193–1269.
- Wood DM, Zumbado MA (2010) Tachinidae (tachinid flies, parasitic flies). In: Brown BV, Borkent A, Cumming JM, Wood DM, Woodley NE, Zumbado MA (Eds) Manual of Central American Diptera. Vol. 2. NRC Research Press, Ottawa, 1343–1417.

Supplementary material 1

Taxa, voucher and GenBank accession numbers used in this study

Authors: Xusheng Liu, Jiayi Ji, Youpeng Lai, Dong Zhang, Pierfilippo Cerretti, Chuntian Zhang

Data type: doc

Copyright notice: This dataset is made available under the Open Database License (<http://opendatacommons.org/licenses/odbl/1.0/>). The Open Database License (ODbL) is a license agreement intended to allow users to freely share, modify, and use this Dataset while maintaining this same freedom for others, provided that the original source and author(s) are credited.

Link: <https://doi.org/10.3897/zookeys.1236.141122.suppl1>

New species of *Plesioaxymyia* Sinclair (Diptera, Axymyiidae) from the Palaearctic Region, including an updated molecular phylogeny of the family

Alexei Polevoi¹, Nikola Burdík², Jan Ševčík²

¹ Forest Research Institute, 185035, Pushkinskaya 11, Petrozavodsk, Russia

² Department of Biology and Ecology, Faculty of Science, University of Ostrava, Chittussiho 10, CZ-710 00 Ostrava, Czech Republic

Corresponding author: Alexei Polevoi (alexei.polevoi@krc.karelia.ru)

Abstract

The family Axymyiidae includes four extant genera and nine species known from the Holarctic and Oriental regions, with only one species *Mesaxymyia kerteszi* (Duda, 1930) occurring in Europe. The genus *Plesioaxymyia* Sinclair, 2013 was first discovered in Alaska in 1962, but officially described only many years later. Up to now, the genus included one species *Plesioaxymyia vespertina* Sinclair, 2013, known from two female specimens from western North America. During the study of the Diptera fauna in Paanajarvi National Park (Northwest Russia), one female specimen of *Plesioaxymyia*, was found. It differs from the Nearctic *P. vespertina* by details of its female terminalia and is recognized as a new species, herein described as *Plesioaxymyia imprevista* sp. nov. The biology and geographic distribution of *Plesioaxymyia* is briefly discussed. The phylogenetic position of the genus, along with the family Axymyiidae is analyzed in the light of new molecular data, including sequences of three mitochondrial (ribosomal 12S and 16S and protein-encoding COI) and three nuclear genes (ribosomal 18S and 28S, protein-encoding CAD) for 72 terminal taxa. Axymyiidae is recovered as a monophyletic group with closest relatives in the infraorder Culicomorpha and *Plesioaxymyia imprevista* sp. nov. representing the sister taxon to all the other species of Axymyiidae included in the analysis.

Key words: Biology, distribution, lower Diptera, Nematocera, new species, Russia, systematics



Academic editor: Vladimir Blagoderov

Received: 29 January 2025

Accepted: 19 March 2025

Published: 5 May 2025

ZooBank: <https://zoobank.org/40535841-E730-44D4-B5D0-D45E54A6FA93>

Citation: Polevoi A, Burdík N, Ševčík J (2025) New species of *Plesioaxymyia* Sinclair (Diptera, Axymyiidae) from the Palaearctic Region, including an updated molecular phylogeny of the family. ZooKeys 1236: 297–315. <https://doi.org/10.3897/zookeys.1236.148218>

Copyright: © Alexei Polevoi et al.
This is an open access article distributed under terms of the Creative Commons Attribution License (Attribution 4.0 International – CC BY 4.0).

Introduction

The family Axymyiidae is often referred to as “enigmatic” in the literature (Wihlm and Courtney 2011; Blagoderov and Lukashovich 2013; Fitzgerald and Wood 2014). This small group of flies includes four extant genera and nine species known in the Holarctic and Oriental regions (Fitzgerald and Wood 2014). Additionally, eight species in four extinct genera have been described from the Jurassic or Early Cretaceous deposits of Asia (Blagoderov and Lukashovich 2013; Shi et al. 2013). Only one species, *Mesaxymyia kerteszi* (Duda, 1930), is so far known from Europe. This is an extremely rare taxon, with a few recent records from eastern Slovakia (Martínovský and Roháček 1993) and Northwest Russia (Polevoi et al. 2018).

As it is known so far, all immature records of Axymyiidae are associated with dead wood. Extremely specialized larvae live inside very wet, often submerged, logs of various tree species (Wood 1981; Krivosheina 2000). The systematic position of this family is still uncertain (see Blagoderov and Lukashovich 2013; Sinclair 2013; Fitzgerald and Wood 2014 for reviews). It is often placed in or as a sister group to Bibionomorpha, but close relationships with this infraorder are not always supported by reconstructions, based on molecular data. In the comprehensive study by Wiegmann et al. (2011), Axymyiidae were placed within Bibionomorpha sensu lato, as a sister group to Bibionomorpha sensu stricto, whereas in other studies this family was represented as a sister group to Culicomorpha (Bertone et al. 2008; Ševčík et al. 2016) or in an unresolved polytomy (Zhang et al. 2023).

During studies of the Diptera fauna in Paanajarvi National Park (Russia, Karelia), an unusual looking female specimen was collected, evidently belonging to the family Axymyiidae. Preliminary examination showed that it was not a representative of any previously known Palaearctic genus, but accords well with the genus *Plesioaxymyia* Sinclair, which includes one North American species, *P. vespertina* Sinclair, 2013. Being morphologically very similar, the Karelian specimen differs from *P. vespertina* by characters of its terminalia. Considering the general rarity of the family Axymyiidae and the evident importance of the new record we feel it necessary to describe the new species and not wait for additional material. Moreover, we could not miss an opportunity to re-evaluate the phylogenetic position of *Plesioaxymyia* and Axymyiidae as a whole, based on new molecular data for extant species.

Material and methods

The type specimen was collected in Paanajarvi National Park, located in the northwestern part of the Republic of Karelia, Russia (Fig. 1). The park was established in 1992, and presently occupies a territory of over 104,000 ha, mostly covered with natural coniferous forests (Bizhon and Systra 1996; Timofeeva and Kutenkov 2009). In 2021, we used three Malaise traps as part of an insect inventory program in the territory of the park. The *Plesioaxymyia* specimen was collected with a trap set in a patch of spruce- and pine-dominated forest of *Vaccinium myrtillus* type, in the vicinity of the abandoned village of Vartolambina. The operation period of the trap was from June 1–27, which corresponds to late spring. Willows and some early-season flowers (e.g., *Tussilago*) were in blossom, and remnants of snow still could be found in shady places.

The trap residue was initially kept in 70% alcohol, and one Axymyiidae specimen was recognized during a preliminary inspection in the laboratory. For a detailed study, the specimen was dried by xylol and amyl acetate baths (Achterberg 2009). Terminalia were detached and macerated in KOH for 24 hours, then neutralized in acetic acid, washed in 70% alcohol, and transferred to glycerine. Finally, terminalia were placed in glycerine vial and pinned together with the rest of the specimen. The holotype is stored in the collection of the Zoological institute, St. Petersburg, Russia (ZISP).

Images of the habitus and wing were taken with a Leica MZ 9.5 stereo microscope and those of the terminalia with a Leica DM1000 compound microscope, both supplied with a LOMO MC6.3 camera. Z-stacked image series



Figure 1. Location of Paanajarvi National Park, Karelia, Russia.

were combined using Helicon Focus v. 8.2.0 software, and final plates prepared with GIMP. The morphological terminology follows Sinclair (2013). The distribution map was created using the online tool SimpleMappr, available at <https://www.simplemappr.net/>.

Molecular methods principally follow those described in Ševčík et al. (2016). A total of 72 terminal taxa are included in the dataset (Appendix 1). Most of the specimens used in this study were collected by Malaise traps during the years 2000–2022. Some sequences were taken from the GenBank database. The material used in the molecular study was stored in ethanol (70% to 96%) or pinned. For DNA extraction, we used a NucleoSpin Tissue Kit (Macherey-Nagel, Düren, Germany) following the manufacturer's protocol. PCRs (total volume = 20 µl) were performed using specific primers for sequences of three mitochondrial (ribosomal 12S and 16S and protein-encoding COI) and three nuclear genes (ribosomal 18S and 28S, protein-encoding CAD). The primers used for PCR amplifications and sequencing are listed in Table 1.

All amplified products were purified using a Gel/PCR DNA Fragments Extraction Kit (Geneaid, New Taipei City, Taiwan) following the manufacturer's

Table 1. Primers used for PCR amplification and sequencing of the mitochondrial 12S, 16S and COI genes and nuclear 18S, 28S and CAD genes.

Gene fragment	Direction	Primer sequences (5'→3')	Source
12S	F	CTGGGATTAGATACCCTGTTAT	Koufopanou et al. 1999
	R	CAGAGAGTGACGGGCGATTTGT	Koufopanou et al. 1999
	F	TACTATGTTACGACTTAT	Kambhampati and Smith 1995
	R	GCCAGCATTGCGGTATAC	M. Žurovcová lab., České Budějovice, Czech Republic
16S	F	TAATCCAACATCGAGGTC	Roháček et al. 2009
	R	CGAAGGTAGCATAATCAGTAG	Roháček et al. 2009
	F	CGCCTGTTTATCAAAAACAT	Palumbi et al. 1991
	R	CCGGTCTGAACTCAGATCACGT	Palumbi et al. 1991
18S	F	AACCTGGTTGATCCTGCCAGT	Katana et al. 2001
	R	TGATCCTTCTGCAGTTTCACCTACG	Katana et al. 2001
	F	AGATACCGCCCTAGTTCTAACC	Campbell et al. 1995
	R	GGTTAGAAGTACGGGCGGTATCT	Campbell et al. 1995
28S	F	AGAGAGAGAGTTCAAGAGTACGTG	Belshaw and Quicke 1997
	R	TAGTTCACCATCTTTCGGGTC	Laurenne et al. 2006
	F	ACCCGCTGAATTTAAGCAT	Dayrat et al. 2001
COI	F	GGTCAACAAATCATAAAGATATTGG	Folmer et al. 1994
	R	TAAACTTCAGGGTGACCAAAAAATCA	Folmer et al. 1994
CAD	F	GGNGTNACNACNGCNTGYTTYGARCC	Moulton and Wiegmann 2004
	R	TTNGGNAGYTGNCNCCCAT	Moulton and Wiegmann 2004
	F	ACNGAYTAYGAYATGTGYGA	Moulton and Wiegmann 2004
	R	TCRTTNTTYTTWGCRTAYAAATGCAT	Moulton and Wiegmann 2004

protocol. Purified products were sequenced by MacroGen Europe (Netherlands) or Eurofins Genomics (Germany). The sequences were assembled and edited in Sequencher v. 5.0 (Gene Codes Corporation, Ann Arbor, MI, USA) or SeqTrace v. 0.9.0 (Stucky 2012). GenBank accession numbers for all the sequences are listed in the Appendix 1. All sequences were checked with the NCBI database using the BLAST and in single-gene trees to avoid possible contamination or other inappropriate results.

Alignments of all genes were created using MAFFT v. 7 on the MAFFT server (<http://mafft.cbrc.jp/alignment/server/>). The resulting alignments were visually inspected and manually refined in BioEdit v. 7.2.5 (Hall 1999) when necessary. All unreliably aligned regions of rRNA genes were removed in the program GBLOCKS v. 0.91b (Castresana 2000); with conditions set as follows: allow smaller blocks, allow gap positions within the final blocks, allow less strict flanking positions and do not allow many contiguous non-conserved positions, or in ClipKIT v. 2.2.2 (Steenwyk et al. 2020) using the -gappy option with a threshold of 0.7. The third positions of COI gene were excluded from the subsequent analyses using software DAMBE (Xia and Xie 2001). The alignments were concatenated using FASconCAT v. 1.0 (Kück and Longo 2014). The final data matrix consisted of 5419 characters: 12S – 301 bp, 16S – 287 bp, 18S – 1985 bp, 28S – 1005 bp, COI – 436 bp (third positions removed) and CAD – 1405 bp.

The final concatenated dataset was partitioned by gene and codon position and subsequently analysed using the maximum likelihood (ML) method. Analyses were conducted using IQ-TREE v. 1 (Nguyen et al. 2015) on the IQ-TREE web server (Trifinopoulos et al. 2016). Best-fitting substitution models were chosen automatically by the IQ-TREE software: 12S – TVM+F+I+G4; 16S – TVM+F+I+G4; 18S – GTR+F+I+G4; 28S – TVM+F+I+G4; CAD_1 – TN+F+I+G4; CAD_2 – SYM+I+G4; CAD_3 – GTR+F+I+G4; COI_1 – TIM2+F+I+G4; COI_2 – TIM3+F+I+G4; without free-rate heterogeneity. Branch supports were evaluated using 1000 ultrafast bootstrap (Hoang et al. 2018). All other settings were left as default. The node support values are given in the form of ultrafast bootstrap (= ufboot). The resulting phylogenetic tree (consensus trees) was visualized using the Interactive Tree of Life (iTOL v. 7.0; Letunic and Bork 2024). A species of Mecoptera, *Boreus hyemalis* (Linnaeus, 1767), was used as a root.

Results

Family Axymyiidae

Plesioaxymyia imprevista Polevoi, sp. nov.

<https://zoobank.org/F101EC9C-CA50-40E2-ABA1-B631CAD5F331>

Figs 2A–C, 3A–C

Specimens examined. Holotype. RUSSIA • ♀; Karelia, Paanajarvi National Park, Vartolambina; 66.246°N, 30.555°E; 80 m a.s.l.; 1–27 Jun. 2021; A. Protasova leg.; Malaise trap; GenBank: accession numbers PV036313, PV036316, PV036319, PV036317, PV035246, PV037681; ZISP, INS_DIP_0001011.

Differential diagnosis. Medium-sized, dark brown species (Fig. 2A); wings hyaline with dark elongated pterostigma, covering apical half of vein R₁; legs yellowish-brown with darkened tarsi, femora and tibiae darkened apically. Similar to *Plesioaxymyia vespertina*, from which it is distinguished by details of female terminalia: sternite 8 with smoothly rounded dorsoapical margin (forming somewhat protruding dorsoapical corner in *P. vespertina*) and completely reduced basal segment of cerci (distinct in *P. vespertina*).

Description. Head. Head dark brown. Face sunken, clypeus convex, mouthparts brown. Palpus brown, 5-segmented, with short (almost hidden) first segment and broadened third segment. Compound eye densely covered with short ommatrichia; divided by fine groove into upper and lower hemispheres of unequal size and with deep triangular excision opposite antennal base (Fig. 2B). Three ocelli arranged in equilateral triangle, placed on elevated tubercle. Frons with a few brownish hairs above antennal bases and between ocellar triangle and compound eye. Posterior part of head with numerous brownish hairs. Antenna 16-segmented, brown; pedicel yellowish apically; middle flagellomeres about twice as wide as long.

Thorax. Mesonotum dark brown, thinly dusted, lacking any larger setae but covered with tiny yellowish hairs; a pair of narrow transverse shiny patches present along prescutal suture (Fig. 2B); prescutum yellowish laterally. Scutellum yellowish-brown, strongly convex, with short hairs along posterior margin. Pleura brown.

Wing. Wing length 4.08 mm. Wing hyaline with light brownish tinge (Fig. 2C); brown elongated pterostigma occupies apical half of R₁. Costa hardly produced

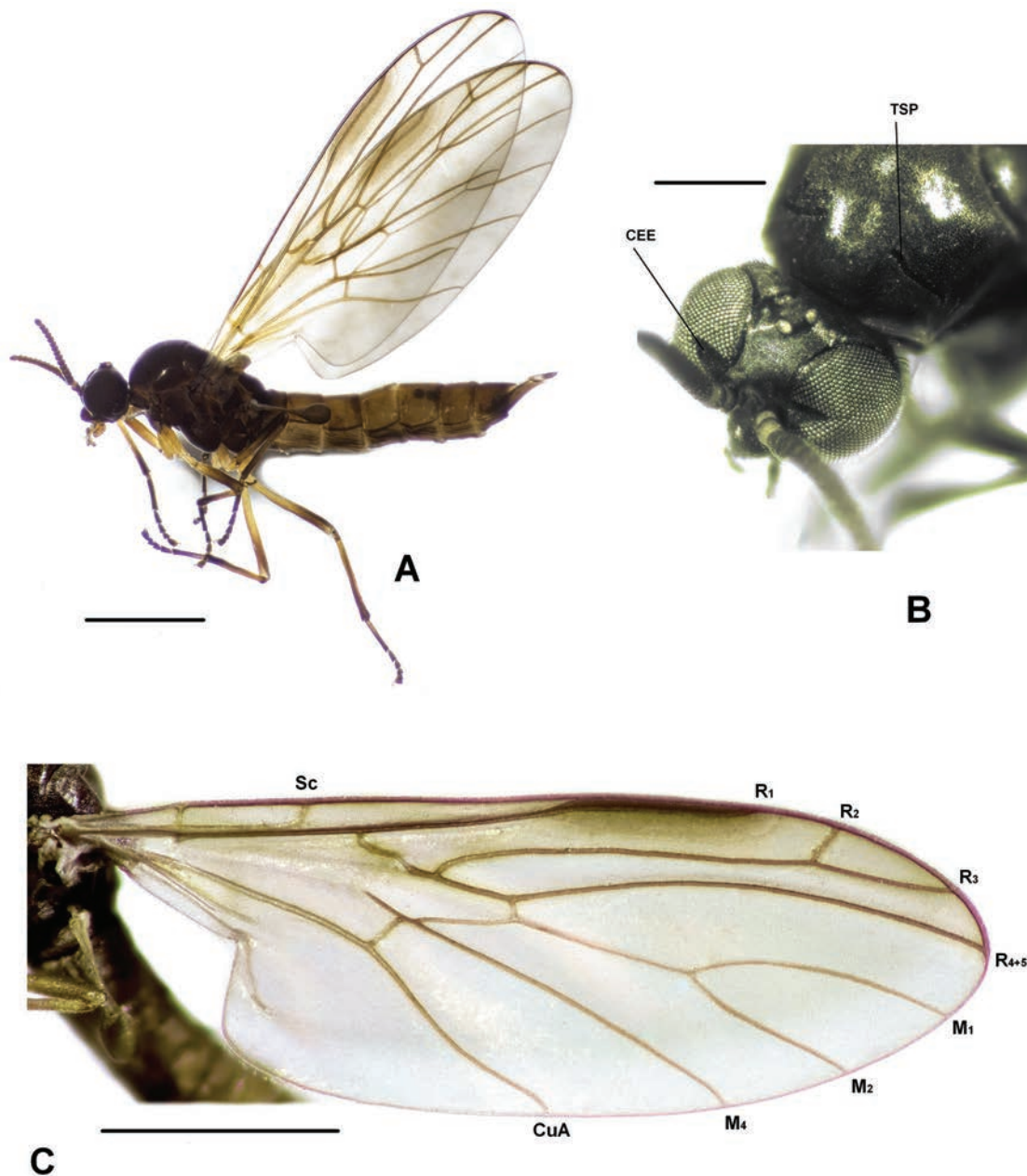


Figure 2. *Plesioaxymyia imprevista* sp. nov., female holotype **A** habitus, lateral view **B** head and thorax, oblique anterodorsal view **C** wing. Abbreviations: CEE – triangular excision of compound eye; CuA – anterior branch of cubital vein; $M_{1,2,4}$ – medial veins; $R_{2,3,4+5}$ – radial vein; Sc – subcostal vein; TSP – transverse shiny patch of mesonotum. Scale bars: 1 mm (**A**, **C**); 0.3 mm (**B**).

beyond R_{4+5} . Sc curved into costa proximally to R_s ; Sc-r reduced. R_s with kink; R_{2+3} forked well beyond apex of R_1 , R_2 deviates in slightly obtuse angle. Crossvein r-m perpendicular to R_{4+5} . M_{1+2} branching slightly before apex of R_1 ; section of M-stem distal to r-m about as long as M_1 , longer than M_2 and about twice as long as its section proximal to r-m. M_4 straight; CuA distinctly sinuous. CuP short, scarcely reaching beyond posteromedial angle of wing. Anal lobe well-developed. Macrotrichia on wing veins not visible. Halter brown.

Legs. Coxa, trochanters, femora and tibiae yellowish-brown; all femora and tibiae darkened apically; tarsi brownish. Hind tibia slightly curved in middle, with brush of bristly hairs posteroapically. Ratio of basitarsus to tibia: bt1:t1 – 0.45, bt2:t2 – 0.43, bt3:t3 – 0.30. Tibial spurs not developed.

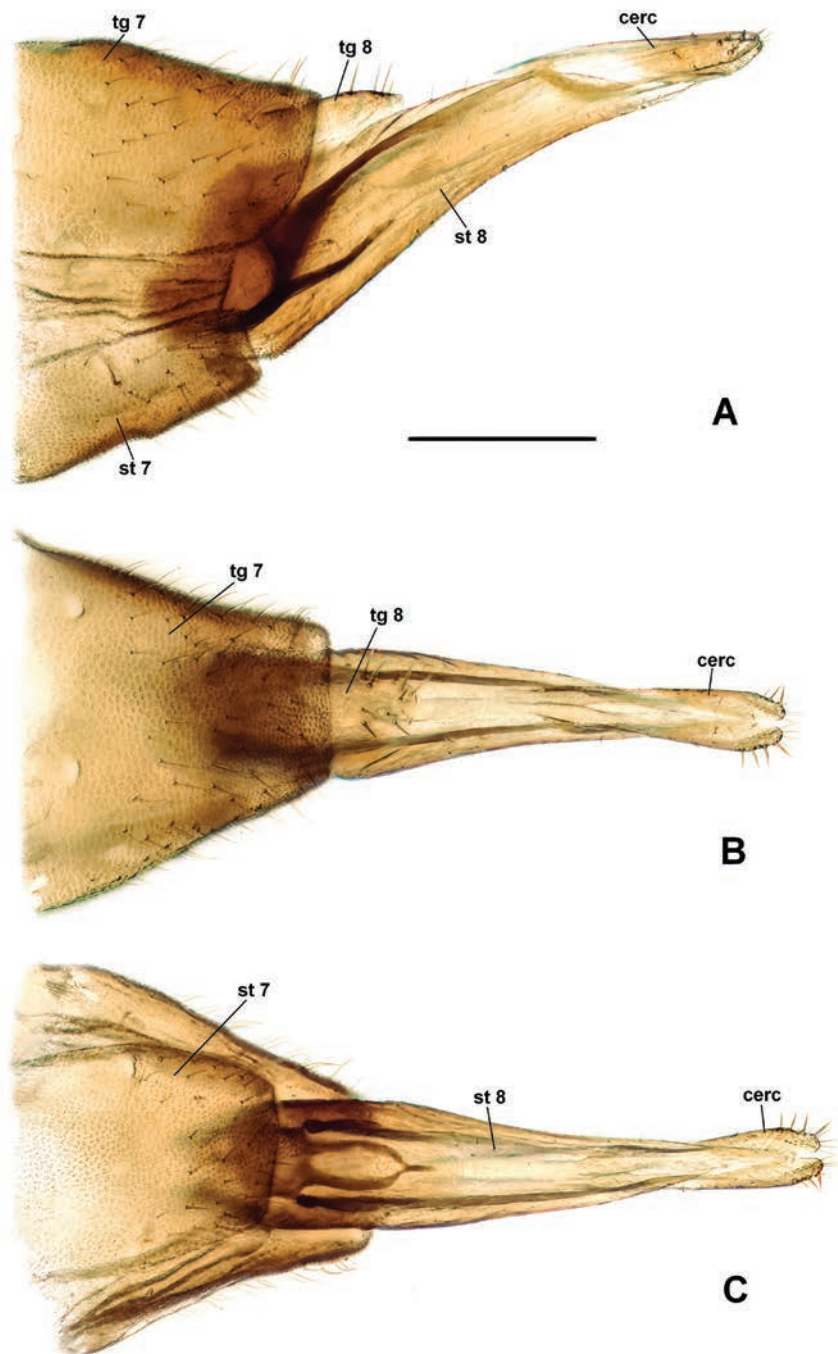


Figure 3. *Plesioaxymyia imprevista* sp. nov., female terminalia **A** lateral view **B** dorsal view **C** ventral view. Abbreviations: cerc—cercus; st 7, 8—sternites; tg 7, 8—tergites. Scale bars: 0.2 mm (A–C).

Abdomen. Abdomen brown. Tergites 1–7 with sparse hairs posteriorly. Terminalia (Fig. 3) brown. Tergite 8 approximately one-third length of sternite 8, rounded and setose apically; sternite 8 lengthened, tapered apically, with sparse short hairs. Cercus one-segmented; basal segment not developed; apical segment about 4 times longer than wide, bearing ca. 10 setae.

Etymology. The species epithet is from the Latin *imprevistus* (unexpected, unforeseen), stressing that the finding of this species in Northwest Russia was a real surprise.

Distribution. The species is currently known only from the type locality in Russian Karelia (Northwest Russia).

Biology. The adult was collected with a Malaise trap set in *Vaccinium myrtillus* type pine- and spruce-dominated forest. The larval biology is unknown.

Key to the Holarctic species of *Plesioaxymyia*, females

- 1 Sternite 8 forming somewhat protruding dorsoapical corner in lateral view, basal segment of cerci distinct (Sinclair 2013, figs 4, 5).....
..... ***P. vespertina* Sinclair, 2013**
- Sternite 8 with smoothly rounded dorsoapical margin in lateral view, basal segment of cerci completely reduced (Fig. 3A, B)***P. imprevista* sp. nov.**

Molecular data

The family Axymyiidae, represented in this dataset by five species from all four extant genera, is recovered as monophyletic with maximum support (ufboot = 100) (see Fig. 4). The new species described in this paper, *Plesioaxymyia imprevista* sp. nov., represents the sister taxon to all other species of Axymyiidae included in the dataset. Surprisingly, two species of *Protaxymyia* are not recovered as sister taxa. Instead, *Protaxymyia thuja* Fitzgerald & Wood, 2014 is sister species (ufboot = 95) to the branch including *Axymyia furcata* McAtee, 1921 and *Mesaxymyia kerteszi*. The sister relationship of the latter two species is, however, weakly supported (ufboot = 61).

The closest relative of the family Axymyiidae appears to be the infraorder Culicomorpha, although their sister relationship is only moderately supported (ufboot = 84). The well-supported clade (Tanyderidae + Psychodidae), represented by *Protoplasa fitchii* Osten Sacken, 1859 and *Clogmia albipunctata* (Williston, 1893), forms a sister group to the clade (Axymyiidae + Culicomorpha), also with moderate support (ufboot = 82).

The infraorder Bibionomorpha sensu stricto is shown to be monophyletic with high support (ufboot = 100), as well as Bibionomorpha sensu lato (ufboot = 98), including also Anisopodidae, Canthyloscelidae and Scatopsidae. The sister clade to Bibionomorpha is the infraorder Brachycera, altogether forming the well-supported group Neodiptera (ufboot = 97), which is sister clade to the large group of aquatic or semi-aquatic lower Diptera formed by the families Ptychopteridae, Blephariceridae, Tanyderidae, Psychodidae, and Axymyiidae and the families of the infraorder Culicomorpha.

Discussion

Biology and distribution

Some species of the family Axymyiidae can be rather abundant in suitable places, at least in respect of the density of larvae (Krivosheina 2000; Wihlm and Courtney 2011). However, representatives of the genus *Plesioaxymyia* apparently are not among them. The Nearctic *P. vespertina* was searched for repeatedly in the location where it was first found (Sinclair 2013). It was encountered again only 50 years later, and far to the south of the earlier known locality. The

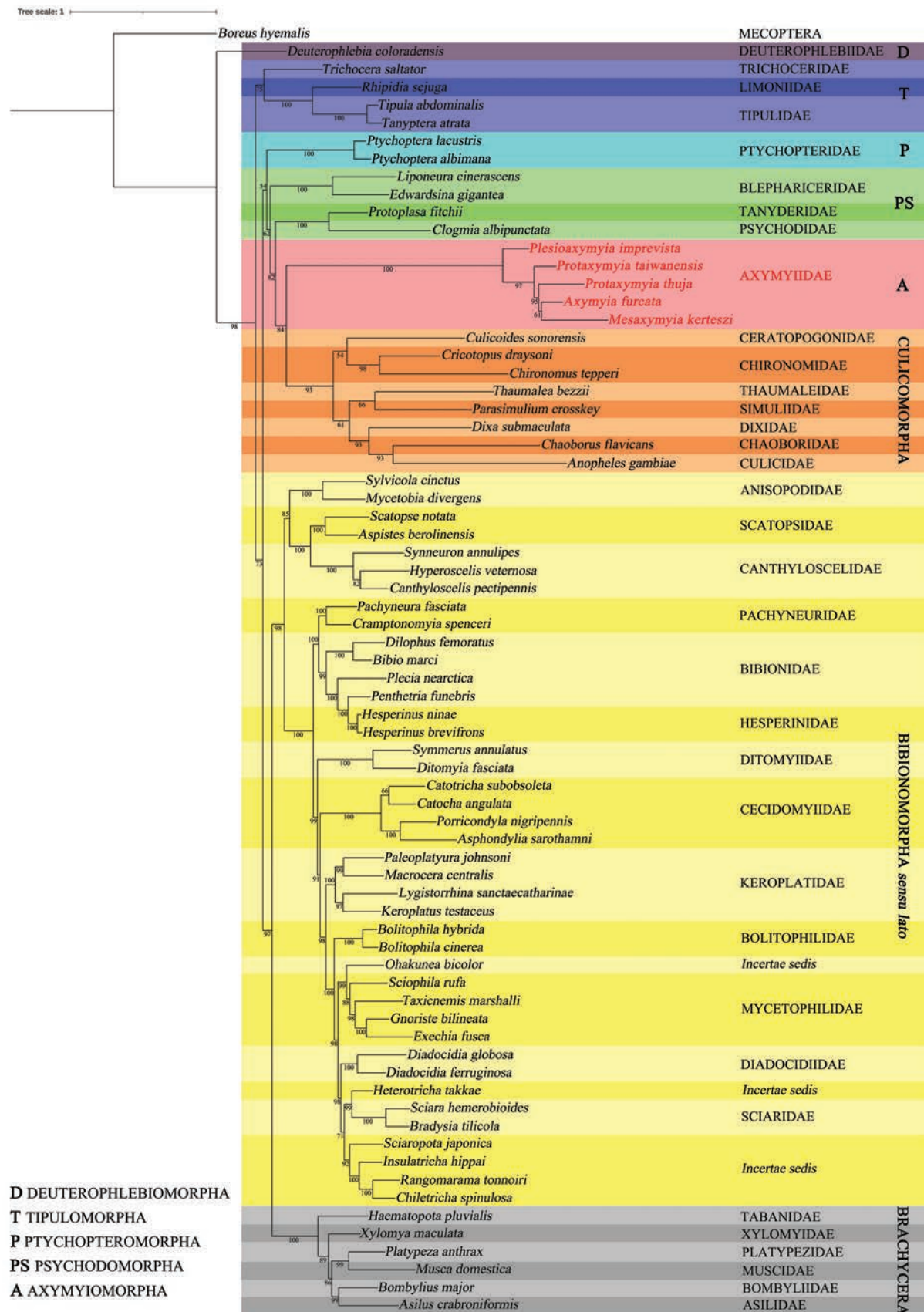


Figure 4. Maximum likelihood hypothesis (IQ-TREE) for relationships among selected taxa of lower Diptera based on DNA sequence data /12S, 16S, 28S, 18S, COI (third positions removed) and CAD/, 5419 characters. Support numbers refer to ultrafast bootstrap values (ufboot) over 50.

Paanajarvi area in Russian Karelia has been known for its relatively well-studied entomofauna since the middle of 20th century (Viramo 1998; Yakovlev et al. 2000), but during this time no Axymyiidae came into any entomologist's view. All known records of *Plesioaxymyia*, both in North America and Russian Karelia, look to be accidental, which may be the result of extremely small populations or a cryptic lifestyle.

Adults of Axymyiidae usually can be found in shady habitats, near rivers, rivulets or other water bodies, close to woody substrates where the larvae develop (Krivosheina 2000; Wihlm and Courtney 2011). The collecting localities of *P. vespertina* in North America well meet these conditions (Sinclair 2013); however, *P. imprevisa* sp. nov. was found in a patch of relatively dry coniferous forest (Fig. 5). The patch is bordered from the north by *Cladonia* type pine stands, and the only available water body around is the Olanga River, about 200 m to the south. Considering unsuccessful attempts to collect immature stages at the Alaskan and Mt. Rainier localities, Sinclair (2013) suggested that the larva of *P. vespertina* may reside in wet litter or decomposing fungi. In Paanajarvi, potentially suitable dead wood sources were totally absent close to the trap location. The distance from the river, however, does not look unreachable (even if Axymyiidae are considered weak fliers), so the wet dead wood, potentially available along the riverbank, cannot be excluded as a larval substrate. In general, the biology of *Plesioaxymyia* remains almost unknown. For now, we only can outline the flight activity period and preferred habitats, while other details of the life history are yet to be discovered.

The current range of *Plesioaxymyia* comprises the western Nearctic and western Palaearctic (Fig. 6). It is highly likely that the current disjunct pattern is just a result of insufficient knowledge. Considering the occurrence of the genus at relatively high latitudes (or high altitudes in more southern regions), a circumpolar, possibly boreo-alpine, distribution can be suggested, and further findings from at least the northern regions of East Russia can be expected.

Molecular phylogeny

The position of Axymyiidae as a sister group of Culicomorpha was initially revealed by Bertone et al. (2008), whose reconstruction was based on four nuclear gene markers and one sequenced taxon, namely *Axymyia furcata*. It was rendered together with *Nymphomyia dolichozepea* Courtney, 1994 (Nymphomyiidae) with relatively low branch support (56%). The authors themselves considered this placement to be ambiguous, suggesting that it may have been influenced by the long-branch attraction effect. The subsequent study by Ševčík et al. (2016), which was based on six gene markers, focused on Bibionomorpha. However, it also included two species of Axymyiidae (*Axymyia furcata* and *Protaxymyia thuja*) among numerous taxa in the broad outgroup. In this study, the sister group relation to Culicomorpha was identified again, though with similarly low support. The recent reconstruction, based on the complete mitochondrial genome (Zhang et al. 2023), included one taxon (*Protaxymyia* sp.) and did not demonstrate any clear relations for Axymyiidae, whose position appeared in an unresolved polytomy.

Sinclair (2013) proposed that *Plesioaxymyia* is sister group to the remaining Axymyiidae based on morphological characters. This hypothesis is now



Figure 5. Collecting biotope of *Plesioaxymyia imprevista* sp. nov. **A** position of Malaise trap (yellow circle), displayed on a satellite image (<https://www.bing.com/maps>) **B** general view of the biotope.



Figure 6. Distribution of the genus *Plesioaxymyia* in the Holarctic Region. *Plesioaxymyia vespertina* is indicated by red circles and *P. imprevista* sp. nov. by a green circle.

corroborated by genetic data. However, the grouping of other species deviates from expectations. Notably, *Protaxymyia thuja* is not rendered as sister taxon to *P. taiwanensis* Papp, 2007, being placed closer to species described in different genera (*Axymyia furcata* and *Mesaxymyia kerteszi*).

The distinction between the genera of Axymyiidae (except the very peculiar *Plesioaxymyia*) is not clearly defined. Separation of adults largely relies on wing characters (Krivosheina 2000; Zhang 2010; Shi et al. 2013); however, with the

accumulation of new materials, it has become evident that wing venation is not stable and its significance in the generic classification of Axymyiidae, including extinct genera, should be re-evaluated (Martinovský and Roháček 1993; Blagoderov and Lukashovich 2013; Fitzgerald and Wood 2014). The importance of larval and pupal characters (Krivoshchina 2000; Fitzgerald and Wood 2014) is similarly unclear, given that preimaginal stages of several species have not yet been discovered.

Conclusion

Our reconstruction of the molecular phylogeny is the first to incorporate representatives of all extant genera of Axymyiidae, although this still represents only approximately half of the known species. Axymyiids constitute a relatively isolated group, with the Culicomorpha families representing its closest evolutionary relatives. Both groups share an aquatic or semi-aquatic larval habitat. The sister group relation of Axymyiidae to Culicomorpha is in agreement with the findings of Bertone et al. (2008) and Ševčík et al. (2016) and is now evidenced with much better (ufboot = 84) support. While this may not yet be considered as strongly reliable, it is assumed that it could be even better supported if more taxa were included.

The current, unexpected placement of the species in relation to the Axymyiidae genera may be an artefact caused by the incomplete DNA data for *Mesaxymyia kerteszi* and *Axymyia furcata*. However, new molecular data provide additional background for the necessity of a revised generic classification of Axymyiidae. It is likely that such a revision will not be possible until details of the morphology of preimaginal stages and, preferably, also genetic data on all extant species are available.

Acknowledgements

We express our sincere gratitude to the staff of Paanajarvi National Park, and especially to Anastasiya Protasova for their assistance during the field studies. We also highly appreciate help from Elena Lukashovich (Moscow, Russia) and Andrei Przhiboro (St. Petersburg, Russia) with some important literature sources on the family Axymyiidae. The field research in Taiwan was carried out in cooperation with the National Chung Hsing University, Taichung, and the National Museum of Natural Science, Taichung. We are especially grateful to Sheng-Feng Lin and Michal Tkoč for their help with the field work in Taiwan. Peter Chandler (Melksham, UK), Bradley Sinclair (Ottawa, Canada) and Scott Fitzgerald (Corvallis, USA) kindly read the manuscript and provided useful comments.

Additional information

Conflict of interest

The authors have declared that no competing interests exist.

Ethical statement

No ethical statement was reported.

Funding

The work of A.P. was carried out under state order to the Karelian Research Center of the Russian Academy of Sciences (Forest Research Institute). The research of N.B. and J.Š. was funded by the Ministry of Education of the Czech Republic by institutional financing of the long-term conceptual development of the research institution (University of Ostrava).

Author contributions

Conceptualization: AP. Formal analysis: NB. Investigation: JŠ. Methodology: AP, JŠ. Software: NB. Visualization: NB, AP. Writing – original draft: AP, JŠ. Writing – review and editing: AP, JŠ.

Author ORCIDs

Alexei Polevoi  <https://orcid.org/0000-0003-2932-9574>

Nikola Burdíková  <https://orcid.org/0009-0009-0735-4411>

Jan Ševčík  <https://orcid.org/0000-0001-7174-593X>

Data availability

All of the data that support the findings of this study are available in the main text or Supplementary Information. Sequence data used in this article are available in the GenBank Nucleotide Database at <https://www.ncbi.nlm.nih.gov/genbank>.

References

- Achterberg K van (2009) Can Townes type Malaise traps be improved? Some recent developments. *Entomologische Berichten* 69: 129–135.
- Belshaw R, Quicke DLJ (1997) A molecular phylogeny of the Aphidiinae (Hymenoptera: Braconidae). *Molecular Phylogenetics and Evolution* 7: 281–293. <https://doi.org/10.1006/mpev.1996.0400>
- Bertone MA, Courtney GW, Wiegmann BM (2008) Phylogenetics and temporal diversification of the earliest true flies (Insecta: Diptera) based on multiple nuclear genes. *Systematic Entomology* 33: 668–687. <https://doi.org/10.1111/j.1365-3113.2008.00437.x>
- Bizhon AV, Systra YJ (1996) The Paanajarvi National Park – a remarkable piece of the world natural heritage. *Oulanka Reports* 16: 11–16.
- Blagoderov VA, Lukashevich ED (2013) New Axymyiidae (Insecta: Diptera) from the Mesozoic of East Siberia. *Polish Journal of Entomology / Polskie Pismo Entomologiczne* 82: 257–271. <https://doi.org/10.2478/v10200-012-0040-9>
- Campbell BC, Steffen-Campbell JD, Sorensen JT, Gill RJ (1995) Paraphyly of Homoptera and Auchenorrhyncha inferred from 18S rDNA nucleotide sequences. *Systematic Entomology* 20: 175–194. <https://doi.org/10.1111/j.1365-3113.1995.tb00090.x>
- Castresana J (2000) Selection of conserved blocks from multiple alignments for their use in phylogenetic analysis. *Molecular Biology and Evolution* 17: 540–552. <https://doi.org/10.1093/oxfordjournals.molbev.a026334>
- Dayrat B, Tillier A, Lecointre G, Tillier S (2001) New clades of Euthyneuran Gastropods (Mollusca) from 28S rRNA Sequences. *Molecular Phylogenetics and Evolution* 19: 225–235. <https://doi.org/10.1006/mpev.2001.0926>
- Fitzgerald SJ, Wood DM (2014) A new species of Axymyiidae (Diptera) from western North America and a key to the Nearctic species. *Zootaxa* 3857: 101–113. <https://doi.org/10.11646/zootaxa.3857.1.4>

- Folmer O, Black M, Hoeh W, Lutz R, Vrijenhoek R (1994) DNA primers for amplification of mitochondrial cytochrome c oxidase subunit I from diverse metazoan invertebrates. *Molecular Marine Biology and Biotechnology* 3: 294–299.
- Hall TA (1999) BioEdit: A user-friendly biological sequence alignment editor and analysis program for Windows 95/98/NT. *Nucleic Acids Symposium Series* 41: 95–98.
- Hoang DT, Chernomor O, Von Haeseler A, Minh BQ, Vinh LS (2018) UFBoot2: Improving the Ultrafast Bootstrap Approximation. *Molecular Biology and Evolution* 35: 518–522. <https://doi.org/10.1093/molbev/msx281>
- Kambhampati S, Smith PT (1995) PCR primers for the amplification of four insect mitochondrial gene fragments. *Insect Molecular Biology* 4: 233–236. <https://doi.org/10.1111/j.1365-2583.1995.tb00028.x>
- Katana A, Kwiatowski J, Spalik K, Zakryś B, Szalacha E, Szymańska H (2001) Phylogenetic position of *Koliella* (Chlorophyta) as inferred from nuclear and chloroplast small subunit rDNA. *Journal of Phycology* 37: 443–451. <https://doi.org/10.1046/j.1529-8817.2001.037003443.x>
- Koufopanou V, Reid DG, Ridgway SA, Thomas RH (1999) A molecular phylogeny of the Patellid Limpets (Gastropoda: Patellidae) and its implications for the origins of their antitropical distribution. *Molecular Phylogenetics and Evolution* 11: 138–156. <https://doi.org/10.1006/mpev.1998.0557>
- Krivosheina MG (2000) Family Axymyiidae. In: Papp L, Darvas B (Eds) *Contributions to a Manual of Palaearctic Diptera*. Appendix. Science Herald, Budapest, 31–39.
- Kück P, Longo GC (2014) FASconCAT-G: extensive functions for multiple sequence alignment preparations concerning phylogenetic studies. *Frontiers in Zoology* 11: 81. <https://doi.org/10.1186/s12983-014-0081-x>
- Laurenne NM, Broad GR, Quicke DLJ (2006) Direct optimization and multiple alignment of 28S D2–D3 rDNA sequences: problems with indels on the way to a molecular phylogeny of the cryptine ichneumon wasps (Insecta: Hymenoptera). *Cladistics* 22: 442–473. <https://doi.org/10.1111/j.1096-0031.2006.00112.x>
- Letunic I, Bork P (2024) Interactive Tree of Life (iTOL) v6: recent updates to the phylogenetic tree display and annotation tool. *Nucleic Acids Research* 52: 78–82. <https://doi.org/10.1093/nar/gkae268>
- Martinovský J, Roháček J (1993) First records of *Synneuron annulipes* Lundström (Synneuridae) and *Mesaxymyia kerteszi* (Duda) (Axymyiidae) from Slovakia, with notes on their taxonomy and biology (Diptera). *Časopis Slezského zemského muzea. Série A, Vědy přírodní* 42: 73–78.
- Moulton JK, Wiegmann BM (2004) Evolution and phylogenetic utility of CAD (rudimentary) among Mesozoic-aged Eremoneuran Diptera (Insecta). *Molecular Phylogenetics and Evolution* 31: 363–378. [https://doi.org/10.1016/S1055-7903\(03\)00284-7](https://doi.org/10.1016/S1055-7903(03)00284-7)
- Nguyen L-T, Schmidt HA, Von Haeseler A, Minh BQ (2015) IQ-TREE: A fast and effective stochastic algorithm for estimating maximum-likelihood phylogenies. *Molecular Biology and Evolution* 32: 268–274. <https://doi.org/10.1093/molbev/msu300>
- Palumbi S, Martin A, Romano S, Owen McMillan W, Stice L, Grabowski G (1991) *The simple fool's guide to PCR*. University of Hawaii, Honolulu, 45 pp.
- Polevoi AV, Ruokolainen A, Shorohova E (2018) Eleven remarkable Diptera species, emerged from fallen aspens in Kivach Nature Reserve, Russian Karelia. *Biodiversity Data Journal* 6: 1–22. <https://doi.org/10.3897/BDJ.6.e22175>
- Roháček J, Tóthová A, Vaňhara J (2009) Phylogeny and affiliation of European Anthomyzidae (Diptera) based on mitochondrial 12S and 16S rRNA. *Zootaxa* 2054: 49–58. <https://doi.org/10.11646/zootaxa.2054.1.3>

- Ševčík J, Kaspřák D, Mantič M, Fitzgerald S, Ševčíková T, Tóthová A, Jaschhof M (2016) Molecular phylogeny of the megadiverse insect infraorder Bibionomorpha sensu lato (Diptera). PeerJ 4: e2563. <https://doi.org/10.7717/peerj.2563>
- Shi G, Zhu Y, Shih C, Ren D (2013) A new axymyiid genus with two new species from the Middle Jurassic of China (Diptera: Nematocera: Axymyiidae). Acta Geologica Sinica – English Edition 87: 1228–1234. <https://doi.org/10.1111/1755-6724.12123>
- Sinclair BJ (2013) Rediscovered at last: a new enigmatic genus of Axymyiidae (Diptera) from western North America. Zootaxa 3682: 143–150. <https://doi.org/10.11646/zootaxa.3682.1.7>
- Steenwyk JL, Buida TJ, Li Y, Shen X-X, Rokas A (2020) ClipKIT: A multiple sequence alignment trimming software for accurate phylogenomic inference. PLOS Biology 18: e3001007. <https://doi.org/10.1371/journal.pbio.3001007>
- Stucky BJ (2012) SeqTrace: A graphical tool for rapidly processing DNA sequencing chromatograms. Journal of Biomolecular Techniques: JBT 23: 90–93. <https://doi.org/10.7171/jbt.12-2303-004>
- Timofeeva VV, Kutenkov S (2009) Analysis of recreational impact on living ground cover in forests of Paanajärvi National Park (Republic of Karelia, Russia). Oulanka Reports 29: 16–26.
- Trifinopoulos J, Nguyen L-T, von Haeseler A, Minh BQ (2016) W-IQ-TREE: a fast online phylogenetic tool for maximum likelihood analysis. Nucleic Acids Research 44: 232–235. <https://doi.org/10.1093/nar/gkw256>
- Viramo J (1998) Trips by Finnish entomologists to the Paanajärvi – Kutsa region prior to 1940. Oulanka Reports 19: 11–18.
- Wiegmann BM, Trautwein MD, Winkler IS, Barr NB, Kim J-W, Lambkin C, Bertone MA, Cassel BK, Bayless KM, Heimberg AM, Wheeler BM, Peterson KJ, Pape T, Sinclair BJ, Skevington JH, Blagoderov V, Caravas J, Kutty SN, Schmidt-Ott U, Kampmeier GE, Thompson FC, Grimaldi DA, Beckenbach AT, Courtney GW, Friedrich M, Meier R, Yeates DK (2011) Episodic radiations in the fly tree of life. Proceedings of the National Academy of Sciences 108: 5690–5695. <https://doi.org/10.1073/pnas.1012675108>
- Wihlm MW, Courtney GW (2011) The distribution and life history of *Axymyia furcata* McAtee (Diptera: Axymyiidae), a wood inhabiting, semi-aquatic fly. Proceedings of the Entomological Society of Washington 113: 385–398. <https://doi.org/10.4289/0013-8797.113.3.385>
- Wood DM (1981) Axymyiidae. In: McAlpine JF, Peterson BV, Shewell GE, Teskey HJ, Vockeroth JR, Wood DM (Eds) Manual of Nearctic Diptera. Volume 1. Research Branch Agriculture Canada, Ottawa, 209–212.
- Xia X, Xie Z (2001) DAMBE: Software package for data analysis in molecular biology and evolution. Journal of Heredity 92: 371–373. <https://doi.org/10.1093/jhered/92.4.371>
- Yakovlev E, Scherbakov A, Polevoi AV, Humala A (2000) Insect fauna of Paanajärvi National Park and proposed Kalevala National Park with particular emphasis on saproxylic Coleoptera, Diptera and Hymenoptera. In: Heikkilä R, Heikkilä M, Polevoi A, Yakovlev E (Eds) Biodiversity of old-growth forests and its conservation in the northwestern Russia. North Ostrobothnia Regional Environmental Centre, Oulu, 103–157.
- Zhang J (2010) Two new genera and one new species of Jurassic Axymyiidae (Diptera: Nematocera), with revision and redescription of the extinct taxa. Annals of the Entomological Society of America 103: 455–464. <https://doi.org/10.1603/AN09073>
- Zhang X, Yang D, Kang Z (2023) New data on the mitochondrial genome of Nematocera (lower Diptera): features, structures and phylogenetic implications. Zoological Journal of the Linnean Society 197: 229–245. <https://doi.org/10.1093/zoolin/zlac012>

Appendix 1

Table A1. List of specimens used for the phylogenetic analysis, with GenBank (GB) accession numbers.

Species	Voucher code	Sampling locality and year	12S	16S	18S	28S	COI	CAD
MECOPTERA								
<i>Boreus hyemalis</i> (Linnaeus, 1767)	borhym	from GB	GAYK00000000.2					
DIPTERA								
Anisopodidae								
<i>Mycetobia divergens</i> Walker, 1856	OUT39	USA, 2014	KP288703	KP288735	KP288781	KP288718	KT316870	FJ040587
<i>Sylvicola cinctus</i> (Fabricius, 1787)	SylCin	Czech Republic, 2016	PV156352	PV156360	PV206766	PV230690	PV153731	PV158022
Axymyiidae								
<i>Axymyia furcata</i> McAtee, 1921	axyfur	from GB	n/a	n/a	n/a	KC177639	MG112467	KC177110
<i>Mesaxymyia kerteszi</i> (Duda, 1930)	BA466	Russia, 2016	PV036314	PV036315	n/a	PV036318	PV035247	n/a
<i>Plesioaxymyia imprevisa</i> sp. nov.	BA187	Russia, 2021	PV036313	PV036316	PV036319	PV036317	PV035246	PV037681
<i>Protaxymyia taiwanensis</i> Papp, 2007	ProTai	Taiwan, 2019	PV156350	PV156358	PV206762	PV230687	PV153729	PV158019
<i>Protaxymyia thuja</i> Fitzgerald & Wood, 2014	OUT38	USA, 2014	KP288702	KP288734	KP288780	KP288817	KT316869	KX453744
Blephariceridae								
<i>Edwardsina gigantea</i> Zwick, 1977	edgi	from GB	KC177470	KC177460	KC177283	KC177655	KC192960	FJ040624
<i>Liponeura cinerascens</i> Loew, 1844	LipCin	Slovakia, 2021	PV156349	PV156357	PV206759	PV230686	PV153728	PV158017
Bibionidae								
<i>Bibio marci</i> (Linnaeus, 1758)	OUT1	Czech Republic, 2013	KJ136689	KJ136724	KP288758	KJ136761	KT316846	KX453730
<i>Dilophus femoratus</i> Meigen, 1804	OUT23	Slovakia, 2014	KP288696	KP288728	KP288773	KP288811	KT316864	KX453740
<i>Penthetria funebris</i> Meigen, 1804	OUT14	Slovakia, 2014	KP288689	KP288721	KP288767	KP288804	KT316858	KX453735
<i>Plecia nearctica</i> Hardy, 1940	OUT2	USA, 2013	KJ136690	KJ136725	KP288759	KJ136762	KT316847	n/a
Bolitophilidae								
<i>Bolitophila cinerea</i> Meigen, 1818	B1	Slovakia, 2012	–	KJ136712	–	–	–	–
	BolCin	Czech Republic, 2016	ON601484	–	ON650659	ON601118	MT446881	ON706250
<i>Bolitophila hybrida</i> (Meigen, 1804)	BolHyb	Slovakia, 2021	JANSTU000000000.1					
Canthylosceldidae								
<i>Canthylosceldis pectipennis</i> Edwards, 1930	CanPic	Argentina, 2022	PV156346	PV156355	PV206757	PV230685	PV153726	n/a
<i>Hyperoscelis veterosa</i> Mamaev & Krivosheina, 1969	OUT24	Slovakia, 2014	KP288697	KP288729	KP288774	KP288812	KT316865	KX453741
<i>Synneuron annulipes</i> Lundstrom, 1910	OUT57	Slovakia, 2016	KX453693	KX453701	n/a	KX453713	KX453763	n/a
Cecidomyiidae								
<i>Asphondylia sarotharni</i> (Loew, 1850)	OUT18	Czech Republic, 2014	KP288692	KP288724	KP288770	KP288807	KX453761	KX453738
<i>Catocha angulata</i> Jaschhof, 2009	C26	Slovakia, 2014	KP288677	KP288711	KP288750	KP288792	KT316837	KX453719
<i>Catotricha suboboleta</i> (Alexander, 1924)	OUT42	USA, 2014	KP288706	KP288738	KP288784	KP288821	KT316873	KX453747
<i>Porricondyla nigripennis</i> (Meigen, 1880)	OUT16	Slovakia, 2014	KP288690	KP288722	KP288768	KP288805	KT316859	KX453736

Species	Voucher code	Sampling locality and year	12S	16S	18S	28S	COI	CAD
Ceratopogonidae								
<i>Culicoides sonorensis</i> Wirth & Jones, 1957	culson	from GB	BK065013	BK065013	n/a	n/a	BK065013	GAWM0000000.1
Chaoboridae								
<i>Chaoborus flavicans</i> (Meigen, 1830)	CH-F2	Slovakia, 2019	PV156348	PV156356	PV206758	n/a	PV153727	PV158016
Chironomidae								
<i>Cricotopus draysoni</i> Cranston & Krosch, 2015	cridra	from GB	GFNI00000000.1	GFNI00000000.1	n/a	n/a	GFNI00000000.1	GFNI00000000.1
<i>Chironomus tepperi</i> Skuse, 1889	chitep	from GB	NC_016167	NC_016167	KC177280	KC177658	NC_016167	FJ040616
Culicidae								
<i>Anopheles gambiae</i> Giles, 1902	anogam	from GB	NC_002084	NC_002084	AM157179	KC177663	NC_002084	KC177121
Deuterophlebiidae								
<i>Deuterophlebia coloradensis</i> Pennak, 1945	deucol	from GB	n/a	n/a	GQ465776	FJ040539	GQ465781	KC177114
Diadocidiidae								
<i>Diadocidia ferruginosa</i> (Meigen, 1830)	SJ1	Slovakia, 2010	–	MG554126	KP288786	–	–	–
	diafer	Czech Republic, 2016	PV156347	–	–	ON601121	MT446885	PV158015
<i>Diadocidia globosa</i> Papp & Ševčík, 2005	SJ9	Thailand, 2008	KP288708	KP288740	KP288789	KP288822	KT316878	KX453755
Ditomyiidae								
<i>Ditomyia fasciata</i> (Meigen, 1818)	SJ3	Czech Republic, 2010	KJ136698	MG554125	MG554141	KJ136770	MG554168	KX453753
<i>Symmerus annulatus</i> (Meigen, 1830)	D2	Slovakia, 2012	MT446483	KX453696	–	KX453708	KX453757	–
	symann	from GB	–	–	FJ171934	–	–	KC177112
Dixidae								
<i>Dixa submaculata</i> Edwards, 1920	OUT58b	Czech Republic, 2015	KX453694	KX453702	KX453706	KX453714	KX453764	–
	dixsub	from GB	–	–	–	–	–	KC177123
Hesperinidae								
<i>Hesperinus brevifrons</i> Walker, 1848	OUT41	USA, 2014	KP288705	KP288737	KP288783	KP288820	KT316872	KX453746
<i>Hesperinus ninae</i> Papp & Krivosheina, 2010	OUT12	Georgia, 2013	KP288687	KP288719	KP288765	KP288802	KT316856	KX453734
Keroplattidae								
<i>Keroplatus testaceus</i> Dalman, 1818	B7	Slovakia, 2014	KJ136683	MG554129	KP288746	–	–	KX453716
	KerTes	Czech Republic, 2016	–	–	–	ON601130	MT446947	–
<i>Lygistorrhina sanctaecatharinae</i> Thompson, 1975	lygsan	USA, 2018	–	MT446624	PV206760	ON601102	MT446948	PV158018
	K105	USA, 2018	MT446547	–	–	–	–	–
<i>Macrocera centralis</i> Meigen, 1818	K10	Slovakia, 2013	KP288682	KP288716	KP288755	KP288797	KT316841	KX453723
<i>Paleoplatyura johnsoni</i> Johannsen, 1910	PaJo	Italy, 2016	MT446551	MT446627	PV206761	MT446846	–	–
	K80	Italy, 2016	–	–	–	–	MG049755	MT446675
Limoniidae								
<i>Rhipidia sejuga</i> Zhang, Li & Yang, 2014	rhisej	from GB	GEMJ00000000.1					
Mycetophilidae								
<i>Exechia fusca</i> (Meigen, 1804)	ExFu	Czech Republic, 2016	MG684498	MH114203	MG684611	ON601123	MG684785	–
	E19	Czech Republic, 2015	–	–	–	–	–	MK133002

Species	Voucher code	Sampling locality and year	12S	16S	18S	28S	COI	CAD
<i>Gnoriste bilineata</i> Zetterstedt, 1852	GS4	Czech Republic, 2009	KP288679	KP288713	KP288752	KP288794	KT316839	KX453720
<i>Sciophila rufa</i> Meigen, 1830	SciRuf	Czech Republic, 2021	MT446554	ON601475	PV206765	ON601116	MT446956	PV158021
<i>Taxicnemis marshalli</i> Matile, 1989	NZ1	New Zealand, 2016	ON601489	ON601459	ON650665	ON601136	ON601531	ON706255
Pachyneuridae								
<i>Cramptonomyia spenceri</i> Alexander, 1931	OUT37	USA, 2014	–	–	KP288779	–	–	–
	craspe	from GB	NC_016203	NC_016203	–	KC177653	NC_016203	FJ040632
<i>Pachyneura fasciata</i> Zetterstedt, 1838	OUT40	Finland, 2012	KP288704	KP288736	KP288782	KP288819	KT316871	KX453745
Psychodidae								
<i>Clogmia albipunctata</i> (Williston, 1893)	OUT21	Czech Republic, 2014	KP288695	KP288727	–	KP288810	KT316863	–
	cloalb	from GB	–	–	KC177281	–	–	FJ040622
Ptychopteridae								
<i>Ptychoptera albimana</i> (Fabricius, 1787)	OUT51	Czech Republic, 2015	KX453691	KX453699	KX453704	KX453711	KX453762	KX453750
<i>Ptychoptera lacustris</i> Meigen, 1830	PtyLa	Czech Republic, 2018	PV156351	PV156359	PV206763	PV230688	PV153730	PV158020
Scatopsidae								
<i>Aspistes berolinensis</i> Meigen, 1818	OUT43	Czech Republic, 2013	KP288707	KP288739	KP288785	KX453710	–	–
	AspBer	Czech Republic, 2018	–	–	–	–	PV153725	PV158014
<i>Scatopse notata</i> (Linnaeus, 1758)	OUT3	Czech Republic, 2011	KJ136691	KJ136726	KP288760	KJ136763	KT316848	KX453731
Sciaridae								
<i>Bradysia tilicola</i> (Loew, 1850)	bratil	from GB	GQ387651	GQ387651	KC177279	FJ040522	GQ387651	FJ040621
<i>Sciara hemerobioides</i> (Scopoli, 1763)	SciHem	Czech Republic, 2018	MT446553	MT446628	PV206764	PV230689	MT446955	MT446687
Simuliidae								
<i>Parasimulium crosskeyi</i> Peterson, 1977	parcro	from GB	AF049472	n/a	n/a	KC177660	FJ524493	KC177118
Tanyderidae								
<i>Protoplasma fitchii</i> Osten Sacken, 1859	profit	from GB	KC177472	KC177462	KC177286	KC177670	NC_016202	FJ040626
Thaumaleidae								
<i>Thaumalea bezzii</i> Edwards, 1929	OUT53	Slovakia, 2015	KX453692	KX453700	KX453705	KX453712	–	KX453751
	thabez	from GB	–	–	–	–	KT215925	–
Tipulidae								
<i>Tanyptera atrata</i> (Linnaeus, 1758)	TanAtr	Czech Republic, 2021	PV156353	PV156361	PV206767	PV230691	PV153732	n/a
<i>Tipula abdominalis</i> (Say, 1823)	tipabd	from GB	KC177466	KC177457	KC177288	KC177678	KC192958	GQ265584
Trichoceridae								
<i>Trichocera saltator</i> Harris, 1778	trisal	from GB	GAXZ00000000.2					
<i>Sciaroidea incertae sedis</i>	–	–	–	–	–	–	–	–
<i>Heterotricha takkae</i> Chandler, 2002	HetTak	Greece, 2016	MG684499	MG684543	MG684612	ON601125	MG684786	MH114336
<i>Chiletricha spinulosa</i> Chandler, 2002	MJ16	Chile, 2000	KT316809	KT316814	KT316819	KT316824	KX453760	KX453727

Species	Voucher code	Sampling locality and year	12S	16S	18S	28S	COI	CAD
<i>Insulatricha hippai</i> Jaschhof, 2004	IS4a	New Zealand, 2016	ON601487	ON601480	ON650663	ON601128	ON601501	ON706253
<i>Ohakunea bicolor</i> Edwards, 1927	MJ38	New Zealand, 2002	KT316810	KT316815	KT316820	KT316825	KT316844	KX453728
<i>Rangomarama tonnoiri</i> Jaschhof & Didham, 2002	MJ51	New Zealand, 2002	ON601488	ON601481	ON650664	ON601135	ON601502	–
<i>Rangomarama</i> sp.	MJ54	New Zealand, 2002	–	–	–	–	–	ON706254
<i>Sciaropota japonica</i> Chandler, 2002	DL30	South Korea, 2022	OQ533498	OQ533499	OQ533501	OQ533500	OQ525969	OQ539524
Brachycera								
<i>Asilus crabroniformis</i> Linnaeus, 1758	asicra	from GB	KC177475	KC177451	KC177289	KC177704	KC192962	EF650383
<i>Bombylius major</i> Linnaeus, 1758	bommaj	from GB	KC177474	KC177450	KC177290	KC177708	KC192961	KC177144
<i>Haematopota pluvialis</i> Linnaeus, 1758	haeplu	from GB	KC177479	KC177454	KC177294	KC177694	MZ563333	n/a
<i>Musca domestica</i> Linnaeus, 1758	mucdom	from GB	AY573084	KC347601	KC177313	KC538816	JX438043	AY280689
<i>Platypeza anthrax</i> Loew, 1870	plaaant	from GB	GCGU00000000.1	n/a	n/a	GCGU00000000.1	GCGU00000000.1	n/a
<i>Xylomya maculata</i> (Meigen, 1804)	XylMac	Czech Republic, 2020	PV156354	PV156362	PV206768	PV230692	PV153733	n/a

Supplementary material 1

Linked Data table of specimens used for the phylogenetic analysis

Authors: Alexei Polevoi, Nikola Burdíkova, Jan Ševčík

Data type: xlsx

Explanation note: File includes linked table with taxa used in the phylogenetic analysis and GenBank accession numbers for sequences.

Copyright notice: This dataset is made available under the Open Database License (<http://opendatacommons.org/licenses/odbl/1.0/>). The Open Database License (ODbL) is a license agreement intended to allow users to freely share, modify, and use this Dataset while maintaining this same freedom for others, provided that the original source and author(s) are credited.

Link: <https://doi.org/10.3897/zookeys.1236.148218.suppl1>

